

**Characterisation of a novel STAT3 inhibitor,
VS-43, and the role of STAT3 in the repair of
DNA-interstrand crosslinks**

by

Helen Valentine

A thesis submitted to University College London for the
degree of Doctor of Philosophy

January 2017

Declaration

I, Helen Valentine, confirm that the work presented in this thesis is my own. Where information has been derived from other sources, I confirm that this has been indicated in the thesis.

For my wonderful parents, sister, and boyfriend...

...and for my feline friend, Tinky.

Abstract

Signal Transducer and Activator of Transcription 3 (STAT3) is a transcription factor constitutively activated in cancer, leading to survival, proliferation, angiogenesis and metastasis. STAT3 inhibitors possess anti-cancer properties, however, the selectivity and potency of current inhibitors must be improved. This thesis characterises a novel STAT3 inhibitor, VS-43. VS-43 is a potent and selective STAT3 inhibitor, able to inhibit cancer cell growth and induce apoptosis in cancer cell lines. VS-43 is shown to inhibit STAT3 DNA binding and downstream target expression. VS-43 is also able to synergise with cisplatin, and this combination is more synergistic than the combination of cisplatin with other STAT3 inhibitors.

Cisplatin acts via the formation of adducts with the cellular DNA, and the interstrand crosslink (ICL) is the most toxic of the cisplatin lesions. Resistance to cisplatin can occur via enhanced repair of ICLs. Therefore, the effect of STAT3 inhibition on ICL repair was investigated. STAT3 inhibitors are shown to block the unhooking of cisplatin-induced ICLs and down-regulate the expression of the ICL repair factors EME1, MUS81, BRCA1 and FANCD2. Binding of STAT3 to the MUS81 and EME1 promoters was demonstrated using CHIP assays, suggesting direct transcriptional regulation of the MUS81-EME1 nuclease by STAT3. In contrast, STAT3 inhibitors did not synergise with melphalan and did not block melphalan-ICL unhooking. siRNA knockdown of MUS81 or EME1 demonstrated that the MUS81-EME1 nuclease is selectively involved in cisplatin-ICL repair.

This thesis presents VS-43 as a promising novel STAT3 inhibitor, and provides mechanistic insight into how STAT3 inhibitors synergise with cisplatin through the regulation of ICL unhooking. Understanding the differences in the repair of different ICLs will be essential for the design of future chemotherapy combinations.

Acknowledgements

First I would like to thank my primary supervisor Professor John Hartley, for the opportunity to carry out my PhD in your lab, and for the guidance you have given me along the way. I would also like to thank my secondary supervisor, Dr Kostas Kiakos, for teaching me so much back at the beginning of this project.

Thank you to Professor Moses Lee for providing myself and other members of our lab the opportunity to explore exciting new avenues using the compounds your group has developed. And I must, of course, thank Cancer Research UK for the funding to carry out my PhD and the opportunities they offer to their students.

Thank you to John Ambrose and Javier Herrero for the bioinformatics screening they performed for this project. And to Dimitra Georgopoulou for advising me on the design of the ChIP experiments.

A huge thank you to those of you in the CRUK Drug-DNA interactions research group who made each day great fun: Michael, Juanjo, Simon, Halla and Nari. Special thanks to Luke, for being my PhD buddy from beginning to end, providing me with much needed gossip sessions at least daily! Thank you to Sylwia for being a great friend, always having time for a chat over coffee (or an ice cream!), and for all your sterling advice. And of course, thank you to John Bingham, for educating me both in science, and in your terrible taste in old films!

Thank you also to the former members of the lab: Ruochen, Valeria, Francesca and Miguel, and to the Chester and Boshoff labs where I spent several months during my first year rotations.

Now, my friends Suzi and Jess, what can I say? You have both supported me throughout my PhD. Our chilled-out Friday nights have truly kept me going when it has been a stressful week in the lab. So thank you, especially to you Suzi, for being everything a best friend should be.

Thank you to my big sister, Sarah. Even from a young age you were always someone for me to look up to. So, probably without knowing, you have inspired me to work hard and to achieve what I want to achieve.

I have to say a huge thank you to my boyfriend, James. You have always been there for me, ready with dinner on the table and a glass of wine after a long day in the lab or a terrible commute! I would never have got through the last 4 years without you by my side. I will always be grateful for your support, and I love you very much.

Mum and dad, no one deserves more praise than you two for making this possible. Mum, you are the strongest woman I know, I can only hope that your constant support and advice has made me half as strong a person as you are! Dad, you are always there when I need you, and you never fail to make me laugh, even when my PhD has stressed me out to the limit! You have both been so supportive, not just for the last 4 years, but throughout my life, so thank you!!

And finally, I have to thank my cat, Tinker. She may not consciously realise it, but for the last 17 years she has been the best listener of all, and is probably a scientific genius in the world of cats! I love you Tinky.

Thank you all.

Communications

- **Poster presentation:** Valentine, H., Dixon, E., Hartley, J. A., Kiakos, K. Chemosensitisation to cisplatin by STAT3 inhibitors is mediated through the inhibition of DNA interstrand crosslink unhooking. AACR-NCI-EORTC International Conference on Molecular Targets and Cancer Therapeutics, Boston Massachusetts, USA. November 2015.
- **Poster presentation:** Valentine, H., Satam, V., Patel, P., Sjöholm, R., Lee, M., Lee, Moses., Hartley, J.A., Kiakos, K. Characterisation of a novel and potent STAT3 inhibitor, VS-43. 24TH Biennial Congress of the European Association for Cancer Research, Manchester, UK. July 2016.

Table of Contents

Declaration	2
Abstract	4
Acknowledgements	5
Communications	7
Table of Contents	8
List of Figures	16
List of Tables	25
Abbreviations	27
Chapter 1 Introduction	34
1.1 The epidemiology of cancer	34
1.1.1 Prostate cancer	36
1.1.2 Lung Cancer.....	36
1.2 The biology of cancer.....	37
1.2.1 The hallmarks of cancer and genomic instability	38
1.3 Treatments for cancer	45
1.3.1 Treatments for prostate cancer	45
1.3.2 Treatments for lung cancer	46
1.4 Cancer chemotherapy	50
1.5 DNA as an anti-cancer target.....	52
1.6 DNA-interacting drugs	54
1.6.1 Crosslinking agents.....	56
1.7 Drug resistance.....	64
1.7.1 Cisplatin resistance	65

1.7.2	Melphalan resistance	68
1.7.3	Chemotherapy cross-resistance	70
1.8	DNA repair	72
1.8.1	Major mechanisms of repair	74
1.8.2	ICL repair	89
1.8.3	Fanconi's Anemia and the FA complementation groups.....	95
1.9	The STAT3 signalling pathway	98
1.9.1	Introduction to the STAT transcription factors.....	98
1.9.2	STAT3 signalling	100
1.9.3	STAT3 and cancer	104
1.10	Targeting STAT3 in cancer	107
1.10.1	Direct STAT3 inhibitors	109
1.10.2	Indirect STAT3 inhibitors.....	112
1.10.3	STAT3 Inhibitors as chemosensitisers.....	117
1.11	Thesis aims and objectives	119
Chapter 2	Methods and Materials	120
2.1	Reagents.....	120
2.2	Maintenance of Cell Lines.....	120
2.3	Frozen cell line stocks	121
2.4	Counting of cells.....	121
2.5	Immunoblotting.....	122
2.5.1	Seeding, Treatment and Whole Cell Protein Extraction.....	122
2.5.2	Protein Quantification.....	122
2.5.3	Protein Sample Preparation	123
2.5.4	Immunoblotting Procedure	123
2.6	Cytotoxicity Assays.....	126
2.6.1	Sulphorhodamine B Cell Growth Inhibition Assays.....	126

2.6.2	MTT Assay	127
2.6.3	Quantification of Growth Inhibition	127
2.6.4	Quantification of Drug Interactions: Chou-Talalay Combination Index Analysis.....	128
2.7	STAT Family Specificity ELISA	129
2.7.1	Treatment of Cells and Preparation of Samples	129
2.7.2	ELISA Assay Procedure.....	129
2.7.3	Quantification of STAT Activation and DNA binding	131
2.8	Electrophoretic Mobility Shift Assay (EMSA)	131
2.9	Single Cell Gel Electrophoresis (Comet) Assay	132
2.9.1	Treatment of Cells and Preparation of Samples	132
2.9.2	Comet Assay Procedure	132
2.9.3	Analysis of Slides	133
2.10	Immunofluorescence.....	134
2.10.1	Seeding and Treatment of Cells.....	134
2.10.2	Fixing and Staining of Cells.....	135
2.10.3	Confocal Microscopy.....	136
2.11	Quantitative Reverse-Transcriptase PCR (qRT-PCR):	136
2.11.1	Treatment of Cells.....	136
2.11.2	RNA Extraction and cDNA Generation	137
2.11.3	qRT-PCR Procedure and Analysis.....	138
2.12	Cell Cycle Analysis.....	140
2.12.1	Drug Treatment of cells.....	140
2.12.2	Preparation of cells for flow cytometry	140
2.12.3	Collection of cell cycle data.....	141
2.12.4	Analysis of cell cycle data	141
2.13	siRNA knockdowns	142
2.14	Whole genome screening of STAT3 binding sites	143

2.15 Chromatin Immunoprecipitation (ChIP) Assay	144
2.15.1 Design of primers	144
2.15.2 Seeding, treatment and harvesting of cells	145
2.15.3 Shearing of chromatin and chromatin immunoprecipitation	146
2.15.4 PCR and analysis.....	147
2.16 Statistical Analysis	149
Chapter 3 A Novel, Selective STAT3 Inhibitor: VS-43.	150
3.1 Introduction.....	150
3.1.1 Rationale for the design of a novel STAT3 inhibitor, VS-43.....	150
3.1.2 Why is there a need for selectivity with STAT3 inhibitors?	151
3.1.3 Design of VS-43	154
3.2 Aims	156
3.3 Results.....	157
3.3.1 STAT3 is constitutively activated in cancer cell lines	157
3.3.2 VS-43 inhibits pSTAT3 ^{Tyr705} protein levels	158
3.3.3 VS-43 is more potent than stattic or curcumin	160
3.3.4 VS-43 inhibits STAT3 DNA binding.....	161
3.3.5 VS-43 action is dependent on confluency, treatment time and dose ..	163
3.3.6 Inhibition of pSTAT3 ^{Tyr705} by VS-43 is persistent	165
3.3.7 VS-43 is a selective STAT3 inhibitor.....	166
3.3.8 VS-43 down-regulates STAT3 target genes	168
3.3.9 VS-43 induces apoptosis and inhibits cell growth	168
3.4 Discussion.....	172
3.4.1 How does VS-43 bind to STAT3?	173
3.4.2 How does VS-43 compare to other STAT3 inhibitors?	178
3.4.3 Why is VS-43 potency cell line dependent?.....	181
3.4.4 How does STAT3 inhibition induce apoptosis?.....	182

3.5	Conclusion	183
Chapter 4 STAT3 inhibitors sensitise cancer cells to cisplatin		
4.1	Introduction	184
4.1.1	Resistance mechanisms to Cisplatin	184
4.1.2	Cisplatin-based combination treatments in cancer	187
4.1.3	STAT3 Inhibitors and Cisplatin.....	189
4.2	Aims	191
4.3	Results	191
4.3.1	Stattic and Curcumin inhibit the growth of cancer cell lines	191
4.3.2	Cisplatin inhibits growth of DU145 and A549 cancer cell lines	192
4.3.3	Stattic and curcumin sensitise cancer cell lines to cisplatin with moderate synergy	194
4.3.4	VS-43 sensitises cancer cell lines to cisplatin with greater synergy than other STAT3 inhibitors	202
4.3.5	STAT3 inhibitor and Cisplatin Combination therapy Enhances Apoptosis in Cancer Cell Lines	212
4.3.6	VS-43 can also chemosensitise DU145 cells to doxorubicin	214
4.4	Discussion.....	216
4.4.1	How does VS-43 compare to other STAT3 inhibitors as a chemosensitiser?	216
4.4.2	Which drug treatment schedule produces the greatest synergy?	220
4.4.3	Why is the synergy between VS-43 and cisplatin not greater?	222
4.4.4	How Do STAT3 Inhibitors Sensitise Cells to Cisplatin?	225
4.4.5	Combination of STAT3 inhibitors with other chemotherapy drugs	227
4.5	Conclusion	228
Chapter 5 STAT3 modulates the repair of cisplatin-induced DNA damage		
		229

5.1	Introduction	229
5.1.1	γ H2AX as a marker of the crosslinker-induced DNA damage response 229	
5.1.2	The key stage of ICL repair: crosslink unhooking	230
5.2	Aims	239
5.3	Results	239
5.3.1	VS-43 inhibits the unhooking of cisplatin-induced ICLs	239
5.3.2	Stattic and Curcumin also inhibit cisplatin-induced DNA-ICL unhooking 246	
5.3.3	STAT3 inhibition alters the DNA damage response after treatment with cisplatin	249
5.3.4	VS-43 regulates the expression of DNA repair proteins	257
5.3.5	STAT3 inhibition blocks G1 to S phase cell cycle progression	269
5.3.6	STAT3 consensus binding sites reside within ICL repair gene promoters 276	
5.3.7	STAT3 binds to the promoters of EME1 and MUS81	279
5.4	Discussion	282
5.4.1	The roles of VS-43 regulated DNA repair factors.....	284
5.4.2	Combination of other DNA repair inhibitors with cisplatin	285
5.4.3	Genetic mutations in the ICL unhooking machinery and cisplatin sensitivity.....	287
5.4.4	Does STAT3 regulate the transcription of genes involved in ICL unhooking?.....	290
5.5	Conclusion	293
 Chapter 6 Cisplatin and Melphalan DNA-ICLs repair via different		
	unhooking mechanisms	294
6.1	Introduction	294

6.1.1	Rationale for investigating melphalan: chemosensitisation studies and ICL repair	294
6.1.2	Structural differences between ICL agents	296
6.2	Aims	301
6.3	Results	301
6.3.1	Melphalan inhibits cancer cell line growth.....	301
6.3.2	STAT3 inhibitors do not chemosensitise cancer cell lines to melphalan 302	
6.3.3	Combination with STAT3 inhibitors does not enhance apoptosis or DNA damage in melphalan-treated cells	312
6.3.4	STAT3 inhibition has no effect on melphalan DNA-ICL repair	313
6.3.5	STAT3 knockdown by siRNA blocks cisplatin but not melphalan DNA-ICL unhooking	318
6.3.6	Knockdown of EME1 or MUS81 specifically abolishes cisplatin-ICL repair 322	
6.3.7	Expression of EME1 and MUS81 is interdependent	329
6.4	Discussion.....	330
6.4.1	Differences between cisplatin and melphalan-ICL repair.....	331
6.4.2	The role of MUS81-EME1 in ICL repair: evidence so far	335
6.4.3	Other possible combinations for STAT3 inhibitors	336
6.4.4	The interdependency of EME1 and MUS81.....	340
6.5	Conclusion	341
Chapter 7	Conclusions	342
7.1	Future work	348
7.1.1	Further development of VS-43 as a therapeutic agent	348
7.1.2	Optimisation of combination schedules.....	348
7.1.3	Combination of STAT3 inhibitors with other chemotherapy agents	349

7.1.4	Further investigation of the ICL unhooking mechanism	350
7.1.5	Clinical relevance of MUS81-EME1	353
7.2	Final conclusion	354

References 355

Appendices	418
Appendix A: Gene list for DNA damage signalling arrays.....	418
Appendix B: Synthesis of VS-43	424
Appendix C: STAT3 binding sites upstream of DNA repair genes identified by UCSC Genome Browser.....	426
Appendix D: Radiosensitisation by VS-43	431

List of Figures

Figure 1-1: The twenty most common cancers in the UK, and their incidence.	35
Figure 1-2: Types of tumour heterogeneity.	38
Figure 1-3: The six Hallmarks of Cancer.	39
Figure 1-4: Accumulation of mutations from a fertilised egg to a chemotherapy resistant tumour cell.	43
Figure 1-5: The four DNA binding modes for bifunctional agents:	55
Figure 1-6: Chemical structure of cisplatin before and after hydrolysis.	59
Figure 1-7: Structure of a cisplatin ICL.	60
Figure 1-8: Formation of nitrogen mustard monoadducts (1) and interstrand crosslinks (2) between two N7 guanine atoms.	63
Figure 1-9: Factors contributing to the development of resistance of cisplatin.	66
Figure 1-10: Fates of cells after DNA damage: cell death, cancer, and aging.	72
Figure 1-11: DNA damage detection by the ATR and ATM kinases, and the resulting arrest in cell cycle due to inhibition of cyclin-dependent kinases.	73
Figure 1-12: Simplified model for homologous recombination.	76
Figure 1-13: Model for single strand annealing homologous recombination.	77

Figure 1-14: Simplified model for NHEJ.....	79
Figure 1-15: Mechanism of base excision repair.....	81
Figure 1-16: Mechanism of nucleotide excision repair.....	83
Figure 1-17: Model of the mismatch repair pathway.....	86
Figure 1-18: Lesion bypass can occur by polymerase switch or template switch mechanisms.....	88
Figure 1-19: Cole Model for ICL repair in E.coli.....	90
Figure 1-20: One model for replication-independent ICL repair in mammalian cells.....	92
Figure 1-21: One model for replication-dependent ICL repair.....	94
Figure 1-22: Role of the Fanconi Anaemia proteins in initiation of ICL repair.....	97
Figure 1-23: STAT Family protein domains.....	99
Figure 1-24: STAT3 Signalling Pathway.....	101
Figure 1-25: Different methods for intervention of the STAT3 pathway.....	108
Figure 1-26: Action of EGFR inhibitors.....	114
Figure 3-1: Crystal structure of a STAT3 Dimer binding to DNA, and amino acid conservation between STAT1 and STAT3.....	153
Figure 3-2: Structures of curcumin and stattic.....	154

Figure 3-3: The molecular structures of curcumin, HO-3867, compound 9 and the novel STAT3 inhibitor VS-43.	156
Figure 3-4: Expression of pSTAT3 ^{Tyr705} in the A549 and DU145 cell lines.	157
Figure 3-5: VS-43 inhibits pSTAT3 ^{Tyr705} levels in a dose-dependent manner in both the DU145 and A549 cell lines.	159
Figure 3-6: Confocal microscopy showing pSTAT3 ^{Tyr705} levels in A549 cells treated with VS-43 for 18 hours.	160
Figure 3-7: Stattic and curcumin inhibit pSTAT3 ^{Tyr705} levels in the DU145 and A549 cell lines.	162
Figure 3-8: VS-43 inhibits binding of STAT3 (indicated by arrowhead) to the hSIE consensus binding sequence from the <i>c-fos</i> promoter region, and did so at lower concentrations than stattic.	163
Figure 3-9: pSTAT3 ^{Tyr705} inhibition by VS-43 is dependent on A) exposure time and B) confluency of DU145 cells.	164
Figure 3-10: Inhibition of pSTAT3 ^{Tyr705} by VS-43 persists for at least 24 hours after drug treatment (18 hours) in both the DU145 and A549 cell lines.	165
Figure 3-11: VS-43 is a specific pSTAT3 ^{Tyr705} inhibitor as shown by A) immunoblotting and B) STAT family ELISA assay.	167
Figure 3-12: Treatment of DU145 cells with VS-43 for 1 hour selectively inhibits STAT3 activation and DNA binding.	168

Figure 3-13: VS-43 down-regulates bcl-2 and survivin expression in the DU145 cell line.....	169
Figure 3-14: VS-43 inhibits cell growth in the DU145 and A549 cancer cell lines.	170
Figure 3-15: Treatment of DU145 and A549 cells with VS-43 for 18 hours results in a dose-dependent increase in cleaved PARP expression, indicative of apoptosis.....	171
Figure 3-16: Structures of curcumin and FLLL32.....	174
Figure 3-17: Molecular modelling and conformation of inhibitors targeting the STAT3 DNA binding domain.	177
Figure 3-18: The molecular structures of STAT3 DNA-binding domain inhibitors:..	178
Figure 3-19: Structures of BB-IV-101 and VS-43.....	179
Figure 4-1: A) Stattic and B) curcumin inhibit cell growth in the DU145 and A549 cancer cell lines.....	192
Figure 4-2: Cisplatin inhibits cell growth in the A) A549 and B) DU145 cancer cell lines.....	193
Figure 4-3: Combination of stattic and cisplatin in A549 cells.....	198
Figure 4-4: Combination of stattic and cisplatin in DU145 cells.....	199
Figure 4-5: Combination of curcumin and cisplatin in A549 cells.....	200
Figure 4-6: Combination of curcumin and cisplatin in DU145 cells.....	201

Figure 4-7: Combination of VS-43 and cisplatin in A549 cells using the fixed ratio method.	204
Figure 4-8: Combination of VS-43 and cisplatin in DU145 cells using the fixed ratio method.	205
Figure 4-9: A) Acute 1 hour exposure of DU145 and A549 cells to VS-43 down-regulates pSTAT3 ^{Tyr705} . B) Treatment with 1 hour VS-43 exhibits minimal cell growth inhibition on DU145 and A549 cells, as determined by SRB assay. ...	208
Figure 4-10: Combination of VS-43 and cisplatin in A549 cells using the non-fixed ratio method.	210
Figure 4-11: Combination of VS-43 and cisplatin in DU145 cells using the non-fixed ratio method.	211
Figure 4-12: Combination of STAT3 inhibitors and cisplatin enhances apoptosis.	213
Figure 4-13: Combination of VS-43 and doxorubicin in DU145 cells using the fixed ratio method.	215
Figure 4-14: CI plots for the fixed and non-fixed ratio combination of VS-43 and cisplatin, in the A549 and DU145 cell line.	221
Figure 4-15: Cisplatin and VS-43 independently induce cellular apoptosis.	223
Figure 5-1: Model for initiation of replication-dependent ICL unhooking by BRCA1, FANCD2, SLX4, XPF-ERCC1, MUS81-EME1 and UHRF1.	236
Figure 5-2: Single cell electrophoresis results in “head” and “tail” DNA, for each cell.	238

Figure 5-3: STAT3 inhibitors do not induce DNA damage.	240
Figure 5-4: VS-43 inhibits ICL unhooking. Fixed ratio combination of VS-43 with cisplatin in the A) DU145 and B) A549 cell lines.	242
Figure 5-5: Representative comet images for DU145 cells treated with VS-43 and cisplatin.	243
Figure 5-6: VS-43 inhibits ICL unhooking. Non-fixed ratio combination of VS-43 with cisplatin in the A) DU145 and B) A549 cell lines.	245
Figure 5-7: Stattic inhibits ICL unhooking.....	247
Figure 5-8: Curcumin inhibits ICL unhooking.	248
Figure 5-9: VS-43 enhances cisplatin-induced γ H2AX expression in the DU145 cell line.....	250
Figure 5-10: Quantification of γ H2AX staining in the DU145 cell line after treatment with VS-43, cisplatin or the combination treatment.	251
Figure 5-11: VS-43 enhances γ H2AX expression after a low dose of cisplatin in the DU145 cell line.	253
Figure 5-12: Quantification of γ H2AX staining in the DU145 cell line after treatment with VS-43, low-dose cisplatin or the combination treatment.	254
Figure 5-13: VS-43 enhances cisplatin-induced γ H2AX expression in the A549 cell line.....	255
Figure 5-14: Curcumin enhances cisplatin-induced γ H2AX expression.	256

Figure 5-15: STAT3 inhibitors increase cisplatin-induced γ H2AX expression, as shown by immunoblot analysis.....	257
Figure 5-16: A) STAT3 inhibitors do not regulate ERCC1 or XPF expression. B) VS-43 does not regulate SLX4 expression.	262
Figure 5-17: VS-43 inhibits FANCD2, BRCA1, EME1 and MUS81 mRNA expression in the DU145 cell line.	264
Figure 5-18: VS-43 inhibits expression of BRCA1, FANCD2, EME1 and MUS81 in the A) DU145 and B) A549 cell lines.....	265
Figure 5-19: A) Stattic and curcumin inhibit the expression of BRCA1, FANCD2, EME1 and MUS81. B) Stattic and C) curcumin inhibit the mRNA expression of FANCD2, BRCA1, EME1 and MUS81.	268
Figure 5-20: VS-43 decreases the percentage of S-phase cells.....	270
Figure 5-21: Stattic decreases the percentage of S-phase cells.....	271
Figure 5-22: Curcumin decreases the percentage of S-phase cells.	272
Figure 5-23: STAT3 inhibitors block the progression of cells from G1 to S phase.	274
Figure 5-24: The expression of BRCA1, but not FANCD2, EME1 or MUS81 is cell cycle regulated.	276
Figure 5-25: EME1 STAT3 promoter binding site, shown on Genome browser.	277
Figure 5-26: EME1 and MUS81 promoter STAT3 binding sites shown on Genome Browser.	279

Figure 5-27: The location of the STAT3 binding site upstream of the cFOS gene, and the region to be amplified by PCR.....	280
Figure 5-28: Chromatin immunoprecipitation analysis of STAT3 binding sites in the EME1 and MUS81 promoters.	282
Figure 6-1: Structures of cisplatin and melphalan.....	296
Figure 6-2: The different structures of DNA ICLs induced by various crosslinking agents.....	297
Figure 6-3: Stick representation of the crystal structure of a single cisplatin ICL from the A) minor groove and B) 90 degrees rotated to show the bend induced. ...	299
Figure 6-4: Cell growth inhibition by 1 hour melphalan treatment in DU145 and RPMI8226 cells.	302
Figure 6-5: Combination of VS-43 and melphalan in DU145 cells.....	303
Figure 6-6: VS-43 inhibits growth of the RPMI8226 myeloma cell line.	305
Figure 6-7: Combination of VS-43 and melphalan in RPMI9228 cells.	306
Figure 6-8: Non-fixed ratio combination of VS-43 and melphalan in DU145 cells.	308
Figure 6-9: Combination of stattic and melphalan in DU145 cells.....	310
Figure 6-10: Combination of curcumin and melphalan in DU145 cells.	311
Figure 6-11: Combination treatment with STAT3 inhibitors and melphalan does not enhance apoptosis of DNA damage in the DU145 cell line.....	313

Figure 6-12: Representative comet images for the combination of VS-43 and melphalan.....	314
Figure 6-13: VS-43 has no effect on melphalan-ICL unhooking in the DU145 cell line.....	316
Figure 6-14: Stattic and curcumin have no effect on melphalan-ICL unhooking in the DU145 cell line.	317
Figure 6-15: VS-43 has no effect on melphalan-ICL unhooking in the RPMI8226 cell line.....	318
Figure 6-16: STAT3 siRNA inhibits cisplatin but not melphalan ICL repair.....	320
Figure 6-17: Representative comet images for STAT3 siRNA cells treated with cisplatin or melphalan... ..	321
Figure 6-18: EME1 siRNA inhibits cisplatin but not melphalan ICL repair.	324
Figure 6-19: Representative comet images for EME1 siRNA cells treated with cisplatin or melphalan.	325
Figure 6-20: MUS81 siRNA inhibits cisplatin but not melphalan ICL repair.	327
Figure 6-21: Representative comet images for MUS81 siRNA cells treated with cisplatin or melphalan.	328
Figure 6-22: Expression of EME1 and MUS81 is interdependent.....	330
Figure 6-23: Structures of cisplatin, carboplatin and oxaliplatin.....	339

List of Tables

Table 1-1: Approximate numbers of DNA damages per cell per day. Summarised from (Bernstein et al., 2013).....	44
Table 1-2: Primary and secondary chemotherapy drug combinations for small cell lung cancer.....	48
Table 1-3: Chemotherapy drug combinations for non-small cell lung cancer.	49
Table 1-4: Activated STAT3 in different tumour types, assessed by immunohistochemistry of human tumour samples.....	105
Table 2-1: Details for primary antibodies used in immunoblotting:.....	125
Table 2-2: Symbols and descriptions for interpretation of CI values.....	129
Table 2-3: List of ChIP primers and their sequences.....	145
Table 2-4: P values and the corresponding significance levels.	149
Table 4-1: GI ₅₀ values for cisplatin alone and in combination with stattic or cisplatin, in the A549 and DU145 cell lines.	202
Table 4-2: Fixed Ratio GI ₅₀ values for cisplatin alone and VS-43 plus cisplatin combination treatment in the A549 and DU145 cell lines.....	206
Table 4-3: Non-fixed ratio GI ₅₀ values for growth inhibition by cisplatin alone and VS-43 plus cisplatin combination treatment in the A549 and DU145 cell lines....	212
Table 4-4: Summary table for combination of STAT3 inhibitors with cisplatin.	217

Table 4-5: STAT3 inhibitors reported to sensitise cancer cell lines to cisplatin.....	219
Table 5-1: Fixed ratio comet assay P values and statistical significance.....	243
Table 5-2: Non-fixed ratio comet assay P values and statistical significance.	245
Table 5-3: Stattic and cisplatin comet assay P values and statistical significance.	248
Table 5-4: Curcumin and cisplatin comet assay P values and statistical significance.	249
Table 5-5: DNA damage signalling array: fold regulation and P value for genes up or down-regulated by a 1µM and 2µM 18 hour VS-43 treatment.	260

Abbreviations

5-FU	5-Fluorouracil
A	Adenine
ADC	Antibody-Drug Conjugate
ADCC	Antibody-Dependent Cellular Cytotoxicity
ADP	Adenosine Diphosphate
ALK	Anaplastic Lymphoma Kinase
AML	Acute Myeloid Leukemia
ANOVA	Analysis of Variance
AP	Apurinic/Apyrimidinic
APEX1	Apurinic-apyrimidinic endodeoxyribonuclease
ATM	Ataxia Telangiectasia Mutated
ATP	Adenosine Triphosphate
ATR	Ataxia Telangiectasia and Rad3-related Protein
ATRIP	ATR-Interacting Protein
Bcl	B-cell Lymphoma
BER	Base Excision Repair
BRCA1	Breast Cancer Associated 1
BRCA2	Breast Cancer Associated 2
BRIP1	BRCA1-Interacting Protein 1
BSA	Bovine Serum Albumin
C	Cytosine
c-Fos	Cellular FBJ Murine Osteosarcoma Oncogene
c-Myc	Cellular Myelocytomatosis Oncogene
CBP	CREB-Binding Protein
CD98	Solute Carrier Family 3 Member 2

CDK	Cyclin-Dependent Kinase
CDKN1A	Cyclin-Dependent Kinase Inhibitor 1A
cDNA	Complementary DNA
ChIP	Chromatin Immunoprecipitation
Chr	Chromosome
CI	Combination Index
CO ₂	Carbon Dioxide
COSMIC	Catalogue of Somatic Mutations in Cancer
CPD	Cyclopyridine Dimer
CS	Cockayne Syndrome
CSA/B	Cockayne Syndrome A/B
C _T	Cycle Threshold
CTR	Copper Transporter
DAP	Diarylidene Piperidone
DDB1/2	DNA Damage-Binding Protein 1/2
DDIT3	DNA Damage Inducible Transcript 3
DMEM	Dulbecco's Modified Eagle Medium
DMSO	Dimethyl Sulfoxide
DNA	Deoxyribonucleic Acid
DNA-PKcs	DNA-Dependent Protein Kinase Catalytic Subunit
DSB	Double Strand Break
DTT	Dithiothreitol
ECL	Enhanced Chemiluminescence
EDTA	Ethylenediaminetetraacetic Acid
EGF	Epidermal Growth Factor
EGFR	Epidermal Growth Factor Receptor
ELISA	Enzyme-Linked Immunosorbent Assay

EMA	European Medicines Agency
EME1	Essential Meiotic Structure-Specific Endonuclease 1
EML4	Echinoderm Microtubule Associated Protein Like-4
EMSA	Electrophoretic Mobility Shift Assay
EMT	Epithelial-Mesenchymal Transition
ENCODE	Encyclopedia of DNA Elements
EPR	Enhanced Permeability and Retention
ERCC1	Excision Repair Cross-Complementation Group 1
EXO1	Exonuclease 1
FA	Fanconi Anemia
FAAP24	Fanconi Anemia Core Complex Associated Protein 24
FAN1	FANCD2/FANCI-Associated Nuclease 1
FANC	Fanconi Anemia Complementation Group
FCS	Fetal Calf Serum
FDA	U.S. Food and Drug Administration
G	Guanine
g	Gram
GADD	Growth Arrest and DNA Damage
GAPDH	Glyceraldehyde 3-Phosphate Dehydrogenase
GI50	Growth Inhibitor Concentration 50
GnRH	Gonadotrophin Releasing Hormone
GOI	Gene of Interest
GST	Glutathione S-Transferase
H2AX	H2A Histone Family, Member X
HIF	Hypoxia Inducible Factor
HIFU	High Intensity Focused Ultrasound
HMGB1	High Mobility Group Box 1

HR	Homologous Recombination
HRP	Horseradish Peroxidase
IAP	Inhibitor of Apoptosis
IC50	Inhibitory Concentration 50
ICL	Interstrand Crosslink
IDL	Insertion/Deletion Loop
IFN	Interferon
IgG	Immunoglobulin G
IL	Interleukin
IP	Immunoprecipitation
JAK	Janus Kinase
kDa	Kilodalton
L	Litre
LIF	Leukemia Inhibitory Factor
LIG1	DNA Ligase 1
M	Molar
MAPK	Mitogen Activated Protein Kinase
Mcl-1	Myeloid Cell Leukemia 1
MDC1	Mediator of DNA Damage Checkpoint Protein 1
MDR1	Multidrug Resistance Transporter 1
MES	2-(N-morpholino)ethanesulfonic acid
mL	Millilitre
MLH	MutL Homolog
mM	Millimolar
MMC	Mitomycin C
MMP	Matrix Metalloproteinase
MMR	Mismatch Repair

MOPS	3-(N-morpholino)propanesulfonic acid
mRNA	Messenger RNA
MRP	Multidrug Resistance Protein
MSH	MutS Protein Homolog
mTOR	Mammalian Target of Rapamycin
MTT	Methylthiazolyldiphenyl-Tetrazolium Bromide
MUS81	Methyl Methansulfonate and Ultraviolet-Sensitive Gene Clone 81
NaCl	Sodium Chloride
NaOH	Sodium Hydroxide
NCAPD2	Non-SMC Condensin I Complex Subunit D2
NER	Nucleotide Excision Repair
NF- κ B	Nuclear Factor Kappa-Light-Chain-Enhancer of Activated B Cells
NHEJ	Non-Homologous End Joining
nM	Nanomolar
nm	Nanometer
NSCLC	Non-Small Cell Lung Cancer
OGG1	8-Oxoguanine Glycosylase
p	Phosphate/Phospho
P-gp	P-Glycoprotein
PAGE	Polyacrylamide Gel Electrophoresis
PALB2	Partner and Localiser of BRCA2
PARP	Poly ADP Ribose Polymerase
PBS	Phosphate Buffered Saline
PCNA	Poliferating Cell Nuclear Antigen
PCR	Polymerase Chain Reaction
PDGF	Platelet Derived Growth Factor
PDT	Photodynamic Therapy

PFA	Paraformaldehyde
PI	Propidium Iodide
PIAS	Protein Inhibitor of Activated STAT
PMSF	Phenylmethylsulfonyl Fluoride
PNK	Polynucleotide Kinase
PSA	Prostate Specific Antigen
PVDF	Polyvinylidene Fluoride
qRT-PCR	Quantitative Reverse Transcription PCR
RecA	Recombination Protein A
RFA	Radiofrequency Ablation
RFC	Replication Factor C
RNA	Ribonucleic Acid
RPA	Replication Protein A
rpm	Revolutions per Minute
RPMI	Roswell Park Memorial Institute Medium
RTK	Receptor Tyrosine Kinase
SCLC	Small Cell Lung Cancer
SDS	Sodium Dodecyl Sulfate
SEM	Standard Error of the Mean
SH2	Src Homology 2
SHP1/2	Src Homology Phosphatase 1/2
siRNA	Small Interfering Ribonucleic Acid
SLX	Structure-Specific Endonuclease Subunit
SNM1A	DNA Cross-link Repair 1A Protein
SOCS	Suppressor of Cytokine Signalling
SRB	Sulphorhodamine B
SSA	Single Strand Annealing

SSB	Single Strand Break
STAT	Signal Transducer and Activator of Transcription
T	Thymine
TAD	Transactivation Domain
TBE	Tris/Borate/EDTA
TBS	Tris Buffered Saline
TBS-T	Tris Buffered Saline with 0.1% Tween
TCA	Trichloroacetic Acid
TdT	Human Terminal Deoxynucleotidyltransferase
TFIIH	Transcription Factor 2 Human
TGF- β	Transforming Growth Factor Beta
TKI	Tyrosine Kinase Inhibitor
TLS	Translesion Synthesis
UHRF1	Ubiquitin-Like with PHD and RING Finger Domain 1
UNG	Uracil DNA Glycosylase
UV	Ultraviolet
Uvr	Ultraviolet Resistant
V	Volts
VDJ	Variable, Diversity, Joining
VEGF	Vascular Endothelial Growth Factor
XP	Xeroderma Pigmentosum
XRCC	X-Ray Repair Cross-Complementing
μg	Microgram
μL	Microlitre
μM	Micromolar

Chapter 1 Introduction

1.1 The epidemiology of cancer

Globally, 14.1 million people were diagnosed with cancer in 2012. It is estimated that 8.2 million deaths occurred in 2012 due to cancer: 22,000 per day (American Cancer Society, 2015). In the UK alone, 352,197 new cases of cancer were diagnosed in 2013, and there were 163,444 deaths related to cancer (Cancer Statistics for the UK, Cancer Research UK webpage. Available from: <http://www.cancerresearchuk.org/health-professional/cancer-statistics> [accessed August 2016]). By 2030, the American Cancer Society estimates that the number of new cancer cases will have increased to 21.7 million per year and the number of cancer-related deaths will be 13 million per year. This, however, may still be a huge underestimate due to the increasing number of people adopting behaviours that increase the risk of cancer such as smoking, lack of activity and a poor diet. Globally, the most common cancer is prostate cancer in men and breast cancer in women (American Cancer Society, 2015). The twenty most common types of cancer and their incidence in the UK are shown in Figure 1-1.

Together, breast, lung, prostate and bowel cancer contribute to 53% of all cancers in the UK. Worldwide, cancer incidence varies with geographical location due to different population age ranges, access to medical care and screening programmes, and the presence of risk factors in different regions. For example, worldwide, 16% of cancers are caused by infections, however this is as high as 23% in developing regions compared with only 7% in developed countries (American Cancer Society, 2015). Even though survival rates have improved considerably over the past 40 years (from 25% to 50% survival 10 years post diagnosis), cancer is still a devastating disease, and 1 in 2 people born after 1960 will be diagnosed with cancer in their lifetime (Ahmad et al., 2015).

According to Cancer Research UK, 42% of cancer incidences are classed as preventable. Smoking is the highest cause of preventable cancer in the UK, accounting for 19% of new cancer cases each year. Other lifestyle factors contributing to preventable cancers include a poor diet, lack of exercise, excessive alcohol consumption, and lack of sun protection. Occupational exposure to radiation or carcinogens such as asbestos, and infections with carcinogenic organisms also contribute to preventable cancers (Statistics on Preventable Cancers, Cancer Research UK webpage. Available from: <http://www.cancerresearchuk.org/health-professional/cancer-statistics/risk/preventable-cancers> [accessed August 2016]). Given the current global burden of cancer and the ever-growing incidence of this disease, continued research into new treatments is critical.

The epidemiology of prostate and lung cancer will be discussed in more detail as prostate and lung cancer cell lines are predominantly used in this thesis.

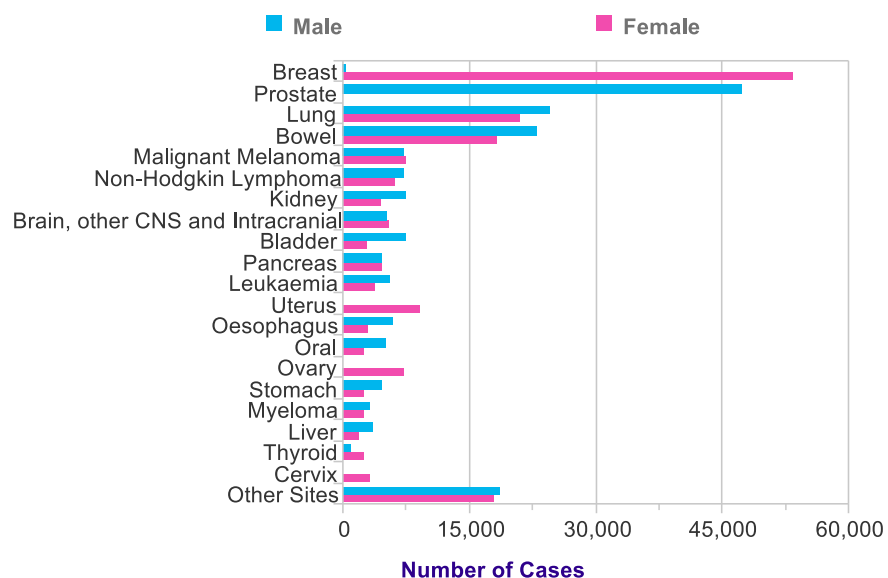


Figure 1-1: The twenty most common cancers in the UK, and their incidence. Figure obtained from: Cancer Incidence for Common Cancers, Cancer Research UK. Available from: <http://www.cancerresearchuk.org/health-professional/cancer-statistics/incidence/common-cancers-compared#heading-Zero> [accessed August 2016].

1.1.1 Prostate cancer

In 2012 there were 1.1 million new cases of prostate cancer and 307,500 deaths due to prostate cancer worldwide. Prostate cancer is most prevalent in the economically developed world, with two thirds of all cases occurring in these regions where only 17% of the worlds population lives. Northern Europe and North America have some of the highest incidence rates for prostate cancer, however this may be correlated to a greater use of prostate specific antigen (PSA) testing in these regions and therefore, greater detection rates. The main risk factor for prostate cancer is age (American Cancer Society, 2015). Prostate cancer is the fifth greatest cause of death globally, however death rates are decreasing due to earlier detection. Between 2010-2011, 10-year survival for men with prostate cancer was 84%, however the number of deaths occurring in the UK was still 11,287 in 2014. Inherited factors contribute to 5-9% of prostate cancers (Prostate Cancer Statistic, Cancer Research UK webpage. Available from: <http://www.cancerresearchuk.org/health-professional/cancer-statistics/statistics-by-cancer-type/prostate-cancer> [accessed August 2016]), with some mutations, for example BRCA2 mutations, being responsible for tumourigenesis. The relative risk of developing prostate cancer is 7.33% in men carrying a BRCA2 mutation under the age of 65 (Consortium, 1999). However, obesity and consumption of processed meat have also been suggested to impact incidence of prostate cancer (American Cancer Society, 2015).

1.1.2 Lung Cancer

In 2012 there were 1.8 million new cases of lung cancer, with again, North America and Northern Europe having the highest incidence rates. Lung cancer is responsible for the most cancer-related deaths in men, and the second most cancer-related deaths in women, with an estimated 1.6 million deaths in 2012 (American Cancer

Society, 2015). In the UK in 2013, there were 45,525 new cases of lung cancer and 38,895 deaths. Only 5% of patients with lung cancer survive for 10 years post-diagnosis. The largest risk factor for developing lung cancer is smoking due to the carcinogens in tobacco smoke and global incidence rates reflect this. For example, Scotland has one of the highest incidence rates of lung cancer in the world and as a country, is also one of the largest consumers of cigarettes (Lung Cancer Statistics, Cancer Research UK webpage. Available from: <http://www.cancerresearchuk.org/health-professional/cancer-statistics/statistics-by-cancer-type/lung-cancer> [accessed August 2016]). The high mortality rate associated with lung cancer is due to the commonly late diagnosis of this disease, due to lack of symptoms until the cancer is more advanced. The most common form of lung cancer is non-small cell lung cancer (NSCLC), which accounts for 87% of cases. Small-cell lung cancer accounts for approximately 12% of cases (Types of Lung Cancer, Cancer Research UK webpage. Available from: <http://www.cancerresearchuk.org/about-cancer/type/lung-cancer/about/types-of-lung-cancer> [accessed August 2016]).

1.2 The biology of cancer

Cancer is a disease of uncontrolled cellular replication, and it places immense strain on the human body either physically, by creating obstructions or putting pressure on a particular organ, or through the deregulation of essential processes such as hormone production, immune response, and haematogenesis. Due to genetic heterogeneity, no two cancers are the same. As illustrated in Figure 1-2, due to the accumulation of genetic mutations in a tumour over time, sub-clones appear within a single tumour, and the sub-clones present can differ between patients with the same cancer type, between different regions in a single tumour, and also between the

primary tumour and metastases (Jamal-Hanjani et al., 2015). Therefore cancer is a collection of diseases, and accordingly, many different treatments are required.

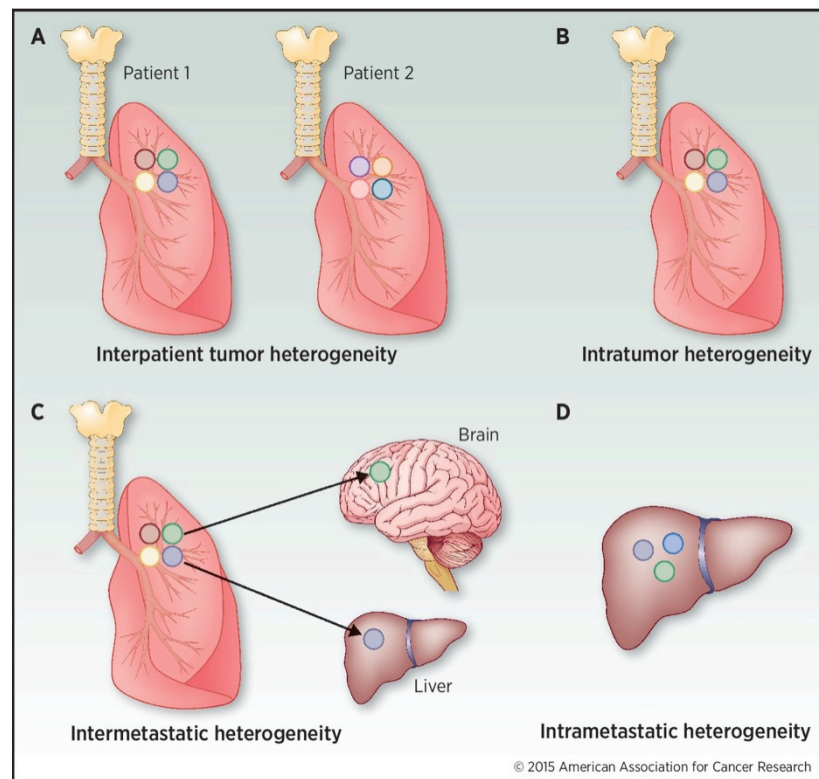


Figure 1-2: Types of tumour heterogeneity. A) Interpatient, B) intratumour, C) intermetastatic and D) intrametastatic. Taken from (Jamal-Hanjani et al., 2015).

1.2.1 The hallmarks of cancer and genomic instability

In 2000, Hanahan and Weinberg identified six key traits which enable tumourigenesis, and coined these “The Hallmarks of Cancer” (Hanahan et al., 2000). These traits are shown in Figure 1-3.

As cancer is a disease of uncontrolled replication, it is not surprising that the ability to sustain proliferative signalling is one of the most important cancer hallmarks. Cancer cells deregulate the signals for proliferation, driving the cell cycle through aberrant production of growth factors and their receptors. Independence from these

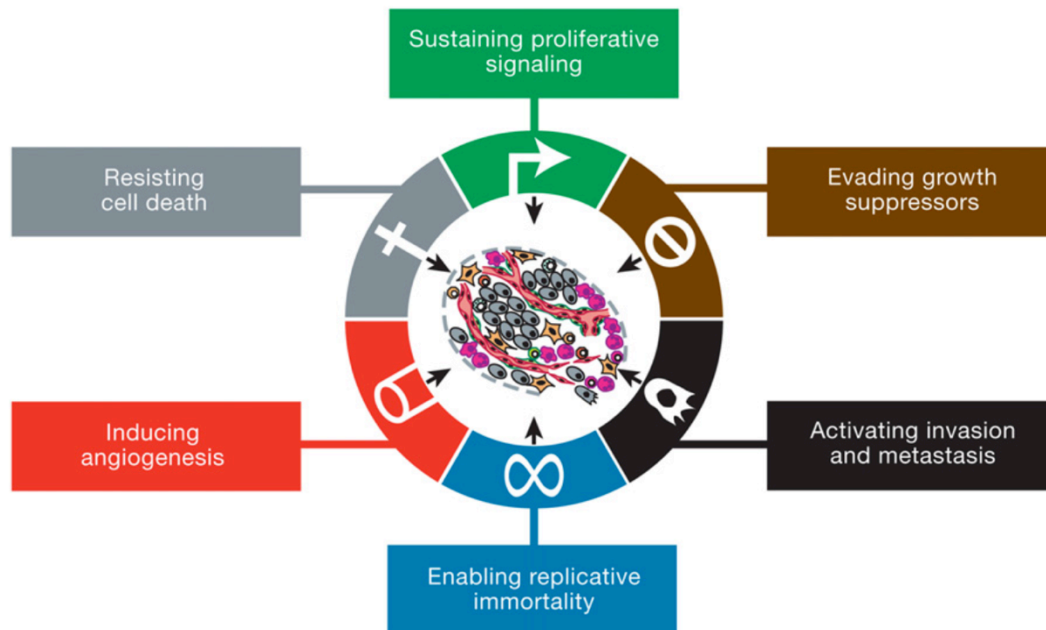


Figure 1-3: The six Hallmarks of Cancer. Proliferation, evasion of growth suppression, invasion and metastasis, replicative immortality, angiogenesis and survival. Taken from (Hanahan and Weinberg, 2011).

growth signals can also arise when components of signalling pathways become constitutively activated (Hanahan and Weinberg, 2011). Genes driving cancer growth in this way are known as oncogenes. An oncogene exists in the normal cell's DNA in its pre-tumourigenic form, the proto-oncogene. Once mutated the gene becomes over-activated or over-expressed, ultimately driving tumourigenesis. Oncogenes are dominant, in that only one mutated allele is required to allow cancer progression. For instance, approximately half of all melanomas have activating somatic mutations in the B-Raf oncogene. B-Raf is a member of the MAP-kinase signalling cascade, and constitutive activation of this pathway drives cellular proliferation (Davies and Samuels, 2010).

In order to continue proliferating, the cancer cell must be able to escape from the signals that restrict proliferation. These growth suppressive signals are often provided by tumour suppressor genes. When tumour suppressors are inactivated by

mutation, deregulation of key cell processes such as the cell cycle occurs. Tumour suppressors are recessive cancer genes in that both alleles must be mutated in order to lose complete function of the gene and allow cancer progression (Stratton, 2011).

A key example of a tumour suppressor is p53 which is mutated in more than half of cancers (Brady and Attardi, 2010). P53 is referred to as the “guardian of the genome”, putting a brake on cell cycle progression when DNA damage is detected, and inducing apoptosis if that damage is irreparable (Lane, 1992). When p53 function is disrupted through mutation, the cancer cell is able to rapidly progress through the cell cycle, acquiring even more mutations as DNA damage is no longer repaired before DNA replication.

The third hallmark is “resisting cell death”. The role of the mutated p53 tumour suppressor gene in evading apoptosis has already been discussed, but tumour cells can also up-regulate the expression of anti-apoptotic regulators such as the bcl2 family of proteins (Hanahan and Weinberg, 2011).

A normal cell can perform a limited number of divisions (known as the Hayflick limit (Shay and Wright, 2000)) before it either enters senescence (a non-replicative but viable state), or undergoes apoptosis. However, a cancer cell must continue replicating. The replicative lifetime of a cell is determined by the length of the telomeres - repetitive DNA sequences protecting the ends of chromosomes from recombination and degradation. Each replicative cycle slightly shortens the telomeres, and once too short, the DNA is no longer protected and the cell is no longer viable. Some cancer cells are able to circumvent telomere shortening by expressing greater levels of the enzyme telomerase which allows for continued replication (Blasco, 2005).

The combination of the first four hallmarks: sustaining proliferation, evading growth suppression, resisting cell death and obtaining replicative immortality, therefore, all contribute to the continued survival and replication of the cancer cell. The fifth hallmark of cancer, angiogenesis, concerns supplying the growing tumour with the required nutrients and oxygen it needs. Angiogenesis is the development of new vasculature, and is usually only temporarily switched on for processes such as wound healing. However, in cancer, angiogenesis is switched on in the pre-tumourigenic stage, and remains switched on in order to continue expanding the vasculature serving the tumour's growth. Expression of the vascular endothelial growth factor (VEGF) and its receptors can induce angiogenesis (Hanahan and Folkman, 1996; Hanahan and Weinberg, 2011).

The final original hallmark is related to the ability of the tumour to spread to other regions of the body: invasion and metastasis. Loss of cell-cell adhesion molecules in the primary tumour, such as E-cadherin, allows for epithelial-mesenchymal transition (EMT) and individual cells can then enter the tumour vasculature, and be carried around the body. Tumour cells then leave the vasculature and develop new tumours at the metastasis site (Talmadge and Fidler, 2010).

These six hallmarks were later expanded upon in 2011 to include two further hallmarks: evading immune destruction and reprogramming energy metabolism. As tumour proliferation is deregulated, the cellular energy demands are higher and therefore metabolism must adapt. Cancer cells derive most of their energy from glycolysis, even in the presence of oxygen. This phenomenon has been coined the Warburg effect. As glycolysis is substantially less efficient at producing ATP than oxidative phosphorylation, the reason why cancer cells undergo this metabolic switch is not fully understood. One hypothesis is that glycolytic intermediates are used for the synthesis of nucleotides and amino acids in order to maintain rapid

tumour cell division (Vander Heiden et al., 2009). The second emerging hallmark, evading immune destruction, allows the tumour to continue growing without being detected and eliminated by the immune system. A tumour may do this through the production of immunosuppressive factors or the recruitment of immunosuppressive inflammatory cells to the tumour microenvironment (Hanahan and Weinberg, 2011). Two enabling characteristics for the development of a tumour have also been identified: genome instability, which provides the genetic alterations required for many of the cancer hallmarks, and tumour-promoting inflammation, which can supply growth factors and enzymes to facilitate hallmark development (Hanahan and Weinberg, 2011).

Cancer cells have inherent genomic instability due to the loss of cell cycle checkpoints and continued proliferation in the presence of unrepaired DNA damage. This damage may be a result of errors in replication, but is also linked to reactive oxygen species and free radicals generated during the reprogrammed metabolism of the cancer cells (Dang, 2012). If a cell acquires mutations in DNA repair genes, the cell becomes less able to correct DNA damage and the stability of the genome worsens.

The hallmarks of cancer are underpinned by genomic instability. Genetic changes can occur via three pathways: aneuploidy (an abnormal number of chromosomes), chromosomal rearrangements such as translocations, or point mutations in specific genes. Mutations can be hereditary, acquired by exposure to external mutagens or a product of random mutations acquired during DNA replication. Cells can acquire two types of mutation: passenger and driver mutations. Passenger mutations have no direct role in tumourigenesis, whereas driver mutations directly contribute to tumour development by allowing the cell some form of growth advantage, contributing to one of the hallmarks (Stratton, 2011). Mutations will begin to

accumulate even before birth due to intrinsic mutational processes. Throughout adulthood, environmental and lifestyle-induced mutations will occur. Further mutations can arise when a cancer cell acquires a mutator phenotype, and also after treatment with chemotherapy, leading eventually to a chemotherapy resistant tumour (Figure 1-4) (Stratton, 2013).

Mutations can arise when DNA damage is incorrectly repaired. On average, tens of thousands of DNA damages occur each day in just one cell. This damage can exist in various forms; a list of the approximate frequencies of some types of DNA damage is shown in Table 1-1.

Epigenetic mutations can also contribute to cancer development. For example, methylation of CpG islands can inhibit the transcription of certain genes. If this

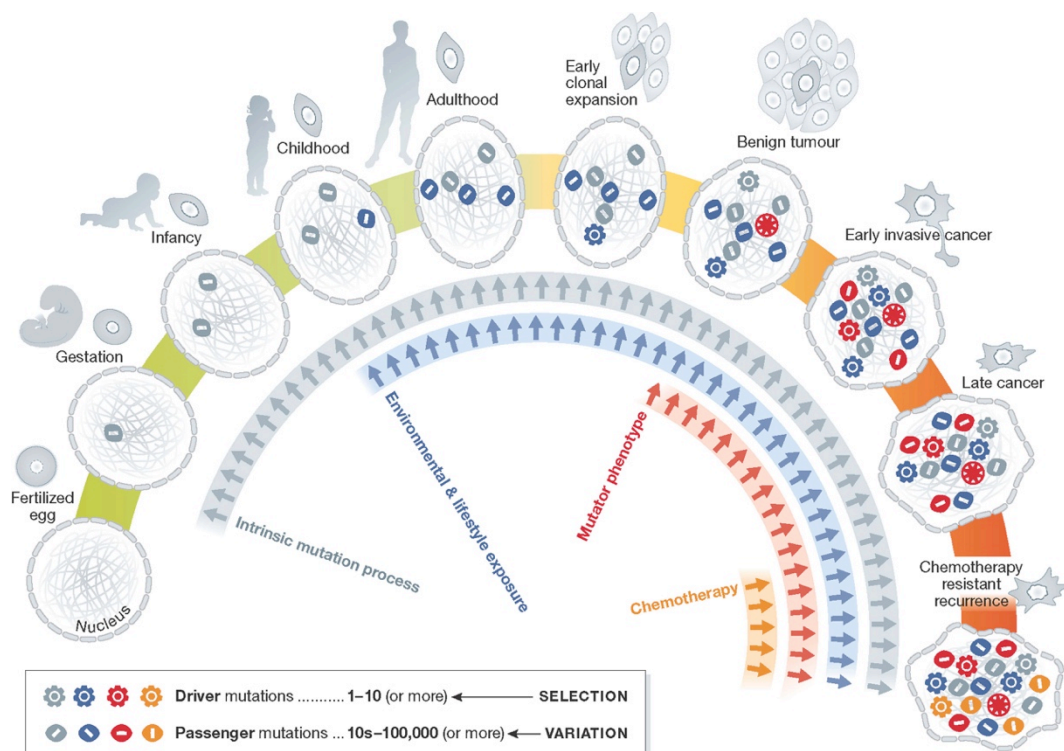


Figure 1-4: Accumulation of mutations from a fertilised egg to a chemotherapy resistant tumour cell. Taken from (Stratton, 2013).

Table 1-1: Approximate numbers of DNA damages per cell per day.
Summarised from (Bernstein et al., 2013).

Damage	Approximate frequency (per cell per day)
Oxidative	10,000
Depurination	10,000
Depyrimidination	700
Single-strand breaks	55,000
Double-strand breaks	10-50 <i>per cell cycle</i>
Methylation	3000
Cytosine deamination	200

occurs in a tumour suppressor gene or a DNA repair gene, this could be considered a driver mutation (Bernstein et al., 2013).

Exogenous carcinogens can cause DNA mutations. As discussed previously, tobacco smoke is the leading cause of lung cancer. The reason for this being that tobacco smoke contains several carcinogens including nitrosamines, benzopyrenes and formaldehyde (Cunningham et al., 2011; Hecht, 2003). As well as chemical carcinogens, biological carcinogens such as *Helicobacter pylori* also exist. Infection with this bacterium increases production of reactive oxygen species in the stomach, resulting in DNA damage such as oxidation of guanines. Infection with *Helicobacter pylori*, therefore, is a significant risk factor for stomach cancer (Wiseman and Halliwell, 1996). Solar UV radiation is another natural carcinogen, which plays a huge role in the development of melanomas due to the formation of cyclopyridine dimers (CPDs) and 6-4 photoproducts in the cellular DNA. The increasing use of commercial tanning sunbeds has also been closely linked to melanomas, with individuals who begin using sunbeds under the age of 30 having a 75% greater chance of developing melanoma (Kanavy and Gerstenblith, 2011).

It is estimated that approximately five driver mutations are required for tumourigenesis (Stratton, 2011), and so given the huge amount of DNA damage that occurs daily from a number of sources, it is understandable why cancer is so prevalent in the human population.

1.3 Treatments for cancer

Surgery is one of the most common treatments for cancer, and is often used when the tumour is confined to one area. Other therapies include radiotherapy, chemotherapy, hormone therapy, biological therapy, and in the case of haematological malignancies, bone marrow or stem cell transplant may be used in conjunction with high dose chemotherapy or radiotherapy.

In this thesis, the main cell lines used are prostate and non-small cell lung cancer; therefore, the treatments currently available for these types of cancer will be discussed in further detail.

1.3.1 Treatments for prostate cancer

The main treatments for prostate cancer in the UK are surgery, radiotherapy and hormone therapy. Radiotherapy can be administered externally or internally and can cure the cancer if it has not yet spread outside of the prostate gland. Hormone therapy works by reducing the level of testosterone in patients, as prostate cancer requires testosterone to continue growing. Hormone therapy drugs include anti-androgens, GnRH blockers, cytochrome p17 blockers and luteinising hormone blockers. Prostate cancers may respond initially to these treatments however they can become hormone-refractory and alternative treatments may be required. The average time to progression after hormone therapy is between 18-24 months (Recine and Sternberg, 2015). Once resistant to hormone-based treatments

metastases can occur and radiotherapy may be used to relieve the painful symptoms of prostate cancer metastases in the bones (Zustovich and Fabiani, 2014). At this stage chemotherapy drugs will also be considered for the treatment of advanced prostate cancer. Drugs currently used include Docetaxel, Paclitaxel, and Cabazitaxel (microtubule inhibitors), Estramustine (both a microtubule inhibitor and alkylating agent), and Mitoxantrone and Epirubicin (DNA intercalating Topoisomerase II inhibitors). All of these drugs act to block cancer cell proliferation. Whether chemotherapy should be given to patients before they become hormone-refractory is currently debated (Recine and Sternberg, 2015).

Other treatments sometimes used for hormone-refractory prostate cancer include steroids, cryotherapy, and High Intensity Focused Ultrasound (HIFU) (Treatment Options for Prostate Cancer, Cancer Research UK webpage. Available from: <http://www.cancerresearchuk.org/about-cancer/type/prostate-cancer/treatment/types/treatment-options-for-prostate-cancer> [accessed August 2016]).

1.3.2 Treatments for lung cancer

Current treatments approved for lung cancer patients in the UK include surgery, radiotherapy and chemotherapy. Surgery is only used for non-small cell lung cancer (NSCLC) as small-cell lung cancers (SCLC) have often already spread by the time of diagnosis. In surgery, one of three procedures can be carried out depending on the tumour size and location. A section, lobe, or whole lung can be removed. Radiotherapy can be used internally or more commonly externally to treat lung cancer (Types of Treatment for Lung Cancer, Cancer Research UK webpage. Available from: <http://www.cancerresearchuk.org/about-cancer/type/lung-cancer/treatment/which-treatment-for-lung-cancer> [accessed August 2016]).

Chemotherapy is the most effective choice of treatment for those with SCLC or for where a cancer has metastasised around the body to multiple locations. Different chemotherapy combinations are used depending on whether a patient has SCLC or NSCLC. For SCLC, most primary treatment combinations include either cisplatin or carboplatin. However, if a cancer becomes resistant to these therapies and recurs, secondary chemotherapy combinations must be used (Table 1-2). For NSCLC, chemotherapy is used after surgery, alongside radiotherapy or for advanced NSCLC that has metastasised (Types of Treatment for Lung Cancer, Cancer Research UK. Available from: <http://www.cancerresearchuk.org/about-cancer/type/lung-cancer/treatment/which-treatment-for-lung-cancer> [accessed August 2016]). Again, chemotherapy drug combinations almost always include cisplatin or carboplatin combined with another agent (Table 1-3). Therefore, platinum agents are the most commonly used class of chemotherapy drugs in the treatment of lung cancer. Which other chemotherapy agent is combined with platinum may be determined by the histology of the tumour (Fennell et al., 2016). However, platinum-based therapy is not curative. Novel platinum agents may be required in the future to overcome acquired resistance to platinum chemotherapy as up to 63% and 68% of NSCLC tumour cultures display resistance to cisplatin and carboplatin, respectively (Chang, 2011).

Biologically targeted therapeutics may be used for NSCLC, including Erlotinib, Gefitinib, and Afatinib. These are all Tyrosine Kinase Inhibitors (TKIs) that target EGFR (Epidermal Growth Factor Receptor). Crizotinib and ceritinib are TKI's that target the EML4-ALK fusion protein and are also approved treatments for some NSCLCs. Overactive EGFR and ALK activity are known to contribute to carcinogenesis of NSCLC, therefore, these proteins are valid targets for directed biological therapy. However, the incidence of driver mutations in these proteins is

only 10% and 4% for EGFR and ALK, respectively. Therefore, approximately 85% of NSCLC patients cannot be treated with these targeted agents and depend upon platinum-based therapy (Fennell et al., 2016).

Table 1-2: Primary and secondary chemotherapy drug combinations for small cell lung cancer. (Types of Treatment for Lung Cancer, Cancer Research UK. Available from: <http://www.cancerresearchuk.org/about-cancer/type/lung-cancer/treatment/which-treatment-for-lung-cancer> [accessed August 2016])

Small Cell Lung Cancer	
Primary Chemotherapy	Cisplatin + Etoposide (EP)
	Carboplatin + Etoposide
	Carboplatin + Gemcitabine
Secondary Chemotherapy	Cyclophosphamide + Doxorubicin + Vincristine (CAV)
	CAV + Etoposide (CAVE)
	Doxorubicin + Cyclophosphamide + Etoposide (ACE)

Table 1-3: Chemotherapy drug combinations for non-small cell lung cancer.(Types of Treatment for Lung Cancer, Cancer Research UK. Available from: <http://www.cancerresearchuk.org/about-cancer/type/lung-cancer/treatment/which-treatment-for-lung-cancer> [accessed August 2016])

Non-Small Cell Lung Cancer		
After Surgery	Cisplatin/Carboplatin +...	Vinorelbine
		Gemcitabine
		Paclitaxel
		Docetaxel
Alongside Radiotherapy	Cisplatin/Carboplatin +...	Doxorubicin
		Etoposide
		Pemetrexed
Advanced or Metastatic NSCLC	Cisplatin/Carboplatin +...	Gemcitabine
		Paclitaxel
		Vinorelbine
		Docetaxel
		Pemetrexed

Combinations of chemotherapy with radiotherapy are also used, and other less commonly used treatments include Radiofrequency Ablation (RFA) where the heat from microwaves is targeted to the cancer cells, or Photodynamic Therapy (PDT) where a photosensitising drug is administered followed by exposure to a laser light source (Types of Treatment for Lung Cancer, Cancer Research UK webpage, available from: <http://www.cancerresearchuk.org/about-cancer/type/lung-cancer/treatment/which-treatment-for-lung-cancer> [accessed August 2016]).

1.4 Cancer chemotherapy

In the early 1900s, the German chemist Paul Ehrlich described the term “chemotherapy” as the use of chemicals to treat disease (DeVita and Chu, 2008). The discovery of the first chemotherapy agent arose from the observation that soldiers exposed to sulphur mustard gas had depleted bone marrow and lymphoid cells. In 1942, pharmacologists Goodman and Gilman at the Yale School of Medicine hypothesised that these gases might also act on tumours of the hematopoietic system. Having demonstrated therapeutic benefit in a mouse model, a more stable nitrogen mustard was tested in its first cancer patient. The nitrogen mustard compound (mechlorethamine) was administered intravenously to an individual with non-Hodgkins lymphoma, and marked regression of the patient’s cancer was observed (Gilman and Philips, 1946). Whilst the cancer did return after a short remission period, this discovery paved the way for the use of chemical compounds in the treatment of cancer (Chabner and Roberts, 2005; DeVita and Chu, 2008).

The second class of chemotherapy compounds to be developed was the anti-folates. Shortly after the Second World War it was noted that folic acid could stimulate the proliferation of some leukemia cells, and that deficiency in folic acid produced similar effects on the hematopoietic system as was previously observed for nitrogen mustards (Farber, 1949). One of the first anti-folate drugs developed was methotrexate, which is still used in the clinic today, and since then other anti-folates have been developed including pemetrexed. These compounds act by inhibiting the enzyme required for folic acid synthesis, which itself is a precursor for thymidine. Therefore, inhibition of the folic acid pathway inhibits DNA replication (Bertino, 2009; DeVita and Chu, 2008). Methotrexate was noted to have anti-tumour effects in a range of cancers including ovarian, breast, head and neck and bladder

cancer. It was even suggested to completely cure some patients with choriocarcinoma, a rare malignancy of the placenta (Chiu Li et al., 1958).

The development of the purine analogues quickly followed in the early 1950s. This class of compounds included mercaptopurine, which is still used today to treat some forms of leukemia. The first form of “targeted cancer therapy” was also brought to light in the 1950s, when scientists at the University of Wisconsin observed that rat hepatocellular cancer cells uptake higher levels of uracil than normal cells. They modified uracil by adding a fluorine atom, creating 5-fluorouracil (5-FU) which was demonstrated to have anti-tumour activity in a variety of solid cancers. 5-FU is still one of the most commonly used chemotherapy drugs in the clinic today (DeVita and Chu, 2008).

In 1963 the natural alkaloids from the *Vinca rosea* plant were identified to have anti-proliferative effects on tumour cells through their ability to inhibit the polymerisation of microtubules which is essential for mitosis (Bensch and Malawista, 1968; Johnson et al., 1963). This class of compounds included vincristine, which was later administered as part of one of the earliest combination chemotherapy treatment regimes alongside methotrexate, prednisone and mercaptopurine. This treatment demonstrated long-lasting remission in children with acute lymphoblastic leukemia (Chabner and Roberts, 2005). Another microtubule-targeting chemotherapy agent discovered in the 1960's was paclitaxel, but due to its difficulty to synthesise and relative insolubility, it wasn't until 1989 that this drug was demonstrated to have significant anti-tumour activity in ovarian cancer (Chabner and Roberts, 2005). The camptothecin class of natural chemotherapy compounds was also discovered in the 1960's but like paclitaxel, these compounds took time to demonstrate clinical efficacy due to their instability. In 1996, irinotecan was the first camptothecin to gain FDA approval for the treatment of colorectal cancer. Irinotecan works by targeting

DNA topoisomerase I (Saltz et al., 2000). This will be reviewed in more detail in the following sections.

Another major class of chemotherapy agents discovered in this period was the platinum compounds, which form adducts and crosslinks with the DNA, blocking replication and transcription. Cisplatin was the first of this class, discovered in 1965 (Rosenberg et al., 1969, 1965) and later approved by the FDA in 1978. In a bid to overcome cisplatin's adverse effects including nephrotoxicity, second and third generation platinum compounds have been developed such as carboplatin and oxaliplatin. During the 1970's the chloroethyl nitrosoureas, a group of DNA-alkylating chemotherapy agents, were also developed. However, in the 1980's, there was little development of new chemotherapy agents that didn't fit into one of the already identified groups: antimetabolites, alkylators, crosslinkers, anti-mitotics and topoisomerase inhibitors. Therefore, more recently there has been a change of direction, with drug discovery focussing more on targeted cancer therapy such as monoclonal antibodies and tyrosine kinase inhibitors. However, traditional chemotherapy is still very much at the core of cancer treatment, and therefore, these agents will be discussed in further detail, with a focus on those which act through targeting the cancer cell DNA.

1.5 DNA as an anti-cancer target

DNA is the most successful anti-cancer target, as demonstrated by the number of traditional chemotherapy agents discussed above which target this molecule. The double helical structure of DNA, and the pairing of adenine with thymine and cytosine with guanine, was resolved in 1953 by geneticists James Watson and Francis Crick (Watson and Crick, 1953), so at the time of the development of the earliest chemotherapy agents, the details of their molecular target were unknown.

Since then, the importance of what is known as the “central dogma” has emerged. This concept was first described by Francis Crick in 1958, and detailed the transfer of information between DNA, RNA and protein (Crick, 1970). The information encoded by DNA is first transcribed by RNA polymerase to form messenger RNA, which is subsequently translated into proteins by ribosomes. Therefore, intact and functional DNA is crucial for the survival of a cell, and so agents that disrupt the integrity of the cellular DNA exert their toxicity in this way.

Agents which target the DNA are not, however, selective in their activity. Every cell contains DNA and is dependent upon its integrity for survival. Accumulation of DNA damage will halt the cell cycle and if left unrepaired, eventually cause apoptosis, whether the cell is a cancer cell or not. DNA-targeting chemotherapy agents do, however, gain some degree of selectivity through the more rapid proliferation of cancer cells versus most normal tissues. Cancer cells typically lose cell cycle regulation and so continue to replicate their DNA even with accumulated DNA damage, leading to replication-induced DSBs and ultimately cell death. Therefore, exposure to DNA-damaging agents can more effectively push cancer cells into apoptosis than normal cells. However, the basis of this selectivity also means that the adverse effects of DNA-damaging agents are often associated with areas of the body with a high cellular proliferation rate (Hurley, 2002).

Nonetheless, DNA damaging agents are still the most frequently used drugs in cancer therapy, although they are more often administered as part of a combination regimen to lower the individual drug toxicities (see Table 1-2 and Table 1-3) for treatment combinations in lung cancer). Future directions for overcoming the adverse effects associated with DNA-damaging agents rely on the development of targeting modules so that the effect of these compounds on normal tissues is minimised. Examples of these include antibody-drug conjugates (ADCs) which

carry a cytotoxic compound to the tumour cell by binding to antigens expressed selectively on tumour cells, such as Kadcyła[®] (trastuzumab emtansine), which is used in HER2 positive breast cancers. Liposomal or nanoparticle formulations of chemotherapy drugs may also be used. These can be coated in tumour-targeting ligands (Thomas and Pommier, 2016). The liposomal form of irinotecan was approved for use in advanced metastatic pancreatic cancer in 2015 (Drummond et al., 2006), and works via a passive accumulation of the liposomes in the tumour tissue due to the enhanced permeability and retention, “EPR”, effect (Greish, 2010).

1.6 DNA-interacting drugs

As described above, many chemotherapy agents interact with the DNA to exert their cytotoxic effects. Drugs may covalently bond to the DNA in the minor or major groove, or may intercalate into the DNA helix. There are four main ways in which a bifunctional alkylating agent can interact with the DNA and these are illustrated in Figure 1-5. Initially, the agent may bind to the DNA in one region, forming a monoadduct. This may be converted in a second step to an adduct with two contacts to the DNA – either an intrastrand crosslink where the drug contacts two bases of the same strand, or an interstrand crosslink (ICL) where the drug bridges two bases on opposite strands of the DNA. The second step is the rate limiting step and so monoadducts are often more common than crosslinks. A fourth type of adduct that may form is a DNA-protein crosslink (McHugh et al., 2001).

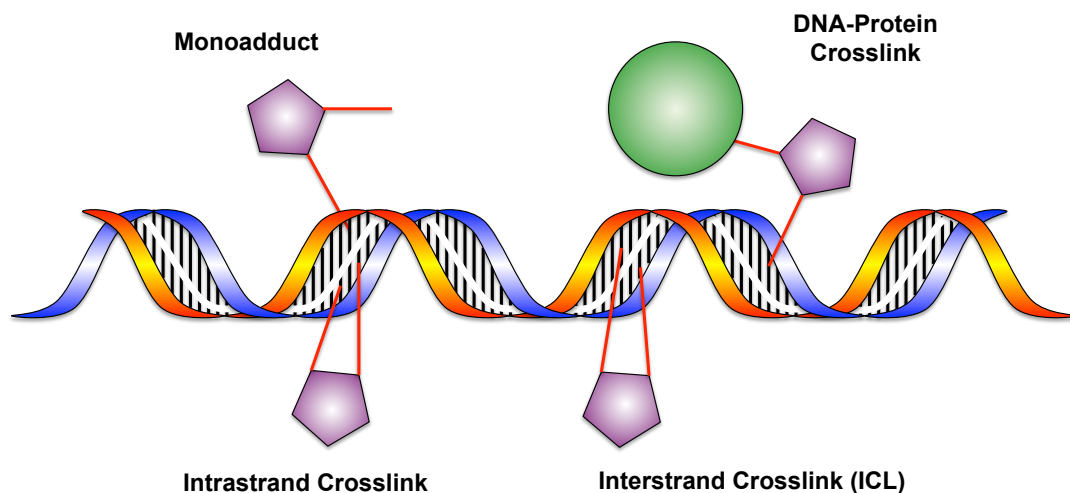


Figure 1-5: The four DNA binding modes for bifunctional agents: monoadduct, DNA-protein crosslink, intrastrand crosslink or interstrand crosslink (ICL). Adapted from (McHugh et al., 2001).

One of the largest group of DNA-interacting drugs is the alkylating agents. These include both mono-functional and bi-functional agents which transfer alkyl groups ranging from small methyl adducts to larger bulky adducts onto the DNA bases. Both types of agents are used in the clinic such as the monofunctional alkylators, procarbazine and temozolomide, and the bifunctional nitrogen mustards melphalan and chlorambucil (D. Fu et al., 2012).

The platinum class of chemotherapy agents are considered “alkylating-like”, in that they perform similar reactions with the DNA but do not contain alkyl groups. Platinum agents consist of a central platinum ion surrounded by ligands that can be displaced by nucleophilic atoms in the DNA bases. This displacement allows platinum agents to form covalent bonds with one base (mono-functional) or two bases (bi-functional) (Colvin et al., 2003).

As well as agents that form mono-adducts and crosslinks, agents that can inhibit topoisomerase complexes are used in cancer therapy. Topoisomerases are required to induce transient breaks in the genome in order to avoid supercoiling and

“knots” in the DNA when regions are unwound for transcription or replication. Therefore, inhibition of these enzymes results in abnormal DNA structures and stalling of DNA replication and transcription. The camptothecins, for example irinotecan, stabilise the topoisomerase I-DNA complex, therefore inhibiting re-ligation of the cleaved DNA and inducing DSBs. Doxorubicin is able to act similarly on the topoisomerase II-DNA complex, doing so through its intercalation into the DNA double helix (Pommier et al., 2010), and etoposide, a non-intercalating topoisomerase II poison, likely inhibits topoisomerase II through direct protein-drug interactions (Nitiss, 2009).

The final class of DNA-interacting chemotherapeutics are the nucleoside analogues, for example, gemcitabine, which is an analogue of cytidine. Upon entering the cell, nucleoside analogues like gemcitabine are phosphorylated and incorporated into the DNA during replication instead of the natural nucleotides. This causes termination of elongation, DNA strand breaks and subsequently apoptosis. Gemcitabine also potentiates its own effect by inhibiting ribonucleotide reductase, an enzyme involved in synthesis of deoxyribonucleotides from ribonucleotides. This lowers the level of competing deoxyribonucleotides in the cell, and ensures that a greater amount of gemcitabine is incorporated into the DNA (Galmarini et al., 2002; Mini et al., 2006).

Therefore, there are several mechanisms by which chemotherapy drugs may interact with DNA and as a result interfere with the correct functioning of this molecule, and this has been exploited from the very beginning of cancer therapy.

1.6.1 Crosslinking agents

Nitrogen mustards, mitomycin C, platinum and psoralens are all successful chemotherapy agents that are still used in the clinic today. These drugs have one thing in common: they produce DNA interstrand crosslinks (ICLs). ICLs are

considered to be one of the most toxic DNA lesions possible, as they covalently link the two DNA strands and as such, cannot be bypassed during replication or transcription. Therefore, these essential processes are blocked by unrepaired ICLs, and stalling of replication forks at these structures results in DSBs and eventual apoptosis (McHugh et al., 2001; Muniandy et al., 2010). The contribution of the ICL in the toxicity of these agents was demonstrated by Clingen et al. Mono-functional melphalan was demonstrated to have an IC_{50} 4-fold higher than bi-functional melphalan, and the novel crosslinker SJG-136 was 60-fold more potent as a bi-functional agent than its mono-functional counterpart (Clingen et al., 2005). As the mono-functional forms of these drugs can only form monoadducts, whereas the bi-functional forms are able to produce ICLs, this suggests that the ICL is a critical cytotoxic lesion. It is estimated that just 20 unrepaired ICLs can cause cell death in sensitive cell lines (Lawley and Phillips, 1996). Therefore, agents that produce ICLs are highly effective for chemotherapy.

1.6.1.1 Cisplatin

The first of the platinum class of agents, cis-platinum diamminodichloride (cisplatin), was initially synthesised in 1844 by Michael Peyrone and named Peyrone's Chloride. 50 years passed before the structure of cisplatin was elucidated in 1893 by Alfred Werner (Desoize and Madoulet, 2002; Florea and Büsselberg, 2011). More than 70 years then passed before cisplatin was re-discovered serendipitously in 1965. Rosenberg et al. intended to observe the effects of an electric current on bacterial processes using platinum electrodes. Instead, they noticed an effect on the replication of the bacteria and identified that this was in fact due to several platinum-based compounds that had formed in the media (Rosenberg et al., 1965). Later, they demonstrated the anti-cancer effects of these platinum-based compounds in mice – one of which was cisplatin (Rosenberg et al., 1969). Cisplatin was given to

the first cancer patient in a phase I clinical trial in 1971, and this was followed by positive results from trials in ovarian and testicular cancer patients (Lebwohl and Canetta, 1998).

Cisplatin was eventually approved for use by the FDA in 1978 and today, more than 170 years after its initial discovery, cisplatin is one of the most commonly used drugs for treating lung, ovarian, testicular, head and neck, cervical, bladder and germ cell cancers. It is typically administered every 3-4 weeks intravenously. As cisplatin is given systemically many side effects can occur with a tendency for a lower tolerance of the drug as age increases. This has been suggested to be due to an inverse relationship between the ability of cells to repair ICLs and the patients age (McHugh et al., 2001). 10% of patients typically experience at least one of the more common side effects of cisplatin which include: vulnerability to infections due to a lower white blood cell count, tiredness and a shortness of breath due to a lower red blood cell count, bruising due to the effect of cisplatin on platelets, nausea, some high-range hearing loss and kidney damage. Less than 10% of patients will experience one of the less common side effects such as amenorrhoea, fertility problems, loss of appetite and taste, tinnitus, or numbness (Cisplatin, Cancer Research UK webpage, available from: <http://www.cancerresearchuk.org/about-cancer/cancers-in-general/treatment/cancer-drugs/cisplatin> [accessed August 2016]). Strategies exist to manage some of these side effects such as increasing drug elimination with intravenous hydration, and alleviation of nausea by administration of antiemetics (Florea and Büsselberg, 2011).

Due to these side effects, cisplatin is often administered in combination with other drugs that have non-overlapping toxicities (see treatment of lung cancer, section 1.3.2) as this allows lower doses of each component of the combination to be used to obtain the same therapeutic effect. Development of other platinum chemotherapy

drugs was also intended to reduce the side effects observed with cisplatin. These include oxaliplatin and carboplatin, now widely used in colon cancer and ovarian cancer, respectively (Florea and Büsselberg, 2011).

1.6.1.1.1 Molecular mechanism of cisplatin

Cisplatin has been suggested to enter the cell by one of three processes: passive diffusion across the membrane, facilitated transportation through the copper transporter CTR1 or active transport via ATPases such as the Na^+/K^+ ATPase (Basu and Krishnamurthy, 2010).

Once inside the cell, cisplatin undergoes two spontaneous hydrolysis reactions, displacing the chloride ions for water molecules (Figure 1-6). Hydrolysis is only favourable inside the cell as the chloride ion concentration is 25-fold lower in the cytoplasm than it is in the bloodstream (Basu and Krishnamurthy, 2010). It is in this hydrolysed form, $\text{cis-}[\text{Pt}(\text{NH}_3)_2(\text{H}_2\text{O})_2]^{2+}$, that the now electrophilic cisplatin may interact with and form adducts to the cellular DNA. Cisplatin binds to the nucleophilic N7 of purine bases to form monoadducts and subsequently crosslinks. The most common adduct formed is the intrastrand crosslink at either 5'-GpG-3' (65%) or 5'-ApG-3' (25%) sites. ICLs constitute up to 8% of cisplatin-DNA adducts and form at 5'-GpC-3' sites, crosslinking the N7 of the opposite guanines (Figure 1-7) (Muniandy et al., 2010).

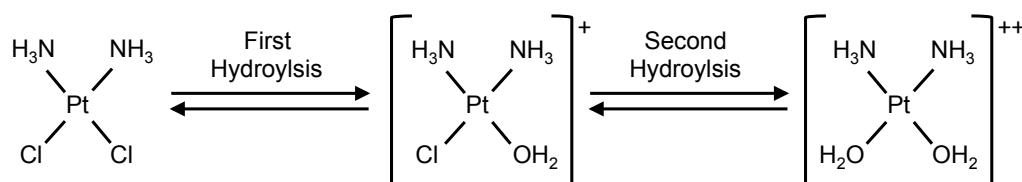


Figure 1-6: Chemical structure of cisplatin before and after hydrolysis.

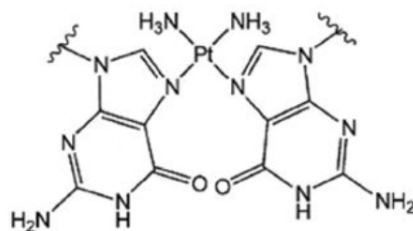


Figure 1-7: Structure of a cisplatin ICL. Cisplatin covalently bonds to the N7 of each cross-linked Guanine. Taken from (Wilson and Seidman, 2010).

1.6.1.2 Melphalan

The discovery of the nitrogen mustards as chemotherapy agents occurred serendipitously in the 1940s as a result of observations with the chemical warfare agent sulphur mustard, as was discussed in section 1.4. These were the first chemotherapy drugs to be discovered, and so the development of derivatives of the first nitrogen mustard occurred soon after its discovery. In 1954, melphalan was first synthesised when searching for new anti-tumour drugs derived from phenylalanine (Bergel and Stock, 1954). Melphalan, previously known as sarcolysine, was demonstrated to completely inhibit tumour growth in mouse sarcoma models. A year later, similar experiments with melphalan demonstrated complete tumour regression in 240 mice with sarcoma (Larionov et al., 1955), providing further evidence towards the usefulness of this compound in the fight against cancer. Throughout the late 1950s and early 1960s clinical trials with melphalan were carried out and in 1964 melphalan was approved by the FDA.

Today, melphalan is primarily used to treat multiple myeloma. Melphalan is administered either intravenously or with oral tablets. As with cisplatin, melphalan has many side effects due to the action of the drug on the normal cells of the body. The most common side effects with melphalan are similar to those of cisplatin,

including tiredness, vulnerability to infection and bruising, which are all due to the effects of chemotherapy on the components of the blood. 33% of patients receiving melphalan may experience nausea and at least 10% of patients receiving melphalan may experience a loss in fertility. Less common side effects associated with melphalan include hair loss, mouth ulcers or development of a second cancer, although this is very rare (Melphalan (Alkeran), Cancer Research UK webpage, available from: <http://www.cancerresearchuk.org/about-cancer/cancers-in-general/treatment/cancer-drugs/melphalan> [accessed August 2016]).

As with cisplatin, melphalan can be administered as part of a combination of drugs. In myeloma, melphalan can be given with prednisolone, thalidomide or bortezomib, which may help to reduce side effects. Myeloma patients are also treated with melphalan in a high dose setting in combination with a stem cell transplant.

1.6.1.2.1 Molecular mechanism of melphalan

The mechanism of cellular uptake of melphalan has not been extensively investigated. However, melphalan uptake has been suggested to occur via an active process, using amino acid transporters due to the structural similarities between melphalan and amino acids (Goldenberg et al., 1979). Competitive inhibition of melphalan uptake has been demonstrated by leucine, which was also able to reduce the anti-tumour effect of melphalan (Vistica et al., 1979).

Nitrogen mustards can form monoadducts, intrastrand crosslinks and interstrand crosslinks. However, melphalan, unlike cisplatin and other nitrogen mustards such as mechlorethamine, does not readily form intrastrand crosslinks. This is proposed to be due to the interaction of melphalan with different regions of the DNA, drawing the reactive chlorine atom away from the conformation favourable for intrastrand crosslink formation (Bauer and Povirk, 1997). The inability of melphalan to form

intrastrand crosslinks highlights the importance of ICLs in the toxicity of crosslinking drugs. Cells treated with doses of mechlorethamine and melphalan that produce similar peak levels of ICLs are more sensitive to melphalan than to mechlorethamine (Ross et al., 1978). As mechlorethamine also produces many more intrastrand crosslinks than ICLs, and the kinetics of ICL repair indicate more persistent ICLs for melphalan, this may suggest that the ICL is the most cytotoxic crosslink (Bauer and Povirk, 1997).

To form DNA-adducts, nitrogen mustards become electrophilic through the loss of one chloride atom, and subsequently covalently bind to the N7 atom of a guanine residue. These adducts constitute 90-95% of nitrogen mustard-DNA adducts. The remaining 5-10% of adducts are ICLs (Muniandy et al., 2010), however early experiments with melphalan suggested that up to 30-40% of melphalan-DNA adducts may be ICLs (Hansson et al., 1987), therefore there may be differences between the proportion of adducts formed by different nitrogen mustards. The formation of a crosslink can occur through a second covalent linkage to another guanine N7 on the opposite strand of DNA (Muniandy et al., 2010; Rajski and Williams, 1998). This mechanism is shown in Figure 1-8 for mechlorethamine, which has a simpler methyl group compared to the phenylalanine group in melphalan. This reaction is particularly slow for melphalan in comparison with other nitrogen mustards, however, the resulting ICLs are considerably more stable (Bauer and Povirk, 1997).

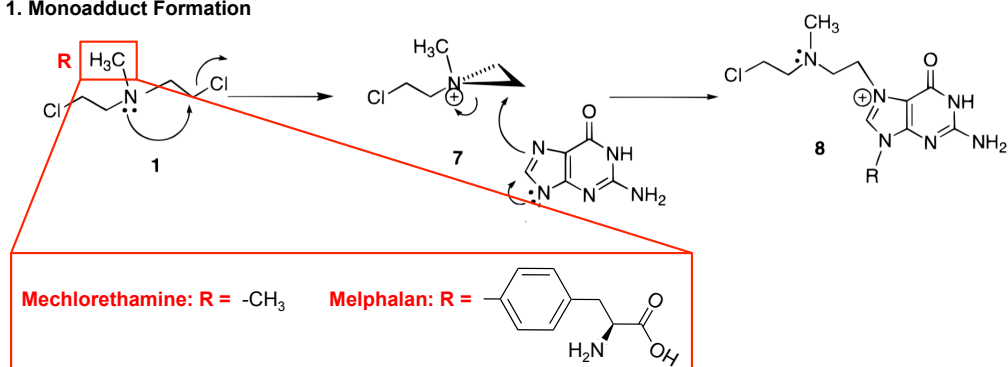
For nitrogen mustards, as the chlorine atoms are separated by 5 atoms, the crosslinked guanines are separated by another base pair, with these adducts occurring at 5'-GpNpC-3' sites. The differences between nitrogen mustard and

cisplatin ICLs in terms of structure and helical distortion are discussed in detail in the introduction to Chapter 6.

In addition to DNA-DNA crosslinks, nitrogen mustards can also crosslink DNA to proteins. This includes chromatin remodelling factors, DNA repair proteins and transcriptional regulation factors.

These crosslinks occur between the guanine N7 and cysteine residues on cellular proteins, although, these interactions are not well characterised. However, the DNA-protein crosslinks induced by nitrogen mustards such as melphalan may also contribute towards the cytotoxicity of these compounds (Loeber et al., 2009).

1. Monoadduct Formation



2. ICL Formation

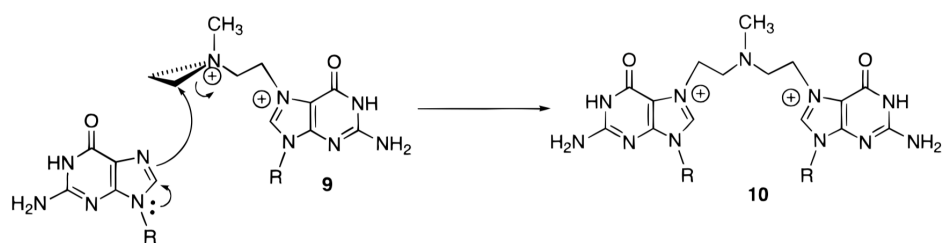


Figure 1-8: Formation of nitrogen mustard monoadducts (1) and interstrand crosslinks (2) between two N7 guanine atoms. The differences in the R group for mechlorethamine and melphalan are highlighted. Adapted from (Rajski and Williams, 1998).

1.7 Drug resistance

Unfortunately, treatment with chemotherapy agents rarely results in a complete cure, as acquired resistance to treatment will occur. Drug resistance is one of the most common reasons for patient discontinuation of treatment with a particular agent (Luqmani, 2005). Resistance to chemotherapy agents can be intrinsic to the tumour. It is estimated that 1 in 10^6 - 10^7 cells in a tumour will have intrinsic resistance to a chemotherapy drug. Given that there are at least 10^9 cells in a clinically detectable tumour, there could be 1000 drug-resistant cells capable of evading chemotherapy. Therefore, the size of the tumour at the onset of chemotherapy is proportional to the chance of intrinsic resistance (Luqmani, 2005). Therefore, treatment with a chemotherapy agent in this setting puts selective pressure on the tumour, with the result being that the intrinsically resistant cancer cells survive and continue to proliferate. Another form of resistance can develop after treatment with an agent. An initial response to the agent will be achieved, but relapse will occur. This is known as acquired resistance, and is also product of natural selection of the tumour cells that are able to evade the cytotoxic actions of the chemotherapy drug. With acquired resistance, however, the ability to evade the tumour develops only after exposure to the chemotherapy agent in question due to acquired mutations.

Several methods can be used in order to overcome resistance to chemotherapy drugs. These include administering higher doses of the chemotherapy whilst controlling side-effects with other drugs in the combination treatment, developing novel combination therapies to target resistance pathways directly, or developing new chemotherapy drugs that do not have the same resistance mechanisms (Giaccone, 2000).

1.7.1 Cisplatin resistance

Although many types of cancer are initially sensitive to cisplatin, high levels of relapse are seen. For example, in NSCLC initial response rate is only 20% due to inherent resistance to cisplatin whereas SCLC tumours are initially very sensitive to cisplatin (80-95% response rate) and only after prolonged exposure will relapse occur, with rates of up to 95% reported. 70-80% of advanced ovarian cancer patients typically respond to cisplatin therapy initially, however, relapse due to cisplatin resistance occurs in 56% (Giaccone, 2000). Resistance to cisplatin is determined in clinical scenarios by the time to progression in the absence of chemotherapy. For example in ovarian cancer, patients that relapse more than 6 months after finishing platinum therapy are considered platinum-sensitive, whereas patients that relapse within 6 months from finishing platinum therapy are considered resistant (Giaccone, 2000).

As discussed previously, cisplatin exerts its toxicity through the adducts it forms with the cancer cell DNA. There is a direct correlation between cisplatin sensitivity and extent of platinated DNA in ovarian cancer patient samples (Reed et al., 1987) and therefore, any process which interferes with the ability of cisplatin to interact with the DNA could result in clinical resistance. This may include changes in cisplatin accumulation within the cell either through enhanced efflux or reduced uptake, inactivation of cisplatin inside the cell, or enhanced DNA repair. The various factors that can contribute to cisplatin resistance are summarised in Figure 1-9 (Siddik, 2003). Ironically, many of the mechanisms behind resistance to chemotherapy drugs like cisplatin are likely to have evolved in order to protect normal cells against natural carcinogens and toxins (Luqmani, 2005). However, these proposed resistance mechanisms, of which many have been demonstrated in cell line models, may not occur in patients. Some proposed mechanisms such as expression of the

GST- π enzyme and the ATP7a transporter have been correlated with cisplatin resistance in patient samples (Bai et al., 1996; Yang et al., 2015), however, data from this research group has suggested that in ovarian cancer patients, cisplatin resistance is acquired through enhanced ICL repair. The level of ICLs formed in paired cisplatin-naïve and cisplatin-treated samples was equal, implying that upstream factors such as cisplatin accumulation or detoxification are not responsible for the acquired resistance found in ovarian cancer patients (Wynne et al., 2007). The mechanisms contributing to cisplatin resistance will be explored in more detail in the introduction to Chapter 4.

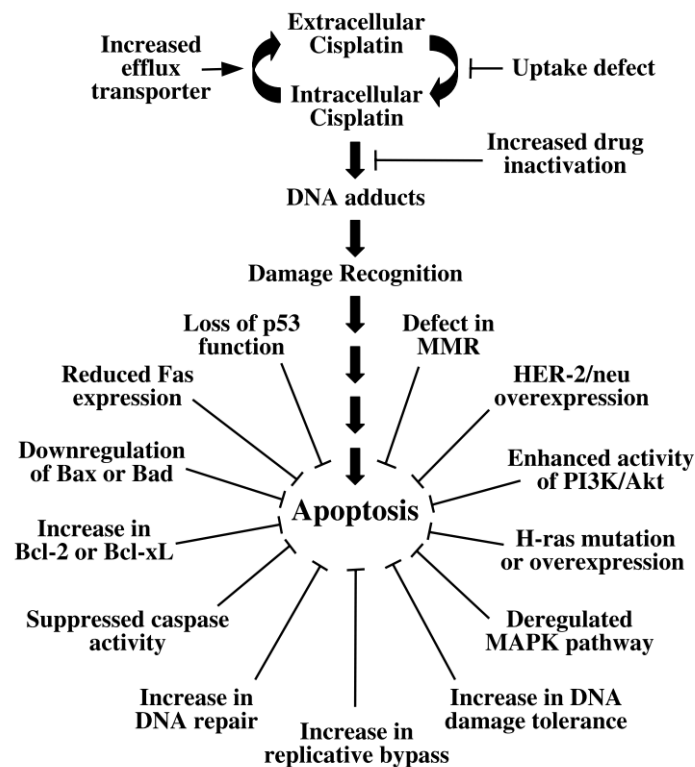


Figure 1-9: Factors contributing to the development of resistance of cisplatin. Taken from (Siddik, 2003).

1.7.1.1 Biomarkers for cisplatin sensitivity

One approach to tackle failure of cisplatin therapy is to select for those patients most likely to respond well using biomarkers for cisplatin sensitivity. This method would improve response rates, save money, and also benefit the non-responding patients greatly as time would not be wasted on platinum-based therapy, increasing the chance of finding an effective treatment sooner.

Biomarkers can be screened for histologically by staining tumour sections, or genetically by identifying mutations in target genes associated with sensitivity or resistance to cisplatin. One such potential biomarker is ERCC1, a component of the XPF-ERCC1 nucleotide excision repair nuclease. This nuclease is essential for the repair of both intrastrand crosslinks (repaired by NER) and ICLs (repaired by a unique pathway), and its role in these repair pathways will be covered in sections 1.8.1.2.2 and 1.8.2.2. Patients classified as clinically resistant to cisplatin have been shown to exhibit significantly higher levels of ERCC1 (Dabholkar et al., 1992). Additionally, single nucleotide polymorphisms in the ERCC1 gene, which reduces expression of the ERCC1 protein, are correlated with survival following platinum-based therapy, and patients expressing higher levels of ERCC1 prior to platinum-based therapy have a reduced overall survival (Ting et al., 2013).

In order to assess the usefulness of ERCC1 as a biomarker for cisplatin treatment, a phase III trial was carried out in 364 NSCLC patients and the results were reported in 2007. The control group received cisplatin and docetaxel therapy, whereas the remainder of the patients received docetaxel and gemcitabine if they had high ERCC1 levels, and cisplatin and docetaxel if they had low ERCC1 levels, as determined by ERCC1 mRNA expression. In the control group 39.3% of patients obtained an objective response whereas in the stratified treatment group (both high and low ERCC1), 50.7% of patients obtained an objective response. This is the first

large scale demonstration that ERCC1 status could be used to successfully assign patients to cisplatin-based treatment schedules (Cobo et al., 2007). However, not all studies have found a correlation between ERCC1 and cisplatin sensitivity, though this may be due to the combination of cisplatin with other drugs making consistent analysis of correlation more complex (Rose and Huang, 2014). Also, the technical issue of ERCC1 antibodies lacking specificity for the active isoform of ERCC1 over other inactive isoforms remains to be overcome if ERCC1 status is to be determined histologically, as this factor may be responsible for the difficulty in validation of ERCC1 as a biomarker for cisplatin sensitivity (Friboulet et al., 2013). Therefore, there is potential in the use of ERCC1 as a biomarker for the selection of patients who would benefit from cisplatin treatment, and this avenue must be explored further in order to improve response to cisplatin.

ERCC1 is by far the most well characterised potential biomarker for cisplatin sensitivity, however, the expression of other factors has also been correlated with cisplatin sensitivity. These include the NER factor, XPA, and transporters involved in the uptake and efflux of cisplatin including the copper transporters CTR1 and CTR2, and the ATP7a and ATP7b ATPase transporters. Additionally, low levels of the glutathione-S-transferase pi (GST π) enzyme have been correlated with cisplatin sensitivity, due to decreased inactivation of cisplatin (Rose and Huang, 2014). However, all of these factors require more clinical evidence in order to demonstrate their potential use as biomarkers for cisplatin sensitivity.

1.7.2 Melphalan resistance

Many of the mechanisms of resistance reported for melphalan are similar to those reported for cisplatin, and act by interfering with the ability of melphalan to form DNA adducts.

Melphalan can be inactivated in the cell through the action of GST enzymes, however whilst the GST- π isoform is involved in detoxification of cisplatin, the microsomal GST (MGSTII) isoform is reportedly involved in melphalan detoxification, and its introduction into cells can confer resistance to melphalan (Harkey et al., 2005). As with cisplatin, expression of thiol-containing molecules such as metallothioneins can also reduce melphalan sensitivity (Kelley et al., 1988) by covalently binding to and inactivating melphalan directly (Yu et al., 1995).

Reduced accumulation of melphalan in the cell is another mechanism by which resistance can occur. Decreased uptake of melphalan in cells with reduced levels of amino acid transporters such as CD98 is correlated with resistance (Harada et al., 2000; Moscow et al., 1993). Alternatively, enhanced efflux of GSH-conjugated melphalan mediated by the multidrug resistance protein, MRP1, has been reported (Barnouin et al., 1998), and a correlation between expression of the multidrug resistance transporter, MDR1, decreased intracellular accumulation and reduced sensitivity to melphalan has been observed (Kuhne et al., 2009). Therefore, both uptake and efflux of melphalan may contribute to cellular melphalan resistance.

Direct effects on the formation and repair of melphalan-DNA adducts has also been linked to cellular melphalan resistance. In resistant cell lines a 50% decrease in melphalan-DNA binding was observed, and 50% less melphalan-ICLs were present when compared to the parental cell line (Parsons et al., 1981). In patient samples, whilst no difference in the formation of ICLs was observed after *ex vivo* treatment with melphalan, cells from individuals previously exposed to melphalan were able to more effectively repair melphalan-ICLs than cells from melphalan-naïve individuals, and the ability to repair melphalan-ICLs negatively correlated with *ex vivo* melphalan sensitivity (Spanswick et al., 2002). This suggests that resistance to melphalan in

myeloma patients is due to DNA repair processes rather than an “upstream” mechanism such as melphalan accumulation or inactivation.

Therefore, melphalan resistance may occur via many processes that interfere with the ability of melphalan to bind cancer cell DNA. However, most of these resistance mechanisms have only been demonstrated *in vitro*, and so their clinical relevance is as yet undetermined. A role for DNA repair in melphalan resistance currently has the most support from clinical data. Whether the melphalan resistance pathways discussed here can be exploited to develop novel biomarkers for melphalan sensitivity has not yet been thoroughly investigated.

1.7.3 Chemotherapy cross-resistance

The mechanisms of resistance to cisplatin and melphalan have significant cross over. This is true for many chemotherapy drugs, and therefore, a phenomenon known as “cross-resistance” can occur. This is when a patient that has been treated with one drug and has subsequently developed acquired resistance to that drug, will now fail to respond to another chemotherapy drug due to similar resistance mechanisms.

This is common within a class of chemotherapy agents. For instance, cells resistant to cisplatin often demonstrate cross-resistance to carboplatin (Eckstein, 2011). Similarly, cross-resistance within the nitrogen mustard class can also exist *in vitro* (Goldenberg, 1975). This can be overcome by the development of similar agents that have alternative mechanisms of resistance. For example, some cisplatin resistant cells are not cross-resistant to oxaliplatin (Eckstein, 2011; Raymond et al., 2002).

Cross-resistance can also occur between classes of drugs if a common resistance mechanism is shared. For example high levels of cellular glutathione has been implicated in cross-resistance to a group of chemotherapy agents including cisplatin, melphalan, carboplatin, etoposide and doxorubicin. This was proposed to be due to inactivation of these compounds by glutathione (Hamaguchi et al., 1993). Similarly, overexpression of metallothionein confers resistance to cisplatin, melphalan and chlorambucil (Kelley et al., 1988). Cross-resistance has also been observed between nitrogen mustards (mechlorethamine, chlorambucil and melphalan), cisplatin and MMC. These are all crosslinking agents and so cells exhibiting cross-resistance to these agents may have enhanced DNA repair pathways common to the repair of these crosslinks (Bramson et al., 1995). However, not all cells that are able to repair interstrand crosslinks induced by one agent are able to repair ICLs induced by all crosslinkers, as was demonstrated by this research group (Spanwick et al., 2012). Therefore, the molecular events responsible for cross-resistance to crosslinking chemotherapy drugs requires further investigation.

Due to cross-resistance, selection of a second chemotherapy agent after resistance has emerged must be considered carefully so as to avoid selecting a drug the patient is already cross-resistant to. However, exploitation of cross-resistance may also provide the potential to develop agents that interfere with common resistance pathways, such as DNA repair or drug inactivation, allowing re-sensitisation of patients to more than one chemotherapy drug.

1.8 DNA repair

As described in section 1.2.1, the human genome is constantly under attack from both exogenous and endogenous sources, producing adducts, intercalations, nicks and breaks in the genetic material. If accumulating DNA damage is not repaired, the cell may undergo apoptosis, or depending on the proliferation status of the cell, the damage may contribute to the development of cancer or the aging process (Bernstein et al., 2013) (Figure 1-10).

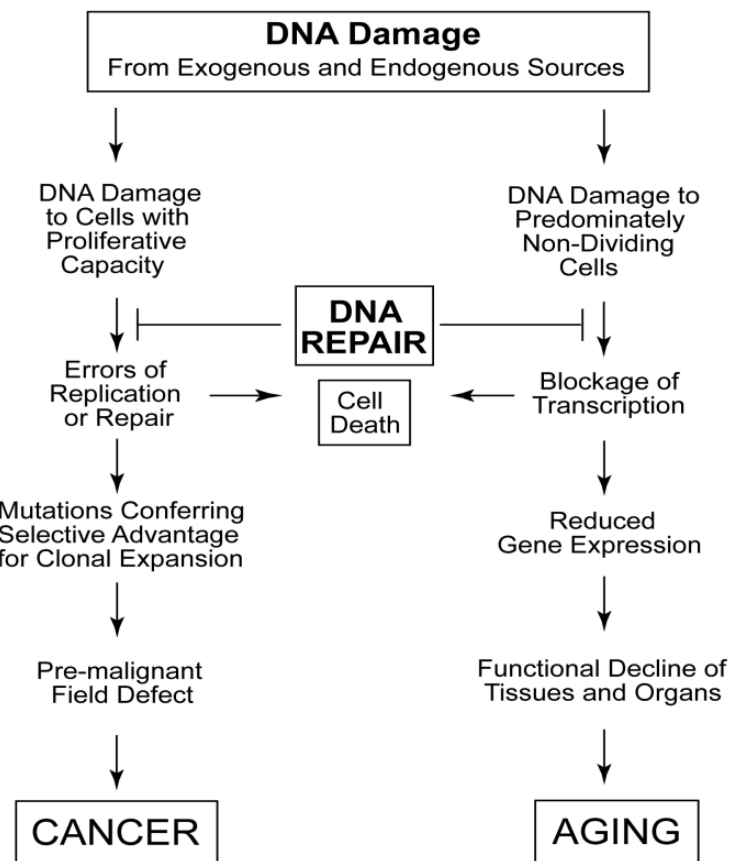


Figure 1-10: Fates of cells after DNA damage: cell death, cancer, and aging. Taken from (Bernstein et al., 2013).

Many thousands of individual DNA damages occur each day (as was summarised in Table 1-1). Fortunately, the cell has evolved a comprehensive defence mechanism in the form of several DNA repair pathways in order to cope with endogenous DNA damages. In a normal cell, upon detection of DNA damage, the cell cycle is halted at one of the checkpoints (either prior to S phase DNA replication or prior to mitosis), and DNA repair is allowed to occur before the cell cycle proceeds again. In cancer cells, these checkpoints are often lost (mainly due to mutations in the p53 and pRb tumour suppressors) and so this allows DNA damage to accumulate and results in enhanced mutation rates (Lapenna and Giordano, 2009). The signalling network from detection of DNA damage to arrest of the cell cycle is shown in Figure 1-11.

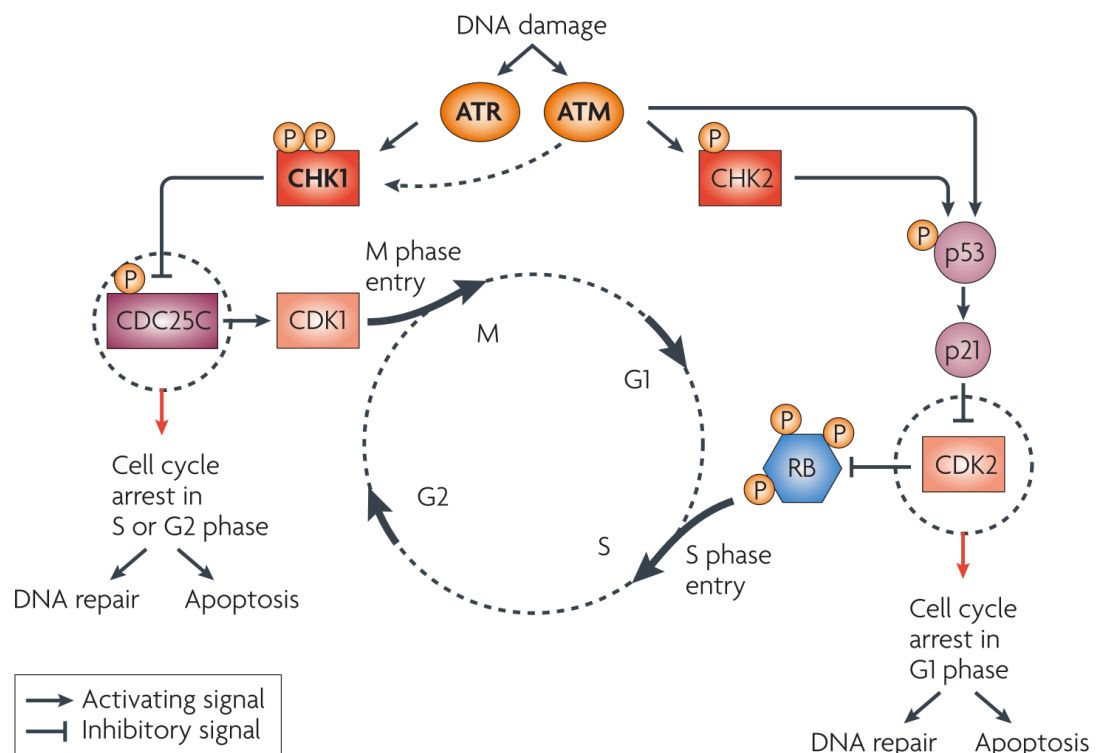


Figure 1-11: DNA damage detection by the ATR and ATM kinases, and the resulting arrest in cell cycle due to inhibition of cyclin-dependent kinases. Taken from (Lapenna and Giordano, 2009).

Many DNA damages induced by exogenous agents are also repaired via these pathways, which at least in part accounts for the resistance to DNA damaging chemotherapy drugs observed, as discussed previously. Defects in these repair processes can result in persistent DNA damage, which causes errors in replication leading to mutations. If a mutation is in a significant region of a driver gene, this event can spark tumourigenesis. Therefore DNA repair pathways are critical in preventing the development of cancer.

1.8.1 Major mechanisms of repair

1.8.1.1 Double strand break repair

Double strand breaks (DSBs) arise when both strands of the DNA are broken close together, resulting in two free DNA ends which are able to dissociate away from each other (Jackson, 2002). An estimated 10 DSBs occur in each cell, each day (Lieber, 2010). DSBs can be caused intentionally by endogenous processes such as VDJ recombination in antibody production (Bassing et al., 2002) as well as crossover during meiosis which produces greater genetic diversity (Youds and Boulton, 2011), or unintentionally by endogenous species such as reactive oxygen species generated during aerobic respiration (Lieber, 2010). Exogenous factors such as exposure to ionizing radiation and topoisomerase inhibitors also induce DSBs. If left unrepaired or incorrectly repaired, DSBs can induce mutations, amplifications, deletions and translocations, and just one DSB can cause cell death if the break occurs in an essential gene. Equally, mis-repaired DSBs can result in tumourigenesis if an oncogene or tumour suppressor is affected (Khanna and Jackson, 2001). Therefore, several repair mechanisms exist depending on the situation, for example cell cycle phase (Jackson, 2002). The three forms of DSB repair and in which scenarios they are used will be discussed.

1.8.1.1.1 Homologous recombination

Where a second copy of the damaged gene is available, for example in S phase immediately after DNA replication, a process known as homologous recombination (HR) can be utilised (Figure 1-12). This type of repair will be employed particularly for DSBs arising from collapsed replication forks (Lieber, 2010). Here, detection of the DSB by ATM and ATR leads to phosphorylation of key repair proteins such as BRCA1, p53 and H2AX. BRCA1 acts as a scaffold for other HR proteins (Walsh, 2015). The RAD50/MRE11/NBS1 nuclease then digests the two ends of the DSB in a 5'-3' direction (known as end resection), creating single-stranded overhangs with 3'OH ends which are substrates for RPA binding. Recombination mediators such as BRCA2 are able to facilitate the displacement of RPA and loading of RAD51 onto the single strand regions, forming a nucleoprotein filament. Rad51 is a recombinase and so is able to search for a homologous sequence (in S phase this is provided by the sister chromatid, often in close proximity due to the action of cohesins) and initiate strand invasion of the template DNA. This forms a "D-loop" structure and allows for highly accurate re-synthesising of the damaged DNA followed by ligation. (Hoeijmakers, 2001; San Filippo et al., 2008). Changes can however occur when the branched holliday junction structures are resolved to separate the two DNA molecules during the last step of HR. These structures can be cleaved in two ways by structure-specific endonucleases such as MUS81-EME1 (Heyer, 2004), and depending on the orientation of the incisions made, a cross-over of genetic material can occur. Alternatively, dissolution of the holliday junctions by the BLM helicase and topoisomerase III can occur, resulting exclusively in non-crossover products, and subsequently a more accurate repair process (Li and Heyer, 2008; San Filippo et al., 2008). Crossover can however be beneficial, for instance during meiosis where this process helps to produce genetic diversity in offspring.

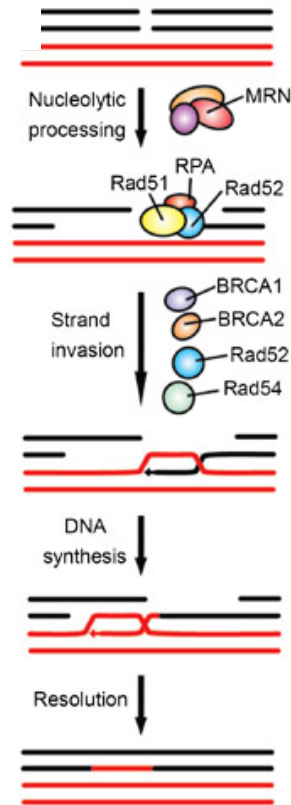


Figure 1-12: Simplified model for homologous recombination. Taken from (Weterings and Chen, 2008).

1.8.1.1.2 Single strand annealing

A second method of DSB repair also involves homology, however, this method occurs between repetitive DNA on the same chromosome. This is known as single strand annealing (SSA, Figure 1-13) and depending on the length of the repetitive sequences, can be classed as long-homology SSA or micro-homology SSA. As with HR, the first stage of SSA involves resection of the DSB site. However, unlike HR, Rad51 is not required for SSA whereas Rad52 is. Rad52 is thought to bind to the ends of the single strand overhangs as a heptameric ring structure, and promotes association of the two complimentary regions (Valerie and Povirk, 2003). Therefore, instead of strand invasion occurring to copy back the missing DNA, when two

repetitive sequences are present, these are paired together, and the resulting single-strand "tails" of DNA are cleaved by nucleases such as XPF-ERCC1. This method deletes the genetic information between the two sites, including one of the repeated sequences (San Filippo et al., 2008). Long-homology SSA likely follows this pathway however it has been suggested that micro-homology SSA may occur in a manner similar to non-homologous end joining (see next section) (Valerie and Povirk, 2003).

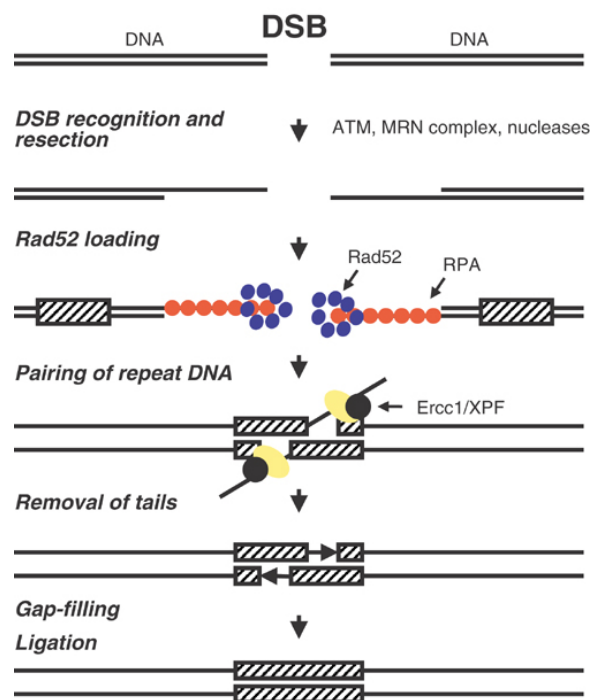


Figure 1-13: Model for single strand annealing homologous recombination. Taken from (Valerie and Povirk, 2003).

1.8.1.1.3 Non-homologous end joining

When a second copy of the gene is not present in the cell and no repetitive regions flank the DSB, non-homologous end joining (NHEJ, Figure 1-14) can be used to repair the DSB. For this reason, NHEJ is thought to be the prevalent method of DSB repair for two-sided DSBs rather than replication-induced DSBs, and also in G1 phase. This pathway involves direct joining of the DNA either side of the DSB. The Ku70/80 complex is largely involved in this process, as it has extremely high affinity for DNA ends and so immediately after DSB induction, Ku70/80 encapsulates the two free DNA ends in its ring-like structure and acts as a scaffold to recruit the other members of the NHEJ machinery. The kinase DNA-PKcs (DNA-dependent protein kinase catalytic subunit) is recruited by Ku70/80, and is able to bridge the two DNA ends together. Autophosphorylation of DNA-PKcs induces a conformation change in the NHEJ complex, which allows the processing enzymes and ligase to access the site. Ligase IV/XRCC4 is then recruited to the repair site, which performs the final ligation step. However, in order to generate compatible ends for ligation, either resection or gap-filling is often necessary. Gap-filling may be carried out by DNA polymerases μ and λ , or by Human terminal deoxynucleotidyltransferase (TdT); all of these enzymes are recruited to the DSB site by Ku70/80. For resection of the overhangs, the nuclease Artemis is required. Phosphate groups may also need to be added at the 5'-end as this is required for successful ligation of the two DNA ends. Once the DNA ends have been processed into ligatable ends, the Ligase IV/XRCC4 is able to complete NHEJ. Due to this end-processing step, NHEJ results in insertions or deletions of genetic information at the site of the repaired DSB. For this reason, NHEJ is considered a less accurate mechanism for DSB repair (Weterings and Chen, 2008).

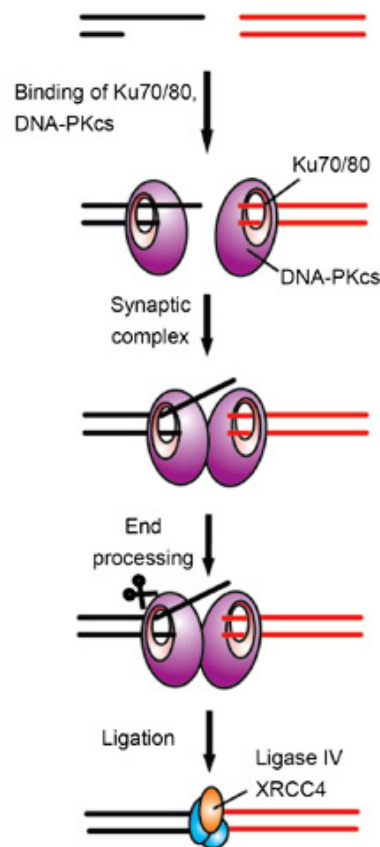


Figure 1-14: Simplified model for NHEJ. Taken from (Weterings and Chen, 2008).

1.8.1.2 Excision repair

There are three main types of excision repair: base excision, nucleotide excision and mismatch repair. These repair pathways deal with damage to bases where DSBs are not present.

1.8.1.2.1 Base excision repair

Base excision repair (BER) is employed by the cell to remove adducts to single bases such as alkylations, base oxidations, depurination/depyrimidations and deaminations, and this can be achieved through two routes: removal of the single affected nucleotide (known as short-patch BER) or removal of a length of nucleotides surrounding the damage site (known as long-patch BER). The core

mechanism for the single-adduct removal BER pathway is illustrated in Figure 1-15. Recognition of the damage is performed by a DNA glycosylase specific for the particular lesion, for example Uracil DNA Glycosylase (UNG) recognises misincorporated uracil nucleotides, and OGG1 recognises 8-oxo-guanine lesions (Krokan et al., 2000). This recognition is followed by excision of the affected base by the glycosylase enzyme. The glycosylase flips the affected nucleotide out of the DNA helix and excises the nucleotide by cleaving the N-glycosidic bond, leaving an abasic site. Spontaneous hydrolysis of the affected nucleotide can also result in an abasic site. The backbone is then nicked either up or down-stream of the lesion by an AP endonuclease (such as APEX1) or an AP lyase (which can be provided by bifunctional glycosylase enzymes such as OGG1 (Jacobs and Schär, 2012)), respectively. When BER is required after induction of a SSB, PARP and polynucleotide kinase (PNK) may be required to process the break for BER. In short-patch BER the resulting abasic site filled by DNA polymerase β adding in a single nucleotide, followed by ligation of the DNA backbone by DNA ligase III (Krokan et al., 2000).

For long-patch BER, between 2-10 nucleotides are replaced via processive polymerisation by DNA Pol δ in a PCNA-dependent manner. This results in a displaced DNA flap, therefore the FEN1 endonuclease is required to cleave the flap before ligation of the newly synthesised DNA by DNA ligase I (Hoeijmakers, 2001; Robertson et al., 2009). What determines whether short- or long-patch BER takes place is not fully understood, however, the glycosylase used to remove the lesion, the cell cycle stage, and the ATP concentration have all been suggested to play a role in this decision (Krokan et al., 2000; Robertson et al., 2009).

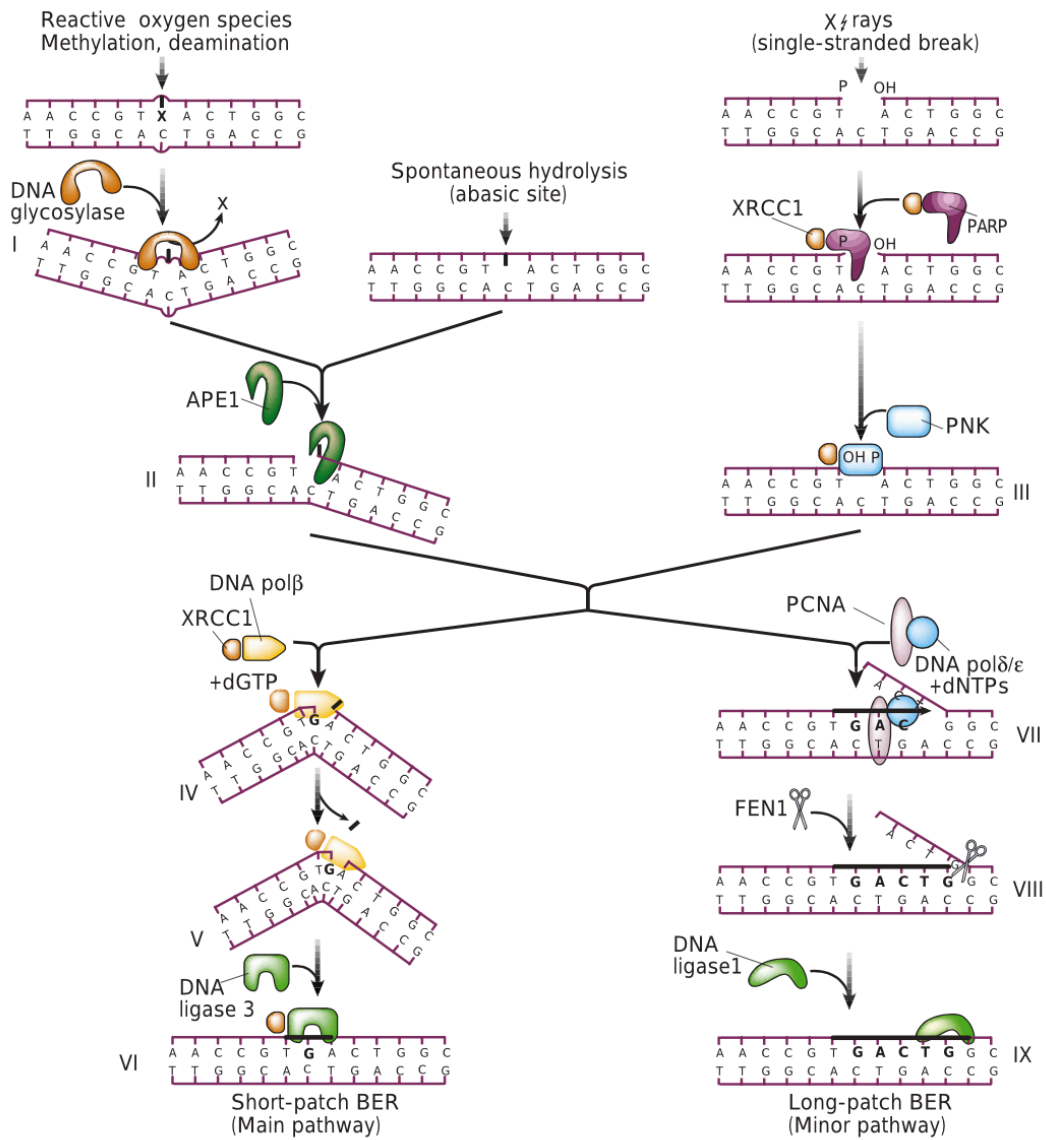


Figure 1-15: Mechanism of base excision repair. Taken from (Hoeijmakers, 2001).

1.8.1.2.2 Nucleotide excision repair

Where bulkier adducts are present, nucleotide excision repair (NER) is employed (Figure 1-16). NER can repair intrastrand crosslinks, UV-induced lesion such as 6-4 pyrimidine-pyrimidone (6,4-PP) photoproducts and cyclopurimidine dimers, as well as

some more complex oxidative lesions. NER is also viewed to be critical for ICL repair alongside other repair pathways (Noussipiel, 2009).

NER can only repair bulky adducts due to the machinery responsible for damage detection in this pathway - the XPC complex. XPC is only able to recognise lesions that considerably distort the double helix. Upon DNA damage, XPC becomes polyubiquitinated, which is thought to stimulate its binding to DNA. Where smaller helix distortions are present, the damage binding complex DDB1/2 will bind the lesion first and induce a larger helical distortion, which allows for XPC recognition. During this process, DDB polyubiquitinates XPC and also auto-polyubiquitinates itself. The result of this is handover of repair from DDB1/2 to XPC through enhancement of XPC binding to DNA and proteasomal degradation of DDB2. The TFIIH complex of proteins is recruited and two components of this complex, XPB and XPD unwind the DNA around the lesion using their helicase and ATPase activities to create a "denaturation bubble". XPA binding is known to be critical for the NER process but it is not fully understood whether XPA has a role in damage recognition or in determination of the damaged strand for excision purposes. The single-strand binding protein, RPA, binds to the now exposed DNA strands in order to stabilise this intermediate. The next stage involves excision at both the 5' and 3' ends, which is carried out by the endonucleases XPF-ERCC1 and XPG, respectively. A 25-30 nucleotide fragment is excised by this process and DNA polymerase $\delta/\epsilon/\kappa$, along with PCNA, synthesises across the gap using the undamaged strand as a template. The excision of the fragment may be coupled to re-synthesis across the gap, beginning as soon as the 5' incision has been made. This prevents the exposure of large single-stranded regions during the repair process and, therefore, prevents further DNA damage signalling (Martelijn et al., 2014). DNA ligase I/III is then recruited to complete re-synthesis and ligation (Friedberg, 2001; Noussipiel, 2009).

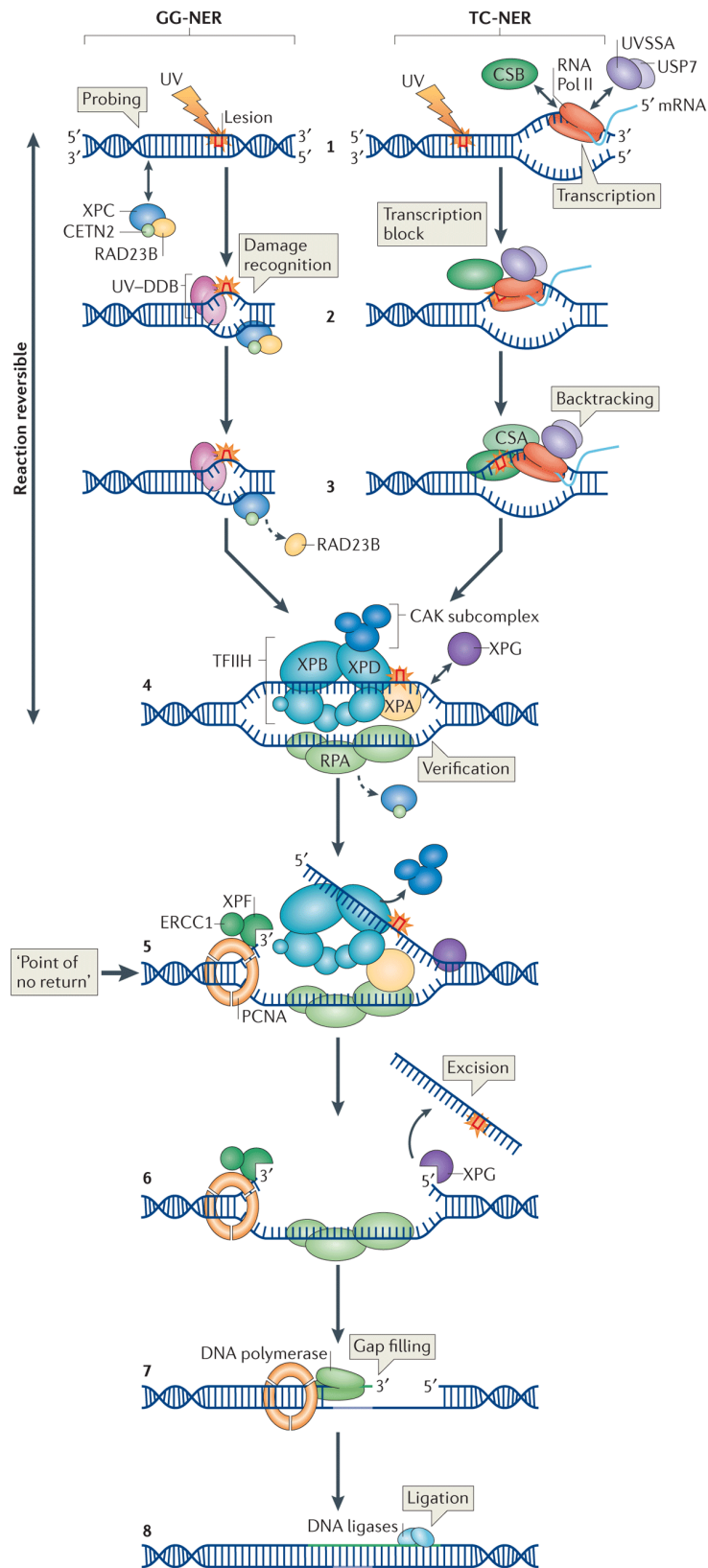


Figure 1-16: Mechanism of nucleotide excision repair. Taken from (Marteijn et al., 2014).

Bulky adducts can also be detected by the RNA polymerase whilst transcribing – this is known as transcription-coupled repair (TCR). When RNA polymerase stalls at a lesion, two factors are recruited to induce RNA polymerase backtracking which allows repair factors access to the damage site: these are CSA and CSB. The repair process post recognition follows the same pathway as classical NER, with the exception that the XPC and DDB proteins are no longer required (Hoeijmakers, 2001; Marteijn et al., 2014).

Defects in many of the NER genes leads to Xeroderma Pigmentosum (XP) syndromes. These are autosomal recessive diseases, of which there are eight complementation groups with varying symptoms. One of the most common symptoms is the high sensitivity to sunlight and subsequent high predisposition to skin cancers. The median age of onset for skin cancer in the XP population is just 8 years, at least 50 years lower than the age of onset for the normal population (Friedberg, 2001). This is due to the inability of these patients to repair UV-induced DNA damage, thus leading to acquired mutations and eventually tumourigenesis. Other internal cancers are also more common in XP individuals due to their inability to repair lesions produced by internalised carcinogens such as tobacco smoke and other pollutants (Noussipiel, 2009).

Cockayne Syndrome (CS) is caused by a mutation in CSA or CSB and is characterised by extreme photosensitivity, and neurological and growth problems. The average life expectancy for a patient with CS is just 12 years. This disease is caused by an inability to perform TCR (Marteijn et al., 2014). Therefore the importance of NER, both global and transcription-coupled, is evident from the severity of the diseases that occur due to failures in this pathway.

1.8.1.2.3 Mismatch repair

Where the lesion in question is an incorrect nucleotide inserted by error during polymerisation of the DNA, or an insertion/deletion loop (IDL) the mismatch repair system (MMR) is required. This pathway is shown in Figure 1-17. Here the MutS α complex (MSH2 and MSH6) is the primary recognition protein complex. For larger IDLs, the MutS β (MSH2 and MSH3) complex is required for recognition. MutS α recruits MutL α (composed of MLH1 and PMS2) and together they form a sliding clamp that uses ATP to move up or down-stream from the mismatch in search of a strand discrimination signal, thought to be in the form of a strand nick. At this site the Exo1 exonuclease is loaded onto the DNA and subsequently, degradation of the intervening DNA between the nick and the mismatch occurs. Exo1 is a 5'-3' exonuclease, however, it is also able to perform digestion of the DNA in a 3'-5' manner with the aid of PCNA and the endonuclease function of MutL α which creates a nick 5' to the mismatch site that Exo1 can digest from. This digestion may occur from multiple Exo1-loading events. Exo1 is blocked from digesting 5'-3' away from the mismatch in this scenario by the replication factor RFC. The resulting gap is filled and ligated with DNA polymerase δ and ligase I. The importance of the MMR pathway in genome protection is highlighted by its link with hereditary non-polyposis colon cancer. Individuals with mutations in MSH2 or MLH1 are predisposed to developing colon cancer (Jiricny, 2006; Li, 2008).

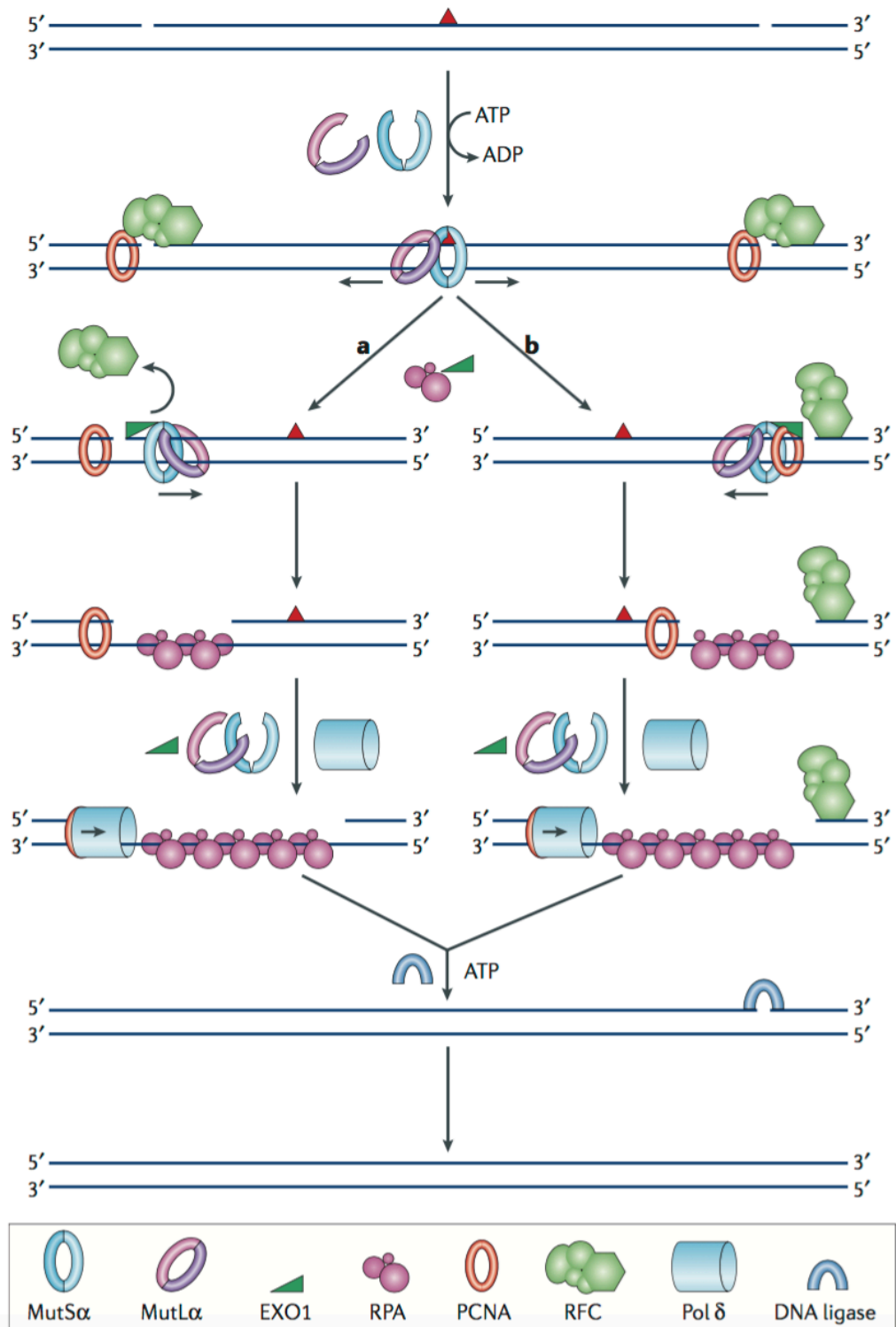


Figure 1-17: Model of the mismatch repair pathway. Taken from (Jiricny, 2006).

1.8.1.3 Lesion bypass and tolerance

In some scenarios, damage is not recognised by the appropriate repair systems and so upon DNA replication, bypass of this lesion must occur for the cell to avoid replication fork breakdown and successfully divide. There are two mechanisms for lesion bypass, both of which are summarised in Figure 1-18. The first mechanism involves the polymerisation of DNA past a lesion. This process is carried out by Y-family polymerases as the high fidelity polymerases used for general DNA replication are not capable of replicating past an adduct. Y-family polymerases such, as DNA Pol η , have significant structural differences which allows them to bypass the damaged bases albeit with higher error than the general DNA polymerases. These structural differences render the catalytic site wider and more able to incorporate damaged nucleotides and dimers such as CPDs. Often two bypass polymerases will cooperate: one performing the nucleotide insertion opposite the damaged base and the other performing the extension stage (Prakash et al., 2005). Rad6-Rad18 mediated mono-ubiquitination of the PCNA sliding clamp is thought to play a key role in the switch from general polymerases to bypass polymerases after encountering a replication-blocking lesion (Waters et al., 2009). Extension past the damaged nucleotide can result in mutations. For example, if an abasic site is present, TLS polymerases prefer to insert an adenine. If the correct sequence should have been C•G and the guanine was lost, the mutation induced would be A•T (Helleday et al., 2014).

Defects in lesion bypass can occur in individuals with mutated DNA polymerase η , which results in the XPV complementation group of xeroderma pigmentosum. These individuals exhibit hypersensitivity to UV light and a high predisposition to skin cancer due to their inability to bypass UV-induced lesions rather than a defect in NER (Friedberg, 2001).

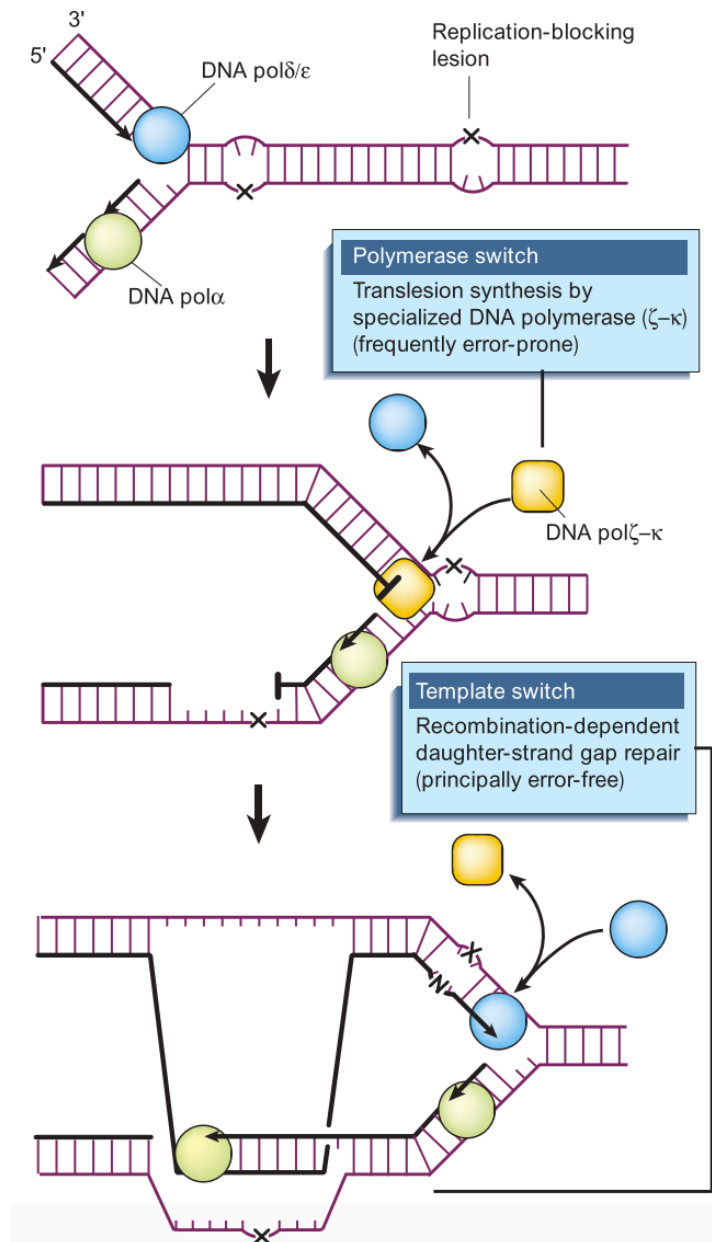


Figure 1-18: Lesion bypass can occur by polymerase switch or template switch mechanisms. Taken from (Hoeijmakers, 2001).

The second mechanism for lesion bypass is via the template switch. Here, the normal polymerase is able to replicate the DNA accurately by using a process called recombinatorial strand exchange whereby the undamaged newly synthesised strand of DNA is used as a template. Regression of the replication fork can also provide an undamaged template for the normal DNA polymerase to copy from (Hoeijmakers, 2001). It is thought that the choice between TLS and template switching is

influenced by the ubiquitination status of PCNA, with monoubiquitinated PCNA stimulating TLS through the interaction with ubiquitin binding domains on the Y-family polymerases, and polyubiquitinated PCNA stimulating template switching. The mechanism for the latter is not yet fully understood, however, binding of a translocase-like protein, ZRANB3, to PCNA's polyubiquitin chains is suggested to promote replication fork regression (Cipolla et al., 2016; Sale, 2012). However, in both TLS and template switching the damage is not removed.

1.8.2 ICL repair

ICLs can be formed endogenously from aldehydes and the ingestion of alcohol and lipids (Clouston et al., 2013) and so a repair system has evolved to protect cells from these lesions.

However the repair of interstrand crosslinks is not yet fully elucidated. This is due to the complexity of these lesions and the requirement for many repair pathways to work together in order to achieve their repair. For example, the NER process alone is able to repair intrastrand crosslinks as only one strand is affected, so the unaffected strand is available as a template for repair. However, ICLs involve both strands of the DNA, which makes forming the "denaturation bubble" impossible, and also means there is no intact template strand for repair. Components of the NER machinery are, however, still important for ICL repair as will be discussed.

1.8.2.1 Model for ICL repair in *E.coli*

ICL repair was first investigated in the prokaryotic *E.coli* system and this led to the basic repair model, known as the Cole model (Figure 1-19) (Cole, 1973). In this model incisions are made either side of the ICL by the Uvr endonucleases (components of the *E.coli* NER system) and DNA Pol I exonuclease activity. This is known as unhooking where the ICL and attached excised fragment are flipped out of

the DNA helix. Recombination events dependent upon RecA lead to the repair of the incised strand and further incisions on the opposite strand remove the ICL from the DNA. The resulting gap is filled and ligation reactions complete the repair process. This model is in agreement with the sensitivity of Uvr and RecA mutants to crosslinking agents (Cole et al., 1976). Where recombination is not possible it has been suggested that after the unhooking stage, bypass polymerases may replicate past the unhooked ICL, before classical NER processes remove the lesion, treating it as a bulky adduct (Berardini et al., 1997).

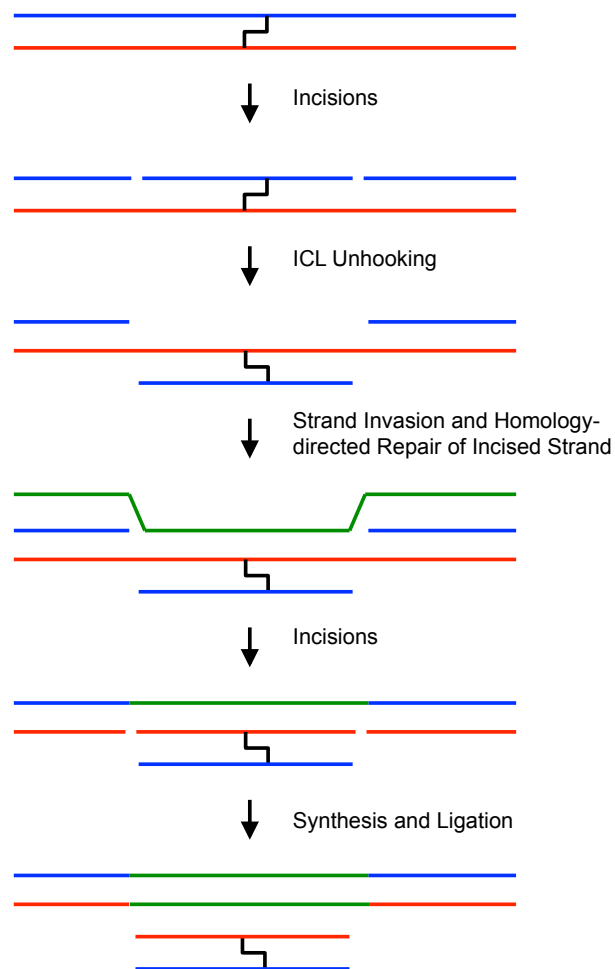


Figure 1-19: Cole Model for ICL repair in E.coli.

1.8.2.2 Model for ICL repair in mammalian cells

Mammalian ICL repair is considerably more complicated than repair in *E.coli* however the key stages remain constant, with the unhooking of the ICL being the critical event.

Detection of the ICL can occur either by damage-recognition proteins, by stalling of transcription, or by stalling of replication. Which recognition method is utilised will depend on the cell cycle stage and the cellular processes occurring at the time of detection.

For replication-independent repair (Figure 1-20), where recognition proteins from other repair pathways such as NER contribute to ICL detection it seems there is a certain degree of lesion specificity. This specificity may be related to the differences in helix distortion various crosslinking agents cause. For instance psoralen ICLs are readily bound by the XPC recognition protein whereas XPC negative cells are not sensitive to cisplatin (Muniandy et al., 2010). The protein HMGB1 has also been suggested to bind cisplatin-induced ICLs (Kasparkova et al., 2003), as has the Fanconi Anemia factor FANCM and components of the MMR system (Fink et al., 1998; Niedernhofer, 2007). Therefore, the initial replication-independent recognition of the ICL is currently not well understood, but may involve several recognition factors.

Post-detection, it is thought that the typical NER machinery is recruited for the unhooking of the ICL, with the XPF-ERCC1 complex being critical for this process. Cells deficient in XPF or ERCC1 are considerably more sensitive to crosslinking agents than other NER mutants (Andersson et al., 1996) and are deficient in ICL unhooking (De Silva et al., 2000). The role of other nucleases in the unhooking stage has also been discussed with a common model suggesting that a scaffold

protein, SLX4, orchestrates ICL unhooking by recruiting XPF-ERCC1 as well as the MUS81-EME1 nuclease (Muñoz et al., 2009). SLX4 is also thought to stimulate the activity of these nucleases (Muñoz et al., 2009), and cells deficient in either nuclease or the SLX4 scaffold express sensitivity to ICL-inducing agents (Abraham et al., 2003; Hanada et al., 2006; Sengerová et al., 2011). The exact mechanism of unhooking is yet to be confirmed, however, this stage of ICL repair will be discussed in more detail in the introduction to Chapter 5. After the crosslink is unhooked, bypass polymerases synthesise past the damage site.

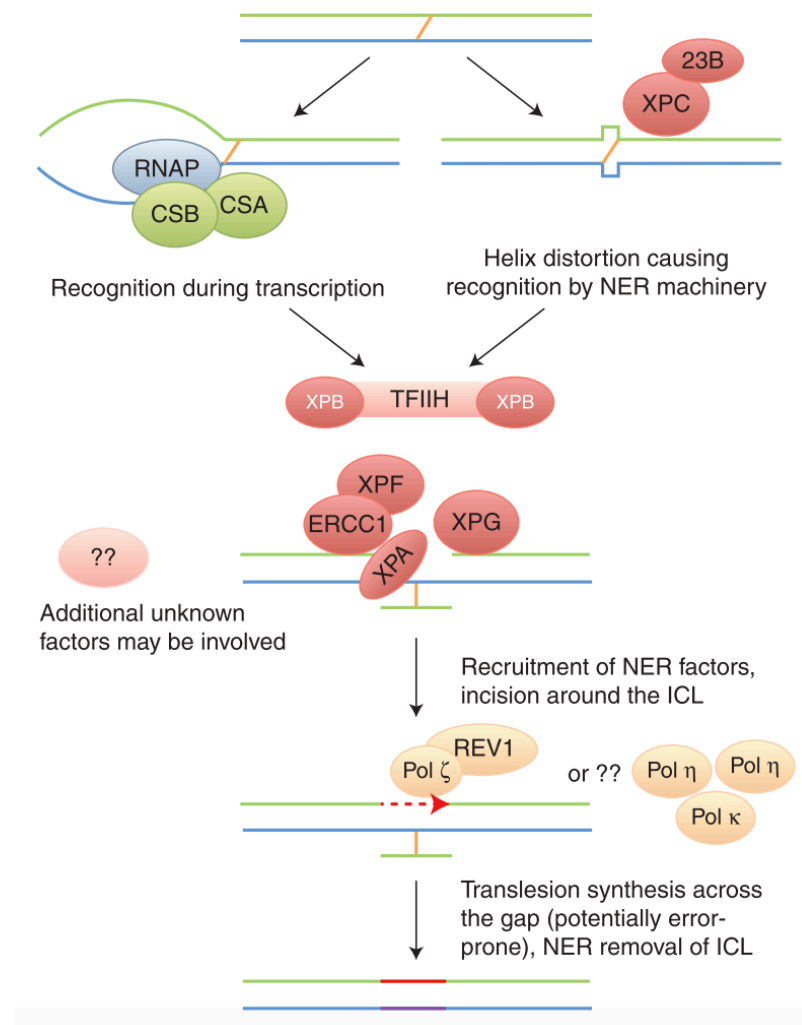


Figure 1-20: One model for replication-independent ICL repair in mammalian cells. Taken from (Clauson et al., 2013).

In replication-dependent repair (Figure 1-21), the replication fork stalls 20-40 nucleotides before the ICL, causing disassembly of the replicative helicase and allowing the fork to approach to within 1 nucleotide of the ICL. The Fanconi Anaemia (FA) pathway is activated through monoubiquitination of the FANCD2/I complex which is essential for replication-coupled ICL repair, most likely in order to recruit structure-specific nucleases to the ICL (Knipscheer et al., 2009). ICL unhooking then proceeds as described for replication-independent repair, and gap filling occurs through translesion synthesis.

However, ICL unhooking at a replication fork results in the formation of a DSB. Replication is therefore restarted through homologous recombination. This model is supported by evidence showing that recombination defective cells (cells negative for BRCA1 or RAD51 paralogs XRCC2 and XRCC3) are highly sensitive to crosslinking agents. However, it should be noted that BRCA1 is also thought to have a HR-independent additional role in the early stages of ICL repair, which will be discussed in Chapter 5 (Bunting et al., 2012; De Silva et al., 2000).

There is a second model for replication-dependent ICL repair, which involves the convergence of two replication forks on one ICL. As the replicative helicase cannot be re-loaded during S-phase, convergence of two replication forks on an ICL negates the need to restart replication after one fork has collapsed. However, this is likely to only occur during late S-phase due to the distance between replication forks (Zhang and Walter, 2014).

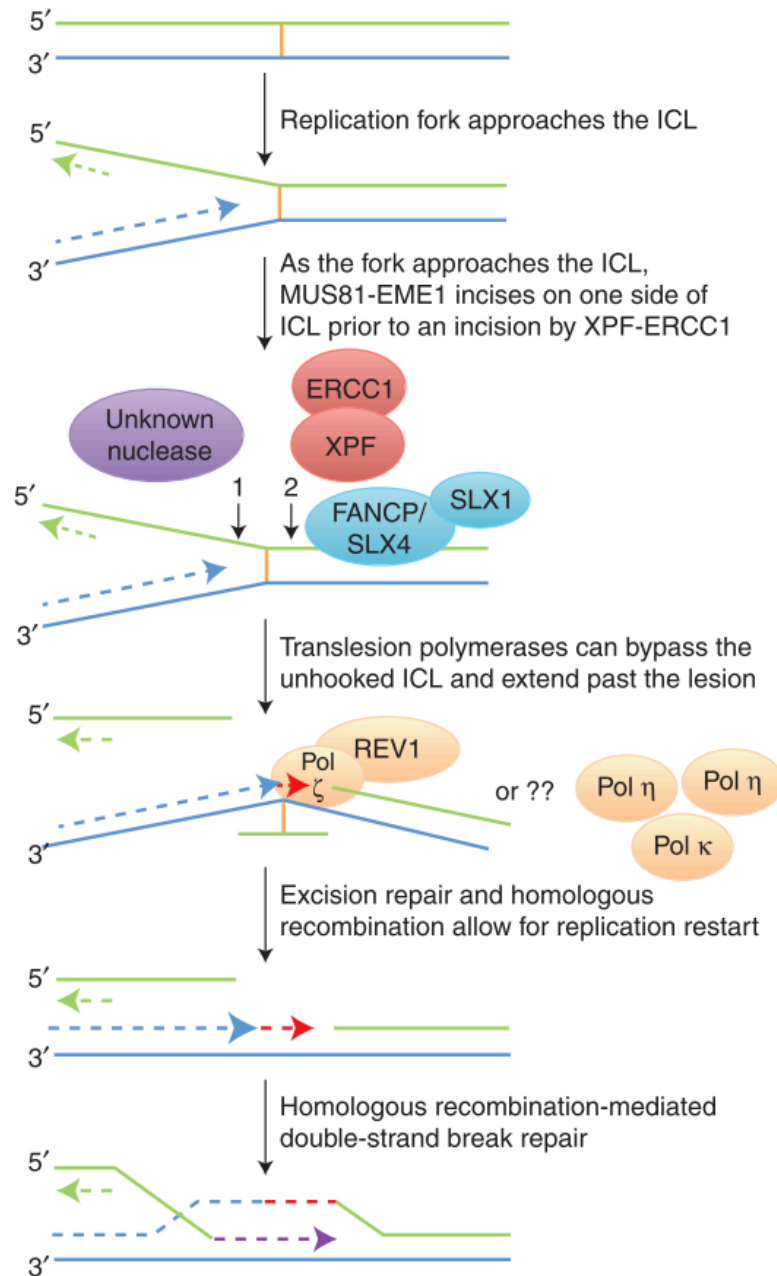


Figure 1-21: One model for replication-dependent ICL repair. Taken from (Clauson et al., 2013).

1.8.3 Fanconi's Anemia and the FA complementation groups

Briefly discussed already, the FA pathway assumes a significant role in the repair of ICLs. This pathway comprises the FANC proteins, which were discovered through genetic studies of individuals with a rare autosomal recessive disease, Fanconi's Anaemia. Discovered in 1927 by Guido Fanconi, a Swiss paediatrician, FA is characterised by bone marrow failure, congenital abnormalities and increased risk of cancer development (de Winter and Joenje, 2009). The occurrence rate is approximately 1 in 360,000 and the median survival only 20 years. 9% of FA patients develop leukemia, >90% of these are AML, and the median diagnosis age is just 14, however, FA patients are also susceptible to solid tumours (Crossan and Patel, 2012). Currently, the only treatment for FA is hematopoietic stem cell transplantation which treats the bone marrow failure, however, this does not alleviate the patient's susceptibility to solid tumours or growth defects (Risitano et al., 2016). FA is a disease of genomic instability, and as such, FA individuals are incredibly sensitive to crosslinking agents (Sasaki, 1975). This characteristic can be used to diagnose FA through chromosomal breakage analysis after treatment of patient blood cells with MMC or diepoxybutane (Oostra et al., 2012). However, this sensitivity also presents one of the hurdles when treating cancer in FA patients, as ICL-inducing agents cannot be used due to increased toxicity.

Complementation analysis and cell fusion studies were employed to discover the key genes involved in the FA phenotype and this resulted in the discovery of 19 FA-associated genes: FANCA, B, C, D1, D2, E, F, G, I, J, L, M, N, O, P, Q, R, S, T) (Dong et al., 2015; Moldovan and D'Andrea, 2009; Walden and Deans, 2014). Some of the FA genes are better known by other names, such as BRCA2 (FANCD1), RAD51C (FANCO), SLX4 (FANCP) and BRCA1 (FANCS) as they were discovered to be FA genes after their initial discovery as DNA repair proteins. Many

of the FA proteins are part of a larger complex, the FA core complex (FANCA, B, C, E, F, G, L, M), which is responsible for the monoubiquitination of the FANCD2/I complex.

The most commonly mutated FA gene is FANCA, contributing to 65% of FA cases. Mutations in FANCA, C and G together account for 85% of FA cases, with the most common form of mutation being an intragenic deletion. The remaining FA complementation groups are considerably rarer (Dong et al., 2015).

1.8.3.1 Roles of the FANC proteins in ICL repair

Upon detection of an ICL at a replication fork (which may occur via the FANCM DNA binding protein and its cofactors (Kim et al., 2008; Walden and Deans, 2014)), the ATR kinase is activated. ATR phosphorylates the FANCD2/I complex, and the core FA complex E3 ubiquitin ligase protein FANCL monoubiquitinates FANCD2/I. The importance of the core FA complex in the functioning of the FA pathway is highlighted by the fact that the majority of FA patients have mutations in core complex proteins, and mutation of these factors results in a loss of FANCD2/I ubiquitination and FA pathway activity (Crossan and Patel, 2012; Dong et al., 2015).

Ubiquitination of FANCD2 is considered essential for FA pathway activation, as it allows the FANCD2/I complex to bind chromatin at DNA damage foci which contain the damage marker γ H2AX and repair factors including BRCA1 and RAD51 (Moldovan and D'Andrea, 2009). Once bound at the DNA damage foci, FANCD2/I may take part in several stages of ICL repair. In terms of early repair events, FANCD2 is thought to be required for efficient recruitment of the unhooking nucleases via interaction with the SLX4 (FANCP) scaffolding protein (Klein Douwel et al., 2014), whereas in later stages of ICL repair, FANCD2 is thought to recruit BRCA2 (FANCD1) for HR (Wang et al., 2004). Other FANC proteins involved in ICL

repair through regulation of homologous recombination include BRCA1, Rad51C and PALB2 (a BRCA2 interacting protein required for HR) (Bunting et al., 2012; Moldovan and D'Andrea, 2009; Vaz et al., 2010). The roles of the FA proteins in ICL repair are illustrated in Figure 1-22. Therefore the importance of the Fanconi Anemia pathway in multiple stages of ICL repair is clear.

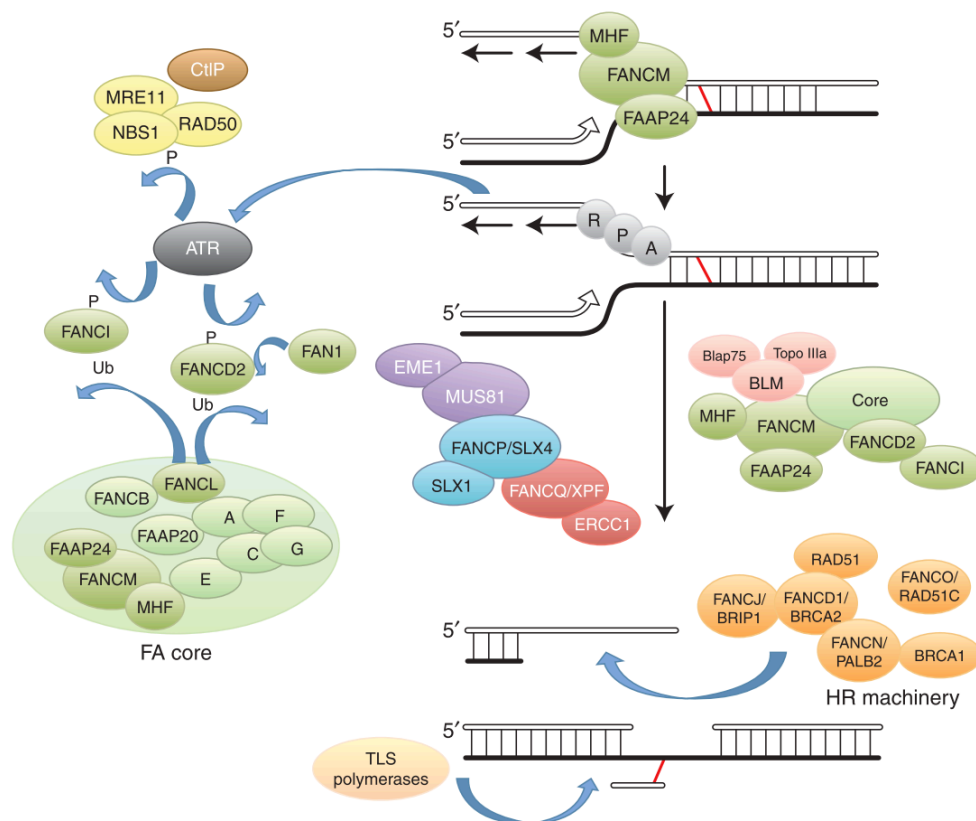


Figure 1-22: Role of the Fanconi Anaemia proteins in initiation of ICL repair. Taken from (Clauson et al., 2013).

1.9 The STAT3 signalling pathway

1.9.1 Introduction to the STAT transcription factors

There are seven signal transducer and activator of transcription (STAT) proteins within the STAT family of transcription factors: STAT1, 2, 3, 4, 5a, 5b, and 6. These proteins relay signals from extracellular ligands binding to cell surface receptors in the plasma membrane, to the nucleus where they initiate a cellular response to that signal through the regulation of gene expression. The STATs were first identified as mediators of IFN-triggered gene expression. The promoters of genes regulated by IFNs revealed a consensus motif (TT(N)₅AA) that was required for expression from those promoters. Proteins bound to this motif were biochemically isolated and purified, and the STAT1 and STAT2 genes were identified. STAT3 was later identified with a cDNA library screen using the SH2 domain of STAT1 aiming to identify further STAT family members (Clevenger, 2004; Zhong et al., 1994).

The general domain structure of STAT proteins is shown in Figure 1-23. The key domains are the DNA binding domain which allows these proteins to bind the DNA in order to regulate the transcription of genes, the transactivation domain (TAD) which contains tyrosine and serine phosphorylation residues that control the activation of these proteins, and the SH2 domain which allows binding to phosphorylated tyrosine kinase receptors and dimerisation of STAT monomers. The N-terminal region is essential for the interaction of both STAT3 and STAT5 with the CBP/p300 transcriptional activating proteins, and the coiled-coil and DNA binding domains contain interaction sites for other transcription factors such as c-Jun and the glucocorticoid receptor. These interactions allow for the formation of “enhanceosomes” which facilitate the recruitment of RNA polymerase to allow for transcription from that site (Bromberg, 2001; Clevenger, 2004; Hou et al., 2008; Lerner et al., 2003; Zhang et al., 1999).

Although the STATs have similar structural properties and are considered one family of proteins, they function in the regulation of diverse processes. The function of each STAT family member in normal cell processes has been investigated with knockout studies in mice. STAT1 knockout mice do not respond to interferon signalling and are highly susceptible to infections, whereas mice lacking STAT4 or STAT6 have impaired IL-12 and IL-14-mediated T-cell proliferation, respectively. STAT5A knockout mice have defective development of the mammary gland, and both STAT5A and STAT5B female knockout mice are infertile. Deletion of STAT2 and STAT3 in mice is embryonic lethal and so these family members have been studied with tissue-specific cre-lox-mediated deletion. Therefore, both STAT2 and STAT3 are required for normal embryo development, and in addition to this, STAT3 knockout keratinocytes display reduced migration, suggesting a role for STAT3 in wound healing (Akira, 1999; Bowman et al., 2000). Additionally, STAT proteins can have opposing effects. Through IFN γ signalling, STAT1 functions as a tumour suppressor, enhancing the expression of genes involved in apoptosis and cell cycle arrest, and suppressing the expression of pro-survival genes. On the other hand, STAT3 promotes the expression of pro-survival and cell cycle progression genes, and is therefore considered an oncogene (Regis et al., 2008).



Figure 1-23: STAT Family protein domains. Adapted from (Aggarwal et al., 2006). Activating phosphorylations occur on tyrosine 705 and serine 727 of the transactivation (TAD) domain.

1.9.2 STAT3 signalling

The third member of the STAT family, STAT3, was discovered in 1994 (Zhong et al., 1994) as a response factor activated by interleukin-6 (IL6) and epidermal growth factor (EGF).

The STAT3 pathway is activated by cytokines or growth factors binding their respective receptors, which subsequently dimerise and become phosphorylated. These phospho-residues on the intracellular domains of the transmembrane receptors are substrates for binding by STAT3 monomers via the SH2 domain. Once bound, the STAT3 monomers are phosphorylated on the Tyrosine-705 residue (by the tyrosine kinase activity of the receptor itself for growth factor receptors, or by an associated kinase such as the Janus Kinase 2 (JAK2) for cytokine receptors), causing dissociation from the receptor, and dimerisation with another phospho-STAT3 monomer. The p-STAT3^{Tyr705} dimer is translocated into the nucleus where it binds to consensus sequences within gene promoters, regulating transcription (Figure 1-24). Where tandem consensus sequences are present, multiple STAT3 dimers may bind, and form tetramers through interaction of the N-terminal domains (Zhang and Darnell, 2001).

A further phosphorylation event on residue Serine-727 does not impact DNA binding but allows a greater level of STAT3 activation (Wen and Darnell, 1997). There has also been some evidence that unphosphorylated STAT3 dimers are able to translocate into the nucleus, however, only phosphorylated dimers are retained there to activate transcription. Therefore, in this model, phosphorylation results in nuclear retention of STAT3 rather than translocation, and in the absence of phosphorylation, STAT3 is able to shuttle between the nucleus and cytoplasm (Liu et al., 2005; Mitchell and John, 2005; Pranada et al., 2004). However, activated STAT3 dimers have been reported to translocate into the nucleus at a faster rate

than non-activated STAT3, which may suggest an alternative mechanism for the accumulation of activated STAT3 in the nucleus (Herrmann et al., 2007).

The N-terminal and coiled coil domains of STAT3 are required for nuclear translocation of STAT3, which is thought to be mediated by the $\alpha 3/\beta 1$ -importin heterodimer (Cimica et al., 2011; Liu et al., 2005; Prana da et al., 2004). Evidence also exists for the interaction of STAT3 with the $\alpha 5$ importin (Ma and Cao, 2006), therefore, this mechanism is not yet fully elucidated. Nuclear export of STAT3 is thought to occur after dephosphorylation by nuclear phosphatases, which renders STAT3 a substrate for exportin-1 mediated transport (Herrmann et al., 2007).

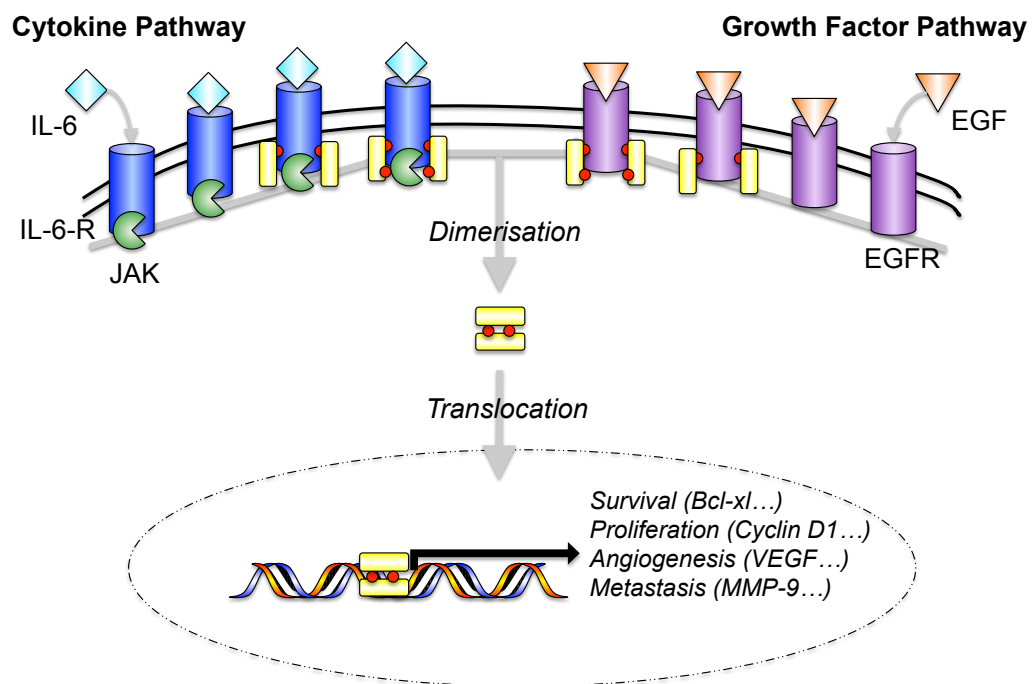


Figure 1-24: STAT3 Signalling Pathway. Adapted from (Johnston and Grandis, 2011).

As well as STAT3 homodimers, STAT3:STAT1 heterodimers have been observed (Zhong et al., 1994), and in the inflammatory response, where STAT3 and STAT1 have opposing effects, STAT3 is able to sequester STAT1 in heterodimers and reduce STAT1-mediated gene expression (Ho and Ivashkiv, 2006). Whether this occurs in tumourigenesis, where STAT3 and STAT1 also exhibit opposing functions, is not yet known.

1.9.2.1 STAT3 upstream activators

The two main events that feed into STAT3 activation are stimulation of either the IL-6-receptor/JAK2 cytokine signalling pathway or the EGF-receptor growth factor signalling pathway (Zhong et al., 1994). Src-family kinases have also been shown to stimulate STAT3 activation, both directly and as downstream mediators of RTK signalling (Silva, 2004), and G-protein coupled receptors are also able to activate STAT3 through their interaction with Src (Ram and Iyengar, 2001). As well as EGF and IL-6, many other growth factors and cytokines including PDGF, LIF, TGF- β , IL-10 and IL-11 have been demonstrated to activate STAT3 (Johnston and Grandis, 2011). As well as stimulatory molecules, cell-cell interactions through cadherins are able to activate the Rac-GTPase which induces IL-6 expression and subsequently increases STAT3 activation (Arulanandam et al., 2009). In many of these activating components, overexpression or activating genetic mutations has been shown to occur in cancers and often correlates with a poor prognosis (Allgayer et al., 2002; Alvarez et al., 2006; Baxter et al., 2005; Engers et al., 2007; Irby et al., 1999; Salgado et al., 2003).

1.9.2.2 Negative regulation of STAT3

Negative regulation of the STAT3 pathway can be carried out by phosphatase action on STAT3 or any of the phosphorylated components of the pathway; for instance, the SHP1 and SHP2 phosphatases remove the activating phosphorylation

from STAT3, terminating signalling. Alternatively, inhibitors such as PIAS3 (protein inhibitor of activated STAT3) can bind to STAT3 directly and block DNA binding. SOCS3 can also negatively regulate STAT3 signalling by acting as a negative feedback loop. SOCS are activated by the JAK/STAT pathway itself and function by binding either upstream JAK molecules, competing for STAT3 binding sites and thus excluding STAT3, or by binding other STAT3 signalling components and targeting them for proteasomal degradation by ubiquitination (Wormald and Hilton, 2004).

As well as protein-mediated negative regulation of STAT3 signalling, miRNAs are able to control STAT3 activation by targeting mRNA expression. The let-7 miRNA is able to induce SOCS3 expression, thus inhibiting STAT3 activation indirectly. Also, lower levels of some STAT3-regulating miRNAs, such as miRNA-20a, are correlated with poorer recurrence-free survival in patients (Fan et al., 2013). These tumour suppressor-like miRNAs have been shown to be down-regulated in tumour cell lines and patient tumour tissue compared with normal tissue (Fan et al., 2013; Patel et al., 2014).

1.9.2.3 STAT3 downstream effectors

STAT3 is an oncogene, which when constitutively activated can drive cells into oncogenesis. The genes that STAT3 modulates the expression of, which includes factors involved in proliferation, anti-apoptosis and survival, angiogenesis, and metastasis, mediate this outcome. Cyclin D1 and c-Myc, key regulators of the cell cycle, as well as anti-apoptosis proteins Bcl-xl, survivin and Mcl-1 are all regulated by STAT3 and these allow cancer cells to survive and proliferate (Aoki et al., 2003; Bromberg et al., 1999; Epling-Burnette et al., 2001; Gritsko et al., 2006; Kiuchi et al., 1999; Masuda et al., 2002; Zushi et al., 1998). Also regulated by STAT3 are VEG-F and MMP-9, which ensure a good blood supply to the tumour (angiogenesis) as well

as the capacity for tumour cells to migrate and form metastases (Dechow et al., 2004; Niu et al., 2002). STAT3 also regulates the expression of other cancer-related transcription factors such as c-Fos and HIF-1 α which potentiates STAT3's tumourigenic effect (Niu et al., 2008; Xu et al., 2005; Yang et al., 2003)

1.9.3 STAT3 and cancer

Several lines of evidence suggest a key role for STAT3 in tumourigenesis. Firstly, cells transformed with the oncogene, Src, depend upon activated STAT3 and expression of a dominant-negative STAT3 will inhibit this transformation (Bromberg et al., 1998). In addition, overexpressing constitutively activated STAT3 causes transformation in fibroblasts and tumourigenesis when these cells are injected into mice (Bromberg et al., 1999). Finally, high levels of constitutively activated STAT3 are seen in many cancer types, including prostate, lung, breast, head and neck, ovarian, gastric, kidney, liver, skin, colorectal, pancreatic and haematological cancers, and in several of these, STAT3 levels are correlated with a poor prognosis (Aggarwal et al., 2006; Johnston and Grandis, 2011). For example, a meta analysis of 1314 gastric cancer patients concluded that positive pSTAT3 expression was significantly associated with poorer overall survival (hazard ratio = 1.87) (Yu et al., 2015), and NSCLC patients with high STAT3 expression exhibited a 5-year overall survival rate of 42.3% compared with 58.8% in patients with low STAT3 expression (Yin et al., 2012).

Table 1-4 summarises several immunohistochemistry experiments where the percentage of pSTAT3^{Tyr705} in human tissue samples has been analysed. As high as 38-50% of non-small cell lung cancers (Cortas et al., 2007; Gao et al., 2007) and 86% of recurrent prostate cancers (Abdulghani et al., 2008) express constitutively active STAT3, and as normal adult tissues do not harbour constitutively active STAT3 (activation is a transient event, tightly regulated by negative feedback

mechanisms (Yoshimura et al., 2007; Zhang and Lai, 2014)), this highlights the potential for the use of STAT3 inhibitors in the clinic.

Table 1-4: Activated STAT3 in different tumour types, assessed by immunohistochemistry of human tumour samples.

Cancer Type	% with STAT3 activated	Reference
Non-small cell lung (NSCLC)	38-50%	(Cortas et al., 2007; Gao et al., 2007)
Prostate:	Up to 100%	(Barton et al., 2004)
-----	-----	
Lymph node metastasis	77%	(Abdulghani et al., 2008)
-----	-----	
Bone metastasis	67%	
-----	-----	
Recurrent human prostate cancers	86%	
Breast	>50%	(Kunigal et al., 2009)
Cervical	25.2%	(Chen et al., 2007)
Endometrial	20.8%	(Chen et al., 2007)
AML	25-44%	(Benekli, 2002; Redell et al., 2011; Schuringa et al., 2000)
Liver	54.3%	(W. Y. Wu et al., 2011)
Colon	55.1%	(Lin et al., 2011)
Gastric	49.5%	(Yakata et al., 2007)
Squamous cell (SCC)	56.7%	(Suiqing et al., 2005)
Basal cell (BCC)	20%	(Suiqing et al., 2005)
Pancreatic	30%	(Toyonaga et al., 2003)
Renal cell	51%	(Guo et al., 2009)

Mutations in the STAT3 gene that lead to its constitutive activation have been reported. In hepatocellular adenomas, several somatic mutations in the STAT3 SH2 domain were identified, and these mutations were shown to cause constitutive STAT3 activation and enhanced STAT3 phosphorylation, nuclear translocation and DNA binding (Pilati et al., 2011). 40% of patients with T-cells leukaemia were shown to have mutations in the SH2 domain of STAT3. Again, these mutations enhanced STAT3 dimerisation by increasing the hydrophobicity of the amino acids lining the SH2 pocket, and therefore, enhanced STAT3 activation and nuclear translocation (Koskela et al., 2012). Mutations in the TAD and DNA binding domains have also been reported in patients with autoimmune diseases (Flanagan et al., 2014).

As well as activating mutations in the STAT3 gene, constitutive STAT3 activation can arise through mutations in the signalling machinery upstream of STAT3. For example, high IL-6 levels contribute significantly to the constitutive activation of STAT3 activation in prostate cancers (Giri et al., 2001). Also, stimulating mutations occur in positive regulators of STAT3 signalling such as the EGF-receptor (EGFR) (Gao et al., 2007), and the V617F activating mutation in the JAK2 kinase occurs in 50-97% of patients with myeloproliferative neoplasms (Baxter et al., 2005; Thomas et al., 2015). Conversely, inhibitory mutations may occur in negative regulators of STAT3 such as SOCS proteins. A deletion in the suppressor of cytokine signalling 1 (SOCS1) gene has been described in B-cell lymphomas, and inactivation of the SOCS1 promoter by methylation has also been described in over 50% of melanomas and hepatocellular carcinomas (Inagaki-Ohara et al., 2013; Yoshikawa et al., 2001). Methylation of the SOCS3 promoter also occurs in up to 90% of head and neck cancers (Inagaki-Ohara et al., 2013). Therefore, constitutive STAT3 signalling can occur via the deregulation of several stages in the STAT3 pathway.

1.10 Targeting STAT3 in cancer

As STAT3 is frequently activated in a broad spectrum of cancers and is involved in tumourigenesis, it is a viable target for therapeutic intervention. *In vivo* studies demonstrated that complete STAT3 knockout is embryonic lethal in mice (Takeda et al., 1997), however, selective knockout is tolerated by normal cells but not transformed cells (Schlessinger and Levy, 2005), therefore, STAT3 has potential as a target for novel anti-cancer therapeutics.

STAT3 signalling can be interfered with at various stages of the pathway. The possible stages of intervention are illustrated in Figure 1-25. Direct inhibition of STAT3 can block the dimerisation of STAT3 monomers, or the binding of activated STAT3 to DNA. Inhibition of the STAT3 pathway could also be achieved by inhibition of the nuclear translocation process. Alternatively, the upstream signalling molecules that lead to STAT3 activation can be inhibited, including the growth factor and cytokine pathways, and stimulation of the factors which negatively regulate STAT3 would also achieve inhibition of this pathway. Each of these modes of intervention will be discussed in further detail.

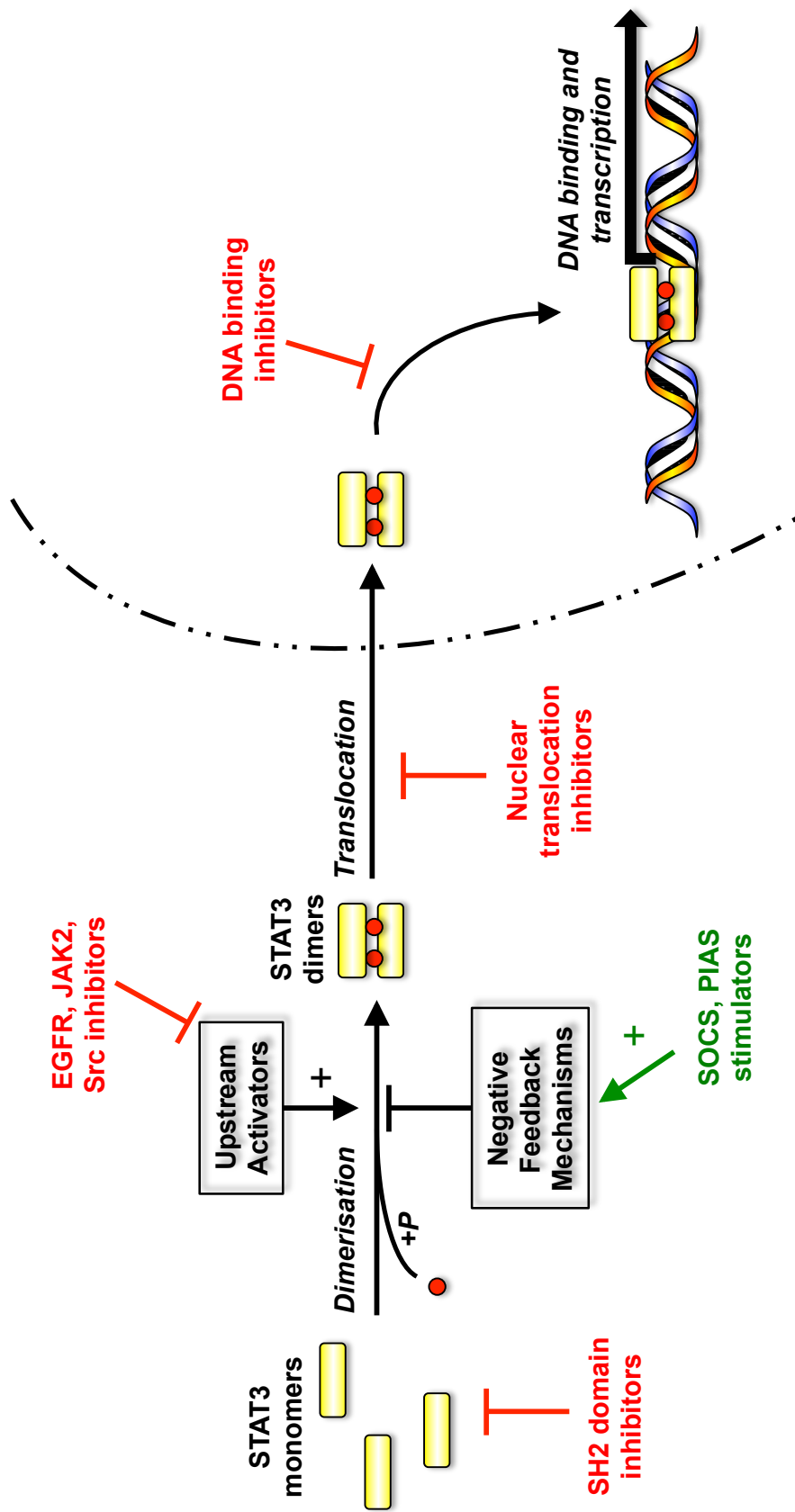


Figure 1-25: Different methods for intervention of the STAT3 pathway.

1.10.1 Direct STAT3 inhibitors

Direct targeting of STAT3 is desirable as many upstream oncogenic signalling pathways lead into STAT3 activation, so blocking one of these pathways may lead to feedback-related resistance, and sustained STAT3 signalling (Zhao et al., 2016). Therefore, by targeting the transcription factor directly, the central cancer-signalling node can be blocked. However, one of the main problems with targeting a transcription factor is how specificity is attained. Transcription factors have classically been considered “undruggable” targets, as they lack individual enzymatic activities to target and many share similar DNA binding mechanisms with large surface areas used for these interactions (Frank, 2012; Yan and Higgins, 2013). Nonetheless, progress has been made in the development of small molecule inhibitors targeting STAT3 directly.

1.10.1.1 SH2 domain inhibitors

STAT3 dimerisation is the first stage of STAT3 signalling where multiple signalling pathways converge, therefore, it represents an attractive target for interference, and as such, most of the STAT3 inhibitors currently reported target the SH2 domain. Inhibition of the SH2 domain can prevent these pockets from binding phosphotyrosine residues on activating receptors and other STAT3 monomers and, therefore, prevent both phosphorylation and dimerisation of STAT3.

There are many natural compounds derived from various plant materials that have been shown to inhibit STAT3 dimerisation. Curcumin, from the Indian spice saffron, or *Curcuma longa*, is one of the most widely known natural inhibitors of STAT3. In its keto form it can bind to SH2 domains (Lin et al., 2010a). Curcumin has, however, been demonstrated to affect many other signalling pathways: it was first discovered as an anti-bacterial compound and since then was shown to regulate an array of

molecules such as hormones, blood sugars, cytokines, cholesterol, growth factors, antioxidants, and cyclooxygenases (Gupta et al., 2013a).

Dried roots of *Salvia miltiorrhiza* contain the active component Cryptotanshinone which has also been shown to have anti-cancer properties through the inhibition of the STAT3 SH2 domain. Cryptotanshinone also has anti-bacterial and anti-inflammatory action (Shin et al., 2009). Another natural STAT3 inhibitor, Scoparone, comes from the Chinese herb *Artemisia capillaris*. Scoparone was predicted by computational studies to bind the STAT3 SH2 domain. Alongside its anti-cancer activity, Scoparone also harbours anti-coagulant, anti-inflammatory, and vasodilator activities as well as being used as a common treatment for jaundice in Asia (Kim et al., 2013).

One of the key limitations when using natural compounds for therapeutic purposes has been highlighted here: lack of specificity. Additionally, natural compounds like curcumin have low bioavailability (Anand et al., 2007). Therefore, the development of synthetic derivatives of these natural compounds has aimed to achieve specificity and improved bioavailability.

High-throughput screening techniques led to the discovery of small molecule inhibitors of the STAT3 SH2 domain, and one of the first of these was stattic (Schust et al., 2006). Many other synthetic STAT3 SH2 inhibitors have since been discovered, including STA-21 (Song et al., 2005), S3I-201 and its derivatives (Siddiquee et al., 2007), 5,15-DPP (Uehara et al., 2009), the CPD compounds (Xu et al., 2009), STX-0119 (Matsuno et al., 2010), 17o (Page et al., 2011), XZH-5 (Liu et al., 2011) and many other synthetic curcumin analogues (Bill et al., 2012; Hutzen et al., 2009; Kumar et al., 2014; Lin et al., 2010a; Selvendiran et al., 2011). Many of these STAT3 inhibitors harbour anti-proliferative activity, however, most lack

potency or have not been demonstrated to be specific for STAT3 over the other STAT transcription factors.

Given the lack of small binding pockets on transcription factors such as STAT3, peptides have also been designed to block the dimerisation of STAT3 monomers, with the rationale that biological macromolecules will be more effective competitors for STAT3 protein-protein interactions (Borghouts et al., 2012; Ren et al., 2003; Wei Zhao et al., 2010). However, peptide-based therapeutics suffer from instability due to cleavage of the peptide bond, and lack of selectivity in terms of tumour delivery versus uptake by normal cells, therefore, both targeting and the use of peptidomimetics should be investigated for further development of peptide-based inhibitors.

1.10.1.2 DNA binding domain inhibitors

Small molecules targeting the DNA binding domain of STAT3 are less common than those targeting the SH2 domain, however, these compounds have exhibited greater selectivity for STAT3. DNA-binding domain inhibitors block STAT3 dimers from binding to consensus DNA sequences and therefore, block transcription. Examples of DNA binding domain inhibitors include the curcumin analogues, HO-3867 and H-4073 (Selvendiran et al., 2011, 2010), and inS3-54 and its derivatives which were initially identified by virtual docking of 200,000 compounds to the STAT3 DNA binding domain (Huang et al., 2016, 2014). A natural compound isolated from a particular type of fungus, galiellalactone, was also demonstrated to inhibit STAT3 DNA binding without affecting STAT3 phosphorylation by covalently binding to cysteine residues in the DNA binding domain (Don-Doncow et al., 2014). A peptide inhibitor of the STAT3 DNA binding domain has also been described (Nagel-Wolfrum et al., 2004), however, the shortcomings of peptide-based molecules remain to be addressed.

1.10.1.2.1 Decoy oligonucleotide inhibitors

The DNA-binding domain of STAT3 has also been investigated as a target for inhibition by decoy oligonucleotides that mimic the STAT3 binding site (Leong et al., 2003; Zhang et al., 2007), however, as with peptide-based inhibitors, cellular stability and delivery of oligonucleotides to the tumour is challenging. A recent phase 0 trial of a STAT3 decoy in head and neck cancer has begun to make advances in this area by using a cyclic oligonucleotide to increase stability (Sen et al., 2012).

1.10.1.3 N-terminal domain inhibitors

Peptide inhibitors targeting the N-terminal domain of STAT3 have also been described (Timofeeva et al., 2007). The rationale behind targeting this domain is to disrupt the interactions between STAT3 dimers and other transcriptional proteins, leading to an impaired enhanceosome formation. However, no small molecule inhibitors of this domain have yet been discovered.

1.10.2 Indirect STAT3 inhibitors

Many inhibitors that target elements upstream of STAT3 activation in the STAT3 pathway have already been approved for use by the FDA and EMA. These indirect inhibitors will be discussed.

1.10.2.1 EGFR inhibitors

EGFR itself is activated or over-expressed in many cancers, and its signalling leads to STAT3 activation (see Figure 1-26a), and so in the 1980s inhibitors targeting this receptor were developed. EGFR can be blocked by monoclonal antibodies targeting the extracellular domain or by small molecule kinase inhibitors targeting the intracellular domain.

1.10.2.1.1 Tyrosine kinase inhibitors

The first class of molecules that target the EGFR pathway are small molecules targeting the EGFR kinase domain. These include erlotinib and gefitinib, which compete with ATP for the EGFR kinase domain. This inhibits EGFR autophosphorylation-induced activation and therefore blocks signalling downstream of EGFR (see Figure 1-26b). However, acquired resistance can develop in response to tyrosine kinase inhibitors (TKIs) through mutations in the EGFR kinase domain. The T790M mutation accounts for approximately half of all cases of resistance to EGFR TKIs. This mutation enhances the affinity of the receptor for ATP, reducing the efficacy of inhibitors such as erlotinib and gefitinib (Yun et al., 2008). The second generation EGFR inhibitor, afatinib, was designed to overcome resistance by irreversibly inhibiting the EGFR kinase domain. However, T790M-mediated resistance to afatinib also occurs (Wu et al., 2016). Development of improved TKIs for patients with the T790M mutation is on-going. The third generation EGFR TKIs include osimertinib, which was approved in late 2015 by the FDA and in early 2016 by the EMA for use in metastatic NSCLC patients with the T790M mutation (Wang et al., 2016). Olmutinib has also been recently approved for use in NSCLC in South Korea based on positive clinical trial results (J. S. Lee et al., 2015). Mutations incurring resistance to these third generation TKIs have, however, already been reported (Wang et al., 2016).

1.10.2.1.2 Monoclonal antibodies

Monoclonal antibodies (mAbs) directed against EGFR are designed to bind the extracellular domain of the receptor. This competes with the EGF ligand and therefore blocks EGF-induced activation of the EGFR pathway. This subsequently blocks downstream STAT3 activation (see Figure 1-26c). EGFR mAbs are also able to elicit cytotoxicity through antibody-dependent cellular cytotoxicity (ADCC).

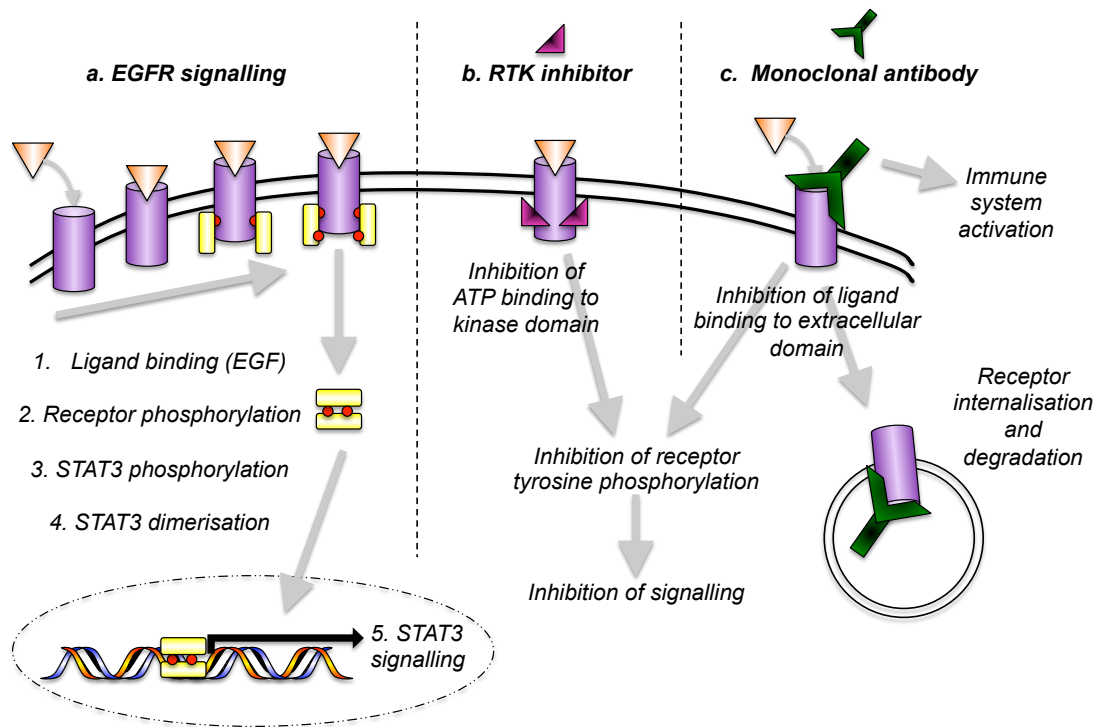


Figure 1-26: Action of EGFR inhibitors. A) EGFR signalling to STAT3, b) tyrosine kinase inhibitors and c) monoclonal antibodies

This is where the Fc domain of the antibody (the domain not bound to the target antigen, EGFR) is bound by Fc-receptors on immune cells and triggers an immune response against the cancer cell (Adams and Weiner, 2005). Additionally, binding of monoclonal antibodies to EGFR is able to induce internalisation and subsequent degradation of the receptor, diminishing the signal to STAT3 (Sunada et al., 1986). The most frequently used monoclonal EGFR antibody is cetuximab (Ciardiello and Tortora, 2008).

1.10.2.2 JAK2 inhibitors

The cytokine signalling pathway can also be targeted. The inhibitor of the JAK2 kinase, ruxolitinib, was approved in 2011 for the treatment of myeloproliferative cancer. This inhibitor targets the kinase domain of both wild-type JAK2 and the V617F mutant, competing with ATP (Mascarenhas and Hoffman, 2012; Seavey and

Dobrzanski, 2012). The natural compound bergamottin was also recently found to inhibit JAK1/2 as well as inducing levels of the STAT3-deactivating phosphatase SHP-1 (Kim et al., 2014).

As with STAT3 inhibitors, many novel JAK2 inhibitors are also being developed. One such inhibitor is AZ1480 which underwent a phase I trial in solid tumours. This trial revealed that AZD1480 induced neuropsychiatric dose-limiting side effects and therefore, the development of this drug was discontinued. The authors hypothesised that these effects were due to lack of specificity of the inhibitor, highlighting the need for specificity in targeting the STAT3 pathway (Plimack et al., 2013).

1.10.2.3 Src inhibitors

The Src kinase is also reported to activate STAT3 and so theoretically, targeting Src would also inhibit STAT3 (Silva, 2004). The Src inhibitor, Dasatinib, was approved in 2011 for patients with elevated Src kinase levels. However, STAT3 inhibition by Dasatinib is not maintained, and with prolonged dasatinib exposure, STAT3 phosphorylation is enhanced. It is thought that other STAT3 activating pathways may compensate for the inhibition Src-mediated STAT3 activation (Sen et al., 2009), For instance, dual inhibition of JAK and Src is able to block STAT reactivation (Byers et al., 2009). Therefore, as many pathways converge on STAT3, it may not be sufficient to focus on one STAT3-activating pathway. It is for this reason that much research has been directed towards the direct inhibition of STAT3.

Other Src inhibitors with FDA approval for the treatment of malignancies include bosotunib, ponatinib and vandetanib, which all target the Src kinase domain (Roskoski, 2015). However, none of these inhibitors are selective for Src, as they also target many other kinases. Development of novel, more selective compounds is underway to address this, with studies suggesting that a more selective Src inhibitor is more efficient at inhibiting cancer cell growth (Brandvold and Steffey, 2012).

1.10.2.4 Nuclear translocation inhibitors.

Another possible target is the nuclear machinery that translocates STAT3 dimers into the nucleus. Translocation is thought to be mediated by the importin class of proteins, including importin α 3, α 5 and β 1 (Cimica et al., 2011; Liu et al., 2005; Ma and Cao, 2006; Pranada et al., 2004), however, small molecule inhibitors of the importins have not yet been investigated for their effect on STAT3 activation. Importin inhibitors discovered to date include importazole, which has been demonstrated to exhibit toxicity against multiple myeloma cells by blocking the import of NF- κ B, an oncogenic transcription factor (Yan et al., 2015). However, the effect of this inhibitor on STAT3 translocation has not yet been investigated. On the other hand, decoy oligonucleotides that interfere with STAT3-importin interactions have been shown to have anti-cancer activity (Souissi et al., 2011).

As well as import, export of STAT3 from the nucleus could be targeted. Blocking the export of STAT3 with ratjadona A, an inhibitor of exportin-1, was shown to interfere with the STAT3 reactivation cycle. STAT3 phosphorylation occurs in the cytoplasm, and STAT3 dephosphorylation occurs in the nucleus, therefore, nuclear shuttling of STAT3 is required to maintain a persistent STAT3 signal (Herrmann et al., 2007). Also, the exportin-1 inhibitor, selinexor, was able to inhibit STAT3 transcriptional activity and is currently undergoing clinical trials in various cancers (Cheng et al., 2014). Consequently, interfering with either STAT3 nuclear import or export is a valid target for future research.

1.10.2.5 Stimulators of STAT3 negative regulation

Negative regulation of the STAT3 signalling pathway occurs through dephosphorylation by SHP1/SHP2, or by activation of PIAS and SOCS proteins. Up-regulating the activity of these negative regulators could inhibit STAT3 signalling. To date, research into this area has focussed on natural compounds. Morin, a natural

compound isolated from figs, was shown to inhibit STAT3 activation by inducing the expression of the SHP1 phosphatase and PIAS3 (Gupta et al., 2013b). Another natural compound, brassinin, was demonstrated to block STAT3 signalling through the up-regulation of PIAS3 expression (J. H. Lee et al., 2015). The flavanoids naringenin and flavone were shown to inhibit STAT3 activation by up-regulating the expression of SOCS3 (Wiejak et al., 2013). However, no stimulators of these STAT3-inhibitory proteins are currently in clinical development, therefore, this particular area for intervention requires more research.

1.10.3 STAT3 Inhibitors as chemosensitisers

Resistance to chemotherapeutics is an important limitation that must be overcome. To achieve this, new compounds can be designed entirely, or drug combinations can be employed where one agent modifies the cancer cell biochemistry in order to re-sensitise the tumour to the chemotherapy agent.

STAT3 inhibitors have been shown to act as both radiosensitisers, and chemosensitisers to a range of chemotherapy agents. The natural compound, curcumin, has been the focus of much research into STAT3-mediated chemosensitisation. Curcumin and its synthetic derivatives are able to sensitise cancer cell lines to a range of chemotherapy agents. These include doxorubicin, etoposide, camptothecin, 5-fluorouracil, vincristine, melphalan, gemcitabine, paclitaxel, celecoxib, oxaliplatin, thalidomide, bortezomib and cisplatin (Dhandapani et al., 2007; Goel and Aggarwal, 2010; Kumar et al., 2014; Lev-Ari et al., 2007; Notarbartolo et al., 2005; Patel et al., 2008; Ye et al., 2012). Additionally, curcumin has been demonstrated to act as a chemosensitiser in murine models (Li et al., 2007; Sreekanth et al., 2011).

Stattic, the first synthetic SH2-domain targeting STAT3 inhibitor, has also been demonstrated to sensitise nasopharyngeal and ovarian cancer cells to cisplatin and

radiotherapy (Pan et al., 2013; Teng et al., 2013), and novel synthetic STAT3 inhibitors such as 5,15-DPP and XZH-5 are also able to sensitise cells to cisplatin and doxorubicin/gemcitabine, respectively (Huang et al., 2012; Liu et al., 2012). As cisplatin features recurrently in these studies, the ability of STAT3 pathway inhibitors to chemosensitise to cisplatin will be discussed in greater detail in the introduction to Chapter 4.

Many of the agents that STAT3 inhibitors chemosensitise cells to are cytotoxic due to the DNA damage they cause, as is the same for radiation therapy. Therefore, what remains to be answered is whether STAT3 inhibitors chemosensitise through an ability to directly modify the DNA damage response or DNA repair pathways of cancer cells.

1.11 Thesis aims and objectives

Given the importance of the STAT3 pathway in tumourigenesis, and the interest in targeting this pathway therapeutically, this thesis details two projects concerning STAT3. First, the anti-cancer potential of a novel STAT3 inhibitor, VS-43, both as a single agent and in combination with cisplatin is investigated. Second, the role of STAT3 in DNA-ICL repair is investigated, in order to better understand the molecular mechanisms contributing to more effective drug combinations.

The summarised aims for each chapter of this thesis are, therefore, as follows:

- **Chapter 3:** Initial characterisation of a novel STAT3 inhibitor, VS-43.
- **Chapter 4:** Determination of the effect of STAT3 inhibitors in combination with cisplatin, and comparison of VS-43 to known STAT3 inhibitors.
- **Chapter 5:** Investigation into the molecular mechanism of sensitisation to cisplatin by STAT3 inhibitors, focusing on the repair of DNA-ICLs.
- **Chapter 6:** Extension of STAT3 combination and mechanistic studies to melphalan.

Chapter 2 Methods and Materials

Methods used in this thesis were assessed for hazards and COSHH risk assessments were carried out in order to perform the following protocols safely.

2.1 Reagents

Cisplatin was kindly provided as a 3.3mM aqueous solution by the UCLH Macmillan Centre. Melphalan, Stattic, Curcumin, and doxorubicin hydrochloride were purchased from Sigma-Aldrich and solubilised to 10mM in DMSO. VS-43 was synthesised and supplied by Professor Moses Lee, Georgia State University, USA. VS-43 was solubilised in DMSO to a 10mM stock solution.

2.2 Maintenance of Cell Lines

DU145 human prostate cancer and A549 human non-small cell lung cancer cells were obtained from the American Type Culture Collection (ATCC) and cultured in DMEM (*Sigma Aldrich*) supplemented with 10% FCS (*Gibco*) and 2mM L-glutamine (*Sigma Aldrich*). Both cell lines were grown at 37°C with 5% CO₂. The RPMI8226 human multiple myeloma cell line was cultured in RPMI 1640 medium (*Sigma Aldrich*) supplemented with 10% FCS and 2mM L-glutamine.

Adherent cell lines (DU145 and A549) were passaged every 2-3 days by trypsinisation. Media was removed, cells were rinsed in 2-3mL Trypsin-EDTA (*Sigma Aldrich*), and then incubated for 5 minutes at 37°C with a further 5mL Trypsin-EDTA. Detached cells were collected and the trypsin was neutralised by adding an equal volume of culture media. Cells were pelleted by centrifugation at 1200rpm for 5 minutes and subsequently resuspended in culture media for counting and seeding. Both cell lines were passaged 2-3 times per week in order to maintain them in exponential growth.

RPMI8226 suspension cells were passaged every 2-3 days by centrifuging at 1200rpm for 5 minutes and resuspending in the appropriate culture media. These cells were maintained within the optimal density range of 5×10^5 and 2×10^6 cells/mL.

2.3 Frozen cell line stocks

To freeze down cell line stocks for future use, one exponentially growing T75 flask of cells was detached by trypsinisation as for cell line maintenance (for suspension cell lines no trypsinisation was required). Cells were spun down at 1200rpm for 5 minutes and subsequently resuspended in 6mL freezing media (FCS with 10% DMSO). This cell suspension was transferred into 6x 1mL cryovials and the vials were placed in a cryo freezing container (*NalgeneTM*) at -80°C in order to achieve a cooling rate of $-1^{\circ}\text{C}/\text{min}$. After 24 hours, cryovials containing cells were transferred to a liquid nitrogen tank for long-term storage.

To set up fresh cultures from frozen down stocks, cryovials were placed in a 37°C water bath to thaw cells quickly. 9mL of culture medium was added to the cell suspension, and centrifugation at 1200rpm for 5 minutes was performed to pellet the cells. The pellet was resuspended in culture medium and seeded into a T75 flask.

2.4 Counting of cells

In order to seed cells at specific densities, an improved Neubauer haemocytometer (*Appleton Woods*) was used to count cells in suspension. $10\mu\text{L}$ of cell suspension was pipetted into the gap between the haemocytometer chamber and cover glass. Under a microscope, the number of cells in 5 of the larger squares on the haemocytometer grid were counted. Cells touching the upper and left limits of each square were counted whereas cells touching the lower and right limits of each

square were not included in the count. The total number of cells counted was divided by 5 to give the number of cells $\times 10^4/\text{mL}$.

2.5 Immunoblotting

2.5.1 Seeding, Treatment and Whole Cell Protein Extraction

Cells were seeded in 6-well plates (*Corning*) and grown until they reached 70% confluency. Cells were then drug treated and incubated for the duration of the treatment time at 37°C with 5% CO₂.

To harvest cells, plates were placed on ice and rinsed twice in cold PBS before adding 1mL cold PBS per well and collecting cells using scrapers. Samples were spun down at 1200rpm, 4°C for 5 minutes. The supernatant was aspirated and the cell pellet was resuspended in CelLytic M Lysis Buffer (*Sigma Aldrich*) containing 1x cComplete™ protease and PhosSTOP™ phosphatase inhibitors (*Roche*). Lysis was performed on ice for at least 30 minutes, with regular vortexing. Samples were then spun down for 15 minutes at 4°C and the supernatant containing the whole-cell lysates collected.

2.5.2 Protein Quantification

The BioRad DC™ protein assay kit was used determine the concentration of protein in lysates. The standard curve method was used, where Bovine Serum Albumin (BSA) standards are included in the assay to create a curve. From this curve, a $y = mx + c$ equation relating absorbance to protein concentration can be obtained. BSA was dissolved in water to reach 1000µg/mL, 800µg/mL, 600µg/mL, 400µg/mL, 200µg/mL, and 100µg/mL for the standard curve. These standards were stored at -20°C.

Whole cell lysates were diluted 1:5 in distilled water and 10 μ L of each sample, including BSA standard samples, was added per well on a 96-well plate (*Corning*). Two replicates of each sample were performed. 25 μ L of a mixture of Reagent A and Reagent S (20 μ L of A : 1mL of S) was then added per well, followed by 200 μ L of Reagent B. Upon adding Reagent B, the contents of each well was mixed by pipetting. The colour was then allowed to develop by placing the plate on a rotating platform for 15 minutes. Absorbance at 630nm was read using the Variskan Flash Multimode Reader (*Thermo-Scientific*). Average absorbance versus BSA concentration was plotted for the standard curve and using the best-fit equation given by Microsoft Excel, the corresponding protein concentration for unknown samples was calculated from their absorbance.

2.5.3 Protein Sample Preparation

4x SDS-PAGE sample loading buffer (NuPAGE®, with 500mM DTT) was added to 30 μ g of each sample lysate to obtain a final 1x concentration. Samples were then denatured by incubating at 95°C for 5 minutes. Samples were allowed to cool and spun down briefly before loading into an SDS-PAGE pre-cast gel.

2.5.4 Immunoblotting Procedure

Proteins were separated on pre-cast 7% Tris-Acetate or 4-12% Bis-Tris NuPAGE® SDS-PAGE gels with either 1x NuPAGE® Tris-Acetate, MOPS or MES running buffers depending on the gel and the separation required (*Thermo Fisher Scientific*). Voltage applied was 150V and 200V for Tris-Acetate and Bis-Tris gels respectively. Proteins were then transferred to Immobilon-P PVDF membrane (*Merck Millipore*) in an XCell transfer module using 1x transfer buffer (10x: 30.3g Tris-base, 144.1g glycine in 1L distilled water, pH 8.3) with 20% methanol added immediately before use. PVDF membrane was activated in methanol for 2 minutes and soaked in

transfer buffer before use. The voltage applied for the transfer was 35V for 2.5 hours.

Membranes were then blocked for 1 hour in 5% w/v BSA in TBS 0.1% Tween-20 (TBS-T) (*Sigma Aldrich*). Membranes were incubated with primary antibodies diluted in 5% w/v milk or BSA overnight at 4°C on a rotating platform. A list of primary antibodies used can be seen in Table 2-1. After washing three times with TBS-T for 5 minutes per wash, secondary horseradish peroxidase-coupled anti-rabbit or anti-mouse antibodies (*Cell Signaling*) were incubated on membranes for 1 hour with rocking at room temperature. After three further TBS-T and one TBS wash, membranes were soaked in enhanced chemiluminescence (ECL, *Amersham, GE Healthcare*) reagent and exposed in a dark room to film.

Where there was a need to probe for proteins of a similar molecular weight, duplicate gels were run where possible. In some cases, stripping of the membrane using Restore PLUS Western Blot Stripping Buffer (*Thermo Fisher Scientific*) and re-blocking was required before re-probing the membrane for a second protein target.

Table 2-1: Details for primary antibodies used in immunoblotting: supplier, species, dilution and diluting buffer.

Primary Antibody Target	Supplier	Species	Dilution	Diluting Buffer
pSTAT3-Tyr ⁷⁰⁵	Cell Signaling	Rabbit	1:1000	5% BSA in TBS-T
STAT3	Cell Signaling	Rabbit	1:1000	5% BSA in TBS-T
pSTAT1-Tyr ⁷⁰¹	Cell Signaling	Rabbit	1:1000	5% BSA in TBS-T
pSTAT5-Tyr ⁶⁹⁴	Cell Signaling	Rabbit	1:1000	5% BSA in TBS-T
β -Actin	Cell Signaling	Rabbit	1:2000	5% BSA in TBS-T
Cleaved PARP	Cell Signaling	Rabbit	1:1000	5% BSA in TBS-T
Cleaved Caspase-3	Cell Signaling	Rabbit	1:1000	5% Milk in TBS-T
γ -H2AX	Cell Signaling	Rabbit	1:500	5% BSA in TBS-T
XPF	Cell Signaling	Rabbit	1:1000	5% BSA in TBS-T
ERCC1	Cell Signaling	Rabbit	1:1000	5% BSA in TBS-T
MUS81	Santa Cruz Biotechnology	Mouse	1:500	5% milk in TBS-T
EME1	Santa Cruz Biotechnology	Mouse	1:500	5% milk in TBS-T
SLX4	Abcam	Mouse	1:500	5% BSA in TBS-T
FANCD2	Abcam	Rabbit	1:1000	5% BSA in TBS-T
BRCA1	Cell Signaling	Rabbit	1:1000	5% BSA in TBS-T

2.6 Cytotoxicity Assays

2.6.1 Sulphorhodamine B Cell Growth Inhibition Assays

2.6.1.1 Seeding and Treatment of Cells

DU145 and A549 cells were seeded in 96-well flat-bottomed plates (*Corning*) at a density of 2.5×10^4 cells/mL and 2×10^4 cells/mL respectively and left to adhere overnight before drug treatment.

Cells were then treated with 100 μ L/well of drug diluted in fully complemented media. For combination treatments cells were treated with drug A, drug B or a successive combination of the two drugs. For instance, in the "Fixed Ratio" regime, cells were treated with VS-43 for 18 hours, media removed, and then immediately treated with cisplatin for 1 hour. The treatment ratio chosen for each combination was based on estimated GI₅₀ values for each drug in the DU145 cell line. The same ratios were applied for A549 cells to allow for a direct comparison between cell lines. Non-fixed ratio combination treatments were also carried out in a successive manner.

After all drug treatments, the media was replaced and plates were incubated at 37°C with 5% CO₂ for 96 hours.

2.6.1.2 SRB Staining

SRB (*Sigma Aldrich*) was used to stain the cells remaining after drug incubation. Cells were first fixed with 100 μ L 10% TCA per well for 20 minutes at 4°C, and then washed with distilled water four times. 100 μ L SRB stain (0.4% w/v SRB in 1% acetic acid) was added to each well and the plates were incubated for 20 minutes at room temperature, followed by four washes with 1% acetic acid. Excess acetic acid was then patted out onto tissue paper and the plates were left to dry overnight at room temperature. SRB was re-suspended in 100 μ L of 10mM Tris-base (*Sigma Aldrich*)

pH 10.5 per well the following morning and the absorbance at 540nm was read using the Variskan Flash Multimode Reader (*Thermo-Scientific*).

2.6.2 MTT Assay

For suspension cell lines the MTT assay is the preferable method of GI₅₀ determination.

2.6.2.1 Seeding of cells and drug treatment

RPMI8226 cells were counted and resuspended to a concentration of 1×10^5 cells/mL in culture media. The appropriate volume of drug was then added directly to the cell suspension and incubated for the required time at 37°C with 5% CO₂. After this time the cells were centrifuged at 1200rpm for 5 minutes and the media was aspirated. Cells were resuspended in drug-free media and plated in 96-well round-bottom plates (*Corning*) with 200µL per well. Plates were incubated for 96 hours post drug treatment.

2.6.2.2 Staining of viable cells with MTT

At the end of the 96 hour incubation period 20µL of 5mg/mL MTT (*Sigma Aldrich*) was added per well and plates were incubated at 37°C with 5% CO₂ for a further 4 hours. Plates were then centrifuged at 1200rpm for 5 minutes and the media was aspirated from each well without disturbing the cell pellets. To resuspend the MTT 200µL DMSO was added per well and mixed by pipetting. The absorbance at 540nm was read using the Variskan Flash Multimode Reader (*Thermo-Scientific*).

2.6.3 Quantification of Growth Inhibition

Absorbances were normalised to the absorbance value of untreated wells and expressed as a percentage of the control absorbance. At least three repeats of each experiment were performed and the results were presented as the mean ± SEM.

Dose-response graphs were plotted using GraphPad Prism 6. GraphPad was also utilised to calculate GI₅₀ values using non-linear regression analysis.

2.6.4 Quantification of Drug Interactions: Chou-Talalay Combination Index Analysis

To determine whether the drug combinations tested were synergistic (total effect is greater than the sum of the effect of the two drugs individually), the Chou-Talalay Combination Index (CI) method was utilised. The two types of drug combination ratio described by Chou were tested for the combination of VS-43 and cisplatin (fixed and non-fixed ratio) (Chou, 2006). For combination of other STAT3 inhibitors with cisplatin, and for combinations involving melphalan, only the fixed ratio combination method was used.

Using the percentages for growth inhibition obtained from the SRB assay, the fraction affected was calculated using the equation:

$$Fraction\ Affected = \frac{100 - Drug\ Treated\ Percentage}{100}$$

Fraction Affected values were inputted into the Calcosyn software and the manual drug wizard was used to generate CI values.

Table 2-2 shows the descriptions and symbols used to interpret CI values. A CI value of less than 0.9 indicates synergism. CI values in the region of 0.9-1.1 indicate an almost additive interaction. This is as described by Chou and Talalay in the Calcosyn manual.

Table 2-2: Symbols and descriptions for interpretation of CI values. (Chou, 2006)

Range of CI	Symbol	Description
<0.1	+++++	Very strong synergism
0.1-0.3	++++	Strong synergism
0.3-0.7	+++	Synergism
0.7-0.85	++	Moderate synergism
0.85-0.90	+	Slight synergism
0.90-1.10	±	Nearly additive
1.10-1.20	-	Slight antagonism
1.20-1.45	--	Moderate antagonism
1.45-3.3	---	Antagonism
3.3-10	----	Strong antagonism
>10	-----	Very strong antagonism

2.7 STAT Family Specificity ELISA

2.7.1 Treatment of Cells and Preparation of Samples

DU145 cells were seeded in 6 well plates (*Corning*) and allowed to reach 70% confluency before treating with VS-43. Treatments of 0, 0.8, 1.2 and 2 μ M in culture media were carried out for 18 hours. For the 1 hour VS-43 treatment, 5 and 10 μ M VS-43 was used. Whole cell extracts were harvested as for immunoblotting (section 2.5.1) and protein quantification carried out as described in section 2.5.2.

2.7.2 ELISA Assay Procedure

The Active Motif TransAM[®] STAT Family ELISA was used according to the manufacturers protocol (TransAM[®] STAT3 and STAT Family Kits, Available from: <http://www.activemotif.com/catalog/232/transam-stat3-stat-family-kits> [accessed

May 2016]). Components of the kit were stored at 4°C, -20°C or -80°C according to the manufacturers guide.

Provided in the kit is a 96-well plate coated with oligos encoding the STAT consensus binding site. 30µL of complete binding buffer was added per well, followed by 20µL of 1µg/µL sample diluted in complete lysis buffer. Each sample was repeated in triplicate for each of the four STAT proteins to be observed; therefore, twelve wells of each sample were required. For positive control wells, the Nb2 (prolactin stimulated) nuclear extract was used at 5 µg/well. The plate was covered with plastic film and incubated for 1 hour at room temperature with gentle rocking.

STAT1, STAT3, STAT5a and STAT5b primary antibodies were diluted 1:1000 in antibody binding buffer and 100µL of antibody added per well. The plate was covered again and incubated at room temperature for 1 hour without agitation. The plate was then washed three times with 200µL of wash buffer.

Secondary HRP-conjugated antibody was diluted 1:1000 in antibody binding buffer and 100µL added per well. The plate was then covered and incubated at room temperature for 1 hour without agitation. During this incubation period the developing solution was placed at room temperature. The plate was then washed four times with 200µL of wash buffer.

To develop the ELISA, 100µL of developing solution was added to each well and incubated away from direct light for 5 minutes to allow for colour development. To prevent over-development of the ELISA, 100µL of stop solution was added per well immediately after the 5 minutes development time. Absorbance was then read at 450nm using the Variskan Flash Multimode Reader (*Thermo-Scientific*) immediately after the addition of stop solution.

2.7.3 Quantification of STAT Activation and DNA binding

Activation and DNA binding of STAT proteins after treatment with VS-43 was quantified as percentage activation compared to control (0 μ M) wells. The average absorbance of the technical repeats was calculated and expressed as a percentage of the average absorbance of the control wells for each STAT protein. Two biological repeats were performed and the average and SEM calculated for the 18 hour VS-43 treatments. For the 1 hour VS-43 treatments, only one biological repeat was performed due to the limited size of the TransAM[®] ELISA kit.

2.8 Electrophoretic Mobility Shift Assay (EMSA)

The following protocol was performed by Dr K. Kiakos.

Nuclear extracts from DU145 cells were prepared using the Active Motif Nuclear Extract kit following the manufacturer's protocol, in the presence of 1x cComplete protease and 1x phosphatase inhibitors (Roche). The concentration of protein was determined as with immunoblotting (section 2.5.2). 20 μ g of nuclear extract was incubated with increasing concentrations of VS-43 or Stattic for 1 hour. Subsequently extracts were incubated for 1 hour with ³²P-labeled double-stranded oligonucleotide containing the high-affinity sis-inducible element (hSIE) probe SIE (5'-AGCTTCATTTCCCGTAAATCCCTA-3'; *Eurofins MWG Operon*) derived from the *c-fos* gene. Binding reactions contained 0.9 μ g poly(dI-dC). Competition assays were performed by adding 100x excess cold SIE oligonucleotide (lane C) and non-specific competitor (lane M; FIRE; 5'-AGCGCCTCCCCGGCCGGGG-3'). The DNA-protein complexes were subjected to electrophoresis on a 5% non-denaturing polyacrylamide gel (30% acrylamide/Bis solution, *Bio-Rad*) in 0.5% TBE buffer containing 2.5% glycerol (pH 7.8) at 4°C for 2 hours. Once dried, the radioactive signal of the gel was visualised by exposure to Fuji medical X-ray film.

2.9 Single Cell Gel Electrophoresis (Comet) Assay

2.9.1 Treatment of Cells and Preparation of Samples

Cells were seeded in 6 well plates (*Corning*) and allowed to reach 70% confluency before treatment. Four treatment conditions were required for this assay: untreated-unirradiated, untreated-irradiated, crosslinker treated-irradiated, and combination treated-irradiated. One well of a 6-well plate was used for each treatment and time-point. Drugs were diluted in culture media for drug treatments and cells were washed with fresh media after treatment. To observe the formation and repair of cisplatin-induced ICLs, cells were harvested at four time-points: 0, 9, 24, and 48 hours, where 0 hours is immediately after 1 hour cisplatin exposure. For melphalan-induced ICLs, cells were harvested at 0, 16, 24 and 48 hours.

To harvest cells for the comet assay, wells were washed briefly in trypsin-EDTA and incubated with 1mL trypsin-EDTA for 5 minutes. An equal volume of culture media was added and cells were collected and spun down at 1200rpm for 5 minutes. Cells were resuspended in 2ml freezing media (FCS with 10% DMSO), counted and aliquotted into two cryo-vials. Samples were immediately placed on ice and frozen at -80°C until all time-points had been harvested.

2.9.2 Comet Assay Procedure

The modified single cell gel electrophoresis (comet) assay was performed as previously described (Spanswick et al., 2010).

Cells were diluted to 2.5×10^4 cells/mL in DMEM and irradiated on ice with 15Gy using the A.G.O. HS 321 kV X-ray system (untreated-unirradiated control cells were diluted but not irradiated). Irradiation with a set dose of X-rays delivers a fixed number of strand breaks to the cellular DNA. Samples were then diluted 1:3 in 1%

low gelling temperature molten agarose and applied to slides pre-coated with 1% type 1-A agarose.

Embedded cells were lysed for 1 hour in the dark on ice in lysis buffer (100mM disodium EDTA, 2.5M NaCl, 10mM Tris-HCl, 1% triton X-100, pH 10.5) and then slides were washed four times with distilled water for 15 minutes per wash. Subsequently, slides were transferred to large electrophoresis tanks and incubated in the dark in ice-cold alkali buffer (50mM NaOH, 1mM disodium EDTA, pH 12.5) for 45 minutes. Electrophoresis was carried out for 25 minutes at 18V in the dark. Slides were then removed from the tanks and placed onto racks where they were washed once with cold neutralisation buffer (0.5M Tris-HCl, pH 7.5) for 10 minutes and once with sterile PBS for 10 minutes before removing excess liquid and leaving to dry at room temperature overnight.

Slides were re-hydrated for 30 minutes in distilled water and the DNA stained with 2.5µg/ml propidium iodide (*Sigma Aldrich*) for 30 minutes in the dark. Slides were then washed twice with distilled water – for 10 and then 30 minutes, and finally dried in an oven at 40°C for 1 hour before reading.

2.9.3 Analysis of Slides

Slides were analysed using the Komet 6.0 analysis software (Andor Technology). Images were captured using a Nikon inverted microscope with a high-pressure mercury light source, 510-560 nm excitation filter, 590 nm barrier filter and an on-line CCD camera. 25 images at 20x were taken per slide with 2 duplicate slides per experimental condition and time point. The tail moment is defined as the “product of the amount of DNA in the tail, and the mean distance of migration in the tail” (Olive et al., 1990). The extent of crosslinking is expressed as a percentage decrease in tail moment.

The following formula was used to calculate the tail moment:

$$\% \text{ Decrease in tail moment} = \left[1 - \frac{(TM_{di} - TM_{cu})}{(TM_{ci} - TM_{cu})} \right] \times 100$$

Where TM_{di} = tail moment of drug treated irradiated sample

TM_{cu} = tail moment of untreated unirradiated control

TM_{ci} = tail moment of untreated irradiated control.

These experiments were performed in parallel when a direct comparison between the crosslink unhooking in two treatment regimes was being made (for example cisplatin alone and VS-43 plus cisplatin treated cells were treated and harvested together, and run in the same electrophoresis tank with the same untreated controls). It should be noted that cells treated only with STAT3 inhibitors were also analysed for any strand breaks caused by these inhibitors, as the outcome of this would determine which tail moment calculation to use.

Three repeats for each experiment were performed, with the mean and SEM of these data sets plotted using GraphPad Prism 6.

2.10 Immunofluorescence

2.10.1 Seeding and Treatment of Cells

13mm round coverslips (*VWR International*) were placed into 24-well culture plates (*Corning*) and cells were seeded on top of these coverslips at a density of 2.5×10^4 or 2×10^4 cells per well for DU145 or A549 cells, respectively. Cells were drug treated 24 hours after seeding once they had reached 70% confluency.

For experiments observing γ -H2AX foci, four time-points were considered: 0, 9, 24 and 48 hours after cisplatin exposure, in accordance with the time-points observed by the comet assay. Therefore, after the allotted drug exposure time, the media was replaced with fresh media and cells incubated for the required amount of time before proceeding with the fixing and staining stages.

2.10.2 Fixing and Staining of Cells

Media was aspirated and cells were washed with 1mL of sterile PBS per well. Cells were subsequently fixed in 500 μ L 4% PFA (*Alfa Aesar*) in water for 10 minutes at room temperature. Two further washes with PBS were carried out before cells were permeabilised by adding 500 μ L 0.5% PBS-Triton-X100 per well for 10 minutes at room temperature. Blocking was carried out with 500 μ L 5% PBS-BSA per well for 1 hour at room temperature. For timecourse experiments each sample was fixed and stored at 4°C in PBS until all samples had been fixed. Permeabilisation onwards was carried out for all samples together.

Coverslips were then removed from the 24-well plate using tweezers and placed cell-side up on parafilm coated microscope slides. Primary antibodies were prepared in 1% PBS-BSA at a dilution of 1:100, and 70 μ L applied to each coverslip for incubation at room temperature for 1 hour. For pSTAT3 detection, the same primary antibody as was used for immunoblotting was used here. For γ H2AX foci detection, the Anti-phospho-Histone H2A.X (Ser139) Antibody, clone JBW301 from Merck Millipore was used. After primary antibody incubation, three 10 minute 0.1% PBS-Triton-X100 washes (70 μ L per wash, removed each time carefully with an aspirator) were then performed before applying 70 μ L AlexaFluor 488 anti-Rabbit/anti-Mouse secondary antibody (*Invitrogen*) at 1:100 and incubating at room temperature for 4 hours. Three 10 minute washes in 0.1% PBS-Triton-X100 were carried out again before applying 70 μ L 1 μ g/mL propidium iodide (PI) and incubating

for 3 minutes at room temperature. Finally, three 10 minute washes in PBS were carried out before mounting coverslips on microscopy slides using mounting media (*Dako*). Coverslips were further secured in place with clear nail varnish. Slides were then stored at 4°C until the time of reading.

2.10.3 Confocal Microscopy

The Leica DM 2500 microscope (fitted with a Leica TCS SPE confocal head) was used to obtain z-stack images at 40x magnification. Leica LASX software was used for image collection.

To quantify γ -H2AX foci from images obtained using the protocol above, the program CellProfiler (Carpenter et al., 2006) was utilised. First, ImageJ (Schneider et al., 2012) was used to split each captured image into the two channels (PI and 488nm). These images were loaded into CellProfiler and each cell nucleus was identified from the PI channel. The number of foci within each nucleus was computationally counted using the 488nm channel. The number of foci was taken as an average from the first 30 cells measured with a detection threshold of 0.3.

Post-capture, confocal images were arranged using Microsoft Powerpoint.

2.11 Quantitative Reverse-Transcriptase PCR (qRT-PCR):

2.11.1 Treatment of Cells

One 10cm dish (*Corning*) of cells was prepared for each treatment and cells were allowed to reach 70% confluency before drug treatments. Each plate was then rinsed in 3mL trypsin-EDTA, then 4mL trypsin-EDTA was added and plates were incubated at 37°C with 5% CO₂ for 5 minutes to allow cells to detach. An equal volume of culture media was added to neutralise the trypsin, and cells were subsequently spun down at 1200rpm for 5 minutes. Pellets were re-suspended in

10mL sterile PBS and pelleted by centrifugation again. Excess PBS was aspirated off and pellets resuspended in 2mL sterile PBS. This was aliquotted into sterile 1.5mL eppendorfs and centrifuged at 8000rpm for 5 minutes at 4°C. The supernatant was aspirated off and the remaining pellet processed for RNA extraction.

2.11.2 RNA Extraction and cDNA Generation

RNA was extracted from cell pellets using the RNeasy Plus Mini-kit (*Qiagen*) according to the manufacturers protocol and stored at -80°C. One modification to the manufacturers protocol was made: each cell pellet was resuspended in lysis buffer using a 21G needle and 1mL syringe 6 times followed by vortexing for 30 seconds per pellet to ensure full lysis.

1µg RNA was used for both cDNA generation protocols.

For the DNA Damage Signalling Array the RT² First Strand Kit (*SABiosciences-Qiagen*) was used whereas for the TaqMan gene expression analysis system the High Capacity cDNA Reverse Transcription Kit (*Life Technologies*) was used. These are the recommended cDNA generation kits for each of the qRT-PCR procedures. Both kits were used as per the instructions in the manufacturers protocols. cDNA was stored at -20°C.

RNA and cDNA concentrations were determined using the NanoDrop 2000 spectrophotometer, with an A_{260}/A_{280} reading of ~2.0 for RNA and ~1.8 for cDNA considered as clean.

2.11.3 qRT-PCR Procedure and Analysis

2.11.3.1 DNA Damage Signaling Array Procedure

To analyse the expression of genes involved in DNA repair pathways the Human DNA Damage Signalling Pathway PCR Array (*SABiosciences-Qiagen*) was used. The array contains primer sets for 84 target genes and 5 house-keeping genes. In addition the plates include genomic DNA, reverse-transcription and positive PCR controls. A full gene list of this array can be found in Appendix A.

As stated in the manufacturers protocol, to perform the array 1248µL RNase-free water, 1350µL RT² SYBR-Green qPCR Mastermix (*SABiosciences-Qiagen*) and 102µL cDNA was added to a sterile reagent reservoir and mixed thoroughly by pipetting. 24µL of this solution was then added per well of the array plate, and the plate sealed with the plastic caps provided. The plate was spun down for 10 seconds at 1000rpm.

qRT-PCR was performed using an Applied Biosystems 7500 RT-PCR machine. The qRT-PCR cycle consisted of an initial 10 minutes at 95°C followed by 45 cycles of 95°C/60°C for 15 seconds and 1 minute respectively.

Cycle Threshold (C_T) values were calculated using a threshold of 0.1 and fold-regulation analysis carried out using the online software found at <http://pcrdataanalysis.sabiosciences.com/pcr/arrayanalysis.php>. Three biological repeats were performed for each drug treatment and the C_T values of these repeats inputted into the online analysis software directly.

2.11.3.2 TaqMan Gene Expression Analysis Procedure

To verify and further quantify changes in gene expression discovered by the array analysis system, TaqMan Gene Expression Assays (*Life Technologies*) were

employed. These assays were also used to analyse the expression of genes not included on the array that were of interest. Primer/probe sets for FANCD2, BRCA1, EME1 and MUS81 were diluted 1:10 with TaqMan 2x Universal PCR Mastermix (*Life Technologies*). cDNA was diluted in RNase-free water to reach 50ng cDNA per reaction. For each reaction, 9µL cDNA and 11µL primer/probe/mastermix solution was added, making a total reaction volume of 20µL. Three technical repeats were performed on each plate, with GAPDH used as the housekeeping gene. The qRT-PCR program was identical to that used in section 2.11.3.1.

Fold change was calculated using the comparative C_T method. For each sample the mean C_T was calculated for the gene of interest (GOI) and for the housekeeping gene GAPDH. The ΔC_T was calculated using the formula:

$$\Delta C_T = C_T \text{ Target Gene} - C_T \text{ GAPDH} .$$

$\Delta\Delta C_T$ was calculated for each dose by using the formula:

$$\Delta\Delta C_T = \Delta C_T \text{ Treated} - \Delta C_T \text{ Untreated} .$$

The fold difference was then calculated using the formula:

$$\text{Fold difference} = 2^{-\Delta\Delta C_T} .$$

From three biological repeats, the mean fold difference and the SEM was calculated. Therefore, all relative mRNA levels are comparable to the untreated control, which is set to 1.

2.12 Cell Cycle Analysis

To assess whether the exposure of cell lines to STAT3 inhibitors significantly altered the cell cycle profile, flow cytometry was used.

2.12.1 Drug Treatment of cells

2.12.1.1 Asynchronous cell treatments

DU145 cells were seeded in 10cm dishes and allowed to attach and reach 70% confluency before drug treatment. Cells were treated with 3 doses of VS-43, stattic and curcumin (one dose below the GI_{50} , the approximate GI_{50} and one dose above the GI_{50}) for 18 hours. Cells treated with drug-free medium were used as a control.

2.12.1.2 Synchronisation and treatment of cells

To enrich for cells in S-phase, DU145 cells were seeded in 10cm dishes and allowed to reach 70% confluency. One plate was harvested as a representation of the asynchronous cell population, and the media on the remaining plates was replaced with serum-free media. After a starvation period of 48 hours, another plate was harvested (the starved cell population), and the media on the remaining plates was replaced with 20% serum full media. These plates were then harvested at various time points after release in order to determine the optimum length of release to obtain the maximum percentage of S phase cells. This was found to be 18 hours therefore, to study the effect of STAT3 inhibitors on the cell cycle progression of synchronised cells, cells were released in the presence of VS-43, stattic or curcumin for 18 hours before harvesting. Cells released with drug-free 20% serum media were used as a control.

2.12.2 Preparation of cells for flow cytometry

After the drug treatment period, all media was removed from plates and cells were harvested by trypsinisation. After spinning down at 1200rpm for 5 minutes, cell

pellets were washed in 10mL PBS and spun down again before resuspending in 1mL PBS. 2mL ice cold 100% ethanol was added to each sample dropwise whilst vortexing to avoid clumping of cells. Cells were fixed at -20°C overnight.

Fixed samples were spun down at 1200rpm for 5 minutes at 4°C and the supernatant carefully aspirated. Pellets were washed with PBS before staining. To enable quantification of DNA content each sample was resuspended in 1mL of the following DNA staining solution:

For 1 mL:

950µL PBS 0.05% Triton-X100, 3.2µL RNase A and 50µL PI (1mg/mL)

Samples were incubated at 37°C for 1 hour to allow for the incorporation of PI into cellular DNA.

2.12.3 Collection of cell cycle data

The BD Biosciences Fortessa X20 cell analyser was utilised for collecting cell cycle data. Forward and side scatter gating was used to select for a single, intact cell population, and 10000 events per sample were recorded. The YG610/20 laser was used to excite PI.

2.12.4 Analysis of cell cycle data

Flowjo v10 was used to analyse flow cytometry raw data. As with data collection, forward and side scatter profiles were used to select for a single, intact cell population. This population was analysed for cell cycle profile using the built-in cell cycle modelling tool. Specifically, the Dean-Jett-Fox model was chosen as this gave the best fit. The percentage of cells in G1, S and G2/M phase was then averaged over 3 repeats and the SEM calculated in GraphPad Prism 6.

2.13 siRNA knockdowns

As a non-pharmacological control for experiments where natural and synthetic compounds had been utilised to inhibit STAT3, siRNA was used. siRNA was also used to knock down the DNA repair proteins EME1 and MUS81.

DU145 cells were seeded in 6-well plates (*Corning*) and allowed to adhere and reach 70% confluency. Cells were then transfected with either a targeted siRNA (STAT3, EME1 or MUS81), or a control siRNA targeted against luciferase (both SMARTpool ON-TARGET*plus* siRNAs purchased from *Dharmacon, GE Healthcare*). The final concentration of siRNA used was 10nM with 3µL of DharmaFECT 1 transfection reagent (*Dharmacon, GE Healthcare*) per well.

In detail, siRNAs were resuspended in 1x siRNA buffer to a final concentration of 20µM and aliquotted for storage at -20°C. For transfection, the siRNA stocks were thawed and diluted further in 1x siRNA buffer (*Thermo Fisher Scientific*) to 5µM. The required volume of the siRNA 5µM stock was added to serum-free media, and the required volume of DharmaFECT 1 reagent was also added to serum-free media (total 200µL per well for each of the siRNA and DharmaFECT tubes. These tubes were incubated for 5 minutes at room temperature before combining, mixing by gentle pipetting and incubating for a further 20 minutes at room temperature. The total volume of transfection mix at this point was 400µL per well. After the incubation, 1600µL serum-full media per well was added and 2mL of this final mix was added to each well. All control wells were treated with DharmaFECT reagent alone.

Plates were incubated for 24 hours at 37°C with 5% CO₂ to allow for the transfection to take place.

For preliminary experiments to determine whether 10nM siRNA could sufficiently down-regulate target expression, after 24 hours of transfection these cells were harvested, lysed and analysed by immunoblotting as is described in section 2.5.

For comet assay experiments to determine the effect of STAT3, EME1 and MUS81 siRNAs on cisplatin and melphalan DNA-ICL repair, immediately after the 24 hour transfection period, media was replaced by either fresh serum-full media for control wells or cisplatin or melphalan containing media for 1 hour. After 1 hour of drug treatment media was replaced on all wells again, and plates incubated at 37°C with 5% CO₂ until harvesting at the ICL peak and then again at 24 hours post ICL peak. The ICL peak occurs at 9 and 16 hours post treatment for cisplatin and melphalan ICL peaks respectively. The rest of the comet assay was performed as is described in section 2.9.

2.14 Whole genome screening of STAT3 binding sites

To investigate the possibility of STAT3 regulating the transcription of ICL repair genes by directly binding to promoter regions, the UCSC Human Genome Browser was utilised (Kent et al., 2002). This online database of the human genome is annotated with results from the ENCODE (Encyclopedia of DNA Elements) project (Rosenbloom et al., 2013) which set out to characterise the functional elements of the human genome. This data includes results from chromatin immunoprecipitation sequencing (ChIP-seq) experiments for many transcription factors in various cell lines. For STAT3, data is available from seven ChIP experiments across three cell lines (GM12878, HeLa-S3 and MCF-10A-ER-Src). The raw data for all STAT3 binding sites found in these experiments was downloaded from the database and subsequently sorted into a comprehensive list of genes in which STAT3 may bind the promoter region (defined as <4kb upstream of the transcription start site). To refine search results, only hits present in 4 or more of the ChIP data sets were

shortlisted. From this list, genes known to be involved in DNA ICL repair were identified. This work was performed by John Ambrose and Javier Herrero of the Bill Lyons Informatics Center, UCL.

2.15 Chromatin Immunoprecipitation (ChIP) Assay

The ChIP-IT[®] Express Enzymatic kit (Active Motif) was used to assess the binding of STAT3 to the EME1 and MUS81 promoter regions. Components of the kit were stored at 4°C or -20°C according to the manufacturer's guide. All buffers referred to in this method are included in the kit.

2.15.1 Design of primers

Primers flanking the putative STAT3 binding sites upstream of the EME1 and MUS81 genes were designed using Primer3 version 4.0 (Koressaar and Remm, 2007; Untergasser et al., 2012). The following primers were ordered from ThermoFisher Scientific as 100µM in water.

Table 2-3: List of ChIP primers and their sequences.

Primer Name	Sequence 5'-3'
cFOS Forward	CGAGCAGTTCCCGTCAATC
cFOS Reverse	TCGTGAGCATTTCGCAGTTC
NEGATIVE Forward	CCCTGGACTCCTCATCTGTA
NEGATIVE Reverse	GGAAGAGCCCTGGTGATTCT
EME1 Forward	AGCCAAGTCTTCACGTTTTTC
EME1 Reverse	GGTGGGTCCTTTCTCTGTAG
MUS81 Forward	CCATCTCCAGCCTCCTTCAA
MUS81 Reverse	TTGTGTAGGCGAGAGGAAGG
MUS81 Region 2 Forward	CCTGGGCAAGCTACATAACC
MUS81 Region 2 Reverse	GGAGCCGAGTTTAGGGAAGT
EME1 Region 2 Forward	TTGTTACCAGCAAGCTCTG
EME Region 2 Reverse	TTGTGGTGGCAGTGAAGTTG

2.15.2 Seeding, treatment and harvesting of cells

DU145 cells were seeded in 15cm dishes and allowed to reach 70% confluency. Two 15cm dishes were used for each chromatin preparation. Cells were either harvested untreated, or after various drug treatments. Drug treatments included 100 μ M cisplatin for 1 hour, or 1.5 μ M VS-43 for 18 hours followed by cisplatin for 1 hour. All drug treatments were carried out in a volume of 20mL per 15cm dish.

After drug treatment, cells were fixed for 5 minutes with 1% formaldehyde in 20mL minimal cell culture media. Fixation was performed at room temperature with gentle rocking. Plates were then washed with PBS and the fixation reaction stopped by the addition of glycine buffer for 5 minutes at room temperature. Plates were again washed with PBS. Cells were collected in 6mL PBS containing PMSF using cell

scrapers, and subsequently centrifuged for at 4°C for 10 minutes at 2500rpm. After centrifugation the supernatant was aspirated.

2.15.3 Shearing of chromatin and chromatin immunoprecipitation

To obtain cellular chromatin, cells were first lysed by resuspending the pellets in lysis buffer containing both a protease inhibitor cocktail and PMSF. Lysis was performed for 30 minutes on ice with frequent agitation. To ensure complete nuclei release, lysates were transferred into a 2mL dounce homogenizer and dounced on ice for 50 strokes. Lysates were then centrifuged at 4°C for 10 minutes at 5000rpm. The supernatant was removed and the remaining pellet was resuspended in digestion buffer containing a protease inhibitor cocktail and PMSF. The samples were warmed to 37°C before incubation with the enzymatic shearing cocktail for 10 minutes at 37°C. During this incubation the samples were vortexed every 2 minutes to increase the shearing efficiency. The shearing reaction was stopped by adding ice cold EDTA and after a 10 minute incubation on ice, nuclear debris was pelleted by centrifugation at 4°C for 10 minutes at full speed. The supernatant containing the chromatin was transferred into a new tube and stored at -80°C until the time of immunoprecipitation. 50µL of the chromatin was removed to analyse shearing efficiency by electrophoresis on a 1% agarose gel. Enzymatic shearing produced fragment sizes of predominantly 150bp, with 300bp and 450bp fragments also present (due to enzymatic cleavage occurring between nucleosomes).

For immunoprecipitation, 10µL of chromatin was set aside as the “input” sample. ChIP reactions were performed with 25µg chromatin and 3µg of either STAT3 (*Santa Cruz Biotechnology*) or rabbit IgG antibody (*Cell Signaling*). Tubes were incubated at 4°C on an end-to-end rotator for 4 hours. A magnetic stand was subsequently used to pellet the magnetic protein G beads used in the ChIP reaction, and beads were washed with the kit wash buffers. Chromatin was eluted from the

beads and reverse cross-linked using the kit buffers. Immunoprecipitated chromatin was isolated by pelleting the magnetic beads using the magnetic stand and collecting the supernatant.

Both the immunoprecipitated and input chromatin were incubated for 15 minutes at 95°C and subsequently incubated with proteinase K for 1 hour at 37°C. After this incubation the chromatin was purified using the Chromatin IP DNA Purification Kit (*Active Motif*) before use in PCR.

2.15.4 PCR and analysis

Input chromatin was diluted 1:10 for PCR whereas immunoprecipitated chromatin was not diluted. 2µL of chromatin was used for each PCR reaction. Primers were diluted 1:10 with water and used at a final concentration of 0.75µM. Power SYBR™ Green 2x Master Mix (*ThermoFisher Scientific*) was used for PCR reactions. The PCR was performed using an Applied Biosystems 7500 RT-PCR machine. The PCR cycle consisted of an initial 10 minutes at 95°C followed by 45 cycles of 95°C/60°C for 15 seconds and 1 minute respectively. C_T values were calculated using a threshold of 0.1. Primer efficiencies were previously calculated using a serial dilution of input DNA ranging from 0.005ng to 50ng. All primers had efficiencies of 100% ± 10%.

To calculate fold enrichment, the relative quantity of DNA amplified in each reaction was calculated using the following formula:

$$DNA\ quantity = 2^{-C_T}$$

The DNA quantity in each reaction was calculated as a percentage of the quantity of input DNA, accounting for the 10-fold dilution factor.

The fold enrichment was calculated using the following formula:

$$\text{Fold enrichment} = \frac{\text{STAT3 ChIP \% input}}{\text{IgG ChIP \% input}}$$

This fold enrichment for the negative control region was then subtracted from the fold enrichment for the target regions in order to normalise for the variation in off-target immunoprecipitation between experiments. Data was presented as mean \pm SEM using GraphPad Prism 6.

2.16 Statistical Analysis

GraphPad Prism 6 was utilised for statistical analysis.

For assessing statistical difference between cytotoxicity data sets, the one-tailed unpaired students t-test was performed. For comet assays, statistical difference was assessed using the two-tailed unpaired students t-test.

For determining statistical difference between a control group and more than two further groups of data analysis of variance (one-way ANOVA) was employed with a Dunnett's post-hoc test. For determining statistical difference between all groups the Tukey's post-hoc test was used. P values and their corresponding significance for all statistical tests are shown in Table 2-4.

Table 2-4: P values and the corresponding significance levels.

P Value	Significance
<0.0001	****
0.0001-0.001	***
0.001-0.01	**
0.01-0.05	*
≥0.5	ns

Chapter 3 A Novel, Selective STAT3 Inhibitor: VS-43.

3.1 Introduction

In this chapter, the novel STAT3 inhibitor VS-43 is investigated in terms of potency, selectivity and effect on cancer cell growth.

3.1.1 Rationale for the design of a novel STAT3 inhibitor, VS-43

STAT3 is constitutively active in many cancer types, and its downstream targets feed the development of cancer by controlling cell survival, angiogenesis, metastasis and proliferation. It has been suggested that some cancers which harbour constitutively active STAT3 develop a phenomenon known as oncogene addiction (Frank, 2007; Masuda et al., 2010). This is where a cancer cell with an activated oncogene driving its survival becomes dependent on the activity of that oncogene to continue proliferating. Removal of that driving force results in the death of the cancer cell (Weinstein, 2002). Therefore, this transcription factor is a viable target for inhibition by novel anti-cancer drugs.

Additionally, STAT3 inhibitors are chemosensitisers to various chemotherapy agents, including cisplatin. As acquired resistance to chemotherapeutics is common, a compound that can effectively re-sensitise patients when given in combination with the chemotherapy agent would be desirable. The most effective combinations will result in a synergistic interaction whereby the effect on cell growth is greater than the effect of the two drugs independently. This will allow for the use of lower doses of each component of the combination, resulting in decreased adverse effects. Therefore, a potent STAT3 inhibitor that is able to chemosensitise cancer cell lines to cisplatin is of clinical interest.

Inhibitors of the EGFR pathway have been successful anti-cancer agents for many years now. As STAT3 lies downstream of EGFR in the EGF signalling pathway one

question that might be asked is: why target STAT3 instead of EGFR? However, several pathways feed into STAT3 activation, not just the EGF pathway. STAT3 can be phosphorylated through the IL-6 cytokine pathway or by individual kinases such as Src (Cao et al., 1996; Zhong et al., 1994). In fact, development of feedback-related resistance has been reported with EGFR inhibitors (reviewed in (Zhao et al., 2016)). In this model, resistance to EGFR inhibitors is said to occur via compensatory activation of STAT3 through the alternative cytokine pathway. Therefore, targeting the central node that is the STAT3 transcription factor itself may overcome these feedback-related issues.

The inhibition of STAT3 has been documented using various natural and novel synthetic inhibitors, however, these are rarely particularly potent, requiring long exposure times and high doses (often above 10 μ M) to reach 50% cell growth inhibition. Additionally, selectivity for STAT3 is an issue that is extremely important and yet is rarely addressed. Therefore, the need for a STAT3 inhibitor that can act alone, or as a sensitising agent, with improved potency and selectivity is required.

3.1.2 Why is there a need for selectivity with STAT3 inhibitors?

There are seven STAT family members, STAT3 being the predominant target for novel anti-cancer drugs due to its function as an oncogene. Other members of the STAT family can, however, function as tumour suppressor genes. For example, STAT1 acts to induce apoptosis through the transcriptional regulation of caspase-8 (Fulda and Debatin, 2002). STAT1 also inhibits the progression of the cell cycle through the p21 CDK inhibitor (Chin et al., 1996). These processes stimulated by STAT1 are in direct contrast to the actions of STAT3 (Regis et al., 2008). STAT1 also actively represses genes stimulated by STAT3 including c-Myc and the bcl-2 family of anti-apoptotic proteins (Ramana et al., 2000; Stephanou et al., 2000), as

well as directly interacting with cyclin D1 to inhibit cell cycle progression (Dimco et al., 2010).

STAT3 is closely related to STAT1, sharing 50% amino acid similarity (Szelag et al., 2015). The x-ray structure of a STAT3 dimer binding to DNA, and the location of the SH2 and DNA binding domains is shown in Figure 3-1A for reference. The SH2 domains of STAT3 and STAT1 have 59% homology at the sequence level (Mankan and Greten, 2011), and residues are highly conserved in both the SH2 and DNA binding domains of STAT3 and STAT1 (Figure 3-1B (Szelag et al., 2015)). Therefore, the design of STAT3 inhibitors must address selectivity in order to avoid inhibition of the tumour suppressor function of STAT1.

Curcumin (Figure 3-2) has been shown to lack selectivity for STAT3, also targeting STAT1 and STAT5 activation (Bill et al., 2009). Conflicting opinions exist on the selectivity of stattic (Figure 3-2) for STAT3, with some groups observing no inhibition of STAT1 activation by stattic (Schust et al., 2006) and other groups reporting that stattic does in fact target STAT1 activation (Sanseverino et al., 2012). Szelag et al. suggest that the small size of stattic would allow for binding to all STAT proteins, reducing its selectivity significantly (Szelag et al., 2015). Even the most successful direct STAT3 inhibitor in clinical trials to date, OPB-31121, was shown to lack selectivity for STAT3, down-regulating STAT1 and STAT5 phosphorylation (M. J. Kim et al., 2013). Therefore, selectivity must be addressed at earlier phases of STAT3 inhibitor development.

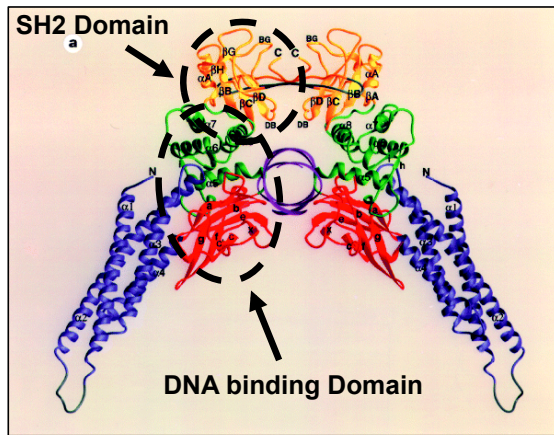
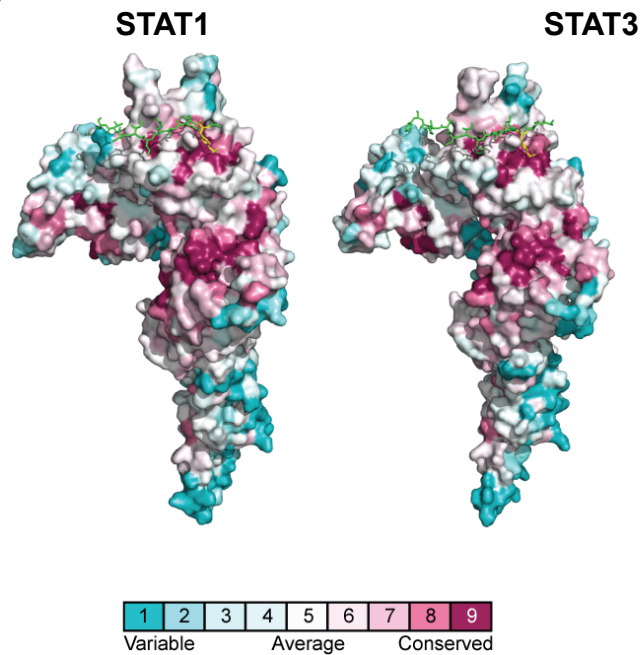
A**B**

Figure 3-1: Crystal structure of a STAT3 Dimer binding to DNA, and amino acid conservation between STAT1 and STAT3. A) The SH2 domain (yellow/orange) is immediately adjacent to the DNA binding domain (red/green). Taken from (Becker et al., 1998). B) purple regions in the SH2 and DNA binding domains are well conserved. Taken from (Szelag et al., 2015).

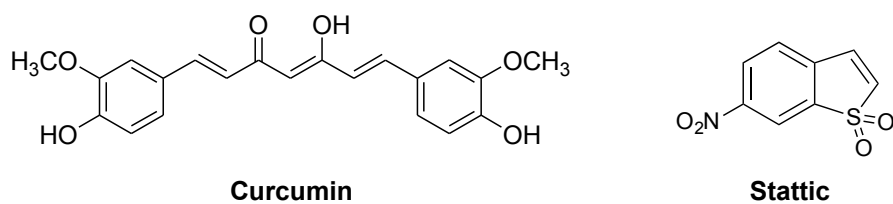


Figure 3-2: Structures of curcumin and stattic.

3.1.3 Design of VS-43

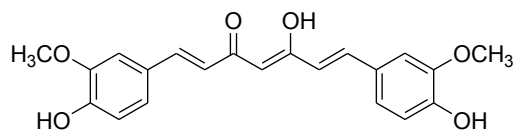
VS-43 was designed and synthesised by collaborator Professor Moses Lee and colleagues (Georgia State University, Atlanta, Georgia, USA).

Curcumin has been repeatedly demonstrated to have substantial anti-tumourigenic activity in many different cancer cell line models (Dhandapani et al., 2007; Goel and Aggarwal, 2010; Notarbartolo et al., 2005; Yallapu et al., 2010), however, its poor absorption and low bioavailability hamper the use of curcumin in patients (Anand et al., 2007). Therefore, the development of synthetic curcumin analogues through structural modifications improving both the potency and the bioavailability of this compound have been of significant interest in recent years.

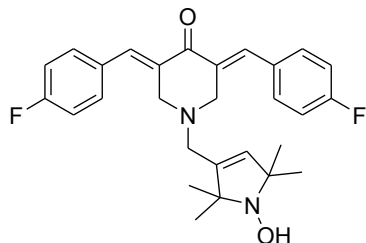
The diarylidene piperidone (DAP) class of compounds are one such group of curcumin derivatives. These compounds have a piperidone ring in place of curcumin's β -diketone moiety (Adams et al., 2004). Two such derivatives, HO-3867 (Figure 3-3) and H-4073, have been shown to inhibit the JAK/STAT pathway in ovarian cancer murine xenografts (Selvendiran et al., 2011, 2010).

Aiming to further improve curcumin's potency and bioavailability, Moses Lee and colleagues have synthesised two groups of curcumin analogues: NH and N-methyl DAPs (Gregory et al., 2013), and 2,6-bis(arylidene)-4-phenylcyclohexanone

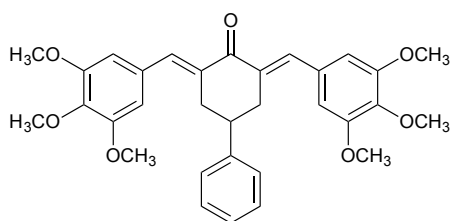
analogues (Davis et al., 2008). Of the second class, one compound (compound 9, Figure 3-3) exhibited excellent cytotoxicity in preliminary MTT cytotoxicity studies with GI_{50} values of 0.51 and 1.2 μ M against the murine B16 and L1210 cancer cell lines respectively. The chemical structure of compound 9 was, therefore, further developed in order to optimise binding to the polar regions of STAT3's DNA binding domain. In VS-43, the N-phenyl moiety was introduced to enhance the interaction of the molecule with the non-polar pocket in this domain. In a bid to address bioavailability, the N-phenyl group also provides the potential for improved water solubility through salt formation. The N-phenyl-DAP design is considered relatively novel as only one such analogue has been reported (identified through SciFinder in March 2016), with no biological results published with this compound as of yet (Yuan et al., 2008). The structural similarities between curcumin, HO-3867, compound 9 and VS-43 can be seen in Figure 3-3. The full synthesis of VS-43 can be found in Appendix B.



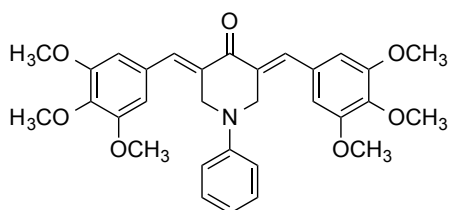
Curcumin



HO-3867



Compound 9



VS-43

Figure 3-3: The molecular structures of curcumin, HO-3867, compound 9 and the novel STAT3 inhibitor VS-43.

3.2 Aims

The aims regarding the initial investigation of VS-43 were as follows:

1. To determine whether VS-43 inhibits the activation and DNA binding ability of STAT3.
2. To test VS-43 for selectivity with respect to other STAT proteins.
3. To investigate whether VS-43 can induce apoptosis in cancer cell lines.
4. To compare VS-43 against other widely used STAT3 inhibitors.

3.3 Results

3.3.1 STAT3 is constitutively activated in cancer cell lines

To select cancer cell lines for use in this thesis, basal STAT3 activation was considered. Cell lines with constitutively active STAT3, that is, high levels of pSTAT3^{Tyr705} without pathway stimulation, would be good models to test the STAT3 inhibitor VS-43.

Previous research suggests that the DU145 prostate cancer cell line and the A549 NSCLC cell line both express constitutively active STAT3 (Ni et al., 2000; Song et al., 2003), therefore, these cell lines were grown and harvested at two growth phases: exponential (E, 50-60% confluency) and confluent (C, 100% confluency).

Western blot analysis of the cell extracts illustrated that both of these cell lines harbour constitutively activated STAT3. DU145 cells express higher levels of pSTAT3^{Tyr705} than A549 cells, and in both cell lines a direct relationship between confluency and pSTAT3^{Tyr705} expression was observed (Figure 3-4). These results suggested that cell confluency must be kept constant for all experiments where STAT3 inhibition is studied so that the level of activated STAT3 remains constant. Therefore, a confluency level of 70% was chosen for all further studies.

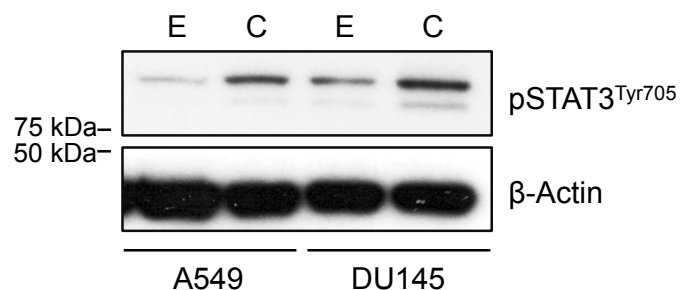


Figure 3-4: Expression of pSTAT3^{Tyr705} in the A549 and DU145 cell lines. Cell density is indicated by E = exponential and C = confluent. Blot is representative of more than 1 experiment.

3.3.2 VS-43 inhibits pSTAT3^{Tyr705} protein levels

To establish whether VS-43 has inhibitory activity on pSTAT3^{Tyr705} levels in the DU145 and A549 cell lines, these cells were treated for 18 hours with increasing concentrations of VS-43. Immunoblot analysis confirmed that pSTAT3^{Tyr705} is down-regulated by an 18 hour treatment with VS-43 at concentrations including and lower than 2 μ M (Figure 3-5).

The potency of VS-43 is cell line specific as A549 cells require higher doses of VS-43 to inhibit pSTAT3^{Tyr705}. In A549 cells, inhibition of pSTAT3^{Tyr705} is not seen until 1.2 μ M, where a dose-dependent inhibition is then present. Approximately 50% pSTAT3^{Tyr705} inhibition occurs at 1.5 μ M. At 2 μ M the majority of pSTAT3^{Tyr705} is depleted. In the DU145 cell line a more gradual inhibition of pSTAT3^{Tyr705} is observed. From 0.5 μ M moderate inhibition can be seen, with approximately 50% pSTAT3^{Tyr705} inhibition occurring at 1 μ M. This inhibition is also dose-dependent and by 2 μ M VS-43, pSTAT3^{Tyr705} is almost completely depleted. The requirement for higher concentrations of VS-43 in A549 cells is not understood but could be related to differences in uptake or efflux of the inhibitor.

To determine whether VS-43 specifically inhibits the activation of STAT3, un-phosphorylated STAT3 was also probed for with the conclusion that whole STAT3 levels are unaffected by VS-43 (Figure 3-5), therefore, VS-43 specifically down-regulates constitutively active STAT3 in the DU145 and A549 cell lines, without altering the cellular stability of the STAT3 protein.

Confocal microscopy was also employed to visualise the effect of VS-43 on pSTAT3^{Tyr705} cellular levels and localisation. This was performed in the A549 cell line. Figure 3-6 shows that with VS-43 treatment, the pSTAT3^{Tyr705} staining

decreases, confirming that this inhibitor can block the activation of STAT3 and thus decrease the amount of transcriptionally active STAT3.

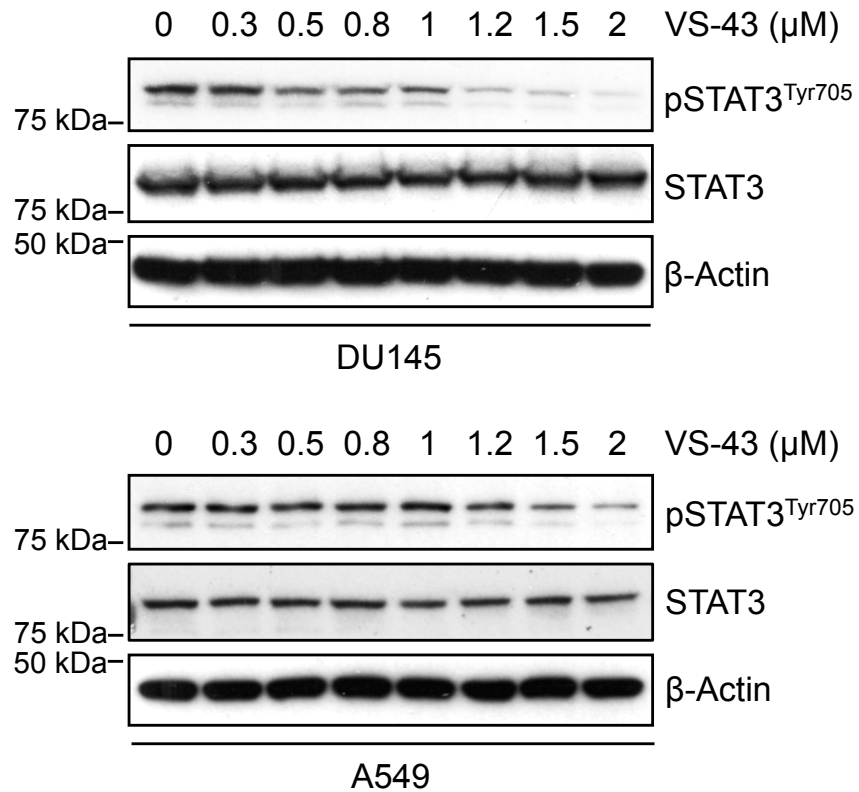


Figure 3-5: VS-43 inhibits pSTAT3^{Tyr705} levels in a dose-dependent manner in both the DU145 and A549 cell lines. STAT3 expression is unaffected. Blots are representative of more than 1 experiment.

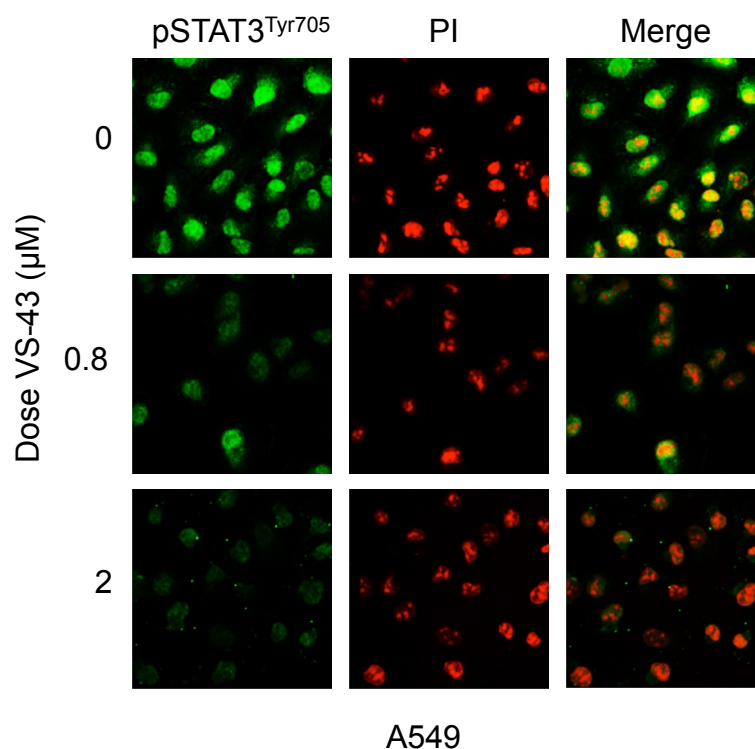


Figure 3-6: Confocal microscopy showing pSTAT3^{Tyr705} levels in A549 cells treated with VS-43 for 18 hours. pSTAT3^{Tyr705} is decreased upon treatment with VS-43. Images are representative of more than 1 experiment.

3.3.3 VS-43 is more potent than stattic or curcumin

In order to compare the potency of VS-43 as a STAT3 inhibitor with other compounds, two commercially available STAT3 inhibitors were used: stattic, a synthetic inhibitor and curcumin, the natural compound which is also the parent compound of VS-43. The ability of these compounds to inhibit pSTAT3^{Tyr705} levels in both the DU145 and A549 cell lines was assessed by immunoblotting. Figure 3-7 shows that both stattic and curcumin are capable of completely diminishing pSTAT3^{Tyr705} levels in both cell lines. Drug treatments were carried out for 18 hours, as with VS-43 in Figure 3-5. Concentrations of approximately 7 μ M and 20 μ M were required for stattic and curcumin respectively, in order to see approximately 50% inhibition of pSTAT3^{Tyr705} expression in both cell lines. These concentrations are

much higher than the doses of VS-43 required to observe a similar degree of pSTAT3^{Tyr705} inhibition – approximately 1 μ M and 1.5 μ M in the DU145 and A549 cell lines respectively (Figure 3-5). Therefore, these inhibitors are considerably less potent than VS-43. Curcumin, the parent compound of VS-43, is approximately 10-fold less potent than VS-43 in terms of pSTAT3^{Tyr705} inhibition.

3.3.4 VS-43 inhibits STAT3 DNA binding

The ability of STAT3 to regulate transcription depends on its ability to bind consensus DNA binding sites located in the promoter regions of its target genes. This is in part regulated through the phosphorylation status of STAT3 as only phosphorylated monomers may dimerise and translocate into the nucleus. However, measuring pSTAT3^{Tyr705} levels does not directly measure STAT3 DNA binding, therefore, an EMSA was performed to measure binding of STAT3 to a consensus STAT3 binding site located in the *c-fos* promoter region. This EMSA was also performed with stattic. This experiment was performed by Dr Konstantinos Kiakos in the research group.

Figure 3-8 shows that while VS-43 can inhibit STAT3 DNA binding at concentrations of 0.8 μ M, stattic requires up to 7 μ M to significantly inhibit STAT3 DNA binding. These concentrations correlate well with the concentrations required to inhibit STAT3 phosphorylation discussed previously, therefore, the level of pSTAT3^{Tyr705} is a good indicator of DNA binding ability.

However, to complete this experiment, a super-shift using a STAT3 antibody must be performed to confirm the identity of the indicated band as DNA-bound STAT3.

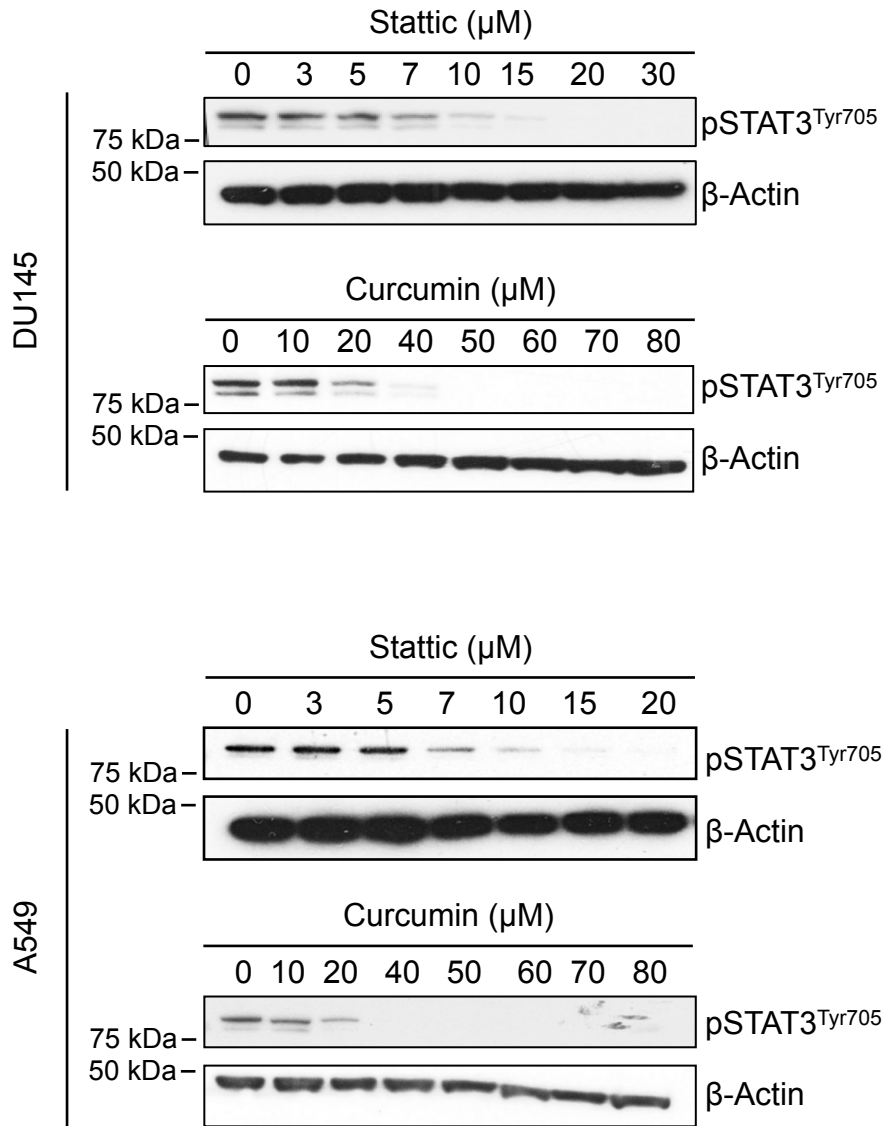


Figure 3-7: Stattic and curcumin inhibit pSTAT3^{Tyr705} levels in the DU145 and A549 cell lines. Blots are representative of more than 1 experiment.

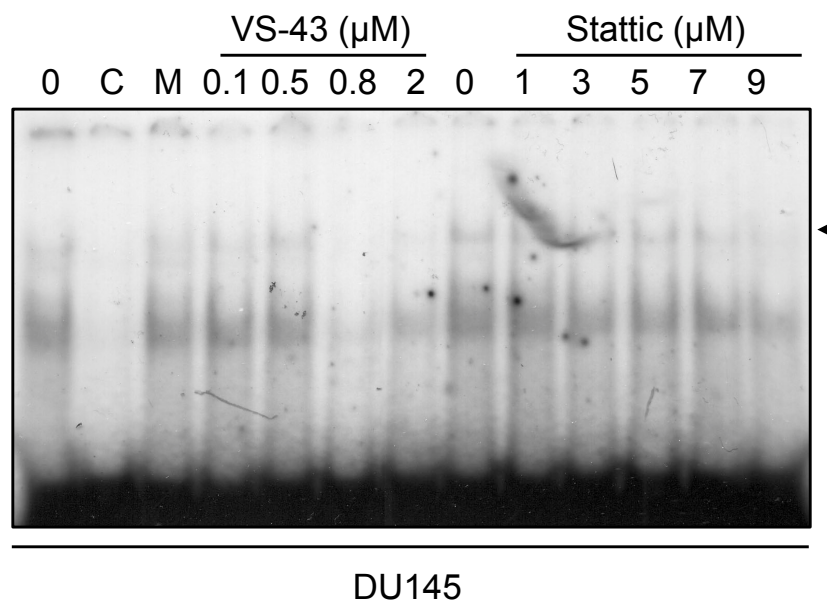


Figure 3-8: VS-43 inhibits binding of STAT3 (indicated by arrowhead) to the hSIE consensus binding sequence from the *c-fos* promoter region, and did so at lower concentrations than stattic. This experiment was carried out with DU145 cell nuclear extract. C = cold oligonucleotide, M = non-specific competitor. Figure supplied by Dr Konstantinos Kiakos.

3.3.5 VS-43 action is dependent on confluency, treatment time and dose

The ability of VS-43 to inhibit pSTAT3^{Tyr705} has already been shown to be dependent on the cell line. The extent of inhibition has also been demonstrated to be dose-dependent in both cell lines tested, with a direct relationship between dose and extent of pSTAT3^{Tyr705} inhibition as confirmed by immunoblotting (Figure 3-5).

Next, the effect of the length of drug treatment time and the cell confluency at the time of drug treatment was investigated in the DU145 cell line by immunoblotting. Inhibition of pSTAT3^{Tyr705} by VS-43 was found to be dependent on the drug treatment time, with a shorter 6 hour exposure requiring 1.5-2 μM to down-regulate pSTAT3^{Tyr705} levels in comparison to an 18 hour drug treatment where down-

regulation of pSTAT3^{Tyr705} can be seen with concentrations as low as 0.8 μ M (Figure 3-9A).

VS-43 was also tested for its ability to inhibit pSTAT3^{Tyr705} at two different confluencies of DU145 cells: low (~30%) and high (~100%). At the lower confluency, 0.5 μ M VS-43 completely depleted activated STAT3 levels whereas at the higher confluency pSTAT3^{Tyr705} levels were not affected until approximately 1.5-2 μ M (Figure 3-9B). This is likely due to the relationship between confluency and STAT3 activation levels that was demonstrated in section 3.3.1. At a higher confluency there is more target present in the cell and therefore, a higher concentration of inhibitor is required to see a reduction in pSTAT3^{Tyr705}.

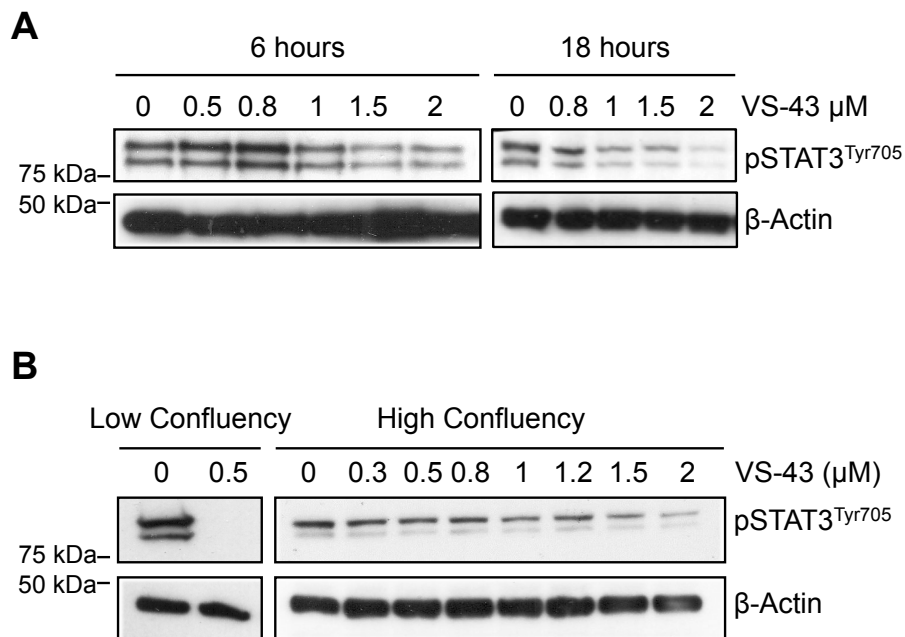


Figure 3-9: pSTAT3^{Tyr705} inhibition by VS-43 is dependent on A) exposure time and B) confluency of DU145 cells. Blots are representative of more than 1 experiment.

3.3.6 Inhibition of pSTAT3^{Tyr705} by VS-43 is persistent

In order to establish whether inhibition of pSTAT3^{Tyr705} by VS-43 is reversible or irreversible, immunoblotting was performed after an 18 hour treatment period and then after a further 24 hours in drug-free media. In both cell lines 24 hours after the end of the VS-43 drug treatment period, the levels of pSTAT3^{Tyr705} remain suppressed (Figure 3-10). This suggests that inhibition of STAT3 by VS-43 is persistent and may be irreversible.

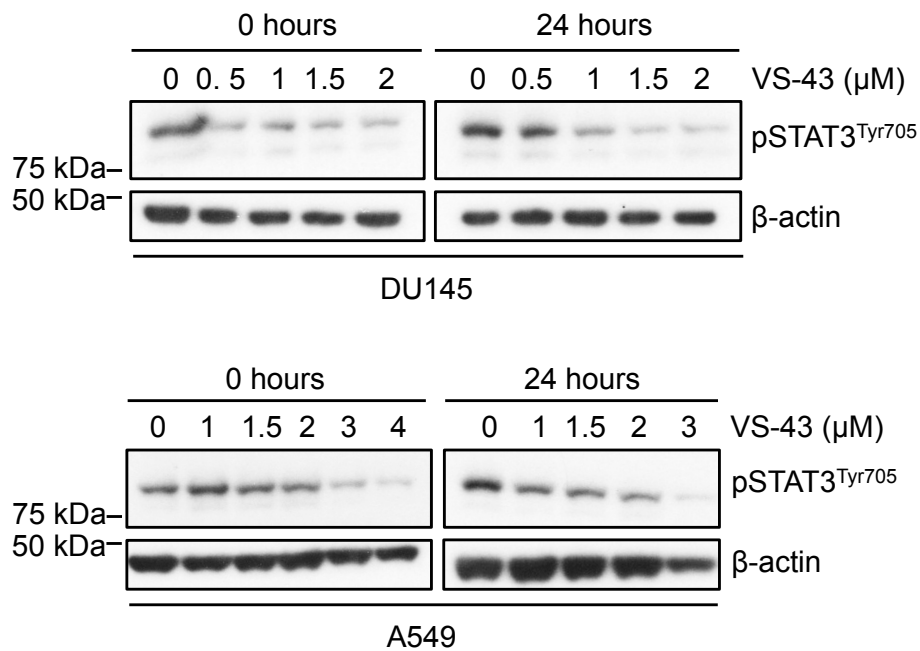


Figure 3-10: Inhibition of pSTAT3^{Tyr705} by VS-43 persists for at least 24 hours after drug treatment (18 hours) in both the DU145 and A549 cell lines. Blots are representative of more than 1 experiment.

3.3.7 VS-43 is a selective STAT3 inhibitor

As has been discussed in the introduction to this chapter, selectivity with STAT3 inhibitors is an important factor that must be considered. This is because all STAT proteins do not regulate the same targets. In particular, STAT1 is a tumour suppressor protein and therefore, inhibition of STAT1 in addition to STAT3 would be counterproductive for an anti-cancer drug. To determine the specificity of VS-43, both immunoblotting and ELISA techniques were employed.

Immunoblot analysis revealed that where pSTAT3^{Tyr705} levels were down-regulated by VS-43 in DU145 cells, pSTAT1^{Tyr701} and pSTAT5^{Tyr694} levels were not down-regulated (Figure 3-11A). The phospho-tyrosine residues observed are the equivalent activating phosphorylations.

The TransAM[®] STAT Family ELISA was used to establish the selectivity of VS-43 for STAT3 over STAT1 α , STAT5a and STAT5b. This kit analyses the activity of STAT proteins by quantifying their binding to a STAT binding consensus oligonucleotide, therefore, it also indirectly observes STAT DNA binding. When incubated with VS-43 for 18 hours, DU145 cells show a significant dose-dependent reduction in STAT3 activation/DNA binding (Figure 3-11B). By 2 μ M VS-43 only 31.4% of control STAT3 DNA binding remains. Whilst a significant effect on STAT1 α and STAT5a DNA binding is also observed, these effects are small. At 2 μ M VS-43, STAT1 α DNA binding is decreased to 92.8% of control binding, and STAT5a DNA binding is decreased to 88.5% of control binding. The DNA binding of STAT5b is not affected by VS-43. Therefore, VS-43 has considerable selectivity for STAT3 over STAT1 or STAT5 and is able to block STAT3 DNA binding.

A shorter drug treatment of 1 hour was also performed for analysis with the STAT Family ELISA. 1 hour treatment of DU145 cells was sufficient to inhibit the

activation/DNA binding of STAT3 by approximately 50% but had no effect on STAT1 α , STAT5a and STAT5b activation (Figure 3-12).

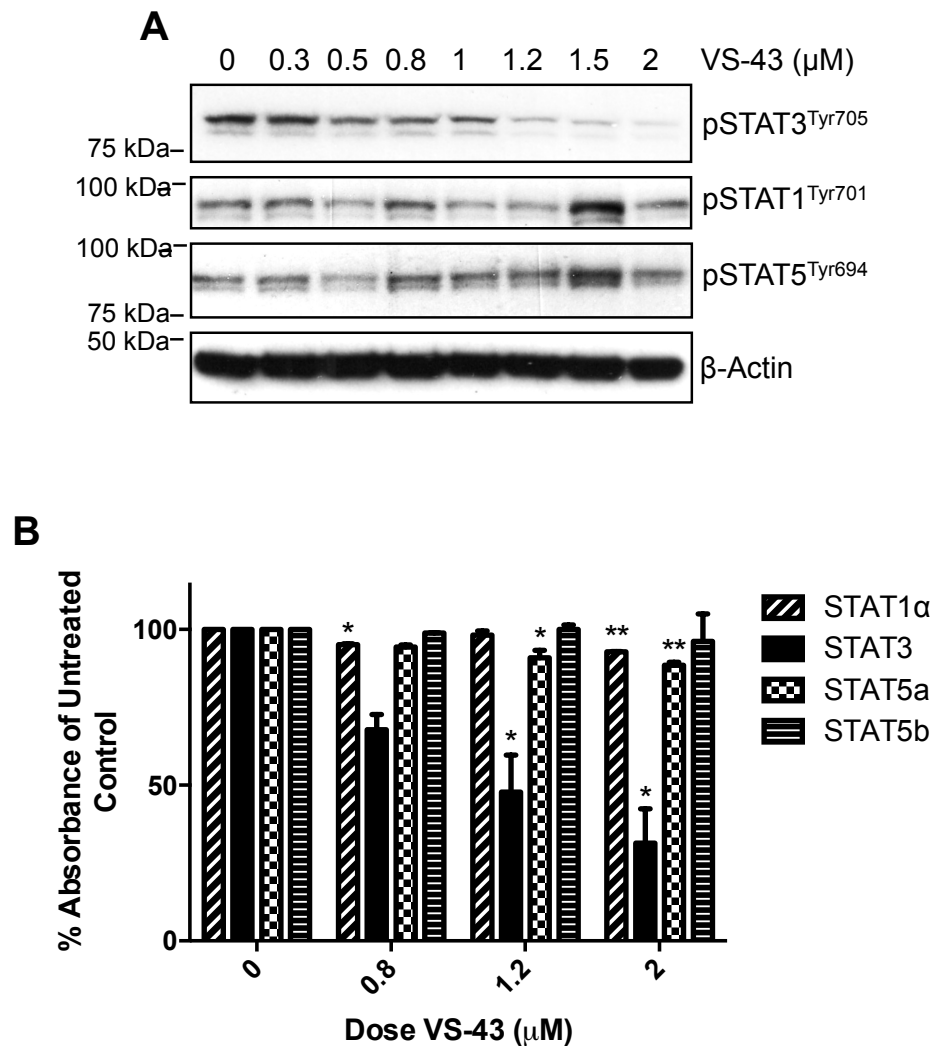


Figure 3-11: VS-43 is a specific pSTAT3^{Tyr705} inhibitor as shown by A) immunoblotting and B) STAT family ELISA assay. VS-43 selectively inhibits activation and DNA binding of STAT3. Blots are representative of more than 1 experiment. For the ELISA, the average of two experiments is presented with the SEM represented as error bars. One-way ANOVA was performed to calculate statistical significance. * = P<0.05, ** = P<0.01.

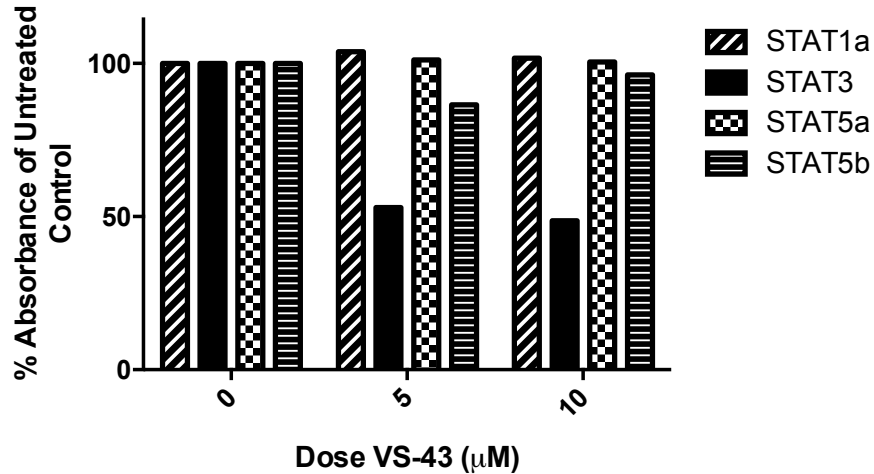


Figure 3-12: Treatment of DU145 cells with VS-43 for 1 hour selectively inhibits STAT3 activation and DNA binding. Data displayed is from one experiment.

3.3.8 VS-43 down-regulates STAT3 target genes

As STAT3 is reported to regulate the transcription of several pro-survival and antiapoptosis genes, the effect of VS-43 on the expression of these proteins was assessed by immunoblotting. Bcl-2 and survivin were both down-regulated in a dose-dependent manner after the treatment of DU145 cells with VS-43 for 18 hours. Survivin inhibition mirrors that of pSTAT3^{Tyr705} inhibition by VS-43, whereas bcl-2 inhibition requires greater doses of VS-43 (Figure 3-13). Therefore, VS-43 successfully down-regulates STAT3 target expression and may therefore, affect cellular survival.

3.3.9 VS-43 induces apoptosis and inhibits cell growth

STAT3 inhibitors have been shown to act as stand-alone agents, capable of inducing apoptosis and cell growth inhibition in many cancer cell lines. To test whether VS-43 inhibits the growth of cancer cell lines, the SRB assay was employed. This assay was chosen as it is reported to have a greater sensitivity than

the alternative MTT assay (Keepers et al., 1991). The assay also has a greater linearity and therefore, is capable of detecting sub-confluent and supra-confluent cell populations. The varying ability of cells to reduce MTT can affect comparisons of MTT data across cell lines however, as the SRB stain is reliant only on protein content, comparability across cell lines is more accurate with this assay (Keepers et al., 1991).

After an 18 hour treatment with VS-43, SRB analysis determined that VS-43 inhibits the growth of these cancer cell lines. GI_{50} concentrations were calculated to be 1.43 μ M and 2.53 μ M for the DU145 and A549 cell lines respectively (Figure 3-14).

The difference between the GI_{50} of VS-43 in different cell lines has not been investigated further; however, this is in agreement with immunoblot analysis where it was found that higher concentrations of VS-43 are required in A549 cells to achieve pSTAT3^{Tyr705} inhibition (section 3.3.2). Both cell lines are, however, sensitive to the cell growth inhibitory effects of VS-43.

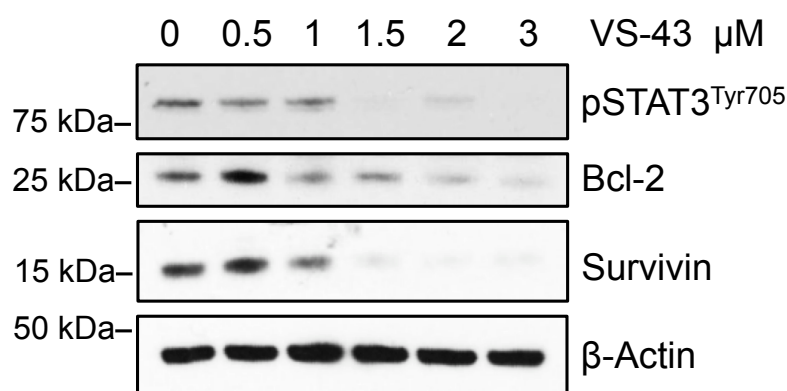


Figure 3-13: VS-43 down-regulates bcl-2 and survivin expression in the DU145 cell line. Blots are representative of more than 1 experiment.

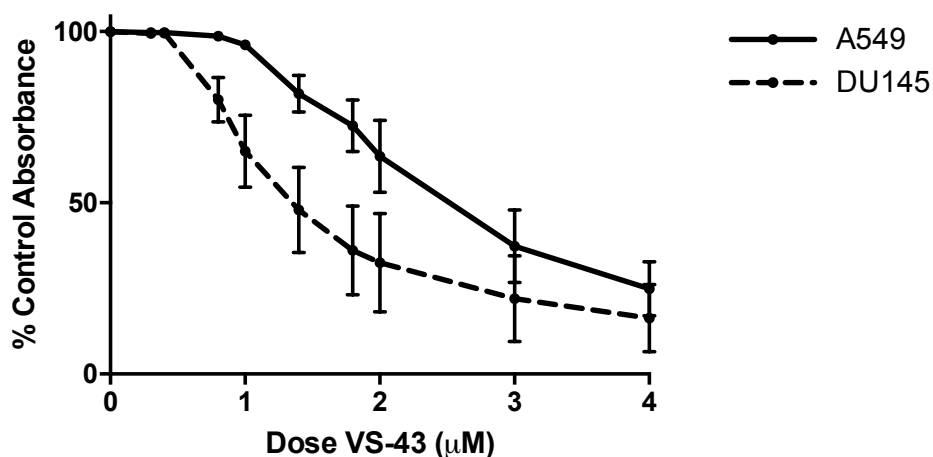


Figure 3-14: VS-43 inhibits cell growth in the DU145 and A549 cancer cell lines. GI_{50} values for DU145 and A549 are $1.43\mu\text{M}$ and $2.53\mu\text{M}$ respectively, obtained by SRB assay. Data is the average of at least 3 independent repeats, with SEM calculated for error bars.

To test whether VS-43 inhibits cell growth by inducing apoptosis, after an 18 hour treatment with VS-43, immunoblotting was performed to probe for cleaved Poly ADP-Ribose Polymerase (PARP), a widely accepted marker of apoptosis.

PARP plays a crucial role in the repair of DNA. It catalyses its own ADP-ribosylation which allows it to bind to SSBs in the early stages of the DNA repair process (Davar et al., 2012; Herceg and Wang, 2001). PARP is also thought to be important in the recognition of other DNA damage that requires BER and NER. In the apoptosis pathway, PARP is cleaved by upstream caspases such as caspase-3, which are themselves activated by cleavage due to extrinsic or intrinsic apoptosis signals. This cleavage inactivates PARP, and results in two products: a 24kDa and an 89kDa fragment. The 24kDa fragment is said to inhibit DNA repair by irreversibly binding SSBs whereas the 89kDa fragment has been suggested to be excluded from the nucleus into the cytosol where it binds un-cleaved PARP, preventing the formation of functional PARP homodimers. These events trigger apoptosis due to unrepaired DNA damage (Chaitanya et al., 2010; Soldani and Scovassi, 2002).

In both the DU145 and A549 cell lines, VS-43 treatment induces cleaved PARP expression. This expression exhibits an inversely proportional relationship with pSTAT3^{Tyr705} inhibition by VS-43 (Figure 3-15). Therefore, inhibition of pSTAT3^{Tyr705} by VS-43 induces apoptosis in these cancer cell lines.

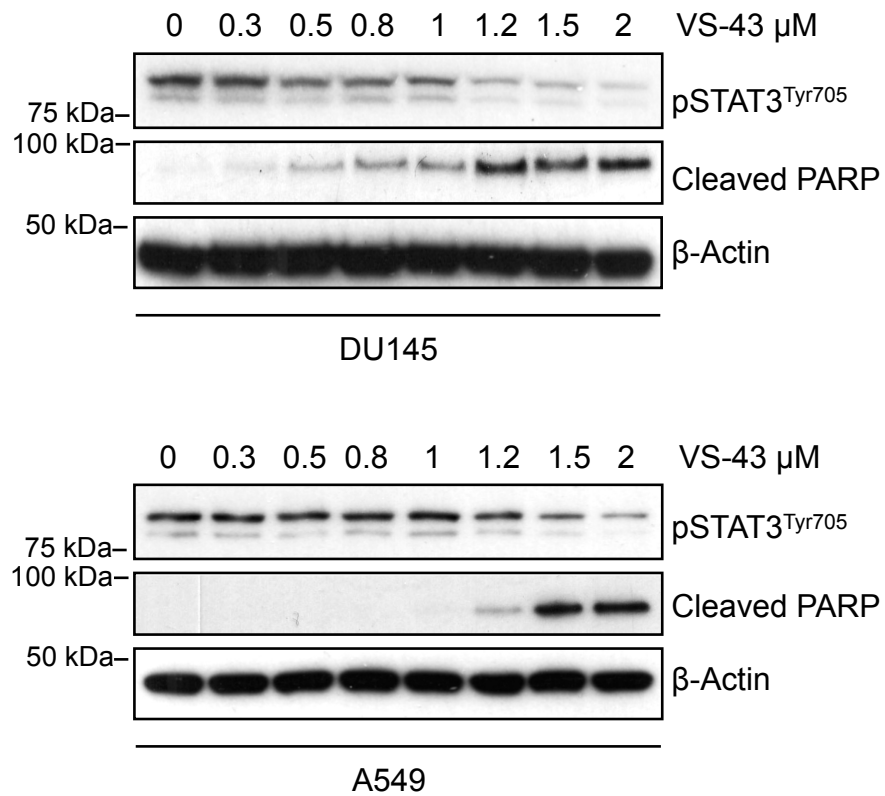


Figure 3-15: Treatment of DU145 and A549 cells with VS-43 for 18 hours results in a dose-dependent increase in cleaved PARP expression, indicative of apoptosis. This expression is inversely proportional to STAT3 inhibition by VS-43. Blots are representative of more than 1 experiment.

3.4 Discussion

As STAT3 is frequently constitutively activated in cancer cell lines and involved in the regulation of many oncogenic pathways, it is a viable target for novel anti-cancer therapeutics.

Here, the initial investigation of a novel synthetic compound, VS-43, has yielded promising results. VS-43 has been shown to specifically inhibit activated STAT3 at low micromolar concentrations in both prostate and lung cancer cell lines, inducing apoptosis and cell growth inhibition.

Studies using proteasome inhibitors and/or protein synthesis inhibitors would aid in confirming that the decrease in pSTAT3^{Tyr705} seen in this chapter is due to inhibition of STAT3 activation rather than an effect on the stability of the STAT3 protein. However, given whole STAT3 levels are unaffected by VS-43 treatment, this is unlikely.

Cell confluency directly correlates with pSTAT3^{Tyr705} levels and therefore, also with the efficacy of inhibition by VS-43. This effect was first noted in 2003 and was attributed to cell-cell interactions and lower CDK2 levels rather than external cytokines or growth factors. CDK2 is hypothesised to inhibit STAT3 activation through interaction with STAT3 inhibitory proteins such as SOCS3 (Steinman et al., 2003), however, this hypothesis has not been proven. In confluency, STAT3 activation acts to promote survival rather than proliferation (Steinman et al., 2003). Due to this effect, a confluency of 70% was chosen for all experiments where cells were to be drug treated. This percentage was chosen so that a significant amount of target, pSTAT3^{Tyr705}, would be present whilst allowing cells to maintain their proliferative phenotype. The effect of confluency on pSTAT3^{Tyr705} expression is scarcely mentioned in studies investigating novel STAT3 inhibitors. Certainly, for *in vivo* studies with STAT3 inhibitors, the effect of cell density and 3D organisation

within the organism must be considered and potentially higher doses of the inhibitor used to account for this should the same relationship be found.

3.4.1 How does VS-43 bind to STAT3?

Whilst no modelling of VS-43 binding the STAT3 monomer has yet been completed, the mechanism by which VS-43 inhibits STAT3 can be predicted based on structural similarities with other STAT3 inhibitors.

Many novel STAT3 inhibitors, including VS-43, are derived from curcumin which exists in both keto and enol forms. However, only the diketone form of curcumin can interact with the STAT3 SH2 domain (Lin et al., 2010a). The design of the JAK2/STAT3 inhibitor FLLL32 (Figure 3-16) utilised this property by locking its structure in the diketone formation. This inhibitor has been shown to bind the SH2 domain of STAT3 and thus block dimerisation, like many STAT3 inhibitors (Bill et al., 2012).

As described in the introduction to this chapter, VS-43 was rationally designed, starting with the DAP class of compounds. Two of these compounds, HO-3867 and H-4073, have been shown to bind to the DNA binding domain of STAT3, directly blocking DNA binding and thus downstream activation of the STAT3 pathway (Kalai et al., 2011; Rath et al., 2014). HO-3867's arylidene groups preferentially bind to pockets within the DNA binding domain lined with polar amino acids whereas its pyrroline-nitroxide group binds in a non-polar pocket (Kalai et al., 2011). Kalai et al. performed molecular modelling of HO-3867 bound to the STAT3 DNA binding domain (Figure 3-17A), and in this model the hydrophobic binding pocket is seen clearly. Another STAT3 inhibitor, inS3-54, has also been demonstrated to bind the DNA binding domain, with its phenyl group binding in the same hydrophobic pocket as was identified for HO-3867 (Figure 3-17B) (Huang et al., 2016, 2014).

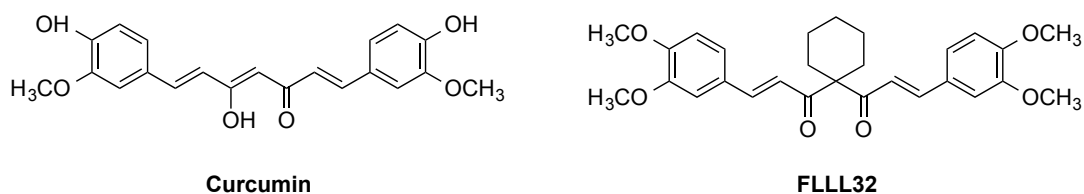


Figure 3-16: Structures of curcumin and FLLL32.

This group also modelled the interaction of their inhibitor with the STAT1 DNA binding domain (Figure 3-17C) and found that the natural conformation of binding was strikingly different to that seen with STAT3. This fit had an unfavourable binding energy, and if the STAT3 binding confirmation of inS3-54 is adopted, a steric clash between the inhibitor and residues T327 and P326 occurs, therefore, binding of this structure to STAT1 is not favourable. This could account for the selectivity seen with STAT3 DNA binding domain inhibitors. While curcumin has been shown to inhibit pSTAT1^{Tyr701} (Bill et al., 2012), both inS3-54 and HO-3867 demonstrated selectivity for STAT3 over STAT1 (Huang et al., 2016; Rath et al., 2014). VS-43 also demonstrates STAT3 selectivity. Interestingly the selectivity of the H-4073 compound has not been addressed in the literature.

H-4073 lacks a central, axial bulky group (see structures in Figure 3-18) therefore, whether this reduces the selectivity of H-4073 due to a loss of interaction with STAT3's hydrophobic pocket would be an interesting observation.

In these docking models, the orientation of the inhibitors represents a "chair" conformation, with an axially orientated hydrophobic group binding to the hydrophobic binding pocket. Computational 3D modelling of VS-40, a compound similarly structured to VS-43, was performed in order to determine the conformation of this novel class of compounds in 3D space. Figure 3-17D and Figure 3-17E show the 3D structure of VS-40 from the front and side views, respectively. VS-40 adopts

a structure that would likely be capable of binding the STAT3 DNA binding domain – with the N-phenyl group positioned axially, maximising interaction with the hydrophobic binding pocket. VS-43 is very similar in structure to VS-40, with the only modifications being the substitution of the phenyl groups with trimethoxyphenyl groups. The structure of VS-43 was chosen with a view to increasing the interaction of the compound with both the polar and non-polar regions of the STAT3 DNA binding domain through the modification of the bis(arylidene) groups and the incorporation of an N-phenyl group.

Therefore, VS-43 most likely inhibits STAT3 via an analogous mechanism of action to the similarly structured compounds discussed here, binding to the STAT3 DNA binding domain rather than the commonly targeted SH2 domain. The structures of HO-3867, H-4073, inS3-54 and VS-43 for comparison are shown in Figure 3-18.

Interestingly, STAT3 inhibitors targeting the DNA binding domain are often seen to down-regulate STAT3 Tyr705 phosphorylation (Huang et al., 2016; Rath et al., 2014). This is also the case for VS-43, despite the phosphorylation event occurring in the SH2 domain. A possible explanation could be that binding of a compound to the DNA binding domain of STAT3 renders the activating phosphorylation site inaccessible to kinases. As the DNA binding domain is located adjacent to the SH2 domain in STAT3 (Figure 3-1A), inhibitor-induced conformational changes in the DNA binding domain could be transferred to the SH2 domain. However, detailed modelling of the full STAT3 protein bound to a DNA binding domain inhibitor would be required to confirm this. Another explanation could be that these inhibitors are actually capable of binding to two sites on the STAT3 monomer – the DNA binding domain and the SH2 domain. The relatively similar chemical structures of the SH2 domain inhibitors curcumin and FLLL32 with the DNA binding inhibitors such as those discussed here could suggest a model where one inhibitor can target the

STAT3 protein in two ways, blocking both phosphorylation and DNA binding. This has, however, not yet been investigated for any STAT3 inhibitor.

Therefore, it is proposed here that VS-43 acts to inhibit STAT3 activation and DNA binding through inhibition of the DNA binding domain. This may result in a decrease in pSTAT3^{Tyr705} levels through conformational changes in the STAT3 protein or a dual binding mechanism. Further investigation would be required to confirm this.

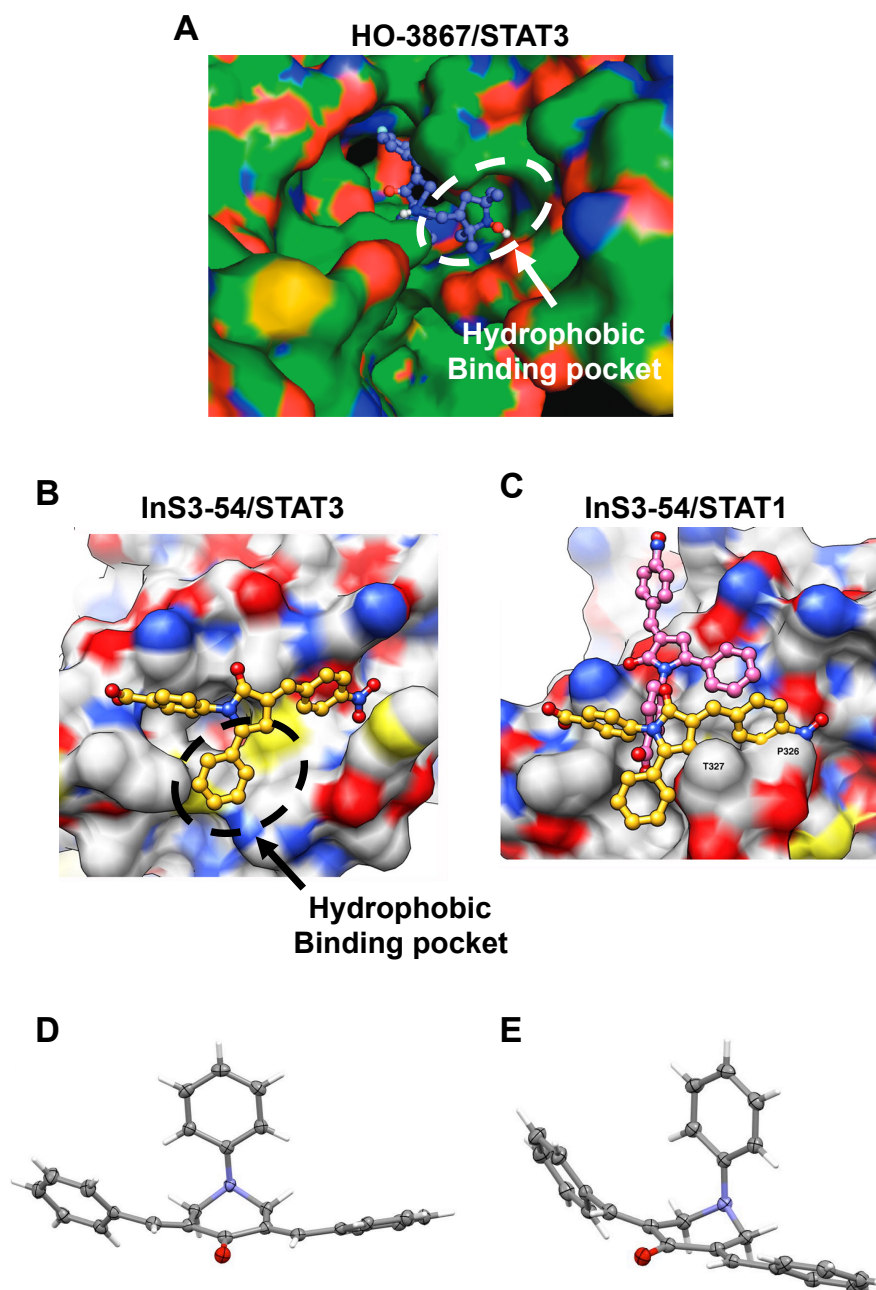


Figure 3-17: Molecular modelling and conformation of inhibitors targeting the STAT3 DNA binding domain. A) molecular modelling of HO-3867 binding to the DNA binding domain of STAT3 (Kalai et al., 2011). B) molecular modelling of inS3-54 binding to the DNA binding domain of STAT3 (Huang et al., 2014). C) molecular modelling of inS3-54 binding to the DNA binding domain of STAT1 – purple represents the natural fit with an unfavourable binding energy. Yellow represents forced binding of inS3-54 in the same conformation as for STAT3 binding (Huang et al., 2014). D) 3D structure of VS-40, a compound related to VS-43, from the front and side (E) view, (unpublished data, courtesy of M. Lee, April 2016).

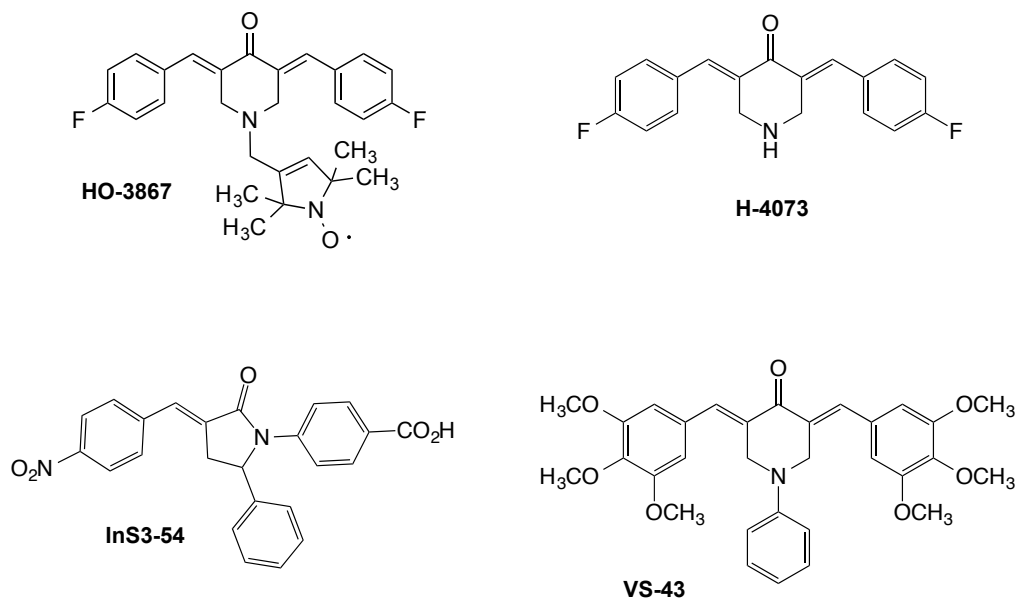


Figure 3-18: The molecular structures of STAT3 DNA-binding domain inhibitors: HO-3867, H-4073 and InS3-54, and the structure of VS-43 for comparison.

3.4.2 How does VS-43 compare to other STAT3 inhibitors?

Direct comparison of inhibitor potency is complex. Here the influence of cell line, cell confluency and duration of treatment on inhibitor potency has been highlighted (section 3.3.5). These factors almost always vary between experiments with novel STAT3 inhibitors. Therefore, this must be kept in mind when making direct comparisons relating to inhibitor potency.

First, a comparison with the similarly structured DNA binding domain inhibitors will be made. Approximately 50% pSTAT3^{Tyr705} inhibition was observed after treatment of cells with 1-1.5 μ M VS-43 for 18 hours (Figure 3-5). For the HO-3867 and H-4073 analogues, a 24 hour treatment with 10-20 μ M was required for inhibition of the pSTAT3^{Tyr705} pathway (Selvendiran et al., 2011, 2010). This is both a higher concentration and a longer duration of drug treatment.

The inS3-54 derivative, A18, exhibited GI_{50} values of 3.2-4.7 μ M after treatment of cancer cell lines for 72 hours continuously (Huang et al., 2016). This is a much longer duration of drug treatment and again at higher concentrations than was observed for VS-43. The GI_{50} range for VS-43 was between 1.4-2.5 μ M after 18 hours of drug treatment (Figure 3-14). It should be noted that the inS3-54 derivative was tested with A549 cells, with a resulting GI_{50} of approximately 4 μ M therefore, these results are comparable with the GI_{50} obtained for VS-43 in A549 cells which was lower at 2.53 μ M. As VS-43 has been shown here to be more potent than these similarly structured curcumin analogues, the structural modifications made during the design of VS-43 may have enhanced binding to the STAT3 DNA binding domain. Additionally, VS-43 exhibits superior water solubility over BB-IV-101, another DAP compound (200 μ M versus 70 μ M, M. Lee personal communication) (structure shown in Figure 3-19). Structurally, VS-43 is identical to BB-IV-101 except for the addition of N-phenyl group. Therefore, this group may enable salt formation as predicted, and could allow VS-43 more favourable pharmacokinetics than have been seen with curcumin in clinical trials.

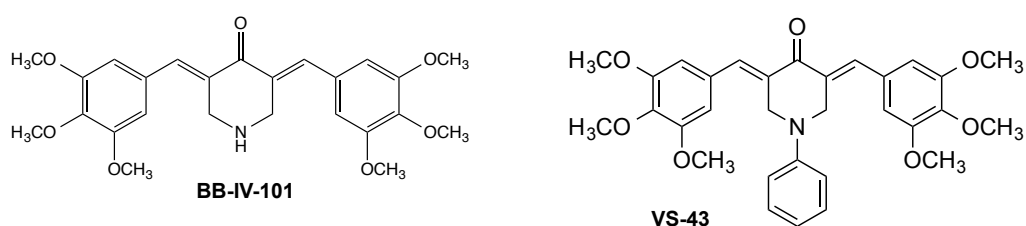


Figure 3-19: Structures of BB-IV-101 and VS-43.

Next, a comparison of VS-43 against the more common class of SH2 domain STAT3 inhibitors will be made. The S3I-201 derivative S3I-1757 was used for an 18 hour treatment period as used for VS-43 in this study. Concentrations of 50-200 μ M were required for pSTAT3^{Tyr705} inhibition by S3I-1757 which is much higher than the low micromolar doses of VS-43 used here (Zhang et al., 2013). A second comparison can be made to the dual JAK2/STAT3 inhibitor cucurbitacin I where with an 18 hour treatment, the median GI₅₀ value across a panel of six patient-derived leukemia cell lines was 5 μ M (Ishdorj et al., 2010). Cryptotanshinone, the natural STAT3 inhibitor, has been studied in DU145 cells and was found to have a GI₅₀ of 7 μ M after a 24 hour treatment period (Shin et al., 2009). Many other synthetic STAT3 inhibitors are administered for 24, 48 or 72 hours (Bill et al., 2012; Huang et al., 2016; Hutzen et al., 2009; Lin et al., 2010b; Page et al., 2011; Selvendiran et al., 2011, 2010; Siddiquee et al., 2007; Song et al., 2005; Uehara et al., 2009) The longest drug treatment with VS-43 carried out here was 18 hours. Therefore, a 72 hour exposure time with VS-43 would likely require sub-micromolar doses.

These studies indicate that VS-43 is considerably more potent than many other synthetic STAT3 inhibitors. However, in order to make a conclusive and true comparison between VS-43 and other inhibitors, the same cell line, treatment time and cell confluency would have to be employed, therefore, these comparisons are somewhat useful but more detailed and controlled comparisons would be required. For example, the studies performed in this thesis with stattic and curcumin are directly comparable to the results presented for VS-43 and it can therefore, be concluded that VS-43 is a more potent STAT3 inhibitor than either of these compounds.

The dependency of efficacy on exposure time indicates that other drug treatment regimes could be investigated. For example, a shorter exposure time to a higher

concentration of VS-43 may be more or less detrimental to cell growth. In this chapter this concept has begun to be investigated – the ability of VS-43 to specifically inhibit STAT3 activation and DNA binding after just a 1 hour drug treatment time has been shown using the TransAM[®] STAT Family ELISA assay (Figure 3-12). Different treatment regimes will be investigated further in the combination studies included in the next chapter.

In section 3.3.6, the inhibition of pSTAT3^{Tyr705} by VS-43 is demonstrated to persist for at least 24 hours post-treatment, suggesting that VS-43 may bind to STAT3 irreversibly. Stattic has been suggested to be an irreversible STAT3 inhibitor, possibly through covalent binding to the STAT3 monomer (Heidelberger et al., 2013; Schust et al., 2006). The inhibition of STAT3 activation by curcumin has however, been shown to be reversible, with pSTAT3^{Tyr705} levels returning to normal after 24 hours in drug free media (Bharti et al., 2003a). Therefore, the structural modifications made during the design of VS-43 may have increased the interaction with STAT3 sufficiently to allow for irreversible binding.

3.4.3 Why is VS-43 potency cell line dependent?

In this chapter, differences between cell line sensitivity to VS-43 have been observed. The DU145 cell line is more sensitive to VS-43 than the A549 cell line. This is the opposite of what would be expected as DU145 cells express higher levels of pSTAT3^{Tyr705} than A549 cells. Therefore, if the same rule were to apply as for confluency, higher doses of VS-43 should be required to induce pSTAT3^{Tyr705} inhibition and cell growth inhibition in DU145 cells. This is, however, not the case, implying that other factors determine a cell line's sensitivity to VS-43. This may be related to impaired drug uptake or enhanced drug efflux. Considering drug efflux mechanisms, the multidrug resistance transporter P-glycoprotein (P-gp) is expressed at high levels in A549 cells (Hamilton et al., 2001; Xu et al., 2014) and

low to undetectable levels in DU145 cells (Brussel et al., 1999). P-gp is a broad specificity ABC transporter that uses energy from ATP to shuttle compounds, including synthetic drugs as well as natural toxins, across the cell membrane. This transporter is known to participate in the resistance to natural product-based anti-cancer agents such as doxorubicin and paclitaxel, through facilitating efflux of the drug (Mechetner et al., 1998; Sarkadi et al., 2006). Therefore, a higher expression level of P-gp may contribute to the lower sensitivity of A549 cells to VS-43 seen here if this compound is a substrate for P-gp mediated efflux. If indeed VS-43 is a substrate for P-gp then sensitivity to this compound could be predicted based on P-gp expression levels.

3.4.4 How does STAT3 inhibition induce apoptosis?

In this chapter, VS-43 is confirmed to induce cellular apoptosis through the induction of cleaved PARP expression (Figure 3-15). As STAT3 activation promotes cell survival, inhibition of this pathway blocks these survival signals, allowing for apoptosis. STAT3 promotes survival through the transcriptional regulation of anti-apoptotic genes such as bcl-xl and survivin (Buettner et al., 2002; Gritsko et al., 2006). Bcl-xl is a member of the bcl-2 family of proteins which act to inhibit apoptosis by preventing the release of mitochondrial cytochrome C into the cytoplasm – an event that leads to activation of the apoptotic caspase cascade (Kharbanda et al., 1997). Survivin is a member of the Inhibitor of Apoptosis (IAP) family of proteins. Survivin acts alongside a cofactor to directly bind and inhibit caspase-9 in the apoptosis cascade. Survivin also plays an essential role in mitosis, ensuring the correct separation of the chromosomes in cytokinesis (Mita et al., 2008). Both bcl-xl and survivin have been shown here to be down-regulated by treatment of DU145 cells with VS-43 (Figure 3-13).

Other survival genes proposed to be regulated by STAT3 but not investigated here also include Mcl-1 (Epling-Burnette et al., 2001), a member of the bcl-2 anti-apoptotic protein family, and bcl-2 itself (Choi and Han, 2012). Additionally, genes driving proliferation which are regulated by STAT3 include cyclin D1 (Bromberg et al., 1999) and c-Myc (Kiuchi et al., 1999). Therefore, the overall effect of inhibiting STAT3 activation would be a decrease in cell proliferation and induction of apoptosis.

The induction of apoptosis seen here by VS-43 can therefore, be attributed to the down-regulation of the anti-apoptotic, survival, and proliferation-stimulating genes regulated by STAT3.

3.5 Conclusion

In conclusion, the novel compound VS-43 has been shown to successfully down-regulate pSTAT3^{Tyr705} levels in both DU145 and A549 cells at concentrations of 2 μ M and below. VS-43 also inhibits STAT3's ability to bind to consensus DNA binding sites and its action on STAT3 is specific: this compound does not inhibit STAT1 or STAT5. Inhibition of STAT3 phosphorylation and DNA binding is achieved at lower doses than with stattic or curcumin, indicating that VS-43 is a potent STAT3 inhibitor.

VS-43 induces programmed cell death in the DU145 and A549 cell lines with GI₅₀ values of 1.43 μ M and 2.53 μ M, respectively, and does so by down-regulating STAT3 target genes including bcl-xl and survivin.

Therefore, VS-43 is a novel, potent and selective STAT3 inhibitor, and a valid compound for potential use as an anti-cancer therapeutic. Further investigation into the use of VS-43 in combination with chemotherapy agents will be described in the following chapter.

Chapter 4 STAT3 inhibitors sensitise cancer cells to cisplatin

4.1 Introduction

The chemotherapy platinum drug cisplatin has been used in the clinic for nearly 40 years since it was approved in 1978 to treat cancer. Unfortunately, resistance to cisplatin therapy is a common occurrence either as intrinsic resistance or as acquired resistance after an initial period of sensitivity to cisplatin. Understanding why resistance occurs is essential in the design of novel sensitising agents that may help to overcome cisplatin resistance.

4.1.1 Resistance mechanisms to Cisplatin

There are many factors that contribute towards cisplatin resistance; the key concepts will be discussed here.

Resistance can occur through the altered accumulation of cisplatin within tumour cells. As for all drugs delivered systemically, the patient's pulse and blood pressure, as well as tumour location and type, can affect the accumulation of cisplatin at the tumour site itself. This can directly impact the concentration of cisplatin in tumour cells. Cisplatin accumulation at the tumour site can also be affected by diet as this regulates the extracellular pH and only an acidic extracellular pH is favourable for cisplatin uptake into cells (Stewart, 2007). Additionally, cisplatin binds plasma proteins irreversibly which lowers its activity due to reduced uptake (Vermorken et al., 1984), and the composition of the plasma membrane has also been postulated to play a role in resistance, as membranes with a higher cholesterol content are more rigid and therefore, allow less cisplatin into the cell via passive diffusion (Todor et al., 2012). Consequently, there are many patient specific physiological and genetic factors that can reduce cisplatin efficacy before it has even reached the tumour cells.

Cisplatin uptake at the cellular level is also believed to contribute to clinical resistance. The effectiveness of cisplatin as a chemotherapy agent has been directly linked to cellular cisplatin concentration in both *in vitro* and *in vivo* studies (Andrews et al., 1988; Kim et al., 2012). Uptake is, in part, mediated via the copper membrane transporter CTR1 therefore, resistance to cisplatin can occur when the expression of this transporter is reduced (Kilari, 2016). Cells deficient in CTR1 are less sensitive to cisplatin (Ishida et al., 2002). However, resistance is more commonly associated with drug efflux. The CTR2 copper transporter has been suggested to be involved in cisplatin efflux. Whilst closely related to CTR1, opposite functionality has been observed, with decreased expression of CTR2 resulting in higher cellular cisplatin levels (Blair et al., 2009). Another transporter involved in cisplatin efflux is the Multidrug Resistance Protein 2 (MRP2), an ABC transporter membrane pump. One study demonstrated a 10-fold increase in resistance following transfection of MRP2 (Cui et al., 1999).

The copper transporter proteins ATP7a and ATP7b have also been shown to have similar effects on cisplatin resistance in human cell lines – the overexpression of both of these transporters correlates with poor cisplatin sensitivity (Komatsu et al., 2000; Samimi et al., 2004; Siddik, 2003).

The inactivation of cisplatin inside the cell can also contribute to resistance. Higher cellular glutathione levels have been reported to correlate with cisplatin sensitivity (Fokkema et al., 2002; Meijer et al., 1992). Glutathione is thought to bind to cisplatin, preventing it binding the DNA therefore, lowering platination. Glutathione-S-transferase (GST) levels have also been shown to correlate with cisplatin resistance (Byun et al., 2005). The GST- π isoform is considered the main isoform involved in resistance to cisplatin. A greater clinical response to cisplatin has been linked to lower GST- π levels (Nishimura et al., 1996), and gene amplification of GST- π has been reported in head and neck cancer (Cullen et al., 2003). It has been

suggested that this enzyme may catalyse the addition of glutathione to cisplatin, resulting in its inactivation (Stewart, 2007). The cellular level of metallothionines has also been linked to cisplatin resistance (Kelley et al., 1988). These thiol-containing species, like GSH, bind to and inactivate cisplatin directly, preventing the formation of cisplatin-DNA adducts.

Cisplatin binding to DNA can also be affected by intra-cellular pH, with a more acidic environment favouring DNA binding. Accordingly, resistant cell lines have been shown to harbour up-regulated proton pumps which increase cellular pH (Urakami et al., 2001).

Some resistance mechanisms act indirectly. The MAPK pathway has been investigated as a mediator of cisplatin resistance as several of its target genes are anti-apoptotic (c-Myc), regulate DNA repair (ERCC1) or increase intracellular thiol levels (GST, Metallothionine) which can all individually contribute to cisplatin resistance (Dempke et al., 2000). Other examples include inhibiting apoptosis by suppressing caspase activation or increasing anti-apoptotic Bcl-2 family proteins – in ovarian cancer Bcl-xL expression correlates with resistance to cisplatin and a reduction in disease-free survival (Williams et al., 2005). The STAT3 pathway has also been suggested to be involved in cisplatin resistance through the regulation of apoptosis (Stewart, 2007), and mutation or loss of p53 functionality has been reported to be involved in resistance; half of all cancers and 60% of NSCLCs have p53 mutations (Giaccone, 2000; Siddik, 2003; Stewart, 2007). Some less well characterised factors contributing to clinical cisplatin resistance include the heat-shock proteins, cyclooxygenase-2 and the kinase SRPK1 (Stewart, 2007).

Heightened repair of cisplatin-DNA adducts has also been reported as a mechanism of resistance. In ovarian cancer, patients with higher levels of platinated DNA showed the best responses to cisplatin (Reed et al., 1987), and cell lines which

exhibited reduced removal of platinum from DNA after treatment also showed greater sensitivity to cisplatin (Köberle et al., 1997). A more recent study on patient derived ovarian tumour cells showed that repair of cisplatin-induced ICLs is enhanced in cells taken from patients previously exposed to cisplatin which may indicate the development of acquired resistance through enhanced DNA repair (Wynne et al., 2007). Genetic mutations and protein over-expressions for various factors involved in DNA repair processes including BER, NER, MMR, TLS, and HR have been connected to cisplatin resistance, however, these will be discussed in detail in Chapter 5.

Therefore, many different factors contribute to cellular cisplatin resistance, and there are subsequently many opportunities to intervene in these processes in order to re-sensitise to cisplatin.

4.1.2 Cisplatin-based combination treatments in cancer

The use of a combination of drugs rather than a single agent to treat cancer is common. The idea behind combination therapy is that two or more pathways driving the cancer are interfered with, thus increasing the overall effect of the treatment. Additionally, combining drugs with non-overlapping toxicities are often used so that if one drug has a dose-limiting adverse effect, combination therapy can enhance the overall chemotherapeutic effect without increasing that toxicity. Currently, cisplatin is given in combination with a large number of other drugs including gemcitabine, flurouracil, topotecan, docetaxel, etoposide, vinorelbine, pemetrexed, capecitabine and trastuzumab (Macmillan.org.uk). These drug combinations are beneficial for the treatment of many different cancer types; however, the drugs combined with cisplatin often have independent mechanisms of action rather than targeting cisplatin resistance. In order to circumvent cisplatin resistance, the additional drug

used should interfere with resistance mechanisms, thereby having a synergistic effect in combination with cisplatin.

One such combination that uses this approach is the use of DNA damage response inhibitors with cisplatin. Mohni et al. demonstrated that ATR inhibitors synergise with cisplatin in human cancer cell lines (Mohni et al., 2015). There are currently three phase I clinical trials investigating the combination of the ATR inhibitor VX-970 with cisplatin (trial identifiers: NCT02723864, NCT02567409, NCT02567422).

The PARP inhibitor olaparib has also demonstrated synergy in combination with cisplatin *in vitro* (Evers et al., 2008) and has had positive results as a combination in a Phase I trial for advanced breast and ovarian tumours with BRCA1/2 mutations (Balmaña et al., 2014). This combination is currently in several other trials including a Phase I clinical trial for advanced solid tumours (trial identifier: NCT00782574). PARP inhibitors act to block the function of PARP in single strand break DNA repair, therefore, in a homologous recombination deficient background (such as BRCA1/2 mutated individuals), these breaks persist and manifest into double strand breaks which causes cellular apoptosis. This is known as synthetic lethality. However, the mechanism by which PARP inhibitors synergise with cisplatin is not clear, as cisplatin does not induce SSBs. Studies regarding the selectivity of PARP inhibitors for other DNA repair proteins may give further information on a mechanism for synergy.

As well as DNA repair, combinations targeting cisplatin cellular uptake have been investigated. The problem of cellular pH in cisplatin resistance is addressed in a phase II clinical trial of the proton pump inhibitor esomeprazole in combination with cisplatin. This combination improved time to progression and overall survival in patients with metastatic breast cancer (Wang et al., 2015). As cisplatin uptake and efflux mechanisms overlap with the transport of copper ions, a phase I clinical trial of

a copper chelator in combination with cisplatin has been carried out. This trial also yielded some promising results, with one patient demonstrating a partial response (S. Fu et al., 2012).

With the knowledge of resistance mechanisms continually increasing, cisplatin-based combination regimens will improve with the use of drugs that target these pathways.

4.1.3 STAT3 Inhibitors and Cisplatin

The relationship between STAT3 inhibition and cellular sensitivity to cisplatin is one that has been reported frequently. As mentioned in the previous section, whilst no direct effect of STAT3 inhibitors on cisplatin resistance mechanisms has been reported as of yet, the involvement of STAT3 in the regulation of apoptosis makes STAT3 a promising target for combination with cisplatin. Compounds that target STAT3 directly or indirectly through the inhibition of upstream factors or negative regulators have been described to enhance cisplatin sensitivity.

There are several natural STAT3 inhibitors that have been shown to act as chemosensitisers to cisplatin both *in vitro* and *in vivo*. These include curcumin (Goel and Aggarwal, 2010; Notarbartolo et al., 2005; Yallapu et al., 2010; Ye et al., 2012) and resveratrol (Weiguo Zhao et al., 2010). Cucurbitacin I is another natural compound reported to sensitise cancer cells to cisplatin in mouse tumour models. In this study enhanced reductions in tumour volume and prolonged survival were demonstrated with the combination therapy (Tseng et al., 2012).

Synthetic inhibitors of STAT3 activity have also been reported to sensitise cells to cisplatin. Many synthetic curcumin analogues including HO-3867 (Selvendiran et al., 2011), H-4073 (Kumar et al., 2014), and FLLL32 (Abuzeid et al., 2011) have demonstrated reduced cell viability and increased apoptosis when combined with

cisplatin treatment. Other synthetic STAT3 inhibitors shown to enhance cisplatin sensitivity include Stattic (Ji et al., 2013; Pan et al., 2013), 5,15-DPP (Huang et al., 2012), YC-1 (Lau et al., 2007), and OPB-31121 (M. J. Kim et al., 2013).

Compounds targeting upstream activators of STAT3 have demonstrated success in combination with cisplatin. These include inhibitors of JAK2 (Catlett-Falcone et al., 1999; Hu et al., 2014; Zhang et al., 2015) and EGFR (Feng et al., 2007). The negative regulation of STAT3 has been targeted using adenoviral delivery of the SOCS1 gene, a suppressor of cytokine signalling. SOCS1 delivery was shown to down-regulate STAT3 signalling and to enhance cisplatin-mediated apoptosis *in vitro*. Additionally this combination inhibited tumour growth in mouse xenografts, although this was also in combination with pemetrexed (Iwahori et al., 2013).

The sheer number of studies reporting positive outcomes from combination of STAT3 inhibitors and cisplatin reinforces the potential for this combination in the clinic. A novel STAT3 inhibitor with increased potency and selectivity would be most beneficial in combination with cisplatin to combat resistance. In this chapter the interaction of STAT3 inhibitors with cisplatin will be investigated. The novel inhibitor VS-43 will be compared against stattic and curcumin in terms of the outcome of combination with cisplatin, and the wider range of use for STAT3 inhibitors in chemotherapy combinations will be investigated through the combination of VS-43 with another chemotherapy agent, doxorubicin.

4.2 Aims

The aims regarding the investigation of STAT3 as a chemosensitising agent were as follows:

1. To determine whether STAT3 inhibitors enhance the cell growth inhibitory effect of cisplatin on cancer cell lines and whether these combinations are synergistic.
2. To compare VS-43 against stattic and curcumin as a chemosensitising agent.
3. To determine whether combination treatment with STAT3 inhibitors and cisplatin enhances apoptosis in cancer cell lines as opposed to single drug treatment.
4. To investigate the ability of VS-43 to chemosensitise cells to doxorubicin.

4.3 Results

4.3.1 Stattic and Curcumin inhibit the growth of cancer cell lines

The effect of the combination treatment of cells with STAT3 inhibitors and cisplatin will first be observed using the commercially available STAT3 inhibitors stattic and curcumin. As Chou-Talalay analysis of a combination treatment consisting of two drugs requires the dose-effect curves of each drug alone to be known (Chou, 2010), first the growth inhibition induced by stattic and curcumin alone was determined by SRB assay.

As with VS-43 in Chapter 3, the DU145 cell line is more sensitive to growth inhibition by both stattic and curcumin than the A549 cell line. Cells were treated with the STAT3 inhibitors for a period of 18 hours before media replacement and incubation for 96 hours.

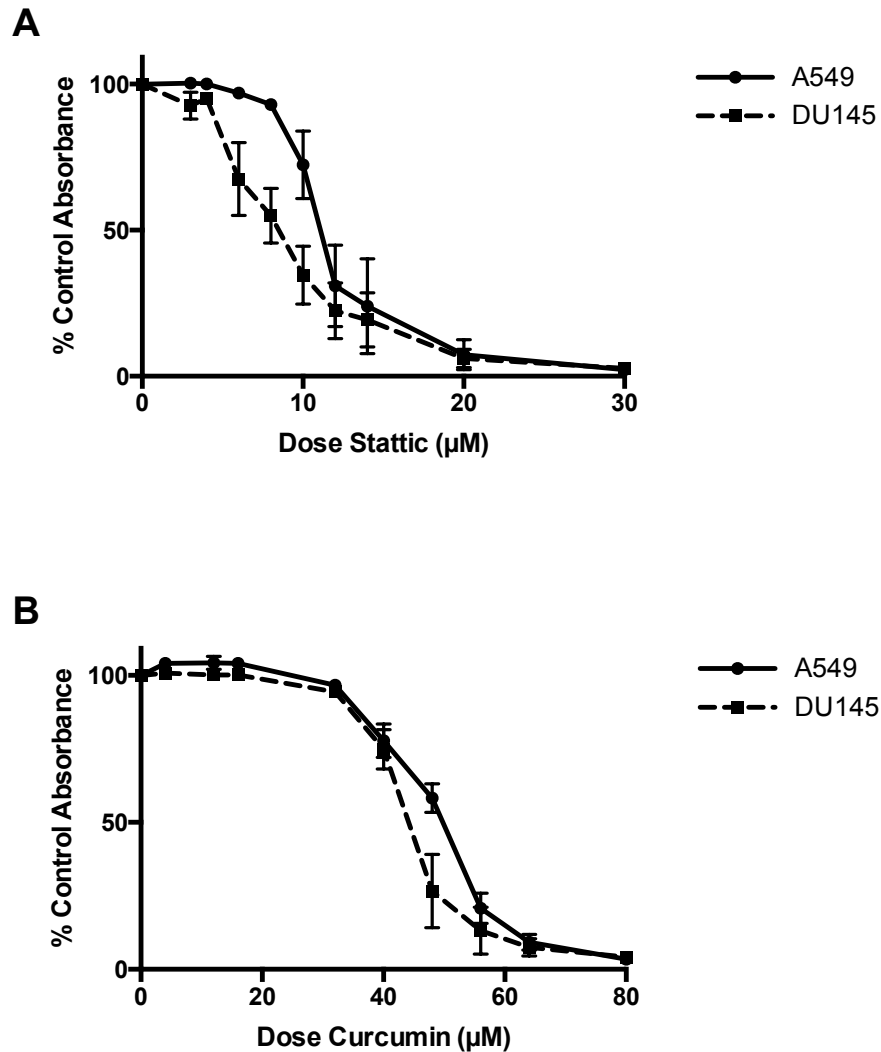


Figure 4-1: A) Static and B) curcumin inhibit cell growth in the DU145 and A549 cancer cell lines. Data plotted was obtained by SRB assay and is the average of at least three individual experiments with SEM calculated for error bars.

The GI_{50} values for static are $8.21\mu\text{M}$ and $11.2\mu\text{M}$ in the DU145 and A549 cell lines, respectively (Figure 4-1A). The GI_{50} values for curcumin are $44.2\mu\text{M}$ and $48.6\mu\text{M}$ in the DU145 and A549 cell lines, respectively (Figure 4-1B).

4.3.2 Cisplatin inhibits growth of DU145 and A549 cancer cell lines

The growth inhibition induced by treatment of cells with cisplatin was also assessed by SRB assay. Two treatment schedules were tested: an acute 1 hour treatment and a continuous treatment whereby cisplatin was present for the duration of the SRB assay incubation time (96 hours). In the A549 cell line GI_{50} values were

57.5 μ M and 4.00 μ M for the 1 hour and continuous treatments, respectively (Figure 4-2A). In the DU145 cell line GI_{50} values were 49.8 μ M and 3.00 μ M for the 1 hour and continuous treatments, respectively (Figure 4-2B). As the aim of this chapter was to observe sensitisation to cisplatin, the acute 1 hour cisplatin treatment was chosen for the combination studies. This was to aid the observation of any benefit of the combination by using a treatment regime with a lower initial effect on cell growth.

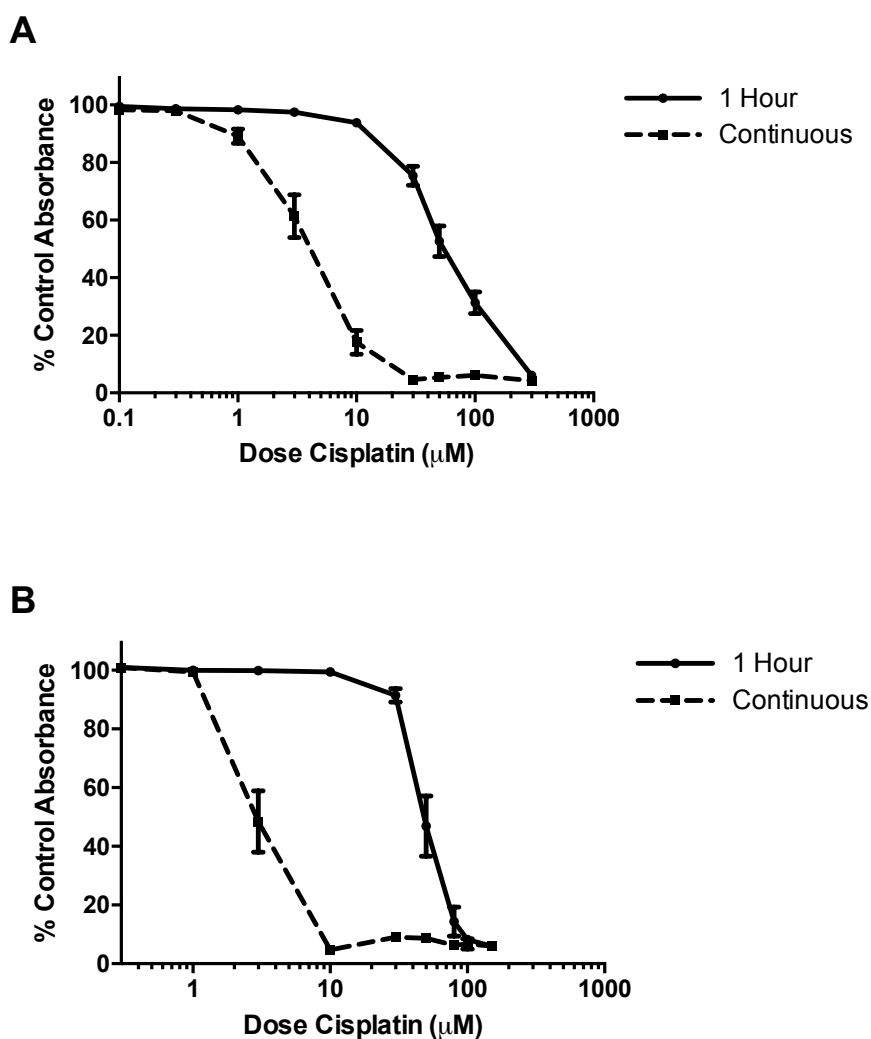


Figure 4-2: Cisplatin inhibits cell growth in the A) A549 and B) DU145 cancer cell lines. Data plotted was obtained by SRB assay is the average of at least three individual experiments with SEM calculated for error bars.

4.3.3 Stattic and curcumin sensitise cancer cell lines to cisplatin with moderate synergy

The fixed ratio drug combination regime was chosen to observe the interaction between STAT3 inhibitors and cisplatin. This ratio is recommended when both drugs have a similar dose-effect curve. Here, the dose-effect curves for stattic, curcumin and cisplatin are all growth inhibitory and are sigmoidal in shape (Bijnsdorp et al., 2011). Ratios of 1:5 for stattic:cisplatin and 4:5 for curcumin:cisplatin were chosen based on the approximate GI_{50} values of the drugs alone. Cells were treated with one of the STAT3 inhibitors for 18 hours, followed by a 1 hour treatment with cisplatin. After drug treatment, the media was replaced and cells were incubated for 96 hours before SRB staining. The decision to treat cells with the STAT3 inhibitors first was made based on the hypothesis that if STAT3 inhibitors interact with one of the cisplatin resistance mechanisms, this pathway would need to be down-regulated prior to cisplatin entering the cell. Therefore, STAT3 inhibitors were given as a pre-treatment to cisplatin.

Figure 4-3 details the combination of stattic and cisplatin in the A549 cell line. The GI_{50} value for cisplatin was reduced from 82.1 μ M to 27.8 μ M after pre-treatment with stattic (Figure 4-3A). This is a 66.1% decrease in cisplatin GI_{50} . By observing changes in GI_{50} values, it can be determined whether a drug combination is more efficient at cell growth inhibition than a single drug, however, this does not tell us whether the drug combination is synergistic. This is a factor that many studies stating chemosensitisation to one drug by another do not address. CI value analysis is required to determine whether a drug combination is synergistic, additive or antagonistic. Synergy occurs when the overall effect is greater than the sum of the effect of the two drugs individually. If the effect is equal to the sum of the individual effects then the drug combination is additive and if the combinatory effect is less than the sum of the individual effects then the drug combination is antagonistic. A

synergistic effect is desirable as this allows for a greater therapeutic benefit with lower drug doses, which may reduce adverse effects. CI value analysis was carried out using the Calcosyn software as detailed in section 2.6.4.

Figure 4-3B shows the CI values for this combination. The majority of CI values are in the “slight synergism” to “moderate synergism” range (see section 2.6.4 for synergy range definitions), with the lowest CI value of 0.802 occurring at 50 μ M cisplatin.

Isobolograms for fixed ratio combinations are interpreted through the relative position of the data points in relation to each of the effect level lines. The effect level lines are drawn between the doses of each drug alone required to achieve that effect. A data point located below and to the left of the associated line implies synergy at that effect level. If the point is above and to the right of the associated line, there is antagonism at that effect level. An additive interaction is indicated by the data point residing close to or on the associated line. The isobologram plot shown in Figure 4-3C indicates that synergy is present between stattic and cisplatin at the 50%, 75% and 90% effect levels in the A549 cell line.

Figure 4-4 shows the same combination of stattic and cisplatin in the DU145 cell line. The cisplatin GI₅₀ is reduced from 60.7 μ M to 25.8 μ M which is a 57.5% decrease. The CI values for this combination are moderately synergistic between 50-70 μ M cisplatin, with the lowest CI value of 0.752 occurring at 60 μ M cisplatin. Some additive and mildly antagonistic CI values are seen at the upper and lower extremities of the dose-effect curve (Figure 4-4B). The isobologram plot indicates that at the 90% effect level synergy is observed between stattic and cisplatin in the DU145 cell line. At the 50% and 75% effect levels, additivity is observed (Figure 4-4C).

Curcumin is the parent compound of the novel STAT3 inhibitor presented in this thesis, VS-43. Therefore, the interaction of curcumin with cisplatin was also assessed by fixed ratio combination SRB assays.

Figure 4-5A illustrates the shift in GI_{50} for cisplatin after combination treatment with curcumin in the A549 cell line. The GI_{50} is reduced from 88.0 μ M to 35.0 μ M (a 60.2% decrease). The CI values for this combination are predominantly synergistic, falling into the “synergism” to “moderate synergism” categories. The lowest CI value is 0.579, achieved at 70 μ M cisplatin (Figure 4-5B). The isobologram depicted in Figure 4-5C indicates synergy at the 75% and 90% effect levels, and additivity at the 50% effect level.

The combination of curcumin and cisplatin was also performed in the DU145 cell line. The GI_{50} for cisplatin was decreased by 45.6% from 67.3 μ M to 36.6 μ M by combination with curcumin (Figure 4-6A). The CI values calculated for this combination fall into the “synergism”, “moderate synergism” and “slight synergism” categories, with the lowest CI value of 0.611 noted at 60 μ M cisplatin (Figure 4-6B). The isobologram shown in Figure 4-6C indicates synergy at the 90% effect level and additivity at the 50% and 75% effect levels.

A summary of the GI_{50} values for combination of stattic or curcumin with cisplatin is presented in Table 4-1. The P values for GI_{50} pairs (cisplatin alone and combination treatment) are all $P < 0.0001$ as determined by non-linear regression analysis.

Clearly the combination of stattic or curcumin with cisplatin is able to produce synergy. Different treatment schedules and doses could be investigated in order to maximise the synergy observed here, as the combinations investigated here produced predominantly moderate synergism. It appears curcumin produces slightly stronger synergy than stattic in combination with cisplatin. This may bode well for

the novel STAT3 inhibitor, VS-43, in combination with cisplatin as the structure of VS-43 is derived originally from curcumin. Therefore, in the following section, the combination of VS-43 with cisplatin will be investigated using similar methods.

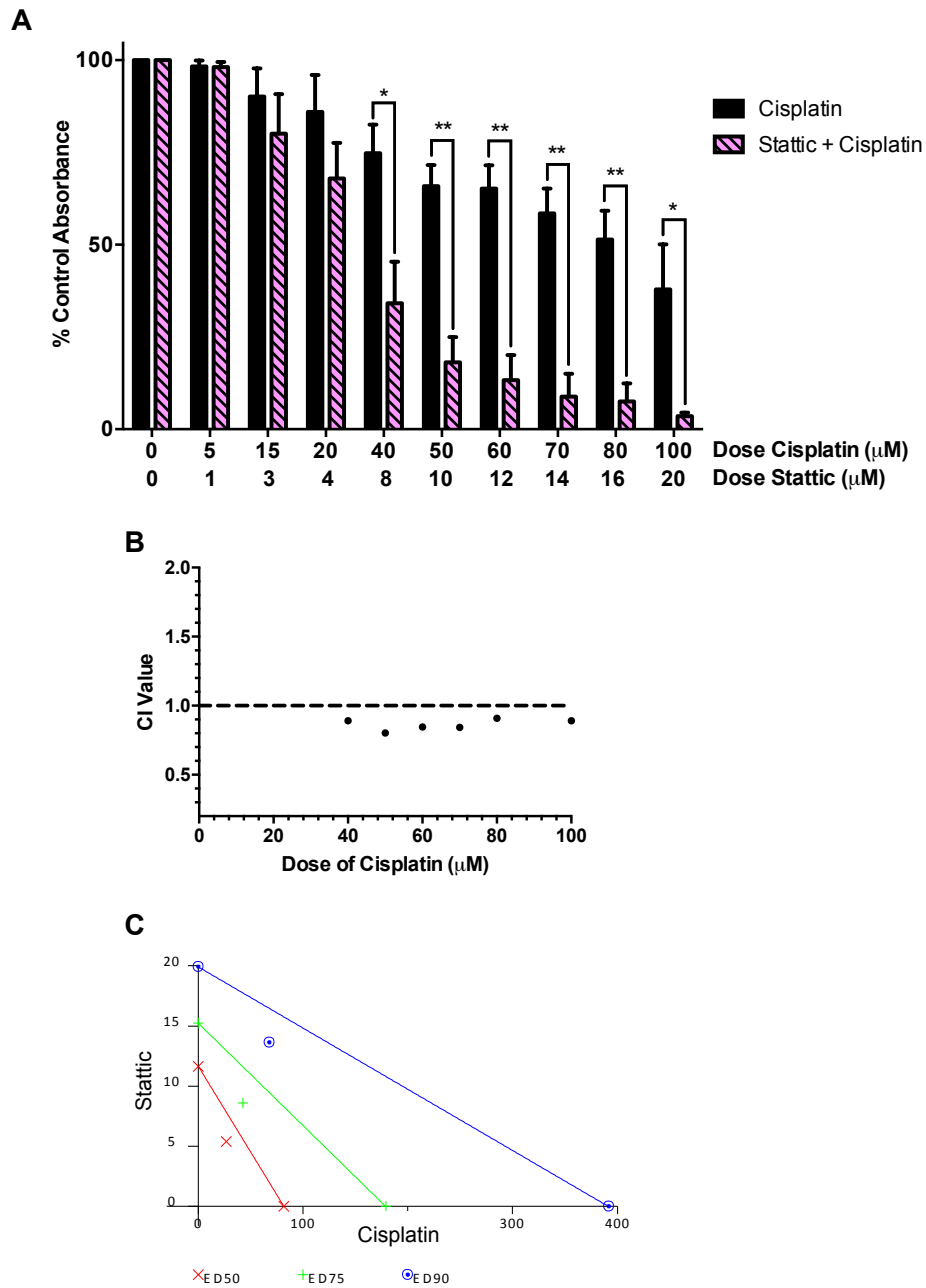


Figure 4-3: Combination of static and cisplatin in A549 cells. A) static plus cisplatin combination treatment results in increased cell growth inhibition. Data plotted was obtained by SRB assay and is the average of at least three individual experiments with SEM calculated for error bars. Students t-test was carried out to determine statistical significance with * = $P < 0.05$, ** = $P < 0.01$. B) Combination indices are predominantly below 1 and C) isobologram plot quantifying drug interactions at the 50%, 75% and 90% effect levels.

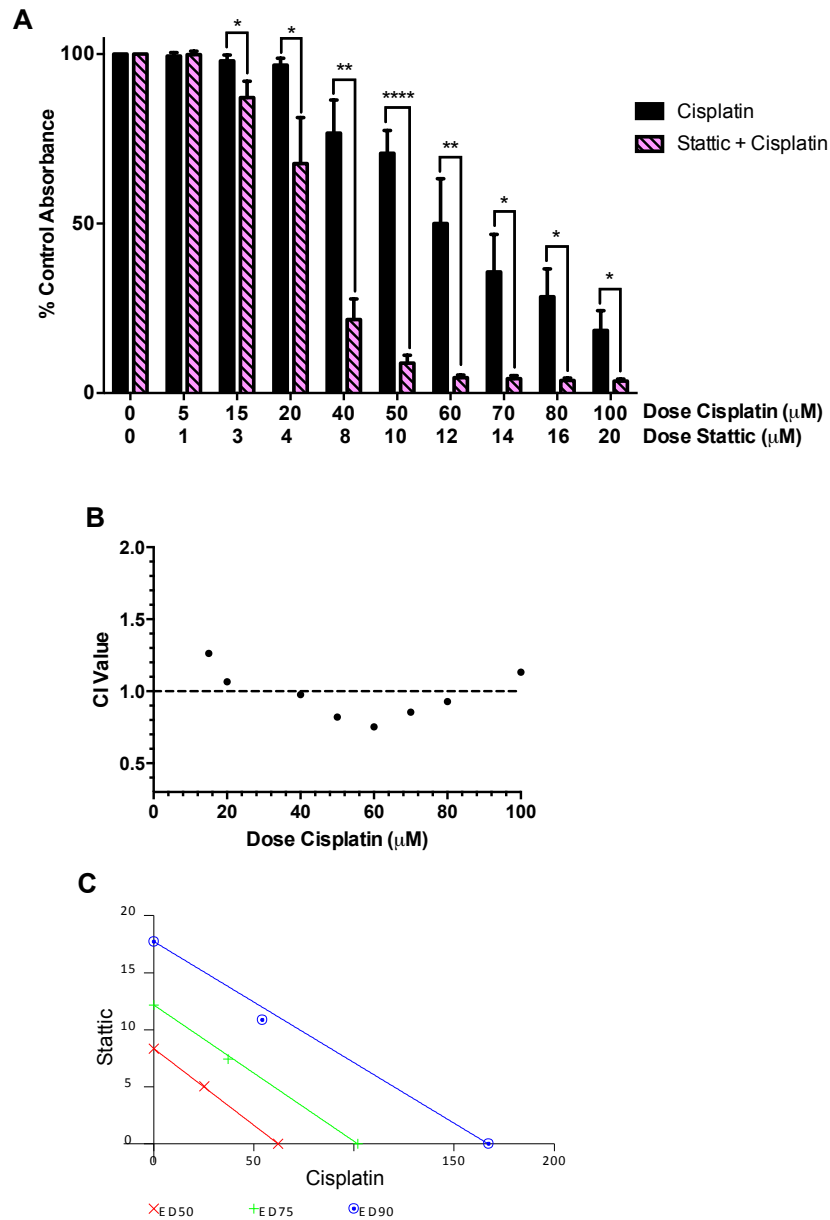


Figure 4-4: Combination of static and cisplatin in DU145 cells. A) static plus cisplatin combination treatment results in increased cell growth inhibition. Data plotted was obtained by SRB assay and is the average of at least three individual experiments with SEM calculated for error bars. Students t-test was carried out to determine statistical significance with * = $P < 0.05$, ** = $P < 0.01$, **** = $P < 0.0001$. B) Combination indices between 50-70 μM fall below 1 and C) isobologram plot quantifying drug interactions at the 50%, 75% and 90% effect levels.

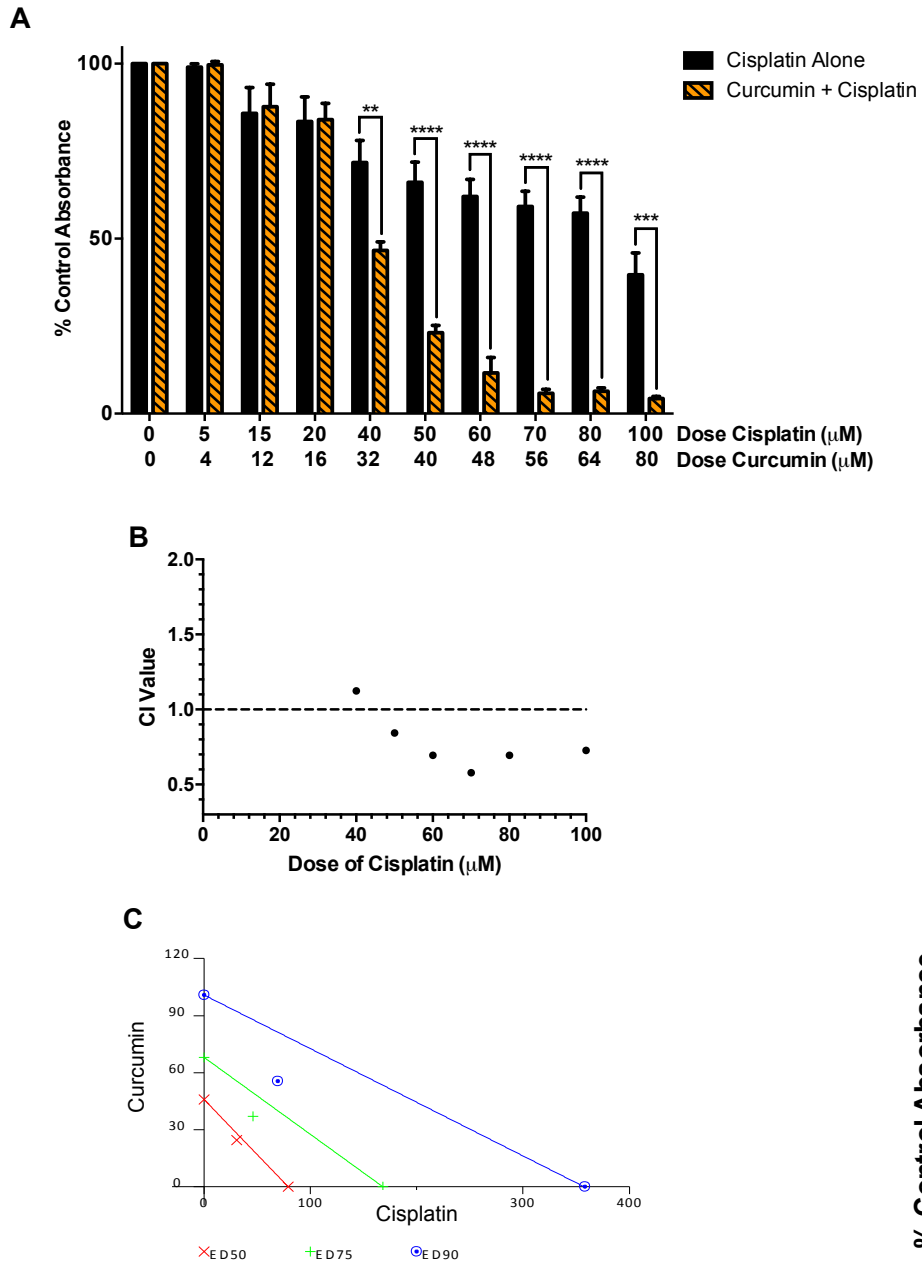


Figure 4-5: Combination of curcumin and cisplatin in A549 cells. A) curcumin plus cisplatin combination treatment results in increased cell growth inhibition. Data plotted was obtained by SRB assay and is the average of at least three individual experiments with SEM calculated for error bars. Students t-test was carried out to determine statistical significance with * = $P < 0.05$, ** = $P < 0.01$, *** = $P < 0.001$ **** = $P < 0.0001$. B) Combination indices are predominantly below 1 and C) isobologram plot quantifying drug interactions at the 50%, 75% and 90% effect levels.

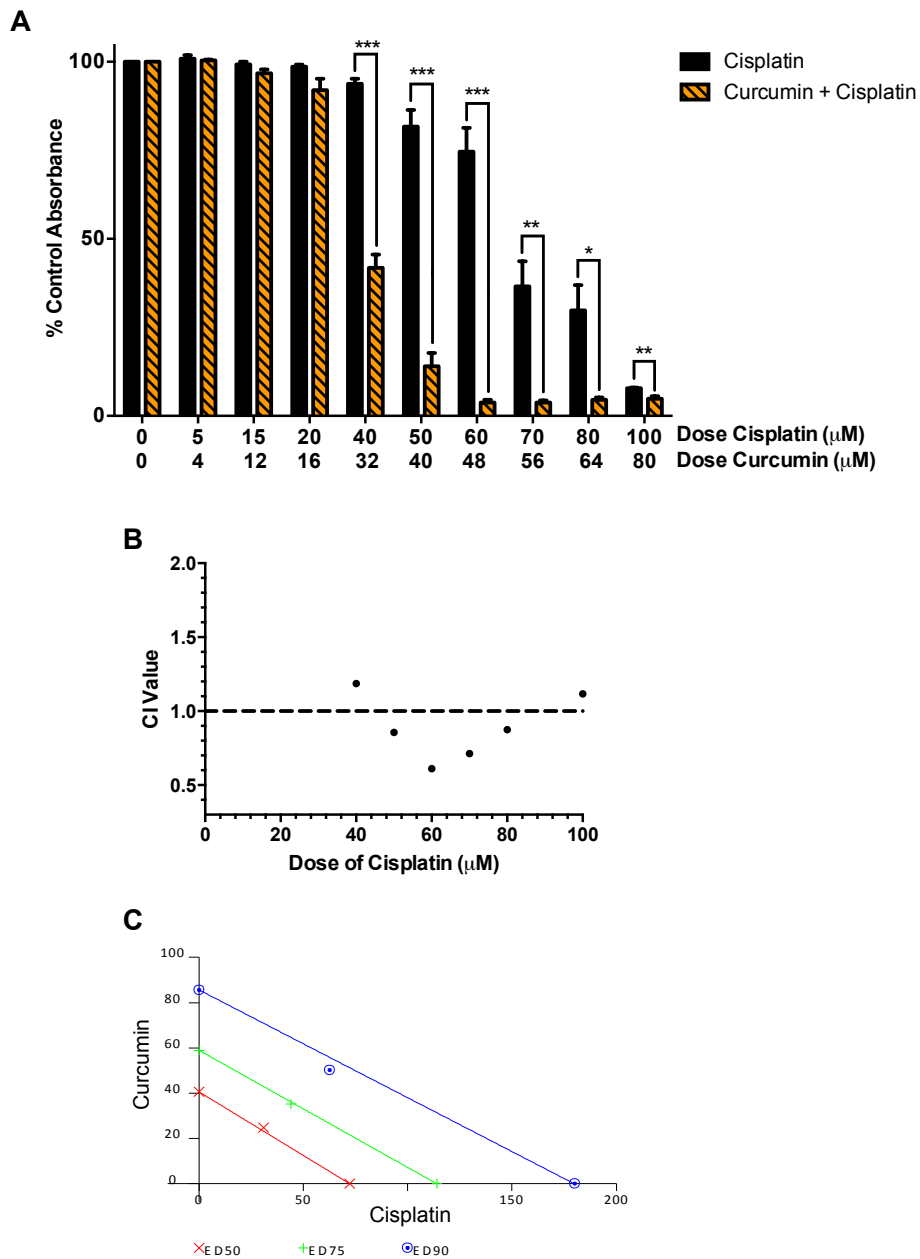


Figure 4-6: Combination of curcumin and cisplatin in DU145 cells. A) curcumin plus cisplatin combination treatment results in increased cell growth inhibition. Data plotted was obtained by SRB assay and is the average of at least three individual experiments with SEM calculated for error bars. Students t-test was carried out to determine statistical significance with * = $P < 0.05$, ** = $P < 0.01$, *** = $P < 0.001$. B) Combination indices are predominantly below 1 and C) isobologram plot quantifying drug interactions at the 50%, 75% and 90% effect levels.

Table 4-1: GI₅₀ values for cisplatin alone and in combination with stattic or curcumin, in the A549 and DU145 cell lines.

Drug treatment	Cisplatin GI ₅₀ (μM)	
	A549	DU145
Cisplatin	82.1	60.7
Stattic + Cisplatin	27.8	25.8
Cisplatin	88.0	67.3
Curcumin + Cisplatin	35.0	36.6

4.3.4 VS-43 sensitises cancer cell lines to cisplatin with greater synergy than other STAT3 inhibitors

As synergy has been observed between the STAT3 inhibitors, stattic and curcumin, and cisplatin in the previous section, the interaction of the novel STAT3 inhibitor VS-43 with cisplatin was investigated. Two drug treatment regimes were tested – the fixed ratio and non-fixed ratio combinations.

4.3.4.1 Fixed Ratio Combination of VS-43 and Cisplatin

For comparison of VS-43 with stattic and curcumin in combination with cisplatin, the “fixed ratio” combination regime was used. As with stattic and curcumin in section 4.3.3, VS-43 drug treatment was carried out for 18 hours prior to a 1 hour cisplatin drug treatment. The ratio of VS-43:cisplatin used was 1:50 based approximately on the preliminary GI₅₀ values of the two drugs independently in the DU145 cell line.

In the A549 cell line, the cisplatin GI₅₀ is reduced from 77.8μM to 45.7μM which is a 41.3% change (Figure 4-7A). The CI values shown in Figure 4-7B are all less than 1 therefore, synergy is evident between VS-43 and cisplatin between 40-100μM cisplatin. The lowest CI value achieved is 0.566 at 100μM cisplatin. These CI values

span the “synergism” to “moderate synergism” range. The isobologram analysis illustrates synergy at the 50%, 75% and 90% effect levels (Figure 4-7C).

For the DU145 cells, combination of cisplatin with VS-43 reduces the GI_{50} from 49.2 μ M to 30.8 μ M (a 37.4% decrease) (Figure 4-8A). The CI value analysis indicates synergy between 40-100 μ M cisplatin, reaching “synergism” and “moderate synergism” on the Chou scale. The lowest CI value obtained was 0.644 at 60 μ M cisplatin (Figure 4-8B). The combination of VS-43 and cisplatin in the DU145 cell line produces one antagonistic CI value at 20 μ M cisplatin. Figure 4-8C shows the isobologram analysis for this combination, which indicates synergy at the 75%, 90% and slight synergy at the 50% effect levels.

These results indicate that there is synergy between VS-43 and cisplatin in both the DU145 and A549 cell lines, as has been shown with stattic and curcumin in the previous section. As these cell lines differ in their sensitivity to STAT3 inhibitors and to cisplatin (section 3.3.2, section 4.3.1, and section 4.3.2), this indicates that STAT3 inhibitors are able to produce chemosensitisation despite varied sensitivities to each drug alone.

Table 4-2 summarises the GI_{50} values for the fixed ratio combination of VS-43 and cisplatin in the A549 and DU145 cell lines. The P values for each GI_{50} pair is <0.0001, as determined by non-linear regression analysis.

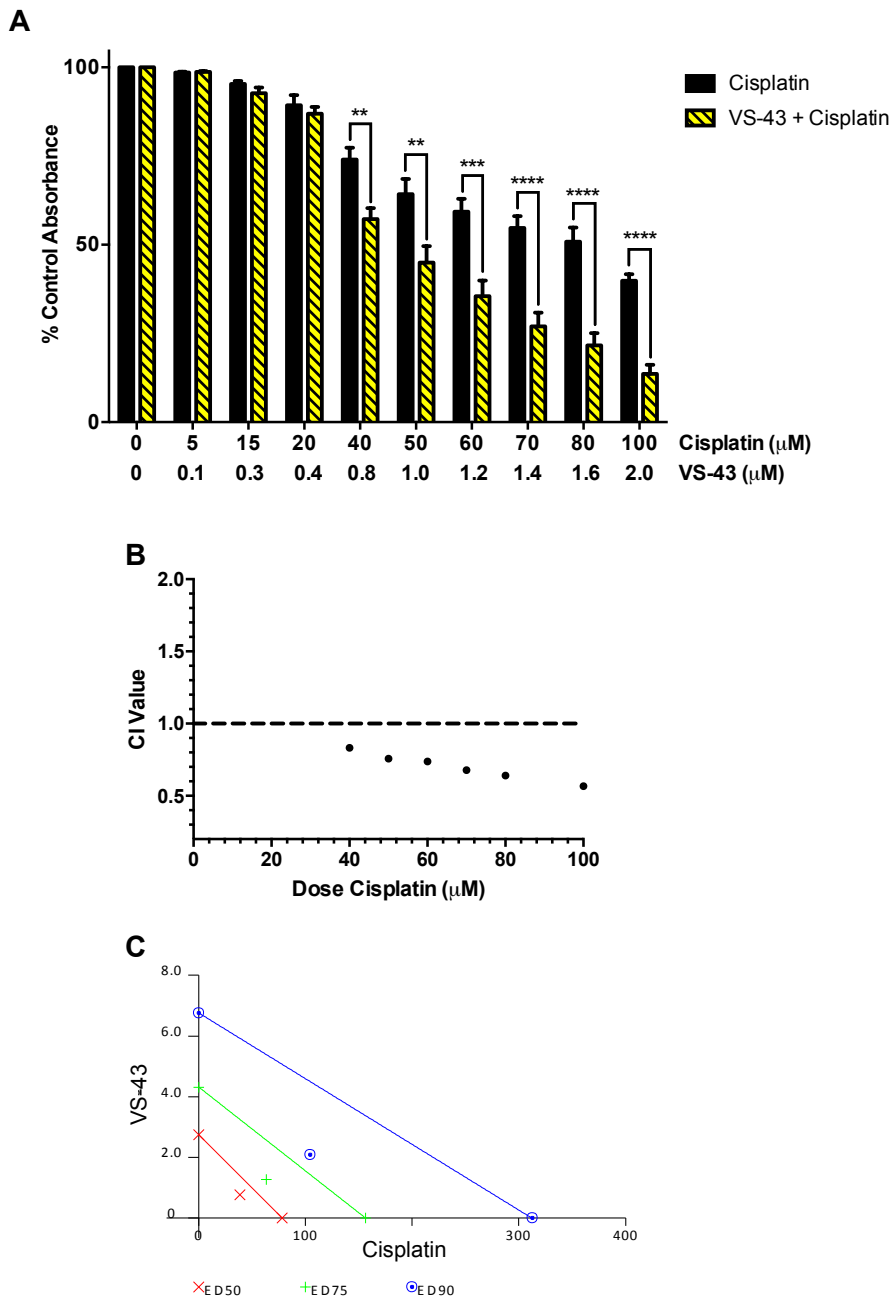


Figure 4-7: Combination of VS-43 and cisplatin in A549 cells using the fixed ratio method. A) VS-43 plus cisplatin combination treatment results in increased cell growth inhibition. Data plotted was obtained by SRB assay and is the average of at least three individual experiments with SEM calculated for error bars. Students t-test was carried out to determine statistical significance with ** = $P < 0.01$, *** = $P < 0.001$ **** = $P < 0.0001$. B) Combination indices are all below 1 and therefore, synergistic C) isobologram plot quantifying drug interactions at the 50%, 75% and 90% effect levels.

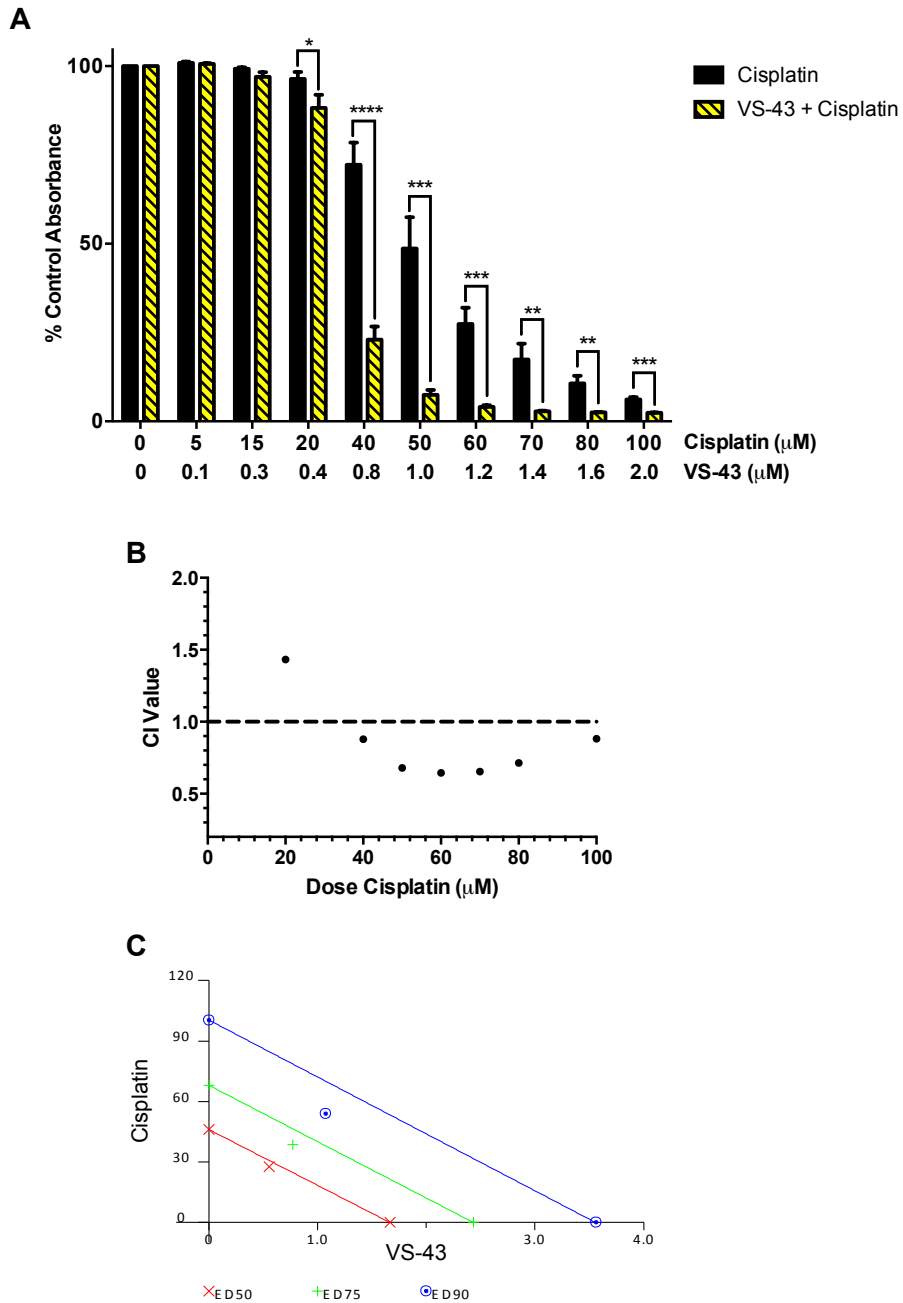


Figure 4-8: Combination of VS-43 and cisplatin in DU145 cells using the fixed ratio method. A) VS-43 plus cisplatin combination treatment results in increased cell growth inhibition. Data plotted was obtained by SRB assay and is the average of at least three individual experiments with SEM calculated for error bars. Students t-test was carried out to determine statistical significance with * = $P < 0.05$, ** = $P < 0.01$, *** = $P < 0.001$ **** = $P < 0.0001$. B) Combination indices are predominantly below 1 and C) isobologram plot quantifying drug interactions at the 50%, 75% and 90% effect levels.

Table 4-2: Fixed Ratio GI₅₀ values for cisplatin alone and VS-43 plus cisplatin combination treatment in the A549 and DU145 cell lines.

Drug treatment	Cisplatin GI ₅₀ (μM)	
	A549	DU145
Cisplatin	77.8	49.2
VS-43 + Cisplatin (Fixed Ratio)	45.7	30.8

4.3.4.2 Non-Fixed Ratio Combination of VS-43 and Cisplatin

As was discussed in section 3.3.5, the inhibition of pSTAT3^{Tyr705} by VS-43 is dependent on several factors, including dose and treatment time. In section 3.3.7 treatment of DU145 cells with VS-43 for 1 hour was able to selectively inhibit STAT3 DNA binding. In this section, the use of VS-43 for an acute period of 1 hour is investigated further.

Immunoblot analysis of cellular pSTAT3^{Tyr705} levels after 1 hour treatment with VS-43 illustrated that an acute VS-43 exposure can also inhibit levels of STAT3 activation in both cell lines. As with an 18 hour VS-43 treatment, a higher concentration of VS-43 is required to achieve pSTAT3^{Tyr705} inhibition in the less sensitive A549 cell line than in the DU145 cell line using this 1 hour treatment. Inhibition of pSTAT3^{Tyr705} is seen at 5μM and 10μM VS-43 in the DU145 and A549 cell lines, respectively (Figure 4-9A), with a dose-dependent effect clear in both cell lines. pSTAT3^{Tyr705} expression is almost completely eliminated at 10μM and 20μM in the DU145 and A549 cell lines, respectively.

Cell growth inhibition studies with 1 hour VS-43 treatments illustrated that an acute exposure to VS-43 results in minimal cell growth inhibition. DU145 cells are more sensitive to this acute VS-43 treatment than A549 cells as is also the case for the 18

hour exposure but neither cell line reaches 50% growth inhibition at the doses tested (Figure 4-9B). As these doses inhibit pSTAT3^{Tyr705} expression but are less detrimental to cell growth, the effect of an acute 1 hour pre-treatment of VS-43 on cisplatin sensitivity was investigated to see if this would provide a more or less synergistic combination.

For the combination of the acute VS-43 treatment with cisplatin, the fixed ratio combination was not appropriate as the dose-response curves for the two drugs are not alike. The non-fixed ratio is the preferable method for combination of drugs where one drug is more active than the other (Bijnsdorp et al., 2011) – in this case cisplatin has a greater effect on cell growth than VS-43 therefore, the non-fixed ratio is appropriate.

A set dose of 5 μ M and 10 μ M of VS-43 was chosen for the combination studies in DU145 and A549 cells, respectively, as these doses exhibited substantial pSTAT3^{Tyr705} inhibition in each cell line. This dose was applied to cells for 1 hour before treatment with increasing doses of cisplatin for 1 hour as for the fixed ratio combination.

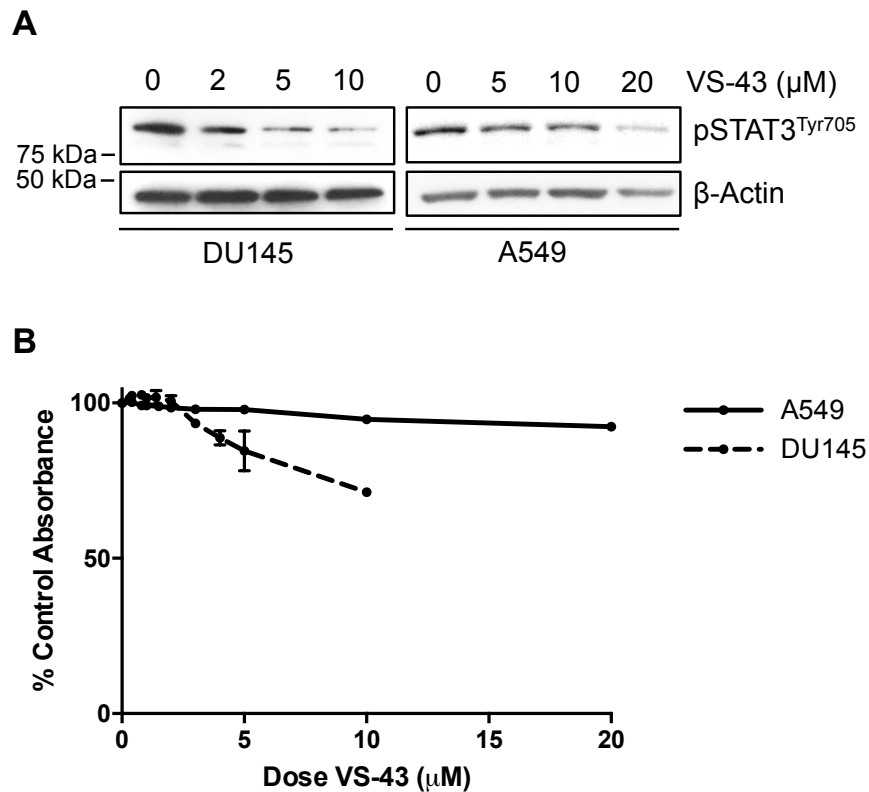


Figure 4-9: A) Acute 1 hour exposure of DU145 and A549 cells to VS-43 down-regulates pSTAT3^{Tyr705}. B) Treatment with 1 hour VS-43 exhibits minimal cell growth inhibition on DU145 and A549 cells, as determined by SRB assay. All data plotted is the average of at least three individual experiments with SEM calculated for error bars. Error bars are present for all data points, including those that are not visible.

In A549 cells the GI₅₀ decreases from 64.6 μM to 39.8 μM - a 38% decrease, similar to what is achieved when a fixed ratio combination is used. The bar chart plot in Figure 4-10A illustrates that 10 μM VS-43 alone has no detrimental effect on cell growth in this combination. Therefore, each difference between the cisplatin alone and combination bars is a result of synergy between VS-43 and cisplatin. These differences are not statistically significant across some doses, however, at the beginning and end of the dose-response curve these differences are significant and through CI analysis are shown to be synergistic (Figure 4-10B). The lowest CI value was 0.437, attained at 15 μM cisplatin.

Non-fixed ratio combinations use normalised isobolograms, where each axis plots the dose of the drug to give X% effect in the combination, divided by the dose of the

drug to give X% effect alone. The line of additivity is drawn between 1 on the Y axis and 1 on the X axis – where the dose of each drug to have a given effect is the same alone and in combination. Any data points to the left and below the line are synergistic and any data points to the right and above the line are antagonistic due to this normalisation.

The isobologram in Figure 4-10C shows all data points to be synergistic for the non-fixed ratio combination of VS-43 and cisplatin in the A549 cell line.

In DU145 cells, the GI_{50} drops from 49.3 μ M to 19.5 μ M (Figure 4-11A). This is a 60% change. This difference between the percentage GI_{50} change in A549 and DU145 cells may be attributed to the higher sensitivity of DU145 cells to VS-43 in terms of growth inhibition. At the doses of VS-43 chosen for combination with cisplatin, DU145 cells exhibit 15.4% growth inhibition whereas A549 cells exhibit 5.5% (Figure 4-9B). This sensitivity to VS-43 alone is also evident in Figure 4-11A where at 0 μ M cisplatin there is already 22.7% growth inhibition by VS-43 alone. Therefore, the increased shift in GI_{50} is likely the result of growth inhibition caused by VS-43 alone in DU145 cells. Table 4-3 summarises the GI_{50} values for the non-fixed ratio combination of VS-43 and cisplatin.

Combination index analysis of the DU145 combination indicates synergy across the full range of cisplatin doses tested, with the greatest synergy achieved at 40 μ M cisplatin with a CI value of 0.596. The isobologram in Figure 4-11C indicates that at all effect levels, the interaction between VS-43 and cisplatin in this combination is synergistic.

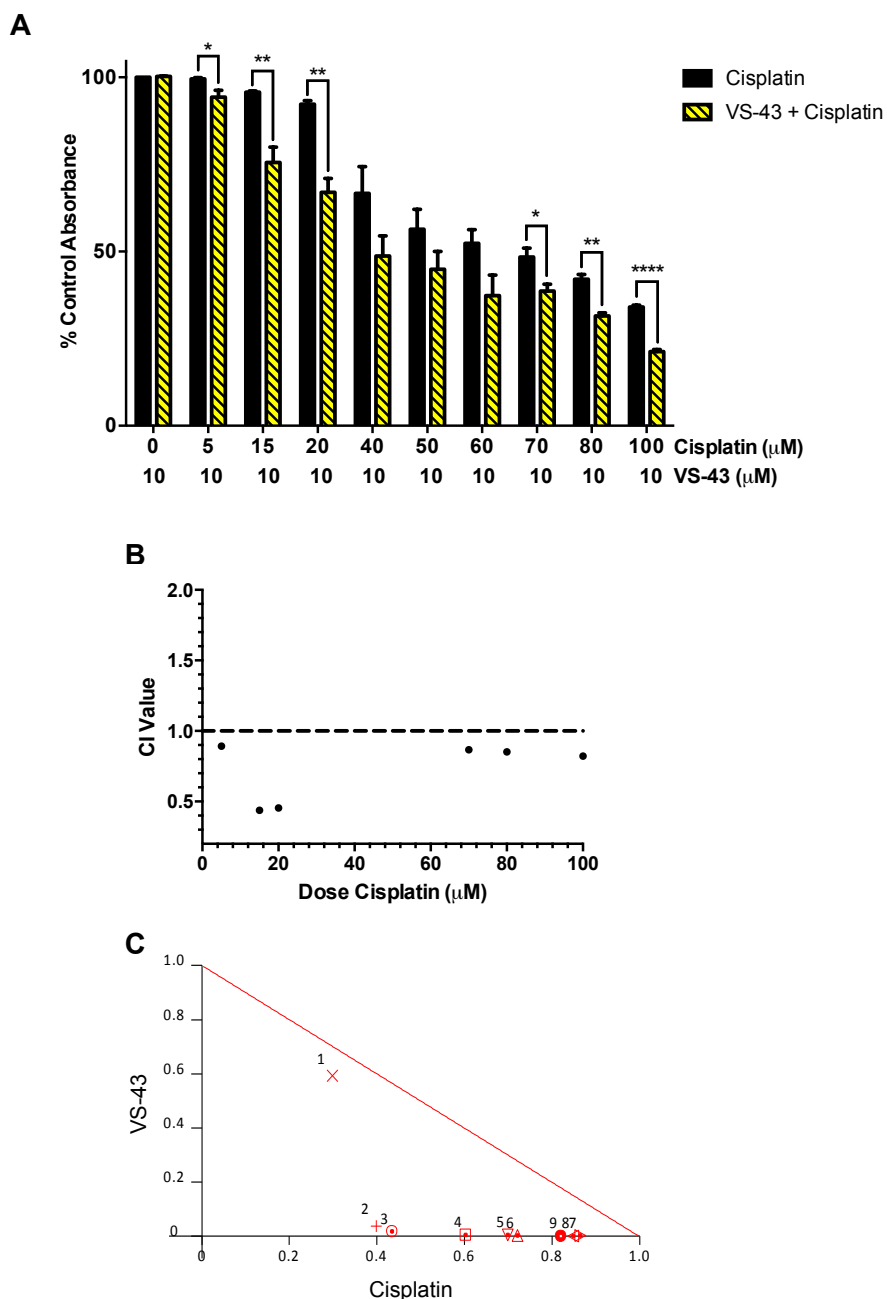


Figure 4-10: Combination of VS-43 and cisplatin in A549 cells using the non-fixed ratio method. A) VS-43 plus cisplatin combination treatment results in increased cell growth inhibition. Data plotted was obtained by SRB assay and is the average of at least three individual experiments with SEM calculated for error bars. Students t-test was carried out to determine statistical significance with * = $P < 0.05$, ** = $P < 0.01$, *** = $P < 0.001$. Absorbance was normalised to 10µM VS-43 alone. B) Combination indices are all below 1 and C) combination data points are mostly left of the line on the isobologram plot.

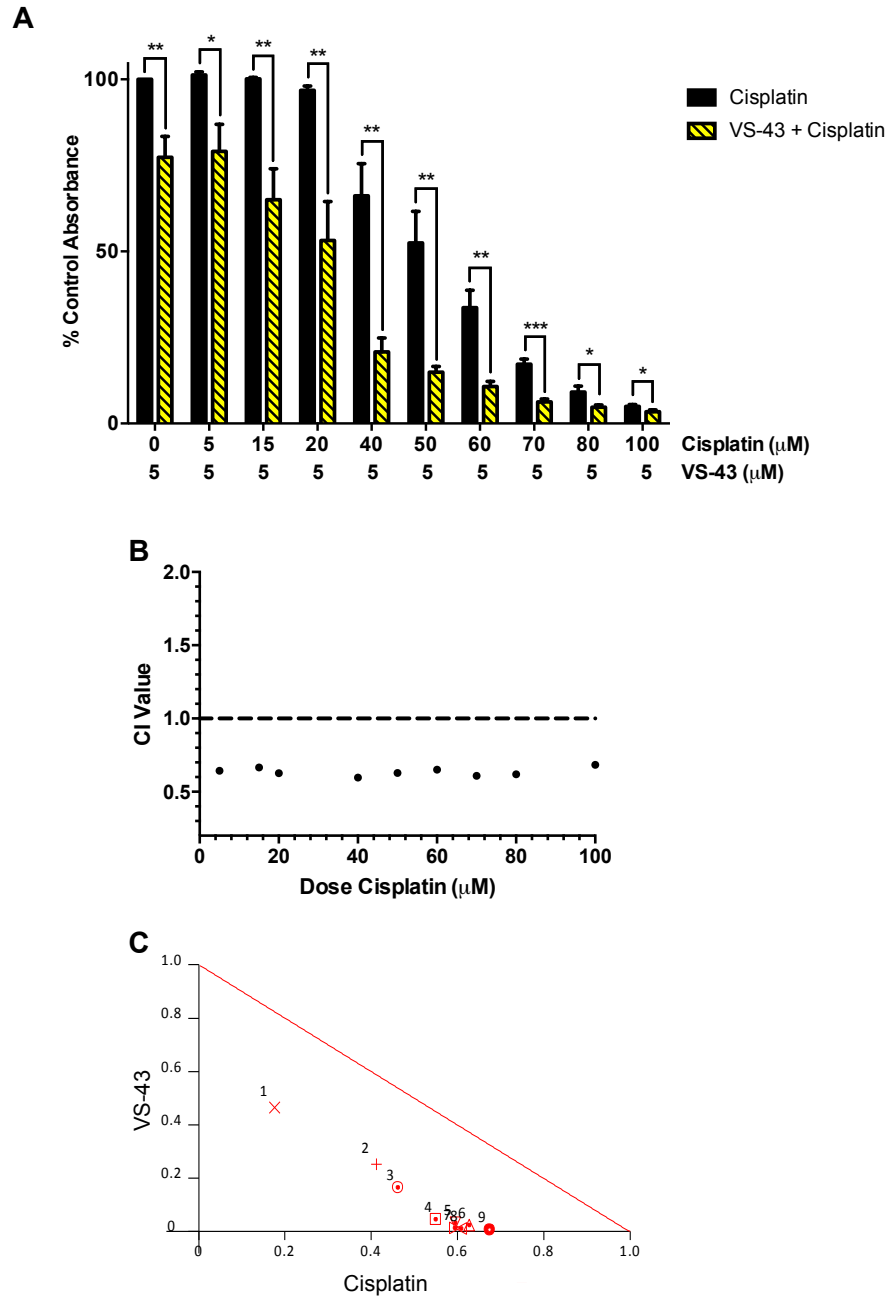


Figure 4-11: Combination of VS-43 and cisplatin in DU145 cells using the non-fixed ratio method. A) VS-43 plus cisplatin combination treatment results in increased cell growth inhibition. Data plotted was obtained by SRB assay and is the average of at least three individual experiments with SEM calculated for error bars. Students t-test was carried out to determine statistical significance with * = $P < 0.05$, ** = $P < 0.01$, *** = $P < 0.001$. Absorbance was normalised to 5μM VS-43 alone. B) All combination indices are below 1 and C) all combination data points are left of the line on the isobologram plot.

Table 4-3: Non-fixed ratio GI₅₀ values for growth inhibition by cisplatin alone and VS-43 plus cisplatin combination treatment in the A549 and DU145 cell lines.

Drug treatment	Cisplatin GI ₅₀ (μM)	
	A549	DU145
Cisplatin	64.6	49.3
VS-43 + Cisplatin (Non-fixed ratio)	39.8	19.5

4.3.5 STAT3 inhibitor and Cisplatin Combination therapy Enhances Apoptosis in Cancer Cell Lines

Both STAT3 inhibitors and cisplatin are known to inhibit cell growth, and VS-43 has been shown in the previous chapter to induce cellular apoptosis via cleaved PARP induction (section 3.3.9). Therefore, the effect of the combination treatment of cells with STAT3 inhibitors and cisplatin on apoptosis induction was investigated.

Immunoblot analysis of key apoptosis markers, cleaved PARP and cleaved caspase-3, was performed for cells treated with STAT3 inhibitors alone, cisplatin alone, and the combination treatment using the fixed ratio combination regime. In the DU145 cell line, whilst some expression of cleaved PARP and cleaved caspase-3 is observed in cells treated with VS-43 and cisplatin alone, the combination treatment enhanced the expression of both of these factors (Figure 4-12A). In the A549 cell line cleaved caspase-3 expression was induced in the combination treated cells where expression was minimal for cells treated with VS-43 and cisplatin alone (Figure 4-12B). DU145 cells treated with statin and curcumin in combination with cisplatin also increased cleaved PARP expression (Figure 4-12C). The observed changes in protein level are visibly greater than additive. This indicates that

combination of STAT3 inhibitors with cisplatin results in enhanced apoptosis of cancer cell lines, and that the synergy observed in terms of growth inhibition is translated into enhanced expression of apoptotic factors at the protein level.

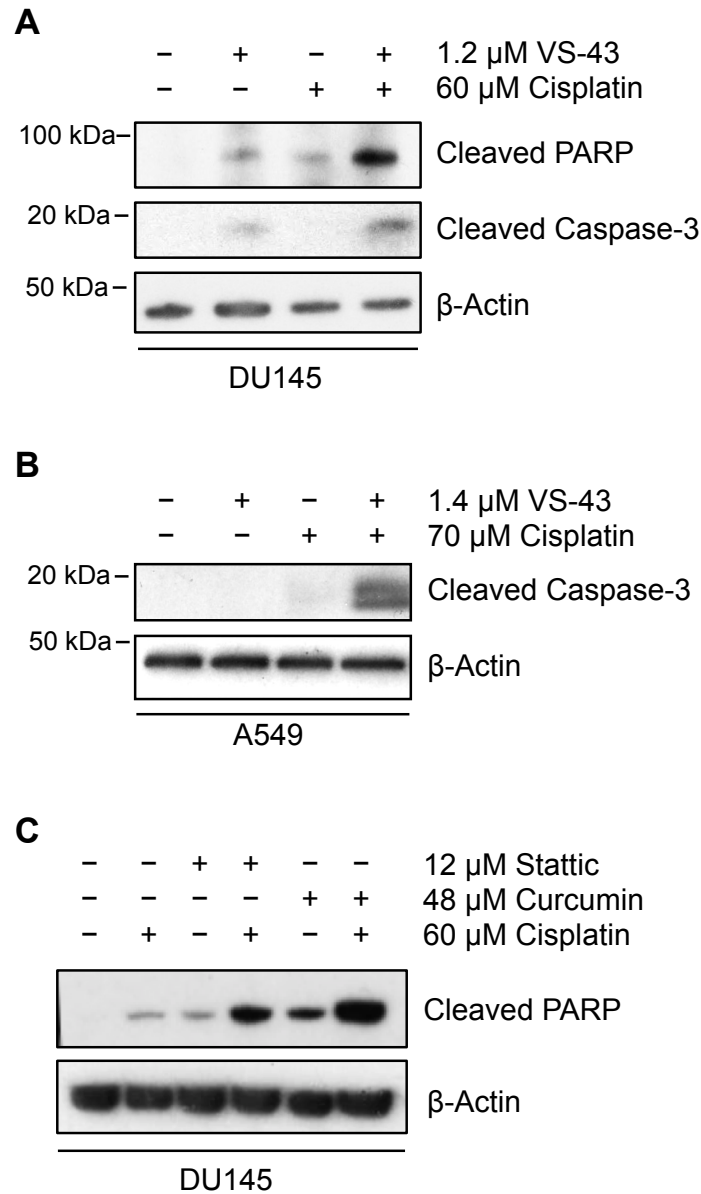


Figure 4-12: Combination of STAT3 inhibitors and cisplatin enhances apoptosis. VS-43 enhances cleaved PARP and cleaved caspase-3 expression in cisplatin treated A) DU145 cells and B) A549 cells. C) Stattic and curcumin enhance cleaved PARP expression in cisplatin treated DU145 cells. Blots are representative of more than 1 experiment.

4.3.6 VS-43 can also chemosensitise DU145 cells to doxorubicin

STAT3 inhibitors have been reported to sensitise cancer cells to many other chemotherapy agents, not just cisplatin. One of the more frequently reported drugs used in combination with STAT3 inhibitors is doxorubicin (Couto et al., 2012; Lin et al., 2010b; Notarbartolo et al., 2005; Rajendran et al., 2011). Like cisplatin, doxorubicin also targets the cancer cell DNA, but through intercalation rather than crosslinking. This intercalation stabilises the topoisomerase II complex, resulting in DNA damage and inhibited DNA replication. Doxorubicin has also been suggested to act via free radical generation (Thorn et al., 2011).

In order to determine whether VS-43, like other STAT3 inhibitors, can synergise with a broader range of chemotherapy drugs, the SRB assay and calcosyn analysis method was used to investigate the interaction of VS-43 and doxorubicin in the DU145 cell line.

Cells were treated with doxorubicin for 1 hour, or in combination with an 18 hour VS 43 pre-treatment at a fixed ratio of 1:1.6. Combination of VS-43 with doxorubicin reduces the GI_{50} from 6.42 μ M to 1.96 μ M (Figure 4-13A) and results in synergistic CI values where statistically significant differences in cell growth inhibition are observed (Figure 4-13B). The point of greatest synergy is at 5 μ M doxorubicin where a CI value of 0.411 is achieved. The isobologram shown in Figure 4-13C demonstrates that this combination is synergistic at the 50%, 75% and 90% effect levels.

Therefore, VS-43, like many other STAT3 inhibitors, is capable of synergising with multiple chemotherapy agents, including doxorubicin.

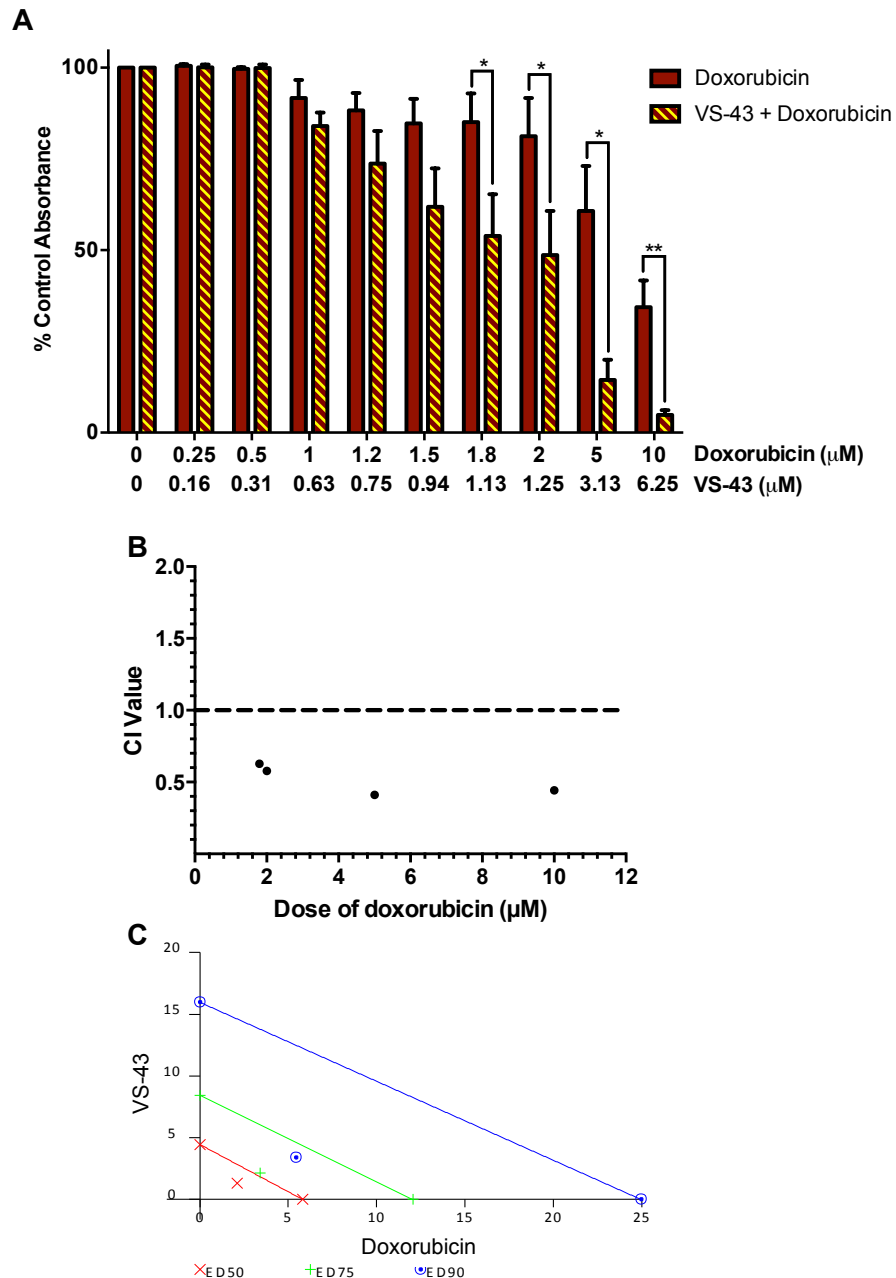


Figure 4-13: Combination of VS-43 and doxorubicin in DU145 cells using the fixed ratio method. A) VS-43 plus doxorubicin combination treatment results in increased cell growth inhibition. Data plotted was obtained by SRB assay and is the average of at least three individual experiments with SEM calculated for error bars. Students t-test was carried out to determine statistical significance with * = $P < 0.05$, ** = $P < 0.01$. B) Combination indices are all below 1 and C) isobologram plot quantifying drug interactions at the 50%, 75% and 90% effect levels. Synergy is observed between VS-43 and doxorubicin in DU145 cells at all effect levels.

4.4 Discussion

In this chapter, STAT3 inhibitors are shown to sensitise both the DU145 and A549 cell lines to cisplatin in a synergistic manner. The combination of STAT3 inhibitors with cisplatin results in a synergistic enhancement in apoptosis in these cell lines. Additionally, the novel STAT3 inhibitor described in chapter 3, VS-43, is demonstrated to produce greater synergy with cisplatin at lower doses than stattic or curcumin.

4.4.1 How does VS-43 compare to other STAT3 inhibitors as a chemosensitiser?

In this chapter, the ability of three STAT3 inhibitors to sensitise cancer cell lines to cisplatin has been investigated: stattic, curcumin and VS-43. All three inhibitors demonstrated synergy in combination with cisplatin as determined by CI analysis.

As similar fixed ratio combinations were used to study each of the inhibitors ability to sensitise cancer cell lines to cisplatin, a direct comparison can be made between VS-43 and the commercially available STAT3 inhibitors. A higher percentage decrease in cisplatin GI_{50} values was observed by combination of cisplatin with stattic and curcumin than was observed in combination with VS-43 (sections 4.3.3 and 4.3.4). However, GI_{50} values alone do not take into account the effect of the second drug, i.e. the STAT3 inhibitor, on cell growth. CI value analysis determines the interaction of the two drugs using the dose-effect curves of each drug alone. Here, a fixed ratio combination of VS-43 with cisplatin produced lower CI values than the combination of stattic with cisplatin. The level of synergy seen with VS-43 is similar to that seen with curcumin in combination with cisplatin, however, VS-43 is able to produce synergy over a greater dose range of cisplatin. These observations are summarised in Table 4-4. The greater GI_{50} reduction but lower synergy seen

with combination of stattic or curcumin with cisplatin may be explained through the contribution of the STAT3 inhibitors alone to cell growth inhibition.

Additionally, the dose of each STAT3 inhibitor used must not be overlooked. VS-43 is used at much lower concentrations than either stattic or curcumin. Five times as much stattic is required to achieve a much lower level of synergy with cisplatin, and 40 times as much curcumin is required to equal the synergy between VS-43 and cisplatin. Therefore, using the fixed ratio combination method, VS-43 is able to sensitise cancer cell lines to cisplatin with greater synergy than stattic or the parent compound curcumin and is clearly a more potent chemosensitiser.

Table 4-4: Summary table for combination of STAT3 inhibitors with cisplatin. The lowest achieved CI value and the number of synergistic CI values is indicated for each combination.

		Lowest CI value	Number of synergistic CI values
A549	Stattic + Cisplatin	0.802	5
	Curcumin + Cisplatin	0.579	5
	VS-43 + Cisplatin	0.566	6
DU145	Stattic + Cisplatin	0.752	3
	Curcumin + Cisplatin	0.611	4
	VS-43 + Cisplatin	0.644	6

Many other STAT3 inhibitors have been reported in the literature to synergise with cisplatin including both natural (curcumin and resveratrol) and synthetic compounds (stattic, HO-3867, and FLLL32 for example). However, in many combination studies the STAT3 inhibitor is given for a minimum of 24 hours, with some inhibitors being present for the duration of the growth assay, which can be up to 96 hours (Table 4-5). VS-43 was able to synergise with cisplatin after both an 18 hour and an acute 1 hour pre-treatment, indicating that VS-43 can be used in a variety of drug schedules in order to maximise synergy. VS-43 has proved potent enough to allow for the possibility of very short drug treatment schedules – an attractive feature for an agent in a clinical setting. This has not yet been demonstrated for any other novel STAT3 inhibitor. Additionally, most of the combination studies referenced in Table 4-5 use doses of STAT3 inhibitors higher than those used for VS-43 here. The majority of these studies do, however, use a wide range of cell lines, which will influence the doses of inhibitors required as well as treatment times as was demonstrated in Chapter 3. Therefore, a truly direct comparison between VS-43 and many of these inhibitors cannot be made, as they did not use either the DU145 or A549 cell lines. The study observing curcumin in combination with cisplatin did use the A549 cell line so this is more comparable, however, within this chapter curcumin has been combined with cisplatin in identical studies to those carried out with VS-43, so a comparison to the work carried out by Ye et. al (2012) does not yield much additional information. Further work in order to verify the activity of VS-43 in a wider panel of cell lines would be necessary to make true comparisons between VS-43 and other STAT3 inhibitors.

A compound that can enter the cell and take effect in as short a time as 1 hour is likely very potent. 1 hour treatment with VS-43 at a high dose is capable of sufficiently down-regulating pSTAT3^{Tyr705} levels in both cell lines tested here with limited longer term cell toxicity. This acute exposure chemosensitised cells to

cisplatin and achieved similar levels of synergy to that of the fixed ratio combination. Therefore, investigation into the use of short drug treatment times, and possibly repeated pulses of VS-43 exposure could be of interest in the future.

Table 4-5: STAT3 inhibitors reported to sensitise cancer cell lines to cisplatin. The dose range and treatment time are reported.

STAT3 Inhibitor	Inhibitor Dose range (μM)	Inhibitor Treatment Time	Reference
5,15-DPP	50	24 hours	(Huang et al., 2012)
Curcumin	5-20	48 hours	(Ye et al., 2012)
Dihydroartemisinin	10-20	24 hours	(Jia et al., 2016)
Diindolylmethane	20-50	24 hours	(Kandala and Srivastava, 2012)
FLLL32	0.85-1.4	96 hours	(Abuzeid et al., 2011)
H-4073	0.6-5	72 hours	(Kumar et al., 2014)
HO-3867	1-10	24 hours	(Selvendiran et al., 2011)
LY5	2.5	24 hours	(Xiao et al., 2015)
OPB-21121	0.15-1	72 hours	(M. J. Kim et al., 2013)
Resveratrol	25-100	48 hours	(Weiguo Zhao et al., 2010)
Stattic	2-8	48 hours	(Pan et al., 2013)
WP1066	5	48 hours	(Zhou et al., 2014)
YC-1	5-10	24 hours	(Lau et al., 2007)

4.4.2 Which drug treatment schedule produces the greatest synergy?

In this chapter, two drug treatment schedules were tested for VS-43 in combination with cisplatin: the fixed ratio and the non-fixed ratio methods. Figure 4-14 shows overlays of the CI value plots for the two drug treatment schedules (fixed and non-fixed) for VS-43 in combination with cisplatin. In both cell lines the degree of synergy obtained is similar for both schedules, with similar CI values being reached. The non-fixed ratio combination does, however, reach slightly lower CI values which is indicative of marginally greater synergy. In terms of consistency of synergy, the non-fixed ratio combination results in universal synergy in the DU145 cell line whereas in the A549 cell line this synergy is interrupted. This is because CI analysis was not carried out for the data points in the centre of the dose-response curve due to the lack of statistical significance. Therefore, the fixed-ratio combination produces more consistent synergy in the A549 cell line here.

For the fixed ratio combination in both cell lines the greatest synergy occurs in the post-GI₅₀ range. The lack of synergy at the lower end of the dose-response curves is due, in part, to the very low doses of VS-43 used. The combination of VS-43 and cisplatin in the DU145 cell line produces one antagonistic CI value at 20µM cisplatin. Chou explains that at the extremities of a dose-response curve, where cell kill is either very high or very low, CI values are less accurate as they lie beyond the sensitivity of the assay used to detect drug effect. This accounts for the antagonistic and additive CI values found at the beginning and end of the dose-response curves presented in this chapter. The synergy begins to appear mid-way through the dose-response curves as the STAT3 inhibitor reaches the dose required to exert the required molecular effect. Synergy in the fixed ratio combination for both cell lines begins at 40µM cisplatin where a dose of 0.8µM VS-43 was used. Doses of VS-43 lower than 0.8µM did not inhibit cell growth (Figure 3-14) and did not produce high levels of pSTAT3^{Tyr705} inhibition (Figure 3-5) therefore, synergy would likely not

occur at those doses as VS-43 is not having a molecular effect. Chou states that in this latter half of the dose-response curve any synergy observed is more relevant to the therapeutic use of anti-cancer drugs (Chou, 2010), therefore, for the remainder of this thesis, the combination of STAT3 inhibitors with cisplatin will be carried out in a fixed ratio combination as this regime produces the most consistent synergy at the relevant effect levels in both cell lines.

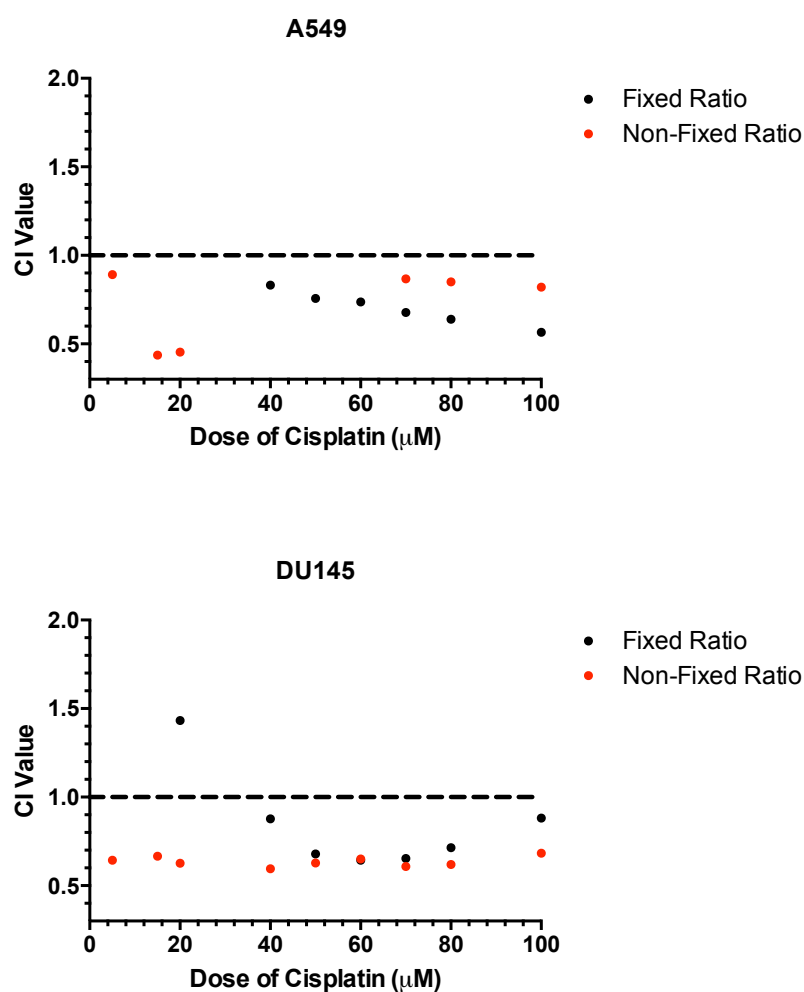


Figure 4-14: CI plots for the fixed and non-fixed ratio combination of VS-43 and cisplatin, in the A549 and DU145 cell line.

4.4.3 Why is the synergy between VS-43 and cisplatin not greater?

CI value analysis has determined that the interaction between cisplatin and VS-43 is synergistic. However, as such large shifts in the GI_{50} values for cisplatin are seen in the combination treated cells, why is this synergy not greater? Chou states that strongly synergistic drug interactions will have a CI in the range of 0.1-0.3 (Chou, 2006). The combination of VS-43 and cisplatin falls into the “synergistic” and “moderately synergistic” CI ranges (0.3-0.7 and 0.7-0.85), as do the combinations of statin and curcumin with cisplatin. An explanation for this lies in the effect of the STAT3 inhibitor alone which has been discussed for VS-43 in Chapter 3.

Treatment of cells with VS-43 alone can induce apoptosis as STAT3 regulates anti-apoptotic and survival genes. Inhibition of STAT3 action suppresses these survival signals and drives the cancer cell into programmed cell death. VS-43 is a potent inducer of apoptosis. Therefore, when cells are treated with VS-43 in combination with cisplatin, they are experiencing two mechanisms of apoptosis induction: one from the DNA damage signalling response induced by cisplatin-DNA adducts, and the other from the withdrawal of anti-apoptotic and survival signals when STAT3 is inhibited by VS-43. These effects are independent. If these were the only effects of cisplatin and VS-43 administration, the CI value upon combination of these compounds would be additive. However, synergy is observed. The effect of treatment with cisplatin plus VS-43 is greater than the sum of each individual effect. This implies a crossover in the effect of the two drugs.

This concept is represented diagrammatically in Figure 4-15. The moderate synergy levels observed between these two drugs is a consequence of the ability of VS-43 itself to induce apoptosis independently of cisplatin (right hand path). Where inhibition of STAT3 impacts the cisplatin-induced apoptosis pathway (interrupted lines), synergy is observed. The CI value analysis method takes into account the dose-effect curves of each drug alone and therefore, if both drugs inhibit cell growth

the synergy observed is more likely to be moderate as is seen here with the fixed ratio combinations. The non-fixed ratio combination of VS-43 and cisplatin resulted in slightly greater synergy, which under this hypothesis would be expected due to the lower cell growth inhibition by VS-43 alone when cells are treated for just 1 hour.

As cisplatin causes cell death via DNA damage, and repair of these adducts can result in resistance, it is hypothesised here that VS-43 inhibition of STAT3 may regulate either the accumulation of DNA damage or inhibit the DNA repair process. This will be addressed in the next chapter.

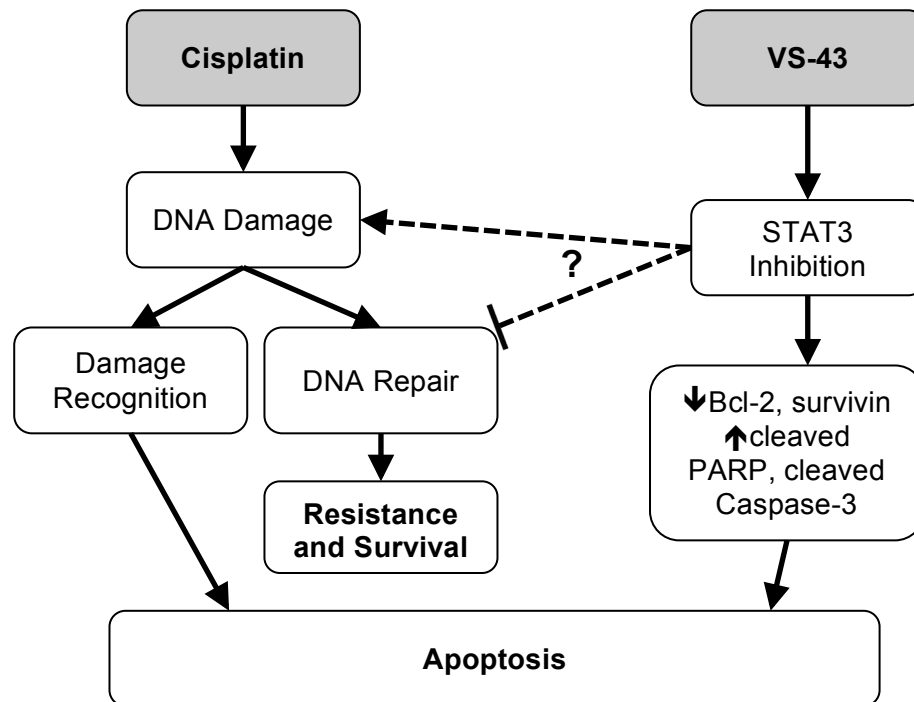


Figure 4-15: Cisplatin and VS-43 independently induce cellular apoptosis. Repair of cisplatin-induced DNA damage leads to resistance and cell survival. Interaction between the two pathways results in synergy and this may occur via STAT3-mediated regulation of DNA damage or DNA repair.

Another factor which may influence the degree of synergy observed in a combination is the treatment scheduling itself. Here, STAT3 inhibitors are given as a pre-treatment, prior to cisplatin treatment. However, many combination studies treat with both drugs simultaneously. Cisplatin treatment could also precede STAT3 inhibitor treatment. The dependence of synergy on drug scheduling has been demonstrated for many combinations. One example being the combination of edatrexate with cisplatin where synergy was exclusively observed when edatrexate was administered as a pre-treatment to cisplatin (Perez et al., 1993). The logic for using the STAT3 inhibitors as pre-treatments to cisplatin was that any cellular changes due to inhibition of STAT3 would need to take effect prior to cisplatin-DNA adduct formation in order to have the greatest effect on cisplatin sensitivity. This idea was adopted by Esaki et al. when they demonstrated reversal of cisplatin resistance by a pre-treatment with 5-FU. This effect was not observed when 5-FU was administered after cisplatin. They suggest that this is due to the effects of 5-FU on cisplatin-ICL repair mechanisms including regulation of ERCC1 mRNA levels, as well as regulation of cellular glutathione content (Esaki et al., 1996).

However, the pre-treatment style sequential scheduling does not always prove to be the best schedule for cisplatin combinations. Combination of histone deacetylase inhibitors with cisplatin was shown to produce the best synergy with simultaneous addition of both drugs. Sequential drug treatments in either order resulted in some additivity and antagonism (Luchenko et al., 2011). Combination of cisplatin with topoisomerase I inhibitors also demonstrated a schedule dependence where the greatest synergy was observed when cisplatin was given as a pre-treatment followed by the topoisomerase I inhibitor (Ma et al., 1998). Similarly, data from our group has demonstrated that cisplatin and gemcitabine only synergise when gemcitabine is given following cisplatin, and not in the reverse order (personal communication, Professor John Hartley). Therefore, further investigation into

whether the sequential method used here produces the greatest synergy could be performed in order to optimise drug scheduling. This is, however, beyond the scope of this thesis.

4.4.4 How Do STAT3 Inhibitors Sensitise Cells to Cisplatin?

Chemosensitisation by STAT3 inhibitors is mostly attributed to deregulation of the anti-apoptotic transcriptional targets of STAT3. However, as has been discussed already, this alone cannot be responsible for synergy between STAT3 inhibition and cisplatin. STAT3 is likely involved in the regulation of one or more cisplatin resistance mechanisms.

The synthetic STAT3 inhibitor, 5,15-DPP, which was demonstrated to sensitise gastric cancer cell lines to cisplatin, was also found to decrease levels of cellular V-ATPase (Huang et al., 2012), a cell membrane proton pump, which has been connected with resistance to several chemotherapy agents including cisplatin. The V-ATPase pumps protons from the cytoplasm to the extracellular environment using the energy from ATP (Pérez-Sayáns et al., 2010). As cisplatin binds DNA more favourably in acidic conditions, increase of cellular pH by up-regulation of proton pumps would have a detrimental effect on cisplatin sensitivity. Accordingly, proton pump inhibitors can sensitise cells to cisplatin (Luciani et al., 2004). Therefore, if a link exists between STAT3 and V-ATPase transcription, this may account for some of the synergy seen between STAT3 inhibitors and cisplatin. However, no other STAT3 inhibitors have been reported to regulate the V-ATPase.

The chemosensitisation to cisplatin by curcumin was hypothesised to be an effect of curcumin-induced Hypoxia Inducible Factor-1 α (HIF-1 α) protein degradation. Ye et al. reported that HIF-1 α transfection reduced cellular sensitivity to cisplatin and HIF-1 α siRNA enhanced sensitivity (2012). HIF-1 α is a transcription factor induced by hypoxia that regulates angiogenesis and also the P-glycoprotein (P-gp) gene *MDR-*

1 (Comerford et al., 2002). P-gp is a membrane drug efflux transporter associated with multidrug resistance. Curcumin has been shown to down-regulate P-gp protein levels in several studies (Ampasavate et al., 2010; Anuchapreeda et al., 2002; Ye et al., 2012), therefore, a link between curcumin, HIF-1 α and cisplatin efflux by P-gp may exist. However, the argument for the involvement of P-gp in cisplatin efflux is weak. Some studies have reported that P-gp expression enhances cisplatin resistance (Gibalová et al., 2012), however, others have stated that cisplatin, being a synthetic compound, is not a substrate for P-gp mediated export and that P-gp does not influence cisplatin resistance (Stordal et al., 2012). However, Gibalová et al. reported that the cisplatin resistance incurred by P-gp was not due to efflux, as the presence of a transport inhibitor did not affect cisplatin sensitivity. Instead, they suggest a mechanism whereby P-gp expression can alter the sensitivity to non-P-gp substrates through the modulation of apoptosis signalling pathways (Gibalová et al., 2012).

As curcumin is a naturally occurring compound and is relatively unspecific, the regulation of P-gp by curcumin cannot be assumed to be a direct effect of STAT3 inhibition. Curcumin also targets other transcription factors including NF- κ B and AP-1 as well as a host of growth factors, enzymes and cytokines (Goel and Aggarwal, 2010; Shehzad et al., 2012). However, STAT3 decoy oligonucleotides and the STAT3 inhibitor cucurbitacin I were also shown to down-regulate P-gp protein and *MDR-1* gene expression (Zhang et al., 2011). In addition, another STAT3 inhibitor, YC-1, also down-regulates HIF-1 α expression (Kong et al., 2014). Therefore, the regulation of cisplatin resistance by P-gp through STAT3 is a possible mechanism of sensitisation.

As of yet, there have been no direct reports of a connection between STAT3 activity and DNA repair in studies discussing chemosensitisation by STAT3 inhibitors to

cisplatin. However, several groups have reported that curcumin sensitises cells to cisplatin through the inhibition of FANCD2 monoubiquitination – a crucial event in early ICL repair (P. Chen et al., 2015; Chirnomas et al., 2006). The effect of other cisplatin sensitising compounds on DNA repair has also been documented. For example cyclosporin A and herbimycin A have been reported to sensitise cancer cells to cisplatin through the down-regulation of ERCC1, a nuclease involved in ICL repair (Li et al., 1999). Therefore, if STAT3 were to regulate the expression of key DNA repair genes, this may contribute to the chemosensitisation produced by STAT3 inhibitors. This will be investigated in the following chapter.

4.4.5 Combination of STAT3 inhibitors with other chemotherapy drugs

In this chapter, the combination of VS-43 with doxorubicin is also investigated using the SRB assay and calcosyn combination index analysis. The interaction between VS-43 and cisplatin is shown to be synergistic at the doses tested (Figure 4-13). STAT3 inhibitors have been previously reported to sensitise cancer cell lines to doxorubicin. The curcumin derivatives FLLL31 and FLLL32 were demonstrated to interact synergistically with doxorubicin in breast cancer cell lines (Lin et al., 2010c), as was the synthetic STAT3 inhibitor LLL12 in canine osteosarcoma cells (Couto et al., 2012). The JAK inhibitor AZD1480 also produced synergy in combination with doxorubicin in myeloma cells (Scuto et al., 2011), contributing further evidence to the JAK/STAT pathway being involved in doxorubicin sensitivity.

Doxorubicin is a DNA intercalator which disrupts topoisomerase II action leading to DNA damage in the form of single and double strand breaks (Tewey et al., 1984; Thorn et al., 2011). STAT3 inhibitors derived from curcumin have also been reported to sensitise cells to etoposide, camptothecin, 5-fluorouracil, gemcitabine, paclitaxel, oxaliplatin and radiotherapy (Aggarwal et al., 2005; Lev-Ari et al., 2007; Pan et al., 2013; Yallapu et al., 2010). Almost all of these agents act by targeting the

cancer cell DNA – either the integrity or the ability of it to replicate. The exception is paclitaxel, which is a microtubule inhibitor. One group did report an increase in DNA damage following paclitaxel treatment of peripheral blood lymphocytes (Branham et al., 2004). This DNA damage could, however, be a result of paclitaxel-induced apoptotic DNA fragmentation. Nevertheless, there is a clear link between STAT3 inhibitors and sensitivity to DNA-interacting chemotherapeutics, including cisplatin and doxorubicin as shown in this chapter. Consequently, STAT3 may regulate the accumulation of DNA damage or efficiency of DNA repair. This will be investigated in the following chapter.

Clearly, the use of STAT3 inhibitors extends beyond that of combination with cisplatin. STAT3 inhibitors may prove useful in combination with many other chemotherapy drugs in the clinic.

4.5 Conclusion

In conclusion, this chapter investigates the chemosensitisation properties of STAT3 inhibitors. Stattic, curcumin and VS-43 are able to sensitise cancer cell lines to cisplatin and increase the level of apoptosis in cisplatin-treated cells. VS-43 produces greater synergy in combination with cisplatin than either stattic or curcumin. Two treatment schedules were tested for the VS-43 combination, with the acute 1 hour VS-43 pre-treatment able to synergise with cisplatin as well as the 18 hour pre-treatment. The combination of VS-43 with doxorubicin was also found to be synergistic. Therefore, STAT3 inhibitors, particularly more potent compounds such as VS-43, are promising candidates for combination with chemotherapy agents including cisplatin and doxorubicin.

Chapter 5 STAT3 modulates the repair of cisplatin-induced DNA damage

5.1 Introduction

STAT3 inhibitors have been shown to sensitise cancer cell lines to cisplatin in a synergistic manner. For synergy to arise, some crossover between the action of STAT3 inhibitors and cisplatin must occur. Therefore, this chapter investigates whether STAT3 inhibitors affect the DNA damage induced by cisplatin. This will help elucidate the mechanism of sensitisation to cisplatin by STAT3 inhibitors.

5.1.1 γ H2AX as a marker of the crosslinker-induced DNA damage response

DNA is packaged into nucleosomes consisting of 145 base pairs of DNA wrapped around a core of eight histone proteins: two each of H2A, H2B, H3 and H4. H2AX is a member of the H2A family, accounting for 2-25% of the H2A protein in mammalian nucleosomes (Rogakou et al., 1998).

Upon DNA damage, thousands of H2AX proteins are phosphorylated at serine-139 by ATM, ATR and DNA-PKc. The phosphorylated form, known as γ H2AX, is able to recruit DNA repair factors (MRN, BRCA1, FANCD2, RAD51, MDC, cohesins) to damage sites (Kuo and Yang, 2008; Lyakhovich and Surrallés, 2007; Paull et al., 2000; Rogakou et al., 1998). Therefore, the phosphorylation of H2AX is essential for the DNA damage response to be triggered effectively.

γ H2AX forms foci in response to DNA damage. Foci persistence has been shown to be effective at predicting patient sensitivity to radiation (Olive and Banáth, 2004). More recently γ H2AX has been found to form foci after treatment with ICL-inducing agents such as cisplatin, mechlorethamine and mitomycin C (Clingen et al., 2008; Huang et al., 2004; Mogi and Oh, 2006). Positive correlation has been found between the number of γ H2AX foci 24 hours after cisplatin treatment and cell

survival (Olive and Banàth, 2009). γ H2AX foci have also proven useful in the determination of DNA damage following treatment with the novel cross-linker SJG-136 in clinical samples (Wu et al., 2013). It is generally accepted that γ H2AX indicates DSB sites; therefore, this suggests that for the detection of crosslink-induced DNA damage, a DSB must arise for γ H2AX foci to form. This may occur if a replication fork encounters an ICL resulting in replication fork collapse, or in the downstream repair of ICLs where nuclease action instigates DSB formation. However, the activation of the ATR kinase occurs through interaction with another protein, ATRIP, which binds to single stranded DNA. Therefore, ATRIP may accumulate at stalled replication forks or at regions where there has been recent repair of a bulky adduct, leaving a single stranded region to fill in (Kinner et al., 2008). Activation of ATR, and subsequently γ H2AX phosphorylation, may therefore, occur without the presence of a DSB, and so γ H2AX foci should be considered as a general DNA damage marker rather than specifically a marker of DSBs.

Therefore, for the purposes of this project, levels of γ H2AX will be used as a marker of the DNA damage response induced by the crosslinking drug cisplatin.

5.1.2 The key stage of ICL repair: crosslink unhooking

The mechanism by which ICLs are repaired is not fully understood but is thought to involve an initial unhooking stage, followed by translesion synthesis and in replicating cells, homologous recombination to reassemble the replication fork (Clauson et al., 2013).

The critical stage of this process is the unhooking of the ICL from one of the two DNA strands.

The process of ICL unhooking is performed by nuclease action either side of the lesion. There is much debate over the identity of the nuclease complexes involved in

this process, however, it is generally accepted that at least one of the incisions is performed by the XPF-ERCC1 complex. This is supported by evidence showing that XPF or ERCC1 knockout cells are highly sensitive to cross-linkers and are deficient in the unhooking stage of ICL repair (De Silva et al., 2000). Additionally, both XPF and ERCC1 expression have been shown to correlate directly with cisplatin sensitivity in patients (Chiu et al., 2011; Dabholkar et al., 1992; Reed et al., 2003; Ting et al., 2013; Vaezi et al., 2011).

Models for ICL unhooking exist with XPF-ERCC1 performing incisions either side of the lesion (Kuraoka et al., 2000), however, ERCC1^{-/-} cells are still capable of DSB formation after treatment with MMC (Niedernhofer et al., 2004). Additionally, data suggesting that a second nuclease complex, MUS81-EME1, could perform one of the incisions contradicts models where XPF-ERCC1 is the sole ICL unhooking nuclease. MUS81-EME1 is structurally similar to XPF-ERCC1, belonging to the same group of nucleases, and shares the ability of XPF-ERCC1 to cleave branched structures, which are likely to be found at replication forks stalled by ICLs. EME1^{-/-} and MUS81^{-/-} cells are hypersensitive to ICL-inducing agents (Abraham et al., 2003; Hanada et al., 2006; McPherson et al., 2004) and some cisplatin resistant cells express higher levels of MUS81 when compared with parental cells. Knockdown of MUS81 in those cells rescues cisplatin sensitivity (Xie et al., 2016). Further evidence suggests that the level of EME1, like ERCC1, correlates with cisplatin sensitivity *in vitro* (Tomoda et al., 2009). Like ERCC1, EME1 is a stabilising factor required for MUS81 nuclease activity (Haber and Heyer, 2001). Therefore, all four components of these nuclease complexes are important for the unhooking step.

If indeed both XPF-ERCC1 and MUS81-EME1 are required for ICL unhooking, one possible model for this process involves the MUS81-EME1 nuclease nicking the DNA on the 3' side of the ICL first, followed by XPF-ERCC1 nuclease action 5' to

the ICL (Rahn et al., 2010). However, which nuclease complex performs the first incision and to which side of the ICL is not yet fully agreed on with some suggesting that the roles of MUS81-EME1 and XPF-ERCC1 are reversed (Zhang and Walter, 2014), and others claiming that MUS81-EME1 is instead required for the removal of ICLs via an insurance pathway should ERCC1-XPF incision fail (Wang et al., 2011).

The SLX4 (FANCP) protein has drawn much interest in recent years with regard to ICL unhooking. SLX4 negative cells are 10-fold more sensitive to cisplatin than control cells. Interestingly, a function as a molecular scaffold has been suggested for SLX4 as this protein interacts with XPF-ERCC1 and MUS81-EME1 along with a nuclease SLX1 (although this nuclease is not thought to actively participate in ICL unhooking). Additionally, XPF and MUS81 nuclease activity is enhanced by SLX4. However, the formation of DSBs is not impaired in cells deficient in SLX4, therefore, it is possible that it may act downstream of unhooking (Muñoz et al., 2009). Conversely, extracts from ERCC1 depleted cells with added recombinant XPF-ERCC1 do not incise ICL-containing substrates unless SLX4 is also present (Klein Douwel et al., 2014). Therefore, the role of SLX4 in ICL unhooking is still undecided.

Another protein important in the process of ICL unhooking is the Fanconi Anemia (FA) factor FANCD2. FANCD2 ubiquitination at lysine 561 is carried out by FANCL, a FA core complex protein and E3 ligase. In a cell-free system, *Xenopus* egg extracts with depleted FANCD2 do not repair ICLs and specifically, cannot incise the DNA around the lesion. This is rescued by reintroduction of FANCD2 but not by reintroduction of a mutated FANCD2 incapable of ubiquitination (Knipscheer et al., 2009).

As SLX4 contains a UBZ ubiquitin-binding domain, this led to studies where FANCD2 was demonstrated to interact with and recruit SLX4 to ICL damage sites.

Both the SLX4 UBZ domain and FANCD2 ubiquitination are required for the recruitment of SLX4 to damage foci by FANCD2 (Klein Douwel et al., 2014; Yamamoto et al., 2011). XPF-ERCC1 was found to be required for the efficient processing of ICLs, however, it is not required for FANCD2 monoubiquitination, implying that XPF-ERCC1 acts in a FA-independent way, and that this modification could occur prior to the recruitment of nucleases to an ICL. In the absence of XPF-ERCC1, FANCD2 ubiquitination persists suggesting that FANCD2 acts upstream of XPF-ERCC1 but that nuclease action is required for the repair of ICLs (Bhagwat et al., 2009). Together, this evidence indicates a direct role of FANCD2 in the ICL unhooking process, possibly through the recruitment of nuclease complexes to the ICL via the scaffold protein SLX4.

FANCD2 has also been found to interact with BRCA1, a protein classically involved in homologous recombination. FANCD2 and BRCA1 co-localise in foci after irradiation or MMC treatment (Garcia-Higuera et al., 2001; Taniguchi et al., 2002), siRNA depletion of BRCA1 significantly decreases FANCD2 ubiquitination (Bruun et al., 2003), and BRCA1^{-/-} cells display the same phenotype as FA cells - hypersensitivity to ICL-inducing agents (Moynahan et al., 2001). Defective BRCA1 in cisplatin sensitive cells causes a reduction in FANCD2 foci formation after treatment, and exogenous BRCA1 introduction to these cells increases resistance to cisplatin implying a key role for BRCA1 alongside FANCD2 in the repair of cisplatin-induced DNA damage (Burkitt and Ljungman, 2007).

Whether BRCA1 interacts with FANCD2 directly is unknown. However, through yeast two hybrid and co-immunoprecipitation assays BRCA1 has been shown to bind FANCA, a component of the FA core complex (Folias et al., 2002). More recent research has suggested opposite roles for BRCA1 and the NHEJ end binding Ku70/80 complex. In BRCA1^{-/-} cells where FANCD2 foci formation is impaired,

depletion of Ku70/80 restores FANCD2 foci. Additionally, depletion of Ku70/80 enhances cell survival in BRCA1^{-/-} cells (Bunting et al., 2012). It is not yet understood why Ku70/80 inhibits FANCD2 foci formation but this could suggest a mechanism whereby Ku70/80 has inhibitory action on the recruitment of FANCD2 to ICLs, and BRCA1 inhibits Ku70/80 action. It is likely therefore, that BRCA1 affects FANCD2 recruitment to ICL damage sites in an indirect manner, either through direct interaction with the core FA complex or through inhibition of Ku70/80. BRCA1 has also been shown to be involved in the unloading of the replicative helicase at replication forks stalled at ICL. This role of BRCA1 allows progression of the replication fork to within 1 nucleotide of the lesion, which was shown to be required for ICL incisions to take place (Long et al., 2014).

More recently, a role for the ubiquitin-like with PHD and RING finger domain 1 (UHRF1) protein in ICL unhooking has been identified. This protein was found to directly bind an ICL-containing substrate and is required for FANCD2 foci formation. Knockdown of UHRF1 causes hypersensitivity of cells to MMC and psoralens, and also mildly increases sensitivity to cisplatin (Liang et al., 2015). Liang et al. propose that UHRF1 acts as a sensor of ICL damage and allows for FANCD2 recruitment and further downstream processing. Another group simultaneously identified UHRF1 as an ICL-interacting protein. Tian et al. found that UHRF1 was able to immunoprecipitate XPF-ERCC1 and MUS81-EME1 in the absence of SLX4, suggesting a direct interaction of UHRF1 with these nuclease complexes. However, UHRF1 deficient cells retain functional FA pathway activation after MMC treatment, and double knockout of the FA pathway and UHRF1 results in enhanced sensitivity to MMC. Therefore, the role of UHRF1 in ICL repair may be distinct from that of the FA pathway. For this reason, they suggest that UHRF1 functions dually to promote FANCD2 recruitment to the ICL site as well as a molecular scaffold parallel to SLX4 for nuclease recruitment (Tian et al., 2015). However, currently these are the only

two reports linking UHRF1 to ICL repair, therefore, further investigation is required to elucidate the detailed role of this protein in the unhooking process.

Taking into consideration all of the components described here, Figure 5-1 illustrates a possible model for the coordination of ICL unhooking during replication. BRCA1 and the FA core complex are involved in the recruitment of FANCD2 to damage sites. FANCD2, once ubiquitinated by the FA core complex, can recruit the scaffold protein SLX4 via interaction with SLX4's UBZ domain. The nuclease complexes XPF-ERCC1 and MUS81-EME1 are brought to the ICL site through their interaction with SLX4. UHRF1 may also stimulate both FANCD2 and nuclease recruitment to the ICL site. This allows for incision reactions, unhooking and progression of ICL repair.

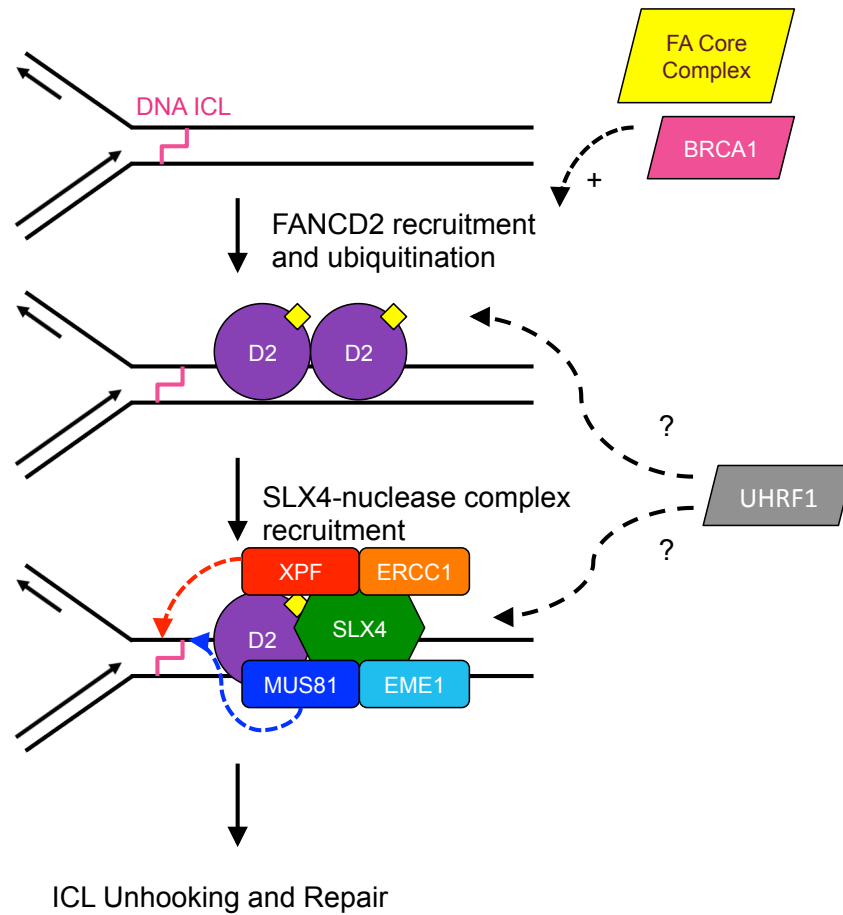


Figure 5-1: Model for initiation of replication-dependent ICL unhooking by BRCA1, FANCD2, SLX4, XPF-ERCC1, MUS81-EME1 and UHRF1.

5.1.2.1 The comet assay as a read-out for ICL unhooking

For many years, the detection of DNA interstrand crosslinks required the use of the alkaline filter elution technique. This technique involved monitoring the elution rates of radiolabelled DNA from a column. Elution time is proportional to DNA fragment size and the presence of ICLs makes DNA fragments behave as if they were larger, therefore, decreasing the elution rate (Kohn, 1991). However, this assay requires large amounts of DNA, collection of fractions is lengthy, radiolabelling is usually required and this technique cannot observe crosslinking in individual cells.

The comet assay was originally utilised to observe strand breaks in cells (Ostling and Johanson, 1984) but was later adapted for use in the detection of ICLs. This assay involves denaturation of cellular DNA in alkaline conditions and electrophoresis to separate the DNA into a “head” region where the main body of intact DNA lies, and a “tail” region where fragmented DNA migrates further (Figure 5-2). Fragmentation of DNA may be caused by irradiation, lesion specific nucleases, DSB-inducing drugs, or apoptosis. Therefore, the comet assay can act as a read-out for several types of DNA damage (Collins, 2004).

To detect ICLs, drug-treated cells are first exposed to a fixed dose of irradiation to induce DSBs, which allows a long “tail” to be seen after alkaline denaturation and electrophoresis. Cells with ICLs will result in a reduction in the amount of DNA in the “tail” region and an increase of DNA in the “head” region of the comet. This is because covalently linking DNA strands with ICLs reduces the ability of fragments to migrate through the agarose gel that the cells are embedded in. When the repair process begins and ICLs are unhooked from one strand, this effect is removed and fragments are able to migrate forming increasingly large tails depending on the extent of ICL unhooking (Spanswick et al., 2010).

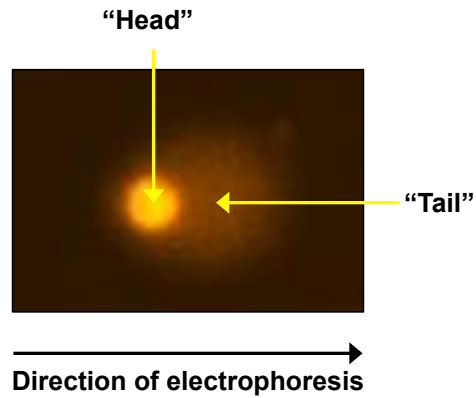


Figure 5-2: Single cell electrophoresis results in “head” and “tail” DNA, for each cell. Image as seen on Komet 6.0 software.

A clear advantage of the comet assay over other methods of crosslink detection is that monoadducts and intra-strand crosslinks do not interfere with the ability of the DNA to migrate through the agarose gel. Therefore, this assay observes solely the ICL lesion. Additionally, the comet assay is more sensitive than the alkaline elution method, capable of detecting lower levels of crosslinking (Wu et al., 2009), and is able to detect crosslinking in single cells. Radiolabelling of DNA is not required for the comet assay and so this technique can be applied to patient samples, extending its use to clinical trials (Hartley et al., 1999; Hochhauser et al., 2009; Spanswick et al., 2012, 2002).

5.2 Aims

The aims regarding the investigation of the DNA repair pathways following STAT3 inhibition were as follows:

1. To determine whether STAT3 inhibitors affect the levels of cellular DNA damage caused by cisplatin.
2. To investigate the effect of STAT3 inhibition on the unhooking of cisplatin-induced ICLs.
3. To determine whether STAT3 inhibitors affect the cellular DNA damage response.
4. To investigate whether STAT3 regulates the expression of DNA repair factors, specifically those involved in ICL repair.

5.3 Results

5.3.1 VS-43 inhibits the unhooking of cisplatin-induced ICLs

In the previous chapter, STAT3 inhibitors were demonstrated to sensitise cancer cell lines to cisplatin in a synergistic manner. As cisplatin exerts its cytotoxic effects through the adducts it forms with DNA, it is logical that the synergy noted between STAT3 inhibitors and cisplatin may arise from an enhancement of DNA damage or reduction of DNA repair in response to cisplatin treatment.

Cisplatin forms several adducts with the DNA – monoadducts, intrastrand crosslinks and interstrand crosslinks (ICLs). As ICLs covalently link the two DNA strands together these are considered highly cytotoxic as they cannot be bypassed in replication or transcription. Therefore, to test the hypothesis that STAT3 inhibitors may affect the level or the repair of cisplatin-induced DNA damage, the formation and repair of cisplatin-ICLs, was followed in cells treated with cisplatin alone, and cells treated with VS-43 followed by cisplatin.

To observe the formation and repair of ICLs in cell culture, the modified single cell gel electrophoresis or comet assay was employed. The tail moment, as discussed in the introduction of this chapter, is a direct measure of the ability of the DNA to migrate. This parameter will be used to determine the amount of ICLs in the DNA of cells treated with either cisplatin alone or cisplatin in combination with STAT3 inhibitors. The data analysis for the comet assay uses one of two equations depending on whether the second drug (the STAT3 inhibitors) cause DNA strand breaks. If the second drug produces strand breaks these must be compensated for in the final calculations. Therefore, to determine whether STAT3 inhibitors induce strand breaks the comet assay was performed on DU145 cells treated with VS-43, stattic and curcumin alone, without irradiation. Figure 5-3 shows that no DNA strand breaks are induced by VS-43, stattic or curcumin, as the tail moments observed are between 0.3-0.5, similar to the untreated cells.

The modified comet assay was then performed with cells treated with cisplatin alone or cisplatin in combination with VS-43 using the fixed ratio combination method.

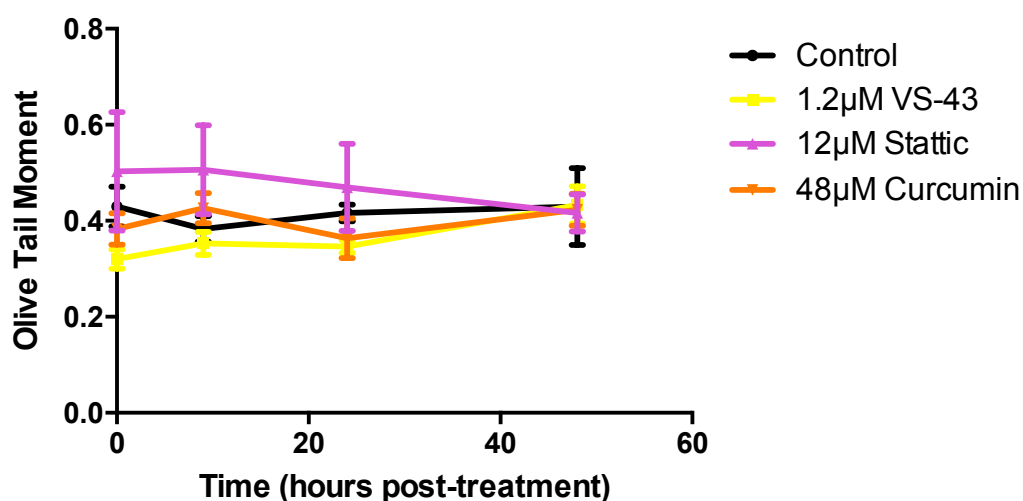


Figure 5-3: STAT3 inhibitors do not induce DNA damage. Cells treated with VS-43, stattic or curcumin did not exhibit any DNA strand breaks as determined by the modified comet assay. Data plotted is the average of at least three individual experiments with SEM calculated for error bars.

Cells were harvested immediately after cisplatin treatment, 9 hours post-treatment (the peak of cisplatin crosslinking), 24 and 48 hours post-treatment. This was to follow the formation and repair of ICLs.

In the DU145 cells, cisplatin alone (Figure 5-4A, solid line) induces a 53.7% decrease in tail moment at the 9 hour ICL peak. By 24 hours post-cisplatin treatment, the decrease in tail moment is less than 10% and this is maintained at 48 hours post-cisplatin. As the decrease in tail moment is representative of the extent of DNA interstrand crosslinking, a reduction in the percentage decrease therefore, indicates that repair to at least the ICL unhooking stage has occurred. Any further repair is not distinguishable from this assay.

In contrast, DU145 cells pre-treated with 1.2 μ M VS-43 before cisplatin exposure (Figure 5-4A, interrupted line) do not unhook the ICLs. The ICLs peak at 9 hours as with cisplatin-treated cells, indicating that VS-43 does not affect the overall level of ICLs at the peak (although a slightly higher level of crosslinking is observed, however, given the results in the rest of this chapter this is not considered to be a real effect). However, the tail moment remains decreased by between 72-73% for at least 48 hours after cisplatin treatment. Representative comet images at 48 hours post-cisplatin are shown in Figure 5-5. Cells treated with cisplatin exhibit visible comet tails similar in size to those of the untreated-irradiated cells. In comparison, VS-43 pre-treated cells have minimal comet tails and the majority of the DNA is in the head of the comet – indicative of high levels of interstrand crosslinking. This same effect is obtained in A549 cells (Figure 5-4B), although the repair of cisplatin-induced ICLs is incomplete in this cell line, where at 48 hours post-cisplatin treatment, a 30% decrease in tail moment is still present. Nonetheless, pre-treatment with VS-43 results in a maintained percentage decrease of 76.9% at 48

hours, indicating inhibition of ICL repair in this cell line also. P values and their corresponding significance levels are displayed in Table 5-1.

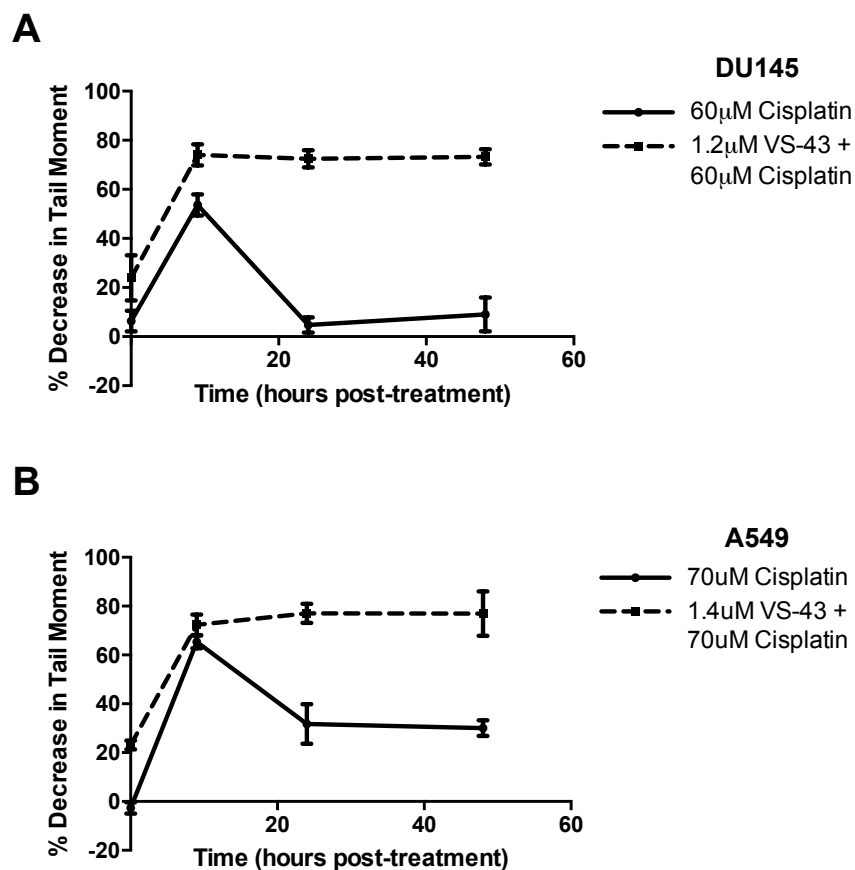


Figure 5-4: VS-43 inhibits ICL unhooking. Fixed ratio combination of VS-43 with cisplatin in the A) DU145 and B) A549 cell lines. VS-43 inhibited cisplatin-ICL repair, as determined by the modified comet assay. Data plotted is the average of at least three individual experiments with SEM calculated for error bars.

48 Hours post cisplatin treatment

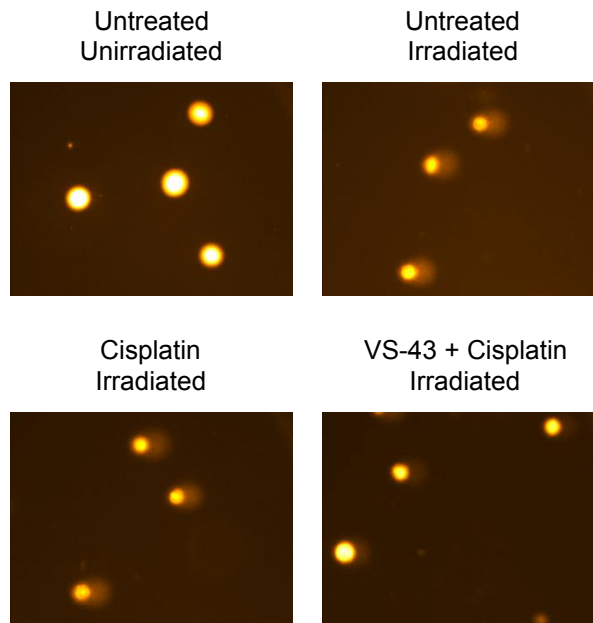


Figure 5-5: Representative comet images for DU145 cells treated with VS-43 and cisplatin.

Table 5-1: Fixed ratio comet assay P values and statistical significance. The students t-test was used as a measure of statistical significance, with the test comparing the % decrease in tail moment at each time point for cells treated with cisplatin alone and with the combination.

Time (Hours)	DU145		A549	
	P Value	Significance	P Value	Significance
0	0.0441	*	0.0115	*
9	0.0074	**	0.1126	ns
24	0.0017	**	0.0107	*
48	0.0077	**	0.0237	*

As the non-fixed ratio combination of VS-43 and cisplatin produced similar synergy to that of the fixed ratio combination in the previous chapter, the non-fixed ratio was also tested for its ability to inhibit ICL unhooking using the modified comet assay.

In the DU145 cells, cisplatin alone (Figure 5-6A, solid line) induces a 60.4% decrease in tail moment at the 9 hour ICL peak. By 24 hours post-cisplatin treatment, the decrease in tail moment is reduced to below 10%. In contrast, DU145 cells pre-treated with 5 μ M VS-43 before cisplatin exposure (Figure 5-6A, interrupted line) do not unhook the ICLs, as with the fixed ratio combination. The tail moment remains decreased by between 60-65% for at least 48 hours after cisplatin treatment. This same effect is obtained in A549 cells (Figure 5-6B), although again, the cisplatin-induced ICLs do not fully repair, as a 20.2% decrease in tail moment persists at 48 hours post-cisplatin treatment. Even so, the cells given a 10 μ M VS-43 pre-treatment have significantly inhibited ICL repair – the percentage decrease in tail moment is 67.1% at 48 hours. P values and their corresponding significance levels are displayed in Table 5-2.

Therefore, both the fixed and non-fixed ratio combination of VS-43 and cisplatin are able to significantly inhibit the unhooking of cisplatin-induced ICLs, which demonstrates persistent DNA damage, and therefore, is likely responsible for the sensitisation of cells to cisplatin by VS-43.

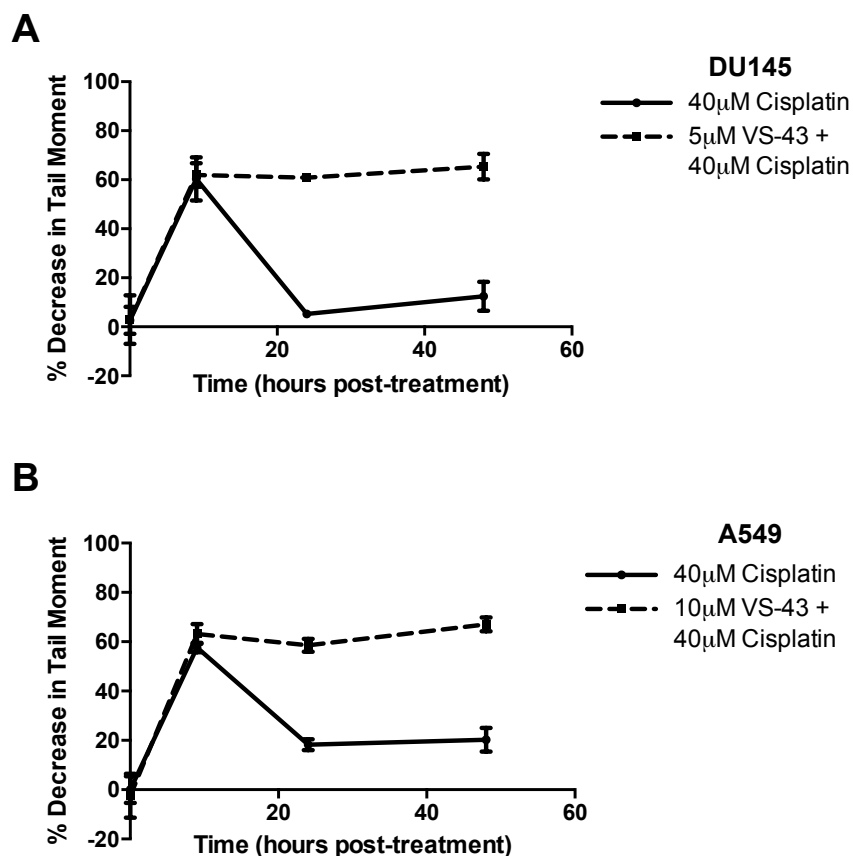


Figure 5-6: VS-43 inhibits ICL unhooking. Non-fixed ratio combination of VS-43 with cisplatin in the A) DU145 and B) A549 cell lines. VS-43 inhibited cisplatin-ICL repair, as determined by the modified comet assay. Data plotted is the average of at least three individual experiments with SEM calculated for error bars.

Table 5-2: Non-fixed ratio comet assay P values and statistical significance. The students t-test was used as a measure of statistical significance, with the test comparing the % decrease in tail moment at each time point for cells treated with cisplatin alone and with the combination.

Time (Hours)	DU145		A549	
	P Value	Significance	P Value	Significance
0	0.4774	ns	0.3134	ns
9	0.3640	ns	0.1026	ns
24	0.0005	***	0.0043	**
48	0.0197	**	0.0049	**

5.3.2 Stattic and Curcumin also inhibit cisplatin-induced DNA-ICL unhooking

In order to determine whether the inhibition of ICL unhooking seen by VS-43 is a property of all STAT3 inhibitors rather than an off-target effect of VS-43, comet assays were performed with cells treated with stattic or curcumin in combination with cisplatin.

Figure 5-7A shows that cisplatin-ICL unhooking in the DU145 cell line is completely inhibited by pre-treatment with stattic. The ICLs peak at 9 hours post-cisplatin treatment at approximately 60% decrease in tail moment. By 24 hours the cells treated with just cisplatin (solid line) have repaired the majority of the ICLs – a 12.3% decrease in tail moment is observed. However, cells treated with a combination of stattic and cisplatin (interrupted line) do not repair the ICLs - a 56.7% decrease in tail moment is still present at 24 hours. This is maintained at 48 hours post-cisplatin treatment.

Similar results were obtained in the A549 cell line, as is shown in Figure 5-7B. At 48 hours cells treated with cisplatin only have a 22.5% decrease in tail moment compared with 55.8% for cells pre-treated with stattic. The P values and their corresponding significance values are shown in Table 5-3.

The combination of curcumin with cisplatin was also tested in the DU145 cell line. Again, the ICL peak at 9 hours is similar between the two treatment groups. The cells treated with cisplatin alone then repair the ICLs, reaching an 11.4% decrease in tail moment by 48 hours (Figure 5-8, solid line). In contrast, cells pre-treated with curcumin (Figure 5-8, interrupted line) do not repair the ICLs and instead an increase in the percentage decrease in tail moment is seen. By 48 hours post-cisplatin a 75.6% decrease in tail moment is seen for the combination treated cells. The P values and their corresponding significance values are shown in Table 5-4.

These results indicate that inhibition of ICL unhooking is a property of all the STAT3 inhibitors tested. Therefore, STAT3 itself may be involved in the regulation of DNA repair factors. This will be investigated in the next section.

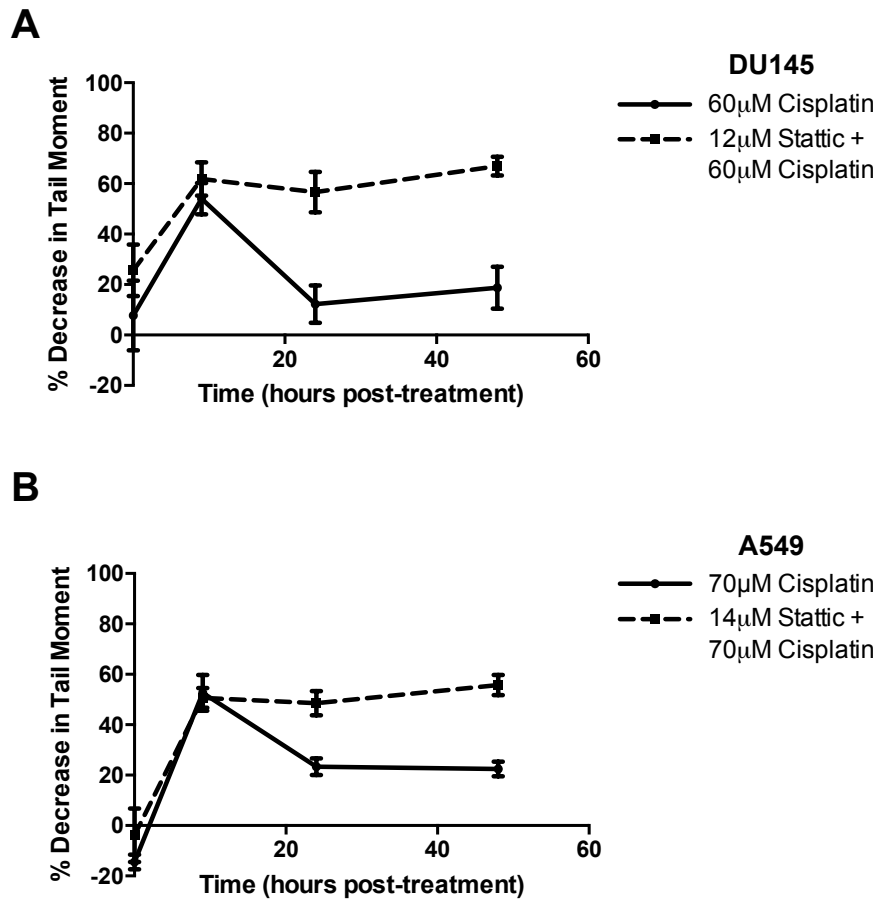


Figure 5-7: Static inhibits ICL unhooking. Fixed ratio combination of static with cisplatin in the A) DU145 and B) A549 cell lines inhibited cisplatin-ICL repair, as determined by the modified comet assay. Data plotted is the average of at least three individual experiments with SEM calculated for error bars.

Table 5-3: Static and cisplatin comet assay P values and statistical significance. The students t-test was used as a measure of statistical significance, with the test comparing the % decrease in tail moment at each time point for cells treated with cisplatin alone and with the combination.

Time (Hours)	DU145		A549	
	P Value	Significance	P Value	Significance
0	0.3589	ns	0.3900	ns
9	0.4389	ns	0.8182	ns
24	0.0154	*	0.0125	*
48	0.0062	**	0.0026	**

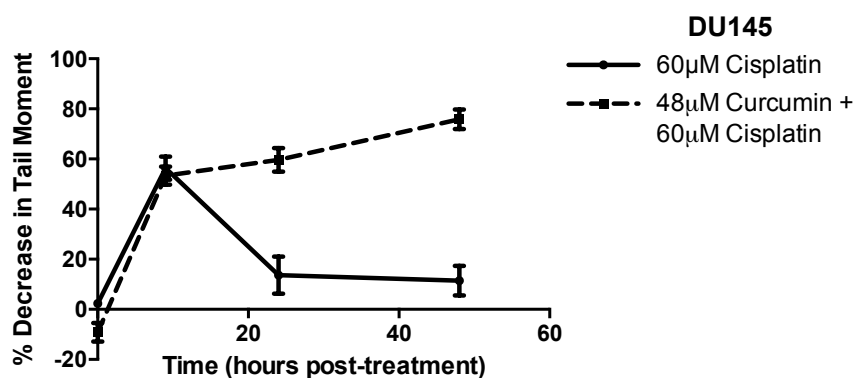


Figure 5-8: Curcumin inhibits ICL unhooking. Fixed ratio combination of curcumin with cisplatin in the DU145 cell line inhibited cisplatin-ICL repair, as determined by the modified comet assay. Data plotted is the average of at least three individual experiments with SEM calculated for error bars.

Table 5-4: Curcumin and cisplatin comet assay P values and statistical significance. The students t-test was used as a measure of statistical significance, with the test comparing the % decrease in tail moment at each time point for cells treated with cisplatin alone and with the combination.

	DU145	
Time (Hours)	P Value	Significance
0	0.0413	*
9	0.6329	ns
24	0.0063	**
48	0.0008	***

5.3.3 STAT3 inhibition alters the DNA damage response after treatment with cisplatin

As STAT3 inhibitors have been shown to inhibit cisplatin-ICL repair, the effect of STAT3 inhibition on the cellular DNA damage response after cisplatin treatment was next observed. The phosphorylated version of histone H2AX (γ H2AX) was employed as a marker of the DNA damage response, as it is recruited to sites of DNA damage. Levels of γ H2AX were assessed by confocal microscopy. Cells were treated with cisplatin, VS-43 or a combination of VS-43 and cisplatin using the fixed ratio treatment method, at concentrations that produced synergy as reported in the previous chapter. The cells were then fixed and stained for γ H2AX at 0, 9, 24 and 48 hours after cisplatin treatment.

Figure 5-9 shows representative images from these experiments in DU145 cells. The top panels show untreated control cells and cells treated with VS-43 alone, neither of which have γ H2AX staining. The lower left panel shows cells treated with cisplatin alone, which do have increasing γ H2AX foci over time. The lower right panel shows cells pre-treated with VS-43 before cisplatin treatment.

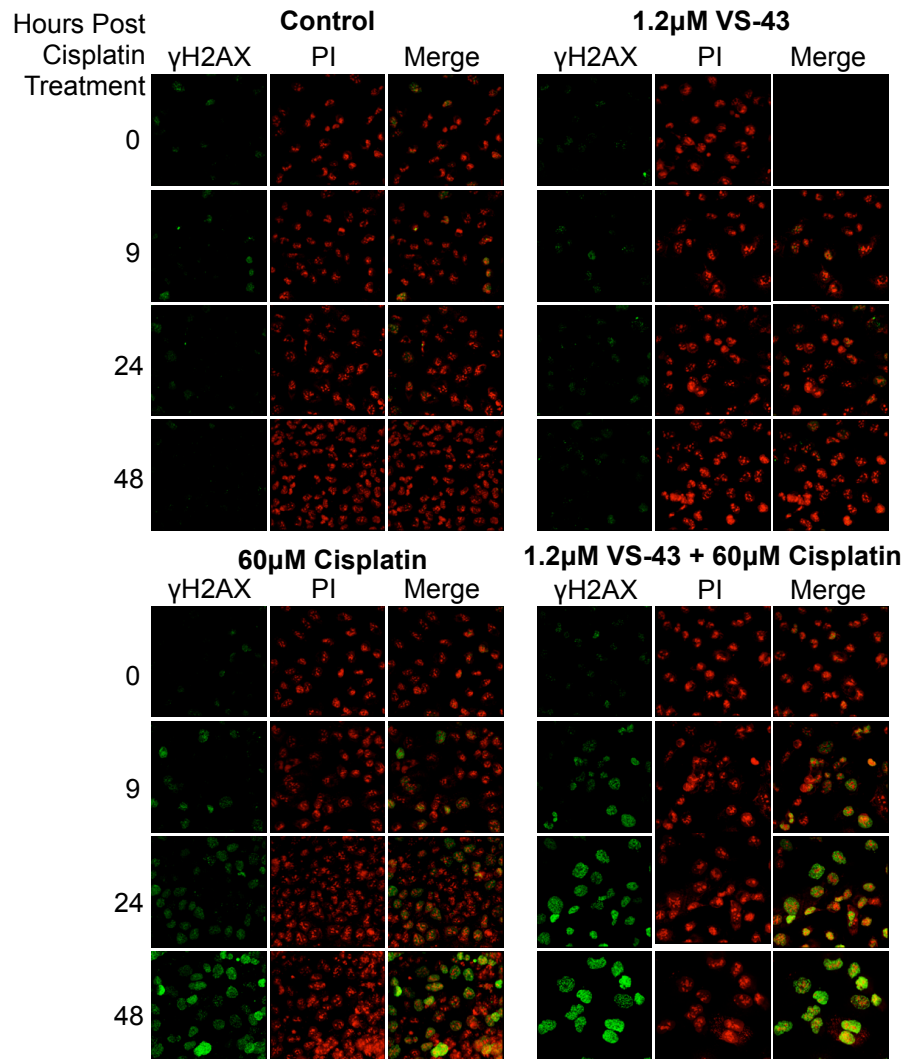


Figure 5-9: VS-43 enhances cisplatin-induced γ H2AX expression in the DU145 cell line. Confocal microscopy showing DU145 cells stained with γ H2AX antibody at four time points: 0, 9, 24 and 48 hours. Top left panel shows control cells (untreated). Top right panel shows cells treated with VS-43 for 18 hours. Bottom left panel shows cells treated with cisplatin for 1 hour, and bottom right panel shows cells treated with a combination of VS-43 and cisplatin. Images are representative of more than 1 experiment.

These cells display greater γ H2AX staining at every time point when compared to the cells treated with cisplatin alone. This staining was quantified for three repeats using the Cell Profiler software, which counts the number of γ H2AX foci per nucleus. Figure 5-10 shows that there is a statistically significant increase in γ H2AX staining in combination treated cells at 9, 24 and 48 hours when compared with cells treated with cisplatin alone. The greatest difference occurs at 24 hours; where cisplatin treated cells show an average of 15.5 foci per cell compared with 52.7 foci per cell for the combination treated cells.

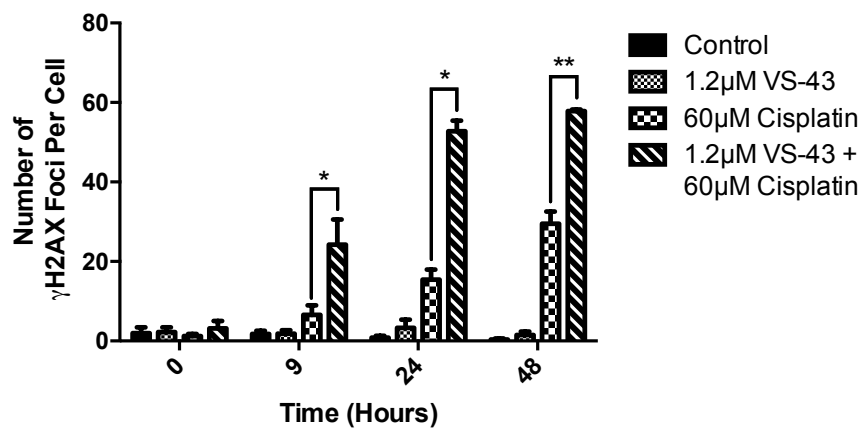


Figure 5-10: Quantification of γ H2AX staining in the DU145 cell line after treatment with VS-43, cisplatin or the combination treatment. Quantification was performed by Cell Profiler with a threshold of 0.3. Data is the average of three independent experiments with the SEM calculated for error bars. Statistical significance was calculated using the one-way ANOVA with * = $P < 0.05$ and ** = $P < 0.01$.

As the dose of cisplatin used (60 μ M) induces approximately 50% cell growth inhibition in DU145 cells, γ H2AX staining was also performed for cells treated with a low-dose of cisplatin (6 μ M) in combination with VS-43. This was to lower the amount of DNA damage that may be occurring due to cisplatin-induced apoptosis. The combination of a low-dose cisplatin treatment with VS-43 resulted in a similar pattern as was seen for the higher dose. Whilst VS-43 itself did not result in γ H2AX staining, in combination with cisplatin, VS-43 enhanced cisplatin-induced γ H2AX staining (Figure 5-11). This effect was most striking at 48 hours post-cisplatin treatment where the combination treatment resulted in an average of 25.6 foci per cell compared with 0.51 foci per cell in cells treated with low-dose cisplatin alone (Figure 5-12).

γ H2AX staining was also carried out in A549 cells treated with VS-43 and cisplatin. Figure 5-13 shows that cells treated with VS-43 and cisplatin in combination exhibit a greater degree of γ H2AX staining. The effect in this cell line is not so clear, however, as there was more non-specific background binding. For this reason, quantification of γ H2AX foci was not possible in this cell line.

In order to test whether other STAT3 inhibitors can enhance the number of γ H2AX foci after cisplatin treatment, curcumin was used in combination in the DU145 cells. Figure 5-14A shows representative images of cells treated with curcumin, cisplatin or the combination at 48 hours post cisplatin. Again, curcumin did not induce γ H2AX foci, and cisplatin treatment resulted in an average of 17.3 foci per cell. When cells were treated with curcumin and cisplatin in combination, this increased to 28.6 foci per cell (Figure 5-14B). This is a 40% increase in γ H2AX staining.

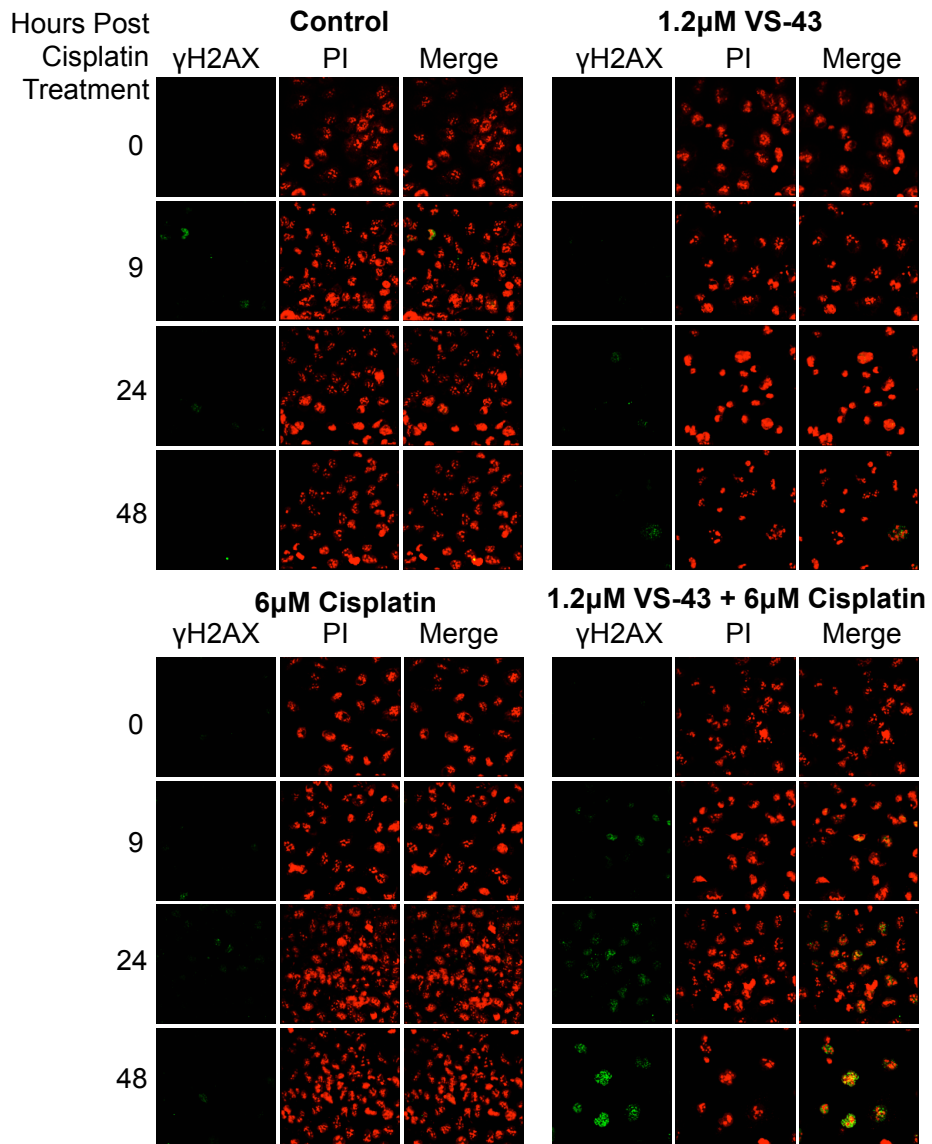


Figure 5-11: VS-43 enhances γ H2AX expression after a low dose of cisplatin in the DU145 cell line. Confocal microscopy showing DU145 cells stained with γ H2AX antibody at four time points: 0, 9, 24 and 48 hours. Top left panel shows control cells (untreated). Top right panel shows cells treated with VS-43 for 18 hours. Bottom left panel shows cells treated with cisplatin for 1 hour, and bottom right panel shows cells treated with a combination of VS-43 and cisplatin. Images are representative of more than 1 experiment.

Immunoblotting for γ H2AX after VS-43 and cisplatin combination treatment in the A549 cell line was performed in addition to confocal microscopy (Figure 5-15A). This shows clearly that γ H2AX expression is greatly increased in the combination treated cells over cells treated with cisplatin alone, where some γ H2AX is detectable. The same immunoblotting was also carried out for combination of stattic and curcumin with cisplatin in the DU145 cell line (Figure 5-15B). Treatment of cells with cisplatin induces γ H2AX expression, whereas treatment with stattic or curcumin does not. The combination of either stattic or curcumin with cisplatin results in an enhanced γ H2AX expression in both instances, however, curcumin appears to have a greater effect in combination with cisplatin than stattic at the equitoxic doses used.

Therefore, as γ H2AX is considered an accepted marker of the DNA damage response, there is a clear link between STAT3 inhibition and the extent of damage response invoked by cisplatin and this is likely to contribute towards the synergy observed between these two agents.

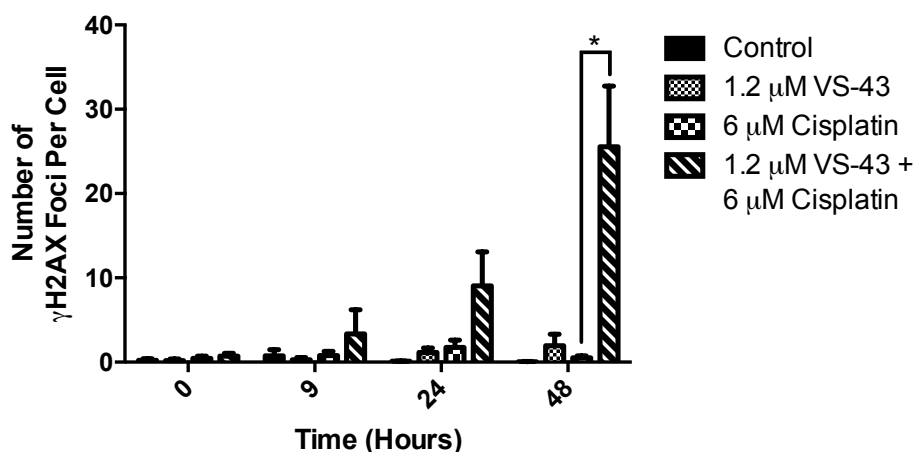


Figure 5-12: Quantification of γ H2AX staining in the DU145 cell line after treatment with VS-43, low-dose cisplatin or the combination treatment. Quantification was performed by Cell Profiler with a threshold of 0.3. Data is the average of three independent experiments with the SEM calculated for error bars. Statistical significance was calculated using the one-way ANOVA with * = $P < 0.05$.

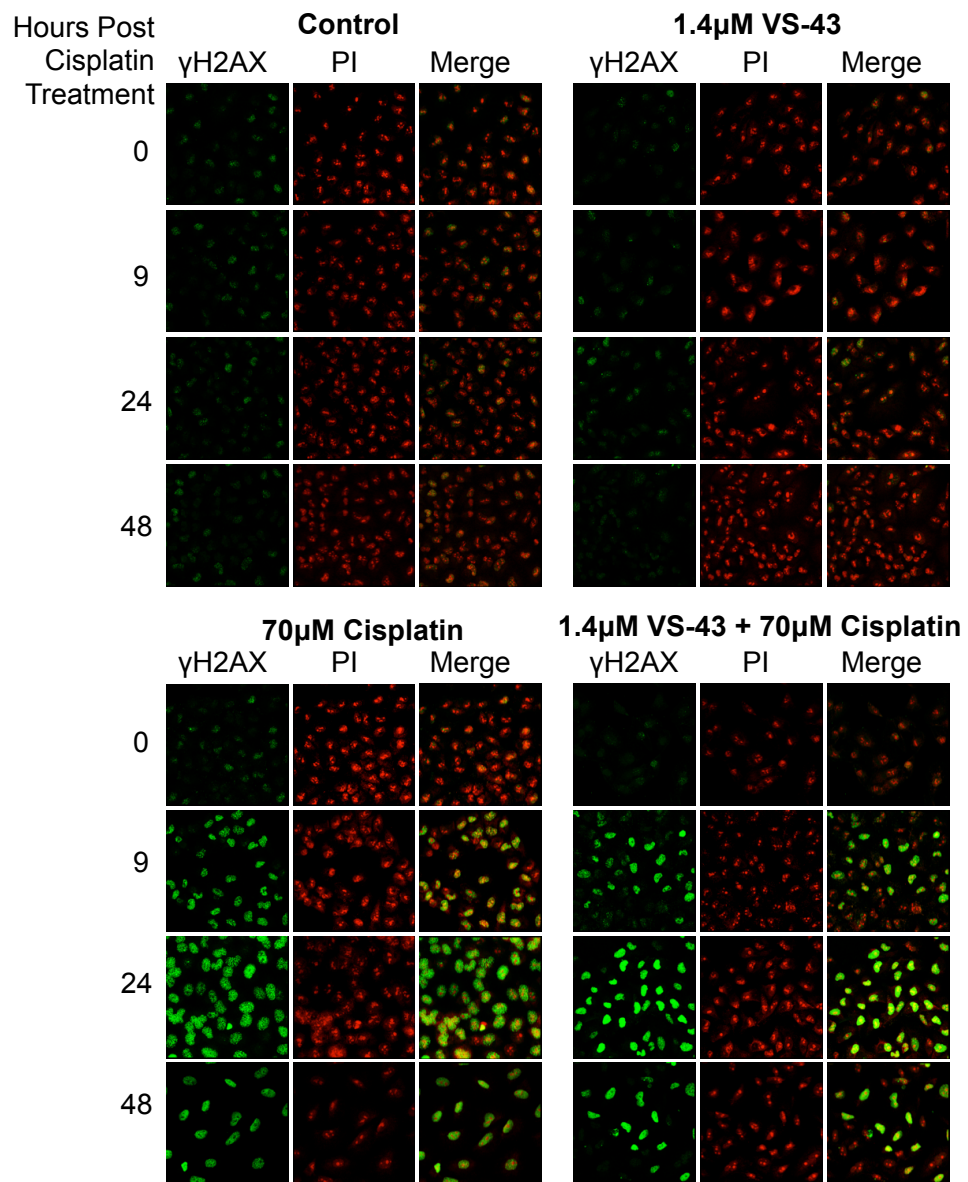


Figure 5-13: VS-43 enhances cisplatin-induced γ H2AX expression in the A549 cell line. Confocal microscopy showing A549 cells stained with γ H2AX antibody at four time points: 0, 9, 24 and 48 hours. Top left panel shows control cells (untreated). Top right panel shows cells treated with VS-43 for 18 hours. Bottom left panel shows cells treated with cisplatin for 1 hour, and bottom right panel shows cells treated with a combination of VS-43 and cisplatin. Images are representative of more than 1 experiment.

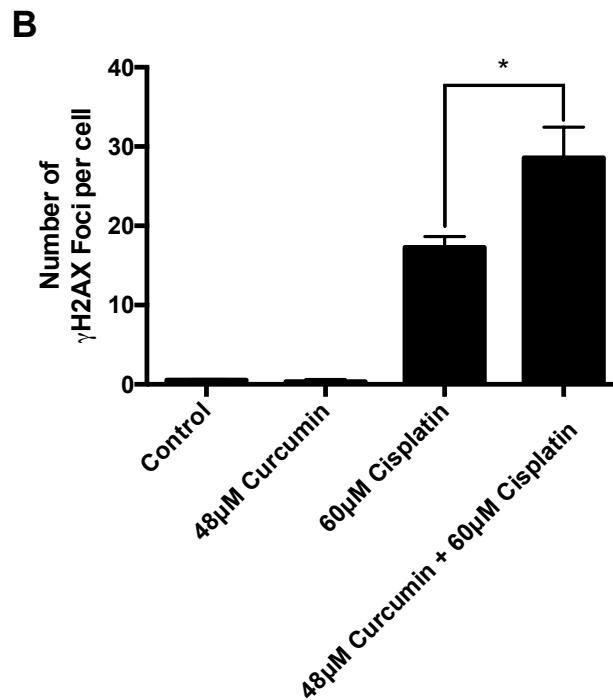
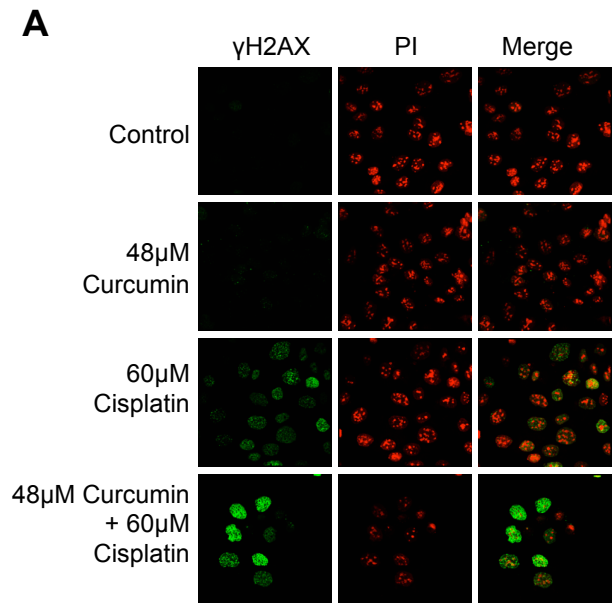


Figure 5-14: Curcumin enhances cisplatin-induced γ H2AX expression. A) Confocal microscopy showing DU145 cells stained with γ H2AX antibody at 48 hours post-drug treatment. Curcumin enhances cisplatin-induced γ H2AX expression. Images are representative of more than 1 experiment. B) Quantification of the above γ H2AX staining. Quantification was performed by Cell Profiler with a threshold of 0.3. Data is the average of three independent experiments with the SEM calculated for error bars. Statistical significance was calculated using the one-way ANOVA with * = P<0.05.

5.3.4.1 Array analysis of DNA damage signalling factors reveals up-regulation of the stress response and down-regulation of DNA repair following VS-43 treatment.

To determine if any DNA repair genes are regulated by STAT3 inhibition, an initial screen using a PCR array with 84 genes involved in DNA damage and damage signalling was employed. DU145 cells were treated with two doses of VS-43 for 18 hours: 1 μ M and 2 μ M. This would allow for the determination of genes regulated in a dose-dependent manner.

The array chosen contained groups of genes involved in apoptosis, cell cycle control and several DNA repair pathways including BER, DSB repair, MMR, and damage binding. The full list of genes can be found in Appendix A.

C_T analysis on the three independent repeats was performed. To be considered a significant change in mRNA expression the following criteria were applied:

1. A dose-dependency in fold regulation must be seen.
2. At 1 μ M VS-43, a fold regulation of $>\pm 1.2$ must be seen.
3. At 2 μ M VS-43, a fold regulation of $>\pm 2.0$ must be seen.
4. P value at both doses tested must be significant (<0.05).

Candidate genes fitting this selection process were then separated into up and down-regulated pools, and ordered from the largest to smallest fold regulation at 1 μ M VS-43. This is because 1 μ M is closer to the concentration used in the comet assays where unhooking of ICLs was shown to be inhibited. The results are displayed in Table 5-5.

Transcription of four genes was up-regulated by VS-43. These include DDIT3 (GADD153) and GADD45a – two stress sensor proteins involved in endoplasmic reticulum stress-mediated apoptosis (Liebermann and Hoffman, 2008; Oyadomari

and Mori, 2004), and CDKN1A (p21) – a cell cycle regulator, considered a marker of cell cycle arrest (Gartel et al., 1996). These genes therefore, are most likely related to the cellular stress induced by exposure to VS-43 and are not involved in DNA damage repair. MLH1, the mismatch repair protein, is also up-regulated by VS-43. No other significant up-regulations were observed.

All of the genes found to be down-regulated by VS-43 treatment are involved in DNA repair pathways (Table 5-5). The top hit was LIG1, a ligase involved in replication and BER. FANCD2 and BRCA1 mRNA were also down-regulated in a dose-dependent manner. These factors have both been linked to ICL repair and therefore, they are viable targets for further investigation. Other down-regulated repair factors with connections to ICL repair include FANCA and BRIP1 (FANCI), however, these were found to be affected less by VS-43 treatment.

Table 5-5: DNA damage signalling array: fold regulation and P value for genes up or down-regulated by a 1 μ M and 2 μ M 18 hour VS-43 treatment.

	1 μ M VS-43		2 μ M VS-43	
Gene	Fold Regulation	P value	Fold Regulation	P value
<i>Up-regulated</i>				
DDIT3	2.98	0.0232	9.44	0.0332
GADD45A	2.02	0.0480	7.96	0.0027
CDKN1A	2.01	0.0492	5.21	0.0052
MLH1	1.69	0.0155	2.01	0.0436
<i>Down-regulated</i>				
LIG1	-1.97	0.0043	-5.70	0.0001
FANCD2	-1.40	0.0222	-2.91	0.0059
BRCA1	-1.34	0.0431	-4.74	0.0005
XRCC1	-1.27	0.0120	-4.75	0.0001
FANCA	-1.26	0.0335	-3.19	0.0000
OGG1	-1.26	0.0391	-2.94	0.0019
RPA1	-1.23	0.0043	-2.72	0.0002
BRIP1	-1.22	0.0067	-4.57	0.0002
MDC1	-1.21	0.0255	-4.33	0.0004

Investigation of every DNA repair factor modulated by VS-43 is beyond the scope of this thesis therefore, only the top hits most relevant to the unhooking of ICLs will be investigated further – these are FANCD2 and BRCA1.

5.3.4.2 VS-43 does not affect levels of XPF-ERCC1 or SLX4

The PCR array used in section 5.3.4.1 did not contain several factors thought to be involved in ICL repair. Namely, the nucleases XPF and MUS81-EME1, and the scaffolding protein SLX4, all thought to play roles in ICL unhooking. Therefore, a combination of immunoblotting and single gene RT-PCR was employed to observe any changes in the protein and/or mRNA levels of these genes after VS-43 treatment.

The primary nuclease complex believed to be involved in ICL unhooking is XPF-ERCC1 (Zhang and Walter, 2014). The PCR array included ERCC1 but did not include XPF therefore, both of these proteins were analysed by immunoblot in cells treated with increasing concentrations of STAT3 inhibitors for 18 hours.

Figure 5-16A illustrates that in the DU145 cell line, protein levels of XPF and ERCC1 are not affected by treatment with VS-43, stattic or curcumin. In agreement with this, the DNA damage signalling RT-PCR array determined the fold regulation of ERCC1 to be 1.11 and -1.46 for 1 μ M and 2 μ M VS-43, respectively. This does not fit the criteria for a significant result. Therefore, STAT3 inhibitors do not inhibit ICL unhooking through the regulation of the XPF-ERCC1 nuclease.

A second factor considered important in the orchestration of ICL unhooking is the scaffold protein SLX4. Immunoblotting for this factor after VS-43 treatment in the A549 and DU145 cell lines showed no effect on cellular SLX4 levels (Figure 5-16B).

Therefore, neither the depletion of XPF, ERCC1 or SLX4 contributes to the inhibition of ICL unhooking seen by STAT3 inhibition.

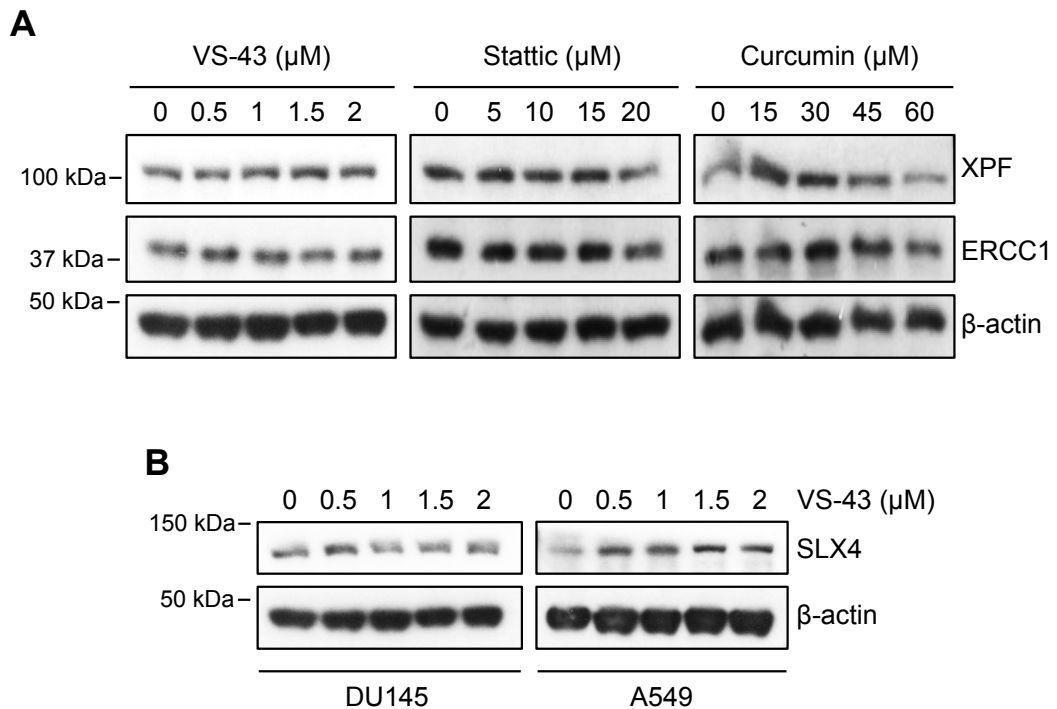


Figure 5-16: A) STAT3 inhibitors do not regulate ERCC1 or XPF expression. B) VS-43 does not regulate SLX4 expression. Blots are representative of more than 1 experiment.

5.3.4.3 VS-43 affects cellular EME1, FANCD2, BRCA1 and MUS81 mRNA and protein levels

The RT-PCR array identified two key ICL repair genes as being significantly down-regulated by VS-43: FANCD2 and BRCA1. To confirm this result, single gene RT-PCR was performed using Taqman gene assays. FANCD2 mRNA levels were down-regulated to 0.806, 0.751 and 0.644 of the control mRNA level by increasing concentrations of VS-43. BRCA1 mRNA levels were down-regulated to 0.623, 0.558 and 0.381 of the control mRNA level by increasing concentrations of VS-43 (Figure 5-17). Therefore, down-regulation of both of these genes at the mRNA level is confirmed.

MUS81-EME1 is thought to be involved in one of the incision reactions during ICL unhooking (Hanada et al., 2006). Therefore, the mRNA level of these targets after VS-43 treatment was also analysed. EME1 mRNA was down-regulated by increasing concentrations of VS-43 to 0.417, 0.427 and 0.270 of the control mRNA level. The changes in MUS81 mRNA after VS-43 treatment were 1.34, 1.07 and 0.633. Therefore, at the higher doses of VS-43, down-regulation of MUS81 mRNA was observed, however, this was not to the same extent as EME1, FANCD2 and BRCA1 mRNA (Figure 5-17).

The protein levels of FANCD2, BRCA1, EME1, and MUS81 were also investigated to observe whether the effect of VS-43 on mRNA levels translates into cellular protein levels of these targets. Figure 5-18 shows that in both DU145 (A) and A549 (B) cells the protein levels of FANCD2, BRCA1, EME1 and MUS81 are down-regulated by 18 hour treatment with increasing concentrations of VS-43. This down-regulation is maintained for at least 24 hours post VS-43 removal, indicating that during the 1 hour cisplatin treatment and the following 23 hours, these repair factors are depleted. Comet assays have shown that the majority of cisplatin-ICL repair occurs within the first 24 hours after cisplatin treatment therefore, lower levels of these factors may impair the unhooking process.

It appears that EME1 is the most heavily down-regulated factor, particularly in the DU145 cell line, where as little as 0.5 μ M VS-43 almost completely abolishes EME1 expression. BRCA1, FANCD2 and MUS81 are all, however, dose-dependently inhibited by VS-43 treatment.

Therefore, VS-43 regulates the cellular levels of BRCA1, FANCD2, EME1 and MUS81 mRNA and protein levels in the cell lines tested here. This may contribute towards the inhibition of ICL unhooking and sensitivity to cisplatin induced by VS-43 treatment.

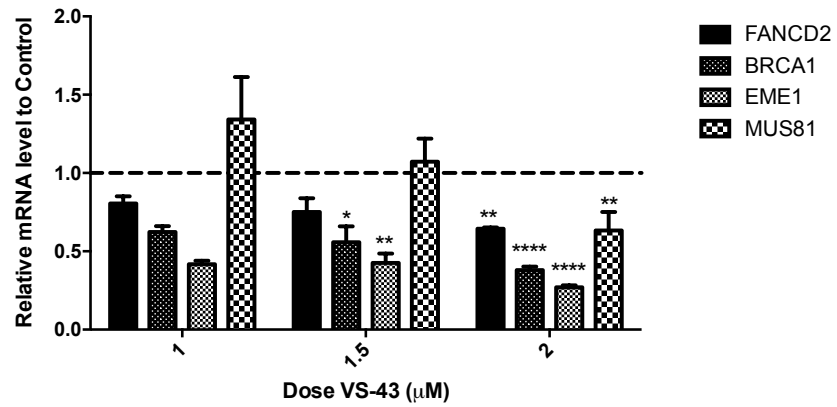


Figure 5-17: VS-43 inhibits FANCD2, BRCA1, EME1 and MUS81 mRNA expression in the DU145 cell line. Data is the average of three independent experiments with SEM calculated for error bars. One-way ANOVA was used to determine statistical significance with * = $P < 0.05$, ** = $P < 0.01$, and **** = $P < 0.0001$. mRNA level was normalised to untreated cells and GAPDH.

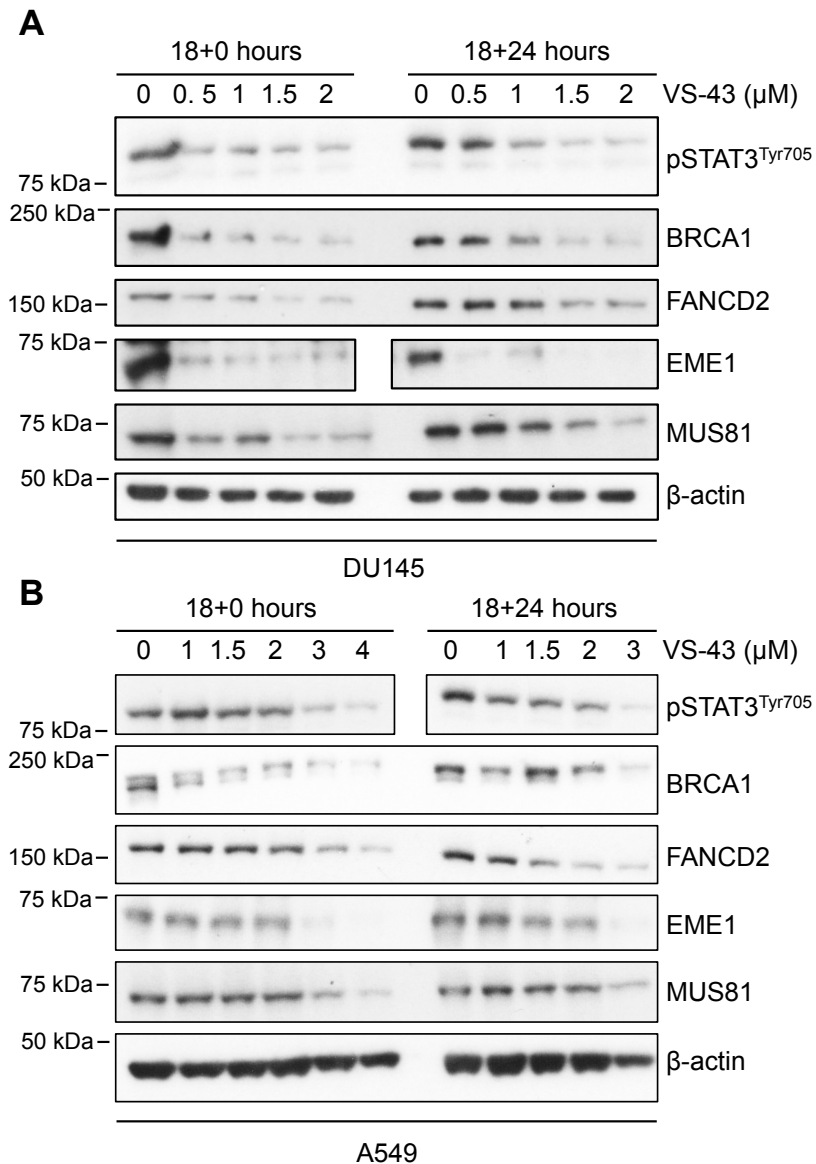


Figure 5-18: VS-43 inhibits expression of BRCA1, FANCD2, EME1 and MUS81 in the A) DU145 and B) A549 cell lines. This effect persists at least 24 hours after VS-43 removal. Blots are representative of more than 1 experiment.

5.3.4.4 *Stattic and curcumin also down-regulate mRNA and protein expression of FANCD2, EME1 and BRCA1*

In order to establish whether the effects seen on BRCA1, FANCD2, EME1 and MUS81 mRNA and protein expression by VS-43 were due to STAT3 inhibition rather than off-target effects of this compound, immunoblotting and RT-PCR was performed for these factors after the treatment of DU145 cells with stattic and curcumin for 18 hours.

Figure 5-19A shows that both stattic and curcumin dose-dependently down-regulate BRCA1, FANCD2, EME1 and MUS81 protein expression. This correlates with inhibition of pSTAT3^{Tyr705} by these compounds. As with VS-43 treatment, EME1 protein expression is down-regulated to the greatest extent, particularly with curcumin where 30µM almost completely abolishes EME1 expression.

Figure 5-19B shows the relative mRNA levels for the four DNA repair factors after treatment with two doses of stattic: one sub-GI₅₀ dose and one supra-GI₅₀ dose. FANCD2 and EME1 mRNA expression are down-regulated by treatment of cells with stattic, however, this effect is not dose-dependent. EME1 mRNA level is decreased to 0.41 and 0.44 of the control cells for 10µM and 20µM stattic, respectively. FANCD2 mRNA is decreased to 0.716 and 0.767 of the control cells at the two doses. BRCA1 does display a dose-dependent inhibition in mRNA expression, with 10µM stattic reducing mRNA to 0.776 that of control cells, and 20µM stattic reducing mRNA to 0.422 that of control cells. The results obtained for MUS81 mRNA expression after stattic treatment demonstrated dose-dependency but no statistically significant change.

The relative mRNA levels of FANCD2, EME1, BRCA1 and MUS81 after treatment of cells with curcumin can be seen in Figure 5-19C. As with stattic, two doses of curcumin were used: one sub-GI₅₀ dose and one supra-GI₅₀ dose. Curcumin has the

greatest effect on mRNA expression when compared with either static or VS-43, which may be due to curcumin's lack of specificity. All four DNA repair factors display a dose-dependent decrease in mRNA expression after treatment with curcumin. As with VS-43, This is strongest for EME1, where at 60 μ M curcumin, mRNA expression is reduced to 0.154 that of control cells. MUS81 mRNA expression is also significantly down-regulated by the higher dose of curcumin, reaching 0.42 relative to control mRNA expression.

Therefore, as STAT3 inhibitors have been demonstrated here to down-regulate the mRNA and protein levels of BRCA1, FANCD2, EME1 and MUS81, it is possible that STAT3 may directly regulate the transcription of these DNA repair factors.

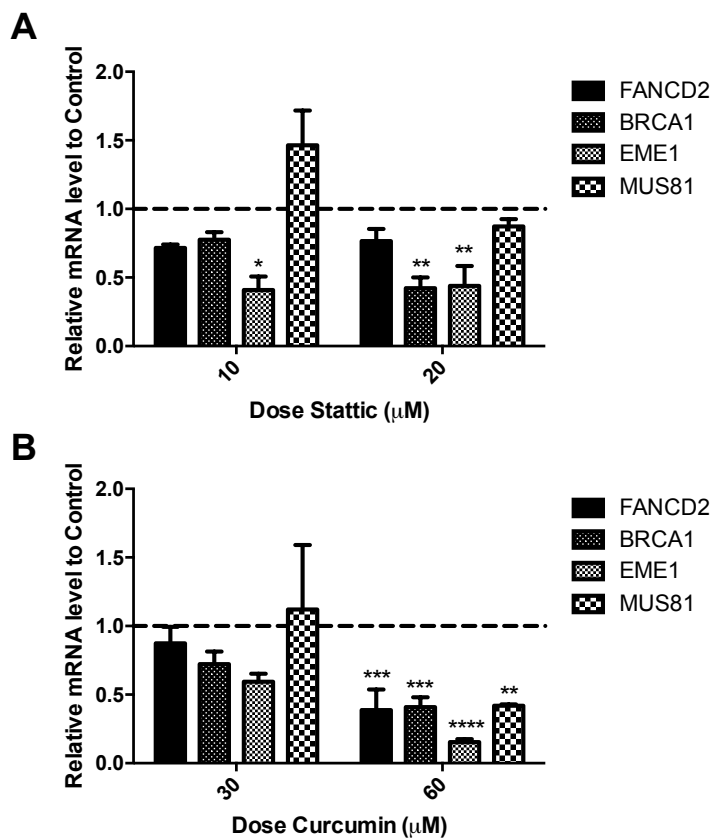
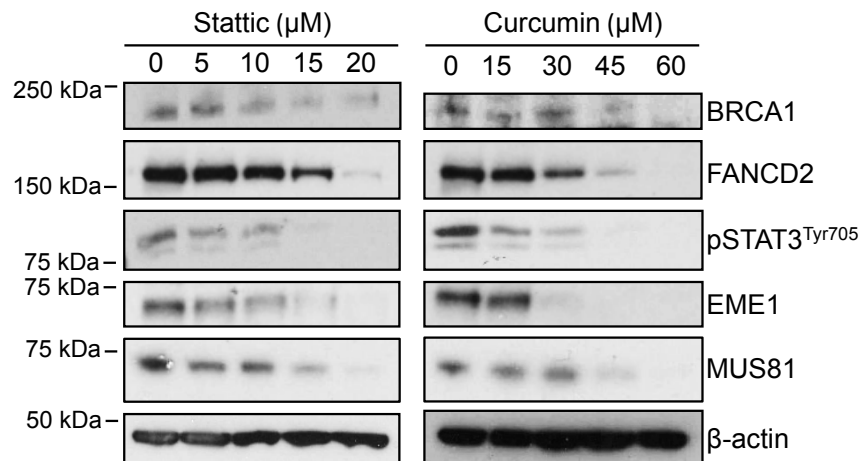


Figure 5-19: A) Stattic and curcumin inhibit the expression of BRCA1, FANCD2, EME1 and MUS81. B) Stattic and C) curcumin inhibit the mRNA expression of FANCD2, BRCA1, EME1 and MUS81. Blots are representative of more than 1 experiment. Data is the average of three independent experiments with SEM calculated for error bars. One-way ANOVA was used to determine statistical significance with * = $P < 0.05$, ** = $P < 0.01$, *** = $P < 0.001$ and **** = $P < 0.0001$. mRNA level was normalised to untreated cells and GAPDH.

5.3.5 STAT3 inhibition blocks G1 to S phase cell cycle progression

Next, the effect of STAT3 inhibition on the cell cycle was assessed by flow cytometry. This was required in order to determine whether the down-regulation of DNA repair factors by STAT3 inhibition is a result of cell cycle phase.

First, asynchronous DU145 cells were treated with VS-43 for 18 hours at increasing doses, and then harvested and stained for cell cycle analysis. Representative cell cycle plots are shown in Figure 5-20A. Treatment with VS-43 does not appear to have a large effect on the cell cycle; however, there does appear to be a lower proportion of cells in S-phase (yellow). These plots were quantified for the percentage of cells in each cell cycle phase using Flowjo v10 (Figure 5-20B). This revealed that the percentage of cells in S phase dose-dependently decreases with VS-43 treatment. There is also a dose-dependent increase in the G1 population, although this is not statistically significant, and also a slight increase in the G2 population.

Identical experiments were performed in DU145 cells treated with stattic and curcumin at equipotent doses to those used for VS-43. The representative cell cycle plots show a similar slight decrease in S phase cells (yellow) after treatment with stattic (Figure 5-21A and Figure 5-21B). Whilst a slight increase in the percentage of G1 phase cells is seen, this is not statistically significant.

For curcumin treated cells, again a dose-dependent decrease in S phase cells is seen on the representative cell cycle plots with increasing doses of curcumin (Figure 5-22A and Figure 5-22B).

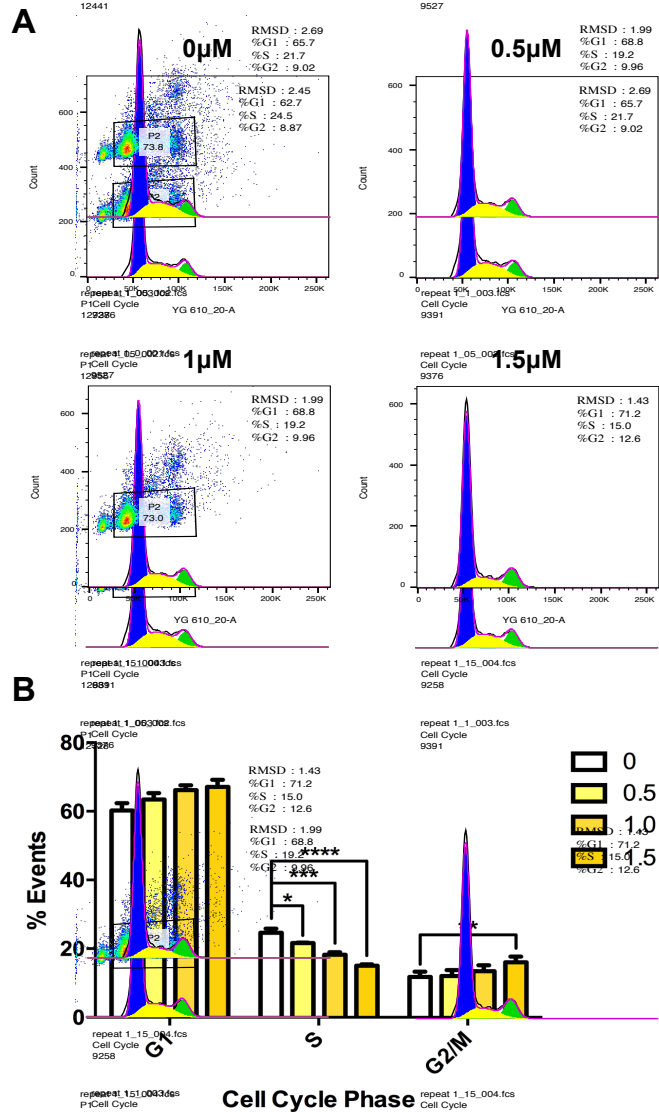


Figure 5-20: VS-43 decreases the percentage of S-phase cells. A) Representative cell cycle plots of DU145 cells treated with increasing doses of VS-43 (μM). B) Quantification of the percentage of cells in each cell cycle phase, performed by Flowjo v10. Data is the average of three independent experiments with SEM calculated for error bars. One-way ANOVA was used to determine statistical significance with * = $P < 0.05$, ** = $P < 0.01$, *** = $P < 0.001$ and **** = $P < 0.0001$.

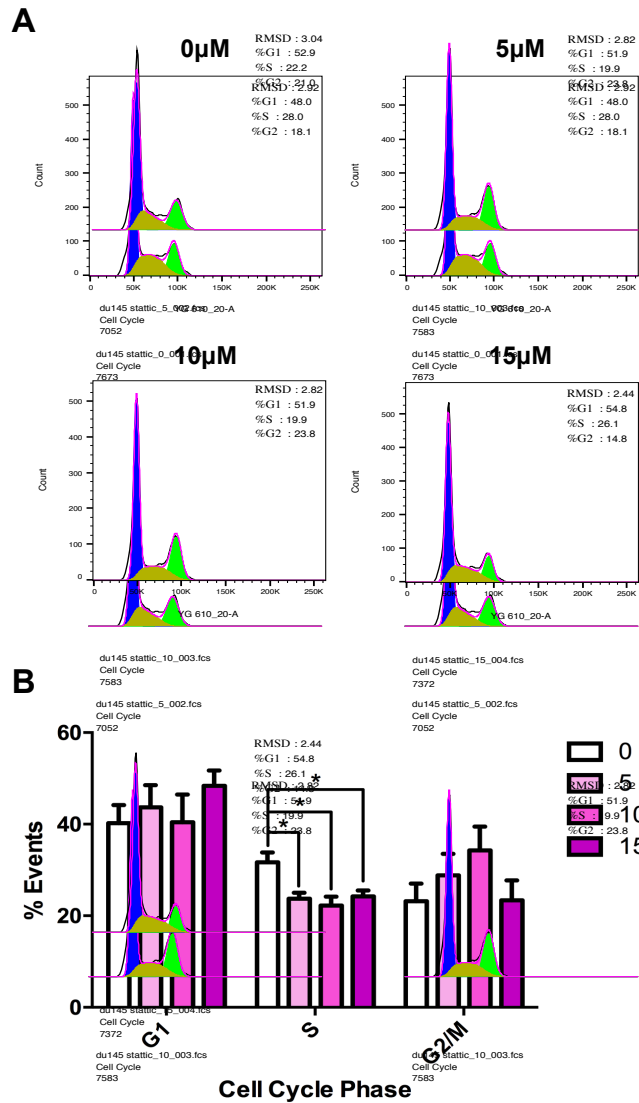


Figure 5-21: Stattic decreases the percentage of S-phase cells. A) Representative cell cycle plots of DU145 cells treated with increasing doses of stattic (μM). B) Quantification of the percentage of cells in each cell cycle phase, performed by Flowjo v10. Data is the average of three independent experiments with SEM calculated for error bars. One-way ANOVA was used to determine statistical significance with * = $P < 0.05$.

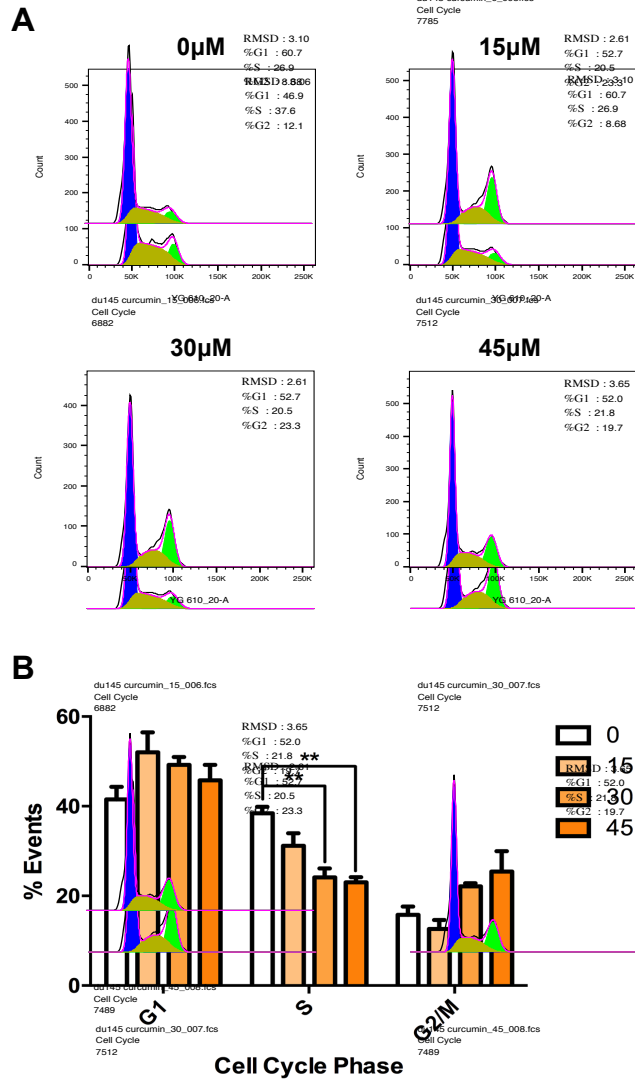


Figure 5-22: Curcumin decreases the percentage of S-phase cells. A) Representative cell cycle plots of DU145 cells treated with increasing doses of curcumin (μM). B) Quantification of the percentage of cells in each cell cycle phase, performed by Flowjo v10. Data is the average of three independent experiments with SEM calculated for error bars. One-way ANOVA was used to determine statistical significance with $** = P < 0.01$.

These experiments demonstrated the effect of STAT3 inhibitors on the cell cycle distribution of an asynchronous cell population. In order to view their effect on cell cycle progression, a similar experiment was performed in synchronised cells. DU145 cells were synchronised by serum starvation for 48 hours. The cell cycle block was then released by addition of serum-full media. This release was also performed in the presence of VS-43, stattic and curcumin. The results of this experiment are shown in Figure 5-23.

Representative cell cycle plots show that the starvation period successfully reduced the percentage of cells in S and G2 phase. Once released, a large proportion of cells progressed through G1 to S phase. The plots showing the cells released in the presence of the STAT3 inhibitors demonstrate that treatment with either VS-43, stattic or curcumin is able to completely block cell cycle progression from G1 to S phase (Figure 5-23A). The quantification of these plots is shown in Figure 5-23B. Starvation increases the G1 population to 75.5% and decreases the S phase population to 12.5%. Upon release of this block, the percentage of G1 cells decreases to 43.1%, and the percentage of S phase cells rises to 46.9% as cells begin to progress through the cell cycle. Release of cells in the presence of VS-43, stattic or curcumin maintains the G1 population at 71.9%, 78.7% and 78.9%, respectively. The percentage of cells in S phase remains at 15.9%, 7.80% and 7.08% for VS-43, stattic and curcumin treated cells, respectively. These results suggest that treatment with STAT3 inhibitors arrests cells in G1 phase.

This may be carried out through the regulation of cyclin D1, which controls the G1-S transition, by STAT3 (Bartek and Lukas, 2011; Bromberg et al., 1999). Additionally, in section 5.3.4.1, p21 was shown to be up-regulated by VS-43 treatment. p21 is a cyclin-dependent kinase inhibitor, which acts to induce cell cycle arrest in G1 (Harper et al., 1995). Therefore, given that STAT3 inhibition likely results in reduced

cyclin D1 and increased p21 levels, a G1 block by VS-43, stattic and curcumin is not unexpected.

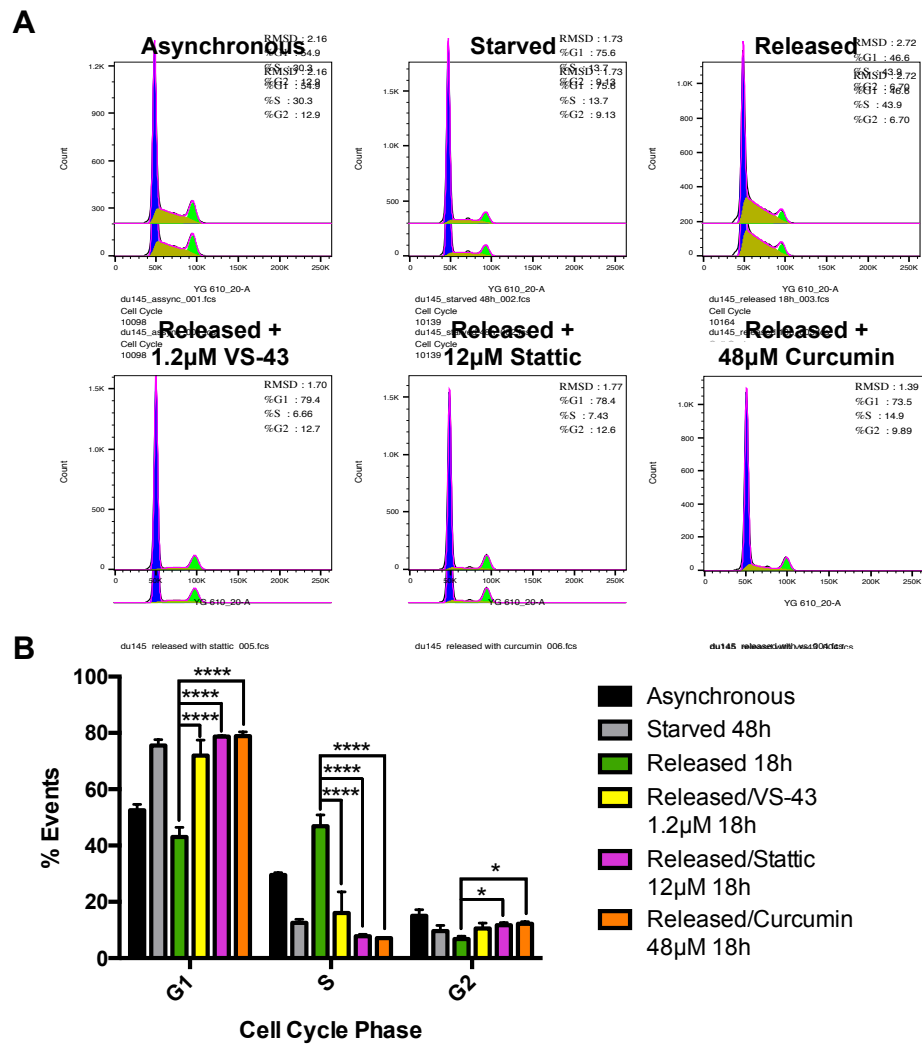


Figure 5-23: STAT3 inhibitors block the progression of cells from G1 to S phase. A) Representative cell cycle plots of asynchronous, serum-starved and serum-released DU145 cells, and cells released in the presence of STAT3 inhibitors. B) Quantification of the percentage of cells in each cell cycle phase, performed by Flowjo v10. Data is the average of three independent experiments with SEM calculated for error bars. One-way ANOVA was used to determine statistical significance with * = $P < 0.05$ and **** = $P < 0.0001$.

5.3.5.1 Cell cycle regulation of BRCA1, FANCD2, EME1 and MUS81.

As the inhibition of STAT3 has been demonstrated to induce cell cycle arrest in G1 phase, the effect of the cell cycle on the expression of BRCA1, FANCD2, EME1 and MUS81 was investigated. This was to establish whether the regulation of these factors by STAT3 was a result of cell cycle dependent expression rather than direct transcriptional regulation.

Three cell populations were harvested for immunoblotting: asynchronous, starved and released cells. The starved group contain a high proportion of G1 cells whereas the released group contains a high proportion of S phase cells. If these proteins are cell cycle regulated a difference in expression should be detectable between these populations.

Figure 5-24 demonstrates that only BRCA1 is cell cycle regulated. A reduced expression of BRCA1 is observed in the starved cells, indicating that BRCA1 expression is lower in G1 phase. As cells treated with STAT3 inhibitors resemble starved cells, it is likely that the decrease in BRCA1 expression by STAT3 inhibition is a result of cell cycle arrest in G1 phase. This agrees with previous reports demonstrating regulation of BRCA1 by the cell cycle (Ruffner and Verma, 1997).

The expression of FANCD2, EME1 and MUS81 is not affected by cell cycle phase. Therefore, these factors may be regulated by STAT3 at the transcriptional level.

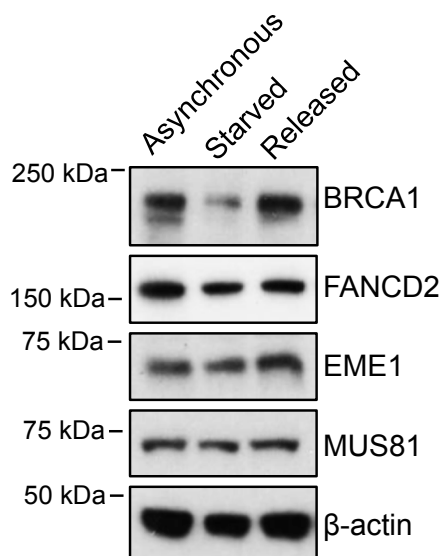


Figure 5-24: The expression of BRCA1, but not FANCD2, EME1 or MUS81 is cell cycle regulated. Assynchronous, serum-starved and serum-released DU145 cells were analysed by immunoblotting for the expression of ICL repair genes. Samples are paired to samples analysed by FACS in Figure 5-23. Blot is representative of more than 1 experiment.

5.3.6 STAT3 consensus binding sites reside within ICL repair gene promoters

To investigate whether STAT3 regulates the transcription of DNA repair genes including FANCD2, EME1 and MUS81, the online UCSC Genome Browser was utilised (Kent et al., 2002). This database contains experimental data from chromatin immunoprecipitation experiments for many transcription factors, including STAT3. This enabled STAT3 binding sites to be located across the human genome. Bioinformatic analysis of this data identified STAT3 binding sites located in the promoter regions of DNA repair genes. This work was performed by John Ambrose and Javier Herrero of the Bill Lyons Informatics Center, UCL.

A full list of the DNA repair genes identified to contain STAT3 binding sites in their promoter regions is included in Appendix C. For the purposes of this thesis, three targets were of particular interest: FANCD2, EME1 and MUS81.

FANCD2 did not contain any STAT3 binding sites in its promoter region. Therefore, it is possible that the regulation of FANCD2 by STAT3 inhibitors seen in this chapter is via an indirect mechanism.

For the EME1 gene, one STAT3 binding site was identified spanning 662-253bp upstream of the EME1 transcription start site. This is shown in the first Genome Browser screenshot in Figure 5-25. The binding site appears as a grey box with the vertical red line indicating the consensus STAT3 binding sequence. Primers were designed to amplify the region between the two black boxes at the bottom of the image.

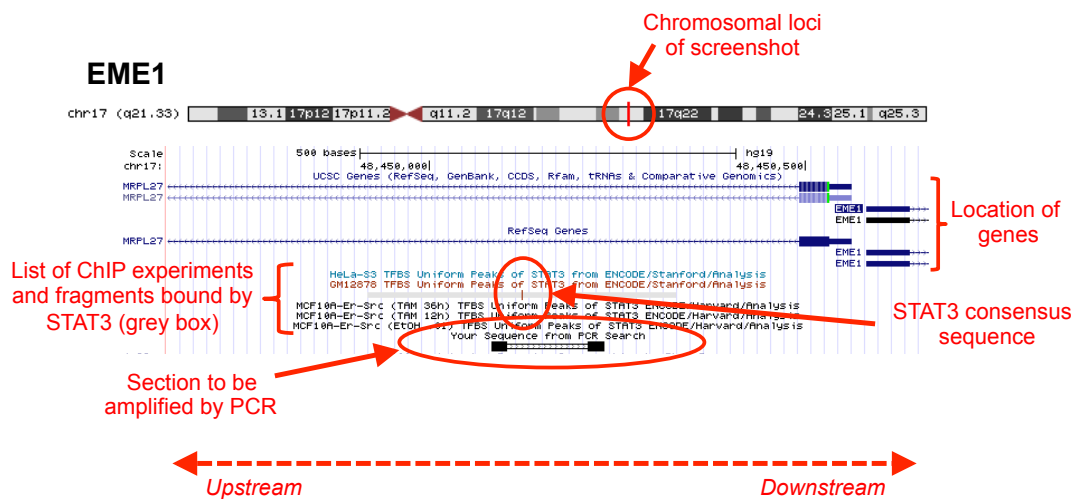


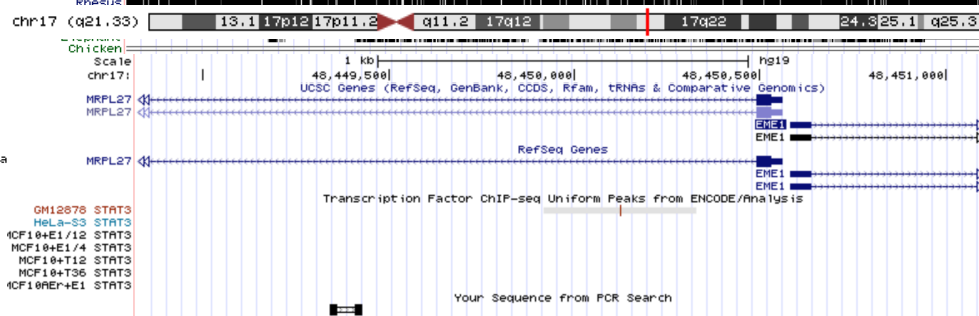
Figure 5-25: EME1 STAT3 promoter binding site, shown on Genome browser. Annotations indicate the location of genes, ChIP fragments bound by STAT3, STAT3 consensus sequence and sequence to be amplified by PCR.

This was the only STAT3 binding site identified on Genome Browser, however, it has previously been reported that STAT3 can bind to a site approximately 1025bp upstream of the EME1 transcription start site (Vigneron et al., 2008). This site is shown in the second screen shot in Figure 5-26 and is labelled EME1 R2. Note that the grey box in this image is the first binding site; the second site is indicated by the location of the PCR amplified sequence.

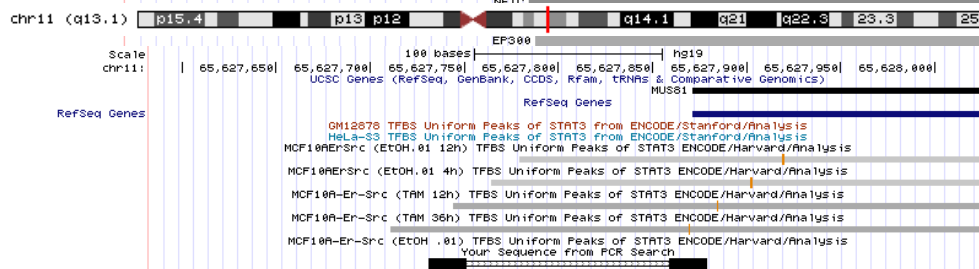
Two STAT3 binding sites were identified upstream of the MUS81 gene. The closest spans from 92bp upstream to 187bp downstream of the transcription start site. The second binding site, MUS81 R2, spans 3267-2992bp upstream of the MUS81 gene. The screenshots illustrating the locations of these binding sites relative to the MUS81 gene and also the regions to be amplified by PCR are shown in Figure 5-26.

As there are putative STAT3 binding sites located upstream of both the EME1 and MUS81 genes, it is possible that STAT3 binds to these sites in order to directly regulate the transcription of these DNA repair factors. This is assessed in the next section.

EME1 R2



MUS81



MUS81 R2

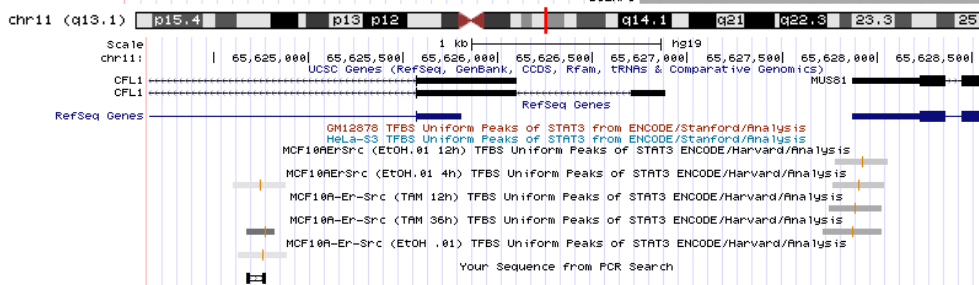


Figure 5-26: EME1 and MUS81 promoter STAT3 binding sites shown on Genome Browser. PCR fragments are also shown.

5.3.7 STAT3 binds to the promoters of EME1 and MUS81

Chromatin immunoprecipitation (ChIP) assays were employed to study the binding of STAT3 to the putative binding sites identified in the previous section. These experiments were performed with DU145 cells. Cells were either harvested as untreated, cisplatin treated, or VS-43 and cisplatin treated. Immunoprecipitation of DNA bound by STAT3 was carried out using a STAT3 antibody, and PCRs were

performed to amplify the regions shown on the genome browser screenshots. An IgG immunoprecipitation was also performed in order to calculate fold enrichment.

For a positive control, primers were designed to amplify the region 305-134bp upstream of the cFOS gene. This region spans a STAT3 binding site identified on the UCSC Genome Browser (Figure 5-27). cFOS is known to be transcriptionally regulated at this site by STAT3 (Yang et al., 2003). A negative control region at chr12: 6637469-6637580 was also amplified in order to obtain a value for non-specific binding. This region lies between the NCAPD2 and GAPDH genes and does not contain any STAT3 binding sites. Fold enrichments were normalised to the non-specific enrichment of the negative control region.

cFOS

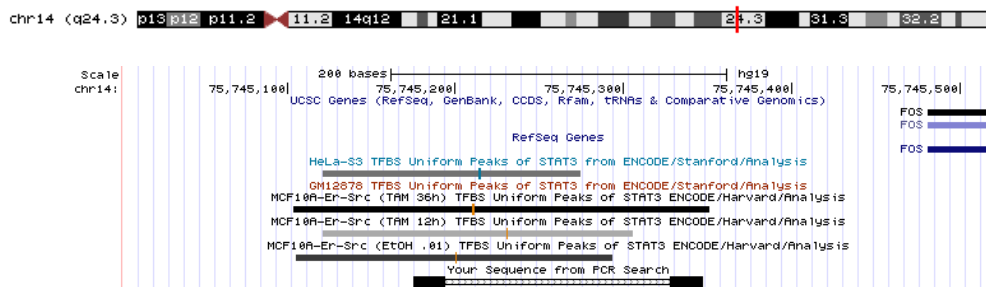


Figure 5-27: The location of the STAT3 binding site upstream of the cFOS gene, and the region to be amplified by PCR.

The result of this ChIP experiment is shown in Figure 5-28. In all treatment groups the cFOS region was amplified in STAT3 immunoprecipitations (IP), indicating that the ChIP was successful. The STAT3 IP also pulled down the EME1 R2, MUS81 and MUS81 R2 regions, which were enriched by 20.5, 8.94 and 21.4 fold, respectively. Upon cisplatin treatment, these regions were enriched similarly to control cells; therefore, cisplatin treatment does not appear to induce STAT3 binding to these sites. The enrichment at the EME1 region was, however, increased upon cisplatin treatment from 0.217 to 16.1 fold.

VS-43 treatment causes a reduction in the fold enrichment at all four sites. The fold enrichment drops to -0.43 for the EME1 site, -1.84 for the EME1 R2 site, 1.21 for the MUS81 site and 3.71 for the MUS81 R2 site. These results are not statistically significant due to the variable nature of ChIP experiments, however, binding to regions upstream of both EME1 and MUS81 by STAT3 is likely, as treatment with the STAT3 inhibitor VS-43 consistently blocks the enrichment seen at these sites. Binding to the cFOS promoter, however, is not inhibited by VS-43 treatment.

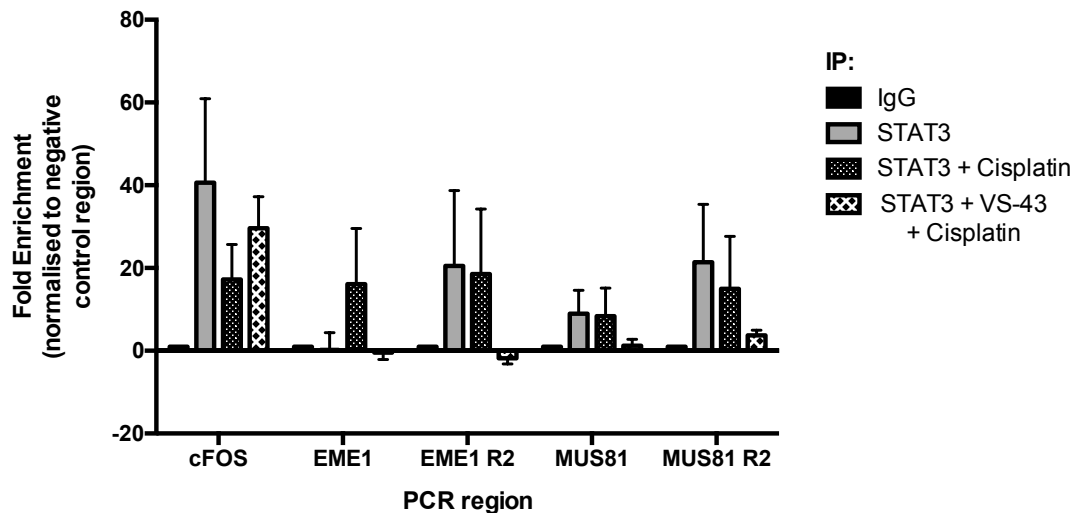


Figure 5-28: Chromatin immunoprecipitation analysis of STAT3 binding sites in the EME1 and MUS81 promoters. Constitutive STAT3 binding was detected at the EME1 R2, MUS81 and MUS81 R2 sites. Cisplatin treatment induced STAT3 binding to the EME1 site. VS-43 pre-treatment blocked STAT3 binding to both EME1 and MUS81 sites. The cFOS promoter region was used as a positive control. Data is the average of at least three independent experiments with SEM calculated for error bars. No statistical significance was observed.

5.4 Discussion

In this chapter the molecular mechanism behind the synergy between STAT3 inhibitors and cisplatin is investigated. As cisplatin primarily acts through the DNA adducts it forms, with ICLs being amongst the most toxic of these adducts, it is logical that sensitisation to cisplatin may involve regulating the repair of these adducts.

Here it is shown that STAT3 inhibitors block the unhooking of cisplatin-ICLs and alter the DNA damage response after treatment with cisplatin. Enhanced γ H2AX staining was observed in cells treated with STAT3 inhibitors followed by cisplatin versus cells treated with cisplatin alone, however, comet assay analysis demonstrated that the level of crosslinks induced by cisplatin was not affected by STAT3 inhibition. Therefore, there is no evidence to suggest that the level of cisplatin-induced DNA damage is enhanced by STAT3 inhibition. Instead,

accumulation of γ H2AX at unrepaired ICL sites may be responsible for the enhanced γ H2AX staining and DNA damage response observed in this chapter.

Through the screening of various DNA repair and signalling factors, STAT3 inhibitors were found to down-regulate EME1, MUS81, BRCA1 and FANCD2 expression in a dose-dependent manner in both the DU145 and A549 cell lines. These proteins are thought to be involved in the unhooking stage of ICL repair, as discussed in the introduction to this chapter, which may account for the reduced repair of cisplatin ICLs and increased sensitivity to cisplatin, which has been observed. BRCA1, FANCD2, EME1 and MUS81 have all been demonstrated to participate in the cellular response to cisplatin.

Colon cancer cells with haploinsufficiency in EME1 (EME1^{+/-}) are hypersensitive to cisplatin, as are EME1-deficient embryonic stem cells, and EME1 levels in cancer cell lines correlate with cisplatin sensitivity *in vitro* (Abraham et al., 2003; Tomoda et al., 2009). This could be a result of the interaction between EME1 and the nuclease MUS81. Accordingly, MUS81^{-/-} cells are also hypersensitive to ICL-inducing agents such as cisplatin and MMC (Hanada et al., 2006; McPherson et al., 2004). McPherson et al. also reported that loss of MUS81 in mice resulted in a predisposition to tumours, suggesting a critical role for MUS81 in genome stability. However, Dendouga et al. reported contradicting evidence where MUS81^{-/-} mice demonstrated hypersensitivity to crosslinking agents with no associated predisposition to tumour development (Dendouga et al., 2005), therefore, a tumour suppressor function for MUS81 is not yet confirmed.

FANCD2 has been connected with cisplatin sensitivity in ovarian cancer cell lines as those that do not express mono-ubiquitinated FANCD2 are hypersensitive to cisplatin (Taniguchi et al., 2003), and siRNA-mediated knockdown of FANCD2 itself in lung cancer cells increases cisplatin sensitivity (Dai et al., 2015). Small molecule

inhibitors of FANCD2 have been shown to sensitise cells to cisplatin and other crosslinking agents (Jacquemont et al., 2012; Jun et al., 2013). These include curcumin, which like VS-43, is also a STAT3 inhibitor (Chirnomas et al., 2006). BRCA1 introduction into sensitive cells has also been shown to increase resistance to cisplatin (Burkitt and Ljungman, 2007).

Therefore, EME1, MUS81 FANCD2 and BRCA1 have each been connected to cisplatin sensitivity, and so the regulation of these proteins by STAT3 inhibitors may be a likely mechanism for the increase in cisplatin sensitivity seen here.

5.4.1 The roles of VS-43 regulated DNA repair factors

In addition to BRCA1, EME1, MUS81 and FANCD2, several other DNA repair factors were shown to be up- or down-regulated by treatment with VS-43 in section 5.3.4.1. The roles of these in ICL repair will be briefly discussed.

MLH1 is the only DNA repair factor found to be up-regulated by VS-43. MLH1 is a component of the MutL complex in the mismatch repair pathway. This complex has been shown to be involved in sensitivity to psoralen induced-ICLs, as MLH1 deficient cells display increased resistance to psoralen (Wu and Vasquez, 2008). However, another study contradicts this and reports that MLH1 negative cells are more sensitive to MMC and cisplatin. Williams et al. also report that MLH1 interacts with FANCD2, however, is not required for FANCD2 ubiquitination and foci formation (Williams et al., 2011). Additionally, lower levels of MLH1 have been correlated with greater progression-free survival in patients after platinum based therapies (Ting et al., 2013). Therefore, the role for MLH1 in ICL repair is still confused, with no direct evidence for a function in ICL unhooking, so the slight up-regulation (1.69 and 2.01 fold at 1 μ M and 2 μ M VS-43, respectively) may be either beneficial or detrimental to cisplatin sensitivity.

All of the genes found to be down-regulated by VS-43 treatment are involved in DNA repair pathways (Table 5-5). The top hit was *LIG1*, a ligase involved in replication and BER. As this enzyme is not thought to function in the early stages of ICL repair, it was not investigated further in this project.

The hits at the lower end of the table included *FANCA* which is also dose-dependently down-regulated by VS-43 and has been suggested to regulate MUS81-EME1 endonuclease activity in ICL repair (Benitez et al., 2014). *BRIP1* (*FANCI*) is also down-regulated by VS-43. *BRIP1* functions as a helicase downstream of *FANCD2* and ICL unhooking (Suhasini and Brosh, 2012). Therefore, although this may affect later stages of ICL repair, *BRIP1* is not involved in unhooking and therefore, was not investigated further in this project.

It is worthwhile noting that VS-43 has an inhibitory effect on the expression of many DNA repair genes. This may explain why STAT3 inhibitors are able to sensitise cells to many DNA damaging chemotherapeutics. For instance, in chapter 4, VS-43 was shown to synergise with doxorubicin, a topoisomerase II inhibitor. Doxorubicin induces DSBs but does not, however, cause ICLs as cisplatin does. Therefore, VS-43 may interfere with the repair of other DNA adducts through the regulation of DNA repair factors involved in other repair pathways such as homologous recombination and non-homologous end joining.

5.4.2 Combination of other DNA repair inhibitors with cisplatin

In this chapter, STAT3 inhibition has been demonstrated to inhibit the repair of cisplatin ICLs, and this is proposed to contribute to the sensitisation to cisplatin by STAT3 inhibitors. The use of inhibitors to re-sensitise cancer cell lines to cisplatin through altering DNA repair mechanisms has been previously reported. For example, a topoisomerase II inhibitor was demonstrated to synergise with cisplatin

and it was suggested that this was in part via an inhibition of cisplatin-ICL repair (Ali-Osman et al., 1993).

This research group previously reported synergy between the EGFR inhibitor, gefitinib, and cisplatin in breast cancer cell lines. Cisplatin-ICL repair after this combination treatment was shown to be delayed (Friedmann et al., 2004). In this chapter, STAT3 inhibitors completely block cisplatin-ICL repair (sections 5.3.1 and 5.3.2). The difference between the effect of EGFR inhibition and STAT3 inhibition may suggest that in order to achieve a greater effect, direct inhibition of STAT3 is preferable to the inhibition of upstream activators. Even with EGFR inhibition, STAT3 could be activated through alternative pathways, which may allow for delayed, but eventual repair of cisplatin-ICLs through continued STAT3 signalling.

One of the DNA repair factors demonstrated here to be down-regulated by STAT3 inhibition was FANCD2. mTOR, a signalling kinase, is also thought to regulate FANCD2 (Shen et al., 2013), and enhanced anti-tumour effect has been demonstrated between mTOR inhibitor rapamycin and cisplatin in mouse tumour xenografts (Hou et al., 2010). Several clinical trials reported promising results with mTOR inhibitors in various combinations with cisplatin (reviewed in (Grandis et al., 2013)), but whether this is due to FANCD2 inhibition has not yet been determined.

Other combinations targeting DNA repair inhibitors to enhance the efficacy of cisplatin include PARP inhibitors and ATR inhibitors, both of which are currently in clinical trials with cisplatin. These combinations were described in more detail in section 4.1.2. PARP inhibitors likely do not target the ICL unhooking mechanism, however, ATR inhibitors may act at this step. ATR acts upstream of FANCD2, phosphorylating its partner protein, FANCI upon DNA damage. This step is required to promote FANCD2 ubiquitination (Crossan and Patel, 2012), and so ATR inhibitors may also block ICL unhooking by interfering with FA pathway activation.

Therefore, research into DNA repair inhibitors for combination with cisplatin is well underway, and the benefit of combinations that target the ICL repair pathway will clearly be worthwhile.

5.4.3 Genetic mutations in the ICL unhooking machinery and cisplatin sensitivity

Identification of genetic mutations in ICL repair factors may offer some insight into the usefulness of an inhibitor that targets those factors as a chemosensitising agent. Activating mutations, increased copy number and up-regulation of gene expression in a particular cancer group may suggest potential for the use of a STAT3 inhibitor in combination with cisplatin in those patients. Alternatively, deactivating mutations or down-regulation of gene expression may provide information about the importance of these factors in sensitivity to cisplatin.

According to the Catalogue of Somatic Mutations in Cancer (COSMIC) online database (Forbes et al., 2015), 96 unique mutations are found for EME1. However, mutations are found only at low frequencies: 1.09% of endometrium cancers and 1% of large intestinal cancers tested harboured EME1 point mutations. The mutations were predominantly missense mutations, substituting one amino acid for another in the final EME1 protein. The outcome of these mutations on EME1 function and patient sensitivity to chemotherapy agents has not been examined. Interestingly, overexpression of EME1 is detected in 21.38% (of 1104 samples) of breast cancer tissues and a gain in copy number of the EME1 gene was found in 6.62% (of 997) of breast cancer tissues. This may be an indication that targeting EME1 in breast cancer may be beneficial.

For the MUS81 gene, 77 unique mutations are listed, with again the majority (65%) being missense mutations. The frequency of these point mutations is low; with 1.85% of melanoma tissues tested carrying a MUS81 mutation. Copy number gains

have been reported in a small number of melanoma samples. As with EME1, the importance of these mutations on MUS81 function and patient sensitivity to cisplatin would need to be investigated. Additionally, overexpression of MUS81 has been detected in 9.4% of ovarian cancer tissue, and similar levels of overexpression have been documented in cervical and breast cancer studies. However, individual studies have reported both down- and up-regulation of MUS81 expression in different cancer tissues. Therefore, the role for MUS81 in tumour progression may be tissue specific (F. Wu et al., 2011; Xie et al., 2016).

COSMIC identifies 297 somatic mutations in the FANCD2 gene across a broad range of cancer types. 55% of these substitutions are missense, again with an unknown outcome. 8% of these mutations are however, nonsense mutations, resulting in a stop codon instead of an amino acid. This truncates the protein being translated and can result in inactive protein product. The substitutions that lead to a truncated FANCD2 may predict tumours that are sensitive to cisplatin or other crosslinking agents however, this has not been tested yet. Around 3% of FANCD2 mutations reported in the COSMIC database are small insertion or deletions of 1 or 2 base pairs. These types of mutation cause a complete frame-shift, and it is likely that these patients also do not express functional FANCD2.

A subset of Fanconi Anaemia patients (3.3%) also carry mutations in the FANCD2 protein and are subsequently predisposed to developing acute lymphoblastic leukaemia. Fanconi Anaemia patients are also characterised by their hypersensitivity to crosslinking agents, such as cisplatin (Borriello et al., 2007; Mathew, 2006; Smetsers et al., 2012), and are often diagnosed through observation of chromosomal breakage after treatment with MMC or diepoxybutane, both ICL-inducing agents (Oostra et al., 2012). Therefore, clinical evidence that an inactive FA pathway increases sensitivity to cisplatin and other crosslinkers is already in

abundance, and so pharmacological targeting of FANCD2, with perhaps a STAT3 inhibitor, may lead to promising drug combinations.

Hereditary BRCA1 mutations contribute towards the tumourigenesis of breast and ovarian cancer through promoting the genetic instability required to gain mutations in oncogenes and tumour suppressors. There are 518 identified mutations in the BRCA1 gene identified on the COSMIC database. 59% of these are missense mutations, 11% account for insertion or deletion based frame-shifts, and 10% nonsense mutations. BRCA1 mutations in patient-derived xenografts have also been associated with cisplatin sensitivity (Lohse et al., 2015), and patients carrying germ-line BRCA1 mutations have been reported to respond well to cisplatin monotherapy (Moiseyenko et al., 2015).

Tumours carrying BRCA1 mutations are often initially sensitive to cisplatin-based chemotherapy due to an impaired ability to remove cisplatin-DNA adducts. BRCA1 may also be inactivated in sporadic breast and ovarian cancers through promoter methylation which inactivates transcription of a gene (Esteller et al., 2000). Acquired resistance can, however, occur. It was found that secondary mutations could reactivate BRCA1. Therefore, repair of cisplatin DNA adducts via reactivation of the BRCA1 gene is correlated with cisplatin resistance (Borst et al., 2008).

Certainly for BRCA1 and FANCD2, and perhaps for EME1 and MUS81, correlation between mutation and cisplatin sensitivity is found. However, BRCA1 expression was demonstrated in this chapter to be regulated by cell cycle phase. As STAT3 inhibition arrests the cell cycle, it was concluded that regulation of BRCA1 expression by STAT3 is indirect. STAT3 is most likely to directly affect cisplatin sensitivity through the transcriptional regulation of EME1 and MUS81, as STAT3 was demonstrated to bind the promoter regions of these genes. Further

investigation into the effect of the mutations reported for EME1 and MUS81 is, therefore, necessary.

5.4.4 Does STAT3 regulate the transcription of genes involved in ICL unhooking?

In this chapter, STAT3 inhibition has been shown to down-regulate the expression of MUS81, EME1, BRCA1 and FANCD2 as a potential mechanism for cisplatin sensitisation.

The transcription factor STAT3 has previously been shown to be involved in the DNA damage response, transcriptionally regulating MDC1, a regulator of the ATM DNA damage response pathway. Additionally cells deficient in STAT3 are less effective at repairing damaged DNA (Barry et al., 2010). It is possible that STAT3 may regulate transcription of other DNA damage response genes such as EME1, MUS81 and FANCD2.

It has been reported that STAT3 binds to the promoter of EME1 and that inhibition of upstream kinases Src and EGFR resulted in down-regulation of STAT3 activation and EME1 expression (Vigneron et al., 2008). STAT3 does not associate with the EME1 promoter after IL-6 exposure but does so only after treatment with a Topoisomerase I inhibitor, suggesting that this effect is in response to DNA damage. Therefore, it is possible that DNA damage as a result of cisplatin exposure could activate the EGFR-Src-STAT3 pathway to up-regulate expression of EME1 in a similar manner. Treatment with a STAT3 inhibitor would block this feedback loop, inhibiting EME1 levels and subsequently inhibiting repair of cisplatin-DNA adducts. In agreement with this hypothesis, activation of EGFR and Src is induced by exposure of cells to cisplatin (Benhar et al., 2002). Interestingly, one study found that treatment of cells with the EGFR inhibitor, cetuximab, resulted in stimulated STAT3 phosphorylation and also EME1 expression. When co-treated with

cetuximab and static, EME1 levels were no longer enhanced (Weinandy et al., 2014), further adding to the evidence for regulation of EME1 by STAT3.

ChIP experiments performed in this chapter investigated whether STAT3 binds to the promoter regions of the EME1 and MUS81 genes. Enrichment of STAT3 occurred at one site upstream of EME1 (the site identified by Vigneron et al.), and two sites upstream of MUS81 in unstimulated DU145 cells (although these cells do harbour constitutive STAT3 activation, as was shown in chapter 3). After cisplatin treatment, no further enrichment of STAT3 binding was seen at the EME1 site identified by Vigneron et al., however, cisplatin-dependent enrichment at a binding site closer to the EME1 transcription start site was observed, though this was not statistically significant. It may be possible that in cells harbouring constitutive STAT3 activation, treatment with cisplatin does not further stimulate STAT3 binding to its target promoters. No reports of regulation of MUS81 by STAT3 exist as of yet, however, the results from this ChIP experiment do suggest that STAT3 transcriptionally regulates both EME1 and MUS81, and that this accounts for the down-regulation of EME1 and MUS81 by VS-43 and other STAT3 inhibitors.

Interestingly, the binding of STAT3 to the cFOS promoter was not inhibited by treatment with VS-43. This could suggest that when active STAT3 is low in the cancer cell, a re-distribution event occurs, with the remaining active STAT3 regulating the transcription of the genes the cell needs to continue to survive, such as those involved in cell survival, including cFOS.

A link between STAT3 and BRCA1 has also been investigated. BRCA1 expression was found to activate STAT3 via the direct activation of upstream kinases JAK1/2 in DU145 cells (Gao et al., 2001). Therefore, a possible positive feedback loop could exist between STAT3 and BRCA1, whereby STAT3 regulates the expression of BRCA1 which enhances the survival signal by further activating STAT3. Inhibition of

STAT3 would disrupt this feedback loop, down-regulating BRCA1 levels. However, as has been shown in this chapter, BRCA1 expression is cell cycle dependent, so STAT3-mediated regulation may be indirect via the arrest of cells in G1 phase.

Regulation of FANCD2 expression by STAT3 has not yet been investigated. The only evidence connecting these two proteins currently is the finding that the natural STAT3 SH2 domain inhibitor Curcumin down-regulates FANCD2 monoubiquitination, sensitising cells to cisplatin (Chirnomas et al., 2006). As FANCD2 mRNA and protein levels appear to be down-regulated to a lesser extent than BRCA1 by VS-43 inhibition of STAT3, it is possible that this is a result of loss of interaction with BRCA1. FANCD2 is known to require BRCA1 to associate to ICL sites (Bruun et al., 2003) therefore, down-regulation of BRCA1 by cell cycle arrest through STAT3 inhibition may destabilise FANCD2. However, whether STAT3 acts to directly or indirectly regulate the expression of FANCD2 is yet to be confirmed.

A link between the ERCC1 component of the XPF-ERCC1 nuclease and STAT3 has also been made, with one study reporting that treatment of cells with the src inhibitor dasatinib, inhibits the STAT3 pathway and also expression of ERCC1 in order to enhance cisplatin sensitivity (J. Chen et al., 2015). However, src acts upstream of STAT3 and also regulates the activation of other signalling pathways such as the Raf/MEK/MAPK pathway. As no down-regulation of ERCC1 was seen by treatment of cells with STAT3 inhibitors in this chapter, src may regulate ERCC1 through another pathway. No connection between any other FANC proteins or the SLX4 scaffolding protein and STAT3 has been reported.

Therefore, currently the strongest evidence exists for the transcriptional regulation of EME1 by STAT3. This combined with the evidence presented here connecting STAT3 to both EME1 and MUS81 expression, could suggest a mechanism whereby

STAT3 regulates the transcription of the MUS81-EME1 nuclease, allowing for STAT3 status to determine the cancer cells ability to repair cisplatin-ICLs.

5.5 Conclusion

In conclusion, this chapter has investigated the mechanism of sensitisation to cisplatin by STAT3 inhibitors. It has been shown that STAT3 inhibitors block the unhooking of cisplatin-ICLs, and alter the DNA damage response in both the DU145 and A549 cancer cell lines.

Investigation of the mRNA and protein levels of key DNA repair factors after treatment of cells with VS-43 and other STAT3 inhibitors has led to the hypothesis that STAT3 inhibitors block ICL unhooking via the down-regulation of EME1, MUS81 BRCA1 and FANCD2. Transcriptional regulation by STAT3 seems most likely for EME1 and MUS81, as STAT3 was demonstrated to bind to genomic locations upstream of the transcription start sites for these genes.

In the following chapter, the involvement of STAT3 in the repair of melphalan-induced ICLs will be investigated to gain an understanding of the range of combinations which STAT3 inhibitors like VS-43 may be useful for in the clinic.

Chapter 6 Cisplatin and Melphalan DNA-ICLs repair via different unhooking mechanisms

6.1 Introduction

The results presented in this thesis so far suggest that STAT3 inhibitors are able to sensitise cancer cell lines to cisplatin, with the hypothesis that this is due to the involvement of STAT3 in ICL repair. The novel STAT3 inhibitor, VS-43, was also shown to synergise with doxorubicin. Therefore, STAT3 inhibitors may be able to synergise with other chemotherapy agents. As STAT3 inhibitors have been shown to block cisplatin-ICL repair, whether these inhibitors have similar effects on other ICL-inducing agents is of interest. This will be investigated for melphalan in this chapter.

6.1.1 Rationale for investigating melphalan: chemosensitisation studies and ICL repair

Melphalan belongs to the nitrogen mustard class of chemotherapy agents which originated from an observation that mustard gas used in the first world war acted through targeting the haematopoietic system, making it useful for the treatment of haematological cancers (Krumbhaar and Krumbhaar, 1919; Lawley and Phillips, 1996). Melphalan is a bifunctional alkylating agent, known react with both guanine and adenine bases to form monoadducts and ICLs (Povirk and Shuker, 1994). Melphalan does not, however, form intrastrand crosslinks as cisplatin does (Bauer and Povirk, 1997). According to early studies, approximately 30-40% of melphalan adducts are ICLs (Hansson et al., 1987).

Whilst not reported as frequently as for cisplatin, some studies have described sensitisation of cancer cells to melphalan by inhibition of STAT3 (Bharti et al., 2003b; Li et al., 2010; Scuto et al., 2011), However, the studies performed by Bharti et al. and Li et al. do not perform combination index analysis to quantify the drug

interactions as synergistic, additive or antagonistic, and whilst Scuto et al. do demonstrate synergy with melphalan, they use a JAK2 inhibitor. As JAK2 has other downstream signalling pathways in addition to STAT3, such as the MAPK pathway, the inhibition of STAT3 may not be responsible for the synergy observed. Therefore, whether STAT3 inhibitors would prove beneficial in combination with melphalan remains to be confirmed. This will be investigated in this chapter.

A second issue this chapter will aim to address is related to the mechanism of ICL repair. Previous research carried out in this group has suggested that melphalan-ICL repair does not occur via the same mechanism as cisplatin-ICL repair. First, Friedmann et al. demonstrated that whilst the EGFR inhibitor, gefitinib, exhibited synergy in combination with cisplatin, when combined with melphalan, no synergy was observed. Using the modified comet assay, the formation and repair of ICLs after treatment of cells with cisplatin or melphalan in combination with gefitinib was followed. Gefitinib delayed the repair of cisplatin-ICLs but had no effect on the repair of melphalan-ICLs (Friedmann et al., 2004). As EGFR is one of the upstream activators of STAT3, it is possible that STAT3 may be selectively involved in cisplatin-ICL repair.

Further evidence gathered by this group demonstrated a clear difference between the mechanism of unhooking for cisplatin and melphalan-induced ICLs. Using the modified comet assay, Spanswick et al. demonstrated that plasma cells from myeloma patients clinically resistant to melphalan could repair melphalan-ICLs but not cisplatin-ICLs. Additionally, cells from ovarian cancer patients pre-platinum therapy could not repair either cisplatin or melphalan ICLs, but post-platinum therapy they were able to repair cisplatin ICLs exclusively. Experiments with the RPMI8226 myeloma cell line were also carried out. These cells behaved similarly to the melphalan-resistant patient cells – comet assays showed successful unhooking

of melphalan-ICLs but persistence of cisplatin ICLs in this cell line. In this study, combination with gemcitabine was also shown to inhibit cisplatin-ICL unhooking but not melphalan-ICL unhooking (Spanswick et al., 2012).

This research group has found two different drug combinations that specifically target cisplatin-ICL repair without affecting the progression of melphalan-ICL repair. Therefore, ICLs induced by different agents, particularly cisplatin and melphalan, may require different repair pathways.

6.1.2 Structural differences between ICL agents

If different mechanisms of repair do exist, the structure of the ICL may determine which repair pathway is taken. The structures of cisplatin and melphalan are very different (Figure 6-1). Melphalan is a more complex molecule than cisplatin, and so even though both link two guanine bases through the displacement of their chloride ions, the impact on the structure of DNA is likely to be different. In fact, the structures of different ICL-forming agents are quite varied. Figure 6-2 illustrates the diversity of crosslinkers and the ICLs they form.

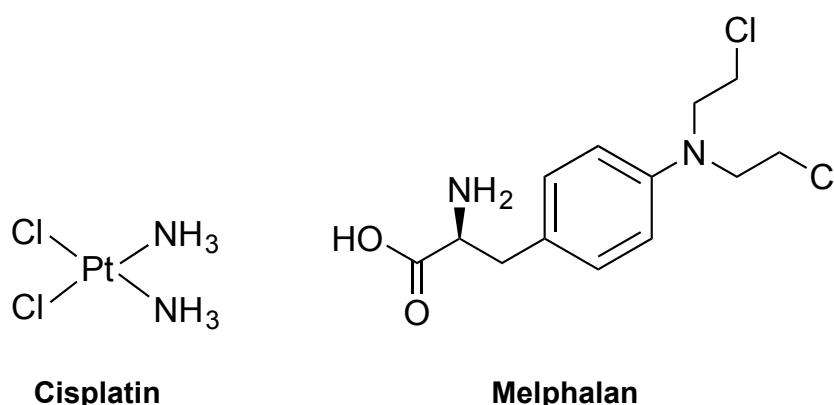


Figure 6-1: Structures of cisplatin and melphalan.

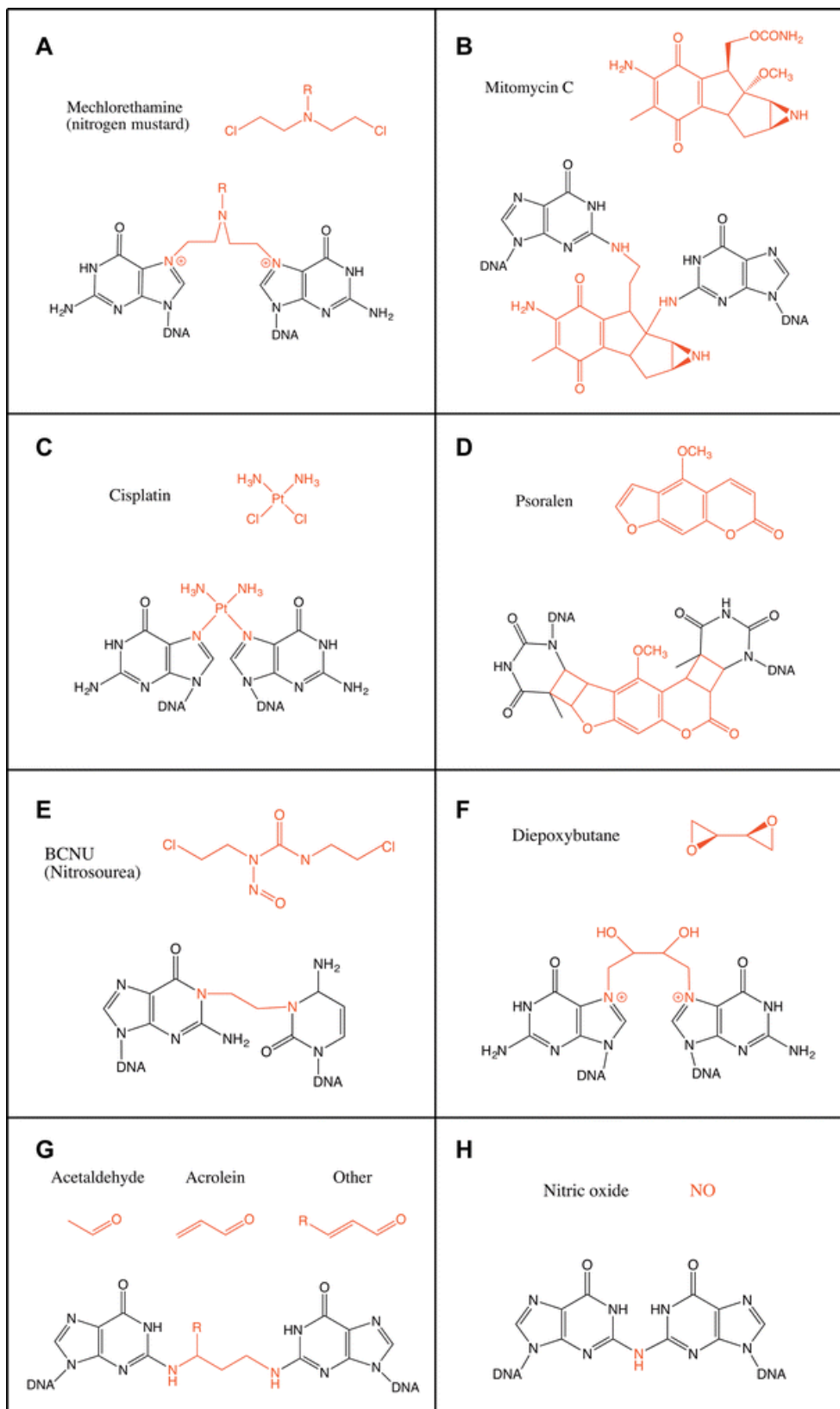


Figure 6-2: The different structures of DNA ICLs induced by various crosslinking agents. A) mechlorethamine, B) MMC, C) cisplatin, D) psoralen, E) nitrosourea, F) diepoxybutane, G) aldehydes and H) nitric oxide. Taken from (Lopez-Martinez et al., 2016).

When an agent binds to the DNA and forms an ICL, the DNA is distorted from its B-DNA form. The degree of distortion and bending achieved will vary depending on the crosslinker. Some crosslinks are considered to be largely distorting whereas others barely distort the DNA at all. The crystal structure of DNA containing a cisplatin ICL was solved in 1999. This structure shows that cisplatin binds in the major groove and bends the DNA double helix by 47° towards the minor groove and unwinds the helix by 70° at the lesion and by 110° five base pairs away from the lesion. The now unpaired cytosine residues complementary to the crosslinked guanines are extruded from the DNA helix. Nine water molecules surround the platinum atom, and another seven water molecules make contacts with the ICL adduct. These water molecules link the platinum adduct to the surrounding phosphate backbone as well as the crosslinked guanines in order to maintain the distorted structure (Coste et al., 1999). The structure of the cisplatin DNA-ICL and the resulting distortion can be seen in Figure 6-3.

The structure of DNA containing a melphalan-ICL has not yet been solved. However, some indication of the physical effect on the DNA structure may be gained from studies using another nitrogen mustard, mechlorethamine (shown in Figure 6-2A). Computer modelling of DNA containing a mechlorethamine-ICL showed that mechlorethamine binds in the major groove, a $12.4\text{-}16.8^\circ$ bend is induced and an over-winding of $2\text{-}6^\circ$ occurs (Rink and Hopkins, 1995). This is a much smaller distortion than that induced by a cisplatin-ICL. However, the effect of melphalan's much bulkier alkyl group on the degree of distortion compared with the single methyl group on mechlorethamine is not known. Other crosslinking agents include MMC which binds the minor groove of the DNA and which induces no detectable distortion of the DNA helix (Rink et al., 1996), and psoralens which have been shown to

induce distortion of the base stacking at the crosslink site, but this does not result in an overall bending of the DNA (Hwang et al., 1996; Sinden and Hagerman, 1984).

The extent of DNA distortion has been linked to the level of lesion repair. ICLs that produce a greater distortion are unhooked more frequently than DNA containing minimally distorting ICLs (Smeaton et al., 2008). The importance of helix distortion on the removal of ICLs has also been highlighted for the novel crosslinker, SJG-136, which binds to the DNA minor groove and exhibits high cytotoxicity and slow ICL repair (Clingen et al., 2005). SJG-136-induced ICLs are reported to induce relatively little distortion to the DNA helix (Jenkins et al., 1994) therefore, this could effectively mask the lesion from recognition by repair proteins, resulting in the slow unhooking of these ICLs.

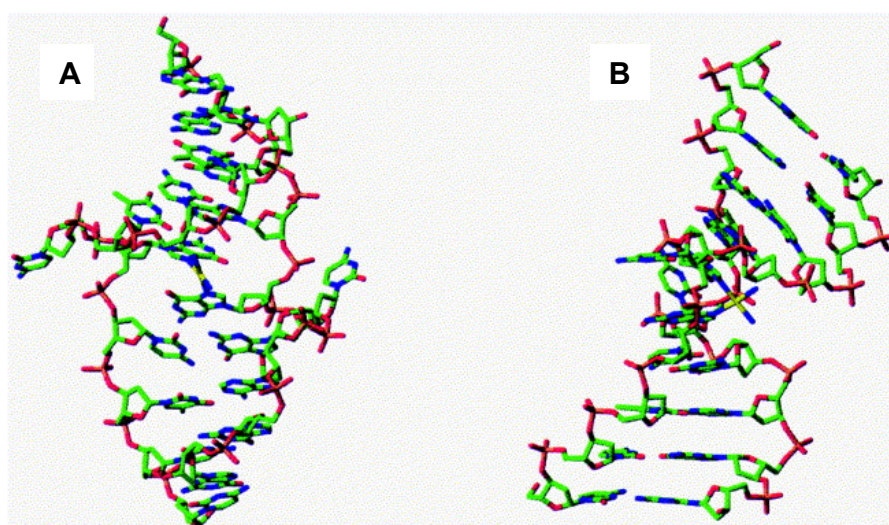


Figure 6-3: Stick representation of the crystal structure of a single cisplatin ICL from the A) minor groove and B) 90 degrees rotated to show the bend induced. Taken from (Malinge et al., 1999).

The trans-isomer of cisplatin, transplatin, is reported to have reduced anti-tumour activity and increased repair of adducts (Heiger-Bernays et al., 1990). Transplatin crosslinks guanine with the complementary cytosine and the distortion produced by the resulting ICL is lower than that of cisplatin – a bend of 24° and 12° unwinding (Brabec et al., 1993). Therefore, the degree of distortion does not always positively correlate with adduct repair or toxicity. The relationship between the structure of ICLs and their biological effects appears to be more complex.

As well as distortion differences, as is shown in Figure 6-2, ICL agents also differ in their base specificity. Cisplatin and melphalan both crosslink guanine residues by reacting with the N7 position, however, the sequence specificity also differs: cisplatin forms ICLs at 5'-GpC-3' sites whereas nitrogen mustards form ICLs at 5'-GpNpC-3' sites (Muniandy et al., 2010). The larger distance between guanines in the nitrogen mustard crosslink is possibly due to the larger distance between the substituted chloride ions. MMC also forms ICLs between guanine residues, though these ICLs crosslink the N2 atoms at 5'-CpG-3' sites (Rink et al., 1996). In contrast, psoralens crosslink the thymine residues at 5'-TpA'3' sites (Hwang et al., 1996).

Therefore, the diverse structures of ICL-inducing agents and the distortions they produce in DNA, combined with the varied sequence and base specificities, results in a wide range of ICLs which must all be recognised and repaired by cellular machinery. Given the structural differences between these lesions, it is possible that different machinery is responsible for the repair of different ICLs.

In this chapter the differences between cisplatin and melphalan ICL repair will be investigated, with an emphasis on the unhooking of these lesions.

6.2 Aims

The aims of this chapter were as follows:

1. To investigate whether STAT3 inhibitors sensitise cancer cell lines to melphalan, and whether this combination is synergistic.
2. To determine whether STAT3 inhibitors block melphalan-ICL unhooking.
3. To investigate the role of STAT3, EME1 and MUS81 in cisplatin and melphalan ICL unhooking.

6.3 Results

6.3.1 Melphalan inhibits cancer cell line growth

In order to establish whether STAT3 inhibitors can sensitise cells to melphalan, the cell growth inhibition produced by melphalan alone was first determined in order to decide the ratio with which to carry out the combination assays.

The effect of 1 hour of melphalan treatment on the DU145 and RPMI8226 cell lines was determined by SRB assay. The DU145 cell line was chosen to allow for a direct comparison to the cisplatin combinations in Chapter 4, and the RPMI8226 myeloma cell line was chosen as melphalan is widely used to treat myeloma and therefore, this is more clinically relevant.

Figure 6-4 shows that in both cell lines melphalan inhibits cell growth. The GI_{50} for melphalan in DU145 cells was 110.3 μ M. RPMI8226 cells were considerably more sensitive to melphalan, with a GI_{50} of 43.75 μ M. These GI_{50} values were taken into consideration when deciding the ratios for the combination assays.

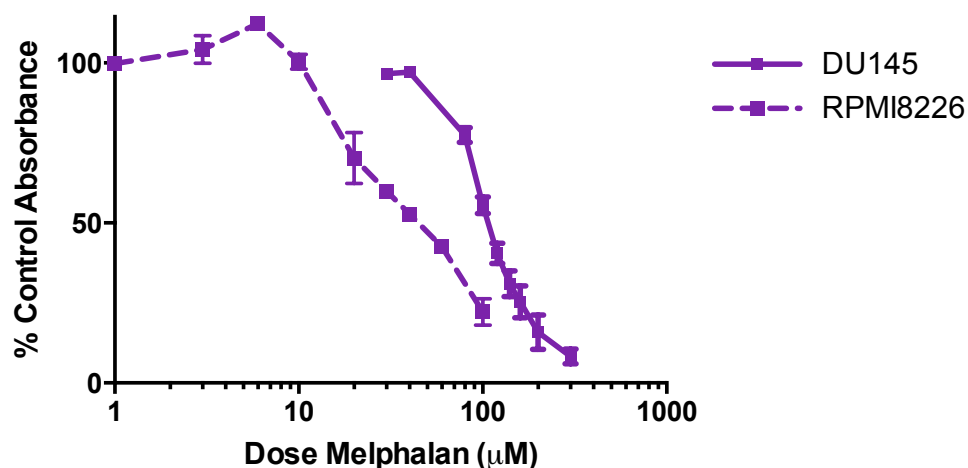


Figure 6-4: Cell growth inhibition by 1 hour melphalan treatment in DU145 and RPMI8226 cells. Determined by SRB and MTT assay for DU145 and RPMI8226 cells, respectively. Data plotted is the average of at least three individual experiments with SEM calculated for error bars.

6.3.2 STAT3 inhibitors do not chemosensitise cancer cell lines to melphalan

The combination of STAT3 inhibitors with melphalan was first trialled in the DU145 cell line using the novel STAT3 inhibitor, VS-43. Due to the approximate GI_{50} values of VS-43 and melphalan alone in this cell line, a ratio of 1:100 was used for VS-43:melphalan, with an 18 hour pre-treatment of VS-43 followed by 1 hour treatment with melphalan. As with all other cell growth inhibition assays, the cells were then incubated for 96 hours before SRB staining.

Figure 6-5A shows that combination of VS-43 with melphalan in the DU145 cell line reduces the melphalan GI_{50} by 19.8% from 91.7 μ M to 73.5 μ M. Non-linear regression analysis determined that these GI_{50} values are significantly different with a P value of $P < 0.0001$. CI value analysis was performed where the differences in cell growth inhibition were statistically significant. Figure 6-5B shows that the CI values obtained were predominantly in the additive range (0.9-1.1). One value was however, in the slight synergy range – a CI of 0.852 was obtained at 160 μ M melphalan. An antagonistic CI value of 1.329 was obtained at 300 μ M melphalan.

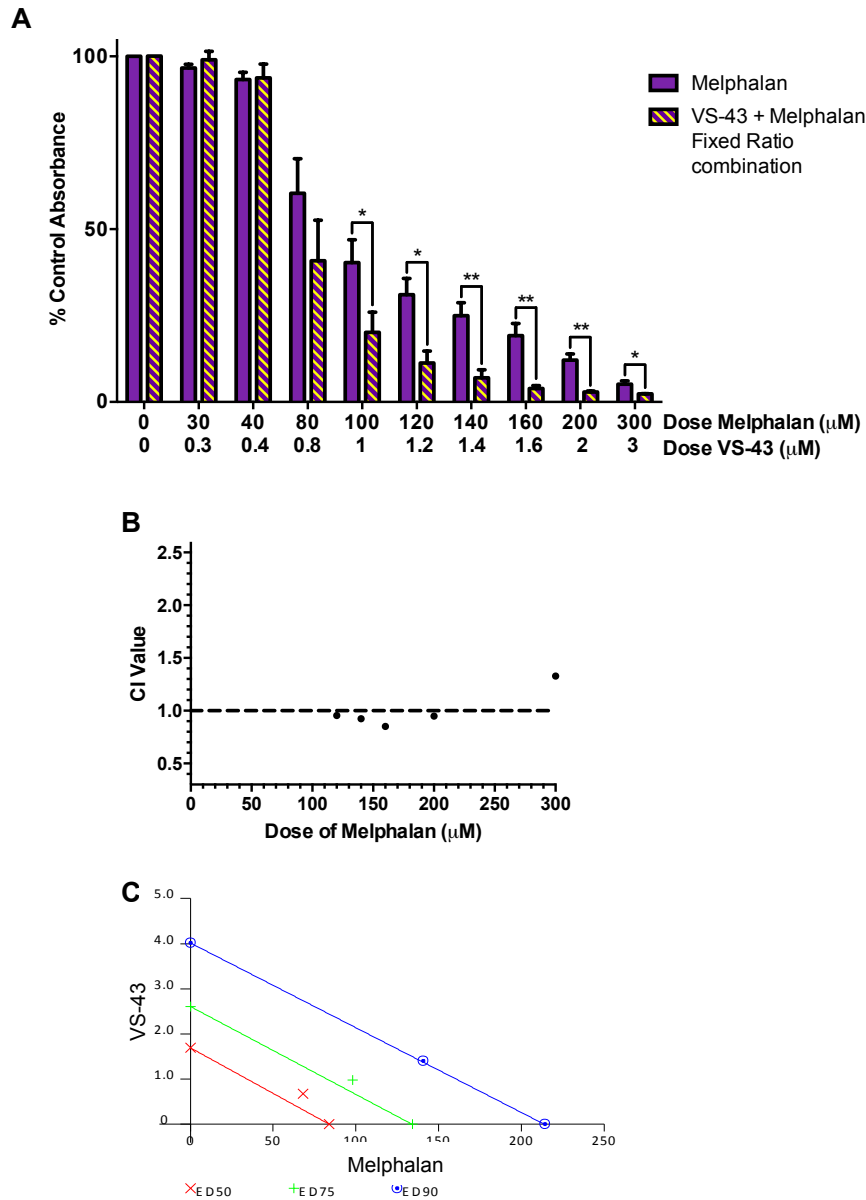


Figure 6-5: Combination of VS-43 and melphalan in DU145 cells. A) VS-43 plus melphalan combination treatment slightly increases cell growth inhibition. Data plotted was obtained by SRB assay and is the average of at least three individual experiments with SEM calculated for error bars. Students t-test was carried out to determine statistical significance with * = $P < 0.05$, ** = $P < 0.01$. B) Combination indices are predominantly in the additive region close to 1 and C) isobologram plot quantifying drug interactions at the 50%, 75% and 90% effect levels. Additivity and slight antagonism is observed between VS-43 and melphalan in DU145 cells.

The isobologram plot, which graphically represents drug interactions at different effect levels, shows that the interaction between VS-43 and melphalan in this particular combination is mildly antagonistic at the 50% and 75% effect levels and additive at the 90% effect level. Therefore, unlike with cisplatin, synergy between VS-43 and melphalan is not observed using the fixed ratio combination in the DU145 cell line.

Next, the combination of VS-43 and melphalan was assessed in the more clinically relevant RPMI8226 cell line. In order to carry out this combination, assessment of the effect of VS-43 treatment alone was required. As RPMI8226 cells are a suspension cell line, the MTT assay was used instead of the SRB assay as a measure of cell growth inhibition. RPMI8226 cells were treated for 18 hours with VS-43, and subsequently incubated for 96 hours before MTT was added.

Figure 6-6 shows that VS-43 inhibits the growth of RPMI8226 cells with a GI_{50} of $2\mu\text{M}$. These cells are less sensitive to VS-43 and more sensitive to melphalan than DU145 cells, therefore, a ratio of 1:100 was not appropriate. Instead, a ratio of 1:20 was chosen as this better represented the relative sensitivity of RPMI8226 cells towards VS-43 and melphalan.

Pre-treating RPMI8226 cells with VS-43 reduces the melphalan GI_{50} from $51.0\mu\text{M}$ to $26.7\mu\text{M}$ – a 47.8% decrease (Figure 6-7A). Non-linear regression analysis determined that these GI_{50} values are significantly different with a P value of $P < 0.0001$. However, only the last three pairs of data points demonstrate a statistically significant difference. CI value analysis was performed for those combinations, with the results shown in Figure 6-7B. The lowest CI value obtained was 0.908 at $60\mu\text{M}$ melphalan, and the highest was 1.465 at $100\mu\text{M}$ melphalan. These values span the additive to antagonistic range. This is confirmed by the

isobologram plot shown in Figure 6-7C, as at all three effect levels the combination data points are to the right and above each line – indicative of antagonism.

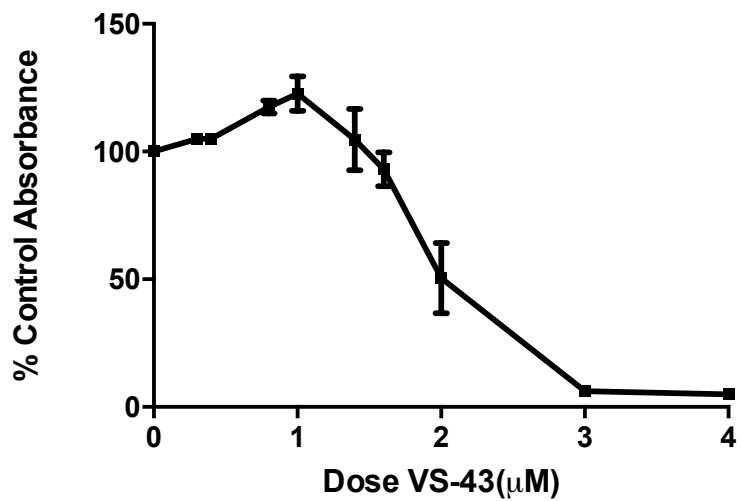


Figure 6-6: VS-43 inhibits growth of the RPMI8226 myeloma cell line. Data plotted was obtained by MTT assay and is the average of at least three individual experiments with SEM calculated for error bars.

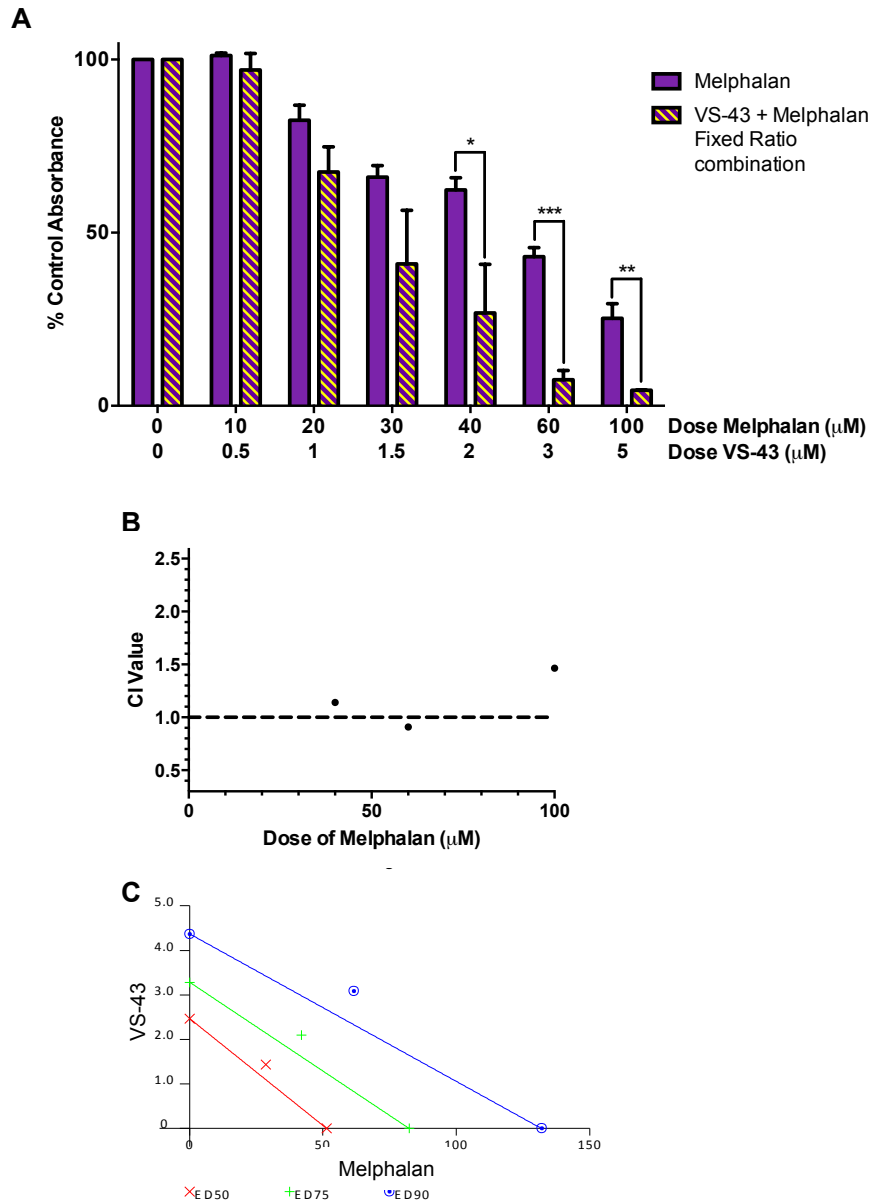


Figure 6-7: Combination of VS-43 and melphalan in RPMI9228 cells. A) VS-43 plus melphalan combination treatment slightly increases cell growth inhibition. Data plotted was obtained by MTT assay and is the average of at least three individual experiments with SEM calculated for error bars. Students t-test was carried out to determine statistical significance with * = $P < 0.05$, ** = $P < 0.01$ and *** = $P < 0.001$. B) Combination indices are predominantly in the additive region close to 1 and C) isobologram plot quantifying drug interactions at the 50%, 75% and 90% effect levels. Slight antagonism is observed between VS-43 and melphalan in RPMI8226 cells at all effect levels.

The combination of VS-43 with melphalan was also assessed using the non-fixed ratio method, as this gave slightly greater synergy for combination of VS-43 with cisplatin in chapter 4. DU145 cells were pre-treated with 5 μ M VS-43 for 1 hour, followed by a 1 hour melphalan treatment at a range of doses. The results of this experiment are shown in Figure 6-8. The GI₅₀ for melphalan is decreased from 109 μ M to 84.9 μ M with a VS-43 pre-treatment. This is a 22.1% change. Non-linear regression analysis determined that these GI₅₀ values are significantly different with a P value of P<0.0001. However, the difference between the pairs of melphalan treated and combination treated cell growth inhibition was not statistically significant. Therefore, no CI analysis was performed, as this combination provided no significant benefit to cell growth inhibition.

To determine whether other STAT3 inhibitors had the potential to synergise with melphalan, DU145 cells were also pre-treated with stattic and curcumin in combination with melphalan.

The ratio of stattic:melphalan used was 1:10 and the ratio of curcumin:melphalan used was 1:2.5. These ratios were based on the approximate GI₅₀ values for each drug alone in the DU145 cell line.

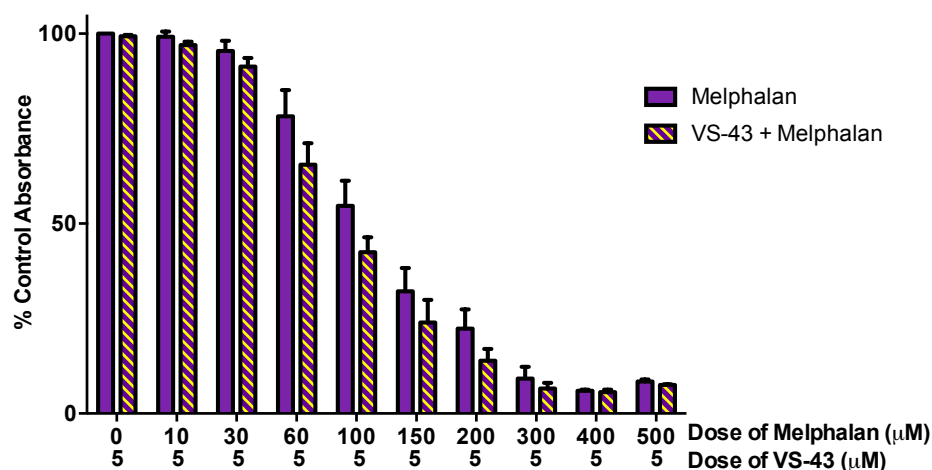


Figure 6-8: Non-fixed ratio combination of VS-43 and melphalan in DU145 cells. VS-43 plus melphalan combination treatment does not significantly affect cell growth inhibition. Data plotted was obtained by SRB assay and is the average of at least three individual experiments with SEM calculated for error bars. No statistical significance was observed. Absorbance was normalised to 5μM VS-43 alone

Figure 6-9A shows the cell growth inhibition for the combination of static and melphalan. The GI_{50} for melphalan decreases from 107.9μM to 49.2μM. This is the largest shift in GI_{50} seen yet with melphalan: a 54% reduction, however, the non-linear regression analysis was not able to establish a P value for this difference due to ambiguous fitting of the curves. The CI value analysis shown in Figure 6-9B shows that irrespective of the GI_{50} shift, the interaction of static and melphalan is predominantly not synergistic. The only mildly synergistic CI value obtained is 0.866 at 120μM melphalan. The remainder of the CI values are in the additive and antagonistic range. The interaction between static and cisplatin is further confirmed with the isobologram indicated in Figure 6-9C. At the 50% and 75% effect levels, the interaction is additive, whereas at the 90% effect level static exhibits slight antagonism in combination with melphalan.

Figure 6-10A shows the effect on cell growth inhibition by combination of curcumin with melphalan. Curcumin pre-treatment lowers the melphalan GI_{50} by 31.2% from 89.7μM to 61.7μM. Non-linear regression analysis determined that these GI_{50} values

are significantly different with a P value of $P < 0.0001$. When CI value analysis was performed no synergistic CI values were obtained. The lowest CI value was 0.961 and the largest was 1.194, indicating additivity and slight antagonism between curcumin and melphalan (Figure 6-10B). Figure 6-10C shows the isobologram analysis of this combination, which indicates antagonism at the 50%, 75% and 90% effect levels.

Therefore, the combination of STAT3 inhibitors with melphalan does not result in synergy. An additive and sometimes antagonistic relationship is found between STAT3 inhibitors and melphalan in both the DU145 and RPMI8226 cell lines.

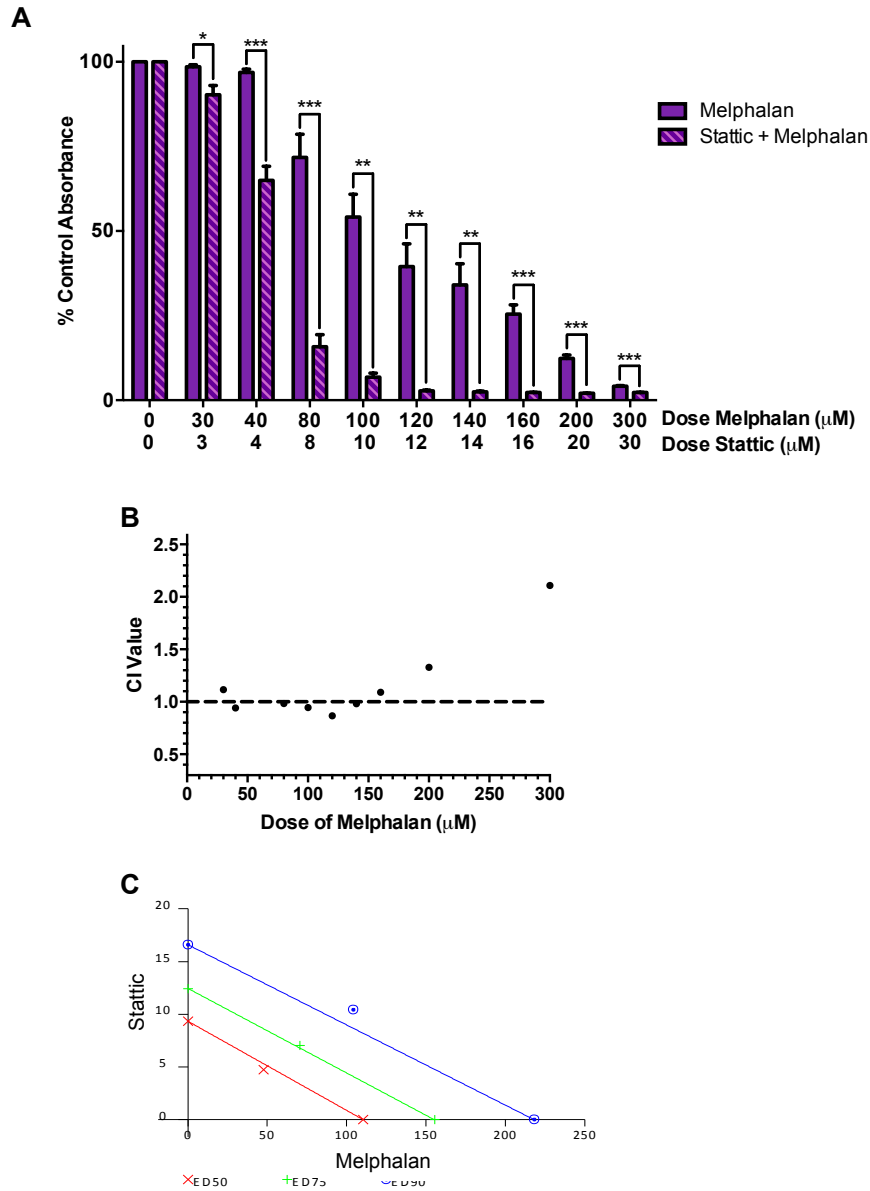


Figure 6-9: Combination of static and melphalan in DU145 cells. A) static plus melphalan combination treatment increases cell growth inhibition. Data plotted was obtained by SRB assay and is the average of at least three individual experiments with SEM calculated for error bars. Student's t-test was carried out to determine statistical significance with * = $P < 0.05$, ** = $P < 0.01$ and *** = $P < 0.001$. B) Combination indices are predominantly in the additive region close to 1 and C) isobologram plot quantifying drug interactions at the 50%, 75% and 90% effect levels. Additivity and slight antagonism is observed between static and melphalan in DU145 cells.

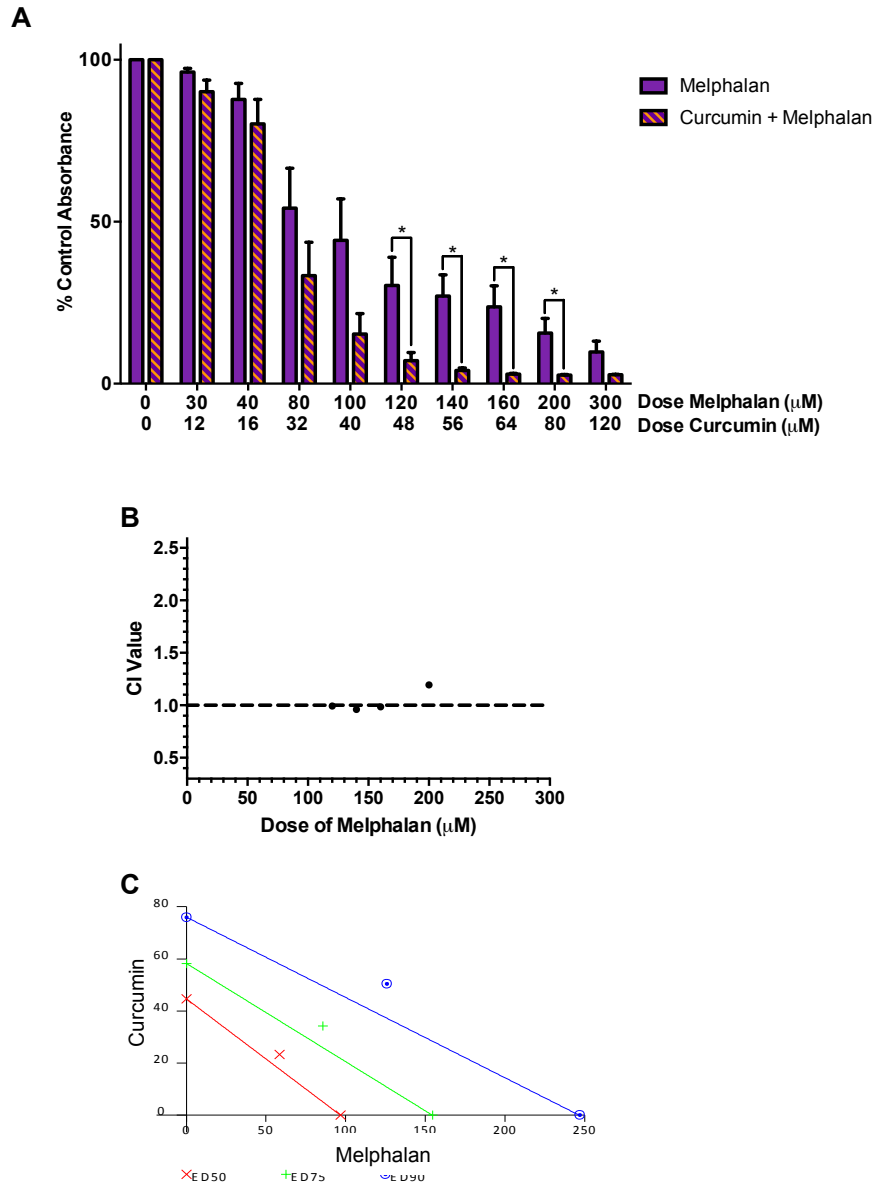


Figure 6-10: Combination of curcumin and melphalan in DU145 cells. A) curcumin plus melphalan combination treatment increases cell growth inhibition. Data plotted was obtained by SRB assay and is the average of at least three individual experiments with SEM calculated for error bars. Student's t-test was carried out to determine statistical significance with * = $P < 0.05$. B) Combination indices are predominantly in the additive region close to 1 and C) isobologram plot quantifying drug interactions at the 50%, 75% and 90% effect levels. Slight antagonism is observed between curcumin and melphalan in DU145 cells at all effect levels.

6.3.3 Combination with STAT3 inhibitors does not enhance apoptosis or DNA damage in melphalan-treated cells

In order to determine whether combination of STAT3 inhibitors with melphalan enhances apoptosis induction, immunoblotting was performed 24 hours after drug treatment. At the same time, immunoblotting for γ H2AX was performed to determine whether STAT3 inhibitors enhance melphalan-induced DNA damage as they do for cisplatin (chapter 5).

Figure 6-11A shows that treatment of DU145 cells with VS-43 induces both cleaved PARP and cleaved caspase-3 expression. Melphalan treatment induced cleaved PARP expression but minimal cleaved caspase-3 expression. Melphalan also resulted in γ H2AX expression. Combination treatment with VS-43 followed by cisplatin did not exhibit higher levels of cleaved PARP, cleaved caspase-3 or γ H2AX expression. Therefore, VS-43 does not enhance apoptosis or DNA damage induced by melphalan.

Figure 6-11B shows similar immunoblotting for DU145 cells treated with stattic and curcumin in combination with melphalan. The combination of stattic and melphalan does not increase γ H2AX expression but does result in a slight increase in cleaved PARP, however, this looks to be no more than additive. Combination of curcumin with melphalan also increases cleaved PARP as well as γ H2AX expression to some extent. However, if compared with the effect of curcumin in combination with cisplatin on these factors (Chapter 4, Figure 4-12), this effect is much lower.

These results suggest that VS-43 and stattic do not enhance melphalan-induced apoptosis or DNA damage, and that curcumin does have some effect on melphalan-induced apoptosis although this is much lower than the enhancement seen in combination with cisplatin. This is consistent with the lack of synergy observed between STAT3 inhibitors and melphalan.

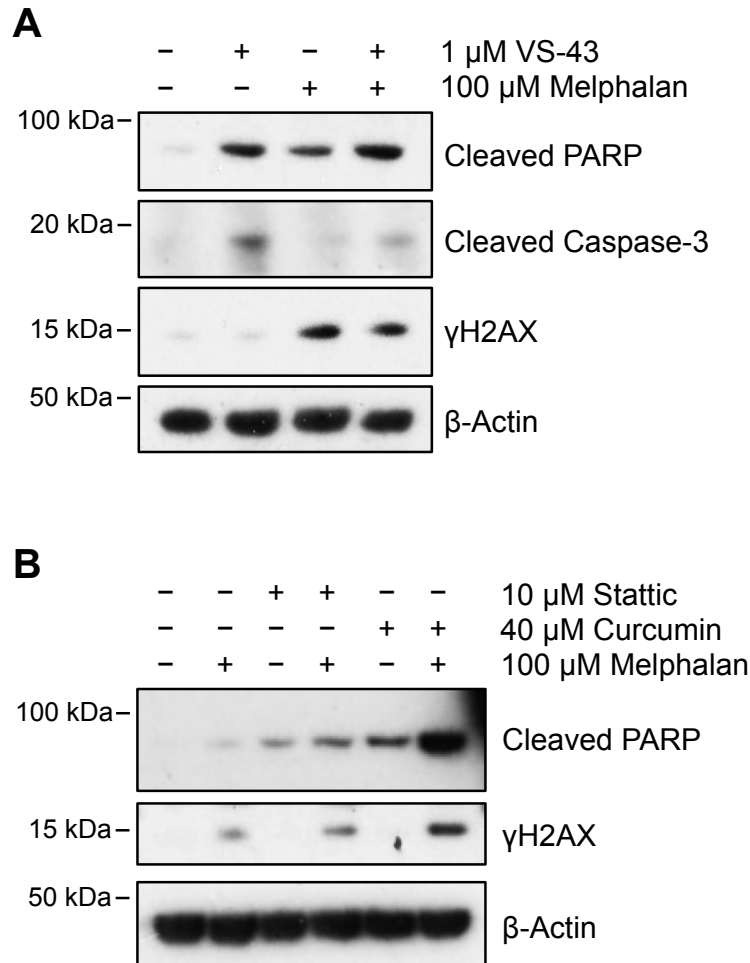


Figure 6-11: Combination treatment with STAT3 inhibitors and melphalan does not enhance apoptosis of DNA damage in the DU145 cell line. A) VS-43 in combination with melphalan does not enhance expression of cleaved PARP, cleaved caspase-3 or γ H2AX. B) combination of stattic with melphalan also does not enhance cleaved PARP or γ H2AX expression. Curcumin slightly increases cleaved PARP and γ H2AX expression in combination with melphalan. Blots are representative of more than 1 experiment.

6.3.4 STAT3 inhibition has no effect on melphalan DNA-ICL repair

In the previous chapter STAT3 inhibitors were demonstrated to enhance cisplatin-induced DNA damage, and block cisplatin-ICL unhooking. So far, the combination of STAT3 inhibitors with melphalan has not resulted in enhanced DNA damage. Therefore, the effect of STAT3 inhibition on melphalan-ICL repair was investigated. First, DU145 cells were treated with VS-43 for 18 hours followed by melphalan for 1

hour and then cells were harvested at 0, 9, 24 and 48 hours post melphalan-treatment for analysis by comet assay.

Figure 6-12 shows representative images of cells 48 hours after melphalan treatment, acquired through the Komet 6.0 software. 48 hours after melphalan treatment there appears to be no difference between cells treated with melphalan alone or cells that have been pre-treated with VS-43: both have similar comet tails, close in size to the comet tails of the untreated irradiated group. This suggests that any crosslinking induced by melphalan treatment has been repaired by 48 hours in both groups.

This is in stark contrast to the representative images shown for the combination of VS-43 with cisplatin in Figure 5-5, where a clear difference in comet tails was observed.

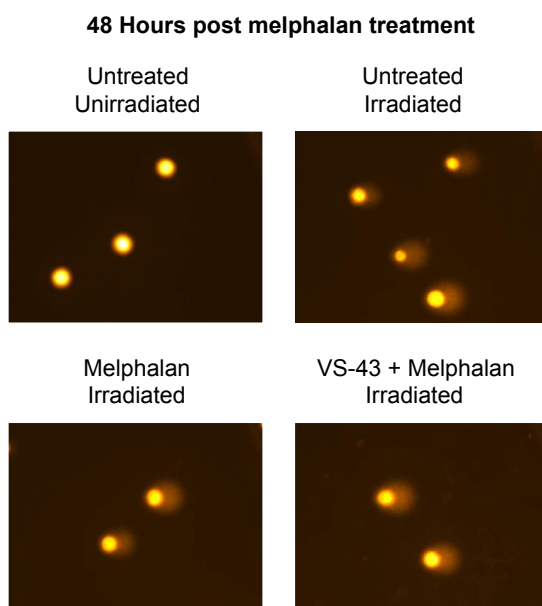


Figure 6-12: Representative comet images for the combination of VS-43 and melphalan. 48 hours after melphalan treatment, cells treated with either melphalan alone or VS-43 in combination with melphalan do not display any difference in extent of crosslinking – both groups have repaired melphalan-induced ICLs.

The representative images represent the overall outcome of the assay, however, this is a snapshot in time. The results from the full time-course comet assay are shown in Figure 6-13A. There is no difference between the formation and repair of melphalan-ICLs in the two treatment groups. Both groups reach the peak of ICL formation at 16 hours post-melphalan treatment (the 16 hour time-point for peak of melphalan-induced ICL formation has been previously demonstrated in this group (Spanswick et al., 2012)), and by 24 hours both groups have begun to repair the ICLs. At 48 hours post-treatment the melphalan-alone treated cells have reached 16.8% decrease in tail moment, and the combination treated cells are at 16.2% decrease in tail moment. This is almost identical. As such, the differences between the two treatment groups were not statistically significant at any time point.

The non-fixed ratio combination of VS-43 and melphalan was also tested for its effect on melphalan-ICL unhooking. Figure 6-13B shows that as with the fixed ratio combination, pre-treatment with 5 μ M VS-43 has no significant effect on the formation or repair of melphalan-induced ICLs.

To determine whether the observed effects were specific for the novel STAT3 inhibitor, VS-43, or apply to all STAT3 inhibitors, comet assays were also performed for cells treated with stattic and curcumin in combination with melphalan. As with VS-43, pre-treatment of DU145 cells with stattic (Figure 6-14A) or curcumin (Figure 6-14B) has no effect on the formation or repair of melphalan-induced ICLs. Again, 16 hours after drug treatment, the peak of ICL formation is observed in all treatment groups. By 24 hours post melphalan treatment, approximately 50% repair has occurred, and by 48 hours post melphalan treatment further repair is evident.

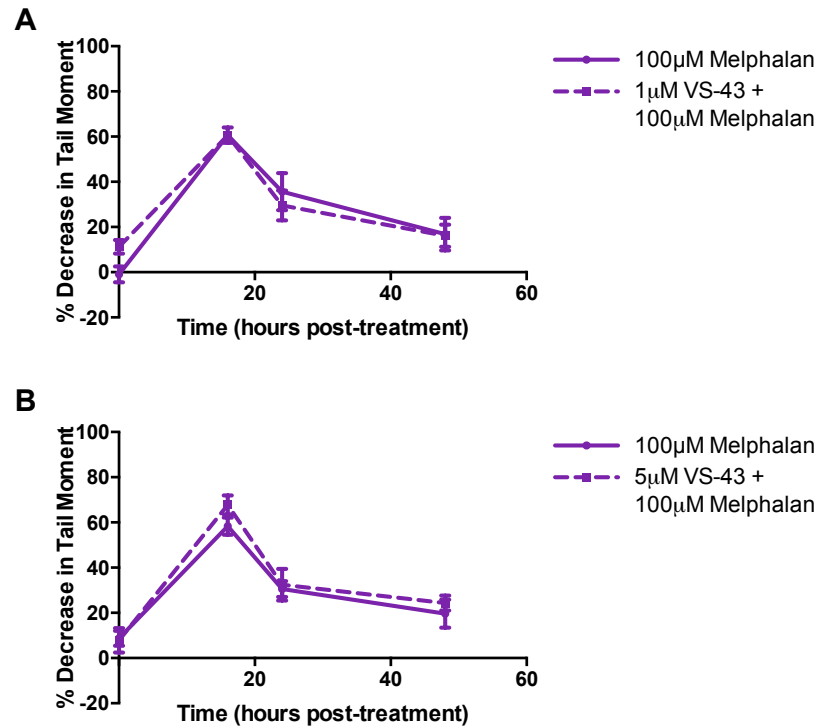


Figure 6-13: VS-43 has no effect on melphalan-ICL unhooking in the DU145 cell line. A) Fixed ratio and B) non-fixed ratio combination of VS-43 with melphalan. Cells pre-treated with VS-43 are able to repair melphalan-ICLs as well as cells treated with melphalan alone. Results are an average of three independent repeats, with SEM calculated for the error bars. No statistical significance was observed.

The combination of stattic and melphalan, however, results in a plateau in the percentage decrease in tail moment. At 24 hours post-treatment 29.6% decrease in tail moment is observed whereas at 48 hours post-treatment this has only reached 25.7%. In contrast, melphalan alone treated cells exhibit a decrease in tail moment of 41.0% at 24 hours and 12.9% at 48 hours. This could suggest potential slowing of melphalan-ICL repair by stattic, however, this is not statistically significant when compared with the melphalan-alone treated cells.

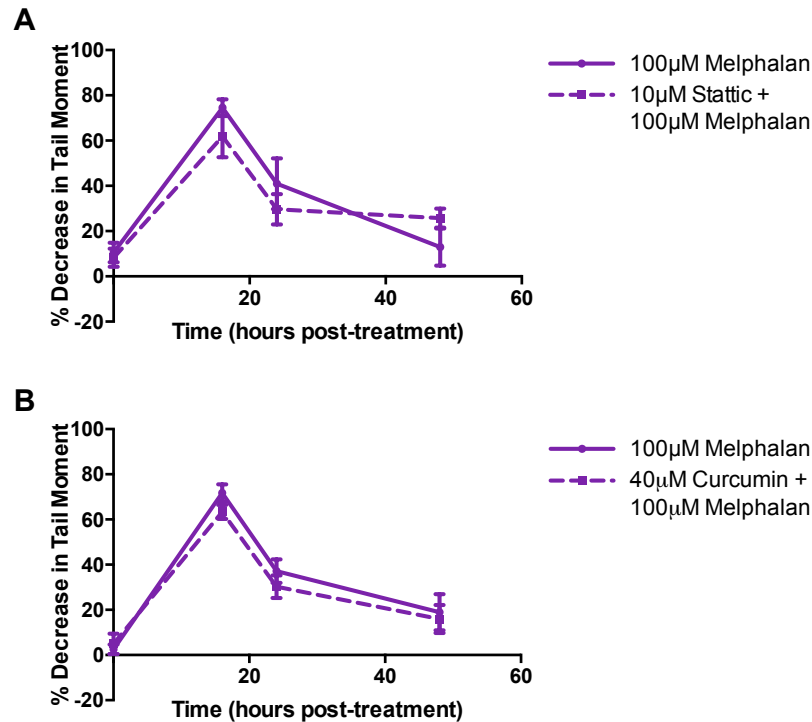


Figure 6-14: Static and curcumin have no effect on melphalan-ICL unhooking in the DU145 cell line. Cells pre-treated with A) static or B) curcumin are able to repair melphalan-ICLs as well as cells treated with melphalan alone. Results are an average of three independent repeats, with SEM calculated for the error bars. No statistical significance was observed.

As melphalan is not clinically used in prostate cancer, the DU145 cell line is not the most relevant model. Therefore, the effect of VS-43 on melphalan-ICL repair was also assessed in the RPMI8226 myeloma cell line. Figure 6-15 illustrates again that the combination of VS-43 with melphalan has no significant effect on the formation or repair of melphalan-ICLs. The tail moments are almost identical between melphalan-alone treated cells and cells that have been pre-treated with VS-43.

Therefore, STAT3 inhibitors do not block the unhooking of melphalan-induced ICLs, in contrast to their role in cisplatin-ICL repair.

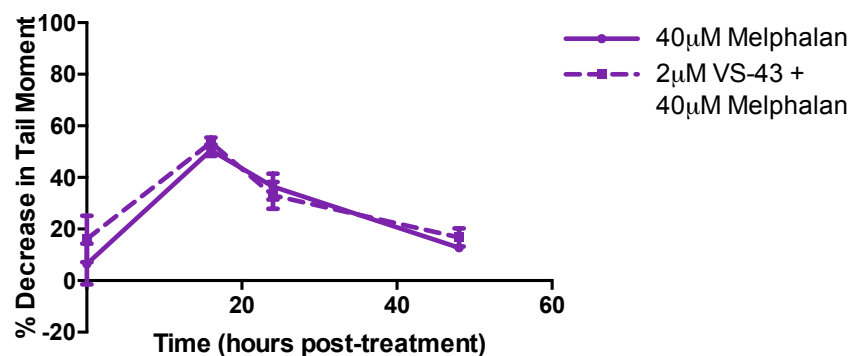


Figure 6-15: VS-43 has no effect on melphalan-ICL unhooking in the RPMI8226 cell line. Cells pre-treated with VS-43 are able to repair melphalan-ICLs as well as cells treated with melphalan alone. Results are an average of three independent repeats, with SEM calculated for the error bars. No statistical significance was observed.

6.3.5 STAT3 knockdown by siRNA blocks cisplatin but not melphalan DNA-ICL unhooking

So far the involvement of STAT3 in the repair of cisplatin and melphalan ICLs has been assessed through the use of pharmacological STAT3 inhibition. As compounds can have off-target effects, specific STAT3 knockdown was carried out using small interfering RNA, and the effect of this on ICL repair observed using the comet assay.

Figure 6-16A shows that partial (approximately 50%) knockdown of pSTAT3^{Tyr705} was achieved using a STAT3 siRNA pool. Luciferase siRNA was used as a negative control. Partial knockdown was used to be comparable to the partial down-regulation of pSTAT3^{Tyr705} levels caused by the doses of STAT3 inhibitors used in the previous comet assays.

For the comet assays, DU145 cells were transfected with STAT3 or luciferase siRNA for 24 hours before treatment with cisplatin or melphalan for 1 hour. Cells

were then harvested at the peak of crosslinking (9 hours for cisplatin and 16 hours for melphalan), and 24 hours after the peak of crosslinking (33 hours for cisplatin and 40 hours for melphalan). This was to determine whether STAT3 siRNA affected either the level of interstrand crosslinking or the overall repair of those crosslinks.

Figure 6-16B shows clearly that partial knockdown of STAT3 by siRNA had no effect on the level of cisplatin or melphalan ICLs at the peak of crosslinking. The percentage decrease in tail moment ranges from 55.0% to 59.3% across the six conditions, and none of these differences are statistically significant, as determined by one-way ANOVA. 24 hours after the ICL peak, however, cells treated with melphalan alone, and with luciferase or STAT3 siRNA in combination with melphalan show ICL repair down to 20.9%, 22.7% and 21.9%, respectively. For cisplatin-treated cells there is a significant difference between the cells treated with cisplatin alone and luciferase siRNA transfected cells, and the STAT3 siRNA transfected cells. Cells treated with cisplatin alone exhibit a 14.7% decrease in tail moment and luciferase siRNA transfected cells exhibit a -1.03% decrease in tail moment. This difference is, however, not statistically significant. Cells transfected with STAT3 siRNA have a 48.4% decrease in tail moment 33 hours after cisplatin treatment. These differences can be seen in the representative comet images in Figure 6-17. At the 9 hours and 16 hours post cisplatin and melphalan treatment, respectively, short tails are observed in all of the cells treated with the crosslinkers, irrespective of siRNA treatment. The images highlighted in red indicate the visible difference between the cells treated with STAT3 siRNA and cisplatin, versus STAT3 siRNA and melphalan, at 24 hours post ICL peak. The cisplatin-treated cells have very short tails, similar to those seen at the ICL peak, whereas the melphalan-treated cells have larger tails, suggesting crosslink unhooking.

This suggests that STAT3 siRNA blocks the repair of cisplatin, but not melphalan-ICLs.

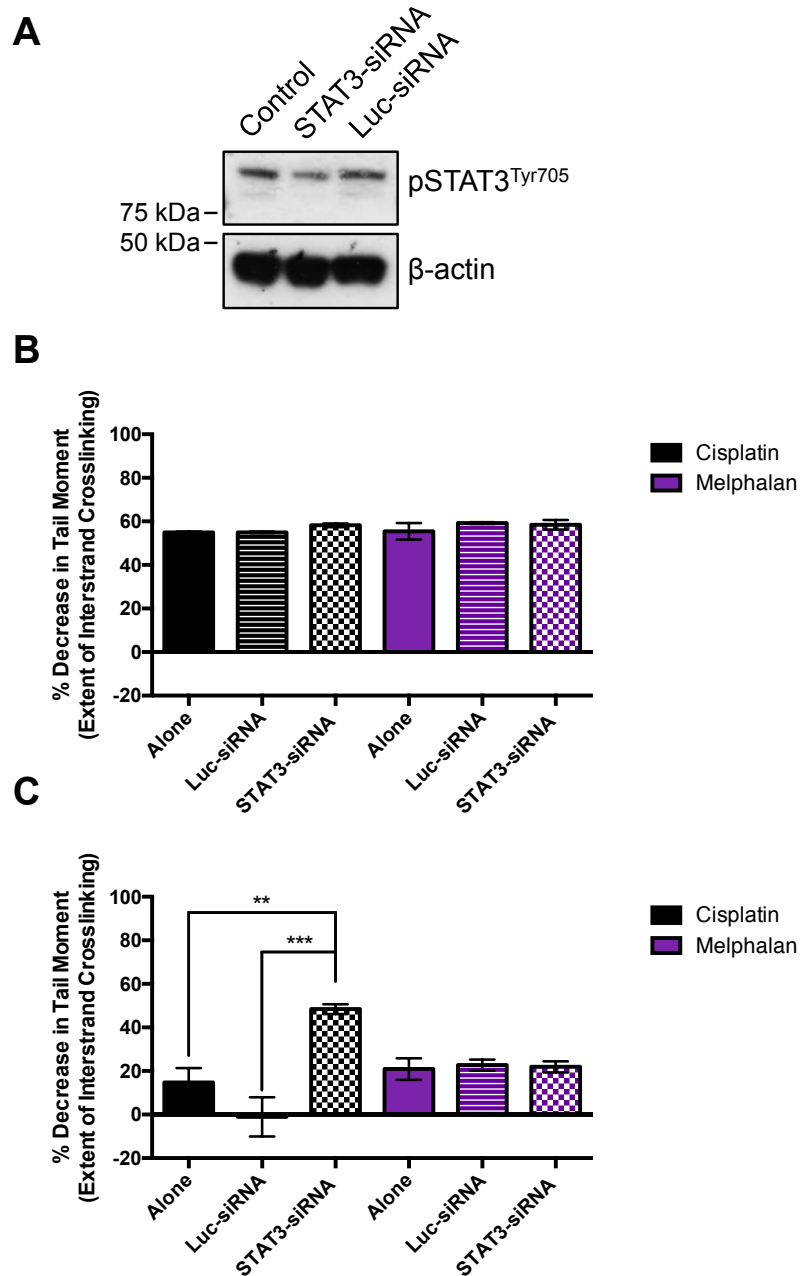


Figure 6-16: STAT3 siRNA inhibits cisplatin but not melphalan ICL repair. A) partial STAT3 knockdown was achieved with STAT3 siRNA in the DU145 cell line, as determined by immunoblotting. B) percentage decrease in tail moment at the peak of crosslinking (9 hours for cisplatin and 16 hours for melphalan). C) percentage decrease in tail moment 24 hours after the peak of crosslinking. The repair of cisplatin ICLs is inhibited by STAT3 siRNA. Melphalan ICLs repair irrespective of siRNA used. Luciferase (Luc) siRNA was used as a control. Results are the mean of three independent experiments with SEM displayed for error bars. One-way ANOVA was used to measure statistical significance. ** = $P < 0.01$ and *** = $P < 0.001$.

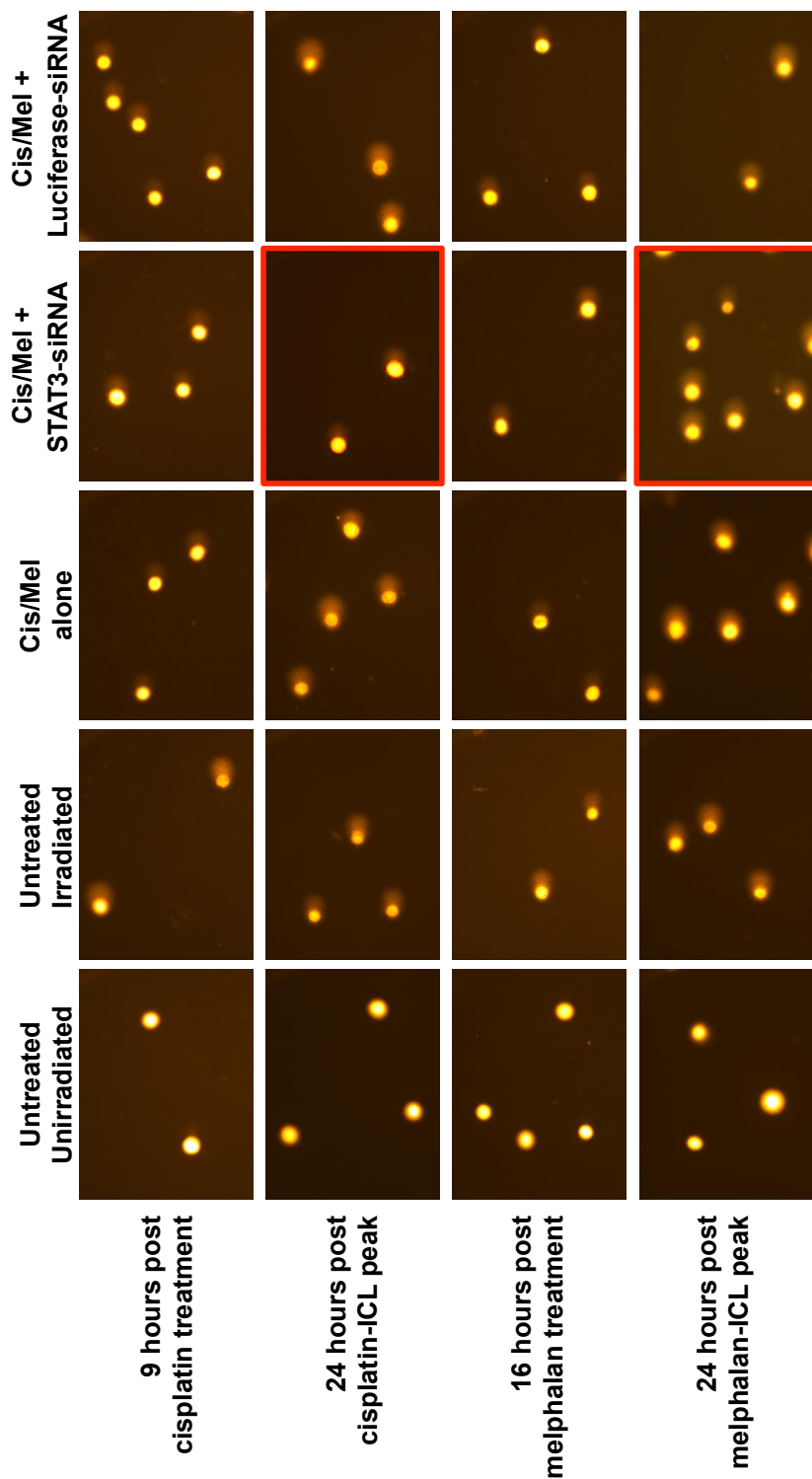


Figure 6-17: Representative comet images for STAT3 siRNA cells treated with cisplatin or melphalan. Images were taken at the cisplatin-ICL peak (9 hours), melphalan ICL peak (16 hours), and also 24 hours after the peak of each crosslinking drug to view repair. Highlighted boxes demonstrate the effect of STAT3 siRNA on cisplatin versus melphalan ICL repair. Luciferase siRNA is used as a control. Images are representative of more than 1 experiment.

6.3.6 Knockdown of EME1 or MUS81 specifically abolishes cisplatin-ICL repair

In Chapter 5, STAT3 inhibitors were identified to down-regulate expression of EME1 and MUS81, the two components of one of the ICL unhooking nuclease complexes. It was hypothesised that the regulation of these DNA repair factors by STAT3 could be responsible for the involvement of STAT3 in cisplatin-ICL unhooking. In order to investigate this, siRNA knockdown of EME1 and MUS81 was carried out before treatment of DU145 cells with cisplatin and melphalan. The extent of ICL repair was quantified by comet assay.

Figure 6-18A demonstrates that a partial EME1 knockdown was achieved in DU145 cells using the EME1 siRNA. As with the STAT3 siRNA comets, the effect of EME1 knockdown on ICL formation was assessed by measuring the tail moment of cells at the ICL peak. All three groups of cells treated with cisplatin reached between 68.7% and 62.1% decrease in tail moment at the ICL peak, whereas the cells treated with melphalan reached between 53.6% and 51.7% decrease in tail moment (Figure 6-18B). The differences between these groups were not statistically significant, indicating that EME1 knockdown has no effect on the formation of cisplatin or melphalan ICLs. At 24 hours post ICL peak, the cisplatin treated cells exhibit 11.1%, 15.7% and 51.9% decrease in tail moment for the cisplatin alone, luciferase siRNA and EME1 siRNA groups. The difference between the EME1 siRNA group was statistically significant when compared with either the cisplatin alone or luciferase siRNA cells. This indicates that EME1 siRNA blocks cisplatin-ICL unhooking, similarly to STAT3 siRNA. The cells treated with melphalan, however, all repaired the melphalan-ICLs to a similar extent: between 6.76% and 16.4% decrease in tail moment was observed, suggesting that melphalan-ICLs are unhooked irrespective of the siRNA treatment. Representative images for this experiment are shown in Figure 6-19. The difference between the role for EME1 in cisplatin-ICL and

melphalan-ICL repair is highlighted in the images outlined in red. After EME1 knockdown, cells treated with cisplatin retain the short comet tails associated with a high level of crosslinking; whereas melphalan treated cells have large comet tails, similar to those seen in cells treated with melphalan alone.

These results are indicative of a role for EME1 in cisplatin-ICL unhooking.

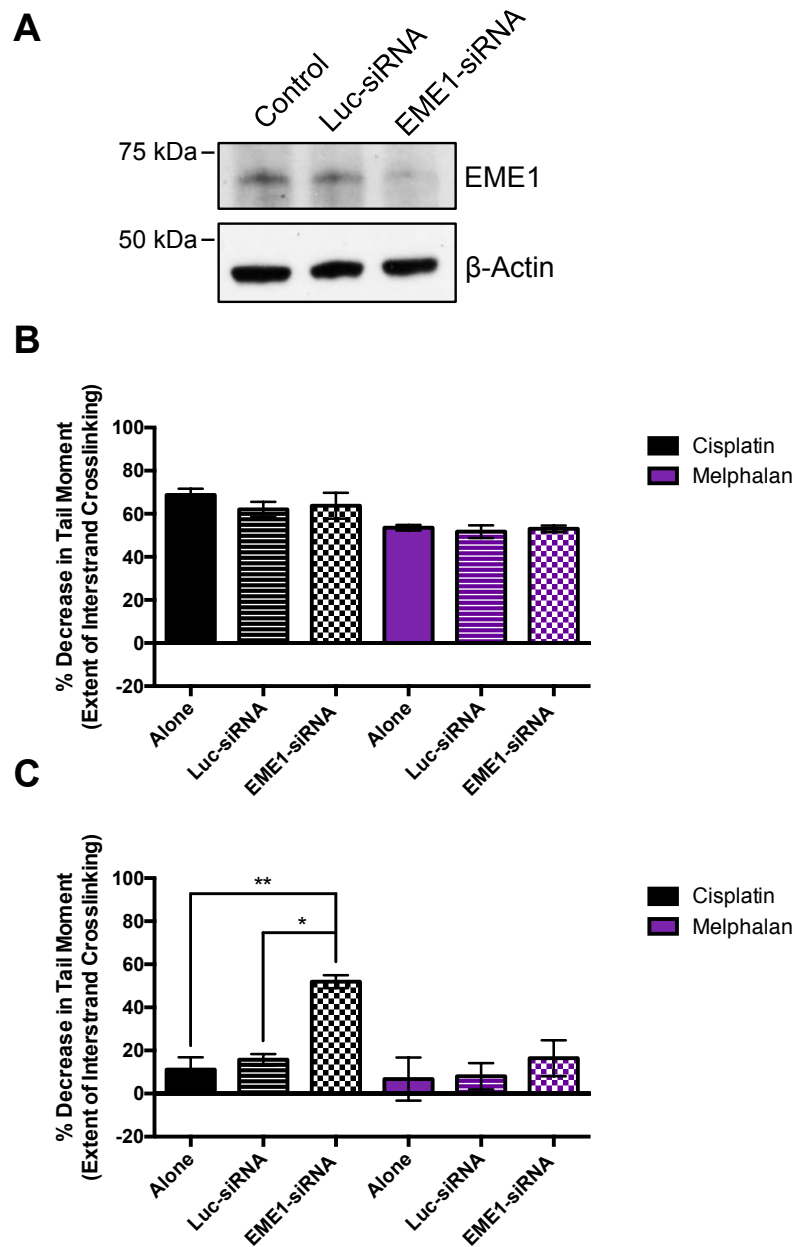


Figure 6-18: EME1 siRNA inhibits cisplatin but not melphalan ICL repair. A) partial EME1 knockdown was achieved with EME1 siRNA in the DU145 cell line, as determined by immunoblotting. B) percentage decrease in tail moment at the peak of crosslinking (9 hours for cisplatin and 16 hours for melphalan). C) percentage decrease in tail moment 24 hours after the peak of crosslinking. The repair of cisplatin ICLs is inhibited by EME1 siRNA. Melphalan ICLs repair irrespective of siRNA used. Luciferase (Luc) siRNA was used as a control. Results are the mean of three independent experiments with SEM displayed for error bars. One-way ANOVA was used to measure statistical significance. * = $P < 0.05$ and ** = $P < 0.01$.

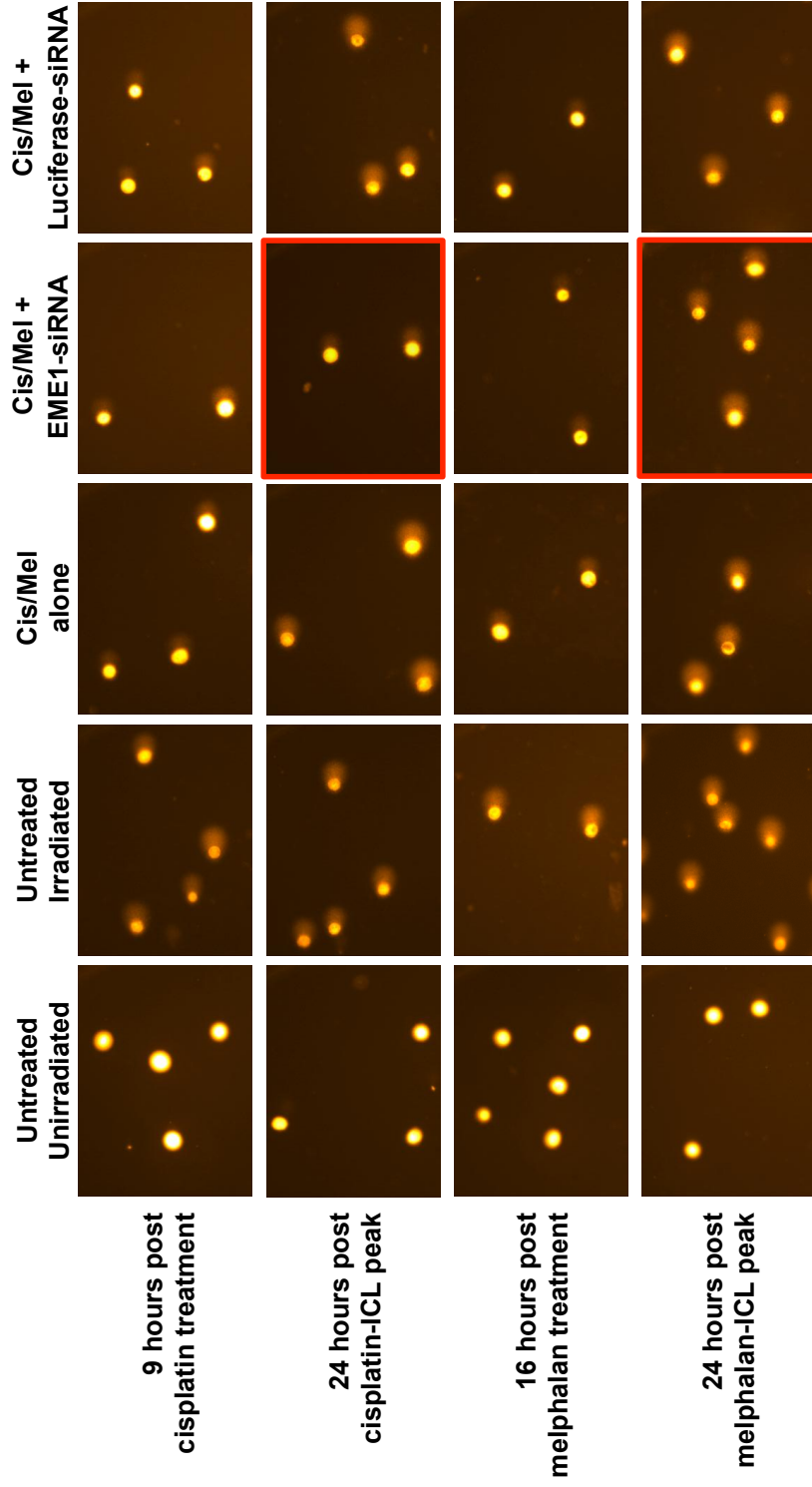


Figure 6-19: Representative comet images for EME1 siRNA cells treated with cisplatin or melphalan. Images were taken at the cisplatin-ICL peak (9 hours), melphalan ICL peak (16 hours), and also 24 hours after the peak of each crosslinking drug to view repair. Highlighted boxes demonstrate the effect of EME1 siRNA on cisplatin versus melphalan ICL repair. Luciferase siRNA is used as a control. Images are representative of more than 1 experiment.

Identical experiments were performed in DU145 cells transfected with MUS81 siRNA. A partial MUS81 knockdown was achieved as is shown in Figure 6-20A, with the luciferase siRNA acting as a negative control. As with both STAT3 and EME1, knockdown of MUS81 has no significant effect on the formation of cisplatin or melphalan ICLs, as the percentage decrease in tail moment at the ICL peak is between 54.8% and 61.7% for cisplatin treated cells, and 47.9% and 51.4% for melphalan treated cells (Figure 6-20B). Figure 6-20C shows that MUS81 siRNA is also capable of inhibiting cisplatin-ICL repair: the percentage decrease in tail moment is 57.6% in MUS81 knockdown cells treated with cisplatin versus 21.8% and 15.9% for cisplatin alone and luciferase knockdown cells treated with cisplatin. Both of these differences are statistically significant. However, MUS81 knockdown has no effect on the repair of melphalan-ICLs. Regardless of siRNA treatment, cells treated with melphalan exhibit a percentage decrease in tail moment of approximately 20%, indicating that ICL unhooking has occurred. Representative images of this experiment are shown in Figure 6-21. Again, the difference between the effect of MUS81 knockdown on cisplatin and melphalan treated cells is visible. 24 hours after the ICL peak, cisplatin treated cells also transfected with MUS81 siRNA have comet tails similar to those seen at the ICL peak, indicating little, if any, repair. In contrast, melphalan treated cells also transfected with MUS81 siRNA have visible comet tails, similar to those seen with melphalan treatment alone or in cells transfected with the luciferase control siRNA.

These results indicate that MUS81, in addition to EME1, is involved in the repair of cisplatin-ICLs but not melphalan-ICLs. STAT3 knockdown has a similar effect to the knockdown of both of these nuclease components, which supports the hypothesis that regulation of EME1 and MUS81 by STAT3 is responsible for the inhibition of cisplatin-ICL unhooking.

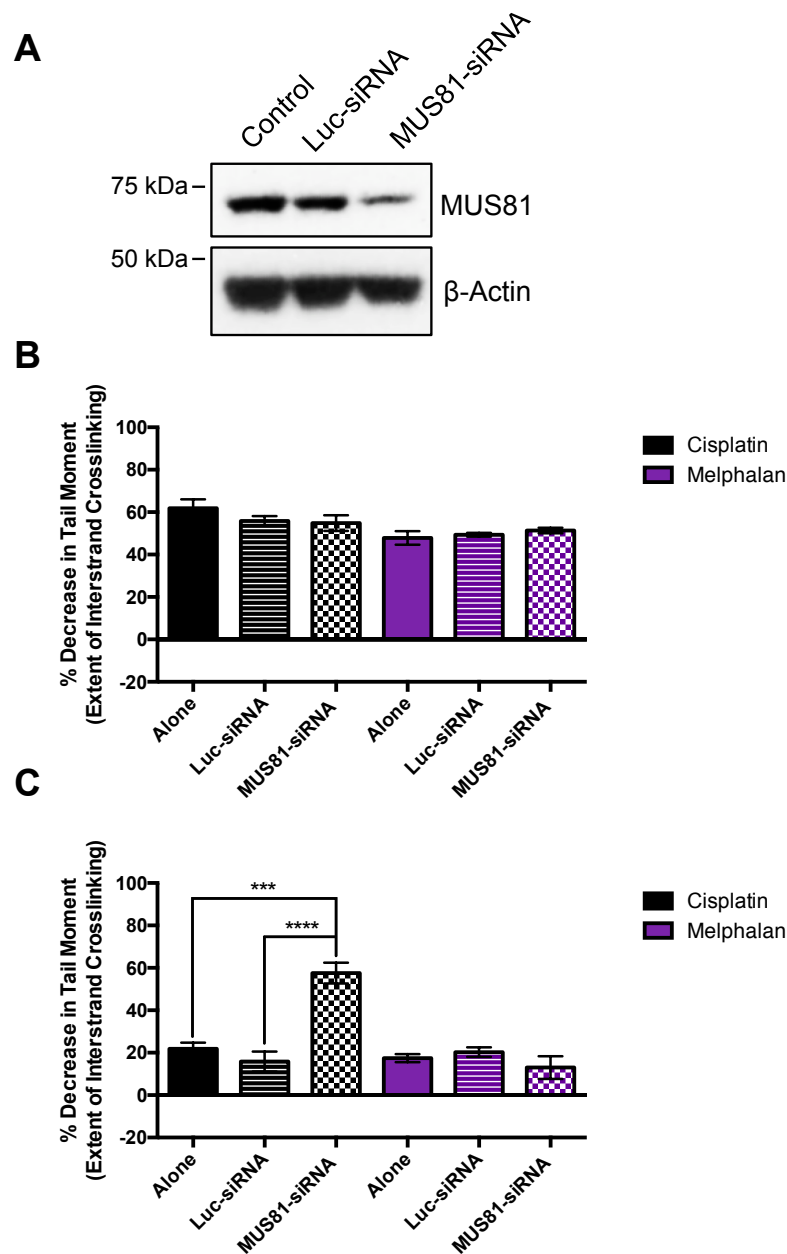


Figure 6-20: MUS81 siRNA inhibits cisplatin but not melphalan ICL repair. A) partial MUS81 knockdown was achieved with MUS81 siRNA in the DU145 cell line, as determined by immunoblotting. B) percentage decrease in tail moment at the peak of crosslinking (9 hours for cisplatin and 16 hours for melphalan). C) percentage decrease in tail moment 24 hours after the peak of crosslinking. The repair of cisplatin ICLs is inhibited by MUS81 siRNA. Melphalan ICLs repair irrespective of siRNA used. Luciferase siRNA was used as a control. Results are the mean of three independent experiments with SEM displayed for error bars. One-way ANOVA was used to measure statistical significance. *** = $P < 0.001$ and **** = $P < 0.0001$.

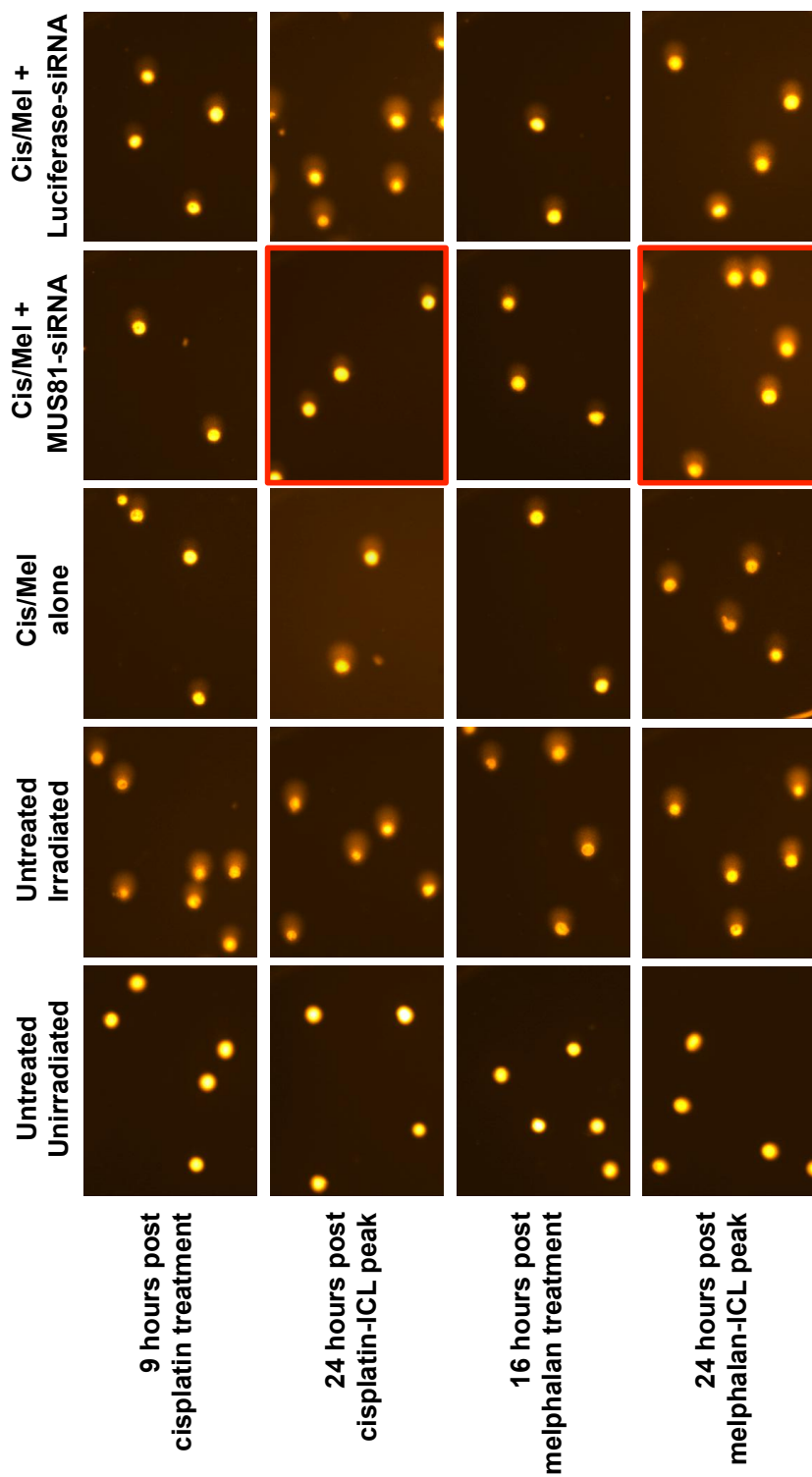


Figure 6-21: Representative comet images for MUS81 siRNA cells treated with cisplatin or melphalan. Images were taken at the cisplatin-ICL peak (9 hours), melphalan ICL peak (16 hours), and also 24 hours after the peak of each crosslinking drug to view repair. Highlighted boxes demonstrate the effect of MUS81 siRNA on cisplatin versus melphalan ICL repair. Luciferase siRNA is used as a control. Images are representative of more than 1 experiment.

6.3.7 Expression of EME1 and MUS81 is interdependent

In this chapter, the involvement of both MUS81 and EME1 in cisplatin-ICL repair has been demonstrated. In Chapter 5, VS-43 and other STAT3 inhibitors were shown to down-regulate the expression of both EME1 and MUS81, and this was suggested to be via the transcriptional regulation of these genes by STAT3.

MUS81 and EME1 form a complex, and this interaction is essential for nuclease activity (Haber and Heyer, 2001), therefore, whether the down-regulation of either EME1 or MUS81 could affect expression of the other component of the complex was investigated. siRNA was used to down-regulate EME1 and MUS81 individually, and immunoblotting was performed for both factors at 24 hours and 48 hours post transfection.

Figure 6-22A shows that cells transfected with 10, 25 and 50nM EME1 siRNA exhibit reduced EME1 expression, which increases from 24 to 48 hours post transfection. MUS81 expression is also down-regulated, and this effect is greater at 48 hours post transfection with EME1 siRNA. There also appears to be a dose-dependent effect. In Figure 6-22B the reverse was performed: MUS81 was knocked down with increasing concentrations of siRNA. Here, the effect is more striking, MUS81 expression is clearly reduced by transfection with MUS81 siRNA, and this is also able to down-regulate expression of EME1. There appears to be a dose-dependent effect, which is, again, greatest at 48 hours post transfection.

Therefore, the expression of EME1 and MUS81 appears to be interdependent, with each factor potentially stabilising the other.

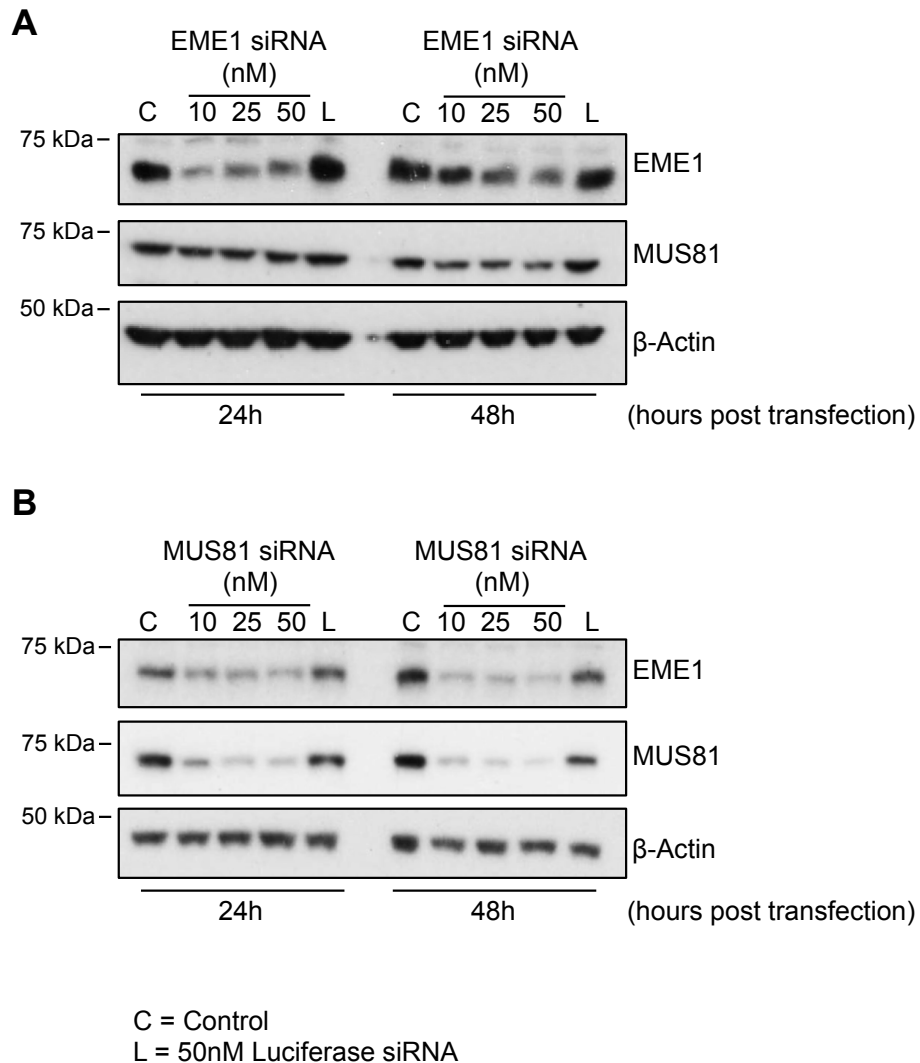


Figure 6-22: Expression of EME1 and MUS81 is interdependent. siRNA knockdown of A) EME1 and B) MUS81 in DU145 cells. Immunoblotting was performed 24 and 48 hours after transfection with three concentrations of siRNA. A luciferase siRNA (L) was used as a non-targeting control. Blots are representative of more than 1 experiment.

6.4 Discussion

In this chapter, the investigation into the role of STAT3 in ICL unhooking has been extended to include the nitrogen mustard crosslinking chemotherapy drug, melphalan. Whereas in Chapter 4 the combination of STAT3 inhibitors with cisplatin was demonstrated to be synergistic, melphalan exhibited no such synergy in

combination with inhibition of STAT3. CI values obtained for the combination of melphalan with STAT3 inhibitors were predominantly additive and at very high effect levels, mildly antagonistic (although the accuracy of the CI values at high effect levels is diminished, as discussed in Chapter 4). In addition, the repair of melphalan-ICLs was not affected by STAT3 inhibitors or STAT3 siRNA knockdown, suggesting that the role of STAT3 in ICL unhooking is not a universal one.

ICLs are considered to be the most toxic of the lesions formed by crosslinkers such as cisplatin and melphalan and, accordingly, the level of these adducts has been shown to correlate with the anti-cancer activity of the crosslinker (Hansson et al., 1987; Kothandapani et al., 2011; Sunter et al., 1992; Zhen et al., 1992). The results presented in this thesis are in agreement with these findings, as the ability of STAT3 inhibitors to block ICL repair correlates with their chemosensitising properties. For melphalan, where ICL repair proceeds in the presence of STAT3 inhibitors, no sensitisation is observed.

Clearly, if STAT3 inhibitors are able to block cisplatin-ICL, but not melphalan-ICL, unhooking, these events must occur via separate pathways, as has been reported by this group previously (Spanswick et al., 2012).

6.4.1 Differences between cisplatin and melphalan-ICL repair

Studies investigating the mechanism for ICL repair often use different crosslinking agents, as the repair pathway is generally considered universal. If, as is demonstrated in this thesis, the repair of different ICLs takes place via different mechanisms, this approach is not appropriate. Experiments performed with the same crosslinking agents should be compared together and the differences and similarities between experiments using different crosslinkers should be noted.

In this chapter, the MUS81-EME1 endonuclease is demonstrated to play a key role for the unhooking of cisplatin-ICLs, but not melphalan-ICLs. Investigations into ICL repair have most frequently used cisplatin, mitomycin C or psoralen. Melphalan is rarely used in these studies. However, work from our laboratory has demonstrated that ERCC1 and XPF mutant cell lines are hypersensitive to melphalan whereas these mutants display only slight increased sensitivity to mono-functional melphalan, indicating the importance of XPF-ERCC1 in melphalan ICL repair (Clingen et al., 2005). Also, another study investigated the role of ERCC1 in melphalan sensitivity and showed ERCC1^{-/-} cells to be hypersensitive to melphalan (Al-Minawi et al., 2009). However, no studies have yet been carried out describing the involvement of MUS81-EME1 in melphalan sensitivity or melphalan-ICL repair.

The role of the MUS81-EME1 endonuclease in cisplatin-ICL repair is more frequently studied. There are several reports of hypersensitivity to cisplatin in cancer cell lines lacking MUS81 or EME1 (Abraham et al., 2003; Hanada et al., 2006; McPherson et al., 2004), as was discussed in Chapter 5. In addition, mouse embryonic stem cells lacking MUS81 expression do not generate DSBs in response to cisplatin whereas wild-type cells do, suggesting that MUS81-EME1 is involved in incising the cisplatin-ICL (Hanada et al., 2006).

In Chapter 5, as well as MUS81-EME1, FANCD2 was shown to be down-regulated by treatment with STAT3 inhibitors. FANCD2 has been reported to be involved in the repair of both cisplatin and melphalan-induced ICLs. Inhibitors of the FANCD2 protein increase sensitivity to cisplatin (Chirnomas et al., 2006) and in myeloma cells a proteasome inhibitor which down-regulates FANCD2 levels is able to sensitise cells to melphalan. In that same study, siRNA directed against FANCD2 was shown to increase the percentage of melphalan-ICLs (Yarde et al., 2009), and Knipsheer et al. have demonstrated that FANCD2 is essential for the incision

reactions to take place on a synthetic cisplatin-ICL (Knipscheer et al., 2009). This evidence combined with the knowledge that FANCD2 acts very early in the ICL repair process suggests that FANCD2 acts in a general ICL repair role. Indeed, the FA core complex protein FANCF, involved in FANCD2 monoubiquitination has also been tied to both cisplatin and melphalan sensitivity, and also melphalan ICL repair (Chen et al., 2005; Dai et al., 2015).

BRCA1 was also shown to be down-regulated by STAT3 inhibition in this thesis. As with FANCD2, the involvement of BRCA1 in both cisplatin and melphalan ICL repair has been proposed. BRCA1^{-/-} cells are hypersensitive to cisplatin, and do not form FANCD2 foci after treatment with cisplatin (Bhattacharyya et al., 2000; Bunting et al., 2012). BRCA1 levels have also been found to be up-regulated in melphalan-resistant cell lines (Chen et al., 2005). These studies do not demonstrate a direct relationship between BRCA1 status and ICL unhooking, however, as BRCA1 is also involved in homologous recombination (Valerie and Povirk, 2003), which occurs downstream of the unhooking process in ICL repair after the lesion has been removed, it is likely to also be involved in the general ICL repair mechanism.

Therefore, the very early stages of ICL repair (FA pathway activation) and later stages (homologous recombination) are possibly the same for all ICLs. What may differ is the initial recognition of the ICL, and the incisions required either side of the ICL for unhooking, as the various ICL structures and distortions produced could influence which proteins are able to bind to the site.

This group has previously reported evidence that the repair of cisplatin and melphalan ICLs occurs via a different mechanism. Friendmann et al. demonstrated that inhibition of EGFR delays cisplatin-ICL but not melphalan-ICL unhooking. They suggested that this effect is due to the inhibition of the NHEJ protein DNA-PK, as an inhibitor of DNA-PK also sensitised cells to cisplatin and delayed cisplatin-ICL

unhooking, but not melphalan-ICL unhooking. EGFR was shown to interact directly with DNA-PK and the possibility of inhibition by sequestration was suggested (Friedmann et al., 2004). The effect of STAT3 inhibition on DNA-PK levels is not reported, however, DNA-PK was one of the genes analysed by RT-PCR array in Chapter 5. DNA-PK was down-regulated by 1.32 and 1.54 fold at 1 μ M and 2 μ M VS-43, respectively. However, neither of these values were statistically significant as P values greater than 0.05 were calculated by the analysis software. Therefore, DNA-PK was not shortlisted as a STAT3 target. It is possible that EGFR may therefore, inhibit cisplatin-ICL unhooking through both the regulation of DNA-PK and STAT3 downstream targets such as MUS81-EME1. Another study, however, reported contradictory evidence for the role of DNA-PK in melphalan sensitivity. Sousa et al. observed sensitisation to melphalan by DNA-PK inhibitors (Sousa et al., 2013). Therefore, the mechanistic role for DNA-PK in ICL unhooking, and whether it does have lesion specificity, requires further investigation. The argument for a link between EGFR and the MUS81-EME1 endonuclease is, however, strengthened by the report by Vigneron et al. which suggested that EGFR regulates EME1 expression through STAT3 (Vigneron et al., 2008).

Spanswick et al. also presented evidence to suggest a different unhooking mechanism for cisplatin and melphalan ICLs. Gemcitabine was shown to selectively inhibit cisplatin ICL unhooking (Spanswick et al., 2012). Gemcitabine is a nucleoside analogue that may inhibit nucleotide excision repair through its incorporation into the repairing DNA patch. As cisplatin also forms intrastrand crosslinks, which are removed by NER (Zamble et al., 1996), Spanswick et al. suggest that the inhibition of intrastrand crosslink repair may sequester DNA repair proteins which also play a role in ICL repair, such as the XPF-ERCC1 endonuclease (Friedberg, 2001). The effects of STAT3 inhibition on the level of cisplatin intrastrand crosslinking could be investigated using adduct-specific antibodies (Liedert et al., 2006). Melphalan does

not form intrastrand crosslinks (Bauer and Povirk, 1997), however, monoadducts are formed which are also repaired by NER (Grant et al., 1998). Therefore, the effect of gemcitabine, and STAT3 inhibitors, on sequestration of NER proteins and whether this selectively targets cisplatin-ICL repair remains to be determined.

6.4.2 The role of MUS81-EME1 in ICL repair: evidence so far

The data presented in this chapter demonstrates the involvement of both components of the MUS81-EME1 endonuclease in cisplatin-ICL repair. Knockdown of either MUS81 or EME1 with siRNA significantly inhibits the unhooking of cisplatin-ICLs in a similar manner to that seen with STAT3 siRNA or STAT3 pharmacological inhibition (Figure 6-16, Figure 6-18, Figure 6-20). However, the role for MUS81-EME1 in ICL repair is still largely debated.

ERCC1^{-/-} cells are able to generate DSBs after treatment with MMC (Niedernhofer et al., 2004), suggesting that ERCC1-XPF may not be the only nuclease involved in the ICL incision reaction. Hanada et al. have demonstrated that DSBs do not form in response to cisplatin and MMC in mouse embryonic stem cells lacking MUS81 (Hanada et al., 2006). However, data from our research group has demonstrated that DSBs do not form after treatment with cisplatin (De Silva et al., 2002). Nonetheless, Hanada et al. also reported that deletion of MUS81 rendered cells hypersensitive to both MMC and cisplatin. In normal cells, the generation of DSBs after cisplatin and MMC treatment was demonstrated to occur in a replication-dependent manner, therefore, suggesting that MUS81-EME1 acts to incise ICLs at stalled replication forks (Hanada et al., 2006). This is in agreement with the structure specificity of MUS81-EME1 for replication fork structures and 3' flaps (Ciccio et al., 2003). Therefore, a role for MUS81-EME1 as the additional nuclease involved in incising cisplatin-induced ICLs remains possible.

Another piece of evidence linking the MUS81-EME1 nuclease to ICL repair is its interaction with the scaffold protein, SLX4. SLX4^{-/-} cells are approximately 10-fold more sensitive to cisplatin than wild-type cells, and SLX4 directly interacts with MUS81, stimulating its nuclease activity as well as the nuclease activity of XPF (Muñoz et al., 2009).

Some studies do not agree with a primary role for MUS81-EME1 in ICL unhooking. Kuraoka et al. demonstrated that the XPF-ERCC1 nuclease is able to incise both sides of the ICL, however, these experiments were performed with psoralen rather than cisplatin (Kuraoka et al., 2000), therefore, it cannot be assumed this is also the case for cisplatin ICLs. Wang et al. suggested that MUS81-EME1 was involved in incising the ICL as an insurance mechanism should XPF-ERCC1 and SNM1A action fail, however, this study did not use cisplatin either, MMC was used to induce ICLs (Wang et al., 2011).

Therefore, the role of MUS81-EME1 in ICL repair remains to be confirmed. However, if a lesion-specific approach is taken, with the results presented in this chapter combined with the evidence put forward by Hanada et al., involvement of MUS81-EME1 in ICL unhooking is likely.

6.4.3 Other possible combinations for STAT3 inhibitors

In this chapter STAT3, via the regulation of the MUS81-EME1 endonuclease, is shown to be involved in the unhooking of cisplatin-ICLs, whilst having no influence on the unhooking of melphalan ICLs. The alternative unhooking mechanisms may be a result of the varying structure of the ICL lesion, which depends on the crosslinking agent used and the resulting degree of DNA helix distortion. As discussed in the introduction to this chapter, cisplatin-ICLs are highly distorting

lesions whereas nitrogen mustard-induced ICLs such as mechlorethamine-ICLs are considerably less distorting (Coste et al., 1999; Rink and Hopkins, 1995).

It is therefore, possible that crosslinkers which produce ICLs with a similar level of DNA distortion to cisplatin-ICLs may be substrates for MUS81-EME1 cleavage, and so may synergise with STAT3 inhibitors. The crosslinkers most likely to produce similar structured ICLs are those from the same family as cisplatin, the platinum crosslinkers. The currently FDA approved platinum compounds other than cisplatin are carboplatin and oxaliplatin. The structures of these compounds are shown in Figure 6-23. Unfortunately there is no structural information regarding the distortions that carboplatin or oxaliplatin produce when they form DNA-ICLs. Therefore, whether the larger size of both of these platinum compounds affects the structure of the DNA-ICL formed is unknown, however, the distance between the two crosslinked sites should be the same as with cisplatin. Sensitivity studies using carboplatin and oxaliplatin with STAT3 inhibitors would provide some indication as to whether all platinum-induced ICLs are repaired via the same unhooking mechanism. One study has already reported synergy between oxaliplatin and curcumin, though whether this is due to STAT3 inhibition is as yet unknown (Li et al., 2007), as our group has previously published an antagonistic interaction between the EGFR inhibitor, cetuximab, and oxaliplatin (Santoro et al., 2015). For carboplatin, a synergistic interaction with curcumin has been described in retinoblastoma cell lines (Sreenivasan and Krishnakumar, 2014). Additionally, combination studies have shown synergy for the combination of carboplatin with gemcitabine (Wang et al., 2010), and the benefit of combining carboplatin with gemcitabine in platinum-resistant ovarian cancer patients has been demonstrated in a phase II trial. This trial also demonstrated a significant reduction in the repair of carboplatin-ICLs in patient cells treated with gemcitabine (Ledermann et al., 2010). As this research group has also previously described gemcitabine to inhibit cisplatin-

ICLs *in vitro* (Spanswick et al., 2012), this could suggest that carboplatin-ICLs repair via a similar mechanism and so combination with STAT3 inhibitors may be beneficial. The differences between the repair of cisplatin, carboplatin and oxaliplatin adducts may also be inferred by the patterns of cross-resistance seen within this class. Cross-resistance exists between cisplatin and carboplatin, whereas cross-resistance is much lower between cisplatin and oxaliplatin (Eckstein, 2011; Raymond et al., 2002). Therefore, this would suggest that cisplatin and carboplatin may have similar repair mechanisms whereas oxaliplatin-induced DNA damage may not be repaired by the same pathway.

Chemosensitivity studies using selective STAT3 inhibitors will determine whether carboplatin is a possible candidate for combination treatment, and comet assays with MUS81-EME1 knockdown will aid in the elucidation of the repair mechanisms at play for the various platinum-ICLs.

In Chapter 4, VS-43 was shown to synergise with doxorubicin, the intercalating topoisomerase II inhibitor, which exerts its toxic effects on cells by inducing DSBs. Interestingly, Friedmann et al. previously reported synergy between the EGFR inhibitor, gefitinib, and etoposide, a topoisomerase II inhibitor. Gefitinib was demonstrated to delay the repair of etoposide-induced DSBs, as measured by comet assay (Friedmann et al., 2004). As discussed previously, EGFR acts upstream of STAT3 therefore, the effects published by Friedmann et al. could be a result of indirect STAT3 inhibition.

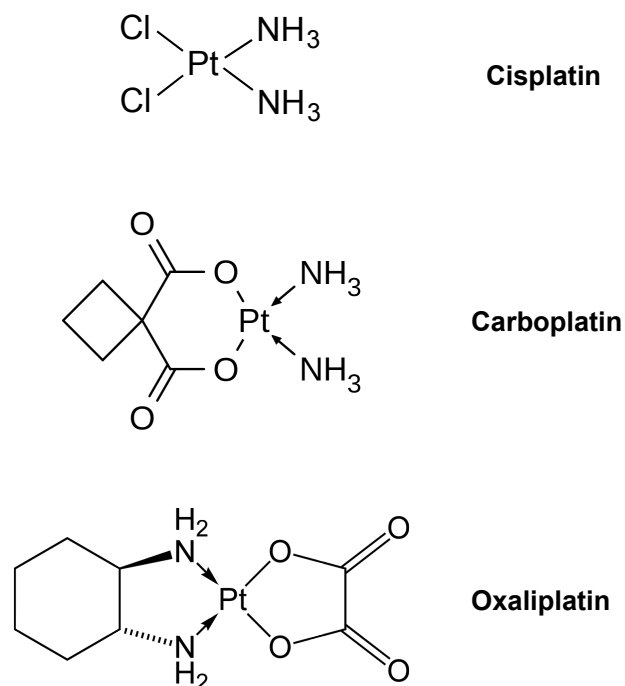


Figure 6-23: Structures of cisplatin, carboplatin and oxaliplatin.

This, along with the results presented in this thesis demonstrating synergy between VS-43 and doxorubicin, could suggest that STAT3 regulates genes involved in DSB repair. Two genes involved in DSB repair via homologous recombination were down-regulated by VS-43 on the DNA damage signalling RT-PCR array in Chapter 5 (section 5.3.4). These were BRCA1 and RPA1. Therefore, through the down-regulation of homologous recombination proteins, STAT3 inhibitors may also chemosensitise to other agents that act via the induction of DSBs, including other topoisomerase inhibitors like irinotecan, or ionising radiation. In fact, previous work carried out by this group has demonstrated radiosensitising properties of VS-43. This data is included in Appendix D.

Therefore, it is proposed here that STAT3 is able to synergise with the ICL-inducing agent, cisplatin, through the inhibition of MUS81-EME1 expression, which is required for the unhooking of cisplatin-ICLs. STAT3 may also be able to sensitise

cells to other crosslinking agents, particularly if MUS81-EME1 is involved in the unhooking of those lesions. Alternatively, the effects of STAT3 inhibition on other DNA repair proteins, including those involved in homologous recombination, may allow for sensitisation to agents inducing DSBs. Further investigation into the DNA repair mechanisms targeted by STAT3 inhibition and the possible therapy combinations as a result of this must be carried out.

6.4.4 The interdependency of EME1 and MUS81

In this chapter, the dependency of each component of the MUS81-EME1 nuclease on its partner protein was investigated using siRNA knockdown of each factor individually. Expression of EME1 and MUS81 was demonstrated to be interdependent, which may be expected due to the reported dependency between MUS81 and EME1 for nuclease activity (Haber and Heyer, 2001).

In Chapter 5, STAT3 inhibitors were demonstrated to down-regulate the expression of both EME1 and MUS81, possibly by directly binding to the promoter regions of these genes and regulating transcription. With the observation that down-regulation of either MUS81 or EME1 is able to produce an effect on the expression of the partner protein, it follows that if STAT3 is involved in the transcription of just one of these genes, inhibitors of this pathway would be able to down-regulate both MUS81 and EME1. The effect of STAT3 inhibition on mRNA expression of EME1 and MUS81 was analysed in sections 5.3.4.3 and 5.3.4.4, with the clear finding that EME1 mRNA expression is inhibited to a greater extent than MUS81 mRNA expression. Therefore, these results could suggest that STAT3 directly regulates the transcription of EME1, and through down-regulation of the EME1 protein, MUS81 expression is also down-regulated. However, STAT3 binding to the MUS81 promoter region was demonstrated by ChIP in Chapter 5, although whether this binding affects transcription of the MUS81 gene is yet to be determined. Therefore,

STAT3 may regulate the expression of MUS81 directly, or through the regulation of its partner protein, EME1. These events lead to an inhibition in cisplatin-ICL unhooking when cells are treated with both a STAT3 inhibitor and cisplatin.

6.5 Conclusion

In this chapter, the combination of STAT3 inhibitors with melphalan has been investigated. STAT3 inhibitors do not chemosensitise to melphalan, and do not enhance melphalan-induced apoptosis or DNA damage. The pharmacological inhibition of STAT3 has no effect on the repair of melphalan-induced ICLs. This is in contrast to what was reported for cisplatin-ICLs in the previous chapter. siRNA knockdown of STAT3 was shown to inhibit cisplatin but not melphalan-ICL repair. The role of the MUS81-EME1 nuclease in the repair of these lesions was also investigated, and it was found that both MUS81 and EME1 are required for the unhooking of cisplatin-ICLs whereas neither component of the nuclease complex is needed for melphalan-ICL repair to proceed. Interdependency between expression of EME1 and MUS81 was also observed.

Therefore, the synergy reported between STAT3 inhibitors and cisplatin is likely due to the regulation of the MUS81-EME1 nuclease by STAT3, which is required for the repair of cisplatin-ICLs. Upon STAT3 inhibition, the MUS81-EME1 nuclease is down-regulated, either through the transcriptional regulation of both factors, or through transcriptional regulation of EME1 and subsequent loss of MUS81 expression due to the interdependency between these factors. Upon down-regulation of MUS81-EME1, cisplatin-ICL unhooking is blocked. As the MUS81-EME1 nuclease is not required for melphalan-ICL unhooking, this provides the mechanistic basis for why STAT3 inhibitors do not synergise with melphalan.

Chapter 7 Conclusions

STAT3 is constitutively activated in many types of cancer, and the targets of this transcription factor drive tumourigenesis through cell survival, metastasis, angiogenesis and differentiation (Frank, 2007; Masuda et al., 2010). STAT3 inhibitors are frequently reported to harbour chemosensitising properties, however, the mechanism behind this is not understood. Therefore, understanding the role of STAT3 and how this interacts with the mechanism of action of chemotherapy agents will enable the development of more successful combination therapies.

This thesis has investigated two projects related to STAT3: the pharmacological characterisation of a novel STAT3 inhibitor, VS-43, and the involvement of STAT3 in the mechanism of ICL repair.

Chapter 3 began with the introduction to the novel STAT3 inhibitor, VS-43. VS-43 was derived from the naturally occurring compound, curcumin, which lacks sufficient potency and bioavailability to be successful in the clinic (Anand et al., 2007). VS-43 was rationally designed by Professor Moses Lee and colleagues to inhibit the STAT3 DNA binding domain. The structural design of VS-43 proved successful as VS-43 was demonstrated to be approximately 10-fold and 40-fold more potent at inhibiting pSTAT3^{Tyr705} than the commercially available STAT3 inhibitors stattic and curcumin, respectively. Additionally, VS-43 may irreversibly inhibit STAT3, as the down-regulation of pSTAT3^{Tyr705} persisted after removal of the drug. As curcumin has been demonstrated to be a reversible STAT3 inhibitor, these results suggest further superiority of VS-43 (Bharti et al., 2003a). A longer duration of action for a compound, could allow for less frequent treatment appointments for a patient. In Chapter 3, the selectivity of VS-43 was also investigated. VS-43 is demonstrated to have selectivity for STAT3 over STAT1, STAT5a and STAT5b. The selectivity of STAT3 inhibitors is an important factor, which is surprisingly rarely addressed for

many novel compounds. In particular, selectivity for STAT3 over STAT1 is critical due to the role of STAT1 as a tumour suppressor, regulating genes involved in apoptosis and cell cycle arrest (Chin et al., 1996; Fulda and Debatin, 2002). The most developed STAT3 inhibitor to date, OPB-31121, even targets STAT1 and STAT5 in addition to STAT3 (M. J. Kim et al., 2013). The clinical consequences of the lack of selectivity and whether it will hamper further clinical development of OPB-31121 remains to be seen. However, it is possible that inhibition of STAT1 could dampen the anti-cancer benefit of a STAT3 inhibitor.

The various factors influencing the activity of a STAT3 inhibitor were also investigated in Chapter 3. Drug treatment times, the confluency of cells and the cell line used were all shown to contribute to the evaluation of potency when treating with a STAT3 inhibitor. These are factors that complicate the comparison of inhibitor potencies from data reported in the literature. A true direct comparison cannot be made unless each of these factors is controlled for. This should be taken into consideration in future studies investigating and comparing inhibitor potencies.

Whilst VS-43 has been demonstrated to have many qualities suitable for a stand-alone anti-cancer agent, today, many chemotherapy regimens consist of a combination of drugs. This provides the rationale for Chapter 4.

In **Chapter 4**, the combination of STAT3 inhibitors with cisplatin was investigated. Curcumin has been frequently reported to enhance cisplatin sensitivity in cancer cell lines (Goel and Aggarwal, 2010; Notarbartolo et al., 2005; Yallapu et al., 2010). Given VS-43 has been proven to be a more potent STAT3 inhibitor than curcumin, whether this affects the interaction with cisplatin was of interest. VS-43 was compared directly to static and curcumin in terms of its interaction with cisplatin. Whilst all three STAT3 inhibitors were able to sensitise cancer cell lines to cisplatin, VS-43 produced greater synergy with cisplatin than either of the commercial STAT3

inhibitors. These results strengthen the argument for the development of more potent STAT3 inhibitors, as they can be used at lower doses to produce greater synergy in combination with cisplatin. Additionally, treatment with VS-43 for just 1 hour was enough to synergise with cisplatin, suggesting that alternative treatment regimes could be investigated to maximise this synergy and perhaps manage side effects in the clinic, as the 1 hour VS-43 treatment was considerably less toxic than the longer 18 hour treatment. A drug that has the flexibility to be used for shorter treatment periods may be beneficial for clinical use, should this observation translate across into clinical trials.

Whilst the combination of VS-43 with cisplatin did result in synergy, this was not considered “strong synergism”, as defined by Chou et al. (Chou, 2010). The effect of VS-43 alone contributed to some of the cell growth inhibition observed in the combination. Therefore, as the analysis of drug combinations takes into account the dose-response curves of both drugs alone, the higher the toxicity of the individual drugs, the lower the synergy observed is likely to be. As such, the non-constant combination of VS-43 and cisplatin produced slightly greater synergy, as VS-43 itself is not particularly toxic after a 1 hour exposure. This should be considered when designing novel combination treatment schedules in the future, and possible alterations in the drug treatment times made in order to obtain the greatest degree of synergy.

Chapter 5 addressed the question of how STAT3 inhibitors synergise with cisplatin. The rationale for looking at DNA repair came from the hypothesis that for synergy to occur between two drugs, their mechanisms of action must overlap. Cisplatin is a DNA-damaging chemotherapy agent, and DNA damage response inhibitors such as ATR inhibitors have previously been shown to synergise with cisplatin (Mohni et al., 2015). Additionally, resistance to cisplatin can occur via the repair of cisplatin-DNA

adducts (Wynne et al., 2007). Therefore, it was logical to observe the effects of STAT3 inhibition on cisplatin-induced DNA damage.

The DNA damage marker, γ H2AX, was significantly increased in cells treated with the combination of STAT3 inhibitor and cisplatin, indicating that cisplatin-induced DNA damage is enhanced by inhibition of STAT3. STAT3 inhibitors were then demonstrated to block the repair, specifically the unhooking, of cisplatin-ICLs, without affecting the initial formation of these adducts. This implied that STAT3 could have a role in the early stages of ICL repair.

As STAT3 is a transcription factor, it was hypothesised that STAT3 may regulate the expression of ICL repair genes. Therefore, inhibition of STAT3 could down-regulate those factors and subsequently block ICL repair. RT-PCR revealed several DNA repair factors to be down-regulated by VS-43 treatment. These included FANCD2 and BRCA1, two proteins known to be involved in the ICL unhooking process, as well as MUS81 and EME1, both components of the MUS81-EME1 endonuclease, which is reported to be involved in incising the ICL site to allow for unhooking (Rahn et al., 2010).

In Chapter 5, STAT3 inhibitors were demonstrated to cause a G1-phase cell cycle arrest. Of the four ICL-repair factor targets, only BRCA1 was found to be cell cycle regulated, consistent with current literature (Ruffner and Verma, 1997). This suggested that the regulation of FANCD2, EME1 and MUS81 by STAT3 may be transcriptional and so the online UCSC Genome Browser database was utilised to identify possible STAT3 binding sites upstream of the MUS81 and EME1 transcription start sites. No STAT3 binding sites were identified upstream of FANCD2. Using CHIP-PCR with a STAT3 antibody, STAT3 was found to be enriched at two sites upstream of the MUS81 gene and one site upstream of the EME1 gene. VS-43 pre-treatment effectively abolished STAT3 binding to these

sites. This data suggested that STAT3 directly regulates the expression of the MUS81-EME1 nuclease, which is in agreement with a study suggesting transcriptional regulation of EME1 by the EGFR-STAT3 axis (Vigneron et al., 2008). These results have expanded the understanding of the synergistic interaction between STAT3 inhibitors and cisplatin, providing a possible mechanistic basis for the frequently reported beneficial co-administration of these drugs. As well as enhancing apoptosis in cisplatin-treated cells, STAT3 inhibitors directly interfere with the cisplatin-ICL repair pathway. This raised the possibility that other ICL-inducing agents may synergise with cisplatin due to the regulation of DNA repair by STAT3.

Therefore, the aim of **Chapter 6** was to investigate the use of STAT3 inhibitors in combination with another crosslinking drug, melphalan. Melphalan was chosen as previous data from this group suggested that melphalan and cisplatin have different mechanisms of ICL unhooking, and that EGFR inhibitors synergise with cisplatin but not melphalan (Friedmann et al., 2004; Spanswick et al., 2012). Whereas cisplatin is used to treat lung, head and neck, testicular and cervical cancer, melphalan is predominantly used in myeloma patients (as well as some ovarian and breast cancer patients) (Cancer Drugs, Cancer Research UK webpage, available from: <http://www.cancerresearchuk.org/about-cancer/cancers-in-general/treatment/cancer-drugs/> [accessed August 2016]), therefore, understanding which chemotherapy drugs STAT3 inhibitors are successful in combination with would indicate which patients would be most likely to benefit from the development of STAT3 inhibitors.

In agreement with the previous findings of this group, STAT3 inhibitors did not synergise with melphalan. Additionally, pre-treatment with a STAT3 inhibitor had no effect on the repair of melphalan-induced ICLs, suggesting that STAT3 is not involved in melphalan-ICL unhooking. Non-pharmacological inhibition of STAT3 was

performed by siRNA knockdown, and the effect of this, as well as siRNA knockdown of MUS81 and EME1, on cisplatin and melphalan ICL unhooking was observed. STAT3, MUS81 and EME1 siRNA knockdown had equivalent effects on ICL repair: cisplatin-ICL repair was inhibited, whereas melphalan-ICL repair was unaffected. Given the potential transcriptional regulation of the MUS81-EME1 nuclease by STAT3 (either by regulation of both components of the nuclease or by regulation of EME1 followed by down-regulation of MUS81 expression due to the interdependency in expression demonstrated between these factors in Chapter 6), these results suggested first that MUS81-EME1 is specifically involved in cisplatin-ICL unhooking, and second, that STAT3 inhibitors synergise with cisplatin through the regulation of the MUS81-EME1 nuclease. This confirms the mechanistic basis for why STAT3 inhibitors synergise with cisplatin, but not melphalan, as MUS81-EME1 is only required for efficient cisplatin-ICL repair.

This data highlights the need for mechanistic ICL repair studies to use the same crosslinking agents in order to elucidate the agent-specific ICL repair pathways. Currently the role of MUS81-EME1 in ICL repair is debated, with some studies suggesting MUS81-EME1 is involved in ICL repair whereas others disagree (Hanada et al., 2006; Kuraoka et al., 2000). However, these studies use different crosslinking agents to make conclusions about ICL repair, and as has been shown in this thesis, this approach is not appropriate as there is not a completely universal ICL repair pathway. Instead, studies using different crosslinkers with select repair proteins knocked out could be compared and contrasted in order to identify which stages of ICL repair are universal and which are variable. Once the differences in ICL repair are established, this will aid in the determination of the most beneficial drug combinations. For instance, here the mechanistic rationale behind combination of STAT3 inhibitors and cisplatin is suggested to be through the MUS81-EME1 nuclease. Combination of STAT3 inhibitors with melphalan in the clinic is not a

viable option as there is no interaction between the STAT3 pathway and melphalan-ICL repair.

7.1 Future work

Several findings presented in this thesis could be carried forward in future work. Each of these areas will be discussed briefly.

7.1.1 Further development of VS-43 as a therapeutic agent

The data presented in this thesis has demonstrated promising results regarding the novel STAT3 inhibitor, VS-43. VS-43 is potent and selective, and has been shown to be a superior chemosensitiser when compared with other STAT3 inhibitors. Therefore, further preclinical development of this compound should be carried out. This will consist of mouse xenograft experiments, initially testing the toxicity of VS-43 *in vivo* and the ability of VS-43 to reach the tumour site and down-regulate STAT3 activation in the tumour. If these studies are successful, combination treatments with cisplatin would be performed to determine whether the synergy demonstrated *in vitro* can be achieved in animal models. After preclinical research, if promising data has been obtained with VS-43, the process of testing VS-43 in clinical trials would begin in order to determine tolerability, dose ranges, treatment schedules and anti-cancer activity. This is, however, a lengthy process. The STAT3 inhibitor, OPB-31121, entered clinical trials in 2010 (Oh et al., 2010) and, 6 years later, is still in phase I/II clinical trials.

7.1.2 Optimisation of combination schedules

The combination of STAT3 inhibitors and cisplatin was reported to be synergistic in this thesis. As discussed in Chapter 4, however, the drug treatment schedule used can affect the degree of synergy achieved. In this thesis, the STAT3 inhibitors were administered as pre-treatments to the crosslinking agents, and synergy was

observed in combination with cisplatin. However, even greater synergy may be obtainable using a different drug schedule, for example simultaneous treatment with both the STAT3 inhibitor and cisplatin.

VS-43 was demonstrated to synergise with cisplatin with both an 18 hour pre-treatment and a 1 hour pre-treatment. Therefore, the length of inhibitor treatment time could also be investigated in order to find the most synergistic treatment scheduling. The importance of the length of time between treatment with the first drug and the second in a combination was demonstrated by Lee et al. Treatment of breast cancer cells with erlotinib followed by doxorubicin was shown to be more beneficial than delivery of the two drugs together or in the opposite order, and a treatment delay of 24 hours was optimal for apoptosis induction when compared with a 4, 8 and 48 hour pre-treatment (Lee et al., 2012).

Whether the best *in vitro* treatment schedules are also the best *in vivo* and even in patients would also need to be addressed.

7.1.3 Combination of STAT3 inhibitors with other chemotherapy agents

STAT3 inhibitors have been described to sensitise cancer cells to various chemotherapy agents, not just cisplatin. This thesis demonstrated that the combination of STAT3 inhibitors with melphalan is not a viable one, however, combination with other crosslinking chemotherapy drugs must be tested. In particular, as discussed in Chapter 6, the combination of STAT3 inhibitors with other platinum crosslinkers should be investigated. Both oxaliplatin and carboplatin are used in the clinic today, and acquired resistance can develop in response to either of these compounds (Giaccone, 2000; Mishima et al., 2002). In the case of oxaliplatin, the extent of DNA platination is lower in more resistant cell lines (Mishima et al., 2002), therefore, if STAT3 inhibitors can sensitise cells to oxaliplatin

or carboplatin, this may overcome resistance through the regulation of ICL repair. As VS-43 is not able to synergise with melphalan, whether this applies to the whole class of nitrogen mustards must also be determined. This will also help to elucidate the differences in ICL repair due to the regulation of MUS81-EME1 by STAT3.

In this thesis, VS-43 is also demonstrated to synergise with the topoisomerase II inhibitor doxorubicin, and it was hypothesised that this may be through the regulation of DSB repair by STAT3. Interestingly, Friedmann et al. previously reported synergy between gefitinib and etoposide, another topoisomerase II inhibitor, and showed that gefitinib can delay the repair of etoposide-induced strand breaks (Friedmann et al., 2004). As gefitinib acts to inhibit EGFR, upstream of STAT3, this suggests that STAT3 inhibitors may also be able to sensitise cells to etoposide. This has, in fact, already been reported for curcumin (Dhandapani et al., 2007). Sensitisation of cancer cell lines to etoposide could possibly occur through the regulation of the DSB repair process, for instance via the transcriptional regulation of factors involved in homologous recombination such as BRCA1 and RPA1, which was demonstrated by VS-43 in Chapter 5. If STAT3 inhibitors are able to sensitise to other DSB-inducing agents, such as IR, whether this is via inhibition of homologous recombination will need to be determined, particularly as melphalan-ICL repair may involve homologous recombination, therefore, why STAT3 inhibitors cannot sensitise to melphalan would also need to be investigated further.

7.1.4 Further investigation of the ICL unhooking mechanism

In this thesis, the differences between cisplatin and melphalan ICL repair have begun to be investigated, with the main finding being that the MUS81-EME1 nuclease is required for the efficient unhooking of cisplatin-ICLs but is not involved in melphalan-ICL repair. In addition to the ERCC1-XPF nuclease, which was

demonstrated to not be regulated by STAT3 in this thesis, there are several other nucleases which have been suggested to play a role in the ICL unhooking process.

SNM1A, a 5'-3' exonuclease, is one candidate. SNM1A has been shown to be capable of digesting past an ICL after an initial incision by ERCC1-XPF - described as an "ICL trimming" activity (Sengerová et al., 2011; Wang et al., 2011). This activity could allow for the unhooking of an ICL in the absence of a second incision. However, the issue of different repair pathways for different crosslinks is evident again, as SNM1A knockout cells are sensitive to MMC and SJG-136, but not melphalan or cisplatin (Dronkert et al., 2000; Wang et al., 2011). Therefore, the role for this nuclease and whether it, as well as MUS81-EME1, acts in a lesion-specific manner, must be investigated further.

The Fanconi Anemia associated nuclease (FAN1), which interacts with FANCD2, has also been suggested to harbour ICL trimming activity due to its 5' nuclease action on nicked DNA, as well as a potential role in the initial ICL incision (Sengerová et al., 2011; Smogorzewska et al., 2010). However, the interaction of FAN1 with FANCD2 is not required, and it has been suggested that FAN1 is not involved in ICL repair, but is instead involved in genomic stability following ICL-inducing agents (Lachaud et al., 2016). Additionally, DSBs are able to form after treatment of FAN1-deficient cells with cisplatin, however, this was demonstrated using immunofluorescence staining of γ H2AX foci therefore, this may not correlate directly with DSB induction (MacKay et al., 2010). Therefore, which nucleases are involved in ICL repair for which types of ICL remains to be investigated, and whether SNM1A or FAN1 are regulated by STAT3 must also be determined.

In this thesis, STAT3 inhibitors have been shown to inhibit cisplatin-ICL unhooking, and it was proposed that this is through the down-regulation of the MUS81-EME1 nuclease. The modified comet assay was utilised to observe ICL formation and

repair in these studies. This assay is capable of detecting ICLs up until the point at which they unhook from the DNA double helix. Therefore, any stage of repair prior to ICL unhooking may have been affected by STAT3 inhibition in order to achieve the observed block in ICL unhooking. Therefore, it is possible that STAT3 also influences repair factors further upstream to the ICL incisions. This could include the machinery that initially recognises the ICL for repair.

The recognition of cisplatin and carboplatin ICLs has been reported to require the mismatch repair pathway, whereas oxaliplatin ICLs are not recognised by this machinery (Fink et al., 1998). The fanconi anemia protein, FANCM, has also been suggested to be involved in ICL recognition. Along with its partner protein FAAP24, FANCM is able to bind unwound DNA at an ICL site and bring with it the FA core complex (Niedernhofer, 2007). Cells deficient in FANCM are not capable of ubiquitylating FANCD2 and demonstrate hypersensitivity to MMC (Meetei et al., 2005). The UHRF1 protein was more recently identified as a potential ICL recognition factor due to its ability to directly bind ICL-containing DNA substrates, as well as the ERCC1 and MUS81 nuclease components (Tian et al., 2015), this study was, however, performed using psoralen-induced ICLs, so again the question of agent-specific ICL repair pathways arises.

As the distortions produced by different ICLs are extremely varied, different mechanisms of ICL recognition are likely to exist, in addition to replication-dependent and independent ICL recognition. Whether STAT3 regulates the expression of ICL-recognition factors should be investigated.

Therefore, much remains to be determined regarding ICL repair, but by using STAT3 inhibitors, and understanding which ICL repair proteins STAT3 regulates, the different pathways within ICL repair may begin to emerge.

7.1.5 Clinical relevance of MUS81-EME1

The MUS81-EME1 nuclease has been demonstrated to be essential for the repair of cisplatin-ICLs, however, the relevance of this nuclease in the clinical setting is not yet known. As discussed in Chapter 5, the COSMIC online database indicates that mutations in EME1 and MUS81 do occur, although the functional consequences of these mutations is unknown. Over-expression of these proteins occurs at greater frequency (21.38% of breast cancer tissues for EME1 and 9.4% of ovarian cancer tissues for MUS81) (Forbes et al., 2015). However, whether this overexpression correlates with resistance to cisplatin in patients is yet to be determined.

If expression of MUS81 or EME1 is correlated with response to cisplatin in patients, as ERCC1 has been suggested to (Chiu et al., 2011; Ting et al., 2013), the expression of either component of the MUS81-EME1 nuclease could be developed as a novel biomarker for cisplatin sensitivity. Additionally, patients expressing high levels of MUS81 or EME1 may respond well to cisplatin combined with a STAT3 inhibitor. Therefore, the potential exists to expand on the findings in this thesis regarding the involvement of MUS81-EME1 in cisplatin-ICL repair, in terms of patient response to platinum-based therapy.

Additionally, a compound which targets the MUS81-EME1 nuclease may be of interest for use in patients with particular genetic backgrounds. MUS81-EME1 has been shown to be synthetically lethal with a number of DNA repair factors such as BLM and other RecQ helicases (Trowbridge et al., 2007).

7.2 Final conclusion

This thesis presents a novel STAT3 inhibitor, VS-43, and demonstrates it to have superior potency and selectivity over other STAT3 inhibitors. VS-43 is also able to produce greater synergy in combination with cisplatin than other STAT3 inhibitors. The second finding of this thesis is that the synergy between STAT3 inhibitors and cisplatin is achieved, in part, through the transcriptional regulation of the MUS81-EME1 endonuclease by STAT3. This nuclease is required for the successful unhooking and downstream repair of cisplatin-ICLs; therefore, down-regulation of MUS81-EME1 by inhibition of STAT3 effectively blocks ICL unhooking. Contrastingly, STAT3 inhibitors do not synergise with melphalan, and do not block melphalan-ICL unhooking, as the MUS81-EME1 nuclease is not essential for melphalan-ICL repair. These findings provide a mechanistic basis for the successful combination of STAT3 inhibitors with cisplatin in the clinic, and also highlight the differences between crosslinking chemotherapeutics, which will be useful in determining successful anti-cancer combination therapies.

References

- Abdulghani, J., Gu, L., Dagvadorj, A., Lutz, J., Leiby, B., Bonuccelli, G., Lisanti, M.P., Zellweger, T., Alanen, K., Mirtti, T., Visakorpi, T., Bubendorf, L., Nevalainen, M.T., 2008. Stat3 promotes metastatic progression of prostate cancer. *Am. J. Pathol.* 172, 1717–28. doi:10.2353/ajpath.2008.071054
- Abraham, J., Lemmers, B., Hande, M.P., Moynahan, M.E., Chahwan, C., Ciccia, A., Essers, J., Hanada, K., Chahwan, R., Khaw, A.K., McPherson, P., Shehabeldin, A., Laister, R., Arrowsmith, C., Kanaar, R., West, S.C., Jasin, M., Hakem, R., 2003. Eme1 is involved in DNA damage processing and maintenance of genomic stability in mammalian cells. *EMBO J.* 22, 6137–47. doi:10.1093/emboj/cdg580
- Abuzeid, W.M., Davis, S., Tang, A., Saunders, L., Chadwick, J., Lin, J., Fuchs, J.R., Light, E., Bradford, C.R., Mark, E.P., Carey, T.E., 2011. Sensitization of head and neck cancer to cisplatin through the use of a novel curcumin analogue. *Arch Otolaryngol Head Neck Surg.* 137, 499–507. doi:10.1001/archoto.2011.63.Sensitization
- Adams, B.K., Ferstl, E.M., Davis, M.C., Herold, M., Kurtkaya, S., Camalier, R.F., Hollingshead, M.G., Kaur, G., Sausville, E.A., Rickles, F.R., Snyder, J.P., Liotta, D.C., Shoji, M., 2004. Synthesis and biological evaluation of novel curcumin analogs as anti-cancer and anti-angiogenesis agents. *Bioorganic Med. Chem.* 12, 3871–3883. doi:10.1016/j.bmc.2004.05.006
- Adams, G.P., Weiner, L.M., 2005. Monoclonal antibody therapy of cancer. *Nat. Biotechnol.* 23, 1147–57. doi:10.1038/nbt1137
- Aggarwal, B.B., Sethi, G., Ahn, K.S., Sandur, S.K., Pandey, M.K., Kunnumakkara, A.B., Sung, B., Ichikawa, H., 2006. Targeting signal-transducer-and-activator-of-transcription-3 for prevention and therapy of cancer: modern target but ancient solution. *Ann. N. Y. Acad. Sci.* 1091, 151–69. doi:10.1196/annals.1378.063
- Aggarwal, B.B., Shishodia, S., Takada, Y., Banerjee, S., Newman, R.A., Bueso-

- Ramos, C.E., Price, J.E., 2005. Curcumin suppresses the paclitaxel-induced nuclear factor-kB pathway in breast cancer cells and inhibits lung metastasis of human breast cancer in nude mice. *Clin. Cancer Res.* 11, 7490–7498. doi:10.1158/1078-0432.CCR-05-1192
- Ahmad, A.S., Ormiston-Smith, N., Sasieni, P.D., 2015. Trends in the lifetime risk of developing cancer in Great Britain: comparison of risk for those born from 1930 to 1960. *Br. J. Cancer* 112, 943–7. doi:10.1038/bjc.2014.606
- Akira, S., 1999. Functional Roles of STAT Family Proteins : Lessons from Knockout Mice. *Stem Cells* 17, 138–146.
- Al-Minawi, A.Z., Lee, Y.F., Hakansson, D., Johansson, F., Lundin, C., Saleh-Gohari, N., Schultz, N., Jenssen, D., Bryant, H.E., Meuth, M., Hinz, J.M., Helleday, T., 2009. The ERCC1/XPF endonuclease is required for completion of homologous recombination at DNA replication forks stalled by inter-strand cross-links. *Nucleic Acids Res.* 37, 6400–6413. doi:10.1093/nar/gkp705
- Ali-Osman, F., Berger, M.S., Rajagopal, S., 1993. Topoisomerase II Inhibition and Altered Kinetics of Formation and Repair of Nitrosourea and Cisplatin-induced DNA Interstrand Cross-Links and Cytotoxicity in Human Glioblastoma Cells Topoisomerase II Inhibition and Altered Kinetics of Formation and Repair. *Cancer Res.* 5663–5668.
- Allgayer, H., Boyd, D.D., Heiss, M.M., Abdalla, E.K., Curley, S.A., Gallick, G.E., 2002. Activation of src kinase in primary colorectal carcinoma: An indicator of poor clinical prognosis. *Cancer* 94, 344–351. doi:10.1002/cncr.10221
- Alvarez, J. V, Greulich, H., Sellers, W.R., Meyerson, M., Frank, D. a, 2006. Signal transducer and activator of transcription 3 is required for the oncogenic effects of non-small-cell lung cancer-associated mutations of the epidermal growth factor receptor. *Cancer Res.* 66, 3162–8. doi:10.1158/0008-5472.CAN-05-3757
- American Cancer Society, 2015. *Global Cancer Facts & Figures 3rd Edition*. Am. Cancer Soc. 1–64. doi:10.1002/ijc.27711
- Ampasavate, C., Sotanaphun, U., Phattanawasin, P., Piyapolrunroj, N., 2010.

Effects of Curcuma spp. on P-glycoprotein function. *Phytomedicine* 17, 506–12. doi:10.1016/j.phymed.2009.09.004

Anand, P., Kunnumakkara, A.B., Newman, R.A., Aggarwal, B.B., 2007. Bioavailability of Curcumin : Problems and Promises. *Mol. Pharm.* 4, 807–818.

Andersson, B.S., Sadeghi, T., Siciliano, M.J., Legerski, R., Murray, D., 1996. Nucleotide excision repair genes as determinants of cellular sensitivity to cyclophosphamide analogs. *Cancer Chemother. Pharmacol.* 38, 406–16. doi:10.1007/s002800050504

Andrews, P., Velury, S., Mann, S., et al, 1988. Cis-Diamminedichloroplatinum (II) accumulation in sensitive and resistant human ovarian carcinoma cells. *Cancer Res* 48, 68–73.

Anuchapreeda, S., Leechanachai, P., Smith, M.M., Ambudkar, S. V., Limtrakul, P. ngarm, 2002. Modulation of P-glycoprotein expression and function by curcumin in multidrug-resistant human KB cells. *Biochem. Pharmacol.* 64, 573–582. doi:10.1016/S0006-2952(02)01224-8

Aoki, Y., Feldman, G.M., Tosato, G., 2003. Inhibition of STAT3 signaling induces apoptosis and decreases survivin expression in primary effusion lymphoma 101, 1535–1542. doi:10.1182/blood-2002-07-2130.BLOOD

Arulanandam, R., Vultur, A., Cao, J., Carefoot, E., Elliott, B.E., Truesdell, P.F., Larue, L., Feracci, H., Raptis, L., 2009. Cadherin-cadherin engagement promotes cell survival via Rac1/Cdc42 and signal transducer and activator of transcription-3. *Mol. Cancer Res.* 7, 1310–1327. doi:10.1158/1541-7786.MCR-08-0469

Bai, F., Nakanishi, Y., Kawasaki, M., Takayama, K., Yatsunami, J., Pei, X.H., Tsuruta, N., Wakamatsu, K., Hara, N., 1996. Immunohistochemical expression of glutathione S-transferase-Pi can predict chemotherapy response in patients with nonsmall cell lung carcinoma. *Cancer* 78, 416–421. doi:10.1002/(SICI)1097-0142(19960801)78:3<416::AID-CNCR6>3.0.CO;2-H [pii]r10.1002/(SICI)1097-0142(19960801)78:3<416::AID-CNCR6>3.0.CO;2-H

- Balmaña, J., Tung, N.M., Isakoff, S.J., Graña, B., Ryan, P.D., Saura, C., Lowe, E.S., Frewer, P., Winer, E., Baselga, J., Garber, J.E., 2014. Phase I trial of olaparib in combination with cisplatin for the treatment of patients with advanced breast, ovarian and other solid tumors. *Ann. Oncol.* 171–178. doi:10.1093/annonc/mdu187
- Barnouin, K., Leier, I., Jedlitschky, G., König, J., Lehmann, W., Keppler, D., 1998. Multidrug resistance protein-mediated transport of chlorambucil and melphalan conjugated to glutathione 77, 201–209.
- Barry, S.P., Townsend, P. a, Knight, R. a, Scarabelli, T.M., Latchman, D.S., Stephanou, A., 2010. STAT3 modulates the DNA damage response pathway. *Int. J. Exp. Pathol.* 91, 506–14. doi:10.1111/j.1365-2613.2010.00734.x
- Bartek, J., Lukas, J., 2011. Cyclin D1 multitasks. *Nature* 474, 0–1.
- Barton, B.E., Karras, J.G., Murphy, T.F., Barton, A., 2004. Signal transducer and activator of transcription 3 (STAT3) activation in prostate cancer: Direct STAT3 inhibition induces apoptosis in prostate cancer lines activation in prostate cancer: Direct STAT3 inhibition induces apoptosis in prostate cancer li 3, 11–20.
- Bassing, C., Swat, W., Alt, F., 2002. The mechanism and regulation of chromosomal V (D) J recombination. *Cell* 109, 45–55.
- Basu, A., Krishnamurthy, S., 2010. Cellular responses to Cisplatin-induced DNA damage. *J. Nucleic Acids* 2010. doi:10.4061/2010/201367
- Bauer, G.B., Povirk, L.F., 1997. Specificity and kinetics of interstrand and intrastrand bifunctional alkylation by nitrogen mustards at a G-G-C sequence. *Nucleic Acids Res.* 25, 1211–1218. doi:10.1093/nar/25.6.1211
- Baxter, J.E., Scott, L.M., Campbell, P.J., East, C., Fourouclas, N., Swanton, S., Vassiliou, G.S., Bench, A.J., Boyd, E.M., Curtin, N., Scott, M.A., Erber, W.N., Cancer Genome Project, T., Green, A.R., 2005. Acquired mutation of the tyrosine kinase JAK2 in human myeloproliferative disorders. *Lancet* 365, 1054–1061. doi:10.1016/S0140-6736(05)71142-9

- Becker, S., Groner, B., Muller, C.W., 1998. Three-dimensional structure of the Stat3beta homodimer bound to DNA. *Nature* 394, 145–151. doi:10.1038/28101
- Benekli, M., 2002. Constitutive activity of signal transducer and activator of transcription 3 protein in acute myeloid leukemia blasts is associated with short disease-free survival. *Blood* 99, 252–257. doi:10.1182/blood.V99.1.252
- Benhar, M., Engelberg, D., Levitzki, A., 2002. Cisplatin-induced activation of the EGF receptor. *Oncogene* 21, 8723–31. doi:10.1038/sj.onc.1205980
- Benitez, A., Yuan, F., Nakajima, S., Wei, L., Qian, L., Myers, R., Hu, J.J., Lan, L., Zhang, Y., 2014. Damage-dependent regulation of MUS81-EME1 by Fanconi anemia complementation group A protein. *Nucleic Acids Res.* 42, 1671–83. doi:10.1093/nar/gkt975
- Bensch, K.G., Malawista, S.E., 1968. Microtubule Crystals: A New Biophysical Phenomenon induced by Vinca Alkaloids. *Nature* 218, 1176–1177. doi:10.1038/222385a0
- Berardini, M., Mackay, W., Loechler, E.L., 1997. Evidence for a recombination-independent pathway for the repair of DNA interstrand cross-links based on a site-specific study with nitrogen mustard. *Biochemistry* 36, 3506–13. doi:10.1021/bi962778w
- Bergel, F., Stock, J.A., 1954. Cyto-active Amino-acid and Peptide Derivatives. *J. Chem. Soc.* 2409–2417.
- Bernstein, C., Prasad, A.R., Nfonsam, V., Bernstein, H., 2013. DNA Damage , DNA Repair and Cancer. *New Res. Dir. DNA Repair* 413–466. doi:10.5772/53919
- Bertino, J.R., 2009. Cancer research: from folate antagonism to molecular targets. *Best Pract. Res. Clin. Haematol.* 22, 577–582. doi:10.1016/j.beha.2009.09.004
- Bhagwat, N., Olsen, A.L., Wang, A.T., Hanada, K., Stuckert, P., Kanaar, R., D'Andrea, A., Niedernhofer, L.J., McHugh, P.J., 2009. XPF-ERCC1 participates in the Fanconi anemia pathway of cross-link repair. *Mol. Cell. Biol.* 29, 6427–37. doi:10.1128/MCB.00086-09

- Bharti, A., Donato, N., Aggarwal, B.B., 2003a. Curcumin (diferuloylmethane) inhibits constitutive and IL-6-inducible STAT3 phosphorylation in human multiple myeloma cells. *J. Immunol.* 171, 3863–71.
- Bharti, A., Donato, N., Singh, S., Aggarwal, B.B., 2003b. Curcumin (diferuloylmethane) down-regulates the constitutive activation of nuclear factor- κ B and I κ B α kinase in human multiple myeloma cells, leading to suppression of proliferation and induction. *Blood* 101, 1053–1062. doi:10.1182/blood-2002-05-1320.Supported
- Bhattacharyya, A., Ear, U.S., Koller, B.H., Weichselbaum, R.R., Bishop, D.K., 2000. The Breast Cancer susceptibility gene BRCA1 is required for subnuclear assembly of Rad51 and survival following treatment with the DNA cross-linking agent cisplatin. *J. Biol. Chem.* 275, 23899–23903. doi:10.1074/jbc.C000276200
- Bijnsdorp, I. V, Giovannetti, E., Peters, G.J., 2011. Analysis of Drug Interactions. *Cancer Cell Cult. Methods Protoc. Second Ed. Methods Mol. Biol., Methods in Molecular Biology* 731, 421–434. doi:10.1007/978-1-61779-080-5
- Bill, M.A., Bakan, C., Benson, D.M., Fuchs, J., Young, G., Lesinski, G.B., 2009. Curcumin induces proapoptotic effects against human melanoma cells and modulates the cellular response to immunotherapeutic cytokines. *Mol. Cancer Ther.* 8, 2726–35. doi:10.1158/1535-7163.MCT-09-0377
- Bill, M.A., Nicholas, C., Mace, T.A., Etter, J.P., Li, C., Schwartz, E.B., Fuchs, J.R., Young, G.S., Lin, L., Lin, J., He, L., Phelps, M., Li, P.-K., Lesinski, G.B., 2012. Structurally modified curcumin analogs inhibit STAT3 phosphorylation and promote apoptosis of human renal cell carcinoma and melanoma cell lines. *PLoS One* 7, e40724. doi:10.1371/journal.pone.0040724
- Blair, B.G., Larson, C., Safaei, R., Howell, S.B., 2009. Copper transporter 2 regulates the cellular accumulation and cytotoxicity of cisplatin and carboplatin. *Clin. Cancer Res.* 15, 4312–4321. doi:10.1158/1078-0432.CCR-09-0311
- Blasco, M.A., 2005. Telomeres and human disease: ageing, cancer and beyond. *Nat Rev Genet* 6, 611–622. doi:10.1038/nrg1656

- Borghouts, C., Delis, N., Brill, B., Weiss, A., Mack, L., Lucks, P., Groner, B., 2012. A membrane penetrating peptide aptamer inhibits STAT3 function and suppresses the growth of STAT3 addicted tumor cells. *JAKSTAT* 1, 44–52.
- Borriello, a, Locasciulli, a, Bianco, a M., Criscuolo, M., Conti, V., Grammatico, P., Cappellacci, S., Zatterale, a, Morgese, F., Cucciolla, V., Delia, D., Della Ragione, F., Savoia, a, 2007. A novel Leu153Ser mutation of the Fanconi anemia FANCD2 gene is associated with severe chemotherapy toxicity in a pediatric T-cell acute lymphoblastic leukemia. *Leukemia* 21, 72–8. doi:10.1038/sj.leu.2404468
- Borst, P., Rottenberg, S., Jonkers, J., 2008. How do real tumors become resistant to cisplatin? *Cell cycle* 7:10bor, 1353–1359.
- Bowman, T., Garcia, R., Turkson, J., Jove, R., 2000. STATs in oncogenesis. *Oncogene* 19, 2474–88. doi:10.1038/sj.onc.1203527
- Brabec, V., Síp, M., Leng, M., 1993. DNA conformational change produced by the site-specific interstrand cross-link of trans-diamminedichloroplatinum(II). *Biochemistry* 32, 11676–81. doi:10.1021/bi00094a025
- Brady, C. a, Attardi, L.D., 2010. P53 At a Glance. *J. Cell Sci.* 123, 2527–32. doi:10.1242/jcs.064501
- Bramson, J., McQuillan, A., Aubin, R., Alaoui-Jamali, M., Batist, G., Christodouloupoulos, G., Panasci, L.C., 1995. Nitrogen mustard drug resistant B-cell chronic lymphocytic leukemia as an in vivo model for crosslinking agent resistance. *Mutat Res* 336, 269–278.
- Brandvold, K., Steffey, M., 2012. Development of a highly selective c-Src kinase inhibitor. *ACS Chem. ...* 7, 1393–1398. doi:10.1021/cb300172e.Development
- Branham, M.T., Nadin, S.B., Vargas-Roig, L.M., Ciocca, D.R., 2004. DNA damage induced by paclitaxel and DNA repair capability of peripheral blood lymphocytes as evaluated by the alkaline comet assay. *Mutat. Res. - Genet. Toxicol. Environ. Mutagen.* 560, 11–17. doi:10.1016/j.mrgentox.2004.01.013

- Bromberg, J.F., 2001. Activation of STAT proteins and growth control. *BioEssays* 23, 161–169. doi:10.1002/1521-1878(200102)23:2<161::AID-BIES1023>3.0.CO;2-0
- Bromberg, J.F., Horvath, C.M., Besser, D., Lathem, W.W., Darnell, J.E., 1998. Stat3 activation is required for cellular transformation by v-src. *Mol. Cell. Biol.* 18, 2553–8.
- Bromberg, J.F., Wrzeszczynska, M.H., Devgan, G., Zhao, Y., Pestell, R.G., Albanese, C., Darnell, J.E., 1999. Stat3 as an oncogene. *Cell* 98, 295–303.
- Brussel, J.P. Van, Steenbrugge, G.J. Van, Romijn, J.C., Schro, F.H., Mickisch, G.H.J., 1999. Chemosensitivity of Prostate Cancer Cell Lines and Expression of Multidrug Resistance-related Proteins. *Eur. J. Cancer* 35, 664–671.
- Bruun, D., Folias, A., Akkari, Y., Cox, Y., Olson, S., Moses, R., 2003. siRNA depletion of BRCA1, but not BRCA2, causes increased genome instability in Fanconi anemia cells. *DNA Repair (Amst)*. 2, 1007–1013. doi:10.1016/S1568-7864(03)00112-5
- Buettner, R., Mora, L.B., Jove, R., 2002. Activated STAT Signaling in Human Tumors Provides Novel Molecular Targets for Therapeutic Intervention
Activated STAT Signaling in Human Tumors Provides Novel Molecular Targets for Therapeutic Intervention 1 945–954.
- Bunting, S.F., Callen, E., Kozak, M.L., Kim, J.M., Wong, N., Lopez-contreras, A.J., Ludwig, T., Baer, R., Faryabi, R.B., Chen, H., Fernandez-capetillo, O., Andrea, A.D., 2012. BRCA1 functions independently of homologous recombination in DNA interstrand cross-link repair. *Mol Cell* 46, 125–135. doi:10.1016/j.molcel.2012.02.015.BRCA1
- Burkitt, K., Ljungman, M., 2007. Compromised Fanconi anemia response due to BRCA1 deficiency in cisplatin-sensitive head and neck cancer cell lines. *Cancer Lett.* 253, 131–7. doi:10.1016/j.canlet.2007.01.017
- Byers, L.A., Sen, B., Saigal, B., Diao, L., Wang, J., Cascone, T., Mills, G.B., Heymach, J. V, Faye, M., 2009. Reciprocal regulation of c-Src and STAT3 in

non-small cell lung cancer Lauren. *Clin. Cancer Res.* 15, 6852–6861. doi:10.1158/1078-0432.CCR-09-0767.Reciprocal

Byun, S.S., Kim, S.W., Choi, H., Lee, C., Lee, E., 2005. Augmentation of cisplatin sensitivity in cisplatin-resistant human bladder cancer cells by modulating glutathione concentrations and glutathione-related enzyme activities. *BJU Int.* 95, 1086–1090. doi:10.1111/j.1464-410X.2005.05472.x

Cao, X., Tay, a, Guy, G.R., Tan, Y.H., 1996. Activation and association of Stat3 with Src in v-Src-transformed cell lines. *Mol. Cell. Biol.* 16, 1595–1603.

Carpenter, A.E., Jones, T.R., Lamprecht, M.R., Clarke, C., Kang, I.H., Friman, O., Guertin, D. a, Chang, J.H., Lindquist, R. a, Moffat, J., Golland, P., Sabatini, D.M., 2006. CellProfiler: image analysis software for identifying and quantifying cell phenotypes. *Genome Biol.* 7, R100. doi:10.1186/gb-2006-7-10-r100

Catlett-Falcone, R., Landowski, T.H., Oshiro, M.M., Turkson, J., Levitzki, a, Savino, R., Ciliberto, G., Moscinski, L., Fernández-Luna, J.L., Nuñez, G., Dalton, W.S., Jove, R., 1999. Constitutive activation of Stat3 signaling confers resistance to apoptosis in human U266 myeloma cells. *Immunity* 10, 105–115. doi:10.1016/s1074-7613(00)80011-4

Chabner, B. a, Roberts, T.G., 2005. Timeline: Chemotherapy and the war on cancer. *Nat. Rev. Cancer* 5, 65–72. doi:10.1038/nrc1529

Chaitanya, G.V., Steven, A.J., Babu, P.P., 2010. PARP-1 cleavage fragments: signatures of cell-death proteases in neurodegeneration. *Cell Commun. Signal.* 8, 31. doi:10.1186/1478-811X-8-31

Chang, A., 2011. Chemotherapy, chemoresistance and the changing treatment landscape for NSCLC. *Lung Cancer* 71, 3–10. doi:10.1016/j.lungcan.2010.08.022

Chen, C.-L., Hsieh, F.-C., Lieblein, J.C., Brown, J., Chan, C., Wallace, J.A., Cheng, G., Hall, B.M., Lin, J., 2007. Stat3 activation in human endometrial and cervical cancers. *Br. J. Cancer* 96, 591–9. doi:10.1038/sj.bjc.6603597

- Chen, J., Lan, T., Zhang, W., Dong, L., Kang, N., Fu, M., Liu, B., Liu, K., Zhang, C., Hou, J., Zhan, Q., 2015. Dasatinib enhances cisplatin sensitivity in human esophageal squamous cell carcinoma (ESCC) cells via suppression of PI3K/AKT and Stat3 pathways. *Arch. Biochem. Biophys.* 575, 38–45. doi:10.1016/j.abb.2014.11.008
- Chen, P., Li, J., Jiang, H.G., Lan, T., Chen, Y.C., 2015. Curcumin reverses cisplatin resistance in cisplatin-resistant lung cancer cells by inhibiting FA/BRCA pathway. *Tumor Biol.* 36, 3591–3599. doi:10.1007/s13277-014-2996-4
- Chen, Q., Sluis, P.C. Van Der, Boulware, D., Hazlehurst, L. a, Dalton, W.S., 2005. The FA / BRCA pathway is involved in melphalan-induced DNA interstrand cross-link repair and accounts for melphalan resistance in multiple myeloma cells. *Mol. Imaging* 106, 698–705. doi:10.1182/blood-2004-11-4286
- Cheng, Y., Holloway, M.P., Nguyen, K., McCauley, D., Landesman, Y., Kauffman, Michael G., Shacham, S., Altura, R.A., 2014. XPO1 (CRM1) inhibition represses STAT3 activation to drive a survivin-dependent oncogenic switch in triple negative breast cancer. *Mol. Cancer Ther.* 13, 675–686. doi:10.3851/IMP2701.Changes
- Chin, Y.E., Kitagawa, M., Su, W.-C.S., You, Z.-H., Iwamoto, Y., Fu, X.-Y., 1996. Cell growth arrest and induction of cyclin-dependent kinase inhibitor p21WAF1/CIP1 mediated by STAT1. *Science* 272, 719–722.
- Chirnomas, D., Taniguchi, T., de la Vega, M., Vaidya, A.P., Vasserman, M., Hartman, A.-R., Kennedy, R., Foster, R., Mahoney, J., Seiden, M. V, D’Andrea, A.D., 2006. Chemosensitization to cisplatin by inhibitors of the Fanconi anemia/BRCA pathway. *Mol. Cancer Ther.* 5, 952–61. doi:10.1158/1535-7163.MCT-05-0493
- Chiu, T.-J., Chen, C.-H., Chien, C.-Y., Li, S.-H., Tsai, H.-T., Chen, Y.-J., 2011. High ERCC1 expression predicts cisplatin-based chemotherapy resistance and poor outcome in unresectable squamous cell carcinoma of head and neck in a betel-chewing area. *J. Transl. Med.* 9, 31. doi:10.1186/1479-5876-9-31
- Chiu Li, M., Hertz, R., Bergenstal, D.M., 1958. Therapy of Choriocarcinoma and

related Trophoblastic tumours with folic acid and purine antagonists. *N. Engl. J. Med.* 259, 66–74.

Choi, H.J., Han, J.S., 2012. Overexpression of phospholipase D enhances Bcl-2 expression by activating STAT3 through independent activation of ERK and p38MAPK in HeLa cells. *Biochim. Biophys. Acta - Mol. Cell Res.* 1823, 1082–1091. doi:10.1016/j.bbamcr.2012.03.015

Chou, T., 2006. Theoretical Basis , Experimental Design , and Computerized Simulation of Synergism and Antagonism in Drug Combination Studies. *Pharmacol. Rev.* 58, 621–681. doi:10.1124/pr.58.3.10.

Chou, T.-C., 2010. Drug combination studies and their synergy quantification using the Chou-Talalay method. *Cancer Res.* 70, 440–6. doi:10.1158/0008-5472.CAN-09-1947

Ciardiello, F., Tortora, G., 2008. EGFR antagonists in cancer treatment. *N. Engl. J. Med.* 358, 1160–74. doi:10.1056/NEJMra0707704

Ciccia, A., Constantinou, A., West, S.C., 2003. Identification and characterization of the human mus81-eme1 endonuclease. *J. Biol. Chem.* 278, 25172–25178. doi:10.1074/jbc.M302882200

Cimica, V., Chen, H.-C., Iyer, J.K., Reich, N.C., 2011. Dynamics of the STAT3 transcription factor: nuclear import dependent on Ran and importin-β1. *PLoS One* 6, e20188. doi:10.1371/journal.pone.0020188

Cipolla, L., Maffia, A., Bertolotti, F., Sabbioneda, S., 2016. The Regulation of DNA Damage Tolerance by Ubiquitin and Ubiquitin-Like Modifiers. *Front. Genet.* 7, 1–12. doi:10.3389/fgene.2016.00105

Clauson, C., Scha, O.D., Niedernhofer, L., 2013. Advances in Understanding the Complex Mechanisms of DNA Interstrand Cross-Link Repair. *Cold Spring Harb. Perspect. Biol.* 5, 1–25.

Clevenger, C. V, 2004. Roles and regulation of stat family transcription factors in human breast cancer. *Am. J. Pathol.* 165, 1449–60. doi:10.1016/S0002-

Clingen, P.H., De Silva, I.U., McHugh, P.J., Ghadessy, F.J., Tilby, M.J., Thurston, D.E., Hartley, J. a., 2005. The XPF-ERCC1 endonuclease and homologous recombination contribute to the repair of minor groove DNA interstrand crosslinks in mammalian cells produced by the pyrrolo[2,1-c][1,4]benzodiazepine dimer SJG-136. *Nucleic Acids Res.* 33, 3283–3291. doi:10.1093/nar/gki639

Clingen, P.H., Wu, J.Y.-H., Miller, J., Mistry, N., Chin, F., Wynne, P., Prise, K.M., Hartley, J. a, 2008. Histone H2AX phosphorylation as a molecular pharmacological marker for DNA interstrand crosslink cancer chemotherapy. *Biochem. Pharmacol.* 76, 19–27. doi:10.1016/j.bcp.2008.03.025

Cobo, M., Isla, D., Massuti, B., Montes, A., Sanchez, J.M., Provencio, M., Vinolas, N., Paz-Ares, L., Lopez-Vivanco, G., Munoz, M.A., Felip, E., Alberola, V., Camps, C., Domine, M., Sanchez, J.J., Sanchez-Ronco, M., Danenberg, K., Taron, M., Gandara, D., Rosell, R., 2007. Customizing cisplatin based on quantitative excision repair cross-complementing 1 mRNA expression: A phase III trial in non-small-cell lung cancer. *J. Clin. Oncol.* 25, 2747–2754. doi:10.1200/JCO.2006.09.7915

Cole, R.S., 1973. Repair of DNA Containing Interstrand Crosslinks 70, 1064–1068.

Cole, R.S., Levitan, D., Sinden, R.R., 1976. Removal of psoralen interstrand crosslinks from DNA of *Escherichia coli*: mechanism and genetic control. *J. Mol. Biol.* 103, 39–59.

Collins, A.R., 2004. The Comet Assay for DNA Damage and Repair. *Mol. Biotechnol.* 26.

Colvin, M., Kufe, D., Pollock, R., Weichselbaum, R., 2003. *Alkylating Agents, Cancer Medicine.* 6th edition.

Comerford, K.M., Wallace, T.J., Karhausen, J., Gene, M.D.R., Louis, N.A., Montalto, M.C., Colgan, S.P., 2002. Hypoxia-inducible Factor-1-dependent Regulation of the Multidrug Resistance (MDR1) Gene Hypoxia-inducible Factor-1-dependent

Regulation of the Multidrug Resistance. *Cancer Res.* 62, 3387–3394.

Consortium, T.B.C.L., 1999. Cancer risks in BRCA2 mutation carriers. *JNCI J. Natl. Cancer Inst.* 91, 1310–6. doi:10.1093/jnci/91.15.1310

Cortas, T., Eisenberg, R., Fu, P., Kern, J., Patrick, L., Dowlati, A., 2007. Activation state EGFR and STAT-3 as prognostic markers in resected non-small cell lung cancer. *Lung Cancer* 55, 349–355. doi:10.1016/j.lungcan.2006.11.003

Coste, F., Malinge, J.M., Serre, L., Shepard, W., Roth, M., Leng, M., Zelwer, C., 1999. Crystal structure of a double-stranded DNA containing a cisplatin interstrand cross-link at 1.63 Å resolution: hydration at the platinated site. *Nucleic Acids Res.* 27, 1837–46.

Couto, J.I., Bear, M.D., Lin, J., Pennel, M., Kulp, S.K., Kisseberth, W.C., London, C. a, 2012. Biologic activity of the novel small molecule STAT3 inhibitor LLL12 against canine osteosarcoma cell lines. *BMC Vet. Res.* 8, 244. doi:10.1186/1746-6148-8-244

Crick, F., 1970. Central dogma of molecular biology. *Nature* 227, 561–563. doi:10.1038/227561a0

Crossan, G.P., Patel, K.J., 2012. The Fanconi anaemia pathway orchestrates incisions at sites of crosslinked DNA. *J. Pathol.* 226, 326–37. doi:10.1002/path.3002

Cui, Y., König, J., Buchholz, J.K., Spring, H., Leier, I., Keppler, D., 1999. Drug resistance and ATP-dependent conjugate transport mediated by the apical multidrug resistance protein, MRP2, permanently expressed in human and canine cells. *Mol. Pharmacol.* 55, 929–937.

Cullen, K.J., Newkirk, K.A., Schumaker, L.M., Haddad, B.R., 2003. Glutathione S - Transferase π Amplification is Associated with Cisplatin Resistance in Head and Neck Squamous Cell Carcinoma Cell Lines and Primary Tumors Advances in Brief in Head and Neck Squamous Cell Carcinoma Cell Lines and Primary Tumors 8097–8102.

- Cunningham, F.H., Fiebelkorn, S., Johnson, M., Meredith, C., 2011. A novel application of the Margin of Exposure approach: Segregation of tobacco smoke toxicants. *Food Chem. Toxicol.* 49, 2921–2933. doi:10.1016/j.fct.2011.07.019
- Dabholkar, M., Bostick-Bruton, F., Weber, C., Bohr, V. a, Egwuagu, C., Reed, E., 1992. ERCC1 and ERCC2 expression in malignant tissues from ovarian cancer patients. *J. Natl. Cancer Inst.* 84, 1512–1517. doi:10.1093/jnci/84.19.1512
- Dai, C.-H., Li, J., Chen, P., Jiang, H.-G., Wu, M., Chen, Y.-C., 2015. RNA interferences targeting the Fanconi anemia/BRCA pathway upstream genes reverse cisplatin resistance in drug-resistant lung cancer cells. *J. Biomed. Sci.* 22, 77. doi:10.1186/s12929-015-0185-4
- Dang, C. V., 2012. Links between metabolism and cancer. *Genes Dev.* 26, 877–890. doi:10.1101/gad.189365.112
- Davar, D., Beumer, J.H., Hamieh, L., Tawbi, H., 2012. Role of PARP inhibitors in cancer biology and therapy. *Curr. Med. Chem.* 19, 3907–21. doi:10.1016/j.biotechadv.2011.08.021.Secreted
- Davies, M.A., Samuels, Y., 2010. Analysis of the genome to personalize therapy for melanoma. *Oncogene* 29, 5545–55. doi:10.1038/onc.2010.323
- Davis, R., Das, U., Mackay, H., Brown, T., Mooberry, S.L., Dimmock, J.R., Lee, M., Pati, H., 2008. Syntheses and cytotoxic properties of the curcumin analogs 2,6-bis(benzylidene)-4-phenylcyclohexanones. *Arch. Pharm. (Weinheim)*. 341, 440–445. doi:10.1002/ardp.200800028
- De Silva, I.U., McHugh, P.J., Clingen, P.H., Hartley, J. a, 2002. Defects in interstrand cross-link uncoupling do not account for the extreme sensitivity of ERCC1 and XPF cells to cisplatin. *Nucleic Acids Res.* 30, 3848–3856. doi:10.1093/nar/gkf479
- De Silva, I.U., McHugh, P.J., Clingen, P.H., Hartley, J. a, 2000. Defining the roles of nucleotide excision repair and recombination in the repair of DNA interstrand cross-links in mammalian cells. *Mol. Cell. Biol.* 20, 7980–90.

- de Winter, J.P., Joenje, H., 2009. The genetic and molecular basis of Fanconi anemia. *Mutat. Res.* 668, 11–9. doi:10.1016/j.mrfmmm.2008.11.004
- Dechow, T.N., Pedranzini, L., Leitch, A., Leslie, K., Gerald, W.L., Linkov, I., Bromberg, J.F., 2004. Requirement of matrix metalloproteinase-9 for the transformation of human mammary epithelial cells by Stat3-C. *Proc. Natl. Acad. Sci. U. S. A.* 101, 10602–7. doi:10.1073/pnas.0404100101
- Dempke, W., Voigt, W., Grothey, A., Hill, B.T., Schmoll, H., Saale, H., Centre, G., Pierre, D.R., Moulin, J., 2000. Cisplatin resistance and oncogenes-a review. *Anticancer. Drugs* 11, 225–236.
- Dendouga, N., Gao, H., Moechars, D., Janicot, M., Vialard, J., McGowan, C.H., 2005. Disruption of murine Mus81 increases genomic instability and DNA damage sensitivity but does not promote tumorigenesis. *Mol. Cell. Biol.* 25, 7569–79. doi:10.1128/MCB.25.17.7569-7579.2005
- Desoize, B., Madoulet, C., 2002. Particular aspects of platinum compounds used at present in cancer treatment. *Crit. Rev. Oncol. Hematol.* 42, 317–325. doi:10.1016/S1040-8428(01)00219-0
- DeVita, V.T., Chu, E., 2008. A history of cancer chemotherapy. *Cancer Res.* 68, 8643–8653. doi:10.1158/0008-5472.CAN-07-6611
- Dhandapani, K.M., Mahesh, V.B., Brann, D.W., 2007. Curcumin suppresses growth and chemoresistance of human glioblastoma cells via AP-1 and NFkappaB transcription factors. *J. Neurochem.* 102, 522–38. doi:10.1111/j.1471-4159.2007.04633.x
- Dimco, G., Knight, R.A., Latchman, D.S., Stephanou, A., 2010. STAT1 interacts directly with cyclin D1/Cdk4 and mediates cell cycle arrest. *Cell Cycle* 9, 4638–4649. doi:10.4161/cc.9.23.13955
- Don-Doncow, N., Escobar, Z., Johansson, M., Kjellstrom, S., Garcia, V., Munoz, E., Sterner, O., Bjartell, A., Hellsten, R., 2014. Galiellalactone is a direct inhibitor of the transcription factor STAT3 in prostate cancer cells. *J. Biol. Chem.* 289, 15969–15978. doi:10.1074/jbc.M114.564252

- Dong, H., Nebert, D.W., Bruford, E.A., Thompson, D.C., Joenje, H., Vasiliou, V., 2015. Update of the human and mouse Fanconi anemia genes. *Hum. Genomics* 9, 32. doi:10.1186/s40246-015-0054-y
- Dronkert, M.L., de Wit, J., Boeve, M., Vasconcelos, M.L., van Steeg, H., Tan, T.L., Hoeijmakers, J.H., Kanaar, R., 2000. Disruption of mouse SNM1 causes increased sensitivity to the DNA interstrand cross-linking agent mitomycin C. *Mol. Cell. Biol.* 20, 4553–61. doi:10.1128/MCB.20.13.4553-4561.2000
- Drummond, D.C., Noble, C.O., Guo, Z., Hong, K., Park, J.W., Kirpotin, D.B., 2006. Development of a highly active nanoliposomal irinotecan using a novel intraliposomal stabilization strategy. *Cancer Res.* 66, 3271–3277. doi:10.1158/0008-5472.CAN-05-4007
- Eckstein, N., 2011. Platinum resistance in breast and ovarian cancer cell lines. *J. Exp. Clin. Cancer Res.* 30, 91. doi:10.1186/1756-9966-30-91
- Engers, R., Ziegler, S., Mueller, M., Walter, A., Willers, R., Gabbert, H.E., 2007. Prognostic relevance of increased Rac GTPase expression in prostate carcinomas. *Endocr. Relat. Cancer* 14, 245–256. doi:10.1677/ERC-06-0036
- Epling-Burnette, P.K., Liu, J.H., Catlett-Falcone, R., Turkson, J., Oshiro, M., Kothapalli, R., Li, Y., Wang, J.M., Yang-Yen, H.F., Karras, J., Jove, R., Loughran, T.P., 2001. Inhibition of STAT3 signaling leads to apoptosis of leukemic large granular lymphocytes and decreased Mcl-1 expression. *J. Clin. Invest.* 107, 351–361. doi:10.1172/JCI9940
- Esaki, T., Nakano, S., Masumoto, N., Fujishima, H., Niho, Y., 1996. Schedule-dependent reversion of acquired cisplatin resistance by 5-fluorouracil in a newly established cisplatin-resistant HST-1 human squamous carcinoma cell line. *Int. J. Cancer* 65, 479–484. doi:10.1002/(SICI)1097-0215(19960208)65:4<479::AID-IJC15>3.0.CO;2-5
- Esteller, M., Silva, J.M., Dominguez, G., Bonilla, F., Matias-Guiu, X., Lerma, E., Bussaglia, E., Prat, J., Harkes, I.C., Repasky, E. a, Gabrielson, E., Schutte, M., Baylin, S.B., Herman, J.G., 2000. Promoter hypermethylation and BRCA1 inactivation in sporadic breast and ovarian tumors. *J. Natl. Cancer Inst.* 92,

564–9.

Evers, B., Drost, R., Schut, E., De Bruin, M., Van Burg, E. Der, Derksen, P.W.B., Holstege, H., Liu, X., Van Drunen, E., Beverloo, H.B., Smith, G.C.M., Martin, N.M.B., Lau, A., O'Connor, M.J., Jonkers, J., 2008. Selective inhibition of BRCA2-deficient mammary tumor cell growth by AZD2281 and cisplatin. *Clin. Cancer Res.* 14, 3916–3925. doi:10.1158/1078-0432.CCR-07-4953

Fan, M., Huang, C., Gu, Y., Xiao, Y., Sheng, J., Zhong, L., 2013. Decrease expression of microRNA-20a promotes cancer cell proliferation and predicts poor survival of hepatocellular carcinoma. *J. Exp. Clin. Cancer Res.* 32, 1. doi:10.1186/1756-9966-32-21

Farber, S., 1949. Some observations on the effect of folic acid antagonists on acute leukemia and other forms of incurable cancer. *Blood* 4, 160–7.

Feng, F.Y., Lopez, C.A., Normolle, D.P., Varambally, S., Li, X., Chun, P.Y., Davis, M.A., Lawrence, T.S., Nyati, M.K., 2007. Effect of epidermal growth factor receptor inhibitor class in the treatment of head and neck cancer with concurrent radiochemotherapy in vivo. *Clin. Cancer Res.* 13, 2512–2518. doi:10.1158/1078-0432.CCR-06-2582

Fennell, D.A., Summers, Y., Cadranet, J., Benepal, T., Christoph, D.C., Lal, R., Das, M., Maxwell, F., Visseren-Grul, C., Ferry, D., 2016. Cisplatin in the modern era: the backbone of first-line chemotherapy for non-small cell lung cancer. *Cancer Treat. Rev. Cancer* 44, 42–50. doi:http://dx.doi.org/10.1016/j.ctrv.2016.01.003

Fink, D., Aebi, S., Howell, S.B., 1998. The role of DNA mismatch repair in drug resistance. *Clin. Cancer Res.* 4, 1–6.

Flanagan, S.E., Haapaniemi, E., Russell, M.A., Caswell, R., Lango Allen, H., De Franco, E., McDonald, T.J., Rajala, H., Ramelius, A., Barton, J., Heiskanen, K., Heiskanen-Kosma, T., Kajosaari, M., Murphy, N.P., Milenkovic, T., Seppänen, M., Lernmark, Å., Mustjoki, S., Otonkoski, T., Kere, J., Morgan, N.G., Ellard, S., Hattersley, A.T., 2014. Activating germline mutations in STAT3 cause early-onset multi-organ autoimmune disease. *Nat. Genet.* 46, 812–4. doi:10.1038/ng.3040

- Florea, A.-M., Büsselberg, D., 2011. Cisplatin as an anti-tumor drug: cellular mechanisms of activity, drug resistance and induced side effects. *Cancers (Basel)*. 3, 1351–71. doi:10.3390/cancers3011351
- Fokkema, E., Groen, H.J.M., Helder, M.N., De Vries, E.G.E., Meijer, C., 2002. JM216-, JM118-, and cisplatin-induced cytotoxicity in relation to platinum-DNA adduct formation, glutathione levels and p53 status in human tumour cell lines with different sensitivities to cisplatin. *Biochem. Pharmacol.* 63, 1989–1996. doi:10.1016/S0006-2952(02)00983-8
- Folias, A., Matkovic, M., Bruun, D., Reid, S., Hejna, J., Grompe, M., D'Andrea, A., Moses, R., 2002. BRCA1 interacts directly with the Fanconi anemia protein FANCA. *Hum. Mol. Genet.* 11, 2591–7.
- Forbes, S.A., Beare, D., Gunasekaran, P., Leung, K., Bindal, N., Boutselakis, H., Ding, M., Bamford, S., Cole, C., Ward, S., Kok, C.Y., Jia, M., De, T., Teague, J.W., Stratton, M.R., McDermott, U., Campbell, P.J., 2015. COSMIC: Exploring the world's knowledge of somatic mutations in human cancer. *Nucleic Acids Res.* 43, D805–D811. doi:10.1093/nar/gku1075
- Frank, D.A., 2012. Targeting STATs for cancer therapy: “Undruggable” no more. *Jak-Stat* 1, 261–2. doi:10.4161/jkst.22528
- Frank, D.A., 2007. STAT3 as a central mediator of neoplastic cellular transformation. *Cancer Lett.* 251, 199–210. doi:10.1016/j.canlet.2006.10.017
- Friboulet, L., Olaussen, K.A., Pignon, J.-P., Shepherd, F.A., Tsao, M.-S., Graziano, S., Kratzke, R., Douillard, J.-Y., Seymour, L., Pirker, R., Filipits, M., André, F., Solary, E., Ponsonailles, F., Robin, A., Stoclin, A., Dorvault, N., Commo, F., Adam, J., Vanhecke, E., Saulnier, P., Thomale, J., Le Chevalier, T., Dunant, A., Rousseau, V., Le Teuff, G., Brambilla, E., Soria, J.-C., 2013. ERCC1 isoform expression and DNA repair in non-small-cell lung cancer. *N. Engl. J. Med.* 368, 1101–10. doi:10.1056/NEJMoa1214271
- Friedberg, E.C., 2001. How nucleotide excision repair protects against cancer. *Nat. Rev. Cancer* 1, 22–33. doi:10.1038/35094000

- Friedmann, B., Caplin, M., Hartley, J. a., Hochhauser, D., 2004. Modulation of DNA repair in vitro after treatment with chemotherapeutic agents by the epidermal growth factor receptor inhibitor Gefitinib (ZD1839). *Clin. Cancer Res.* 10, 6476–6486. doi:10.1158/1078-0432.CCR-04-0586
- Fu, D., Calvo, J.A., Samson, L.D., 2012. Balancing repair and tolerance of DNA damage caused by alkylating agents. *Nat. Rev. Cancer* 12, 104–20. doi:10.1038/nrc3185
- Fu, S., Naing, A., Fu, C., Kuo, M.T., Kurzrock, R., 2012. Overcoming Platinum Resistance through the Use of a Copper- Lowering Agent. *Mol. Cancer Ther.* 11, 1221–1225. doi:10.1158/1535-7163.MCT-11-0864.Overcoming
- Fulda, S., Debatin, K.-M., 2002. IFN γ sensitizes for apoptosis by upregulating caspase-8 expression through the Stat1 pathway. *Oncogene* 21, 2295–2308. doi:10.1038/sj.onc.1205255
- Galmarini, C.M., Mackey, J.R., Dumontet, C., 2002. Nucleoside analogues and nucleobases in cancer treatment. *Lancet Oncol.* 3, 415–424. doi:10.1016/S1470-2045(02)00788-X
- Gao, B., Shen, X., Kunos, G., Meng, Q., Goldberg, I.D., Rosen, E.M., Fan, S., 2001. Constitutive activation of JAK-STAT3 signaling by BRCA1 in human prostate cancer cells. *FEBS Lett.* 488, 179–84.
- Gao, S.P., Mark, K.G., Leslie, K., Pao, W., Motoi, N., Gerald, W.L., Travis, W.D., Bornmann, W., Veach, D., Clarkson, B., Bromberg, J.F., 2007. Mutations in the EGFR kinase domain mediate STAT3 activation via IL-6 production in human lung adenocarcinomas. *J. Clin. Invest.* 117. doi:10.1172/JCI31871.3846
- Garcia-Higuera, I., Taniguchi, T., Ganesan, S., Meyn, M.S., Timmers, C., Hejna, J., Grompe, M., D'Andrea, a D., 2001. Interaction of the Fanconi anemia proteins and BRCA1 in a common pathway. *Mol. Cell* 7, 249–62.
- Gartel, a. L., Serfas, M.S., Tyner, a. L., 1996. p21--Negative Regulator of the Cell Cycle. *Exp. Biol. Med.* 213, 138–149. doi:10.3181/00379727-213-44046

- Giaccone, G., 2000. Clinical perspectives on platinum resistance. *Drugs* 59 Suppl, 9–17.
- Gibalová, L., Šereš, M., Rusnák, A., Ditte, P., Labudová, M., Uhrík, B., Pastorek, J., Sedlák, J., Breier, A., Sulová, Z., 2012. P-glycoprotein depresses cisplatin sensitivity in L1210 cells by inhibiting cisplatin-induced caspase-3 activation. *Toxicol. Vitr.* 26, 435–444. doi:10.1016/j.tiv.2012.01.014
- Gilman, A., Philips, F.S., 1946. The Biological Actions and Therapeutic Applications of the B-Chloroethyl Amines and Sulfides. *Science* 103, 409–415. doi:10.1126/science.103.2675.409
- Giri, D., Ozen, M., Ittmann, M., 2001. Interleukin-6 is an autocrine growth factor in human prostate cancer. *Am. J. Pathol.* 159, 2159–65. doi:10.1016/S0002-9440(10)63067-2
- Goel, A., Aggarwal, B.B., 2010. Curcumin, the golden spice from Indian saffron, is a chemosensitizer and radiosensitizer for tumors and chemoprotector and radioprotector for normal organs. *Nutr. Cancer* 62, 919–30. doi:10.1080/01635581.2010.509835
- Goldenberg, G.J., 1975. The role of drug transport in resistance to nitrogen mustard and other alkylating agents in L518Y lymphoblasts. *Cancer Res.* 35, 1687–1692.
- Goldenberg, J., Lam, H.-Y.P., Begleiter, A., 1979. Active Amino Carrier-mediated Acid Transport Transport of Melphalan by Two Separate Systems in LPC-1 Plasmacytoma Cells in Vitro. *J. Biol. Chem.* 254, 1057–1064.
- Grandis, J., Pendleton, K., Pendleton, K., Dr Grandis, 2013. Cisplatin-Based Chemotherapy Options for Recurrent and/or Metastatic Squamous Cell Cancer of the Head and Neck. *Clin. Med. Insights Ther.* 5, 103. doi:10.4137/CMT.S10409
- Grant, D.F., Bessho, T., Reardon, J.T., 1998. Nucleotide excision repair of melphalan monoadducts. *Cancer Res.* 58, 5196–5200.
- Gregory, M., Dandavati, A., Lee, M., Tzou, S., Savagian, M., Brien, K. a., Satam, V.,

- Patil, P., Lee, M., 2013. Synthesis, cytotoxicity, and structure–activity insight of NH- and N-methyl-3,5-bis-(arylidonyl)-4-piperidones. *Med. Chem. Res.* 22, 5588–5597. doi:10.1007/s00044-013-0557-9
- Greish, K., 2010. Enhanced Permeability and Retention (EPR) Effect for Anticancer Nanomedicine Drug Targeting. *Cancer Nanotechnol.* 624, 25–37. doi:10.1007/978-1-60761-609-2
- Gritsko, T., Williams, A., Turkson, J., Kaneko, S., Bowman, T., Huang, M., Nam, S., Eweis, I., Diaz, N., Sullivan, D., Yoder, S., Enkemann, S., Eschrich, S., Lee, J.-H., Beam, C. a, Cheng, J., Minton, S., Muro-Cacho, C. a, Jove, R., 2006. Persistent activation of stat3 signaling induces survivin gene expression and confers resistance to apoptosis in human breast cancer cells. *Clin. Cancer Res.* 12, 11–9. doi:10.1158/1078-0432.CCR-04-1752
- Guo, C., Yang, G., Khun, K., Kong, X., Levy, D., Lee, P., Melamed, J., 2009. Activation of Stat3 in renal tumors. *Am. J. Transl. Res.* 1, 283–290.
- Gupta, S.C., Patchva, S., Aggarwal, B.B., 2013a. Therapeutic roles of curcumin: lessons learned from clinical trials. *AAPS J.* 15, 195–218. doi:10.1208/s12248-012-9432-8
- Gupta, S.C., Phromnoi, K., Aggarwal, B.B., 2013b. Morin inhibits STAT3 tyrosine 705 phosphorylation in tumor cells through activation of protein tyrosine phosphatase SHP1. *Biochem. Pharmacol.* 85, 898–912. doi:10.1016/j.bcp.2012.12.018
- Haber, J.E., Heyer, W., 2001. The Fuss about Mus81. *Cell* 107, 551–554.
- Hamaguchi, K., Godwin, A.K., Yakushiji, M., O'Dwyer, P.J., Ozols, R.F., Hamilton, T.C., 1993. Cross-resistance to diverse drugs is associated with primary cisplatin resistance in ovarian cancer cell lines. *TL - 53. Cancer Res.* 53 VN-r, 5225–5232.
- Hamilton, K.O., Backstrom, G., Yazdanian, M.A., Audus, K.L., 2001. P-Glycoprotein Efflux Pump Expression and Activity in Calu-3 Cells. *J. Pharm. Sci.* 90, 599–606. doi:10.1002/1520-6017(200105)90

- Hanada, K., Budzowska, M., Modesti, M., Maas, A., Wyman, C., Essers, J., Kanaar, R., 2006. The structure-specific endonuclease Mus81-Eme1 promotes conversion of interstrand DNA crosslinks into double-strands breaks. *EMBO J.* 25, 4921–32. doi:10.1038/sj.emboj.7601344
- Hanahan, D., Folkman, J., 1996. Patterns and emerging mechanisms of the angiogenic switch during tumorigenesis. *Cell* 86, 353–364. doi:10.1016/S0092-8674(00)80108-7
- Hanahan, D., Weinberg, R.A., Francisco, S., 2000. The Hallmarks of Cancer Review University of California at San Francisco 100, 57–70.
- Hanahan, D., Weinberg, R. a, 2011. Hallmarks of cancer: the next generation. *Cell* 144, 646–74. doi:10.1016/j.cell.2011.02.013
- Hansson, J., Lewensohn, R., Ringborg, U., Nilsson, B., 1987. Formation and removal of DNA cross-links induced by melphalan and nitrogen mustard in relation to drug-induced cytotoxicity in human melanoma cells. *Cancer Res.* 47, 2631–2637.
- Harada, N., Nagasaki, a, Hata, H., Matsuzaki, H., Matsuno, F., Mitsuya, H., 2000. Down-regulation of CD98 in melphalan-resistant myeloma cells with reduced drug uptake. *Acta Haematol.* 103, 144–51. doi:41037
- Harkey, M. a, Czerwinski, M., Slattery, J., Kiem, H.-P., 2005. Overexpression of glutathione-S-transferase, MGSTII, confers resistance to busulfan and melphalan. *Cancer Invest.* 23, 19–25. doi:10.1081/CNV-200046508
- Harper, J.W., Elledge, S.J., Keyomarsi, K., Dynlacht, B., Tsai, L.H., Zhang, P., Dobrowolski, S., Bai, C., Connell-Crowley, L., Swindell, E., 1995. Inhibition of cyclin-dependent kinases by p21. *Mol. Biol. Cell* 6, 387–400. doi:10.1111/j.1365-2184.2009.00584.x
- Hartley, J.M., Spanswick, V.J., Gander, M., Giacomini, G., Whelan, J., Souhami, R.L., Hartley, J.A., 1999. Measurement of DNA Cross-linking in Patients on Ifosfamide Therapy Using the Single Cell Gel Electrophoresis (Comet) Assay
Measurement of DNA Cross-linking in Patients on Ifosfamide Therapy Using

the Single Cell Gel Electrophoresis 507–512.

Hecht, S.S., 2003. Tobacco carcinogens, their biomarkers and tobacco-induced cancer. *Nat. Rev. Cancer* 3, 733–44. doi:10.1038/nrc1190

Heidelberger, S., Zinzalla, G., Antonow, D., Essex, S., Piku Basu, B., Palmer, J., Husby, J., Jackson, P.J.M., Rahman, K.M., Wilderspin, A.F., Zloh, M., Thurston, D.E., 2013. Investigation of the protein alkylation sites of the STAT3:STAT3 inhibitor Stattic by mass spectrometry. *Bioorganic Med. Chem. Lett.* 23, 4719–4722. doi:10.1016/j.bmcl.2013.05.066

Heiger-Bernays, W.J., Essigmann, J.M., Lippard, S.J., 1990. Effect of the antitumor drug cis-diamminedichloroplatinum(II) and related platinum complexes on eukaryotic DNA replication. *Biochemistry* 29, 8461–6.

Helleday, T., Eshtad, S., Nik-Zainal, S., 2014. Mechanisms underlying mutational signatures in human cancers. *Nat. Rev. Genet.* 15, 585–598. doi:10.1038/nrg3729

Herceg, Z., Wang, Z.Q., 2001. Functions of poly(ADP-ribose) polymerase (PARP) in DNA repair, genomic integrity and cell death. *Mutat. Res.* 477, 97–110.

Herrmann, A., Vogt, M., Mönningmann, M., Clahsen, T., Sommer, U., Haan, S., Poli, V., Heinrich, P.C., Müller-Newen, G., 2007. Nucleocytoplasmic shuttling of persistently activated STAT3. *J. Cell Sci.* 120, 3249–3261. doi:10.1242/jcs.03482

Heyer, W.D., 2004. Recombination: Holliday Junction Resolution and Crossover Formation. *Curr. Biol.* 14, 56–58. doi:10.1016/j.cub.2003.12.043

Ho, H.H., Ivashkiv, L.B., 2006. Role of STAT3 in type I interferon responses: Negative regulation of STAT1-dependent inflammatory gene activation. *J. Biol. Chem.* 281, 14111–14118. doi:10.1074/jbc.M511797200

Hochhauser, D., Meyer, T., Spanswick, V.J., Wu, J., Clingen, P.H., Loadman, P., Cobb, M., Gumbrell, L., Begent, R.H., Hartley, J. a, Jodrell, D., 2009. Phase I study of sequence-selective minor groove DNA binding agent SJG-136 in

- patients with advanced solid tumors. *Clin. Cancer Res.* 15, 2140–7. doi:10.1158/1078-0432.CCR-08-1315
- Hoeijmakers, J.H., 2001. Genome maintenance mechanisms for preventing cancer. *Nature* 411, 366–74. doi:10.1038/35077232
- Hou, G., Zhang, Q., Wang, L., Liu, M., Wang, J., Xue, L., 2010. mTOR inhibitor rapamycin alone or combined with cisplatin inhibits growth of esophageal squamous cell carcinoma in nude mice. *Cancer Lett.* 290, 248–254. doi:10.1016/j.canlet.2009.09.015
- Hou, T., Ray, S., Lee, C., Brasier, A.R., 2008. The STAT3 NH2-terminal domain stabilizes enhanceosome assembly by interacting with the p300 bromodomain. *J. Biol. Chem.* 283, 30725–30734. doi:10.1074/jbc.M805941200
- Hu, Y., Hong, Y., Xu, Y., Liu, P., Guo, D.-H., Chen, Y., 2014. Inhibition of the JAK/STAT pathway with ruxolitinib overcomes cisplatin resistance in non-small-cell lung cancer NSCLC. *Apoptosis*. doi:10.1007/s10495-014-1030-z
- Huang, S., Chen, M., Shen, Y., Shen, W., Guo, H., Gao, Q., Zou, X., 2012. Inhibition of activated Stat3 reverses drug resistance to chemotherapeutic agents in gastric cancer cells. *Cancer Lett.* 315, 198–205. doi:10.1016/j.canlet.2011.10.011
- Huang, W., Dong, Z., Chen, Y., Wang, F., Wang, C.J., Peng, H., He, Y., Hangoc, G., Pollok, K., Sandusky, G., Fu, X., Broxmeyer, H.E., 2016. Small-molecule inhibitors targeting the DNA-binding domain of STAT3 suppress tumor growth, metastasis and STAT3 target gene expression in vivo. *Oncogene* 35, 783–792. doi:10.1038/onc.2015.215
- Huang, W., Dong, Z., Wang, F., Peng, H., Liu, J.Y., Zhang, J.T., 2014. A small molecule compound targeting STAT3 DNA-binding domain inhibits cancer cell proliferation, migration, and invasion. *ACS Chem. Biol.* 9, 1188–1196. doi:10.1021/cb500071v
- Huang, X., Okafuji, M., Traganos, F., Luther, E., Holden, E., Darzynkiewicz, Z., 2004. Assessment of histone H2AX phosphorylation induced by DNA

- topoisomerase I and II inhibitors topotecan and mitoxantrone and by the DNA cross-linking agent cisplatin. *Cytom. A* 58, 99–110. doi:10.1002/cyto.a.20018
- Hurley, L.H., 2002. DNA and its associated processes as targets for cancer therapy. *Nat. Rev. Cancer* 2, 188–200. doi:10.1038/nrc749
- Hutzen, B., Friedman, L., Sobo, M., Lin, L.I., Cen, L., Angelis, S.D.E., Yamakoshi, H., Shibata, H., Iwabuchi, Y., Lin, J., 2009. Curcumin analogue GO-Y030 inhibits STAT3 activity and cell growth in breast and pancreatic carcinomas. *Int. J. Oncol.* 35, 867–872. doi:10.3892/ijo
- Hwang, G.S., Kim, J.K., Choi, B.S., 1996. The solution structure of a psoralen cross-linked DNA duplex by NMR and relaxation matrix refinement. *Biochem. Biophys. Res. Commun.* 219, 191–7. doi:10.1006/bbrc.1996.0204
- Inagaki-Ohara, K., Kondo, T., Ito, M., Yoshimura, A., 2013. SOCS, inflammation, and cancer. *Jak-Stat* 2, e24053. doi:10.4161/jkst.24053
- Irby, R.B., Mao, W., Coppola, D., Kang, J., Loubeau, J.M., Trudeau, W., Karl, R., Fujita, D.J., Jove, R., Yeatman, T.J., 1999. Activating SRC mutation in a subset of advanced human colon cancers. *Nat. Genet.* 21, 187–90. doi:10.1038/5971
- Ishdorj, G., Johnston, J.B., Gibson, S.B., 2010. Inhibition of constitutive activation of STAT3 by curcubitacin-I (JSI-124) sensitized human B-leukemia cells to apoptosis. *Mol. Cancer Ther.* 9, 3302–14. doi:10.1158/1535-7163.MCT-10-0550
- Ishida, S., Lee, J., Thiele, D.J., Herskowitz, I., 2002. Uptake of the anticancer drug cisplatin mediated by the copper transporter Ctr1 in yeast and mammals 99.
- Iwahori, K., Serada, S., Fujimoto, M., Ripley, B., Nomura, S., Mizuguchi, H., Shimada, K., Takahashi, T., Kawase, I., Kishimoto, T., Naka, T., 2013. SOCS-1 gene delivery cooperates with cisplatin plus pemetrexed to exhibit preclinical antitumor activity against malignant pleural mesothelioma. *Int. J. Cancer* 132, 459–471. doi:10.1002/ijc.27611
- Jackson, S.P., 2002. Sensing and repairing DNA double-strand breaks.

Carcinogenesis 23, 687–696. doi:10.1093/carcin/23.5.687

Jacobs, A.L., Schär, P., 2012. DNA glycosylases: In DNA repair and beyond. *Chromosoma* 121, 1–20. doi:10.1007/s00412-011-0347-4

Jacquemont, C., Simon, J. a, D'Andrea, A.D., Taniguchi, T., 2012. Non-specific chemical inhibition of the Fanconi anemia pathway sensitizes cancer cells to cisplatin. *Mol. Cancer* 11, 26. doi:10.1186/1476-4598-11-26

Jamal-Hanjani, M., Quezada, S.A., Larkin, J., Swanton, C., 2015. Translational implications of tumor heterogeneity. *Clin. Cancer Res.* 21, 1258–1266. doi:10.1158/1078-0432.CCR-14-1429

Jenkins, T.C., Hurley, L.H., Neidle, S., Thurston, D.E., 1994. Structure of a covalent DNA minor groove adduct with a pyrrolobenzodiazepine dimer: evidence for sequence-specific interstrand cross-linking. *J. Med. Chem.* 37, 4529–37. doi:10.1021/jm00052a012

Ji, T., Gong, D., Han, Z., Wei, X., Yan, Y., Ye, F., Ding, W., Wang, J., Xia, X., Li, F., Hu, W., Lu, Y., Wang, S., Zhou, J., Ma, D., Gao, Q., 2013. Abrogation of constitutive Stat3 activity circumvents cisplatin resistant ovarian cancer. *Cancer Lett.* doi:10.1016/j.canlet.2013.08.022

Jia, L., Song, Q., Zhou, C., Li, X., Pi, L., Ma, X., Li, H., Lu, X., Shen, Y., 2016. Dihydroartemisinin as a Putative STAT3 Inhibitor, Suppresses the Growth of Head and Neck Squamous Cell Carcinoma by Targeting Jak2/STAT3 Signaling. *PLoS One* 11, e0147157. doi:10.1371/journal.pone.0147157

Jiricny, J., 2006. The multifaceted mismatch-repair system. *Nat. Rev. Mol. Cell Biol.* 7, 335–46. doi:10.1038/nrm1907

Johnson, I.S., Armstrong, J.G., Gorman, M., Burnett, J.P., 1963. the Vinca Alkaloids: a New Class of Oncolytic Agents. *Cancer Res.* 23, 1390–1427.

Johnston, P.A., Grandis, J.R., 2011. Stat3 Signaling: Anticancer Strategies and Challenges. *Mol. Interv.* 11, 18–26.

- Jun, D.W., Hwang, M., Kim, H.J., Hwang, S.K., Kim, S., Lee, C.-H., 2013. Ouabain, a cardiac glycoside, inhibits the Fanconi anemia/BRCA pathway activated by DNA interstrand cross-linking agents. *PLoS One* 8, e75905. doi:10.1371/journal.pone.0075905
- Kalai, T., Kuppusamy, M.L., Balog, M., Selvendiran, K., Rivera, B.K., Kuppusamy, P., Hideg, K., 2011. Synthesis of N-substituted 3,5-bis(arylidene)-4-piperidones with high antitumor and antioxidant activity. *J. Med. Chem.* 54, 5414–5421. doi:10.1021/jm200353f
- Kanavy, H.E., Gerstenblith, M.R., 2011. Ultraviolet Radiation and Melanoma. *Semin. Cutan. Med. Surg.* 30, 222–228. doi:10.1016/j.sder.2011.08.003
- Kandala, P.K., Srivastava, S.K., 2012. Diindolylmethane suppresses ovarian cancer growth and potentiates the effect of cisplatin in tumor mouse model by targeting signal transducer and activator of transcription 3 (STAT3). *BMC Med.* 10, 9. doi:10.1186/1741-7015-10-9
- Kasparkova, J., Delalande, O., Stros, M., Elizondo-Riojas, M.-A., Vojtiskova, M., Kozelka, J., Brabec, V., 2003. Recognition of DNA interstrand cross-link of antitumor cisplatin by HMGB1 protein. *Biochemistry* 42, 1234–44. doi:10.1021/bi026695t
- Keepers, Y.P., Pizao, P.E., Peters, G.J., Ark-Otte, J. van, Winograd, B., Pinedo, H.M., 1991. Comparison of the Sulforhodamine B Protein and Tetrazolium (MTT) Assays for in vitro Chemosensitivity Testing. *Eur J Cancer* 27, 897–900.
- Kelley, S.L., Basu, a, Teicher, B. a, Hacker, M.P., Hamer, D.H., Lazo, J.S., 1988. Overexpression of metallothionein confers resistance to anticancer drugs. *Science* 241, 1813–1815. doi:10.1126/science.3175622
- Kent, W.J., Sugnet, C.W., Furey, T.S., Roskin, K.M., Pringle, T.H., Zahler, A.M., Haussler, D., 2002. The Human Genome Browser at UCSC The Human Genome Browser at UCSC. *Genome Res.* 12, 996–1006. doi:10.1101/gr.229102.
- Khanna, K.K., Jackson, S.P., 2001. DNA double-strand breaks: signaling, repair and

the cancer connection. *Nat. Genet.* 27, 247–54. doi:10.1038/85798

Kharbanda, S., Pandey, P., Schofield, L., Israels, S., Roncinske, R., Yoshida, K., Bharti, A., Yuan, Z., Saxena, S., Weichselbaum, R., Nalin, C., Kufe, D., 1997. Role for Bcl-xL as an inhibitor of cytosolic cytochrome C accumulation in DNA damage-induced apoptosis. *Proc. Natl. Acad. Sci. U. S. A.* 94, 6939–42.

Kilari, D., 2016. Role of copper transporters in platinum resistance. *World J. Clin. Oncol.* 7, 106. doi:10.5306/wjco.v7.i1.106

Kim, E.S., Lee, J.J., He, G., Chow, C.W., Fujimoto, J., Kalhor, N., Swisher, S.G., Wistuba, I.I., Stewart, D.J., Siddik, Z.H., 2012. Tissue platinum concentration and tumor response in non-small-cell lung cancer. *J. Clin. Oncol.* 30, 3345–3352. doi:10.1200/JCO.2011.40.8120

Kim, J.K., Kim, J.Y., Kim, H.J., Park, K.G., Harris, R.A., Cho, W.J., Lee, J.T., Lee, I.K., 2013. Scoparone Exerts Anti-Tumor Activity against DU145 Prostate Cancer Cells via Inhibition of STAT3 Activity. *PLoS One* 8, e80391. doi:10.1371/journal.pone.0080391

Kim, J.M., Kee, Y., Gurtan, A., Andrea, A.D.D., 2008. Cell cycle – dependent chromatin loading of the Fanconi anemia core complex by FANCM / FAAP24 111, 5215–5222. doi:10.1182/blood-2007-09-113092.An

Kim, M.J., Nam, H.J., Kim, H.P., Han, S.W., Im, S.A., Kim, T.Y., Oh, D.Y., Bang, Y.J., 2013. OPB-31121, a novel small molecular inhibitor, disrupts the JAK2/STAT3 pathway and exhibits an antitumor activity in gastric cancer cells. *Cancer Lett.* 335, 145–152. doi:10.1016/j.canlet.2013.02.010

Kim, S.M., Lee, J.H., Sethi, G., Kim, C., Baek, S.H., Nam, D., Chung, W.S., Kim, S.H., Shim, B.S., Ahn, K.S., 2014. Bergamottin, a natural furanocoumarin obtained from grapefruit juice induces chemosensitization and apoptosis through the inhibition of STAT3 signaling pathway in tumor cells. *Cancer Lett.* 2–12. doi:10.1016/j.canlet.2014.08.002

Kinner, A., Wu, W., Staudt, C., Iliakis, G., 2008. Gamma-H2AX in recognition and signaling of DNA double-strand breaks in the context of chromatin. *Nucleic*

Acids Res. 36, 5678–5694. doi:10.1093/nar/gkn550

Kiuchi, N., Nakajima, K., Ichiba, M., Fukada, T., Narimatsu, M., Mizuno, K., Hibi, M., Hirano, T., 1999. STAT3 is required for the gp130-mediated full activation of the c-myc gene. *J. Exp. Med.* 189, 63–73. doi:10.1084/jem.189.1.63

Klein Douwel, D., Boonen, R.A.C.M., Long, D.T., Szypowska, A.A., Räschle, M., Walter, J.C., Knipscheer, P., 2014. XPF-ERCC1 Acts in Unhooking DNA Interstrand Crosslinks in Cooperation with FANCD2 and FANCP/SLX4. *Mol. Cell* 1–12. doi:10.1016/j.molcel.2014.03.015

Knipscheer, P., Räschle, M., Smogorzewska, A., Enoiu, M., Ho, T.V., Schärer, O.D., Elledge, S.J., Walter, J.C., 2009. The Fanconi anemia pathway promotes replication-dependent DNA interstrand cross-link repair. *Science* 326, 1698–701. doi:10.1126/science.1182372

Köberle, B., Grimaldi, K.A., Sunter, A., Hartley, J.A., Kelland, L.R., Masters, J.R., 1997. DNA repair capacity and cisplatin sensitivity of human testis tumour cells. *Int. J. Cancer* 70, 551–555. doi:10.1002/(SICI)1097-0215(19970304)70:5<551::AID-IJC10>3.0.CO;2-G

Kohn, K.W., 1991. Principles and practice of DNA filter elution. *Pharmacol. Ther.* 49, 55–77.

Komatsu, M., Sumizawa, T., Mutoh, M., Chen, Z.S., Terada, K., Furukawa, T., Yang, X.L., Gao, H., Miura, N., Sugiyama, T., Akiyama, S.I., 2000. Copper-transporting P-type adenosine triphosphatase (ATP7B) is associated with cisplatin resistance. *Cancer Res.* 60, 1312–1316.

Kong, J., Kong, F., Gao, J., Zhang, Q., Dong, S., Gu, F., Ke, S., Pan, B., Shen, Q., Sun, H., Zheng, L., Sun, W., 2014. YC-1 enhances the anti-tumor activity of sorafenib through inhibition of signal transducer and activator of transcription 3 (STAT3) in hepatocellular carcinoma. *Mol. Cancer* 13, 7. doi:10.1186/1476-4598-13-7

Koressaar, T., Remm, M., 2007. Enhancements and modifications of primer design program Primer3. *Bioinformatics* 23, 1289–1291.

doi:10.1093/bioinformatics/btm091

Koskela, H., Eldfors, S., Ellonen, P., Adrichem, A., Kuusanmaki, H., Andersson, E., Lagstrom, S., Clemente, M., Olson, T., Jalkanen, S., Majumder, M., Almusa, H., Edgren, H., Lepisto, M., Mattila, P., Guinta, K., Koistinen, P., Kuittinen, T., Penttinen, K., Parsons, A., Knowles, J., Saarela, J., Wennerberg, K., Kallioniemi, O., Porkka, K., Loughran, T., Heckman, C., Maciejewski, J., Mustjoki, S., 2012. Mutations in Large Granular Lymphocytic Leukemia. *N. Engl. J. Med.* 366, 1905–1913.

Kothandapani, A., Dangeti, V.S.M.N., Brown, A.R., Banze, L.A., Wang, X.H., Sobol, R.W., Patrick, S.M., 2011. Novel role of base excision repair in mediating cisplatin cytotoxicity. *J. Biol. Chem.* 286, 14564–14574. doi:10.1074/jbc.M111.225375

Krokan, H.E., Nilsen, H., Skorpen, F., Otterlei, M., Slupphaug, G., 2000. Base excision repair of DNA in mammalian cells. *FEBS Lett.* 476, 73–77.

Krumbhaar, E.B., Krumbhaar, H.D., 1919. The Blood and Bone Marrow in Yellow Cross Gas (Mustard Gas) Poisoning. *J. Med. Res.* 40, 497–508.3.

Kuhne, A., Tzvetkov, M.V., Hagos, Y., Lage, H., Burckhardt, G., Brockmoller, J., 2009. Influx and efflux transport as determinants of melphalan cytotoxicity: Resistance to melphalan in MDR1 overexpressing tumor cell lines. *Biochem. Pharmacol.* 78, 45–53. doi:10.1016/j.bcp.2009.03.026

Kumar, B., Yadav, A., Hideg, K., Kuppusamy, P., Teknos, T.N., Kumar, P., 2014. A novel curcumin analog (h-4073) enhances the therapeutic efficacy of Cisplatin treatment in head and neck cancer. *PLoS One* 9, e93208. doi:10.1371/journal.pone.0093208

Kunigal, S., Lakka, S.S., Sodadasu, P.K., Estes, N., Rao, J.S., 2009. Stat3-siRNA induces Fas-mediated apoptosis in vitro and in vivo in breast cancer. *Int. J. Oncol.* 34, 1209–1220. doi:10.3892/ijo_00000249

Kuo, L.J., Yang, L.-X., 2008. Gamma-H2AX - a novel biomarker for DNA double-strand breaks. *In Vivo* 22, 305–9.

- Kuraoka, I., Kobertz, W.R., Ariza, R.R., Biggerstaff, M., Essigmann, J.M., Wood, R.D., 2000. Repair of an interstrand DNA cross-link initiated by ERCC1-XPF repair/recombination nuclease. *J. Biol. Chem.* 275, 26632–6. doi:10.1074/jbc.C000337200
- Lachaud, C., Moreno, A., Marchesi, F., Toth, R., Blow, J.J., Rouse, J., 2016. Ubiquitinated Fancd2 recruits Fan1 to stalled replication forks to prevent genome instability. *Science* 5634, aad5634. doi:10.1126/science.aad5634
- Lane, D.P., 1992. Cancer. p53, guardian of the genome. *Nature*. doi:10.1038/358015a0
- Lapenna, S., Giordano, A., 2009. Cell cycle kinases as therapeutic targets for cancer. *Nat. Rev. Drug Discov.* 8, 547–566. doi:10.1038/nrd2907
- Larionov, L.F., Khokhlov, A.S., Shkodinskaja, E.N., Vasina, O.S., Troosheikina, V.I., Novikova, M.A., 1955. Studies on the anti-tumour activity of p-di-(2-chloroethyl)aminophenylalanine (sarcosine). *Lancet* 169–171.
- Lau, C.K., Yang, Z.F., Lam, S.P., Lam, C.T., Ngai, P., Tam, K.H., Poon, R.T.-P., Fan, S.T., 2007. Inhibition of Stat3 activity by YC-1 enhances chemo-sensitivity in hepatocellular carcinoma. *Cancer Biol. Ther.* 6, 1900–7.
- Lawley, P.D., Phillips, D.H., 1996. DNA adducts from chemotherapeutic agents. *Mutat. Res.* 355, 13–40. doi:10.1016/0027-5107(96)00020-6
- Lebwohl, D., Canetta, R., 1998. Clinical Development of Platinum Complexes in Cancer Therapy: an Historical Perspective and an Update. *Eur J Cancer* 34, 1522–1534. doi:10.1016/S0959-8049(98)00224-X
- Ledermann, J.A., Gabra, H., Jayson, G.C., Spanswick, V.J., Rustin, G.J.S., Jitlal, M., James, L.E., Hartley, J.A., 2010. Inhibition of carboplatin-induced DNA interstrand cross-link repair by gemcitabine in patients receiving these drugs for platinum-resistant ovarian cancer. *Clin. Cancer Res.* 16, 4899–4905. doi:10.1158/1078-0432.CCR-10-0832
- Lee, J.H., Kim, C., Sethi, G., Ahn, K.S., 2015. Brassinin inhibits STAT3 signaling

pathway through modulation of PIAS-3 and SOCS-3 expression and sensitizes human lung cancer xenograft in nude mice to paclitaxel. *Oncotarget* 6, 6386–6405.

Lee, J.S., Park, K., Han, J.Y., Lee, K.H., Cho, E.K., Cho, J.Y., Min, Y.J., Kim, J.S., Kim, H.G., Kim, B.S., Juny, J., Kim, D.W., 2015. Clinical activity and safety of the EGFR mutant-specific inhibitor, BI1482694, in patients (pts) with T790M-positive NSCLC. *Ann. Oncol.* 26. doi:10.1093/annonc/mdv532.9

Lee, M.J., Ye, A.S., Gardino, A.K., Heijink, A.M., Sorger, P.K., MacBeath, G., Yaffe, M.B., 2012. Sequential application of anticancer drugs enhances cell death by rewiring apoptotic signaling networks. *Cell* 149, 780–794. doi:10.1016/j.cell.2012.03.031

Leong, P.L., Andrews, G. a, Johnson, D.E., Dyer, K.F., Xi, S., Mai, J.C., Robbins, P.D., Gadiparthi, S., Burke, N. a, Watkins, S.F., Grandis, J.R., 2003. Targeted inhibition of Stat3 with a decoy oligonucleotide abrogates head and neck cancer cell growth. *Proc. Natl. Acad. Sci. U. S. A.* 100, 4138–4143. doi:10.1073/pnas.0534764100

Lerner, L., Henriksen, M.A., Zhang, X., Darnell, J.E., 2003. STAT3-dependent enhanceosome assembly and disassembly: Synergy with GR for full transcriptional increase of the α 2-macroglobulin gene. *Genes Dev.* 17, 2564–2577. doi:10.1101/gad.1135003

Lev-Ari, S., Vexler, A., Starr, A., Ashkenazy-Voghera, M., Greif, J., Aderka, D., Ben-Yosef, R., 2007. Curcumin augments gemcitabine cytotoxic effect on pancreatic adenocarcinoma cell lines. *Cancer Invest.* 25, 411–8. doi:10.1080/07357900701359577

Li, G.-M., 2008. Mechanisms and functions of DNA mismatch repair. *Cell Res.* 18, 85–98. doi:10.1038/cr.2007.115

Li, J., Favata, M., Kelley, J.A., Caulder, E., Thomas, B., Wen, X., Sparks, R.B., Arvanitis, A., Rogers, J.D., Combs, A.P., Vaddi, K., Solomon, K.A., Scherle, P.A., Newton, R., Fridman, J.S., 2010. INCB16562, a JAK1/2 selective inhibitor, is efficacious against multiple myeloma cells and reverses the

protective effects of cytokine and stromal cell support. *Neoplasia* 12, 28–38. doi:10.1593/neo.91192

Li, L., Ahmed, B., Mehta, K., Kurzrock, R., 2007. Liposomal curcumin with and without oxaliplatin: effects on cell growth, apoptosis, and angiogenesis in colorectal cancer. *Mol. Cancer Ther.* 6, 1276–82. doi:10.1158/1535-7163.MCT-06-0556

Li, Q., Tsang, B., Bostick-Bruton, F., Reed, E., 1999. Modulation of excision repair cross complementation group 1 (ERCC-1) mRNA expression by pharmacological agents in human ovarian carcinoma cells. *Biochem. Pharmacol.* 57, 347–53.

Li, X., Heyer, W.-D., 2008. Homologous recombination in DNA repair and DNA damage tolerance. *Cell Res.* 18, 99–113. doi:10.1038/cr.2008.1

Liang, C., Zhan, B., Gygi, S.P., Cohn, M.A., Liang, C., Zhan, B., Yoshikawa, Y., Haas, W., Gygi, S.P., Cohn, M.A., 2015. UHRF1 Is a Sensor for DNA Interstrand Crosslinks and Recruits FANCD2 to Initiate the Fanconi Anemia Pathway. *CellReports* 1–10. doi:10.1016/j.celrep.2015.02.053

Lieber, M.R., 2010. The Mechanism of Double-Strand DNA Break Repair by the Nonhomologous DNA End Joining Pathway. *Annu. Rev. Biochem.* 79, 181–211. doi:10.1146/annurev.biochem.052308.093131.The

Liebermann, D. a, Hoffman, B., 2008. Gadd45 in stress signaling. *J. Mol. Signal.* 3, 15. doi:10.1186/1750-2187-3-15

Liedert, B., Pluim, D., Schellens, J., Thomale, J., 2006. Adduct-specific monoclonal antibodies for the measurement of cisplatin-induced DNA lesions in individual cell nuclei. *Nucleic Acids Res.* 34. doi:10.1093/nar/gkl051

Lin, L., Deangelis, S., Foust, E., Fuchs, J., Li, C., Li, P.-K., Schwartz, E.B., Lesinski, G.B., Benson, D., Lü, J., Hoyt, D., Lin, J., 2010a. A novel small molecule inhibits STAT3 phosphorylation and DNA binding activity and exhibits potent

growth suppressive activity in human cancer cells. *Mol. Cancer* 9, 217. doi:10.1186/1476-4598-9-217

Lin, L., Hutzen, B., Li, P., Ball, S., Zuo, M., Deangelis, S., Foust, E., Sobo, M., 2010b. A Novel Small Molecule , LLL12 , Inhibits STAT3 Phosphorylation and Activities and Exhibits Potent Growth-Suppressive Activity in Human Cancer Cells 12, 39–50. doi:10.1593/neo.91196

Lin, L., Hutzen, B., Zuo, M., Ball, S., Deangelis, S., Foust, E., Pandit, B., Ihnat, M.A., Shenoy, S.S., Kulp, S., Li, P.-K., Li, C., Fuchs, J., Lin, J., 2010c. Novel STAT3 phosphorylation inhibitors exhibit potent growth suppressive activity in pancreatic and breast cancer cells. *Cancer Res.* 70, 2445–2454. doi:10.1016/j.jsbmb.2011.07.002.Identification

Lin, L., Liu, A., Peng, Z., Lin, H.J., Li, P.K., Li, C., Lin, J., 2011. STAT3 is necessary for proliferation and survival in colon cancer-initiating cells. *Cancer Res.* 71, 7226–7237. doi:10.1158/0008-5472.CAN-10-4660

Liu, A., Liu, Y., Jin, Z., Hu, Q., Lin, L., Jou, D., Yang, J., Xu, Z., Wang, H., Li, C., Lin, J., 2012. XZH-5 inhibits STAT3 phosphorylation and enhances the cytotoxicity of chemotherapeutic drugs in human breast and pancreatic cancer cells. *PLoS One* 7, e46624. doi:10.1371/journal.pone.0046624

Liu, A., Liu, Y., Xu, Z., Yu, W., Wang, H., Li, C., Lin, J., 2011. Novel small molecule, XZH-5, inhibits constitutive and interleukin-6-induced STAT3 phosphorylation in human rhabdomyosarcoma cells. *Cancer Sci.* 102, 1381–7. doi:10.1111/j.1349-7006.2011.01932.x

Liu, L., McBride, K.M., Reich, N.C., 2005. STAT3 nuclear import is independent of tyrosine phosphorylation and mediated by importin-alpha3. *Proc. Natl. Acad. Sci. U. S. A.* 102, 8150–5. doi:10.1073/pnas.0501643102

Loeber, R., Michaelson-Richie, E.D., Codreanu, S.G., Liebler, D.C., Campbell, C.R., Tretyakova, N.Y., 2009. Proteomic Analysis of DNA-Protein Cross-Linking by Antitumor Nitrogen Mustards. *Chem. Res. Toxicol.* 22, 1151–1162. doi:10.3851/IMP2701.Changes

- Lohse, I., Borgida, a, Cao, P., Cheung, M., Pintilie, M., Bianco, T., Holter, S., Ibrahimov, E., Kumareswaran, R., Bristow, R.G., Tsao, M.-S., Gallinger, S., Hedley, D.W., 2015. BRCA1 and BRCA2 mutations sensitize to chemotherapy in patient-derived pancreatic cancer xenografts. *Br. J. Cancer* 1–8. doi:10.1038/bjc.2015.220
- Long, D.T., Joukov, V., Budzowska, M., Walter, J.C., 2014. BRCA1 promotes unloading of the CMG helicase from a stalled DNA replication fork. *Mol Cell* 56, 174–185. doi:10.1038/jid.2014.371
- Lopez-Martinez, D., Liang, C.-C., Cohn, M.A., 2016. Cellular response to DNA interstrand crosslinks: the Fanconi anemia pathway. *Cell. Mol. Life Sci.* doi:10.1007/s00018-016-2218-x
- Luchenko, V.L., Salcido, C.D., Zhang, Y., Agama, K., Komlodi-Pasztor, E., Murphy, R.F., Giaccone, G., Pommier, Y., Bates, S.E., Varticovski, L., 2011. Schedule-dependent synergy of histone deacetylase inhibitors with DNA damaging agents in small cell lung cancer. *Cell Cycle* 10, 3119–3128. doi:10.4161/cc.10.18.17190
- Luciani, F., Spada, M., De Milito, A., Molinari, A., Rivoltini, L., Montinaro, A., Marra, M., Lugini, L., Logozzi, M., Lozupone, F., Federici, C., Iessi, E., Parmiani, G., Arancia, G., Belardelli, F., Fais, S., 2004. Effect of proton pump inhibitor pretreatment on resistance of solid tumors to cytotoxic drugs. *J. Natl. Cancer Inst.* 96, 1702–13. doi:10.1093/jnci/djh305
- Luqmani, Y.A., 2005. Mechanisms of drug resistance in cancer chemotherapy. *Med. Princ. Pract.* 14, 35–48. doi:10.1159/000081921
- Lyakhovich, A., Surrallés, J., 2007. New Roads to FA/BRCA Pathway - H2AX. *Cell Cycle* 6, 1019–1023.
- Ma, J., Cao, X., 2006. Regulation of Stat3 nuclear import by importin α 5 and importin α 7 via two different functional sequence elements. *Cell. Signal.* 18, 1117–1126. doi:10.1016/j.cellsig.2005.06.016
- Ma, J., Maliepaard, M., Nooter, K., Boersma, A.W.M., Verweij, J., Stoter, G.,

- Schellens, J.H.M., 1998. Synergistic cytotoxicity of cisplatin and topotecan or SN-38 in a panel of eight solid-tumor cell lines in vitro. *Cancer Chemother. Pharmacol.* 41, 307–316. doi:10.1007/s002800050744
- MacKay, C., Declais, A.C., Lundin, C., Agostinho, A., Deans, A.J., MacArtney, T.J., Hofmann, K., Gartner, A., West, S.C., Helleday, T., Lilley, D.M.J., Rouse, J., 2010. Identification of KIAA1018/FAN1, a DNA Repair Nuclease Recruited to DNA Damage by Monoubiquitinated FANCD2. *Cell* 142, 65–76. doi:10.1016/j.cell.2010.06.021
- Malinge, J.M., Giraud-Panis, M.J., Leng, M., 1999. Interstrand cross-links of cisplatin induce striking distortions in DNA. *J. Inorg. Biochem.* 77, 23–29. doi:10.1016/S0162-0134(99)00148-8
- Mankan, A.K., Greten, F.R., 2011. Inhibiting signal transducer and activator of transcription 3: rationality and rationale design of inhibitors. *Expert Opin. Investig. Drugs* 20, 1263–75. doi:10.1517/13543784.2011.601739
- Marteijn, J. a, Lans, H., Vermeulen, W., Hoeijmakers, J.H.J., 2014. Understanding nucleotide excision repair and its roles in cancer and ageing. *Nat. Rev. Mol. Cell Biol.* 15, 465–81. doi:10.1038/nrm3822
- Mascarenhas, J., Hoffman, R., 2012. Ruxolitinib: The first FDA approved therapy for the treatment of myelofibrosis. *Clin. Cancer Res.* 18, 3008–3014. doi:10.1158/1078-0432.CCR-11-3145
- Masuda, M., Suzui, M., Yasumatu, R., 2002. Constitutive Activation of Signal Transducers and Activators of Transcription 3 Correlates with Cyclin D1 Overexpression and May Provide a Novel Prognostic Marker in Head and Neck Squamous Cell Carcinoma. *Cancer Res.* 62, 3351–3355.
- Masuda, M., Wakasaki, T., Suzui, M., Toh, S., Joe, A.K., Weinstein, I.B., 2010. Stat3 orchestrates tumor development and progression: the Achilles' heel of head and neck cancers? *Curr. Cancer Drug Targets* 10, 117–26.
- Mathew, C.G., 2006. Fanconi anaemia genes and susceptibility to cancer. *Oncogene* 25, 5875–5884. doi:10.1038/sj.onc.1209878

- Matsuno, K., Masuda, Y., Uehara, Y., Sato, H., Muroya, A., Takahashi, O., Yokotagawa, T., Furuya, T., Okawara, T., Otsuka, M., Ogo, N., Ashizawa, T., Oshita, C., Tai, S., Ishii, H., Akiyama, Y., Asai, A., 2010. Identification of a New Series of STAT3 Inhibitors by Virtual Screening. *ACS Med. Chem. Lett.* 1, 371–375. doi:10.1021/ml1000273
- McHugh, P.J., Spanswick, V.J., Hartley, J. a, 2001. Repair of DNA interstrand crosslinks: molecular mechanisms and clinical relevance. *Lancet Oncol.* 2, 483–90. doi:10.1016/S1470-2045(01)00454-5
- McPherson, J.P., Lemmers, B., Chahwan, R., Pamidi, A., Migon, E., Matysiak-Zablocki, E., Moynahan, M.E., Essers, J., Hanada, K., Poonepalli, A., Sanchez-Sweatman, O., Khokha, R., Kanaar, R., Jasin, M., Hande, M.P., Hakem, R., 2004. Involvement of mammalian Mus81 in genome integrity and tumor suppression. *Science* 304, 1822–1826. doi:10.1126/science.1094557
- Mechetner, E., Kyshtoobayeva, A., Zonis, S., Kim, H., Stroup, R., Garcia, R., Parker, R.J., Fruehauf, J.P., 1998. Levels of multidrug resistance (MDR1) P-glycoprotein expression by human breast cancer correlate with in vitro resistance to taxol and doxorubicin. *Clin. Cancer Res.* 4, 389–98.
- Meetei, A.R., Medhurst, A.L., Ling, C., Xue, Y., Singh, T.R., Bier, P., Steltenpool, J., Stone, S., Dokal, I., Mathew, C.G., Hoatlin, M., Joenje, H., de Winter, J.P., Wang, W., 2005. A human ortholog of archaeal DNA repair protein Hef is defective in Fanconi anemia complementation group M. *Nat. Genet.* 37, 958–63. doi:10.1038/ng1626
- Meijer, C., Mulder, N.H., Timmer-Bosscha, H., Sluiter, W.J., Meersma, G.J., De Vries, E.G.E., 1992. Relationship of cellular glutathione to the cytotoxicity and resistance of seven platinum compounds. *Cancer Res.* 52, 6885–6889.
- Mini, E., Nobili, S., Caciagli, B., Landini, I., Mazzei, T., 2006. Cellular pharmacology of gemcitabine. *Ann. Oncol.* 17, 7–12. doi:10.1093/annonc/mdj941
- Mishima, M., Samimi, G., Kondo, A., Lin, X., Howell, S.B., 2002. The cellular pharmacology of oxaliplatin resistance. *Eur. J. Cancer* 38, 1405–1412. doi:10.1016/S0959-8049(02)00096-5

- Mita, A.C., Mita, M.M., Nawrocki, S.T., Giles, F.J., 2008. Survivin: key regulator of mitosis and apoptosis and novel target for cancer therapeutics. *Clin. Cancer Res.* 14, 5000–5. doi:10.1158/1078-0432.CCR-08-0746
- Mitchell, T.J., John, S., 2005. Signal transducer and activator of transcription (STAT) signalling and T-cell lymphomas. *Immunology* 114, 301–312. doi:10.1111/j.1365-2567.2005.02091.x
- Mogi, S., Oh, D.H., 2006. γ -H2AX formation in response to interstrand crosslinks requires XPF in human cells. *DNA Repair (Amst)*. 5, 731–740. doi:10.1016/j.dnarep.2006.03.009.
- Mohani, K.N., Thompson, P.S., Luzwick, J.W., Glick, G.G., Pendleton, C.S., Lehmann, B.D., Pietenpol, J.A., Cortez, D., 2015. A synthetic lethal screen identifies DNA repair pathways that sensitize cancer cells to combined ATR inhibition and cisplatin treatments. *PLoS One* 10, 1–22. doi:10.1371/journal.pone.0125482
- Moiseyenko, V.M., Dolmatov, G.D., Moiseyenko, F. V., Ivantsov, A.O., Volkov, N.M., Chubenko, V.A., Abduloeva, N.K., Bogdanov, A.A., Sokolenko, A.P., Imyanitov, E.N., 2015. High efficacy of cisplatin neoadjuvant therapy in a prospective series of patients carrying BRCA1 germ-line mutation. *Med. Oncol.* 32, 1–5. doi:10.1007/s12032-015-0514-1
- Moldovan, G.-L., D'Andrea, A.D., 2009. How the Fanconi Anemia pathway guards the genome. *Annu Rev Genet* 43, 223–249. doi:10.1146/annurev-genet-102108-134222.How
- Moscow, J.A., Swanson, C.A., Cowan, K.H., 1993. Decreased melphalan accumulation in a human breast cancer cell line selected for resistance to melphalan. *Br. J. Cancer* 68, 732–737. doi:10.1038/bjc.1993.419
- Moynahan, M.E., Cui, T.Y., Jasin, M., 2001. Homology-directed DNA Repair , Mitomycin-C Resistance , and Chromosome Stability Is Restored with Correction of a Brca1 Mutation Stability Is Restored with Correction of a Brca1 Mutation 1. *Cancer res* 61, 4842–4850.

- Muniandy, P., Liu, J., Majumdar, A., Su-ting Liu, Seidman, M.M., 2010. DNA Interstrand Crosslink Repair in Mammalian Cells: Step by Step. *Crit Rev Biochem Mol Biol.* 45, 23–49. doi:10.3109/10409230903501819.DNA
- Muñoz, I.M., Hain, K., Déclais, A.-C., Gardiner, M., Toh, G.W., Sanchez-Pulido, L., Heuckmann, J.M., Toth, R., Macartney, T., Eppink, B., Kanaar, R., Ponting, C.P., Lilley, D.M.J., Rouse, J., 2009. Coordination of structure-specific nucleases by human SLX4/BTBD12 is required for DNA repair. *Mol. Cell* 35, 116–27. doi:10.1016/j.molcel.2009.06.020
- Nagel-Wolfrum, K., Buerger, C., Wittig, I., Butz, K., Hoppe-seyler, F., Groner, B., 2004. The Interaction of Specific Peptide Aptamers With the DNA Binding Domain and the Dimerization Domain of the Transcription Factor Stat3 Inhibits Transactivation and Induces Apoptosis in Tumor Cells. *Mol. Cancer Res.* 2, 170–182.
- Ni, Z., Lou, W., Leman, E.S., Gao, A.C., 2000. Inhibition of Constitutively Activated Stat3 Signaling Pathway Suppresses Growth of Prostate Cancer Cells Advances in Brief Inhibition of Constitutively Activated Stat3 Signaling Pathway Suppresses Growth of Prostate Cancer Cells 1. *Cancer Res.* 60, 1225–1228.
- Niedernhofer, L.J., 2007. The Fanconi Anemia Signalosome Anchor. *Mol. Cell* 25, 487–490. doi:10.1016/j.molcel.2007.02.002
- Niedernhofer, L.J., Odijk, H., Budzowska, M., Drunen, E. Van, Maas, A., Theil, A.F., Wit, J. De, Jaspers, N.G.J., Beverloo, H.B., Hoeijmakers, J.H.J., Kanaar, R., 2004. The Structure-Specific Endonuclease Ercc1-Xpf Is Required To Resolve DNA Interstrand Cross-Link-Induced Double-Strand Breaks. *Mol. Cell. Biol.* 24, 5776–5787. doi:10.1128/MCB.24.13.5776
- Nishimura, T., Newkirk, K., Sessions, B., Andrews, A., Trock, B., Rasmussen, A., Bischoff, K., Montgomery, A., Cullen, K., 1996. Immunohistochemical Staining for Glutathione S-Transferase Predicts Response to Platinum-based Chemotherapy in Head and Neck Cancer. *Clin. Cancer Res.* 2, 1859–1865.
- Nitiss, J.L., 2009. Targeting DNA topoisomerase II in cancer chemotherapy. *Nat.*

Rev. Cancer 9, 338–350. doi:10.1038/nrc2607

Niu, G., Briggs, J., Deng, J., Ma, Y., Lee, H., Kortylewski, M., Kujawski, M., Kay, H., Cress, W.D., Jove, R., Yu, H., 2008. Signal transducer and activator of transcription 3 is required for hypoxia-inducible factor-1 α RNA expression in both tumor cells and tumor-associated myeloid cells. *Mol. Cancer Res.* 6, 1099–1105. doi:10.1158/1541-7786.MCR-07-2177

Niu, G., Wright, K.L., Huang, M., Song, L., Haura, E., Turkson, J., Zhang, S., Wang, T., Sinibaldi, D., Coppola, D., Heller, R., Ellis, L.M., Karras, J., Bromberg, J., Pardoll, D., Jove, R., 2002. Constitutive Stat3 activity up-regulates VEGF expression and tumor angiogenesis. *Oncogene* 21, 2000–2008. doi:10.1038/sj/onc/1205260

Notarbartolo, M., Poma, P., Perri, D., Dusonchet, L., Cervello, M., D'Alessandro, N., 2005. Antitumor effects of curcumin, alone or in combination with cisplatin or doxorubicin, on human hepatic cancer cells. Analysis of their possible relationship to changes in NF- κ B activation levels and in IAP gene expression. *Cancer Lett.* 224, 53–65. doi:10.1016/j.canlet.2004.10.051

Nouspikel, T., 2009. DNA repair in mammalian cells : Nucleotide excision repair: variations on versatility. *Cell. Mol. Life Sci.* 66, 994–1009. doi:10.1007/s00018-009-8737-y

Oh, D., Han, S., Kim, T., Lee, S., Kim, T., Heo, D., Bang, Y., 2010. A phase I, open-label, nonrandomized trial of OPB-31121, a STAT3 inhibitor, in patients with advanced solid tumors. *J. Clin. Oncol.* 2010 ASCO Annu. Meet. Abstr. 28, e13056.

Olive, P.L., Ban, J.P., Durand, R.E., 1990. DNA Damage and Repair in Tumor Heterogeneity in Radiation-Induced and Normal Cells Measured Using the “ Comet ” Assay. *Radiat. Res.* 122, 86–94.

Olive, P.L., Banáth, J.P., 2004. Phosphorylation of histone H2AX as a measure of radiosensitivity. *Int. J. Radiat. Oncol.* 58, 331–335. doi:10.1016/j.ijrobp.2003.09.028

- Olive, P.L., Banàth, J.P., 2009. Kinetics of H2AX phosphorylation after exposure to cisplatin. *Cytom. Part B - Clin. Cytom.* 76, 79–90. doi:10.1002/cyto.b.20450
- Oostra, A.B., Nieuwint, A.W.M., Joenje, H., De Winter, J.P., 2012. Diagnosis of fanconi anemia: Chromosomal breakage analysis. *Anemia* 2012. doi:10.1155/2012/238731
- Ostling, O., Johanson, K., 1984. Microelectrophoretic study of radiation-induced DNA damages in individual mammalian cells. *Biochem. Biophys. Res. Commun.* 123, 291–298.
- Oyadomari, S., Mori, M., 2004. Roles of CHOP/GADD153 in endoplasmic reticulum stress. *Cell Death Differ.* 11, 381–9. doi:10.1038/sj.cdd.4401373
- Page, B.D.G., Fletcher, S., Yue, P., Li, Z., Zhang, X., Sharmeen, S., Datti, A., Wrana, J.L., Trudel, S., Schimmer, A.D., Turkson, J., Gunning, P.T., 2011. Identification of a non-phosphorylated, cell permeable, small molecule ligand for the Stat3 SH2 domain. *Bioorg. Med. Chem. Lett.* 21, 5605–5609. doi:10.1016/j.bmcl.2011.06.056
- Pan, Y., Zhou, F., Zhang, R., Claret, F.X., 2013. Stat3 inhibitor Stattic exhibits potent antitumor activity and induces chemo- and radio-sensitivity in nasopharyngeal carcinoma. *PLoS One* 8, e54565. doi:10.1371/journal.pone.0054565
- Parsons, P.G., Carter, F.B., Morrison, L., Mary, R., 1981. Mechanism of melphalan resistance developed in vitro in human melanoma cells. *Cancer Res.* 41, 1525–1534.
- Patel, B.B., Sengupta, R., Qazi, S., Vachhani, H., Yu, Y., Rishi, A.K., Majumdar, A.P.N., 2008. Curcumin enhances the effects of 5-fluorouracil and oxaliplatin in mediating growth inhibition of colon cancer cells by modulating EGFR and IGF-1R. *Int. J. Cancer* 122, 267–273. doi:10.1002/ijc.23097
- Patel, K., Kollory, A., Takashima, A., Sarkar, S., Faller, D. V., Ghosh, S.K., 2014. MicroRNA let-7 downregulates STAT3 phosphorylation in pancreatic cancer cells by increasing SOCS3 expression. *Cancer Lett.* 347, 54–64.

doi:10.1016/j.canlet.2014.01.020

Paull, T.T., Rogakou, E.P., Yamazaki, V., Kirchgessner, C.U., Gellert, M., Bonner, W.M., 2000. A critical role for histone H2AX in recruitment of repair factors to nuclear foci after DNA damage. *Curr. Biol.* 10, 886–95.

Pérez-Sayáns, M., Somoza-Martín, J.M., Barros-Angueira, F., Diz, P.G., Rey, J.M.G., García-García, A., 2010. Multidrug resistance in oral squamous cell carcinoma: The role of vacuolar ATPases. *Cancer Lett.* 295, 135–43. doi:10.1016/j.canlet.2010.03.019

Perez, E.A., Hack, F.M., Webber, L.M., Chou, T.C., 1993. Schedule-dependent synergism of edatrexate and cisplatin in combination in the A549 lung-cancer cell line as assessed by median-effect analysis. *Cancer Chemother. Pharmacol.* 33, 245–250. doi:10.1007/BF00686223

Pilati, C., Amessou, M., Bihl, M.P., Balabaud, C., Nhieu, J.T. Van, Paradis, V., Nault, J.C., Izard, T., Bioulac-Sage, P., Couchy, G., Poussin, K., Zucman-Rossi, J., 2011. Somatic mutations activating STAT3 in human inflammatory hepatocellular adenomas. *J. Exp. Med.* 208, 1359–1366. doi:10.1084/jem.20110283

Plimack, E.R., Lorusso, P.M., McCoon, P., Tang, W., Krebs, A.D., Curt, G., Eckhardt, S.G., 2013. AZD1480: a phase I study of a novel JAK2 inhibitor in solid tumors. *Oncologist* 18, 819–20. doi:10.1634/theoncologist.2013-0198

Pommier, Y., Leo, E., Zhang, H., Marchand, C., 2010. DNA topoisomerases and their poisoning by anticancer and antibacterial drugs. *Chem. Biol.* 17, 421–433. doi:10.1016/j.chembiol.2010.04.012

Povirk, L.F., Shuker, D.E., 1994. DNA damage and mutagenesis induced by nitrogen mustards. *Mutat. Res. Genet. Toxicol.* 318, 205–226. doi:10.1016/0165-1110(94)90015-9

Prakash, S., Johnson, R.E., Prakash, L., 2005. Eukaryotic translesion synthesis DNA polymerases: specificity of structure and function. *Annu. Rev. Biochem.* 74, 317–53. doi:10.1146/annurev.biochem.74.082803.133250

- Pranada, A.L., Metz, S., Herrmann, A., Heinrich, P.C., Müller-Newen, G., 2004. Real Time Analysis of STAT3 Nucleocytoplasmic Shuttling. *J. Biol. Chem.* 279, 15114–15123. doi:10.1074/jbc.M312530200
- Rahn, J.J., Adair, G.M., Nairn, R.S., 2010. Multiple Roles of ERCC1-XPF in Mammalian Interstrand Crosslink Repair. *Environ. Mol. Mutagen.* 51, 567–581. doi:10.1002/em
- Rajendran, P., Li, F., Manu, K.A., Shanmugam, M.K., Loo, S.Y., Kumar, A.P., Sethi, G., 2011. γ -Tocotrienol is a novel inhibitor of constitutive and inducible STAT3 signalling pathway in human hepatocellular carcinoma: potential role as an antiproliferative, pro-apoptotic and chemosensitizing agent. *Br. J. Pharmacol.* 163, 283–98. doi:10.1111/j.1476-5381.2010.01187.x
- Rajski, S.R., Williams, R.M., 1998. DNA Cross-Linking Agents as Antitumor Drugs. *Chem. Rev.* 98, 2723–2796. doi:10.1021/cr9800199
- Ram, P.T., Iyengar, R., 2001. G protein coupled receptor signaling through the Src and Stat3 pathway: role in proliferation and transformation. *Oncogene* 20, 1601–6. doi:10.1038/sj.onc.1204186
- Ramana, C. V, Grammatikakis, N., Chernov, M., Nguyen, H., Goh, K.C., Williams, B.R.G., Stark, G.R., 2000. Regulation of c-myc expression by IFN-gamma through Stat1-dependent and -independent pathways. *Embo J* 19, 263–72. doi:10.1093/emboj/19.2.263
- Rath, K.S., Naidu, S.K., Lata, P., Bid, H.K., Rivera, B.K., McCann, G.A., Tierney, B.J., ElNaggar, A.C., Bravo, V., Leone, G., Houghton, P., Hideg, K., Kuppusamy, P., Cohn, D.E., Selvendiran, K., 2014. HO-3867, a safe STAT3 inhibitor, is selectively cytotoxic to ovarian cancer. *Cancer Res.* 74, 2316–2327. doi:10.1158/0008-5472.CAN-13-2433
- Raymond, E., Faivre, S., Chaney, S., Woynarowski, J., Cvitkovic, E., 2002. Cellular and Molecular Pharmacology of Oxaliplatin. *Mol. Cancer Ther.* 1, 227–235.
- Recine, F., Sternberg, C.N., 2015. Hormonal therapy and chemotherapy in hormone-naive and castration resistant prostate cancer. *Transl. Androl. Urol.* 4,

Redell, M.S., Ruiz, M.J., Alonzo, T. a, Gerbing, R.B., Tweardy, D.J., 2011. Stat3 signaling in acute myeloid leukemia: ligand-dependent and -independent activation and induction of apoptosis by a novel small-molecule Stat3 inhibitor. *Blood* 117, 5701–9. doi:10.1182/blood-2010-04-280123

Reed, E., Ozols, R.F., Taronet, R., Yuspat, S.H., Poiriert, M.C., 1987. Platinum-DNA adducts in leukocyte DNA correlate with disease response in ovarian cancer patients receiving platinum-based chemotherapy. *Proc. Natl. Acad. Sci. U. S. A.* 84, 5024–5028.

Reed, E., Yu, J.J., Davies, A., Gannon, J., Armentrout, S.L., 2003. Clear Cell Tumors Have Higher mRNA Levels of ERCC1 and XPB Than Other Histological Types of Epithelial Ovarian Cancer Clear Cell Tumors Have Higher mRNA Levels of ERCC1 and XPB Than Other Histological Types of Epithelial Ovarian Cancer. *Clin. Cancer Res.* 9, 5299–5305.

Regis, G., Pensa, S., Boselli, D., Novelli, F., Poli, V., 2008. Ups and downs: the STAT1:STAT3 seesaw of Interferon and gp130 receptor signalling. *Semin. Cell Dev. Biol.* 19, 351–9. doi:10.1016/j.semcd.2008.06.004

Ren, Z., Cabell, L.A., Schaefer, T.S., McMurray, J.S., 2003. Identification of a high-affinity phosphopeptide inhibitor of Stat3. *Bioorganic Med. Chem. Lett.* 13, 633–636. doi:10.1016/S0960-894X(02)01050-8

Rink, S.M., Hopkins, P.B., 1995. A mechlorethamine-induced DNA interstrand cross-link bends duplex DNA. *Biochemistry* 34, 1439–1445. doi:10.1021/bi00004a039

Rink, S.M., Lipman, R., Alley, S.C., Hopkins, P.B., Tomasz, M., 1996. Bending of DNA by the mitomycin C-induced, GpG intrastrand cross-link. *Chem. Res. Toxicol.* 9, 382–389. doi:10.1021/tx950156q

Risitano, A.M., Marotta, S., Calzone, R., Grimaldi, F., Zatterale, A., 2016. Twenty years of the Italian Fanconi Anemia Registry: where we stand and what remains to be learned. *Haematologica* 101, 319–327.

doi:10.3324/haematol.2015.133520

- Robertson, A.B., Klungland, A., Rognes, T., Leiros, I., 2009. DNA repair in mammalian cells: Base excision repair: the long and short of it. *Cell. Mol. Life Sci.* 66, 981–93. doi:10.1007/s00018-009-8736-z
- Rogakou, E.P., Pilch, D.R., Orr, a. H., Ivanova, V.S., Bonner, W.M., 1998. DNA Double-stranded Breaks Induce Histone H2AX Phosphorylation on Serine 139. *J. Biol. Chem.* 273, 5858–5868. doi:10.1074/jbc.273.10.5858
- Rose, M.C., Huang, R.S., 2014. Pharmacogenomics of Cisplatin Sensitivity in Non-small Cell Lung Cancer. *Genomics. Proteomics Bioinformatics* 12, 198–209. doi:10.1016/j.gpb.2014.10.003
- Rosenberg, B., Van Camp, L., Krigas, T., 1965. Inhibition of Cell Division in *Escherichia coli* by Electrolysis products from a platinum Electrode. *Nature* 205, 698–699.
- Rosenberg, B., Van Camp, L., Trosko, J.E., Mansour, V.H., 1969. Platinum Compounds: a New Class of Potent Antitumour Agents. *Nature* 222, 386–387.
- Rosenbloom, K.R., Sloan, C. a., Malladi, V.S., Dreszer, T.R., Learned, K., Kirkup, V.M., Wong, M.C., Maddren, M., Fang, R., Heitner, S.G., Lee, B.T., Barber, G.P., Harte, R. a., Diekhans, M., Long, J.C., Wilder, S.P., Zweig, a. S., Karolchik, D., Kuhn, R.M., Haussler, D., Kent, W.J., 2013. ENCODE Data in the UCSC Genome Browser: year 5 update. *Nucleic Acids Res.* 41, D56–D63. doi:10.1093/nar/gks1172
- Roskoski, R., 2015. Src protein-tyrosine kinase structure, mechanism, and small molecule inhibitors This paper is dedicated to the memory of Prof. Donald F. Steiner (1930-2014) - Advisor, mentor, and discoverer of proinsulin. *Pharmacol. Res.* 94, 9–25. doi:10.1016/j.phrs.2015.01.003
- Ross, W.E., Ewig, R.A.G., Kohn, K.W., 1978. Differences between melphalan and nitrogen mustard in the formation and removal of DNA cross-links. *Cancer Res.* 38, 1502–1506.

- Ruffner, H., Verma, I.M., 1997. BRCA1 is a cell cycle-regulated nuclear phosphoprotein. *Proc. Natl. Acad. Sci. U. S. A.* 94, 7138–43. doi:10.1073/pnas.94.14.7138
- Sale, J.E., 2012. Competition, collaboration and coordination – determining how cells bypass DNA damage. *J. Cell Sci.* 125, 1633–1643. doi:10.1242/jcs.094748
- Salgado, R., Junius, S., Benoy, I., Van Dam, P., Vermeulen, P., Van Marck, E., Huget, P., Dirix, L.Y., 2003. Circulating interleukin-6 predicts survival in patients with metastatic breast cancer. *Int. J. Cancer* 103, 642–646. doi:10.1002/ijc.10833
- Saltz, L.B., Cox, J. V., Blanke, C., Rosen, L.S., Fehrenbacher, L., Moore, M.J., Maroun, J.A., Ackland, S.P., Locker, P.K., Pirotta, N., Elfring, G.L., Miller, L.L., 2000. Irinotecan plus Fluorouracil and Leucovorin for metastatic colorectal cancer. *N. Engl. J. Med.* 343, 905–914. doi:10.1016/S0140-6736(10)61183-X
- Samimi, G., Safaei, R., Katano, K., Holzer, A.K., Rochdi, M., Tomioka, M., Goodman, M., Howell, S.B., 2004. Increased Expression of the Copper Efflux Transporter ATP7A Mediates Resistance to Cisplatin , Carboplatin , and Oxaliplatin in Ovarian Cancer Cells Increased Expression of the Copper Efflux Transporter ATP7A Mediates Resistance to Cisplatin , Carboplatin 4661–4669.
- San Filippo, J., Sung, P., Klein, H., 2008. Mechanism of eukaryotic homologous recombination. *Annu. Rev. Biochem.* 77, 229–57. doi:10.1146/annurev.biochem.77.061306.125255
- Sanseverino, I., Purificato, C., Gauzzi, M.C., Gessani, S., 2012. Revisiting the specificity of small molecule inhibitors: The example of stattic in dendritic cells. *Chem. Biol.* 19, 1213–1214. doi:10.1016/j.chembiol.2012.08.021
- Santoro, V., Jia, R., Thompson, H., Nijhuis, A., Jeffery, R., Kiakos, K., Silver, A.R., Hartley, J.A., Hochhauser, D., 2015. Role of Reactive Oxygen Species in the Abrogation of Oxaliplatin Activity by Cetuximab in Colorectal Cancer. *J Natl Cancer Inst* 108, 1–11. doi:10.1093/jnci/djv394

- Sarkadi, B., Homolya, L., Szakacs, G., Varadi, A., 2006. Human Multidrug Resistance ABCB and ABCG Transporters: Participation in a Chemoimmunity Defense System. *Physiol Rev* 86, 1179–1236. doi:10.1152/physrev.00037.2005.
- Sasaki, M.S., 1975. Is Fanconi's anaemia defective in a process essential to the repair of DNA cross links? *Nature* 257, 501–503.
- Schlessinger, K., Levy, D.E., 2005. Malignant transformation but not normal cell growth depend on STAT3. *Cancer Res.* 65, 5828–5834.
- Schneider, C. a, Rasband, W.S., Eliceiri, K.W., 2012. NIH Image to ImageJ: 25 years of image analysis. *Nat. Methods* 9, 671–675. doi:10.1038/nmeth.2089
- Schuringa, J.J., Wierenga, a T., Kruijer, W., Vellenga, E., 2000. Constitutive Stat3, Tyr705, and Ser727 phosphorylation in acute myeloid leukemia cells caused by the autocrine secretion of interleukin-6. *Blood* 95, 3765–3770.
- Schust, J., Sperl, B., Hollis, A., Mayer, T.U., Berg, T., 2006. Stattic: a small-molecule inhibitor of STAT3 activation and dimerization. *Chem. Biol.* 13, 1235–42. doi:10.1016/j.chembiol.2006.09.018
- Scuto, A., Krejci, P., Popplewell, L., Wu, J., Wang, Y., Kujawski, M., Kowolik, C., Xin, H., Yen, Y., Forman, S., Jove, R., 2011. The novel JAK inhibitor AZD1480 blocks STAT3 and FGFR3 signaling, resulting in suppression of human myeloma cell growth and survival. *Leukemia* 25, 538–550. doi:10.1038/leu.2010.289.The
- Seavey, M.M., Dobrzanski, P., 2012. The many faces of Janus kinase. *Biochem. Pharmacol.* 83, 1136–45. doi:10.1016/j.bcp.2011.12.024
- Selvendiran, K., Ahmed, S., Dayton, A., Kuppusamy, M.L., Rivera, B.K., Kálai, T., Hideg, K., Kuppusamy, P., 2011. HO-3867, a curcumin analog, sensitizes cisplatin-resistant ovarian carcinoma, leading to therapeutic synergy through STAT3 inhibition. *Cancer Biol. Ther.* 12, 837–45. doi:10.4161/cbt.12.9.17713
- Selvendiran, K., Tong, L., Bratasz, A., Kuppusamy, M.L., Ahmed, S., Ravi, Y., Trigg,

- N.J., Rivera, B.K., Kálai, T., Hideg, K., Kuppusamy, P., 2010. Anticancer efficacy of a difluorodiarlylidenyl piperidone (HO-3867) in human ovarian cancer cells and tumor xenografts. *Mol. Cancer Ther.* 9, 1169–79. doi:10.1158/1535-7163.MCT-09-1207
- Sen, B., Saigal, B., Parikh, N., Gallick, G., Johnson, F.M., 2009. Sustained Src Inhibition Results in STAT3 Activation and Cancer Cell Survival via Altered JAK-STAT3 Binding. *Cancer Res.* 69, 1958–1965. doi:10.1158/0008-5472.CAN-08-2944.Sustained
- Sen, M., Thomas, S.M., Kim, S., Yeh, J.I., Ferris, R.L., Johnson, J.T., Duvvuri, U., Lee, J., Sahu, N., Joyce, S., Freilino, M.L., Shi, H., Li, C., Ly, D., Rapireddy, S., Etter, J.P., Li, P.-K., Wang, L., Chiosea, S., Seethala, R.R., Gooding, W.E., Chen, X., Kaminski, N., Pandit, K., Johnson, D.E., Grandis, J.R., 2012. First-in-human trial of a STAT3 decoy oligonucleotide in head and neck tumors: implications for cancer therapy. *Cancer Discov.* 2, 694–705. doi:10.1158/2159-8290.CD-12-0191
- Sengerová, B., Wang, A.T., McHugh, P.J., 2011. Orchestrating the nucleases involved in DNA interstrand cross-link (ICL) repair. *Cell Cycle* 10, 3999–4008. doi:10.4161/cc.10.23.18385
- Shay, J.W., Wright, W.E., 2000. Hayflick, his limit, and cellular ageing. *Nat. Rev. Mol. Cell Biol.* 1, 72–76.
- Shehzad, A., Lee, J., Lee, Y.S., 2012. Curcumin in various cancers. *Biofactors* 39, 56–68. doi:10.1002/biof.1068
- Shen, C., Oswald, D., Phelps, D., Cam, H., Pelloski, C.E., Pang, Q., Houghton, P.J., 2013. Regulation of FANCD2 by the mTOR pathway contributes to the resistance of cancer cells to DNA double-strand breaks. *Cancer Res.* 73, 3393–3401. doi:10.1158/0008-5472.CAN-12-4282
- Shin, D.S., Kim, H.N., Shin, K.D., Yoon, Y.J., Kim, S.J., Han, D.C., Kwon, B.M., 2009. Cryptotanshinone inhibits constitutive signal transducer and activator of transcription 3 function through blocking the dimerization in DU145 prostate cancer cells. *Cancer Res.* 69, 193–202. doi:10.1158/0008-5472.CAN-08-2575

- Siddik, Z.H., 2003. Cisplatin: mode of cytotoxic action and molecular basis of resistance. *Oncogene* 22, 7265–79. doi:10.1038/sj.onc.1206933
- Siddiquee, K., Zhang, S., Guida, W.C., Blaskovich, M. a, Greedy, B., Lawrence, H.R., Yip, M.L.R., Jove, R., McLaughlin, M.M., Lawrence, N.J., Sebt, S.M., Turkson, J., 2007. Selective chemical probe inhibitor of Stat3, identified through structure-based virtual screening, induces antitumor activity. *Proc. Natl. Acad. Sci. U. S. A.* 104, 7391–6. doi:10.1073/pnas.0609757104
- Silva, C.M., 2004. Role of STATs as downstream signal transducers in Src family kinase-mediated tumorigenesis. *Oncogene* 23, 8017–23. doi:10.1038/sj.onc.1208159
- Sinden, R.R., Hagerman, P.J., 1984. Interstrand psoralen cross-links do not introduce appreciable bends in DNA. *Biochemistry* 23, 6299–6303. doi:10.1021/bi00321a002
- Smeaton, M.B., Hlavin, E.M., Mason, T.M., Noronha, A.M., Wilds, C.J., Miller, P.S., 2008. Distortion-dependent unhooking of interstrand cross-links in mammalian cell extracts. *Biochemistry* 16, 9920–9930. doi:10.1038/nmeth.2250.Digestion
- Smetsers, S., Muter, J., Bristow, C., Patel, L., Chandler, K., Bonney, D., Wynn, R.F., Whetton, A.D., Will, A.M., Rockx, D., Joenje, H., Strathdee, G., Meyer, S., 2012. Heterozygote FANCD2 mutations associated with childhood T Cell ALL and testicular seminoma. *Fam. Cancer* 11, 661–665. doi:10.1007/s10689-012-9553-3
- Smogorzewska, A., Desetty, R., Saito, T.T., Schlabach, M., Lach, F.P., Sowa, M.E., Clark, A.B., Kunkel, T. a, Harper, J.W., Colaiácovo, M.P., Elledge, S.J., 2010. A genetic screen identifies FAN1, a Fanconi anemia-associated nuclease necessary for DNA interstrand crosslink repair. *Mol. Cell* 39, 36–47. doi:10.1016/j.molcel.2010.06.023
- Soldani, C., Scovassi, A.I., 2002. Poly (ADP-ribose) polymerase-1 cleavage during apoptosis : An update *Cell death mechanisms : Necrosis and apoptosis* 7, 321–328.

- Song, H., Wang, R., Wang, S., Lin, J., 2005. A low-molecular-weight compound discovered through virtual database screening inhibits Stat3 function in breast cancer cells. *Proc. Natl. Acad. Sci. U. S. A.* 102, 4700–5. doi:10.1073/pnas.0409894102
- Song, L., Turkson, J., Karras, J.G., Jove, R., Haura, E.B., 2003. Activation of Stat3 by receptor tyrosine kinases and cytokines regulates survival in human non-small cell carcinoma cells. *Oncogene* 22, 4150–65. doi:10.1038/sj.onc.1206479
- Souissi, I., Najjar, I., Ah-Koon, L., Schischmanoff, P.O., Lesage, D., Le Coquil, S., Roger, C., Dusanter-Fourt, I., Varin-Blank, N., Cao, A., Metelev, V., Baran-Marszak, F., Fagard, R., 2011. A STAT3-decoy oligonucleotide induces cell death in a human colorectal carcinoma cell line by blocking nuclear transfer of STAT3 and STAT3-bound NF- κ B. *BMC Cell Biol.* 12, 14. doi:10.1186/1471-2121-12-14
- Sousa, M.M.L., Zub, K.A., Aas, P.A., Hanssen-Bauer, A., Demirovic, A., Sarno, A., Tian, E., Liabakk, N.B., Slupphaug, G., 2013. An Inverse Switch in DNA Base Excision and Strand Break Repair Contributes to Melphalan Resistance in Multiple Myeloma Cells. *PLoS One* 8. doi:10.1371/journal.pone.0055493
- Spanswick, V.J., Craddock, C., Sekhar, M., Mahendra, P., Shankaranarayana, P., Hughes, R.G., Hochhauser, D., Hartley, J. a, 2002. Repair of DNA interstrand crosslinks as a mechanism of clinical resistance to melphalan in multiple myeloma. *Blood* 100, 224–9.
- Spanswick, V.J., Hartley, J.M., Hartley, J.A., 2010. Measurement of DNA Interstrand Crosslinking in Individual Cells Using the Single Cell Gel Electrophoresis (Comet) Assay. *Drug-DNA Interact. Protoc. Methods Mol. Biol., Methods in Molecular Biology* 613, 267–282. doi:10.1007/978-1-60327-418-0
- Spanswick, V.J., Lowe, H.L., Newton, C., Bingham, J.P., Bagnobianchi, A., Kiakos, K., Craddock, C., Ledermann, J. a, Hochhauser, D., Hartley, J. a, 2012. Evidence for different mechanisms of “unhooking” for melphalan and cisplatin-induced DNA interstrand cross-links in vitro and in clinical acquired resistant tumour samples. *BMC Cancer* 12, 436. doi:10.1186/1471-2407-12-436

- Sreekanth, C.N., Bava, S. V, Sreekumar, E., Anto, R.J., 2011. Molecular evidences for the chemosensitizing efficacy of liposomal curcumin in paclitaxel chemotherapy in mouse models of cervical cancer. *Oncogene* 30, 3139–52. doi:10.1038/onc.2011.23
- Sreenivasan, S., Krishnakumar, S., 2014. Synergistic Effect of Curcumin in Combination with Anticancer Agents in Human Retinoblastoma Cancer Cells Lines. *Curr. Eye Res.* 3683, 1–13. doi:10.3109/02713683.2014.987870
- Steinman, R. a, Wentzel, A., Lu, Y., Stehle, C., Grandis, J.R., 2003. Activation of Stat3 by cell confluence reveals negative regulation of Stat3 by cdk2. *Oncogene* 22, 3608–15. doi:10.1038/sj.onc.1206523
- Stephanou, A., Brar, B.K., Knight, R.A., Latchman, D.S., 2000. Opposing actions of STAT-1 and STAT-3 on the Bcl-2 and Bcl-x promoters. *Cell Death.Differ.* 7, 329–330.
- Stewart, D.J., 2007. Mechanisms of resistance to cisplatin and carboplatin. *Crit. Rev. Oncol. Hematol.* 63, 12–31. doi:10.1016/j.critrevonc.2007.02.001
- Stordal, B., Hamon, M., McEneaney, V., Roche, S., Gillet, J.P., O’Leary, J.J., Gottesman, M., Clynes, M., 2012. Resistance to paclitaxel in a cisplatin-resistant ovarian cancer cell line is mediated by P-glycoprotein. *PLoS One* 7. doi:10.1371/journal.pone.0040717
- Stratton, M.R., 2013. Journeys into the genome of cancer cells. *EMBO Mol. Med.* 5, 169–172. doi:10.1002/emmm.201202388
- Stratton, M.R., 2011. Exploring the genomes of cancer cells: progress and promise. *Science* 331, 1553–8. doi:10.1126/science.1204040
- Suhasini, A.N., Brosh, R.M., 2012. Fanconi anemia and Bloom’s syndrome crosstalk through FANCD1-BLM helicase interaction. *Trends Genet.* 28, 7–13. doi:10.1016/j.tig.2011.09.003
- Suiqing, C., Min, Z., Lirong, C., 2005. Overexpression of phosphorylated-STAT3 correlated with the invasion and metastasis of cutaneous squamous cell

carcinoma. *J. Dermatol.* 32, 354–60. doi:10.1111/j.1346-8138.2005.tb00906.x

Sunada, H., Magun, B.E., Mendelsohn, J., MacLeod, C.L., 1986. Monoclonal antibody against epidermal growth factor receptor is internalized without stimulating receptor phosphorylation. *Proc. Natl. Acad. Sci. U. S. A.* 83, 3825–9.

Sunters, A., Springer, C.J., Bagshawe, K.D., Souhami, R.L., Hartley, J.A., 1992. The cytotoxicity, DNA crosslinking ability and DNA sequence selectivity of the aniline mustards melphalan, chlorambucil and 4-[bis(2-chloroethyl)amino] benzoic acid. *Biochem. Pharmacol.* 44, 59–64. doi:10.1016/0006-2952(92)90038-K

Szelag, M., Czerwoniec, A., Wesoly, J., Bluysen, H. a. R., 2015. Identification of STAT1 and STAT3 Specific Inhibitors Using Comparative Virtual Screening and Docking Validation. *PLoS One* 10, e0116688. doi:10.1371/journal.pone.0116688

Takeda, K., Koichi, N., Wei, S., Takashi, T., Matsumoto, M., Nobuaki, Y., Tadimitsu, K., Shizuo, A., 1997. Targeted disruption of the mouse Stat 3 gene leads to early embryonic lethality. *Proc. Natl. Acad. Sci. U. S. A.* 94, 3801–3804.

Talmadge, J.E., Fidler, I.J., 2010. AACR centennial series: The biology of cancer metastasis: Historical perspective. *Cancer Res.* 70, 5649–5669. doi:10.1158/0008-5472.CAN-10-1040

Taniguchi, T., Garcia-Higuera, I., Andreassen, P.R., Gregory, R.C., Grompe, M., D'Andrea, A.D., 2002. S-phase-specific interaction of the Fanconi anemia protein, FANCD2, with BRCA1 and RAD51. *Blood* 100, 2414–20. doi:10.1182/blood-2002-01-0278

Taniguchi, T., Tischkowitz, M., Ameziane, N., Hodgson, S. V, Mathew, C.G., Joenje, H., Mok, S.C., D'Andrea, A.D., 2003. Disruption of the Fanconi anemia-BRCA pathway in cisplatin-sensitive ovarian tumors. *Nat. Med.* 9, 568–74. doi:10.1038/nm852

- Teng, J., Gong, D., Han, Z., Wei, X., Yan, Y., Ye, F., Ding, W., 2013. Abrogation of Constitutive Stat3 Activity Circumvents Cisplatin Resistant Ovarian Cancer. *Cancer Lett.*
- Tewey, K., Rowe, T., Yang, L., Halligan, B., Liu, L., 1984. Adriamycin-Induced DNA Damage Mediated by Mammalian DNA Topoisomerase II. *Science* 226, 466–8.
- Thomas, A., Pommier, Y., 2016. Small cell lung cancer: Time to revisit DNA-damaging chemotherapy. *Sci. Transl. Med.* 8, 1–4.
- Thomas, S.J., Snowden, J.A., Zeidler, M.P., Danson, S.J., 2015. The role of JAK/STAT signalling in the pathogenesis, prognosis and treatment of solid tumours. *Br. J. Cancer* 113, 365–371. doi:10.1038/bjc.2015.233
- Thorn, C., Oshiro, C., Marsh, S., Hernandez-Boussard, T., McLeod, H., Klein, T., Altman, R., 2011. Doxorubicin pathways: pharmacodynamics and adverse effects. *Pharmacogenet Genomics* 21, 440–446. doi:10.1097/FPC.0b013e32833ffb56.Doxorubicin
- Tian, Y., Paramasivam, M., Ghosal, G., Chen, D., Shen, X., Huang, Y., Akhter, S., 2015. UHRF1 Contributes to DNA Damage Repair as a Lesion Recognition Factor and Nuclease Scaffold Report UHRF1 Contributes to DNA Damage Repair as a Lesion Recognition Factor and Nuclease Scaffold. *CellReports* 10, 1957–1966. doi:10.1016/j.celrep.2015.03.038
- Timofeeva, O.A., Gaponenko, V., Lockett, S.J., Tarasov, S.G., Jiang, S., Michejda, C.J., Perantoni, A.O., Tarasova, N.I., 2007. Rationally designed inhibitors identify STAT3 N-domain as a promising anticancer drug target. *ACS Chem. Biol.* 2, 799–809. doi:10.1021/cb700186x
- Ting, S., Mairinger, F.D., Hager, T., Welter, S., Eberhardt, W.E., Wohlschlaeger, J., Schmid, K.W., Christoph, D.C., 2013. ERCC1, MLH1, MSH2, MSH6, and β III-tubulin: resistance proteins associated with response and outcome to platinum-based chemotherapy in malignant pleural mesothelioma. *Clin. Lung Cancer* 14, 558–567. doi:10.1016/j.clc.2013.04.013
- Todor, I.N., Lukyanova, N.Y., Chekhun, V.F., 2012. THE LIPID CONTENT OF

CISPLATIN- AND DOXORUBICIN- RESISTANT MCF-7 HUMAN BREAST
CANCER CELLS 2012, 97–100.

- Tomoda, Y., Katsura, M., Okajima, M., Hosoya, N., Kohno, N., Miyagawa, K., 2009. Functional evidence for Eme1 as a marker of cisplatin resistance. *Int. J. Cancer* 124, 2997–3001. doi:10.1002/ijc.24268
- Toyonaga, T., Nakano, K., Nagano, M., Zhao, G., Yamaguchi, K., Kuroki, S., Eguchi, T., Chijiwa, K., Tsuneyoshi, M., Tanaka, M., 2003. Blockade of constitutively activated Janus kinase/signal transducer and activator of transcription-3 pathway inhibits growth of human pancreatic cancer. *Cancer Lett.* 201, 107–116. doi:10.1016/S0304-3835(03)00482-8
- Trowbridge, K., McKim, K., Brill, S.J., Sekelsky, J., 2007. Synthetic lethality of *Drosophila* in the absence of the MUS81 endonuclease and the DmBlm helicase is associated with elevated apoptosis. *Genetics* 176, 1993–2001. doi:10.1534/genetics.106.070060
- Tseng, L.-M., Huang, P.-I., Chen, Y.-R., Chen, Y.-C., Chou, Y.-C., Chen, Y.-W., Chang, Y.-L., Hsu, H.-S., Lan, Y.-T., Chen, K.-H., Chi, C.-W., Chiou, S.-H., Yang, D.-M., Lee, C.-H., 2012. Targeting signal transducer and activator of transcription 3 pathway by cucurbitacin I diminishes self-renewing and radiochemoresistant abilities in thyroid cancer-derived CD133+ cells. *J. Pharmacol. Exp. Ther.* 341, 410–23. doi:10.1124/jpet.111.188730
- Uehara, Y., Mochizuki, M., Matsuno, K., Haino, T., Asai, A., 2009. Novel high-throughput screening system for identifying STAT3-SH2 antagonists. *Biochem. Biophys. Res. Commun.* 380, 627–31. doi:10.1016/j.bbrc.2009.01.137
- Untergasser, A., Cutcutache, I., Koressaar, T., Ye, J., Faircloth, B.C., Remm, M., Rozen, S.G., 2012. Primer3-new capabilities and interfaces. *Nucleic Acids Res.* 40, e115. doi:10.1093/nar/gks596
- Urakami, T.M., Hibuya, I.S., Se, T.I., Hen, Z.C., Kiyama, S.A., Akagawa, M.N., Zumi, H.I., 2001. ELEVATED EXPRESSION OF VACUOLAR PROTON PUMP GENES AND CELLULAR PH IN CISPLATIN RESISTANCE 874, 869–874.

- Vaezi, a., Wang, X., Buch, S., Gooding, W., Wang, L., Seethala, R.R., Weaver, D.T., D'Andrea, a. D., Argiris, a., Romkes, M., Niedernhofer, L.J., Grandis, J.R., 2011. XPF Expression Correlates with Clinical Outcome in Squamous Cell Carcinoma of the Head and Neck. *Clin. Cancer Res.* 17, 5513–5522. doi:10.1158/1078-0432.CCR-11-0086
- Valerie, K., Povirk, L.F., 2003. Regulation and mechanisms of mammalian double-strand break repair. *Oncogene* 22, 5792–5812. doi:10.1038/sj.onc.1206679
- Vander Heiden, M., Cantley, L., Thompson, C., 2009. Understanding the Warburg effect: The metabolic Requirements of cell proliferation. *Science* 324, 1029–1033. doi:10.1126/science.1160809.Understanding
- Vaz, F., Hanenberg, H., Schuster, B., Barker, K., Wiek, C., Erven, V., Neveling, K., Endt, D., Kesterton, I., Autore, F., Fraternali, F., Freund, M., Hartmann, L., Grimwade, D., Roberts, R.G., Schaal, H., Mohammed, S., Rahman, N., Schindler, D., Mathew, C.G., 2010. Mutation of the RAD51C gene in a Fanconi anemia-like disorder. *Nat. Genet.* 42, 406–9. doi:10.1038/ng.570
- Vermorken, J.B., Vijdh, W. van der, Klein, I., A, H., H, G., H, P., 1984. Pharmacokinetics of Free and Total Platinum species after Short-Term infusion of Cisplatin. *Cancer Treat Rep* 68, 505–513.
- Vigneron, A., Gamelin, E., Coqueret, O., 2008. The EGFR-STAT3 oncogenic pathway up-regulates the Eme1 endonuclease to reduce DNA damage after topoisomerase I inhibition. *Cancer Res.* 68, 815–25. doi:10.1158/0008-5472.CAN-07-5115
- Vistica, D.T., Rabon, A., Rabinovitz, M., 1979. Amino acid conferred protection against melphalan interference with melphalan therapy by L-leucine, a competitive substrate for transport. *Cancer Lett.* 6, 7–13.
- Walden, H., Deans, A.J., 2014. The Fanconi anemia DNA repair pathway: structural and functional insights into a complex disorder. *Annu. Rev. Biophys.* 43, 257–78. doi:10.1146/annurev-biophys-051013-022737
- Walsh, C.S., 2015. Two decades beyond BRCA1/2: Homologous recombination,

hereditary cancer risk and a target for ovarian cancer therapy. *Gynecol. Oncol.* 137, 343–350. doi:10.1016/j.ygyno.2015.02.017

Wang, A.T., Sengerová, B., Cattell, E., Inagawa, T., Hartley, J.M., Kiakos, K., Burgess-Brown, N. a, Swift, L.P., Enzlin, J.H., Schofield, C.J., Gileadi, O., Hartley, J. a, McHugh, P.J., 2011. Human SNM1A and XPF-ERCC1 collaborate to initiate DNA interstrand cross-link repair. *Genes Dev.* 25, 1859–70. doi:10.1101/gad.15699211

Wang, B.-Y., Zhang, J., Wang, J.-L., Sun, S., Wang, Z.-H., Wang, L.-P., Zhang, Q.-L., Lv, F.-F., Cao, E.-Y., Shao, Z.-M., Fais, S., Hu, X.-C., 2015. Intermittent high dose proton pump inhibitor enhances the antitumor effects of chemotherapy in metastatic breast cancer. *J. Exp. Clin. Cancer Res.* 34, 85. doi:10.1186/s13046-015-0194-x

Wang, S., Cang, S., Liu, D., 2016. Third-generation inhibitors targeting EGFR T790M mutation in advanced non-small cell lung cancer. *J. Hematol. Oncol.* 9, 34. doi:10.1186/s13045-016-0268-z

Wang, S., Zhang, H., Cheng, L., Evans, C., Pan, C.X., 2010. Analysis of the cytotoxic activity of carboplatin and gemcitabine combination. *Anticancer Res.* 30, 4573–4578.

Wang, X., Andreassen, P.R., Andrea, A.D.D., 2004. Functional Interaction of Monoubiquitinated FANCD2 and BRCA2 / FANCD1 in Chromatin. *Mol. Cell. Biol.* 24, 5850–5862. doi:10.1128/MCB.24.13.5850

Waters, L.S., Minesinger, B.K., Wiltrot, M.E., D'Souza, S., Woodruff, R. V, Walker, G.C., 2009. Eukaryotic translesion polymerases and their roles and regulation in DNA damage tolerance. *Microbiol. Mol. Biol. Rev.* 73, 134–154. doi:10.1128/MMBR.00034-08

Watson, J.D., Crick, F.H.C., 1953. A structure for deoxyribose nucleic acid. *Nature* 171, 737–738.

Weinandy, A., Piroth, M.D., Goswami, A., Nolte, K., Sellhaus, B., Gerardo-Nava, J., Eble, M., Weinandy, S., Cornelissen, C., Clusmann, H., Luscher, B., Weis, J.,

2014. Cetuximab induces eme1-mediated DNA repair: A novel mechanism for cetuximab resistance. *Neoplasia (United States)* 16, 207–220. doi:10.1016/j.neo.2014.03.004
- Weinstein, I.B., 2002. Cancer. Addiction to oncogenes--the Achilles heel of cancer. *Science* 297, 63–4. doi:10.1126/science.1073096
- Wen, Z., Darnell, J.E., 1997. Mapping of Stat3 serine phosphorylation to a single residue (727) and evidence that serine phosphorylation has no influence on DNA binding of Stat1 and Stat3. *Nucleic Acids Res.* 25, 2062–7.
- Weterings, E., Chen, D.J., 2008. The endless tale of non-homologous end-joining. *Cell Res.* 18, 114–24. doi:10.1038/cr.2008.3
- Wiejak, J., Dunlop, J., Mackay, S.P., Yarwood, S.J., 2013. Flavanoids induce expression of the suppressor of cytokine signalling 3 (SOCS3) gene and suppress IL-6-activated signal transducer and activator of transcription 3 (STAT3) activation in vascular endothelial cells. *Biochem. J.* 454, 283–93. doi:10.1042/BJ20130481
- Williams, J., Lucas, P.C., Griffith, K. a, Choi, M., Fogoros, S., Hu, Y.Y., Liu, J.R., 2005. Expression of Bcl-xL in ovarian carcinoma is associated with chemoresistance and recurrent disease. *Gynecol. Oncol.* 96, 287–95. doi:10.1016/j.ygyno.2004.10.026
- Williams, S. a, Wilson, J.B., Clark, A.P., Mitson-Salazar, A., Tomashevski, A., Ananth, S., Glazer, P.M., Semmes, O.J., Bale, A.E., Jones, N.J., Kupfer, G.M., 2011. Functional and physical interaction between the mismatch repair and FA-BRCA pathways. *Hum. Mol. Genet.* 20, 4395–410. doi:10.1093/hmg/ddr366
- Wilson, D.M., Seidman, M.M., 2010. A novel link to base excision repair? *Trends Biochem. Sci.* 35, 247–252. doi:10.1016/j.tibs.2010.01.003
- Wiseman, H., Halliwell, B., 1996. Damage to DNA by reactive oxygen and nitrogen species: role in inflammatory disease and progression to cancer. *Biochem. J.* 313 (Pt 1, 17–29.

- Wormald, S., Hilton, D.J., 2004. Inhibitors of cytokine signal transduction. *J. Biol. Chem.* 279, 821–4. doi:10.1074/jbc.R300030200
- Wu, F., Shirahata, A., Sakuraba, K., Kitamura, Y., Goto, T., Saito, M., Ishibashi, K., Kigawa, G., Nemoto, H., Sanada, Y., Hibi, K., 2011. Down-regulation of MUS81 as a novel prognostic biomarker for patients with colorectal cancer. *Cancer Sci.* 102, 472–477. doi:10.1111/j.1349-7006.2010.01790.x
- Wu, J., Clingen, P.H., Spanswick, V.J., Mellinas-Gomez, M., Meyer, T., Puzanov, I., Jodrell, D., Hochhauser, D., Hartley, J. a, 2013. γ -H2AX Foci Formation as a Pharmacodynamic Marker of DNA Damage Produced by DNA Cross-Linking Agents: Results from 2 Phase I Clinical Trials of SJG-136 (SG2000). *Clin. Cancer Res.* 19, 721–30. doi:10.1158/1078-0432.CCR-12-2529
- Wu, J.H., Wilson, J.B., Wolfreys, A.M., Scott, A., Jones, N.J., 2009. Optimization of the comet assay for the sensitive detection of PUVA-induced DNA interstrand cross-links. *Mutagenesis* 24, 173–81. doi:10.1093/mutage/gen068
- Wu, Q., Vasquez, K.M., 2008. Human MLH1 protein participates in genomic damage checkpoint signaling in response to DNA interstrand crosslinks, while MSH2 functions in DNA repair. *PLoS Genet.* 4, e1000189. doi:10.1371/journal.pgen.1000189
- Wu, S. gin, Liu, Y. nan, Tsai, M. feng, Chang, Y. leong, Yu, C. jen, 2016. The mechanism of acquired resistance to irreversible EGFR tyrosine kinase inhibitor-afatinib in lung adenocarcinoma patients. *Oncotarget* 7, 12404–12413.
- Wu, W.Y., Li, J., Wu, Z.-S., Zhang, C.-L., Meng, X.-L., 2011. STAT3 activation in monocytes accelerates liver cancer progression. *BMC Cancer* 11, 506. doi:10.1186/1471-2407-11-506
- Wynne, P., Newton, C., Ledermann, J. a, Olaitan, a, Mould, T. a, Hartley, J. a, 2007. Enhanced repair of DNA interstrand crosslinking in ovarian cancer cells from patients following treatment with platinum-based chemotherapy. *Br. J. Cancer* 97, 927–33. doi:10.1038/sj.bjc.6603973
- Xiao, H., Bid, H.K., Jou, D., Wu, X., Yu, W., Li, C., Houghton, P.J., Lin, J., 2015. A

novel small molecular STAT3 inhibitor, LY5, inhibits cell viability, cell migration, and angiogenesis in medulloblastoma cells. *J. Biol. Chem.* 290, 3418–3429. doi:10.1074/jbc.M114.616748

Xie, S., Zheng, H., Wen, X., Sun, J., Wang, Y., Gao, X., Guo, L., Lu, R., 2016. MUS81 is associated with cell proliferation and sensitivity to cisplatin in serous ovarian cancer. *Biochem. Biophys. Res. Commun.* 1–8. doi:10.1016/j.bbrc.2016.05.152

Xu, L., Li, H., Wang, Y., Dong, F., Wang, H., Zhang, S., 2014. Enhanced activity of doxorubicin in drug resistant A549 tumor cells by encapsulation of P-glycoprotein inhibitor in PLGA-based nanovectors. *Oncol. Lett.* 7, 387–392. doi:10.3892/ol.2013.1711

Xu, Q., Briggs, J., Park, S., Niu, G., Kortylewski, M., Zhang, S., Gritsko, T., Turkson, J., Kay, H., Semenza, G.L., Cheng, J.Q., Jove, R., Yu, H., 2005. Targeting Stat3 blocks both HIF-1 and VEGF expression induced by multiple oncogenic growth signaling pathways. *Oncogene* 24, 5552–60. doi:10.1038/sj.onc.1208719

Xu, X., Kasembeli, M.M., Jiang, X., Twardy, B.J., Twardy, D.J., 2009. Chemical probes that competitively and selectively inhibit Stat3 activation. *PLoS One* 4, e4783. doi:10.1371/journal.pone.0004783

Yakata, Y., Nakayama, T., Yoshizaki, A., Kusaba, T., Inoue, K., Sekine, I., 2007. Expression of p-STAT3 in human gastric carcinoma: Significant correlation in tumour invasion and prognosis. *Int. J. Oncol.* 30, 437–442.

Yallapu, M.M., Maher, D.M., Sundram, V., Bell, M.C., Jaggi, M., Chauhan, S.C., 2010. Curcumin induces chemo/radio-sensitization in ovarian cancer cells and curcumin nanoparticles inhibit ovarian cancer cell growth. *J. Ovarian Res.* 3, 11. doi:10.1186/1757-2215-3-11

Yamamoto, K.N., Kobayashi, S., Tsuda, M., Kurumizaka, H., Takata, M., Kono, K., 2011. Involvement of SLX4 in interstrand cross-link repair is regulated by the Fanconi anemia pathway. *PNAS* 108, 6492–6496. doi:10.1073/pnas.1018487108/-

- Yan, C., Higgins, P.J., 2013. Drugging the undruggable: Transcription therapy for cancer. *Biochim. Biophys. Acta - Rev. Cancer* 1835, 76–85. doi:10.1016/j.bbcan.2012.11.002
- Yan, W., Li, R., He, J., Du, J., Hou, J., 2015. Importin β 1 mediates nuclear factor- κ B signal transduction into the nuclei of myeloma cells and affects their proliferation and apoptosis. *Cell. Signal.* 27, 851–859. doi:10.1016/j.cellsig.2015.01.013
- Yang, E., Lerner, L., Besser, D., Darnell, J.E., 2003. Independent and cooperative activation of chromosomal c-fos promoter by STAT3. *J. Biol. Chem.* 278, 15794–15799. doi:10.1074/jbc.M213073200
- Yang, T., Chen, M., Chen, T., Thakur, A., 2015. Expression of the copper transporters hCtr1, ATP7A and ATP7B is associated with the response to chemotherapy and survival time in patients with resected non-small cell lung cancer. *Oncol. Lett.* 10, 2584–2590. doi:10.3892/ol.2015.3531
- Yarde, D.N., Oliveira, V., Mathews, L., Wang, X., Villagra, A., Boulware, D., Shain, K.H., Hazlehurst, L.A., Alsina, M., Chen, D.T., Beg, A.A., Dalton, W.S., 2009. Targeting the Fanconi anemia/BRCA pathway circumvents drug resistance in multiple myeloma. *Cancer Res.* 69, 9367–9375. doi:10.1158/0008-5472.CAN-09-2616
- Ye, M.-X., Zhao, Y.-L., Li, Y., Miao, Q., Li, Z.-K., Ren, X.-L., Song, L.-Q., Yin, H., Zhang, J., 2012. Curcumin reverses cis-platin resistance and promotes human lung adenocarcinoma A549/DDP cell apoptosis through HIF-1 α and caspase-3 mechanisms. *Phytomedicine* 19, 779–87. doi:10.1016/j.phymed.2012.03.005
- Yin, Z., Zhang, Y., Li, Y., Lv, T., Liu, J., Wang, X., 2012. Prognostic significance of STAT3 expression and its correlation with chemoresistance of non-small cell lung cancer cells. *Acta Histochem.* 114, 151–8. doi:10.1016/j.acthis.2011.04.002
- Yoshikawa, H., Matsubara, K., Qian, G.S., Jackson, P., Groopman, J.D., Manning,

- J.E., Harris, C.C., Herman, J.G., 2001. SOCS-1, a negative regulator of the JAK/STAT pathway, is silenced by methylation in human hepatocellular carcinoma and shows growth-suppression activity. *Nat. Genet.* 28, 29–35. doi:10.1038/88225
- Yoshimura, A., Naka, T., Kubo, M., 2007. SOCS proteins, cytokine signalling and immune regulation. *Nat. Rev. Immunol.* 7, 454–465. doi:10.1038/nri2093
- Youds, J.L., Boulton, S.J., 2011. The choice in meiosis - defining the factors that influence crossover or non-crossover formation. *J. Cell Sci.* 124, 501–13. doi:10.1242/jcs.074427
- Yu, S., Li, G., Wang, Z., Wang, Z., Chen, C., Cai, S., He, Y., 2015. The prognostic value of pSTAT3 in gastric cancer: a meta-analysis. *J. Cancer Res. Clin. Oncol.* 649–657. doi:10.1007/s00432-015-2023-1
- Yu, X., Wu, Z., Fenselau, C., 1995. Covalent sequestration of melphalan by metallothionein and selective alkylation of cysteines. *Biochemistry* 34, 3377–3385.
- Yuan, L., Sumpter, B.G., Abboud, K. a., Castellano, R.K., 2008. Links between through-bond interactions and assembly structure in simple piperidones. *New J. Chem.* 32, 1924. doi:10.1039/b808818g
- Yun, C.-H., Mengwasser, K.E., Toms, A. V, Woo, M.S., Greulich, H., Wong, K.-K., Meyerson, M., Eck, M.J., 2008. The T790M mutation in EGFR kinase causes drug resistance by increasing the affinity for ATP. *Proc. Natl. Acad. Sci. U. S. A.* 105, 2070–5. doi:10.1073/pnas.0709662105
- Zamble, D.B., Mu, D., Reardon, J.T., Sancar, A., Lippard, S.J., 1996. Repair of cisplatin-DNA adducts by the mammalian excision nuclease. *Biochemistry* 35, 10004–10013. doi:10.1021/bi960453+
- Zhang, H., Kuang, S., Wang, Y., Sun, X., Gu, Y., Hu, L., Yu, Q., 2015. Bigelovin inhibits STAT3 signaling by inactivating JAK2 and induces apoptosis in human cancer cells. *Acta Pharmacol. Sin.* 36, 507–516. doi:10.1038/aps.2014.143

- Zhang, H.F., Lai, R., 2014. STAT3 in cancer-friend or foe? *Cancers (Basel)*. 6, 1408–1440. doi:10.3390/cancers6031408
- Zhang, J., Walter, J.C., 2014. Mechanism and regulation of incisions during DNA interstrand cross-link repair. *DNA repair (Amst)*. 19, 135–142. doi:10.1016/j.dnarep.2014.03.018
- Zhang, X., Darnell, J.E., 2001. Functional Importance of Stat3 Tetramerization in Activation of the α 2-Macroglobulin Gene. *J. Biol. Chem.* 276, 33576–33581. doi:10.1074/jbc.M104978200
- Zhang, X., Sun, Y., Pireddu, R., Yang, H., Urlam, M.K., Lawrence, H.R., Guida, W.C., Lawrence, N.J., Sebti, S.M., 2013. A novel inhibitor of STAT3 homodimerization selectively suppresses STAT3 activity and malignant transformation. *Cancer Res.* 73, 1922–33. doi:10.1158/0008-5472.CAN-12-3175
- Zhang, X., Wrzeszczynska, M.H., Horvath, C.M., Darnell, J.E., 1999. Interacting regions in Stat3 and c-Jun that participate in cooperative transcriptional activation. *Mol. Cell. Biol.* 19, 7138–7146. doi:10.1128/MCB.19.10.7138
- Zhang, X., Xiao, W., Wang, L., Tian, Z., Zhang, J., 2011. Deactivation of signal transducer and activator of transcription 3 reverses chemotherapeutics resistance of leukemia cells via down-regulating P-gp. *PLoS One* 6, e20965. doi:10.1371/journal.pone.0020965
- Zhang, X., Zhang, J., Wang, L., Wei, H., Tian, Z., 2007. Therapeutic effects of STAT3 decoy oligodeoxynucleotide on human lung cancer in xenograft mice. *BMC Cancer* 7, 149. doi:10.1186/1471-2407-7-149
- Zhao, C., Li, H., Lin, H.J., Yang, S., Lin, J., Liang, G., 2016. Feedback Activation of STAT3 as a Cancer Drug-Resistance Mechanism. *Trends Pharmacol. Sci.* 37, 47–61. doi:10.1016/j.tips.2015.10.001
- Zhao, W., Bao, P., Qi, H., You, H., 2010. Resveratrol down-regulates survivin and induces apoptosis in human multidrug-resistant SPC-A-1/CDDP cells. *Oncol. Rep.* 23, 279–86. doi:10.3892/or

- Zhao, W., Jaganathan, S., Turkson, J., 2010. A cell-permeable Stat3 SH2 domain mimetic inhibits Stat3 activation and induces antitumor cell effects in vitro. *J. Biol. Chem.* 285, 35855–35865. doi:10.1074/jbc.M110.154088
- Zhen, W., Link, C.J., O'Connor, P.M., Reed, E., Parker, R., Howell, S.B., Bohr, V.A., 1992. Increased gene-specific repair of cisplatin interstrand cross-links in cisplatin-resistant human ovarian cancer cell lines. *Mol. Cell. Biol.* 12, 3689–98. doi:10.1128/MCB.12.9.3689
- Zhong, Z., Wen, Z., Jr, J.E.D., 1994. Stat3: A STAT Family Member Activated by Tyrosine Phosphorylation in Response to Epidermal Growth Factor and Interleukin-6. *Science* 264, 95–98.
- Zhou, X., Ren, Y., Liu, A., Jin, R., Jiang, Q., Huang, Y., Kong, L., Wang, X., Zhang, L., 2014. WP1066 Sensitizes Oral Squamous Cell Carcinoma Cells to Cisplatin by Targeting STAT3/miR-21 axis. *Sci. Rep.* 4, 7461. doi:10.1038/srep07461
- Zushi, S., Shinomura, Y., Kiyohara, T., Miyazaki, Y., Kondo, S., Sugimachi, M., Higashimoto, Y., Kanayama, S., Matsuzawa, Y., 1998. STAT3 mediates the survival signal in epithelial cells. *Int J. Cancer* 78, 326–330.
- Zustovich, F., Fabiani, F., 2014. Therapeutic opportunities for castration-resistant prostate cancer patients with bone metastases. *Crit. Rev. Oncol. Hematol.* 91, 197–209. doi:10.1016/j.critrevonc.2014.01.003

Appendices

Appendix A: Gene list for DNA damage signalling arrays

Position	Symbol	Description	Gene name
A01	ABL1	C-abl oncogene 1, non-receptor tyrosine kinase	ABL/JTK7/bcr/abl/c-ABL/c-ABL1/p150/v-abl
A02	APEX1	APEX nuclease (multifunctional DNA repair enzyme) 1	APE/APE1/APEN/APEX/APX/HAP1/REF1
A03	ATM	Ataxia telangiectasia mutated	AT1/ATA/ATC/ATD/ATDC/ATE/TEL1/TELO1
A04	ATR	Ataxia telangiectasia and Rad3 related	FCTCS/FRP1/MEC1/SCKL/SCKL1
A05	ATRIP	ATR interacting protein	-
A06	ATRX	Alpha thalassemia/mental retardation syndrome X-linked	ATR2/JMS/MRXHF1/RAD54/RAD54L/SFM1/SHS/XH2/XNP/ZNF-HX
A07	BARD1	BRCA1 associated RING domain 1	-
A08	BAX	BCL2-associated X protein	BCL2L4
A09	BBC3	BCL2 binding component 3	JFY-1/JFY1/PUMA
A10	BLM	Bloom syndrome, RecQ helicase-like	BS/RECQ2/RECQL2/RECQL3
A11	BRCA1	Breast cancer 1, early onset	BRCA1/BRCC1/BROVCA1/IRIS/PNCA4/PPP1R53/PSCP/RNF53
A12	BRIP1	BRCA1 interacting protein C-terminal helicase 1	BACH1/FANCJ/OF
B01	CDC25A	Cell division cycle 25 homolog A (S. pombe)	CDC25A2
B02	CDC25C	Cell division cycle 25 homolog C (S. pombe)	CDC25/PPP1R60
B03	CDK7	Cyclin-dependent kinase 7	CAK1/CDKN7/HCAK/MO15/STK1/p39MO15

Position	Symbol	Description	Gene name
B04	CDKN1A	Cyclin-dependent kinase inhibitor 1A (p21, Cip1)	CAP20/CDKN1/CIP1/MDA-6/P21/SDI1/WAF1/p21CIP1
B05	CHEK1	CHK1 checkpoint homolog (S. pombe)	CHK1
B06	CHEK2	CHK2 checkpoint homolog (S. pombe)	CDS1/CHK2/HuCds1/LFS2/PP1425/RAD53/hCds1
B07	CIB1	Calcium and integrin binding 1 (calmyrin)	CIB/CIBP/KIP1/PRKDCIP/SIP2-28
B08	CRY1	Cryptochrome 1 (photolyase-like)	PHLL1
B09	CSNK2A2	Casein kinase 2, alpha prime polypeptide	CK2A2/CSNK2A1
B10	DDB1	Damage-specific DNA binding protein 1, 127kDa	DDBA/UV-DDB1/XAP1/XPCE/XPE/XPE-BF
B11	DDB2	Damage-specific DNA binding protein 2, 48kDa	DDBB/UV-DDB2
B12	DDIT3	DNA-damage-inducible transcript 3	CEBPZ/CHOP/CHOP-10/CHOP10/GADD153
C01	ERCC1	Excision repair cross-complementing rodent repair deficiency, complementation group 1 (includes overlapping antisense sequence)	COFS4/RAD10/UV20
C02	ERCC2	Excision repair cross-complementing rodent repair deficiency, complementation group 2	COFS2/EM9/TTD/XPD
C03	EXO1	Exonuclease 1	HEX1/hExo1
C04	FANCA	Fanconi anemia, complementation group A	FA/FA-H/FA1/FAA/FACA/FAH/FANCH
C05	FANCD2	Fanconi anemia, complementation group D2	FA-D2/FA4/FACD/FAD/FAD2/FANCD
C06	FANCG	Fanconi anemia,	FAG/XRCC9

Position	Symbol	Description	Gene name
		complementation group G	
C07	FEN1	Flap structure-specific endonuclease 1	FEN-1/MF1/RAD2
C08	GADD45A	Growth arrest and DNA-damage-inducible, alpha	DDIT1/GADD45
C09	GADD45G	Growth arrest and DNA-damage-inducible, gamma	CR6/DDIT2/GADD45gamma/GRP17
C10	H2AFX	H2A histone family, member X	H2A.X/H2A/X/H2AX
C11	HUS1	HUS1 checkpoint homolog (S. pombe)	hHUS1
C12	LIG1	Ligase I, DNA, ATP-dependent	-
D01	MAPK12	Mitogen-activated protein kinase 12	ERK3/ERK6/P38GAMMA/PRKM12/SAPK-3/SAPK3
D02	MBD4	Methyl-CpG binding domain protein 4	MED1
D03	MCPH1	Microcephalin 1	BRIT1/MCT
D04	MDC1	Mediator of DNA-damage checkpoint 1	NFBD1
D05	MLH1	MutL homolog 1, colon cancer, nonpolyposis type 2 (E. coli)	COCA2/FCC2/HNPCC/HNPCC2/hMLH1
D06	MLH3	MutL homolog 3 (E. coli)	HNPCC7
D07	MPG	N-methylpurine-DNA glycosylase	AAG/ADPG/APNG/CRA36.1/MDG/Mid1/PIG11/PIG16/anpg
D08	MRE11A	MRE11 meiotic recombination 11 homolog A (S. cerevisiae)	ATLD/HNGS1/MRE11/MRE11B
D09	MSH2	MutS homolog 2, colon cancer, nonpolyposis type 1 (E. coli)	COCA1/FCC1/HNPCC/HNPCC1/LCFS2
D10	MSH3	MutS homolog 3 (E. coli)	DUP/MRP1
D11	NBN	Nibrin	AT-V1/AT-V2/ATV/NBS/NBS1/P95

Position	Symbol	Description	Gene name
D12	NTHL1	Nth endonuclease III-like 1 (E. coli)	NTH1/OCTS3
E01	OGG1	8-oxoguanine DNA glycosylase	HMMH/HOGG1/MUTM/OGH1
E02	PARP1	Poly (ADP-ribose) polymerase 1	ADPRT/ADPRT1/ADPRT1/ARTD1/PARP/PARP-1/PPOL/pADPRT-1
E03	PCNA	Proliferating cell nuclear antigen	-
E04	PMS1	PMS1 postmeiotic segregation increased 1 (S. cerevisiae)	HNPCC3/PMSL1/hPMS1
E05	PMS2	PMS2 postmeiotic segregation increased 2 (S. cerevisiae)	HNPCC4/PMS2CL/PMSL2
E06	PNKP	Polynucleotide kinase 3'-phosphatase	EIEE10/MCSZ/PNK
E07	PPM1D	Protein phosphatase, Mg ²⁺ /Mn ²⁺ dependent, 1D	PP2C-DELTA/WIP1
E08	PPP1R15A	Protein phosphatase 1, regulatory (inhibitor) subunit 15A	GADD34
E09	PRKDC	Protein kinase, DNA-activated, catalytic polypeptide	DNA-PKcs/DNAPK/DNPK1/HYRC/HYRC1/XRCC7/p350
E10	RAD1	RAD1 homolog (S. pombe)	HRAD1/REC1
E11	RAD17	RAD17 homolog (S. pombe)	CCYC/HRAD17/R24L/RAD17SP/RAD24
E12	RAD18	RAD18 homolog (S. cerevisiae)	RNF73
F01	RAD21	RAD21 homolog (S. pombe)	CDLS4/HR21/HRAD21/MCD1/NXP1/SCC1/hHR21
F02	RAD50	RAD50 homolog (S. cerevisiae)	NBSLD/RAD502/hRad50
F03	RAD51	RAD51 homolog (S. cerevisiae)	BRCC5/HRAD51/HsRad51/HsT16930/MRMV2/RAD51A/RECA

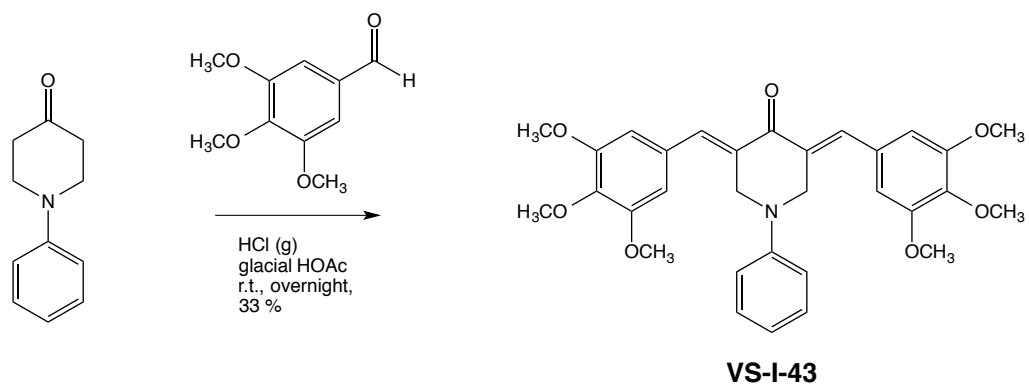
Position	Symbol	Description	Gene name
F04	RAD51B	RAD51 homolog B (<i>S. cerevisiae</i>)	R51H2/RAD51L1/REC2
F05	RAD9A	RAD9 homolog A (<i>S. pombe</i>)	RAD9
F06	RBBP8	Retinoblastoma binding protein 8	COM1/CTIP/JWDS/RIM/SAE2/SCKL2
F07	REV1	REV1 homolog (<i>S. cerevisiae</i>)	REV1L
F08	RNF168	Ring finger protein 168	hRNF168
F09	RNF8	Ring finger protein 8	hRNF8
F10	RPA1	Replication protein A1, 70kDa	HSSB/MST075/REPA1/RFA-A/RP-A/RPA70
F11	SIRT1	Sirtuin 1	SIR2L1
F12	SMC1A	Structural maintenance of chromosomes 1A	CDLS2/DXS423E/SB1.8/SMC1/SMC1L1/SMC1alpha/SMCB
G01	SUMO1	SMT3 suppressor of mif two 3 homolog 1 (<i>S. cerevisiae</i>)	DAP1/GMP1/OFC10/PIC1/SEN2/SMT3/SMT3C/SMT3H3/UBL1
G02	TOPBP1	Topoisomerase (DNA) II binding protein 1	TOP2BP1
G03	TP53	Tumor protein p53	BCC7/LFS1/P53/TRP53
G04	TP53BP1	Tumor protein p53 binding protein 1	53BP1/p202
G05	TP73	Tumor protein p73	P73
G06	UNG	Uracil-DNA glycosylase	DGU/HIGM4/HIGM5/UDG/UNG1/UNG15/UNG2
G07	XPA	Xeroderma pigmentosum, complementation group A	XP1/XPAC
G08	XPC	Xeroderma pigmentosum, complementation group C	RAD4/XP3/XPCC
G09	XRCC1	X-ray repair complementing defective repair in Chinese hamster cells 1	RCC
G10	XRCC2	X-ray repair complementing defective repair in Chinese	-

Position	Symbol	Description	Gene name
		hamster cells 2	
G11	XRCC3	X-ray repair complementing defective repair in Chinese hamster cells 3	CMM6
G12	XRCC6	X-ray repair complementing defective repair in Chinese hamster cells 6	CTC75/CTCBF/G22P1/KU70/ML8/TLAA
H01	ACTB	Actin, beta	BRWS1/PS1TP5BP1
H02	B2M	Beta-2-microglobulin	-
H03	GAPDH	Glyceraldehyde-3-phosphate dehydrogenase	G3PD/GAPD
H04	HPRT1	Hypoxanthine phosphoribosyltransferase 1	HGPRT/HPRT
H05	RPLP0	Ribosomal protein, large, P0	L10E/LP0/P0/PRLP0/RPP0
H06	HGDC	Human Genomic DNA Contamination	HIGX1A
H07	RTC	Reverse Transcription Control	RTC
H08	RTC	Reverse Transcription Control	RTC
H09	RTC	Reverse Transcription Control	RTC
H10	PPC	Positive PCR Control	PPC
H11	PPC	Positive PCR Control	PPC
H12	PPC	Positive PCR Control	PPC

Appendix B: Synthesis of VS-43

Synthesis of VS-43 ((3*E*,5*E*)-3,5-Bis-(3,4,5-trimethoxybenzylidene)-1-phenylpiperid-4-one) was as follows:

A solution of appropriate *N*-phenyl-4-piperidone (100 mg, 0.6 mM) and 3,4,5-trimethoxybenzaldehyde (235 mg, 1.2 mM) in glacial acetic acid (2.0 mL) was purged with dry hydrogen chloride gas for 20-25 minutes. The reaction mixture was stirred at room temperature for 16 hours, poured into ice-water, and neutralised with solid sodium carbonate. The organic product was extracted with ethyl acetate (3 x 10 mL), which was combined and dried with anhydrous sodium sulfate. Removal of the drying agent and solvent gave a residue that was purified by silica gel column chromatography. The desired product, drying in vacuum at 40-45 °C, was isolated as a yellow solid (100 mg, 33%), Mp = 134-136 °C, R_f = 0.55 [ethyl acetate:hexane (2:3)]; FT-IR (KBr) ν 3473, 3020, 2935, 2834, 1659, 1594, 1577, 1497, 1450, 1415, 1385, 1360, 1241, 1213, 1186, 1120, 1046, 1038, 996, 963, 835, 793, 764, 734, 720; ¹H NMR (CDCl₃) δ 7.82 (s, 2H), 7.16 (t, *J* = 8.0 Hz, 2H), 6.81 (t, *J* = 8.0 Hz, 1H), 6.74 (d, *J* = 8.0 Hz, 2H), 6.66 (s, 4H), 4.67 (s br, 4H), 3.86 (s, 6H), 3.84 (s, 12H); ¹³C NMR (CDCl₃) δ 186.9, 153.2, 148.7, 139.3, 137.9, 132.3, 130.6, 129.3, 120.2, 116.5, 107.9, 61.0, 56.3, 51.3; LRMS (EI) *m/z* 531 (M⁺, 100%). HRMS (EI) calcd for C₃₁H₃₃NO₇ 531.2257, found 531.2254.



Appendix B Figure 1: Synthesis of VS-43.

Appendix C: STAT3 binding sites upstream of DNA repair genes identified by UCSC Genome Browser

GENE	STAT3 binding site		
EME1	chr17	48449918	48450328
	chr17	48449918	48450328
MUS81	chr11	65627711	65628059
	chr11	65627711	65628059
BRCA1	chr17	41276552	41276828
	chr17	41277280	41277690
FANCG	chr9	35079960	35080310
	chr9	35079960	35080310
	chr9	35079960	35080310
	chr9	35079960	35080310

GENE	STAT3 binding site		
	chr9	35079960	35080310
	chr9	35079960	35080310
FANCM	chr14	45646302	45646637
FANCI	chr15	89786961	89787287
	chr15	89786961	89787287
CHEK2	chr22	29108348	29108722
	chr22	29138506	29138750
	H2AFX	chr11	118966349
chr11		118966349	118966670
MDC1	chr6	30685155	30685510
	chr6	30685155	30685510

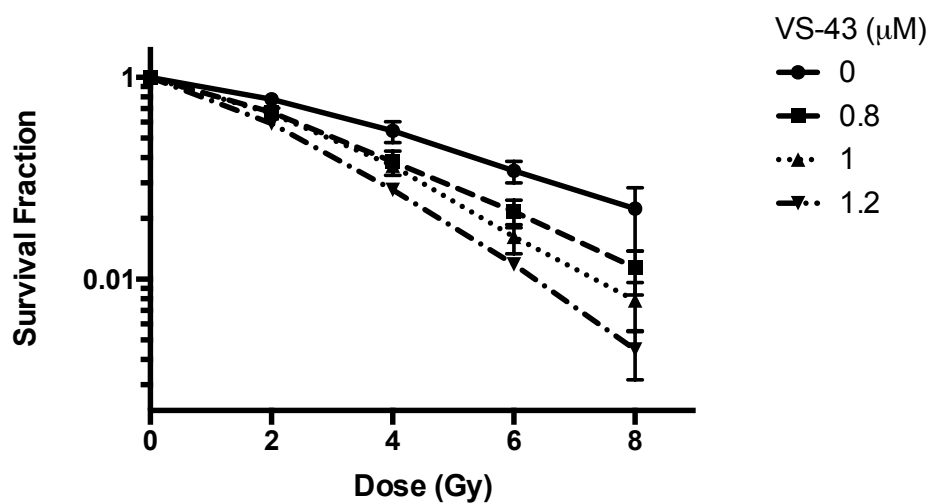
GENE	STAT3 binding site		
MSH6	chr2	48010135	48010490
	chr2	48010135	48010490
	chr2	48010135	48010490
	chr2	48010135	48010490
RAD51AP1	chr12	4647486	4647896
	chr12	4647486	4647896
RAD51B	chr14	69010937	69011262
RAD54B	chr8	95385447	95385727
CHEK1	chr11	125491913	125492229
	chr11	125491913	125492229

GENE	STAT3 binding site		
	chr11	125491913	125492229
ERCC1	chr19	45927618	45927952
	chr19	45982169	45982495
HMGB1P27	chr2	192036449	192036910
MDM2	chr12	69202547	69202858
	chr12	69202547	69202858

GENE	STAT3 binding site		
	chr12	69202547	69202858
MLH3	chr14	75516304	75516585
	chr14	75516304	75516585
MRE11A	chr11	94182617	94182941
	chr11	94183305	94183585
RAD52	chr12	1023485	1023789

Appendix D: Radiosensitisation by VS-43

VS-43 can radiosensitise DU145 cells. Cells were treated with VS-43 for 18 hours and subsequently irradiated. Cell survival was assessed by colony formation assay (supplementary methods). Pre-treatment with VS-43 resulted in a dose-dependent decrease in colony formation following irradiation.



Appendix D Figure 1: Radiosensitisation by VS-43.